NEW ORGANIC CHEMISTRY FOR POLYMER SYNTHESIS WORKSHOP

MAY 21-24, 1995
Santa Fe, New Mexico

The Division of Polymer Chemistry - American Chemical Society

New Organic Chemistry for Polymer Synthesis

Workshop Presentations

"Investigations into the Chemistry of Thermodynamically Unstable Monomers: Direct Polymerization of Vinyl Alcohol, the Enolic Tautomer of Acetaldehyde"

Bruce M. Novak and Anna K. Cederstav

Department of Polymer Science and Engineering
University of Massachusetts
Amherst, MA 01002

A Tale of Two "Monomers"

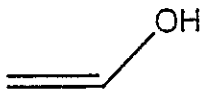

Vinyl Alcohol

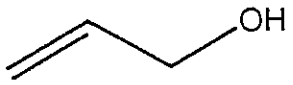

Allylic Alcohol

Poly(vinyl alcohol)

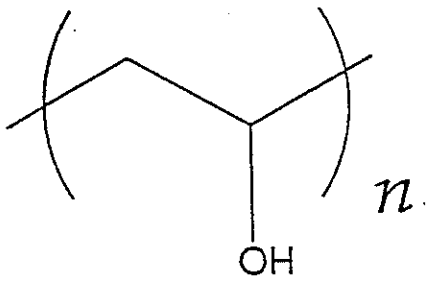

- Thickening agent
- Coatings, adhesives
- Water-soluble packaging
- Cosmetics, personal care products
- Pharmaceuticals
- Poly(vinyl butyral) interlayers in auto safety glass
- Biodegradable

Vinyl Polymerizations: A Primer

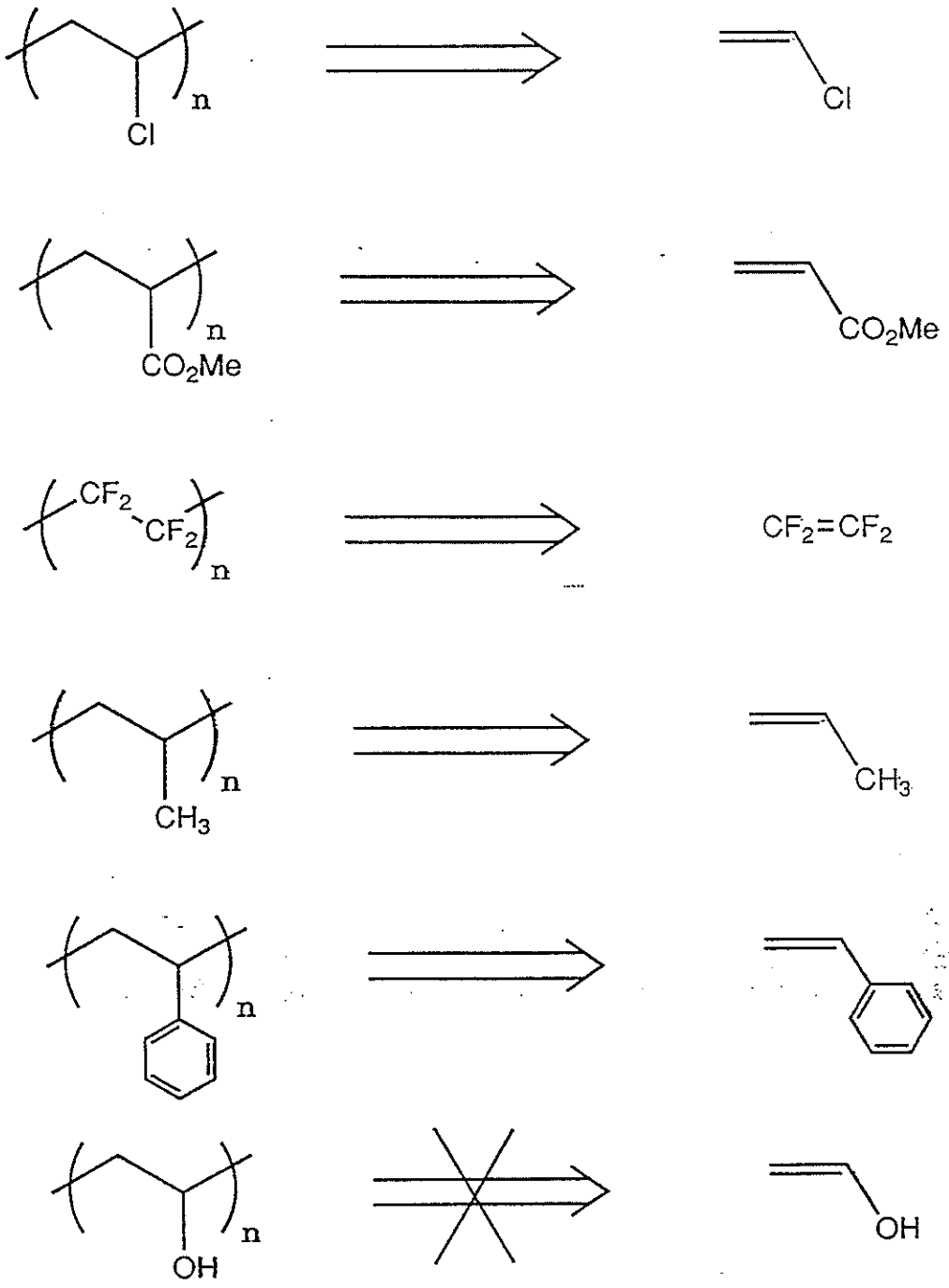

Thermodynamic Considerations

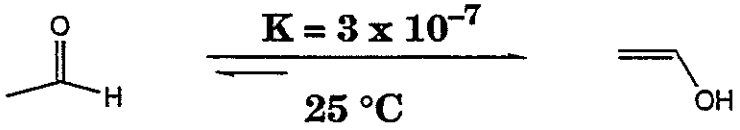

"Vinyl alcohol is an unstable compound that rearranges spontaneously to acetaldehyde."

T. Solomons, "Organic Chemistry", 2d Ed. Wiley, 1980, pg 336

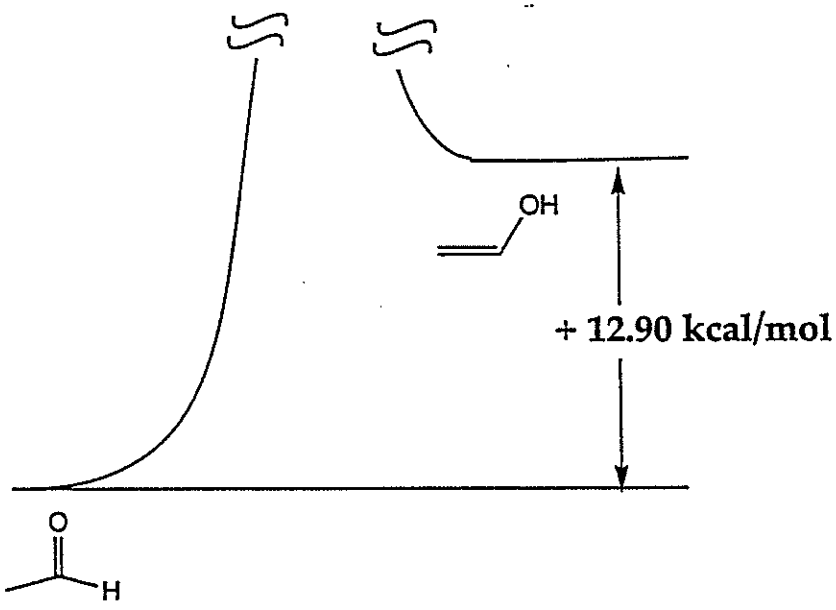

The Synthesis of Poly(Vinyl Alcohol)

"...poly(vinyl acetate) is used to produce two polymers that cannot be synthesized directly since their monomers do not exist."

G. Odian, Principles of Polymerization, 3rd Edition, 1991, pg 711

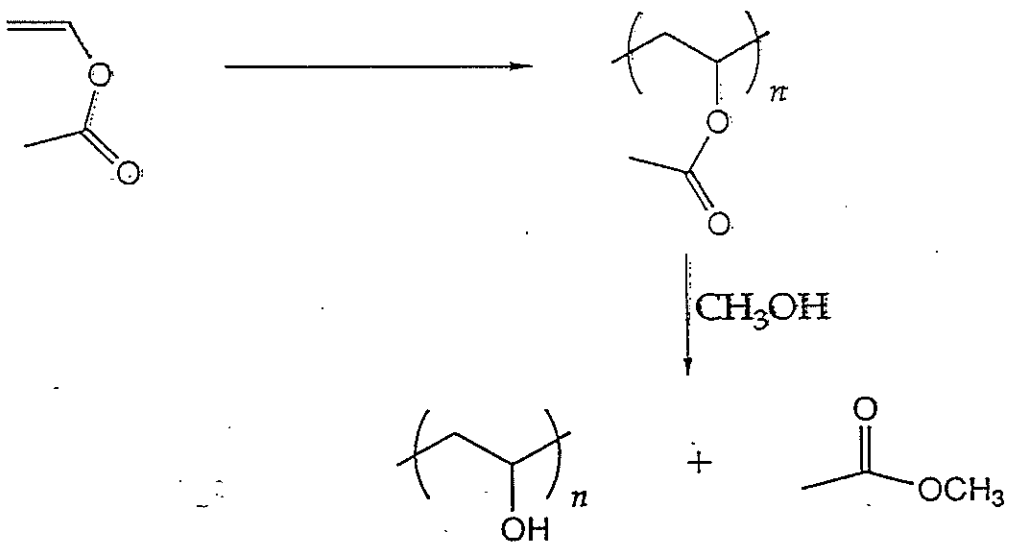

Poly(vinyl alcohol)

- Thickening agent
- Coatings, adhesives
- Water-soluble packaging
- Cosmetics, personal care products
- Pharmaceuticals
- Poly(vinyl butyral) interlayers in auto safety glass
- Biodegradable

Proposal

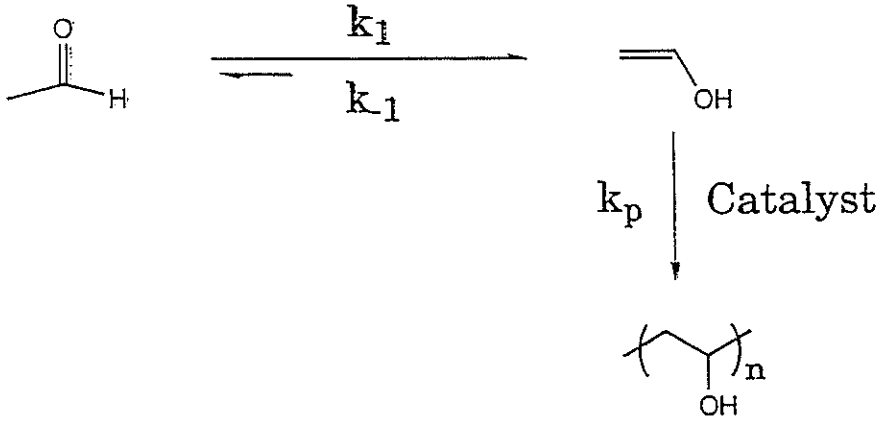

Our Approach
(Kinetics vs. Thermodynamics)

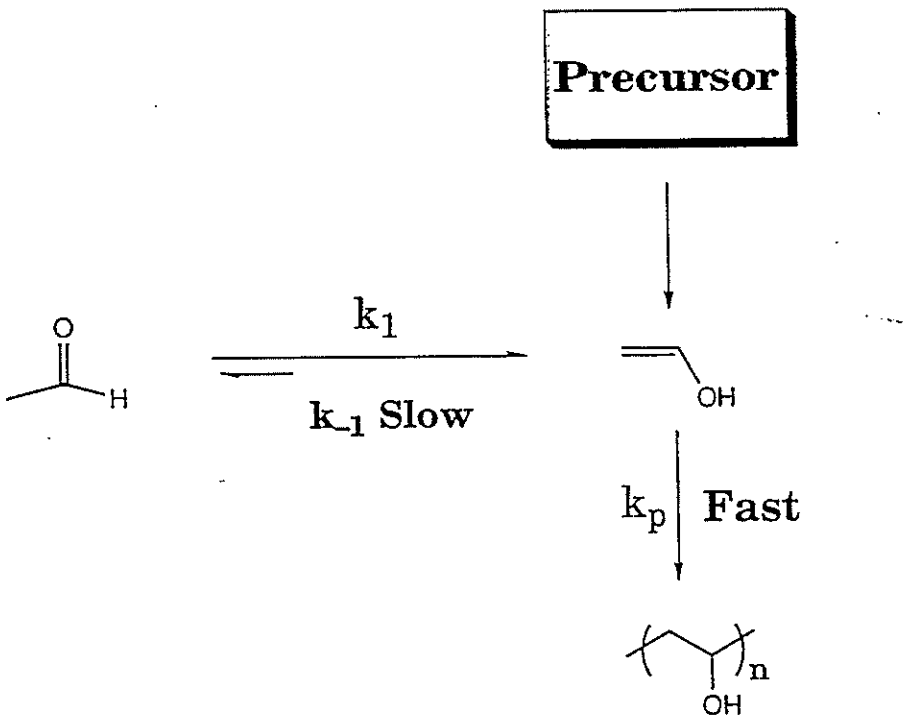

Require Conditions Under Which:

$$k_p >>> k_{-1}$$

Mechanism of Enol Ketonization

Base Catalysis (Fast)

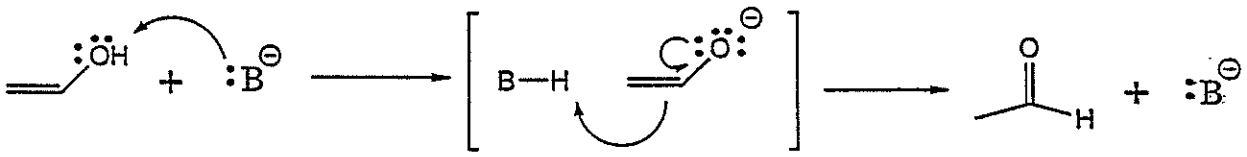

$k_{OH^-} = 1.5 \times 10^7\ M^{-1}s^{-1}$

Acid Catalysis (Slow)

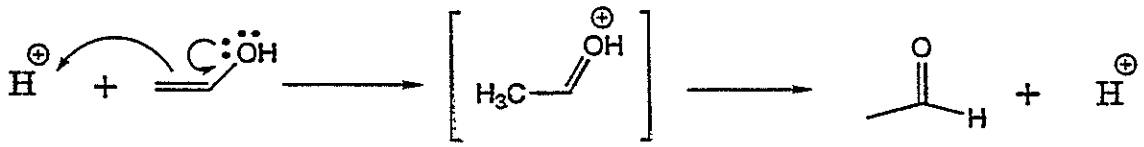

Concerted Water Catalysis

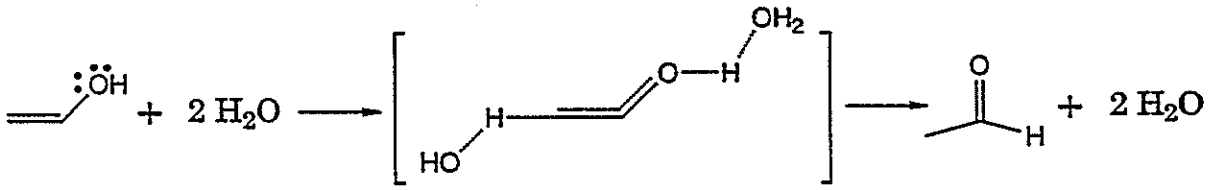

Rate of Tautomerization is Dependent On:

- **pH**
- **Water Content**
- **Vinyl Alcohol Concentration (Upper limit ≈ 0.6 M)**

Hydrolysis of Orthoesters

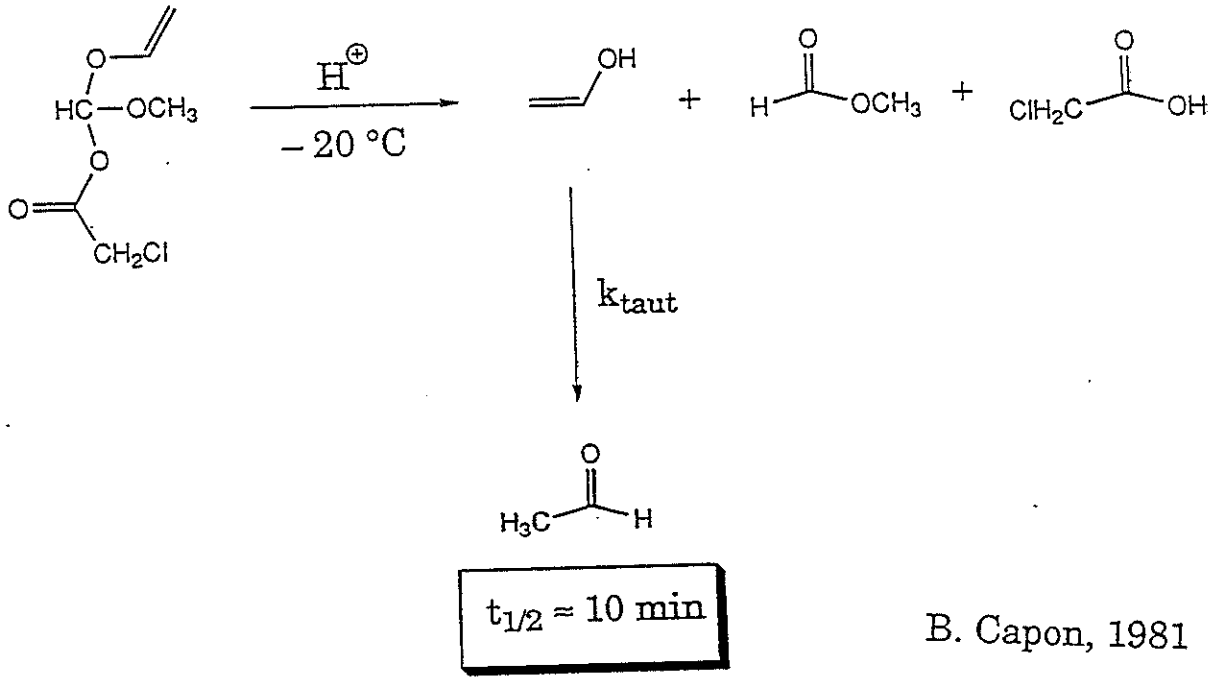

B. Capon, 1981

The Synthesis of Unsaturated Acetals

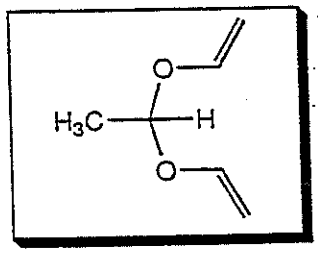

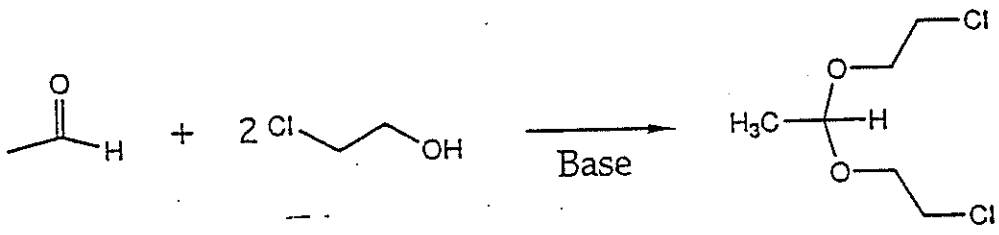

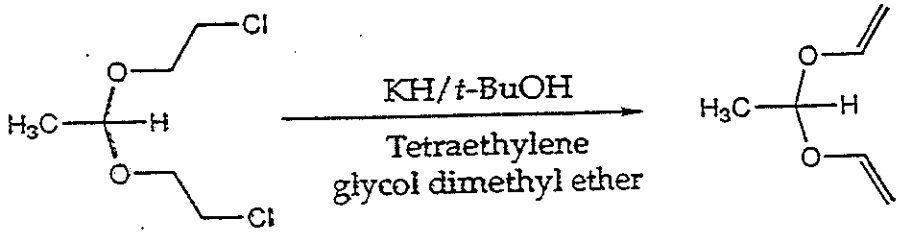

80%

Precursor Method for Vinyl Alcohol Synthesis

Hydrolysis of Acetals and Ketene Acetals

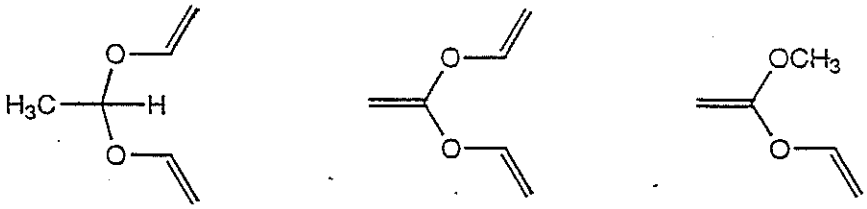

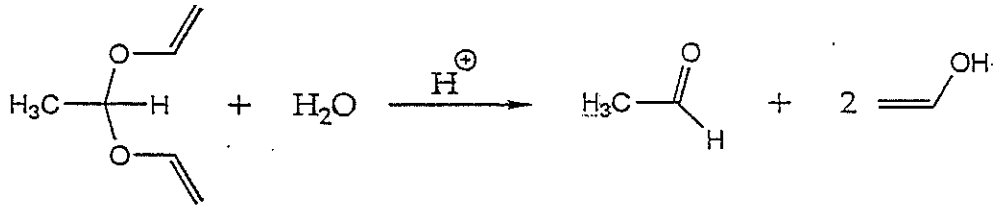

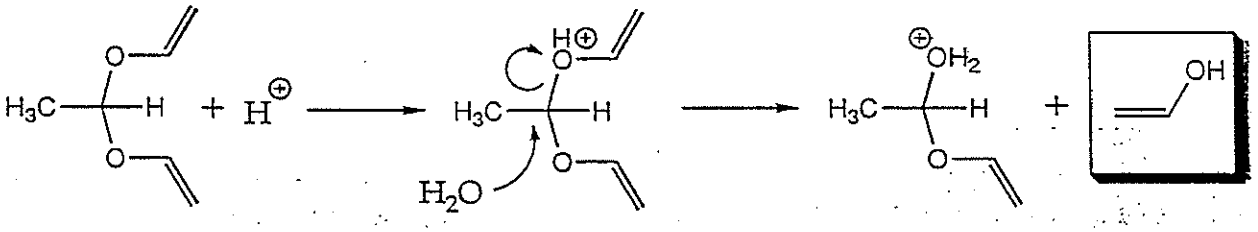

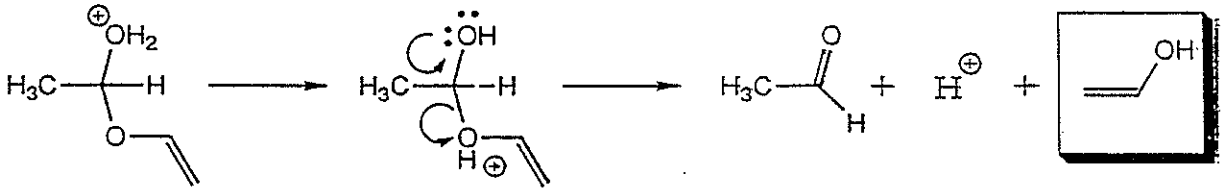

B. Capon, 1982

Kinetics of Tautomerization

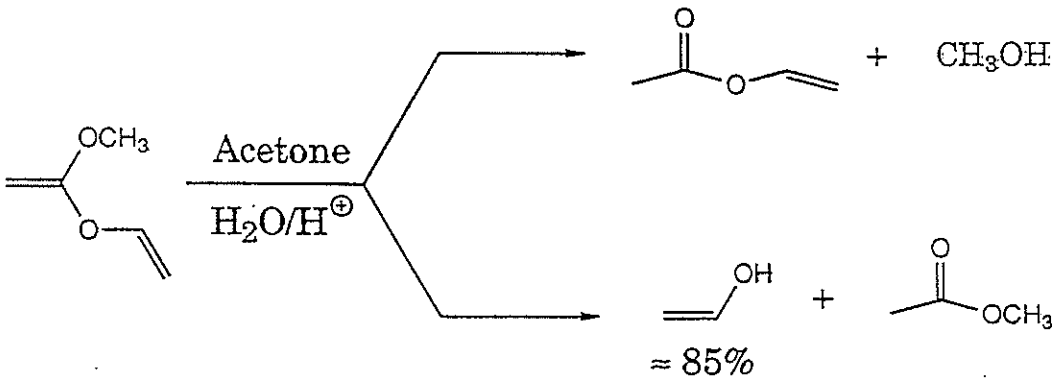

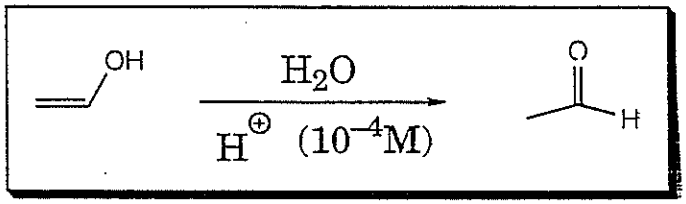

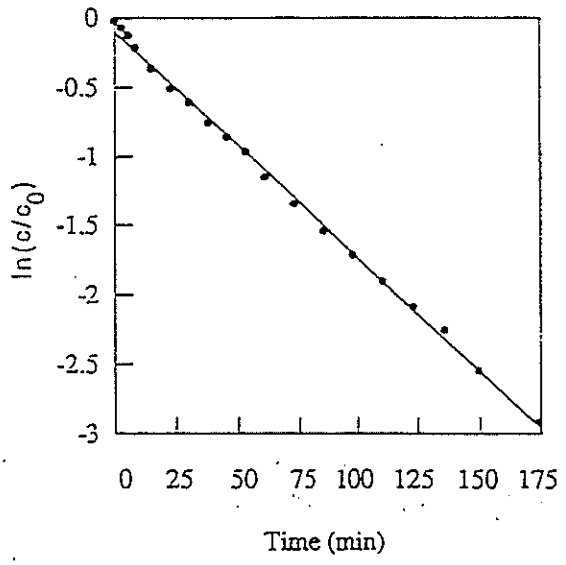

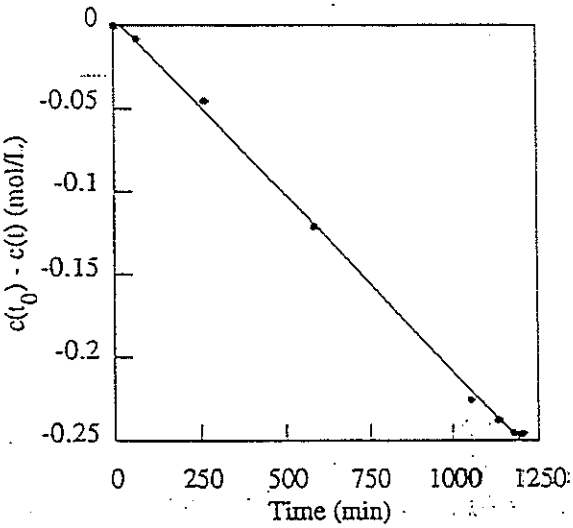

Excess Water

First Order in VA

$k_{obs} = 2.7 \times 10^{-4}\ s^{-1}$

One Equivalent H_2O

Zero Order in VA

$k_{obs} = 3.5 \times 10^{-6}$ M/s

⟹ **Water Catalyzes Tautomerization**

Michaelis-Menten Enzyme Kinetics

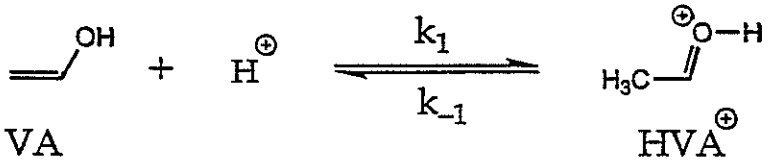

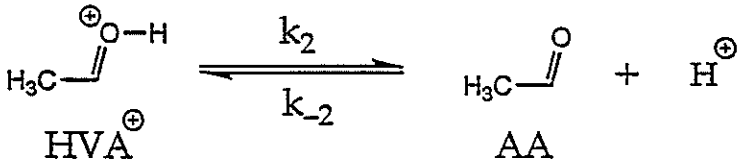

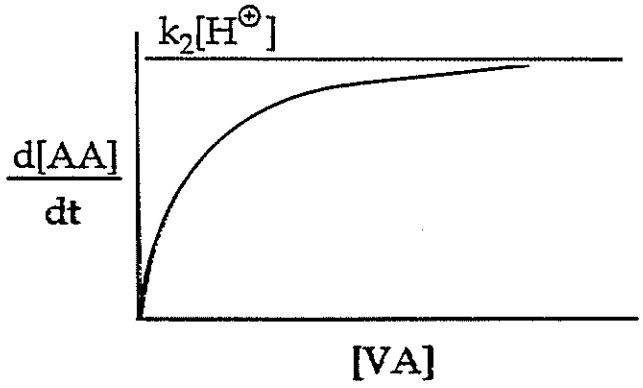

$$\frac{d[AA]}{dt} = \frac{k_2[H^{\oplus}][VA]}{K_M + [VA]}$$

where: $K_M = \dfrac{k_{-1} + k_2}{k_1}$

when: $[VA] >>> K_M$

$$\boxed{\frac{d[AA]}{dt} = k_2[H^{\oplus}]}$$

Extending Vinyl Alcohol's Lifetime

1. Use Acidic Conditions ($[H^{\oplus}] \approx 10^{-4}$)

2. "Dehydrate" Hydrolysis System

"Self Dehydrating" Conditions

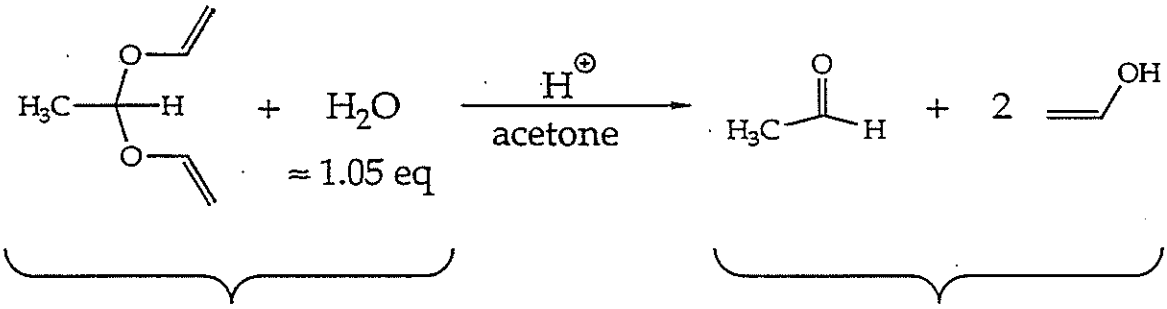

"Wet" "Dry"

Probing the Chemistry of Vinyl Alcohol

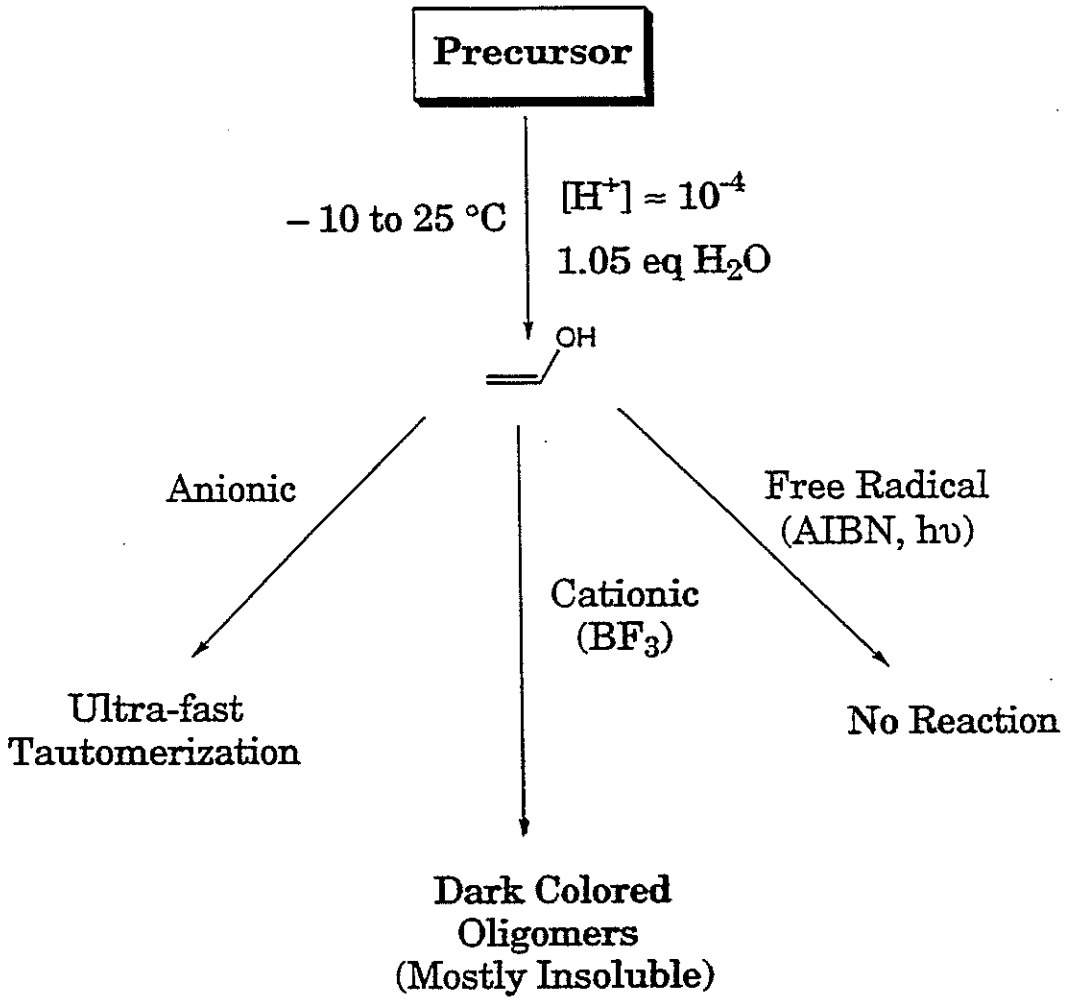

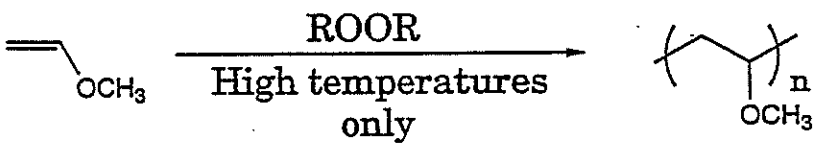

Stabilized, Electron-Rich
Radical Intermediate

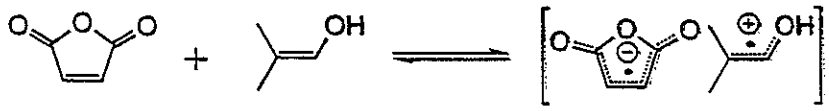

Charge Transfer Complex

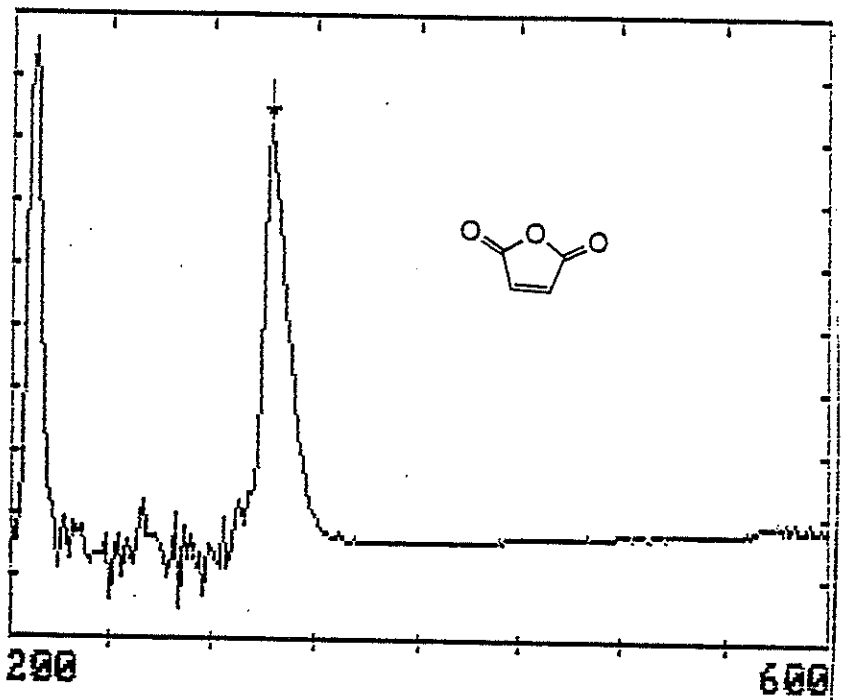

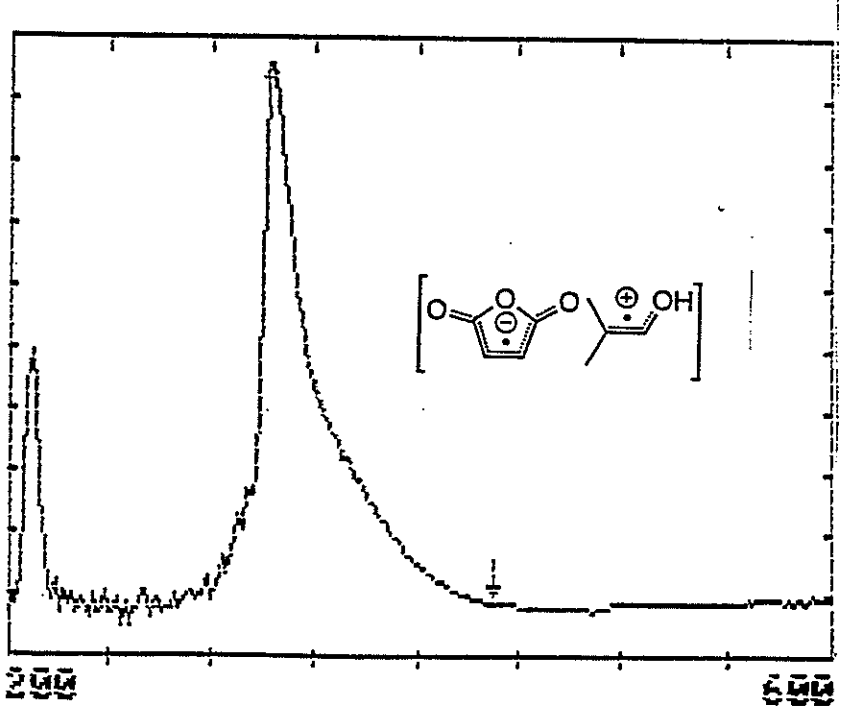

1:1 Alternating Copolymerizations

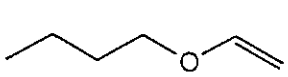

ROOR → No Reaction

ROOR → No Reaction

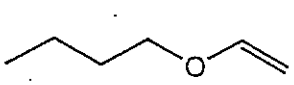

$r_1 = 0$

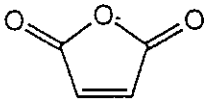

$r_2 = 0.045$

ROOR, 50 °C →

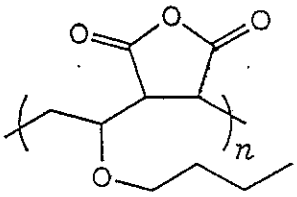

$r_1 \bullet r_2 = 0$

1:1 Alternating copolymer

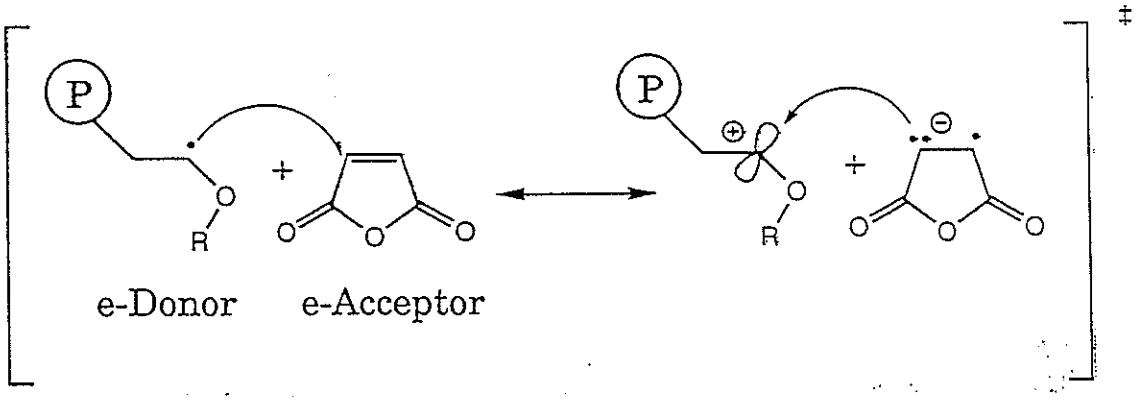

e-Donor e-Acceptor

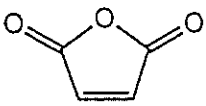

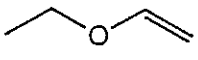

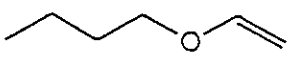

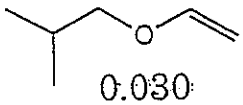

Q	0.86	0.018	0.038	0.030
e	3.69	−1.80	−1.50	−1.27

Donor-Acceptor Copolymerizations

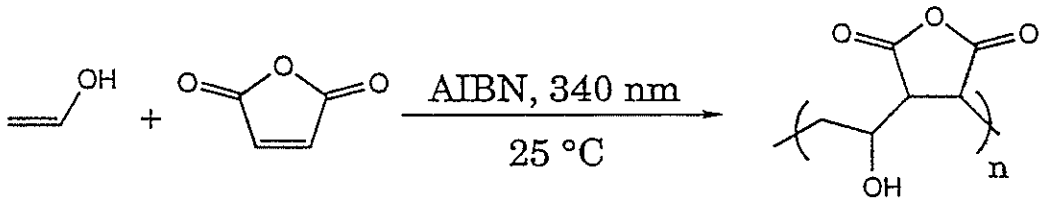

1:1 Copolymer
≈ 100% Yields

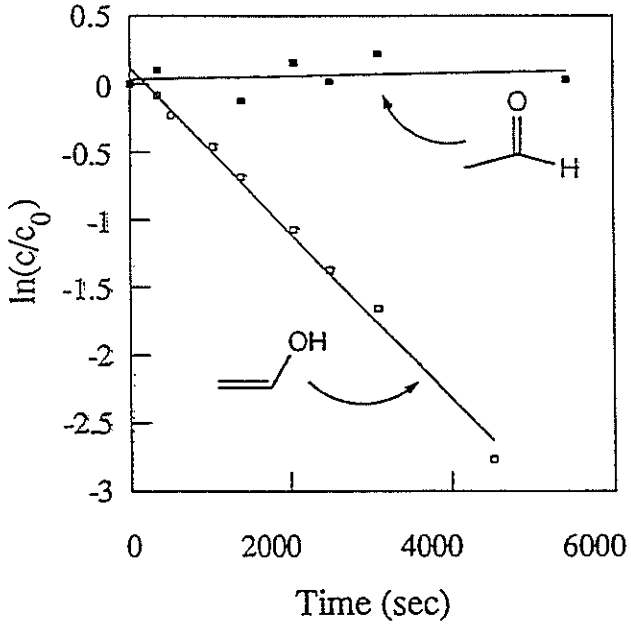

Intramolecular Cyclization

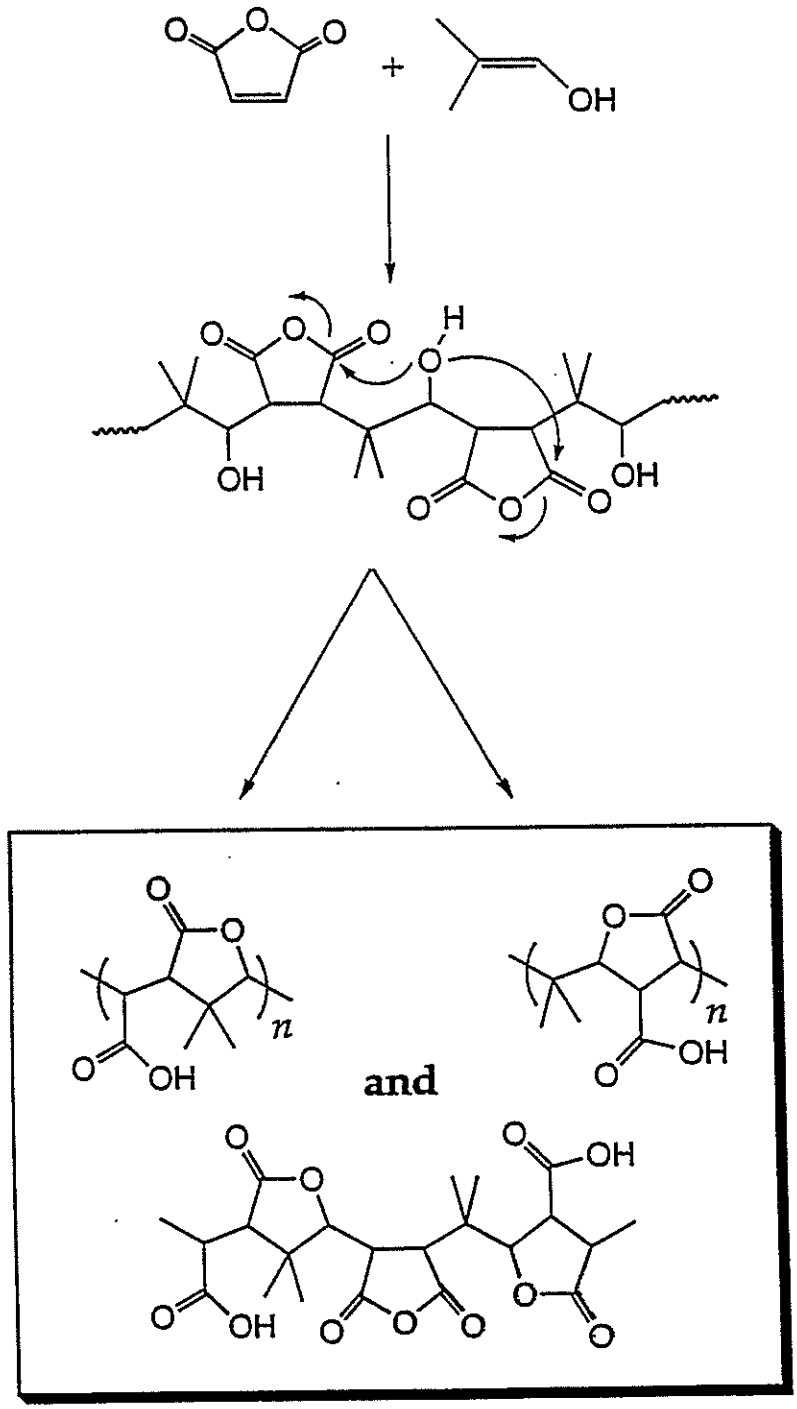

Soluble in: DMSO, acetone, THF

Vinyl Alcohol Copolymer Transformations

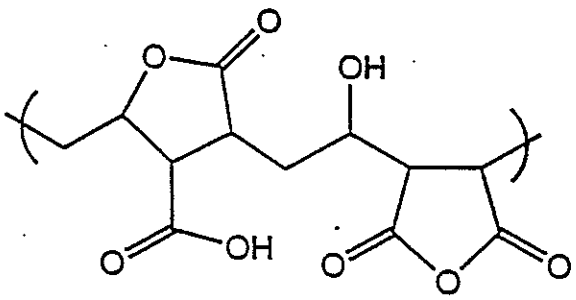

IR (cm^{-1})	Solubility
1716 - acid	DMSO
1732 - ester	
1778 - anhydride	
1849 - anhydride	
3500-2400 - OH	

DMSO
H_2O, H^+

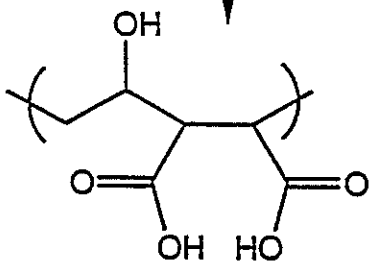

IR (cm^{-1})	Solubility
1718 - acid	H_2O
	MeOH
3500-2400 - OH	

CH_2N_2

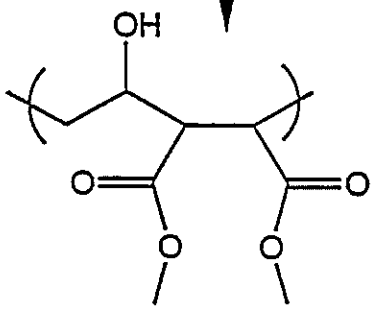

IR (cm^{-1})	Solubility
1731 - ester	THF
3448 (br) - OH	

Mn: 55,900
Mw: 183,600
PDI: 3.3

Non-viable Acceptor Monomers

7,7,8,8 - tetracyanoquinodimethane

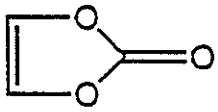

Vinylene Carbonate

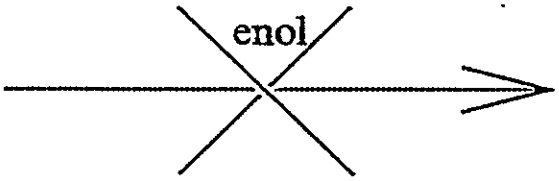

copolymer

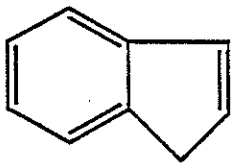

Indene

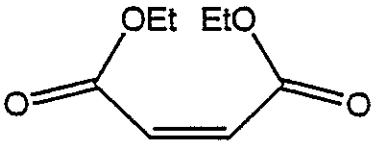

Diethyl Fumarate

New Alternating Copolymers Using Vinyl Alcohol

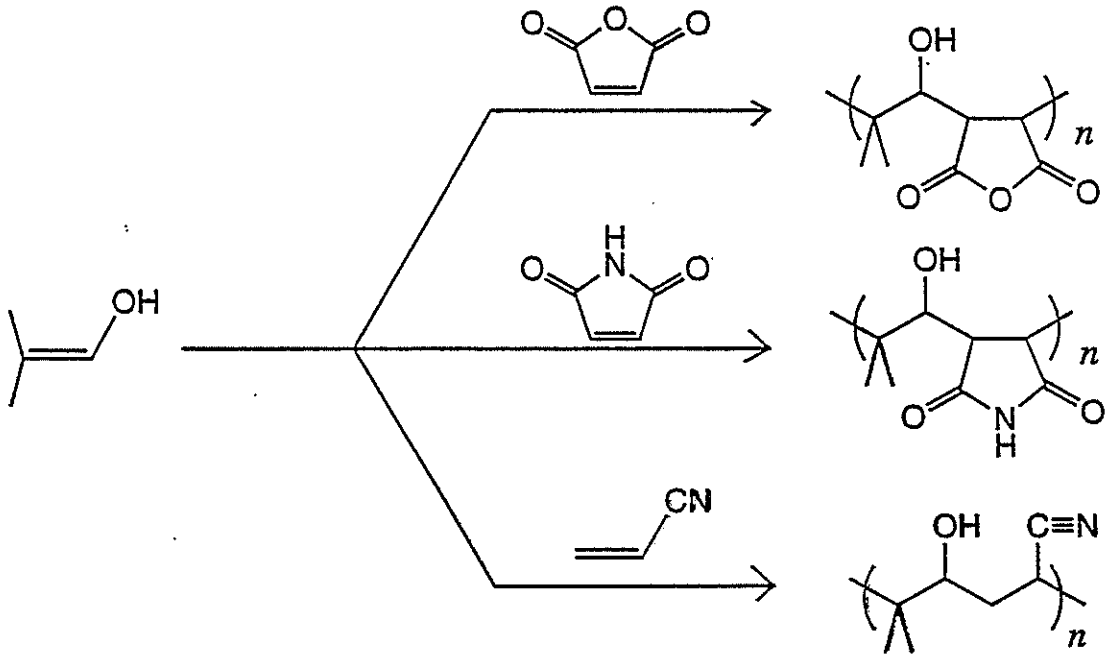

	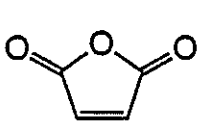	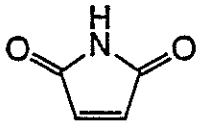	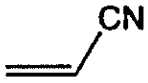
Q	0.86	0.94	0.60
e	3.69	2.86	1.20

^{13}C NMR of N-Ethyl Maleimide Polymers

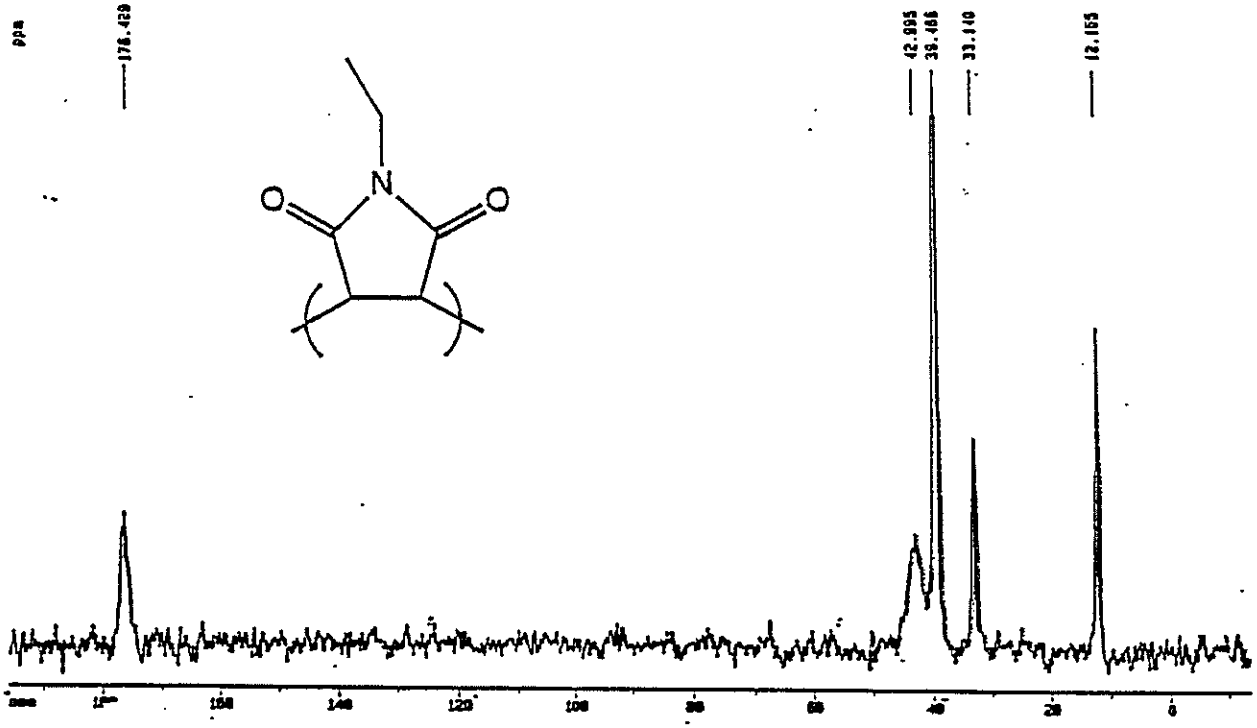

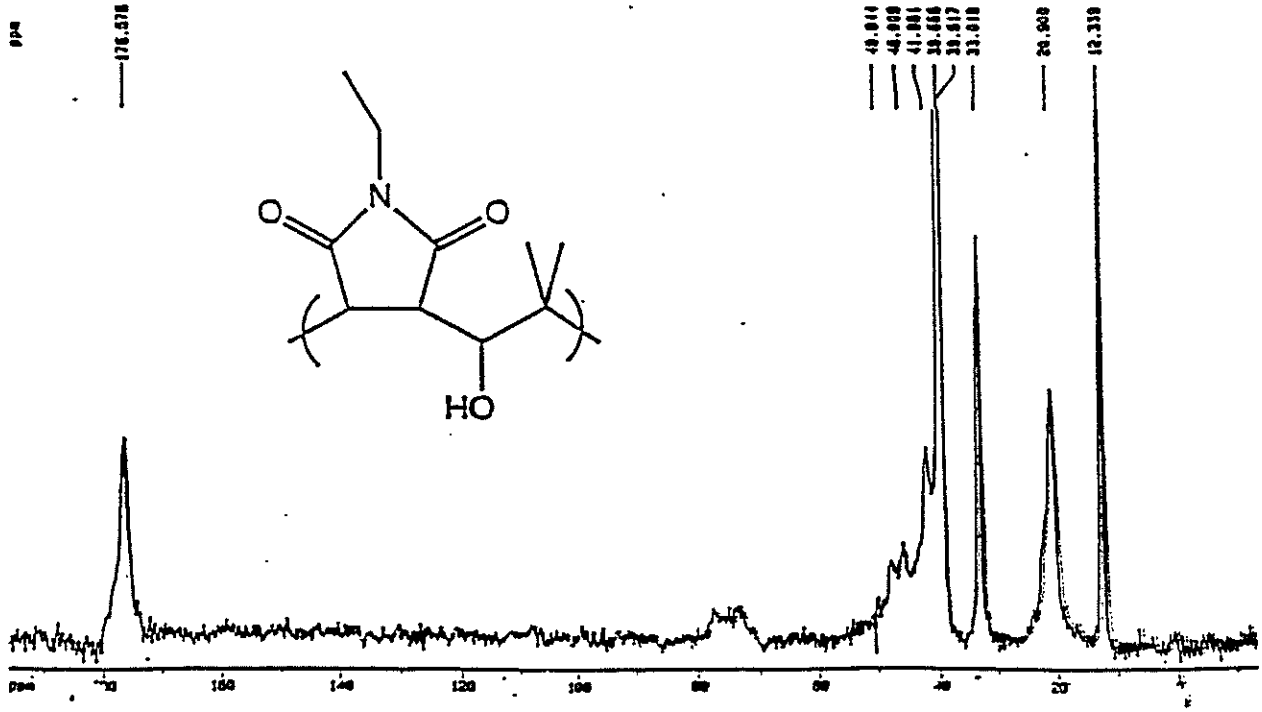

Maleimide Copolymers

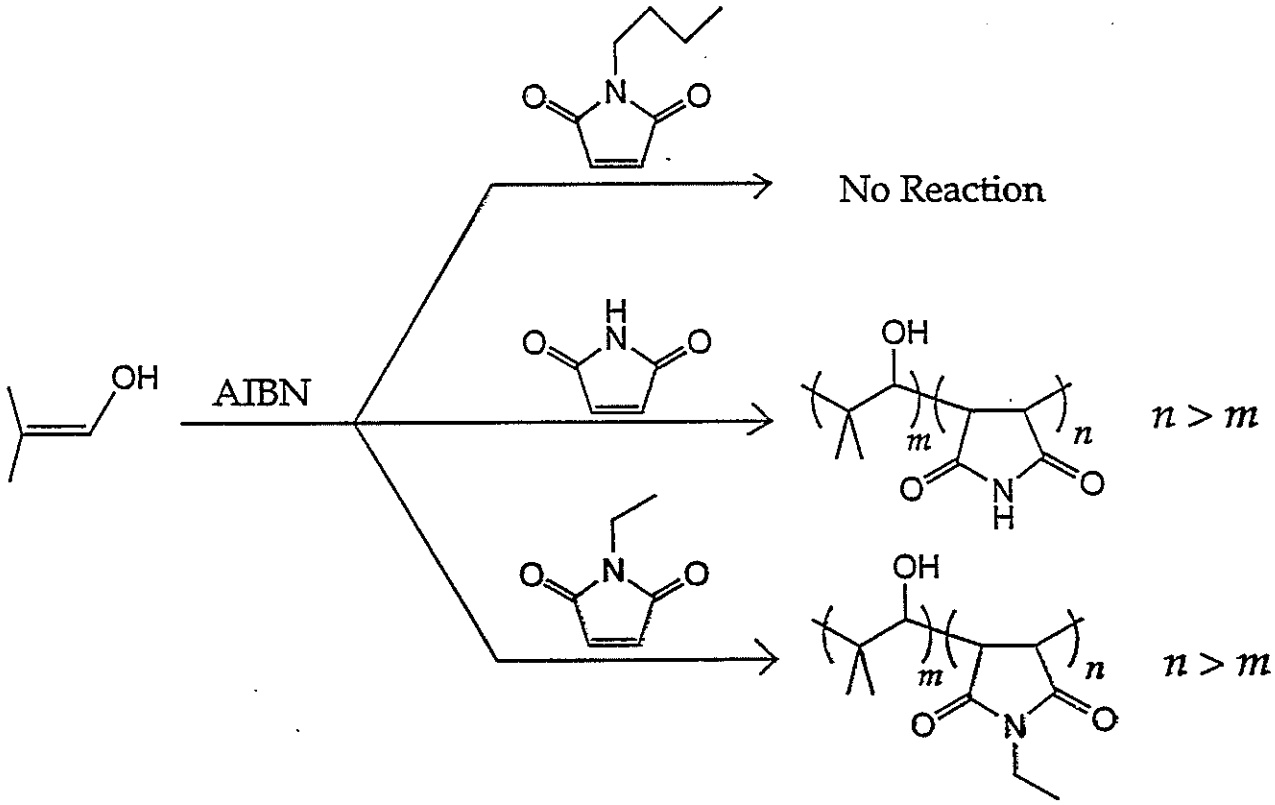

Feed Ratio	Copolymer Ratio (^{1}H NMR)
1.3	1.2
5.8	2.3
10.9	3.2
23.3	4.3

Modified Precursor Route to Poly(Vinyl Alcohol) Copolymers

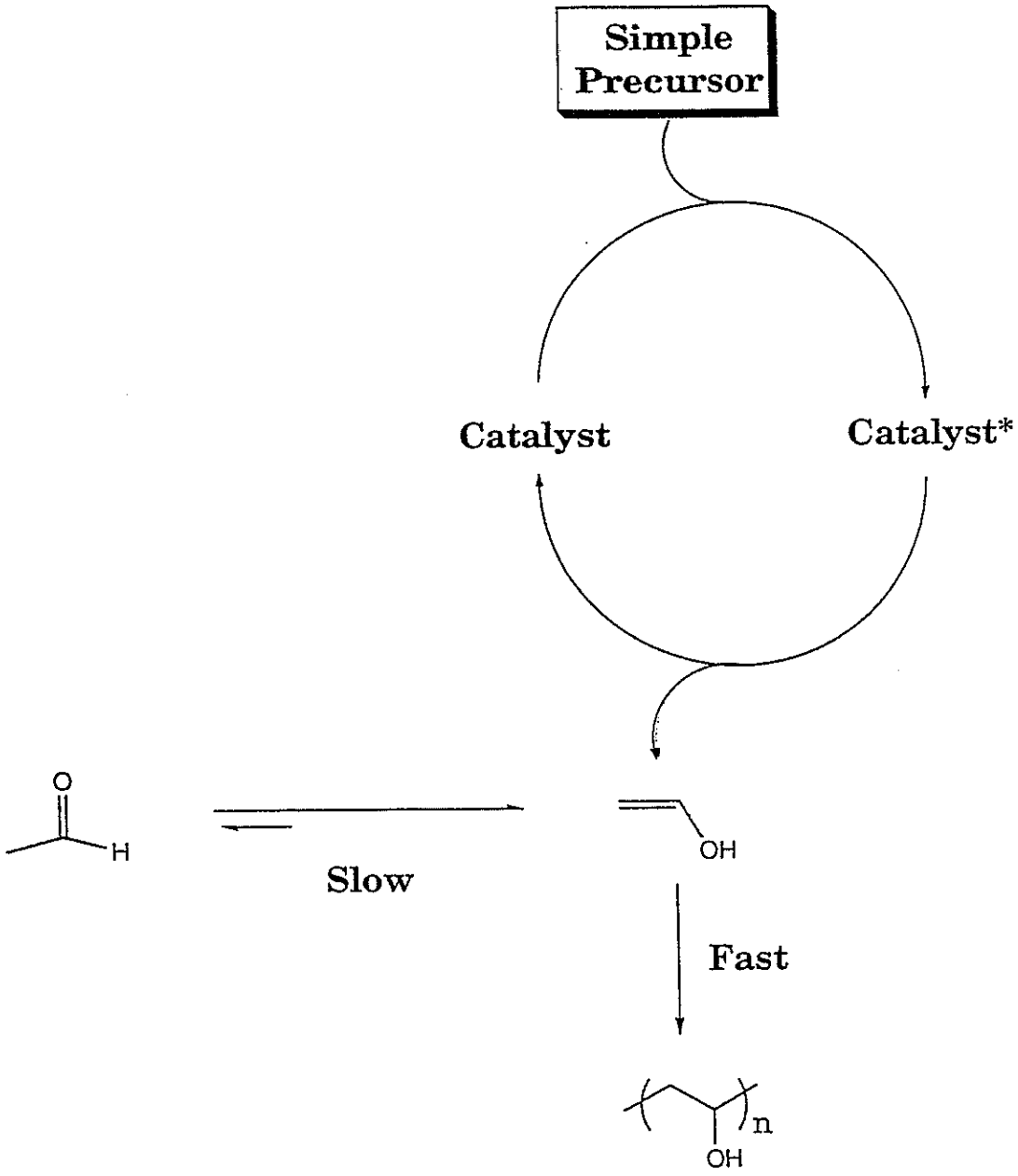

A Tale of Two "Monomers"

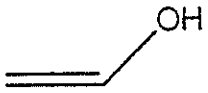

Vinyl Alcohol

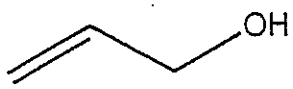

Allylic Alcohol

Allylic Alcohol:
A Cheap But Nonpolymerizable Monomer

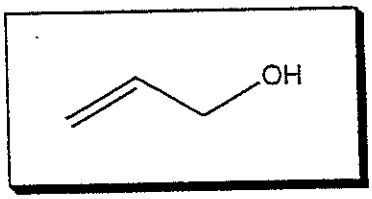

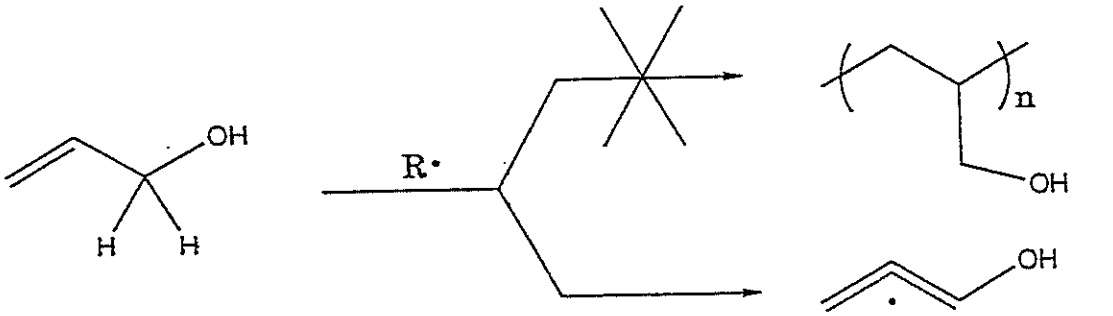

Stabilized, Allylic Radical

Catalytic Enol Formation

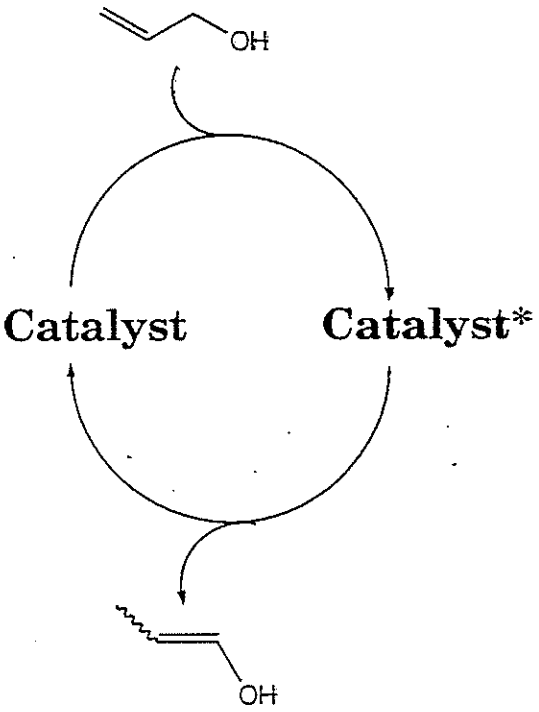

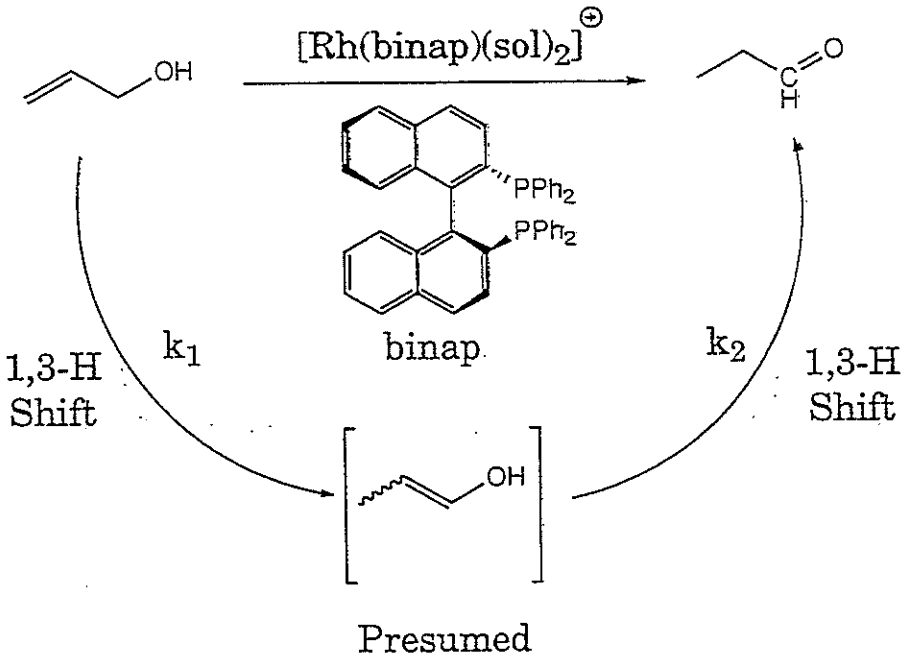

Presumed

K. Tani, 1985

Energy Diagram for the Isomerization of 2-Methyl Propenol to 2-Methyl Propanal

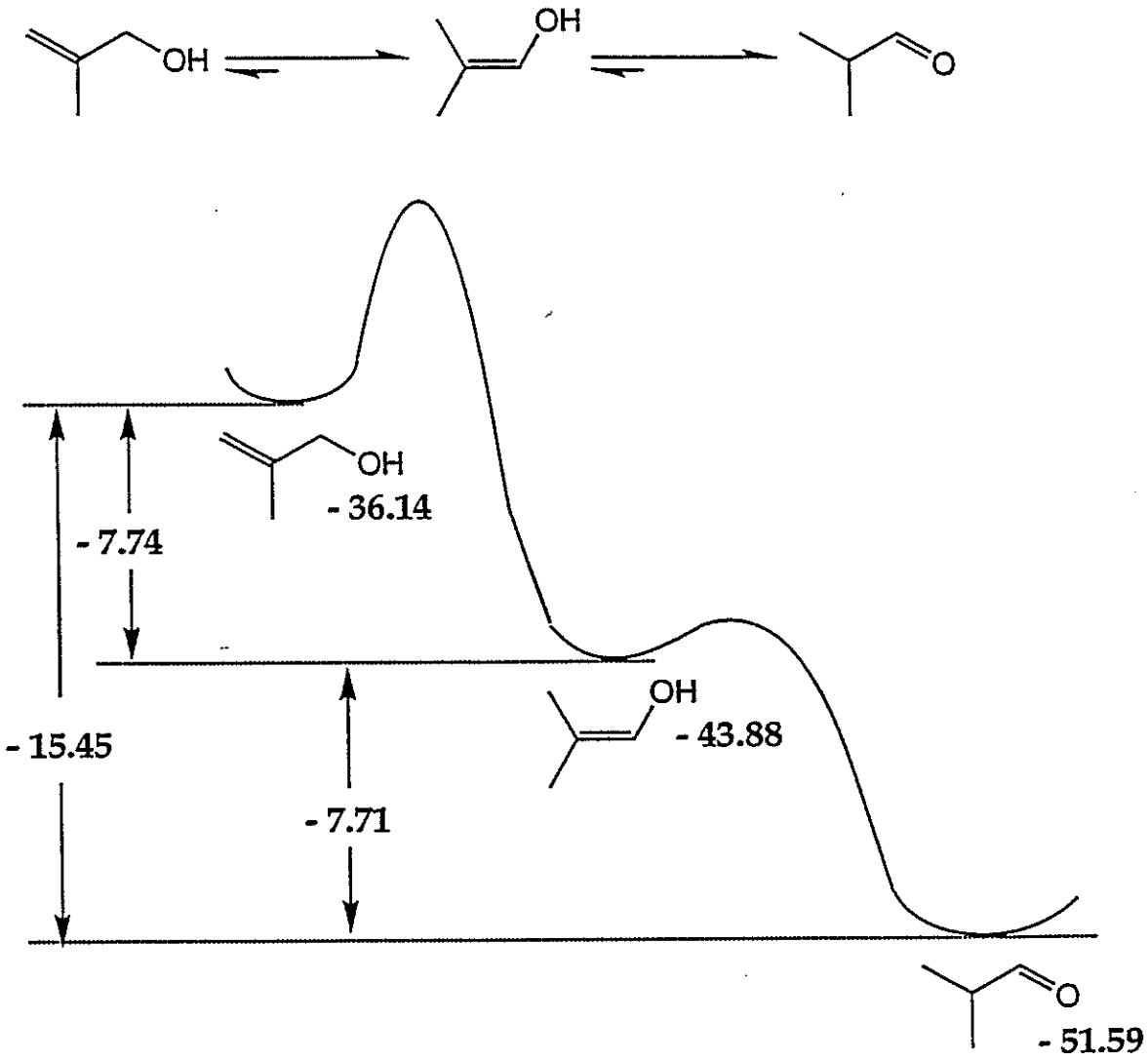

Isomerization Catalysts

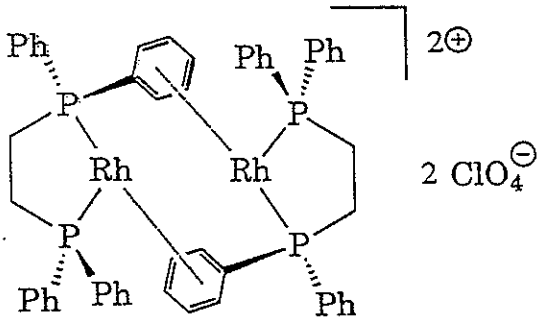

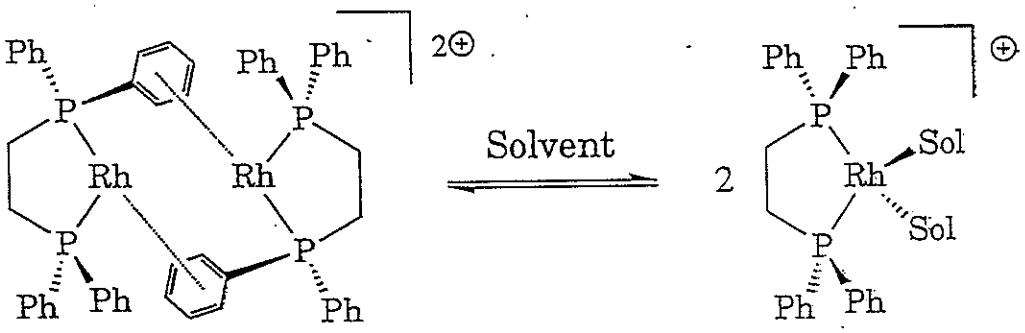

Inactive — Active

Solvent	Structure
Acetone	Monomer
Nitromethane	Dimer

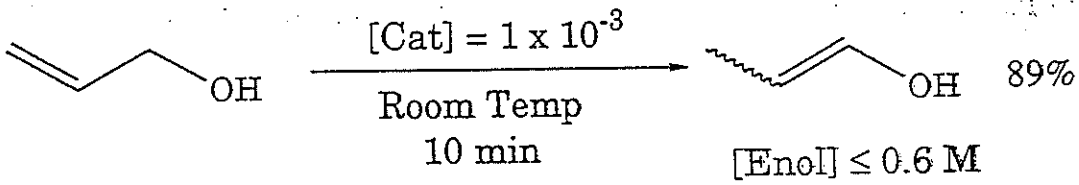

B. Bosnich, 1988, 1991

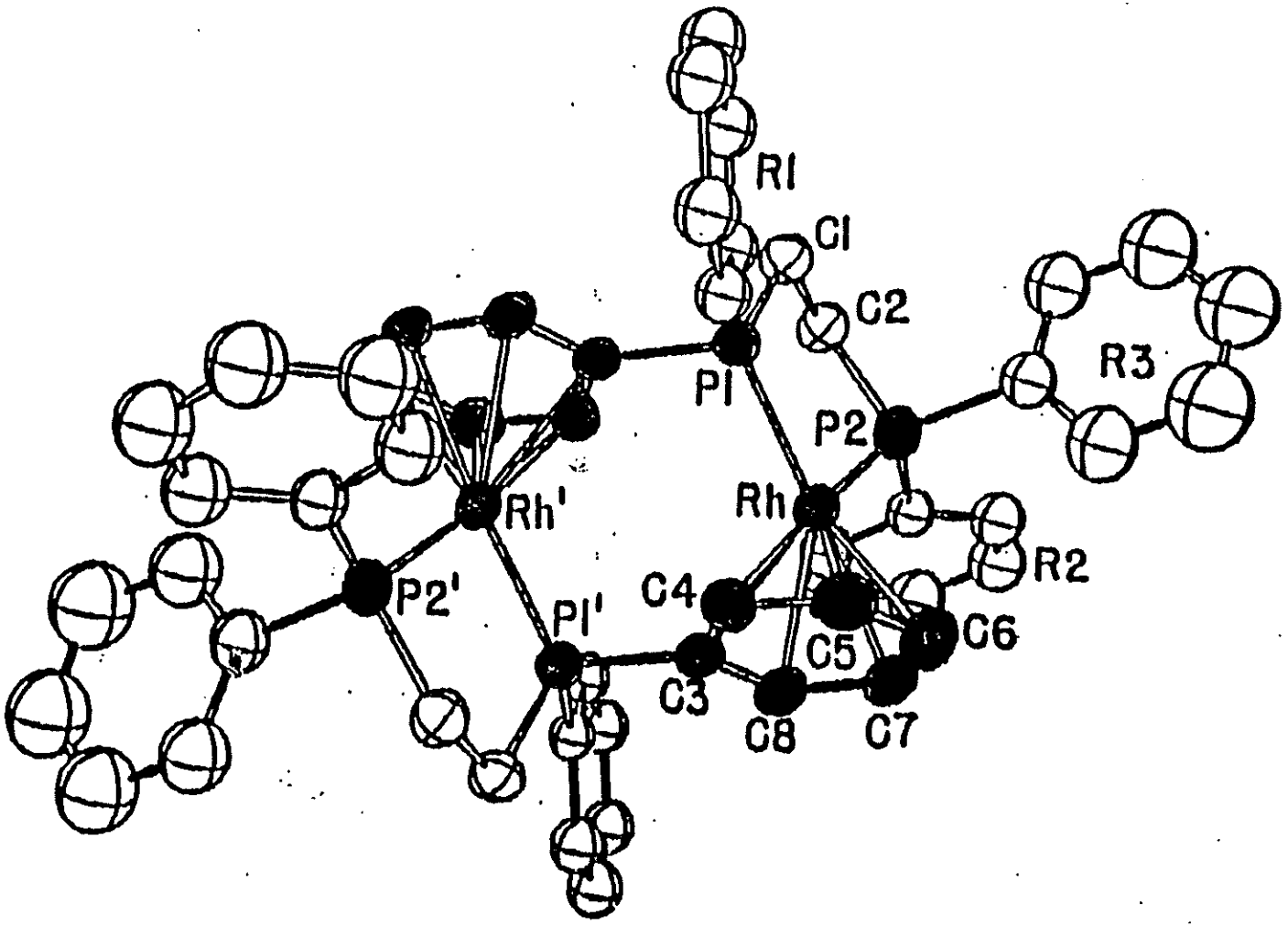

Figure 1. Structure of $[Rh_2(diphos)_2]^{2+}$. Distances (Å): Rh–Rh, 4.275 (1); Rh–P, 2.230 (2), 2.240 (2); Rh–C, range 2.285–2.368, mean 2.33.

Mechanism of Catalytic Enol Formation

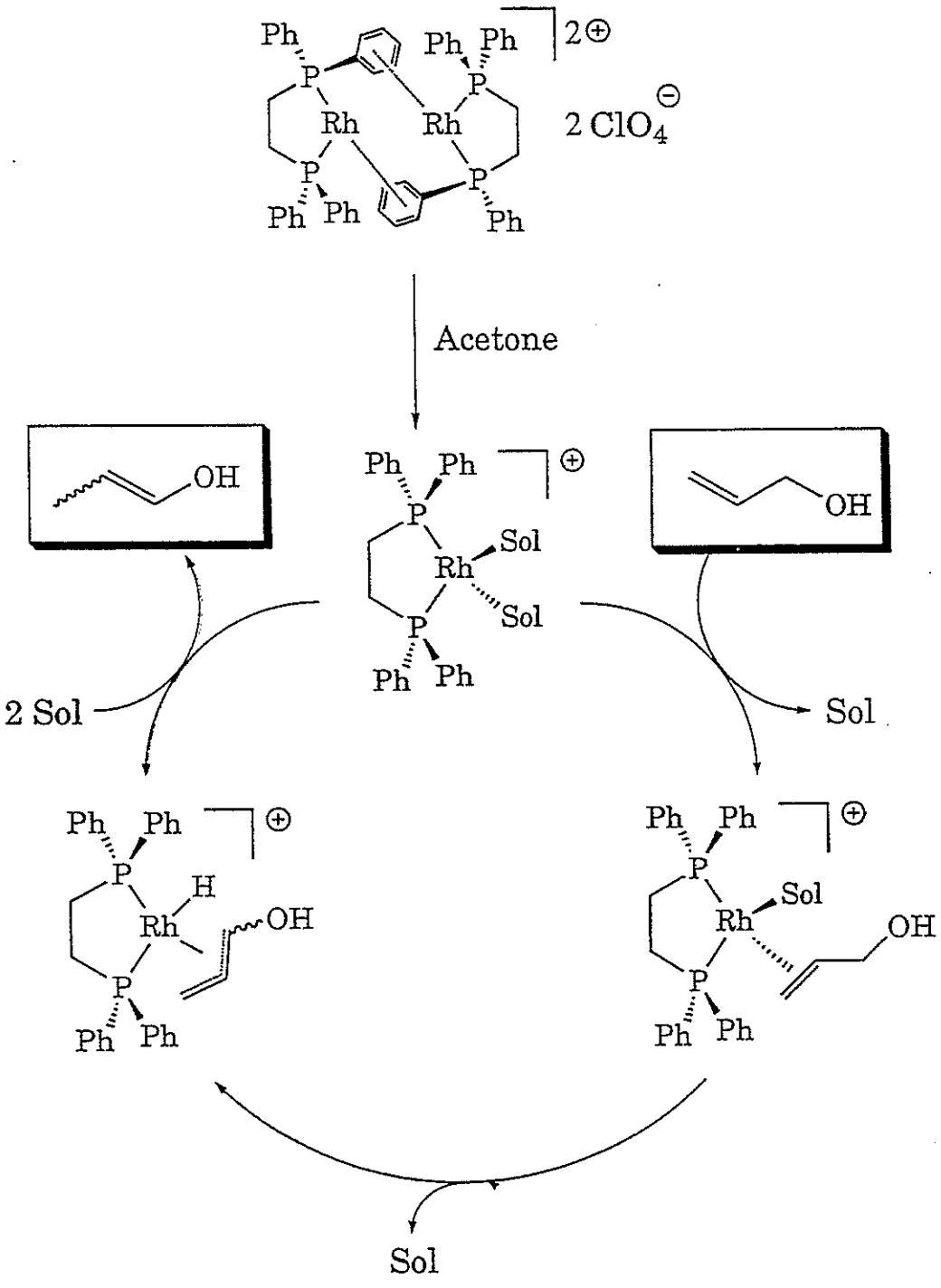

Synthesis of Rhodium PF_6 Catalyst

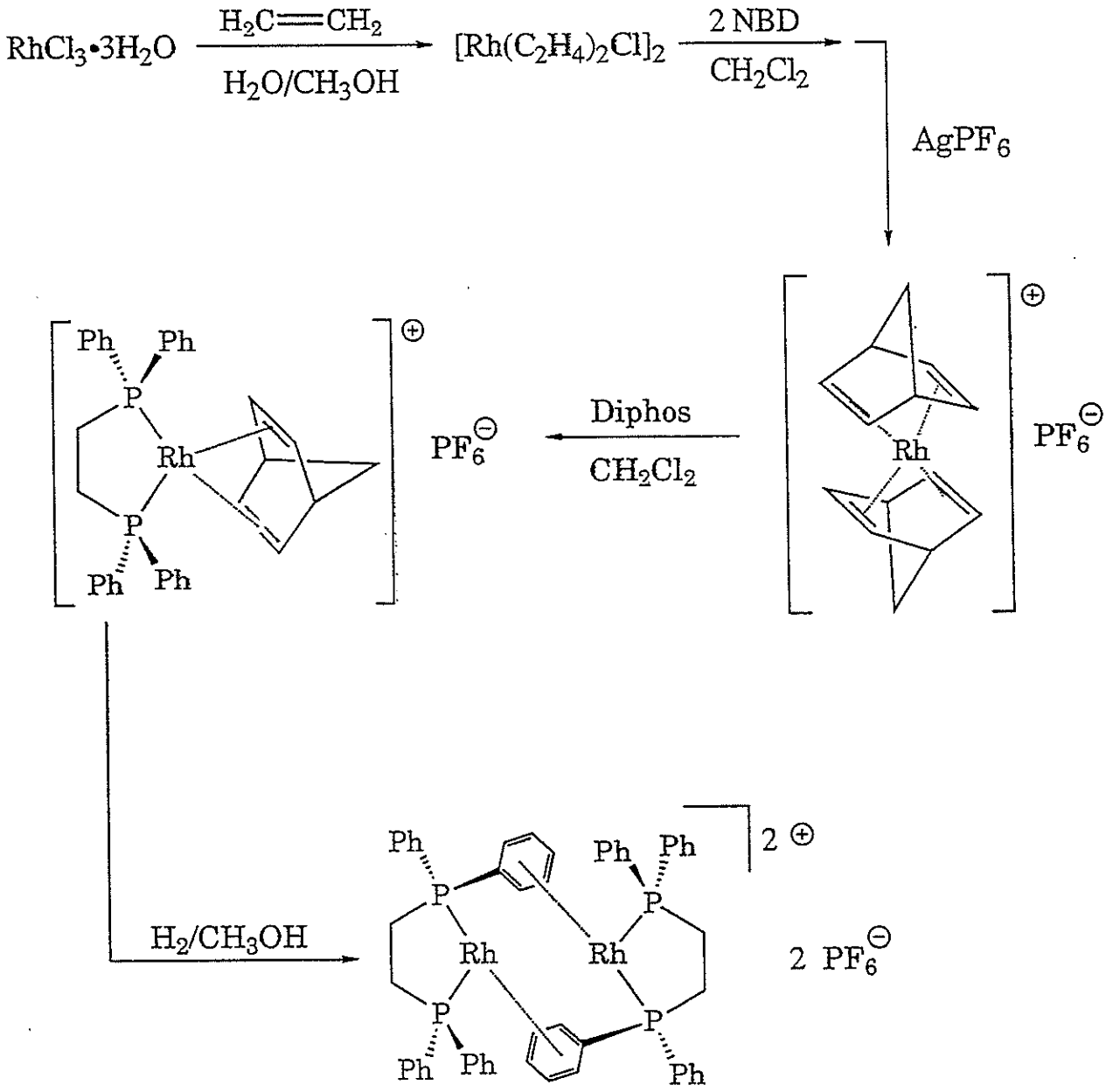

Catalytic Production of Enols

[Cat] = 1×10^{-3}

25 °C

[Substrate] / [Catalyst] ≈ 100 / 1

	% Enol	E/Z Ratio
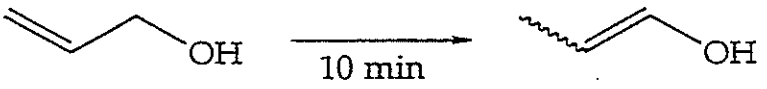	89%	1.1
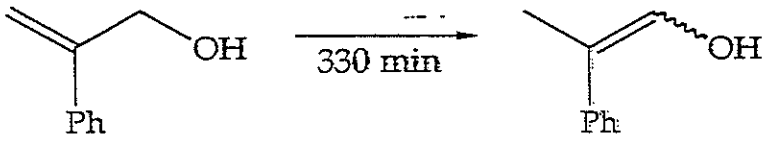	86%	1.0
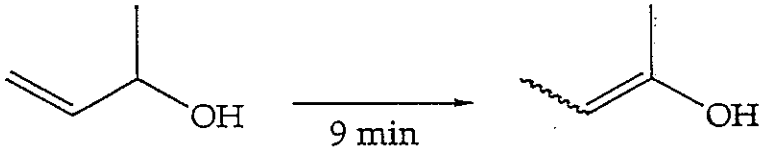	83%	0.19
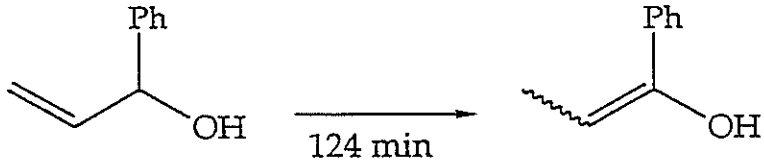	47%	All Z
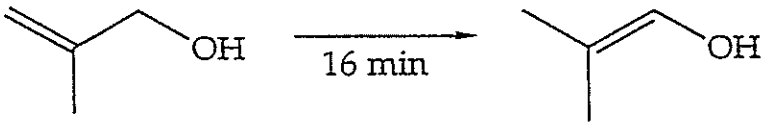	96%	——

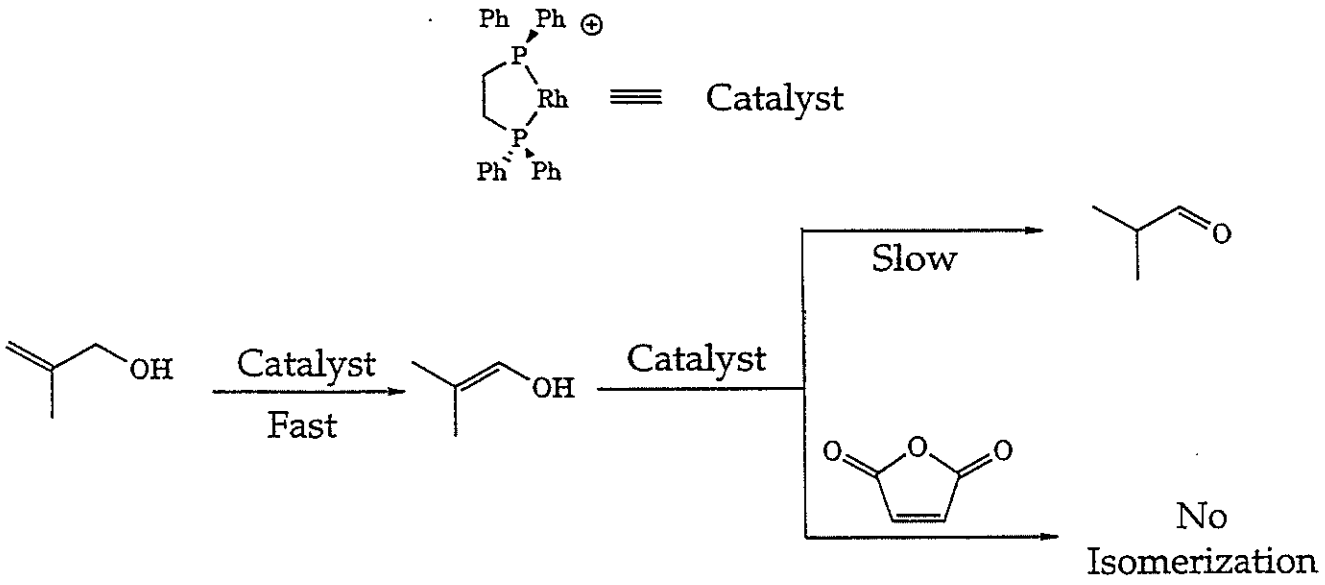
Ph Ph
P
Rh
P
Ph Ph
≡ Catalyst
OH
Catalyst
Fast
OH
Catalyst
Slow
O
O O O
No
Isomerization

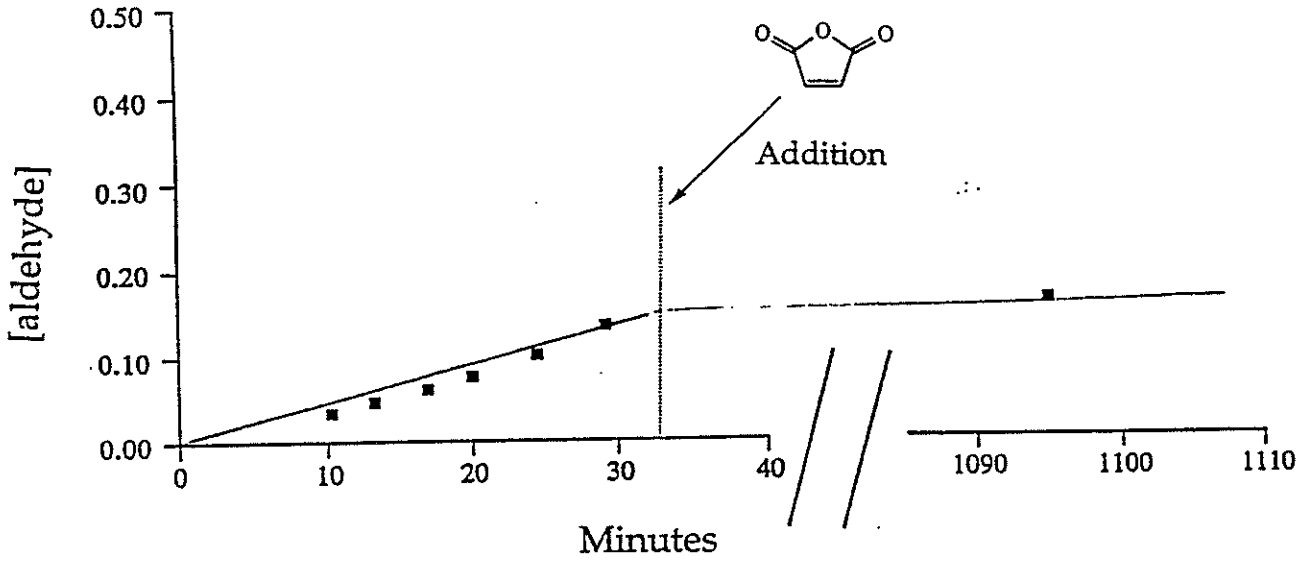
[aldehyde]
0.50
0.40
0.30
0.20
0.10
0.00
0
10
20
30
40
1090
1100
1110
Minutes
O O O
Addition

Copolymerization of Allyl Alcohol and Maleic Anhydride

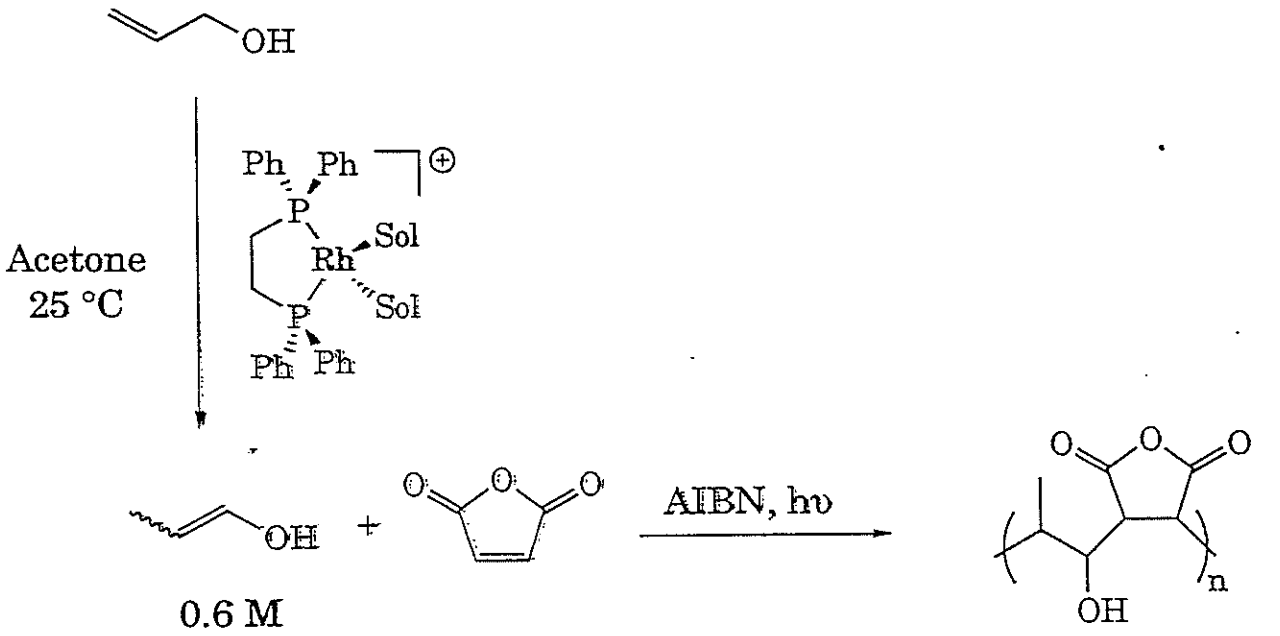

0.6 M
E/Z ≈ 1.1

≈ 100% Yields
1:1 Copolymer

2-Methyl-Propenol Copolymer with Maleic Anhydride

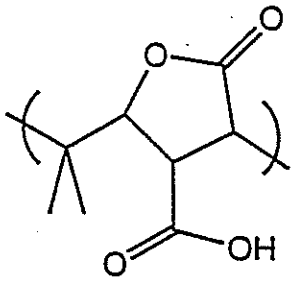

IR (cm^{-1})	Solubility
1717 - acid	DMSO
1781 - lactone	Acetone
3600-2400 - OH	

CH_2N_2

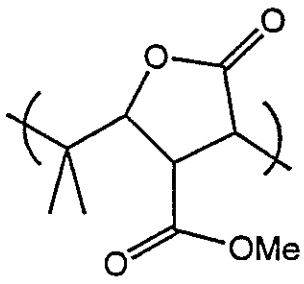

IR (cm^{-1})	Solubility
1736 - ester	$MeCl_2$
1782 - lactone	

Catalytic Activation of Monomers: Routes into Highly Stable Enols

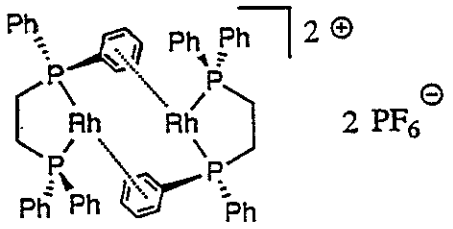

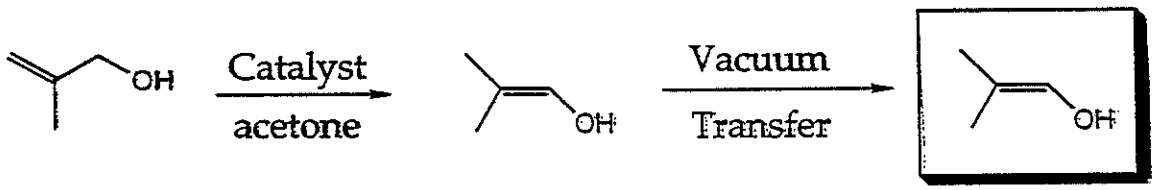

(Solution)
$T_{1/2} \approx 20$ days

(Neat Liquid)
$T_{1/2} \approx$ days

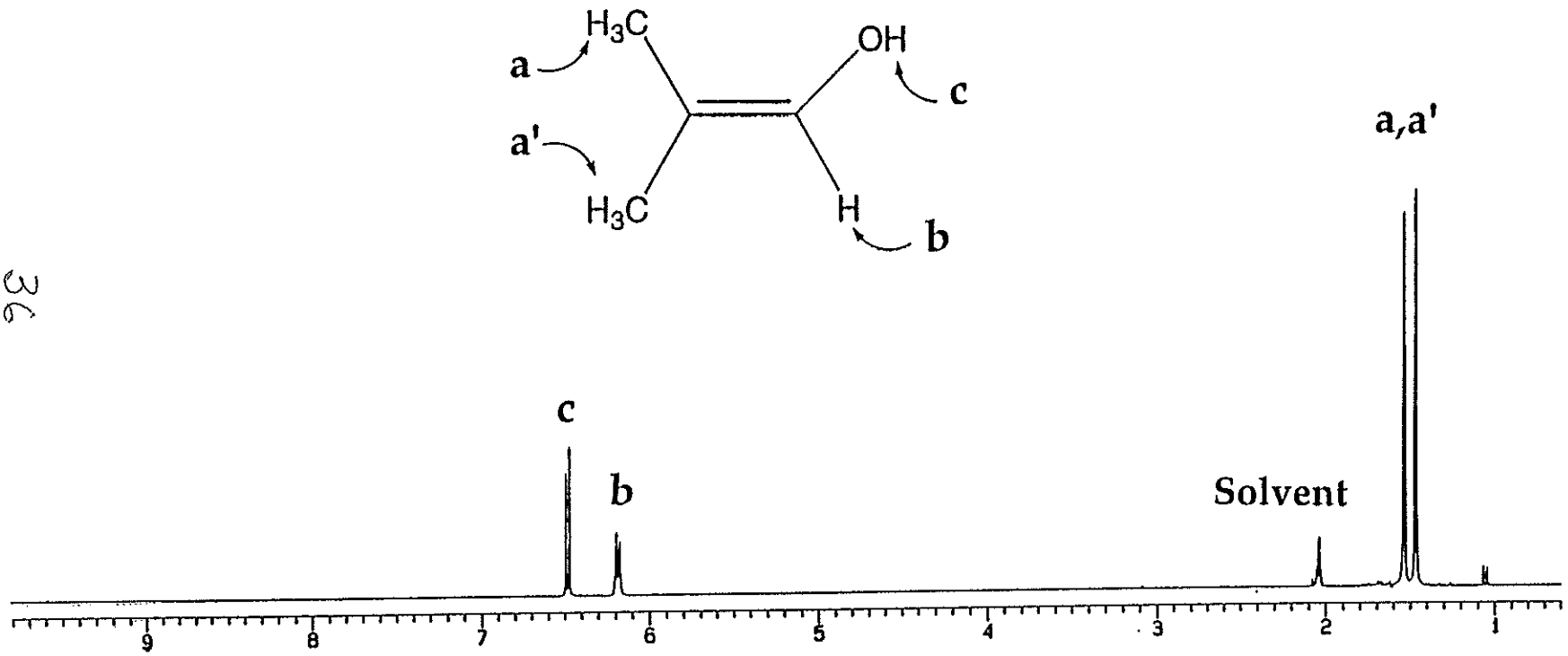
H3C
OH
a
c
a'
H3C
H
b
a,a'
c
b
Solvent
9
8
7
6
5
4
3
2
1

Tautomerization Kinetics of Neat 2,2-Dimethyl Vinyl Alcohol

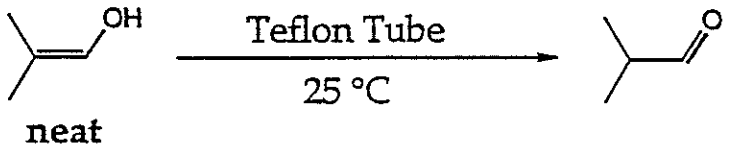

neat

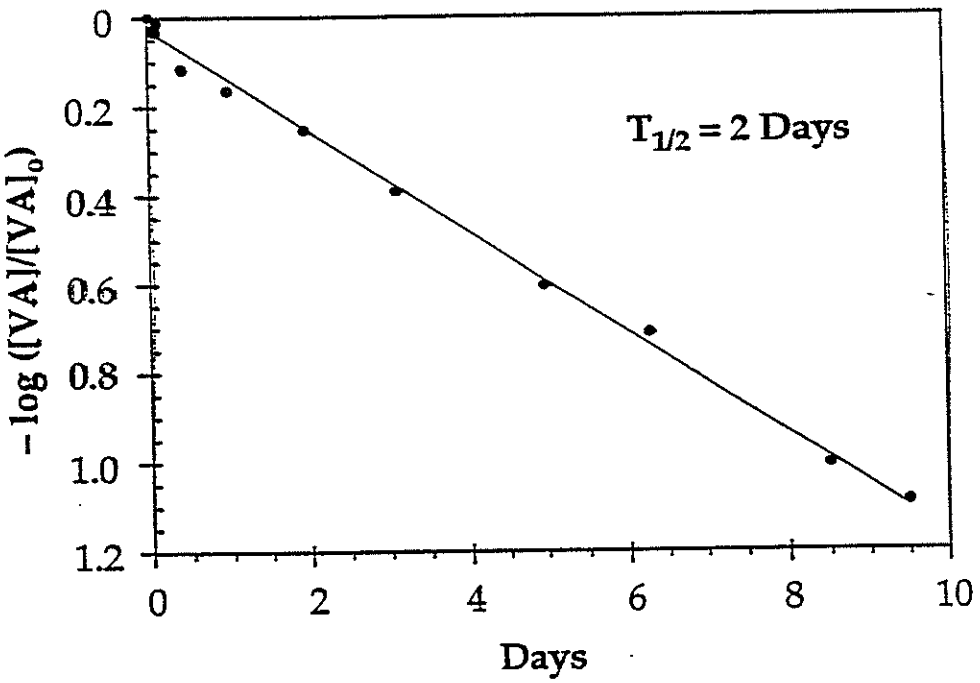

Copolymerization of Stable Enols

Inactive

Active

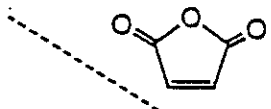

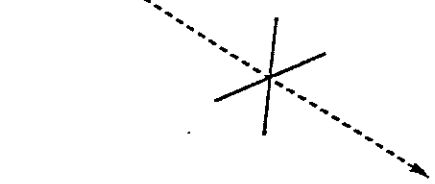

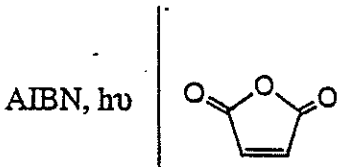

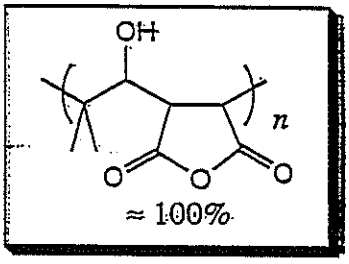

Polymeric Materials Synthesis and Processing in Carbon Dioxide

Joseph M. DeSimone

Department of Chemistry
CB #3290, Venable and Kenan Laboratories
The University of North Carolina at Chapel Hill
Chapel Hill, NC 27599-3290

Outline

- Supercritical CO_2 solvent properties
- Characterization of Poly(FOA), Poly(1,1-dihydroperfluorooctyl acrylate), a CO_2 soluble polymer
- Design and characterization of CO_2-philic/hydrophilic amphiphiles
- Design and characterization of CO_2-philic/lipophilic amphiphiles
- Conclusions

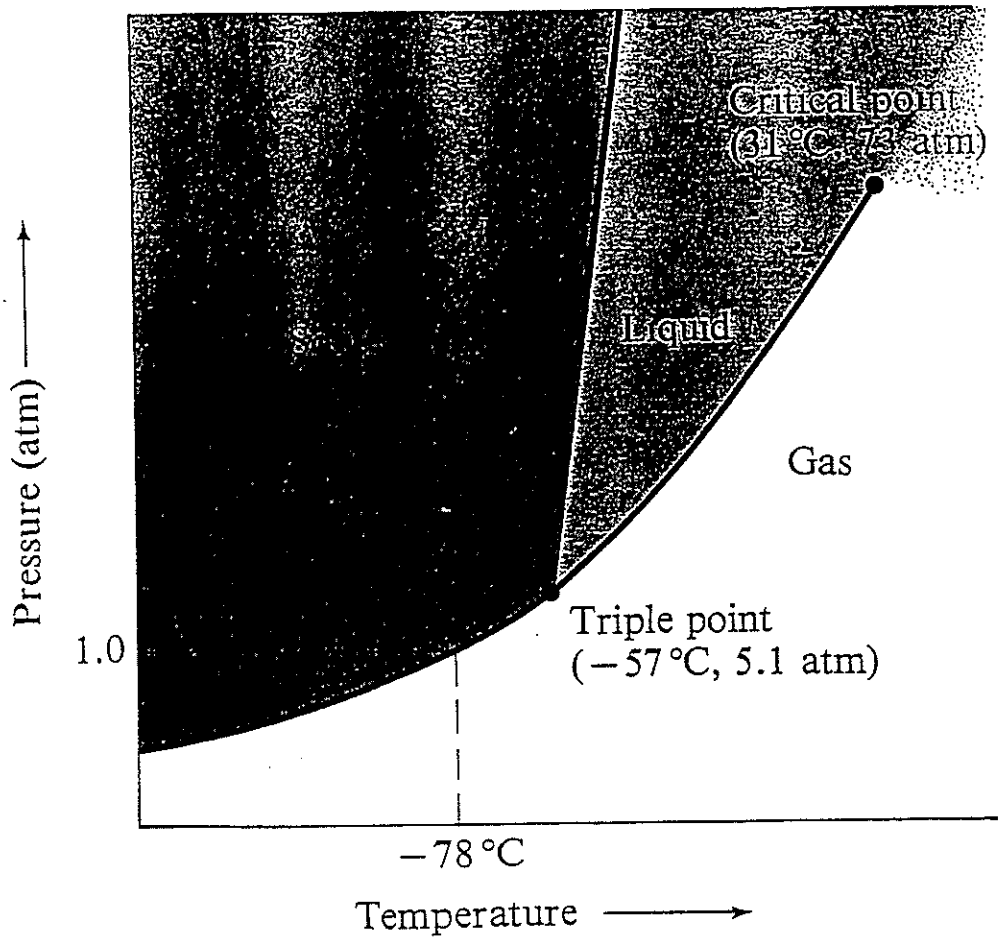

A

Dependence of CO_2 density and dielectric constant on pressure at 59.4 °C

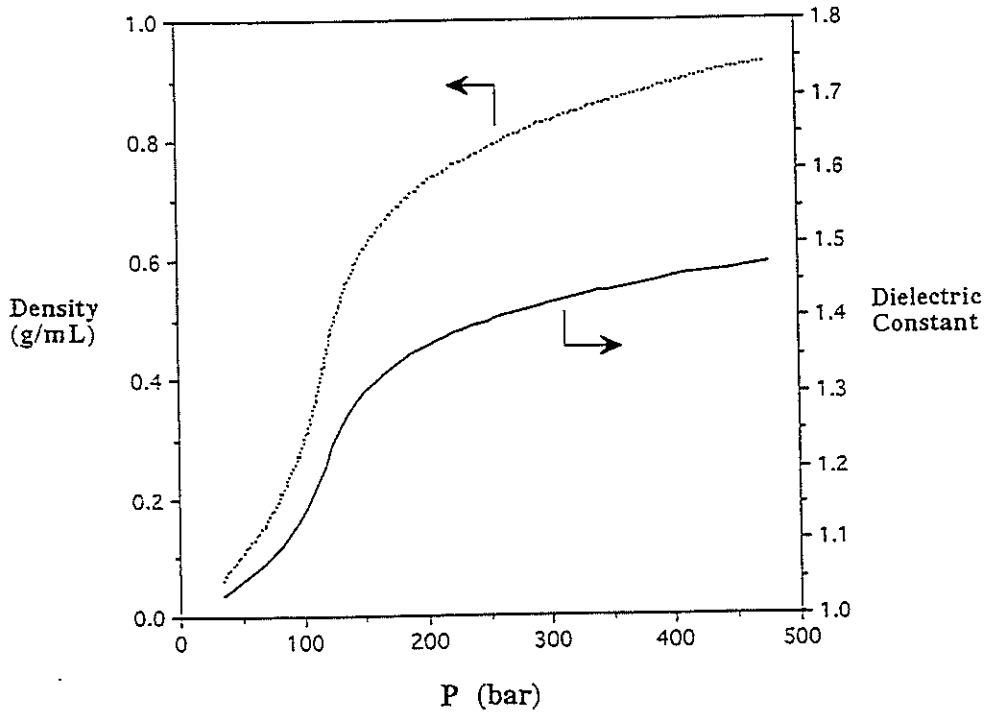

Vapor Pressure of Carbon Dioxide
vs. Temp at Saturation

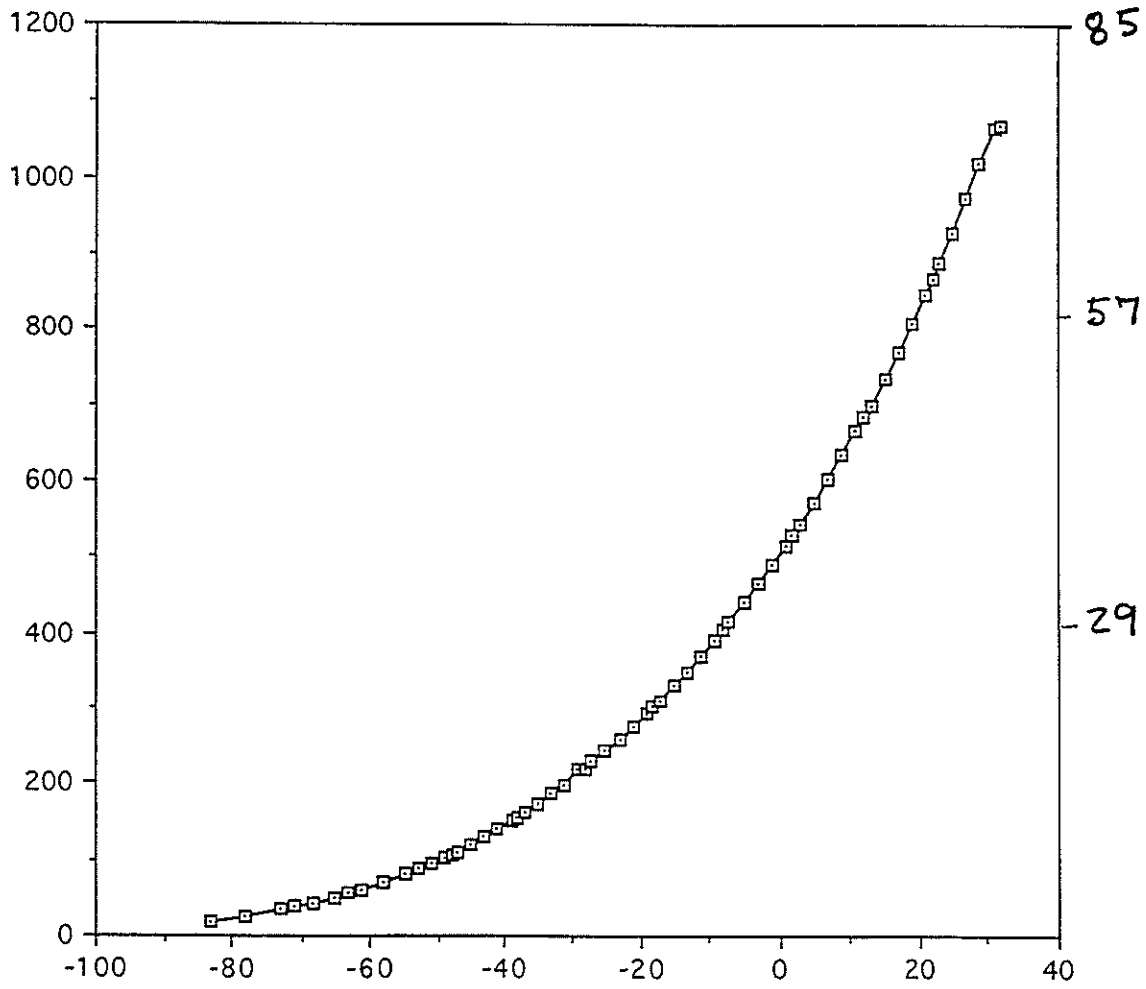

Advantages and Attributes of Supercritcal CO_2 for Synthesis and Processing

"...not just another solvent..."

Compatible Chemistries:

- **Free Radical**
- **ROMP**
- **Others...**
- **Cationic**

Carbon Dioxide

- **Environmentally Responsible**
- **Inexpensive (2.5 ¢ / lb)**
- **Non-toxic**
- **Easily removed**
- **Easily recycled**

Supercritical Carbon Dioxide

- **Tunable Density-dependant Properties**
  - **0.1 - 0.9 g/cc**
  - **Dielectric Constant**
  - **Solubility Parameter**
- **Gas-like Viscosity (< 0.09 cps)**
- **Gas-like Diffusivity**
- **Plasticizing Agent**
  - **Increased rate of solute diffusion in polymers**

Solubility Characteristics of SC Carbon Dioxide

- **Tunable**
- **Similar to Hexane for Small Molecules**
  - **Immiscible with water**
- **Similar to Fluorocarbons for Polymers**
  - **Freon-113**

Topologically Ordered "Soft" Structures

- **Amphiphilic Surfactant Systems**

  Hydrophilic Cores (W / O)
  Lipophilic Cores (O / W ; FC / HC)

- **Emulsions and Microemulsions**

- **Compressible Medium**

  - **Small Angle Neutron Scattering (SANS)**
  - **Small Angle X-ray Scattering (time resolved - SAXS)**

- **Technological Significance**

  - **Polymerizations**
  - **Separations**
  - **Cleaning**

Modified Polymerization Processes Based on CO_2

(A) Bulk:

Traditional ⟶ high temperature and vacuum

Modified ⟶ high temperature with SCFE

(B) Solution:

Fluoropolymers or siloxanes

(C) Heterogeneous:

(1) Precipitation

monomer soluble ⟶ polymer insoluble

(2) Dispersion

monomer soluble ⟶ polymer insoluble but stabilized as colloid

(3) Suspension

monomer soluble
monomer-soluble initiator
stabilizer or dispersant

(4) Emulsion

monomer insoluble
monomer-insoluble initiator
surfactant

(5) Interfacial

water-rich phase / CO_2-rich phase

Homogeneous Free Radical Polymerization in Supercritical CO_2

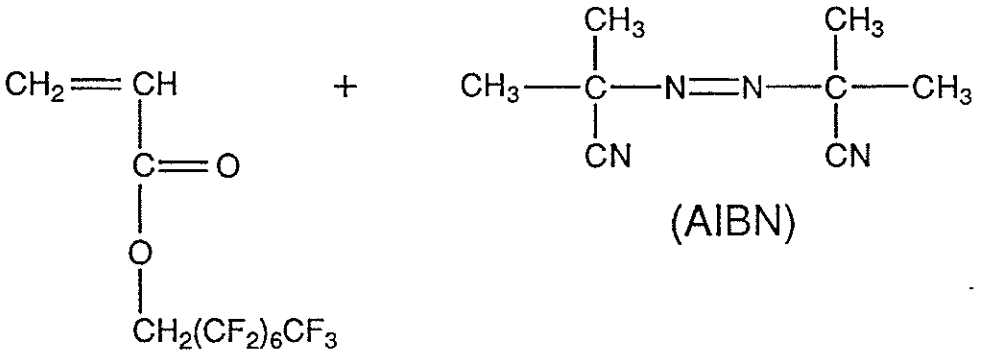

FOA + (AIBN)

CO_2
60 °C, 24 hours
345 bar

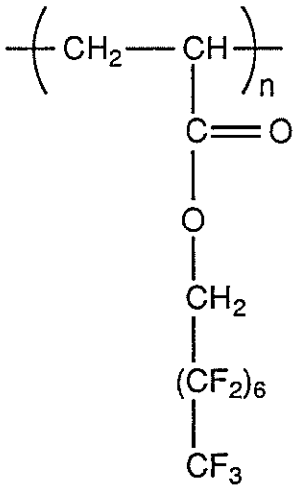

Poly(FOA)

DeSimone, J. M.; Guan, Z.; Elsbernd, C. S. *Science* **1992**, *257*, 945

Small Angle Neutron Scattering Analysis of Polymers in SC-CO_2

- *CO_2 (SLD) = 1.8 x 10^{10} - 2.2 x 10^{10} cm^{-2} {Variable with density}*
- *Poly(FOA) (SLD) = 3.4 x 10^{10} cm^{-2}*
- *Ability to tune both the solvent strength and the scattering contrast*

Typical SANS spectra for a concentration series of poly(FOA), 65 deg. C, 340 bar

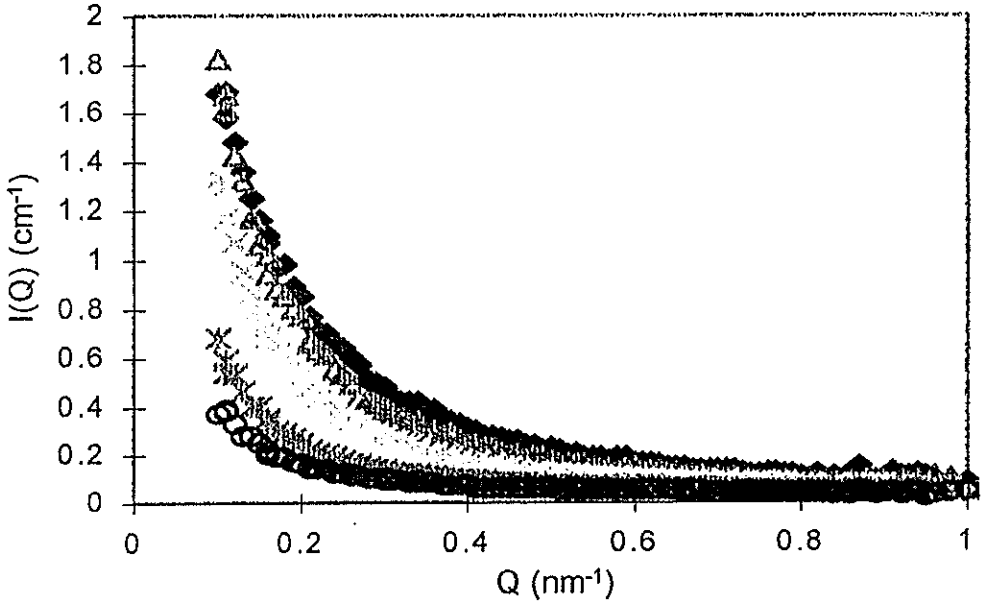

◆ 8 % poly(FOA)
△ 5 % poly(FOA)
3 % poly(FOA)
✕ 1.5 % poly(FOA)
○ 0.8 % poly(FOA)

M_w and A_2 Determination for Poly(FOA)

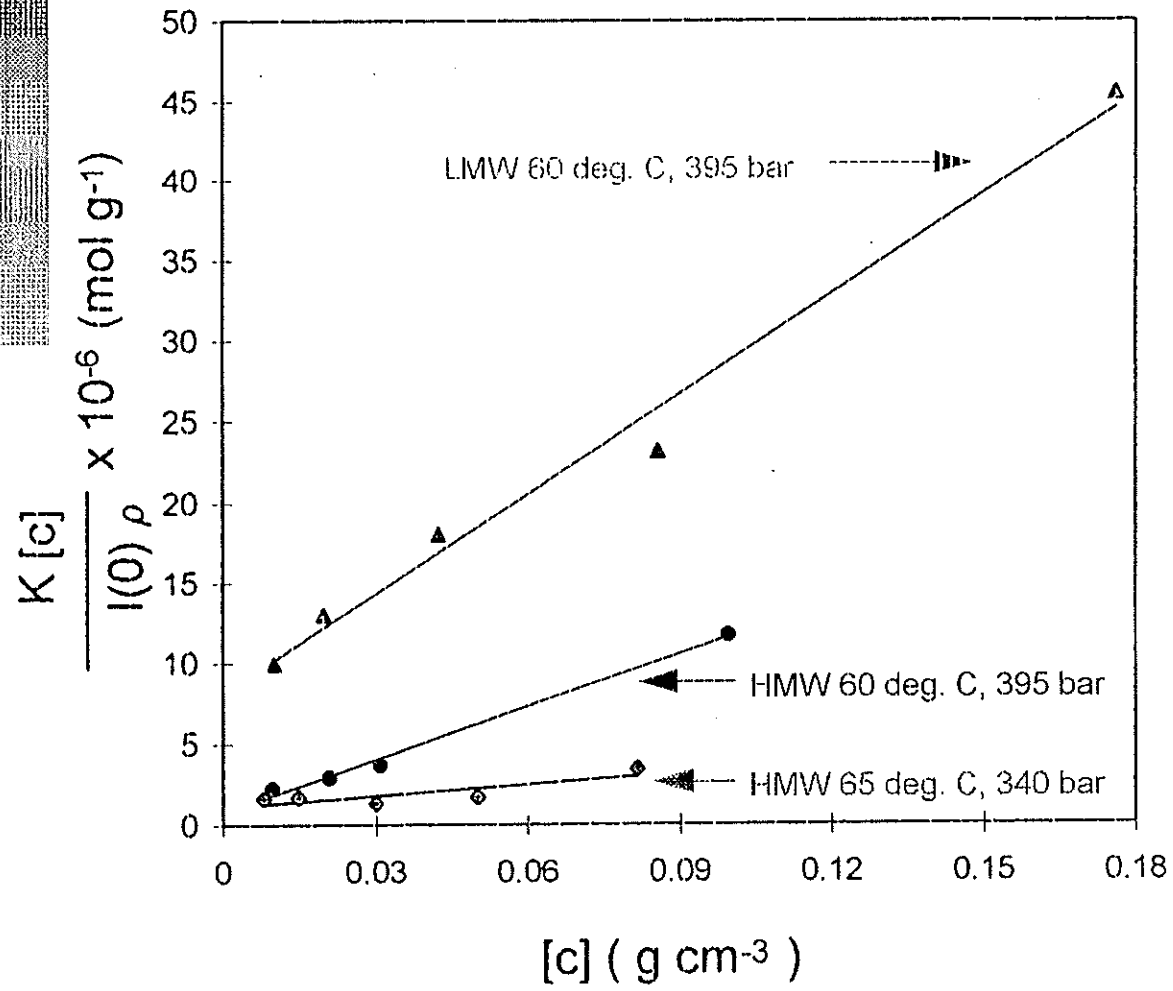

A_2 = 1/2 Slope

M_w = [Intercept]$^{-1}$

Degree of Aggregation of Poly(FOA) as a Function of CO_2 Density

Poly(FOA) Sample	P (psia)	T (°C)	ρ (g cm^{-3})	Degree of Association
High M_W	5,800	60	0.89	Unimer
High M_W	5,000	65	0.84	Unimer
High M_W	4,500	65	0.82	Trimer
High M_W	4,300	65	0.81	10 -mer
High M_W	4,200	65	0.80	40 - mer
High M_W	4,100	65	0.79	Cloudy
High M_W	4,000	65	0.77	Two Phase

- There is signifigant polydispersity (MWD ≈ 1.5 - 2.0) in the polymer.
- We are in a density range where fractionation can be explored.

Tetrafluoroethylene Polymerization

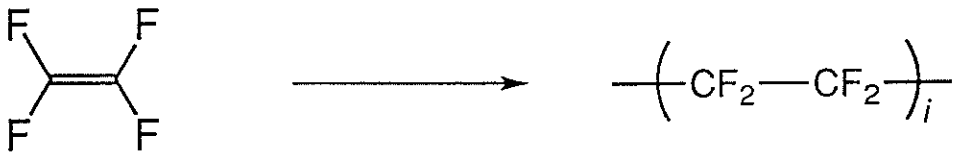

- Aqueous polymerization media
- Ammonium persulfate initiator
  - ionic end groups
  - acid end groups
- Perfluorinated surfactants

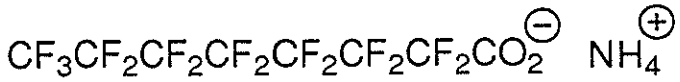

- T_m = 342 °C
- Broad-based applications

Melt Processable Fluoropolymers

	T_m (°C)
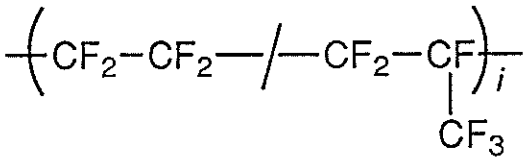	260
FEP	
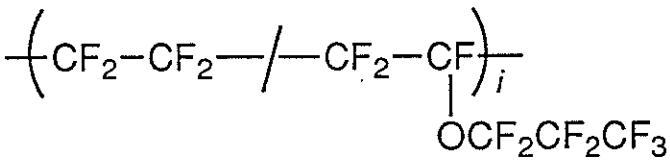	305
PFA	
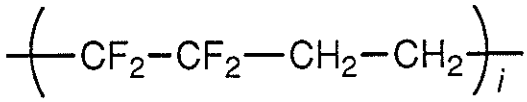	275
ETFE	
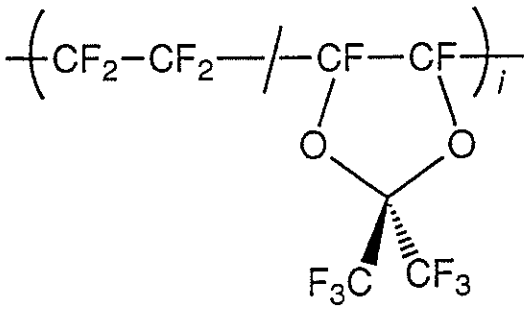	Amorphous T_g = 160, 240
Teflon AF	

Non-Aqueous Polymerizations of Fluoroolefins

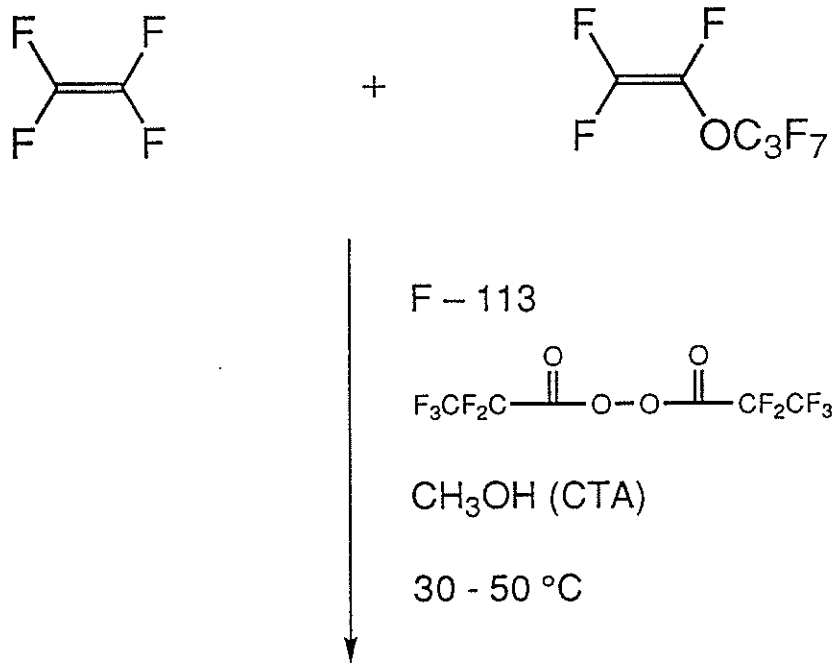

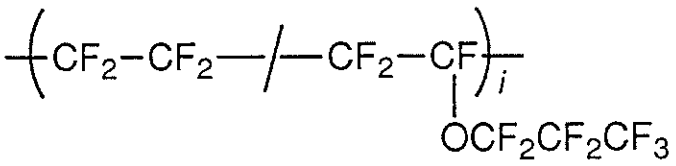

- No hydrocarbons
- Perfluorinated initiators
- Treat with F_2, CH_3OH, or NH_3
  - Stable end groups
  - High molar masses
- Wire coatings, gaskets, microelectronics

7×10^6 kg/yr in U.S. ($15–50/kg)

50

Potential Alternatives to Chlorofluorocarbon Based Solvents

- **Perfluorocarbons** – Hexafluorobenzene, perfluorocyclobutane, perfluorohexane...

1972	US	3,642,742	DuPont
1994	JP	06,157,613	Asahi Glass
1994	JP	06,157,614	Asahi Glass
1994	JP	06,157,615	Asahi Glass
1994	JP	06,157,616	Asahi Glass
1994	JP	06,157,675	Asahi Glass

- **Hydrofluorocarbons** – Tetrafluorocyclobutane, 2,2-bis(trifluoromethyl)-1,3-dioxolane...

1993	US	5,182,342	DuPont
1994	US	5,310,870	DuPont
1994	JP	06,157,617	Asahi Glass
1994	JP	06,184,205	Asahi Glass
1994	JP	06,184,239	Asahi Glass

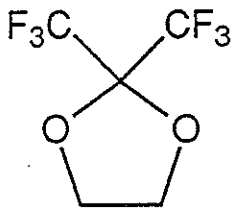

Advantages of CO_2 for Non-Aqueous Polymerizations of Fluoroolefins

- No observable chain transfer to solvent
- Increased initiator efficiency
- Fluorinated initiators and monomers highly soluble
- Environmentally benign
- Non-toxic
- Inexpensive – 0.025 $/lb
- Safe Handling of TFE (US Patent 5,345,013; 1994)

Additional Benifits (potential)

- Plasticization (Dispersion polymerization?)
- Only one fluid phase present in reactor
- Supercritical fluid advantages – Viscosity, mass transport, in-situ extraction/washing, etc...

Bis (Perfluoro-2-propoxy Propionyl) Peroxide (HFPO Dimer Peroxide)

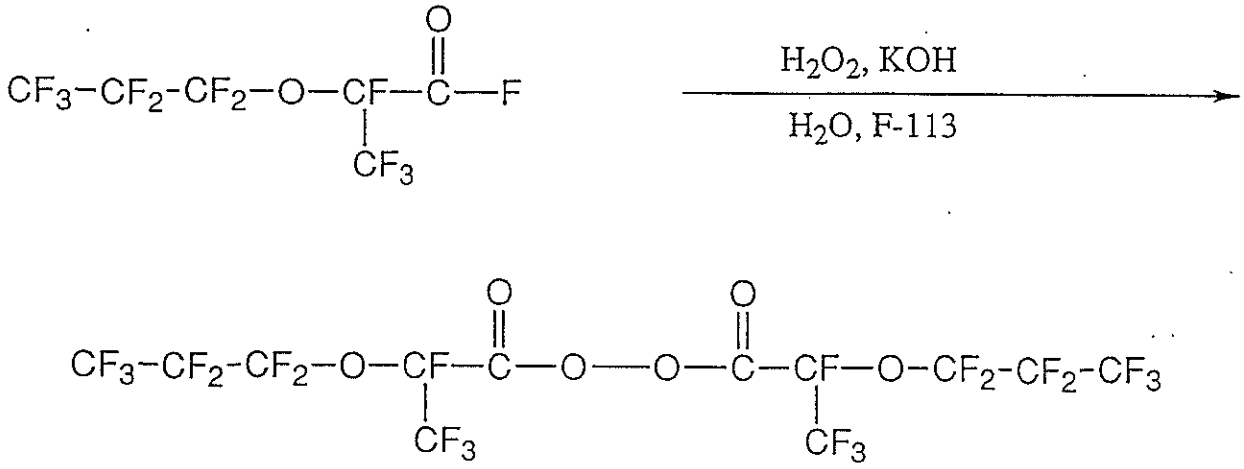

10 hour half life @ 7.6 °C $K_d = 3.5 \times 10^{-4} s^{-1}$ @ 35°C, (half life = 33 min)

Vysokomol. Soyed. **1975**, *A17(6)*, 1235
J. Org. Chem. **1982**, *47*, 2009

Copolymerizations of TFE and PPVE in CO_2 with HFPO Dimer Initiator

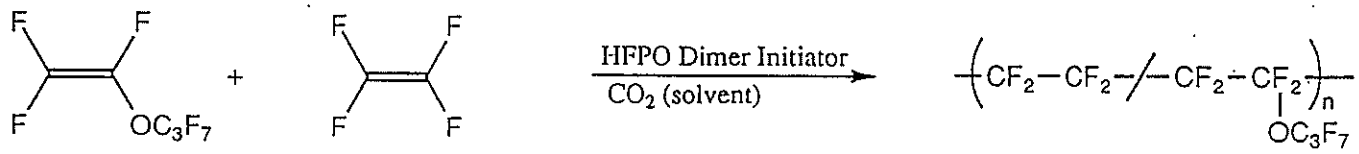

[TFE]	[PPVE]	Yield (%)*	wt. % PPVE	MV (poise)	T_m
2.1	0.18	100	—	—	330.5
1.9	0.18	99	—	—	321.5
2.2	0.55	101	—	—	318.6
2.0	0.55	100	5.2	Too high to	312.7
2.2	0.92	101	5.8	Measure	313.7
1.2	0.35	70	7.8	7.3×10^4 **	297.1

* Based on TFE charge ** Methanol added as chain transfer agent

- End group analysis (FT-IR) showed ≤ 3 CO_2H, CO_2F end groups per 10^6 Carbons
- Mn > 1,000,000 g/mol without chain transfer agent!!

Other Copolymerizations in CO_2 with HFPO Dimer Initiator

- Ethylene / tetrafluoroethylene
- Vinyl Fluoride
- Perfluoro(methyl vinyl ether) / tetrafluoroethylene
- Chlorotrifluoroethylene / vinylidine fluoride
- Hexafluoropropylene / vinylidine fluoride

Rational Design of Surfactants for CO_2

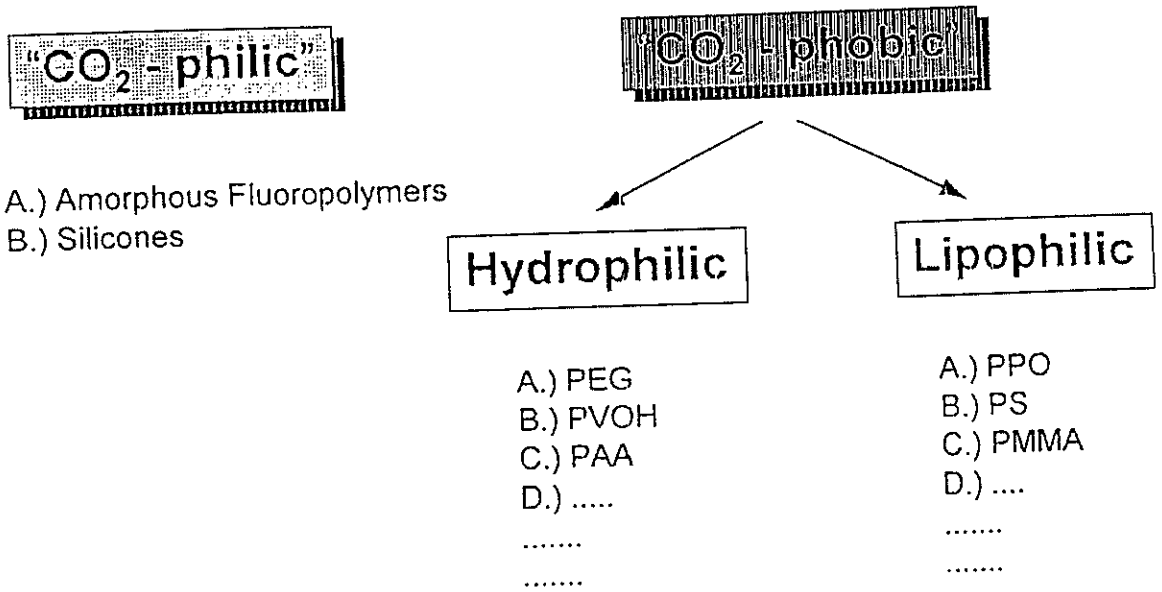

J. M. DeSimone et. al. *Science* **1994**, *265*, 356

Uses of Block Copolymers

- Dispersion polymerizations
- Emulsion polymerizations
- Viscosity modifiers

CO_2 continuous phase

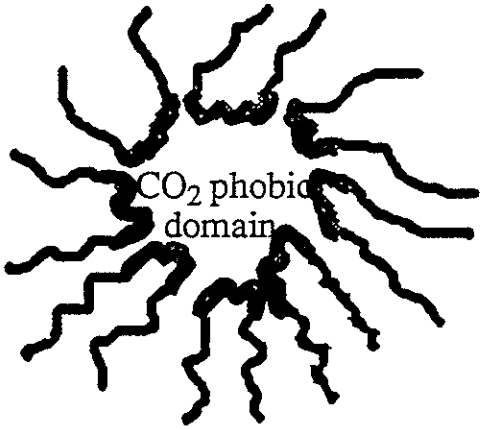

Stabilized micelle in CO_2

CO_2 - philic fluorocarbon | CO_2 - phobic hydrocarbon | CO_2 - philic fluorocarbon

CO_2 - phobic hydrocarbon | CO_2 - philic fluorocarbon | CO_2 - phobic hydrocarbon

55

CO_2-philic/Hydrophilic Surfactant

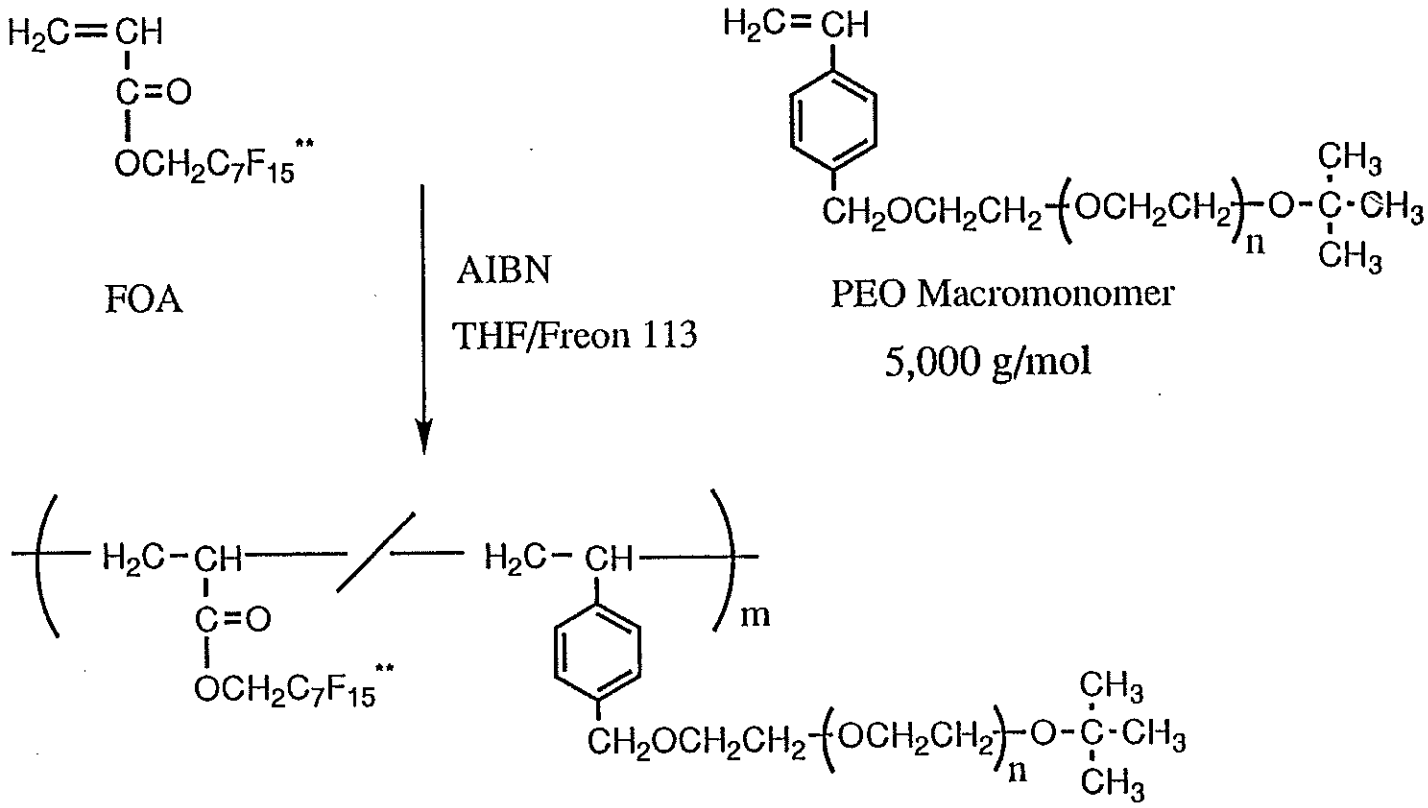

★ 15 wt % EO per molecule

★ Shown to stabilize 5 kg/mol PEO

★ Shown by UV studies to stabilize a CO_2 insoluble water/methyl orange dye phase

Initial Solvatochromic Studies

Dye: Methyl Orange (MO)

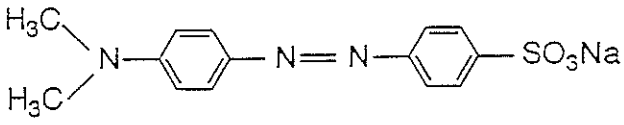

λ_{max} = 464nm (in water)

soluble in water, methanol ...
insoluble in CO_2

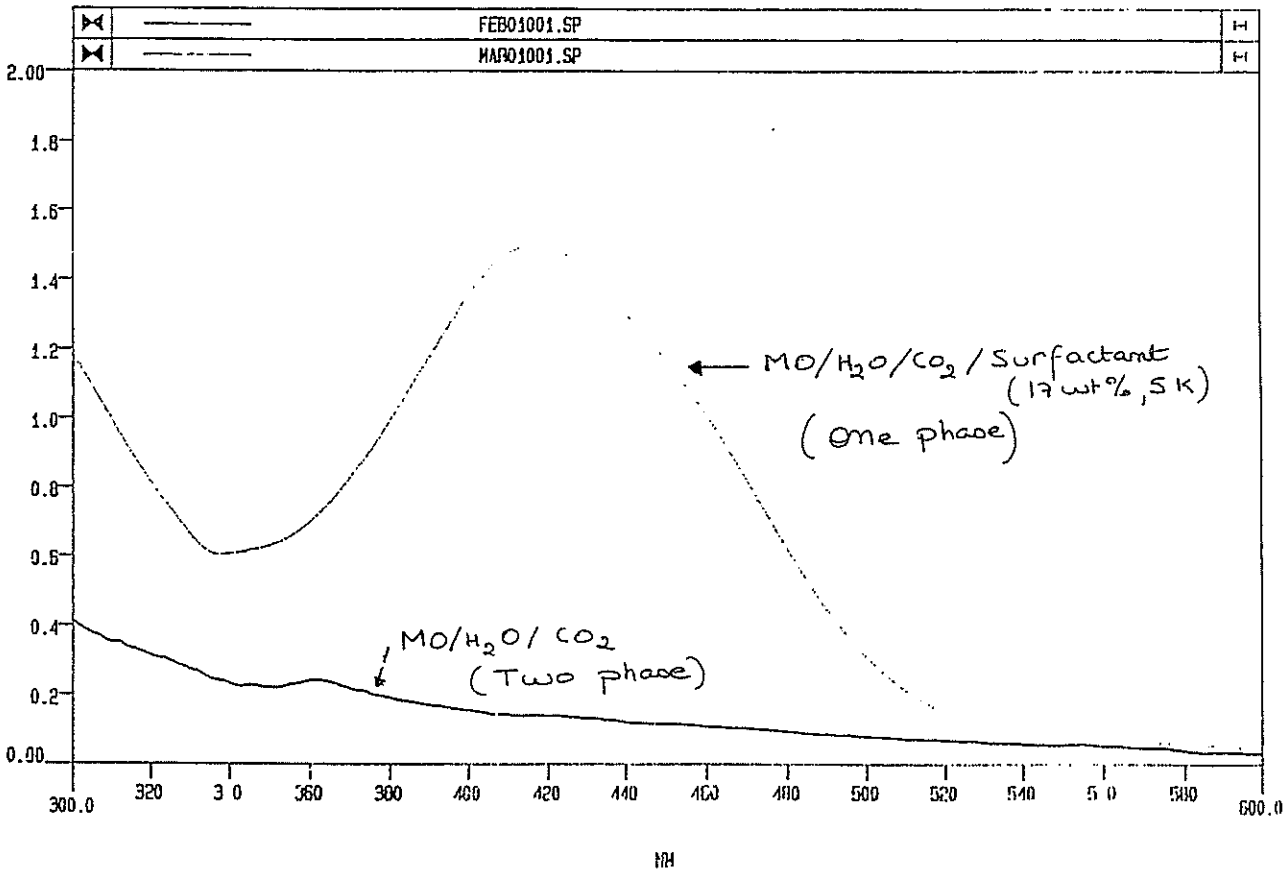

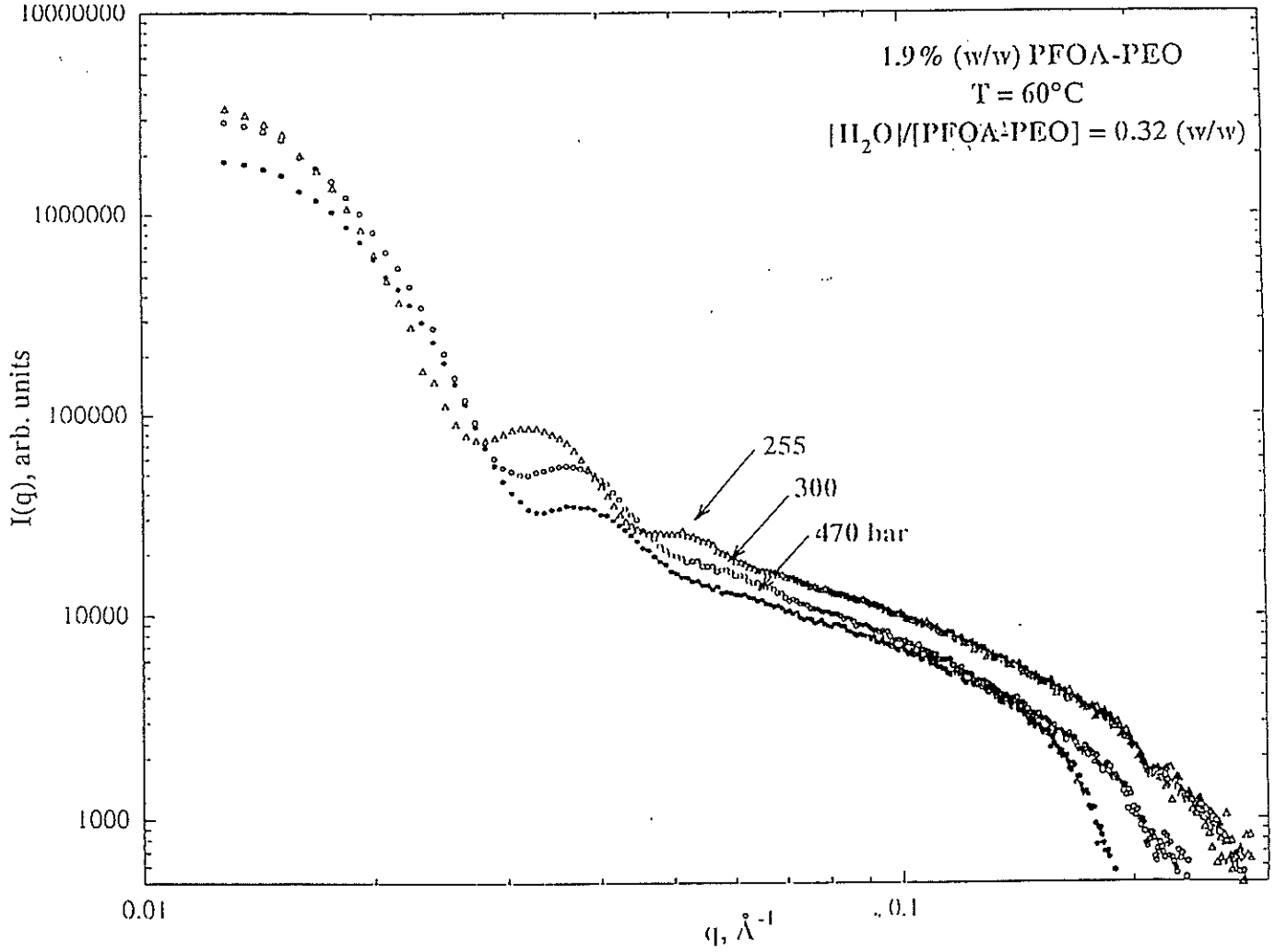

Small Angle x-ray Scattering of Poly(FOA-g-EO)

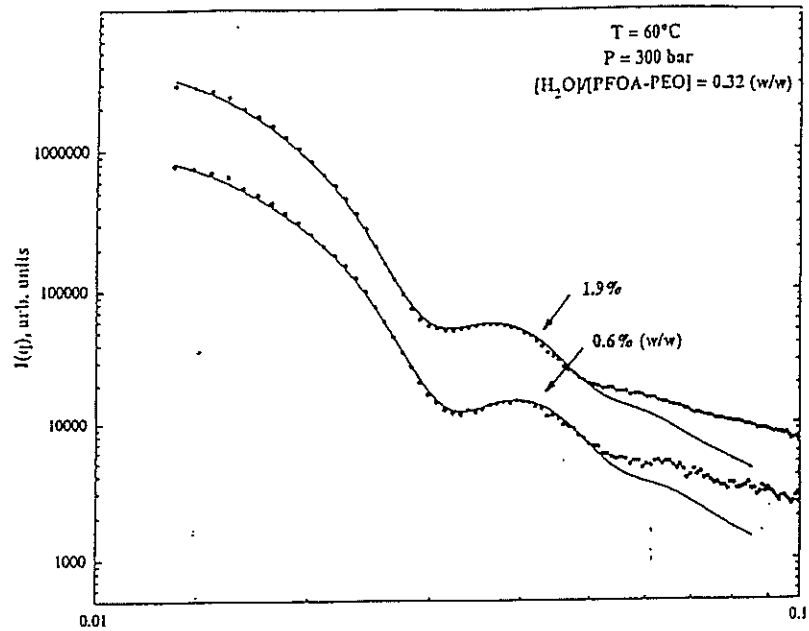

$$P(q) = [V_{core}(\rho_{core}-\rho_{shell})f_o(qR_{core}) + V_{shell}(\rho_{shell} - \rho_{solvent})f_o(qR_{shell})]^2$$

R_{core} = 109 Å Shell Thickness = 11 Å

* 0.32 wt % water based on surfactant promotes aggregation through hydrogen bonding

Association of Poly(FOA-g-EO)

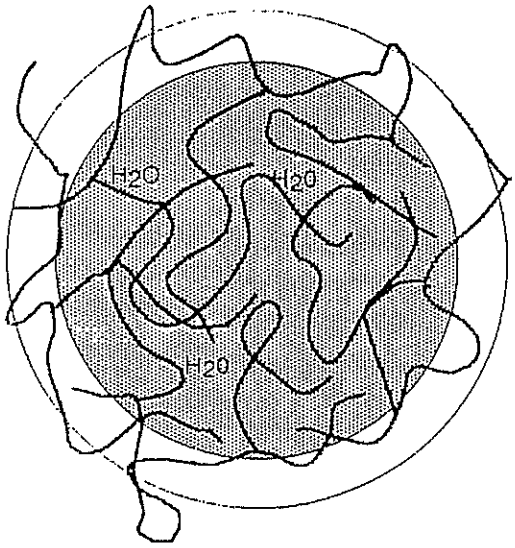

218 Å

240 Å

CO_2-philic/Lipophilic Surfactant

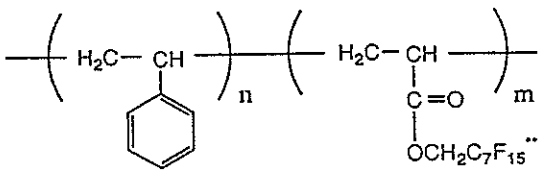

CO_2 phobic block

CO_2 philic block

SANS spectra for a copolymer with n = 35, m = 37

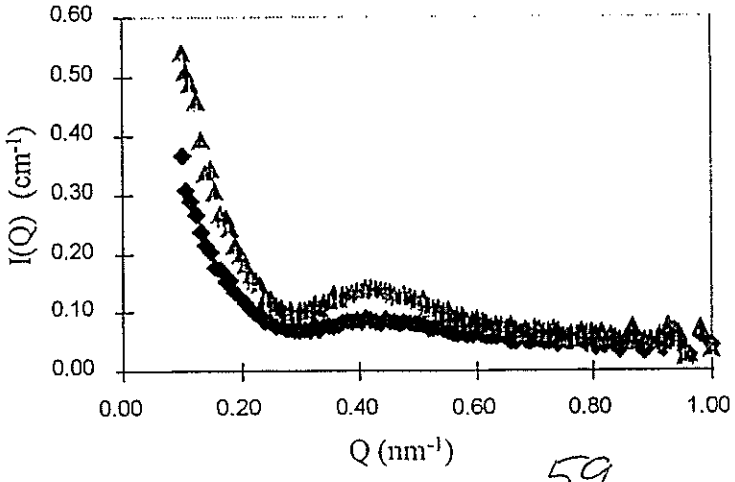

◆ 2 wt/vol % polymer

^ 4 wt/vol % polymer

Aggregation of a Lipophilic - CO_2 philic Block Copolymer in Supercritical CO_2

Poly(FOA-*b*-Sty)

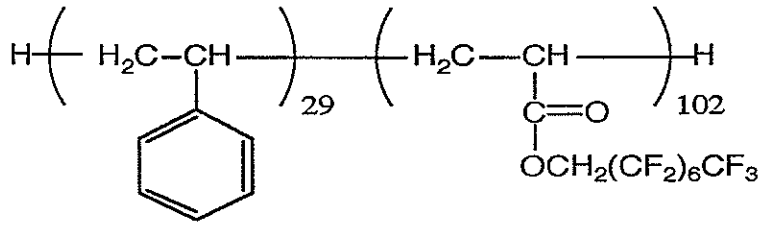

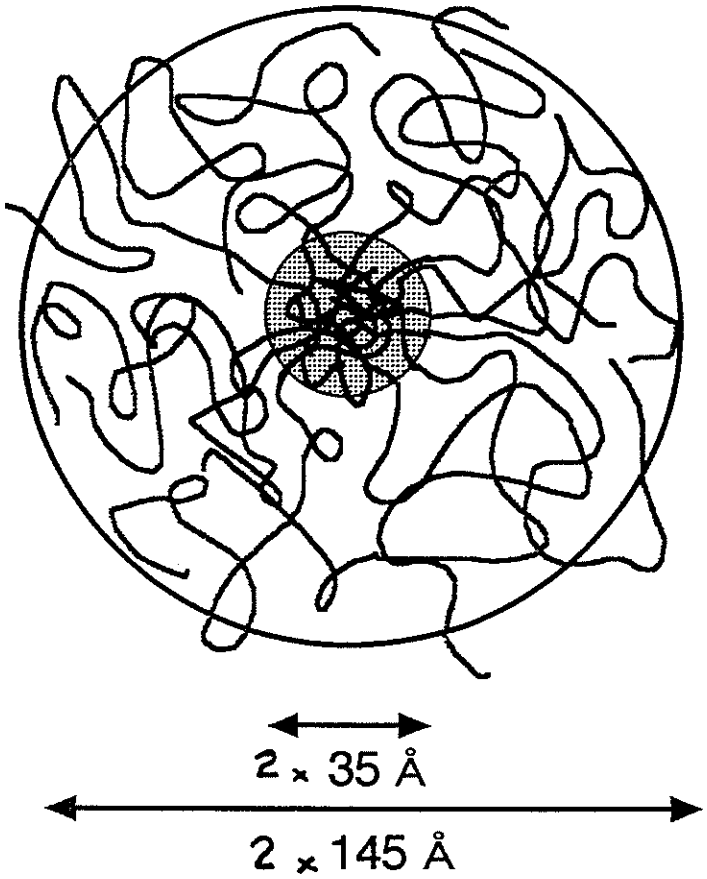

- MW determined from SANS* = 2.1 x 10^6 g/mol
- MW determined from GPC and NMR = 4.9 x 10^4 g/mol
- Estimate degree of aggregation of 40-45 molecules

Addition of Lipophilic, CO_2 Insoluble Material

Comparative SANS spectra for 4.0 wt/vol % surfactant solutions, w/ and w/o added 500 g/mol PS

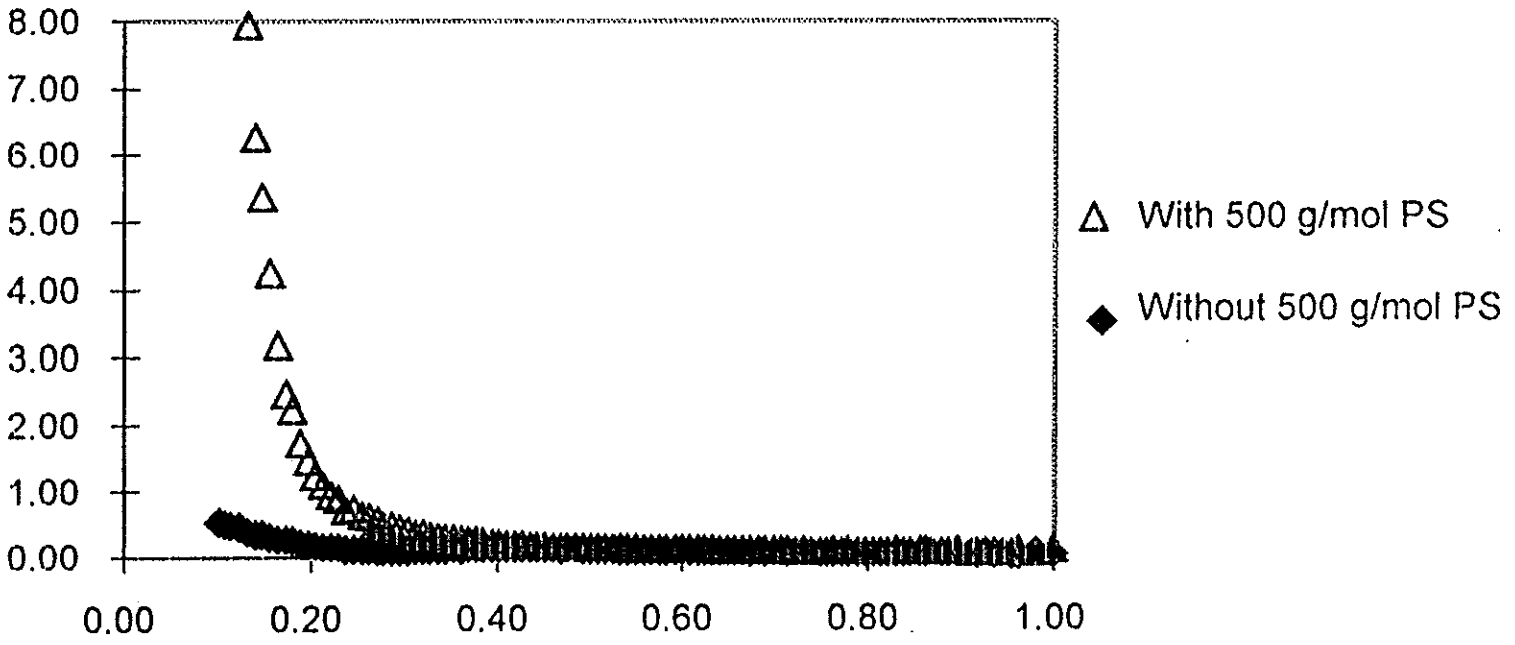

- Addition of CO_2 insoluble PS oligomer swells the interior of the aggregates by approximately 2 orders of magnitude

Dispersion Polymerization in CO_2

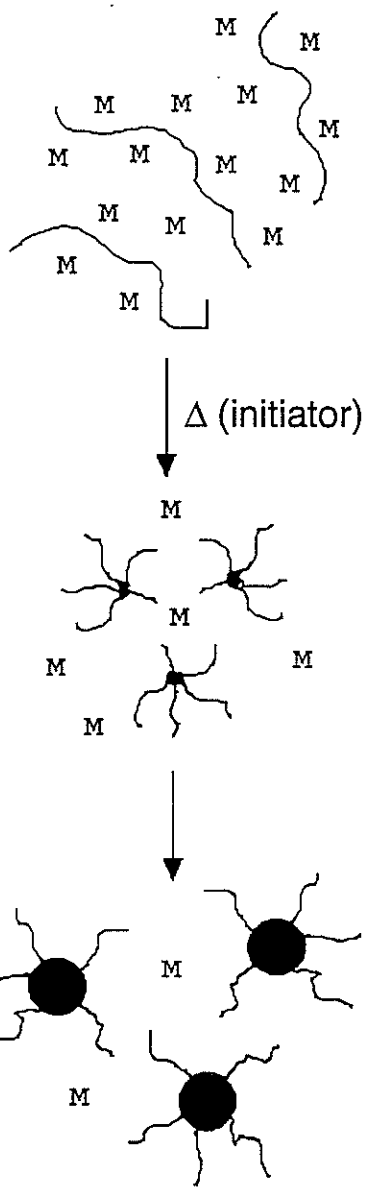

Observations

Clear, colorless solution

↓

Clear solution + intensifying color

↓

black (short

↓

white latex

According to Barrett's Model:

$$R_p = \alpha C_d V^{1/2} k_p (R_i/k_t)^{1/2}$$

where α = monomer partition coefficient
C_d = monomer concentration in the continuous phase
V = particle volume fraction
k_p = propagation rate constant
k_t = termination rate constant
R_i = initiation rate

Barrett, K. E. J. *Dispersion Polymerization in Organic Media*, Wiley, London, **1975**.

Dispersion Polymerization in CO_2

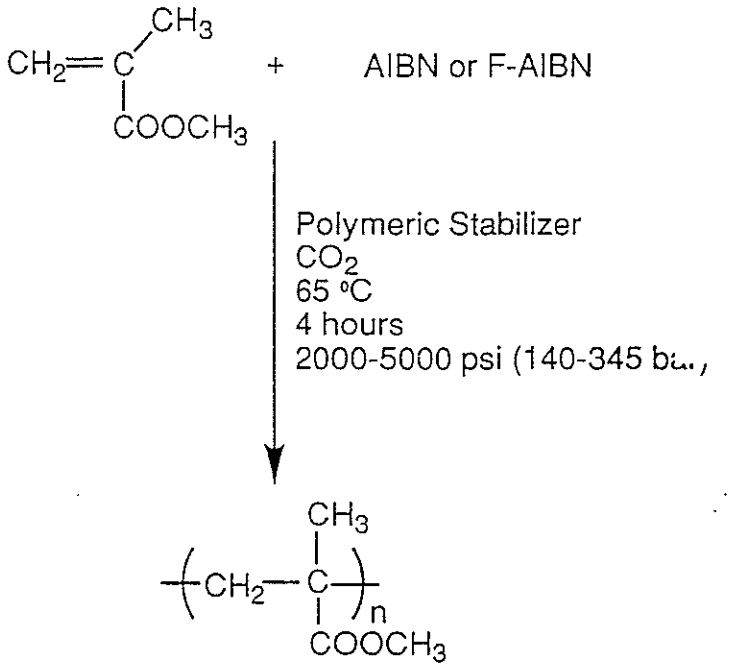

DeSimone, J. M.; Maury, E. E. *et al. Science* 1994, *265*, 356.

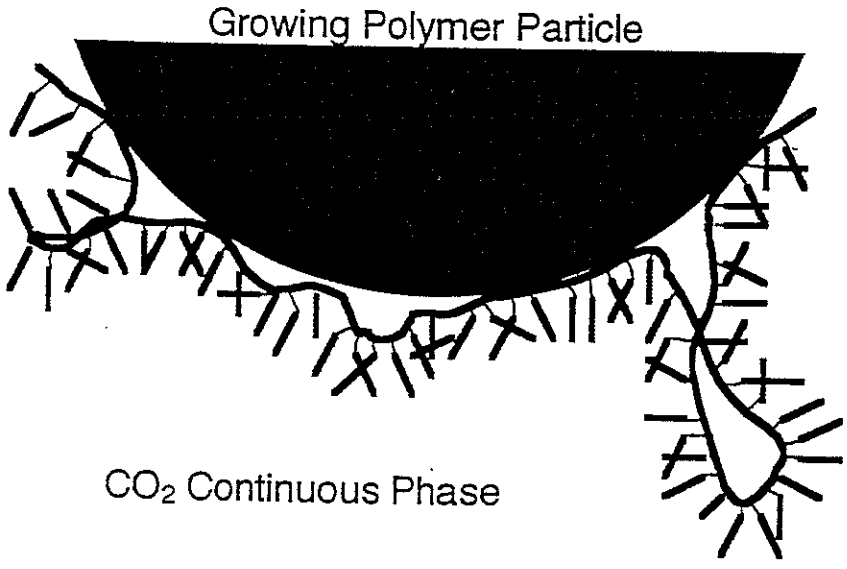

Heterogeneous Dispersion Polymerization of MMA in CO_2

Reaction Conditions: F-AIBN, 65 °C, 204 bar, 4 hours

Initiator	Stabilizer (w/v %)	Yield (%)	$\langle M_n \rangle$ ($\times 10^{-3}$ g/mol)	MWD	Particle Size (μm)
F-AIBN	0% LMW-PFOA	10	77	2.9	
F-AIBN	2% LMW-PFOA	98	277	2.5	2.0 (± 0.2)
F-AIBN	4% LMW-PFOA	91	303	2.3	0.9 (± 0.3)
F-AIBN	1% HMW-PFOA	38	163	2.3	1.6 (± 0.6)
F-AIBN	2% HMW-PFOA	47	193	2.3	2.4 (± 0.2)
F-AIBN	4% HMW-PFOA	74	281	2.5	1.4 (± 0.1)

Particle Isolation

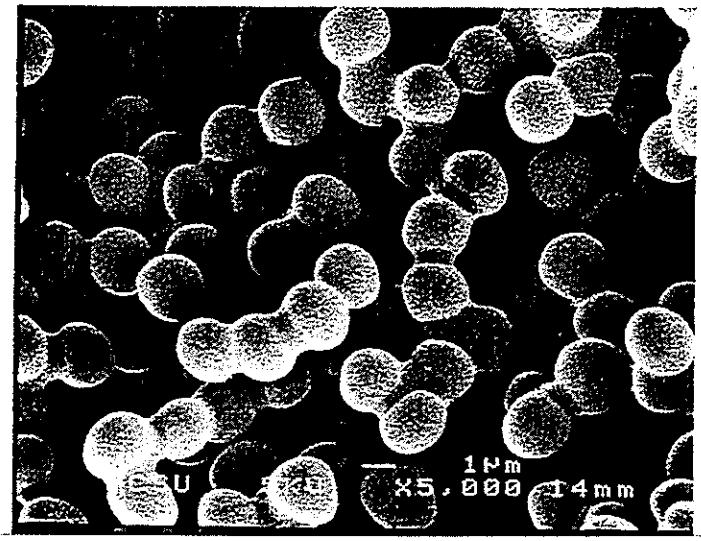

As Polymerized

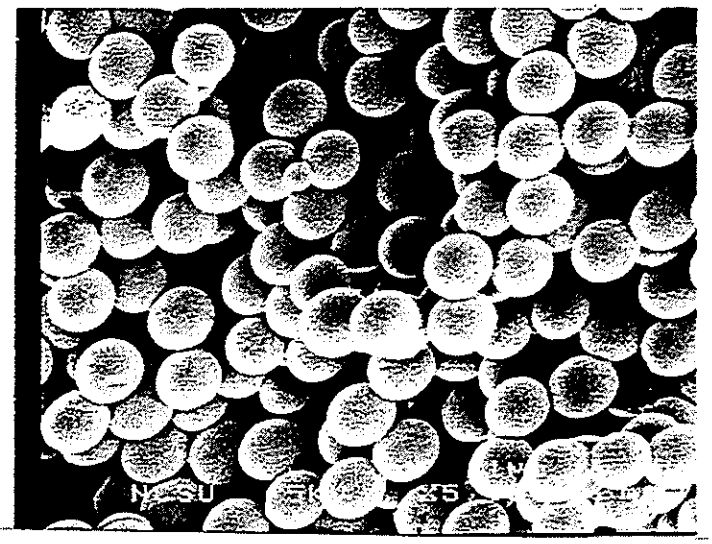

CO_2 Wash

5000 psi
0°C

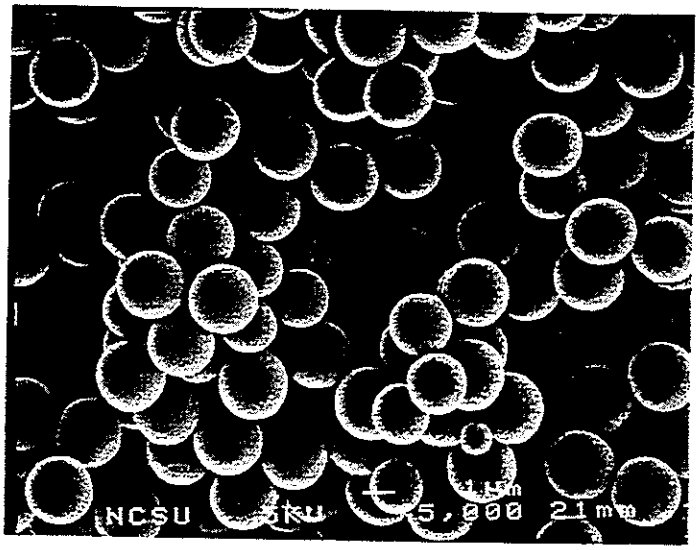

F-113 Wash

Effect of the Concentration of Stabilizer

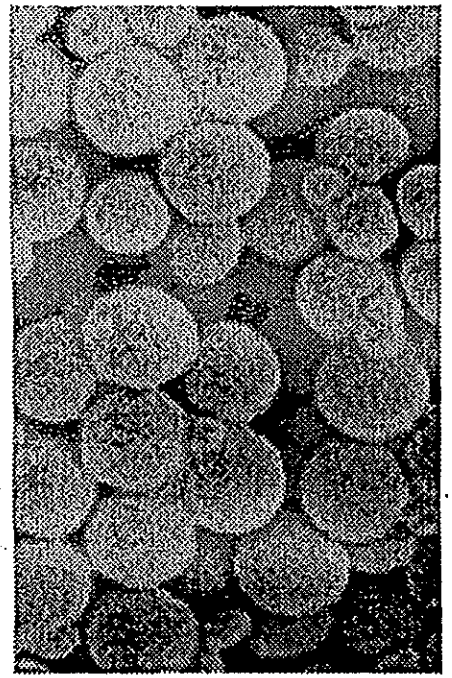

1.5 μm

20w/v% MMA

4w/v% PFOA

90-98% yield

Mn=293K

MWD=2.33

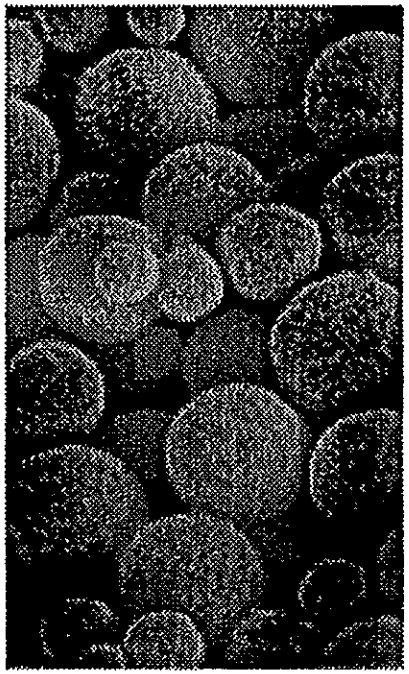

1.9 μm

20w/v% MMA

2w/v% PFOA

94% yield

Mn=230K

MWD=2.51

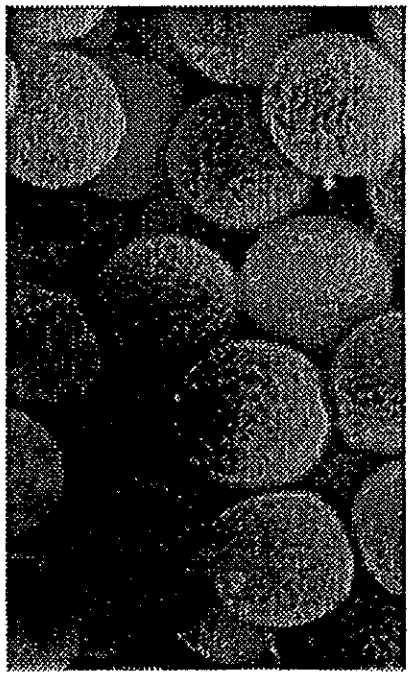

2.2 μm

20w/v% MMA

1w/v% PFOA

96% yield

Mn=274K

MWD=2.41

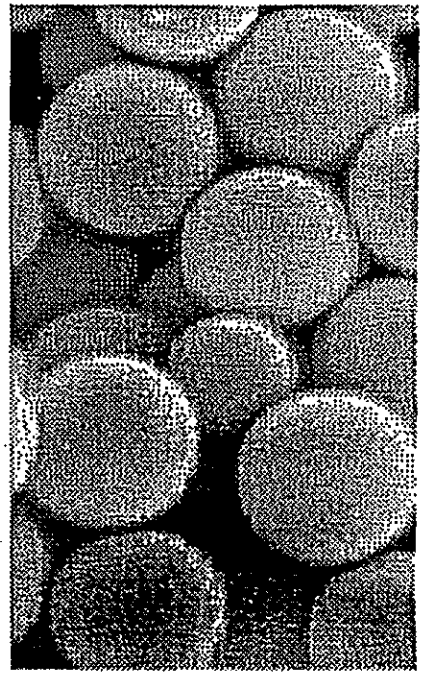

2.7 μm

20w/v% MMA

0.5w/v% PFOA

91% yield

Mn=302K

MWD=2.34

Macromonomer = comonomer *and* stabilizer

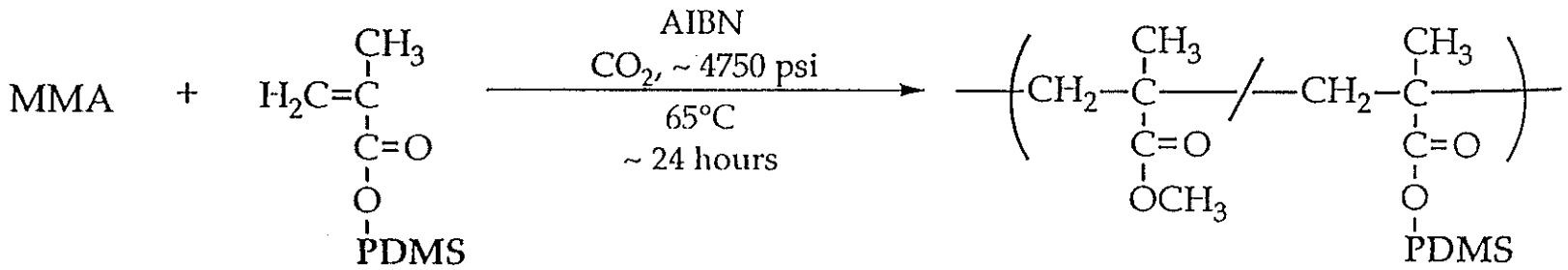

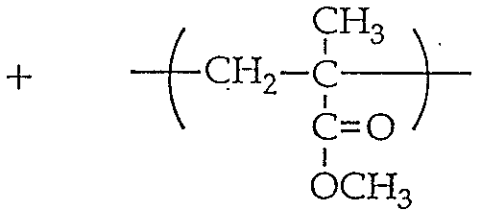

PDMS = C_4H_9—(Si(CH$_3$)$_2$—O)$_{130}$—C_3H_6—

0, 2, 4% based on MMA

X 5000

PMMA (no stabilizer)

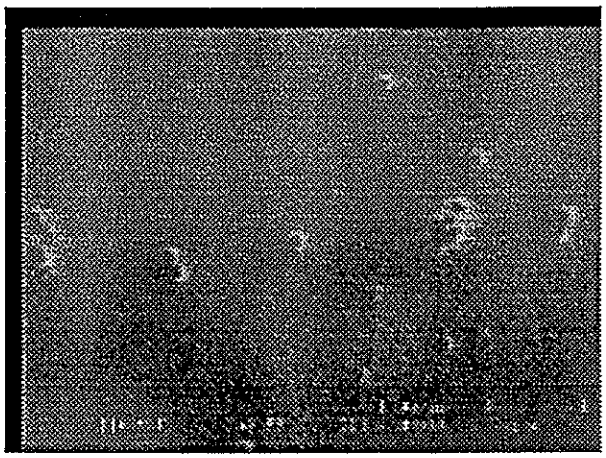

X 1000

PMMA (stabilized)
(4 w/v% PDMS homopolymer

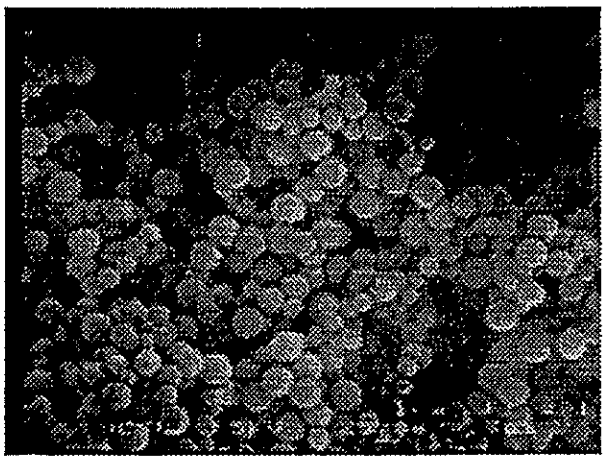

X 5000

PMMA (stabilized + washed)
(4 w/v% PDMS macromonomer

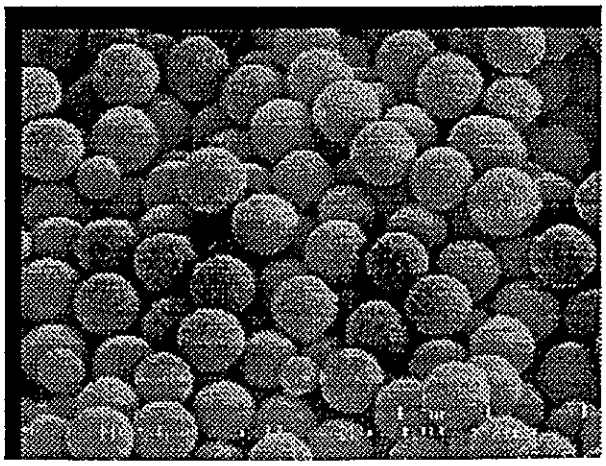

X 5000

PMMA (stabilized)
(0.7 w/v% PDMA macromonomer

PMMA Particles Made in Supercritical Carbon Dioxide

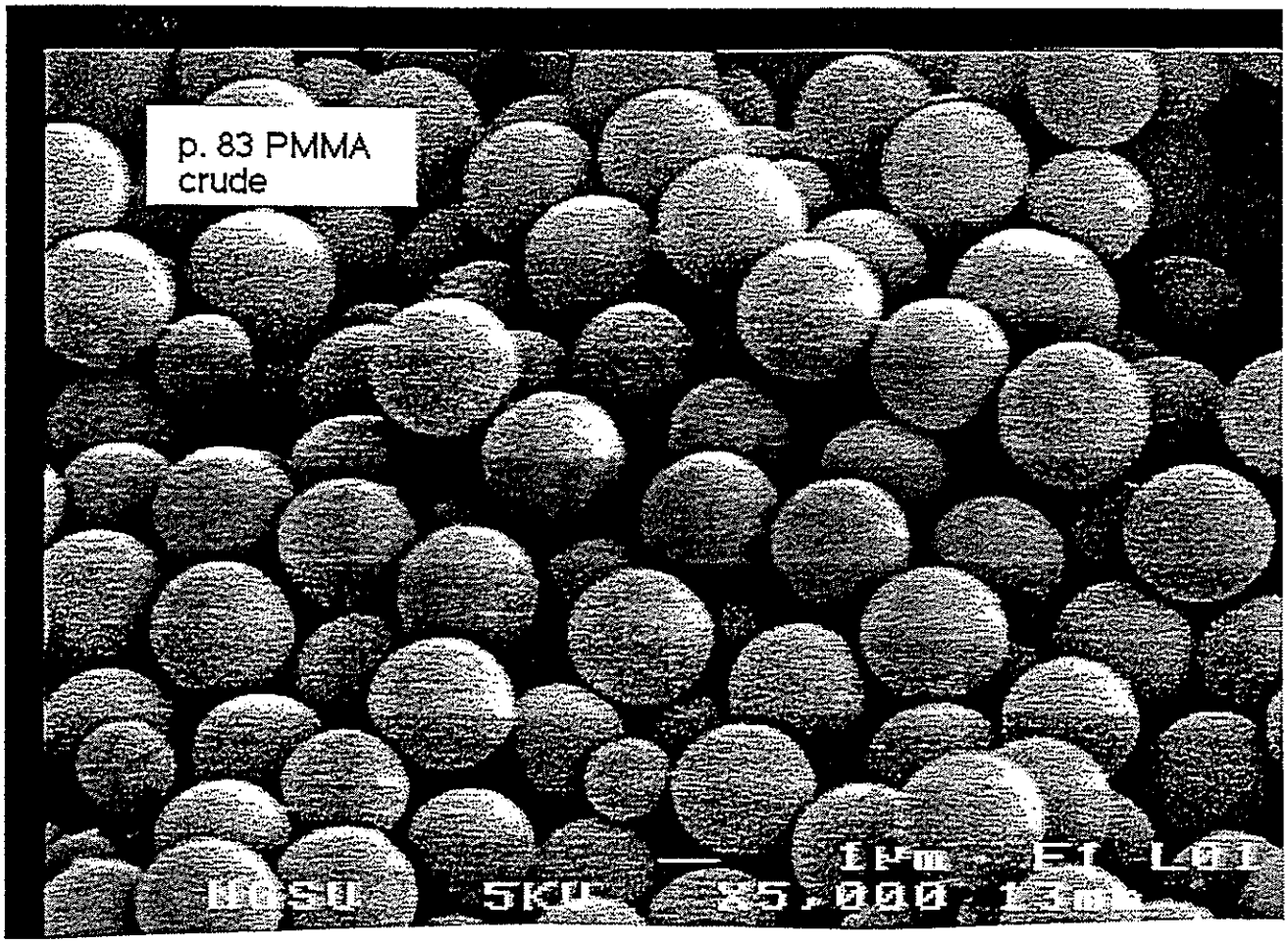

After Washing: 0.2% PDMS by Weight

"...CO_2 is the best solvent for free radical chain reactions..."

- Inert to free radicals
  - **No chain transfer to solvent**
    - **Even with highly electrophilic fluorinated radicals!**
- Liquid-like densities, gas-like transport properties
  - **Viscosity is order of magnitude lower than liquids**
    - **Highest radical initiator efficiencies**
    - **No Tromsdorf effect**
  - **Diffusivities of solutes one to two orders of magnitude higher in CO_2 than in liquids**
- Solubilizes hard to dissolve fluoropolymers
  - **Fluorinated acrylates, styrenics, polyethers, ...**
  - **Pseudoazeotrope w/ terafluoroethylene (safe handling)**
- Plasticizes many CO_2-insoluble polymers
  - **Core-shell structures**
  - **IPNs**
- Emulsions and Microemulsions
  - **Option to have hydrophilic or lipophilic cores!**
- Dispersion Processes
  - **Stable polymer colloids (coatings)**
  - **New materials, new morphologies**
- Precipitation Processes
  - **Free flowing, bone dry powders**
- Immisicible with water
  - **Unique processes possible**

Students and Postdocs

Dr. Kathy Shaffer from University of Pittsburgh

Dr. Yu-Ling Hsiao from Stanford University

Dr. James Combes from University of Texas

Elise Maury (Dispersion Polymerizations)

Tim Romack (Fluoropolymers)

Zhibin Guan (Fluoropolymers)

Jim McClain (Polymer Processing / Composite Materials)

Dorian Canelas (Heterogeneous Polymerizations / Composite Materials)

Doug Betts (Heterophase Fluoropolymers via Living Radical Methods)

Heather Batten (Hydrophilic Surfactant Synthesis)

Collaborators:

E. T. Samulski (UNC-CH, Molecular Dynamics Simulations)

Keith Johnston (UT-Austin, Micellization and Surfactants)

G. Wignall and David Londono (Oakridge National Laboratory, SANS)

J. Fulton (Batelle, SAXS)

Acknowledgments

- National Science Foundation:
  Presidential Faculty Fellowship (J. M. DeSimone 1993-97)
- Environmentally Benign Chemical Synthesis and Processing Initiative:
  NSF, EPA, in collaboration with K. P. Johnston U.T. Austin
- Consortium on Materials Synthesis and Processing in CO_2
  The University of North Carolina at Chapel Hill

DuPont	Air Products and Chemicals
Eastman Chemical	B. F. Goodrich
Hoechst - Celanese Corp.	Xerox
Bayer	G. E.
Oak Ridge National Laboratories	

- The Supercritical Fluids Research Group at UNC

Oscillating Catalysts for Propylene Polymerization

Robert Waymouth
Stanford University

FOCUS:

MECHANISTIC UNDERSTANDING

⇓

MOLECULAR DESIGN OF NEW POLYMERS

- POLYMERIZATION MECHANISM

INIITIATION, PROPAGATION, CHAIN TRANSFER ⟹ MOLECULAR WEIGHT, END GROUPS ⟹ PHYSICAL PROPERTIES

- POLYMERIZATION STEREOCHEMISTRY

CATALYST GEOMETRY ⟹ POLYMER MICROSTRUCTURE ⟹ PHYSICAL PROPERTIES

- POLYMERIZATION OF FUNCTIONALIZED MONOMERS

FUNCTIONALIZED MONOMERS ⟹ FUNCTIONALIZED POLYMERS ⟹ PHYSICAL PROPERTIES, CHEMICAL PROPERTIES

INSERTION AND TERMINATION STEPS OF HOMOGENEOUS ZIEGLER-NATTA POLYMERIZATION

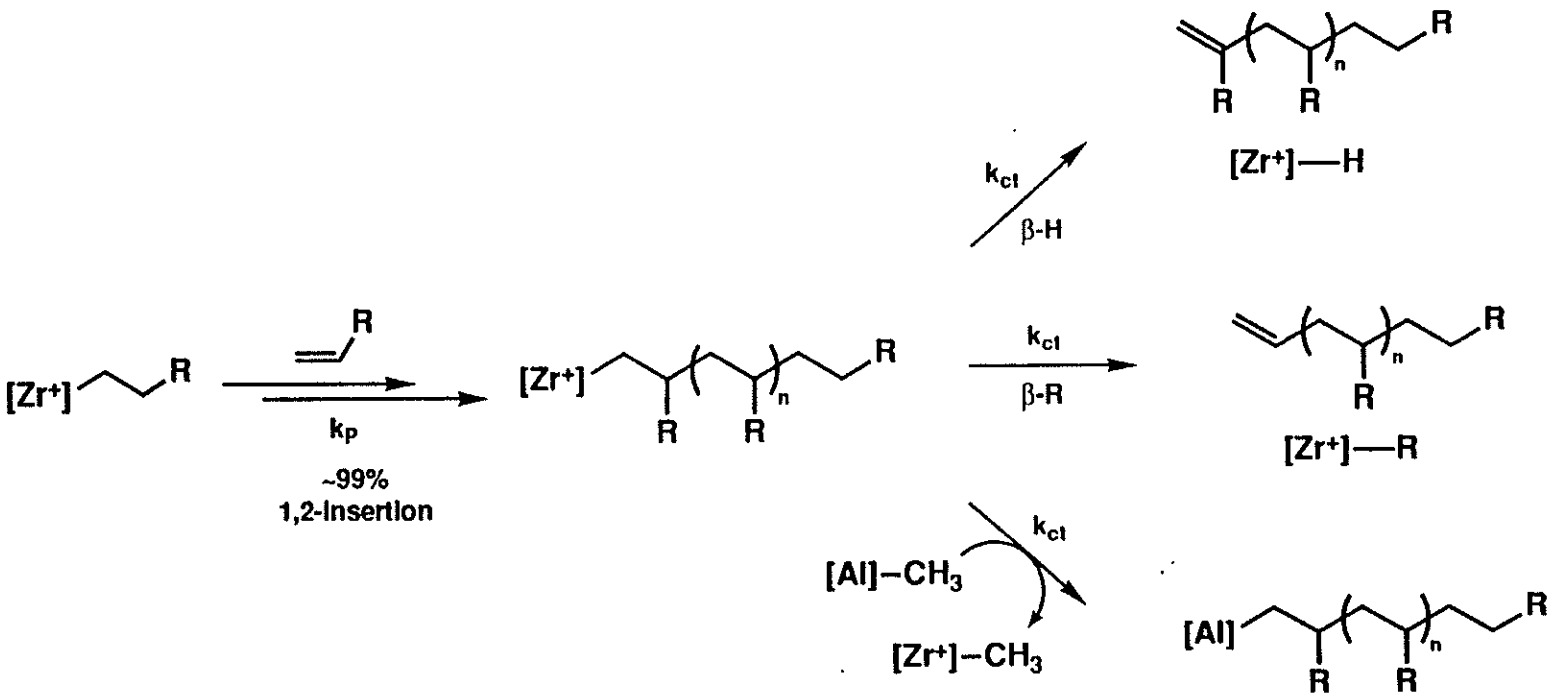

THE FIRST EXAMPLE OF A COMMERCIALLY VIABLE HOMOGENEOUS ZIEGLER-NATTA CATALYST

1980 Sinn, Kaminsky (Adv. Organomet. Chem. p99)

M = Ti, Zr, Hf
X = Halogen, Methyl

+

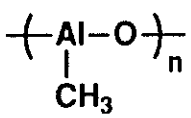

Aluminoxane
Al/Zr = 1000:1
10 < n < 30

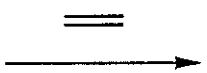

Linear HDPE
- Long-lived catalyst
- Single-sited behavior (M_w/M_n ~ 2)
- Activity = 10^7 g_P/mol_{Zr} h bar

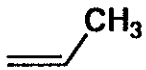

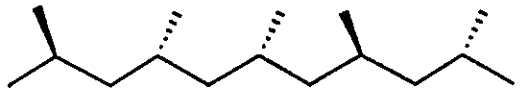

Atactic Polypropylene
- Long-lived catalyst
- Single-sited behavior (M_w/M_n ~ 2)
- Activity = 10^6 g_P/mol_{Zr} h bar

$AlMe_3 + H_2O \longrightarrow$ 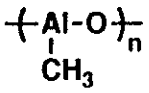

- Poorly defined mixture of linear and cyclic oxo-bridged aluminum alkyls

Proposed active species:

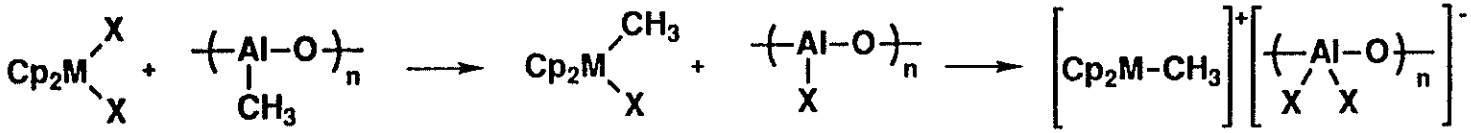

STEREOCHEMISTRY OF POLYMERIZATION

1980 Sinn, Kaminsky

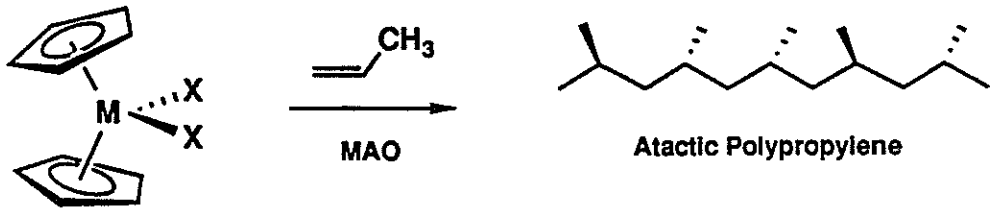

1984 Ewen, 1985 Brintzinger, Kaminsky

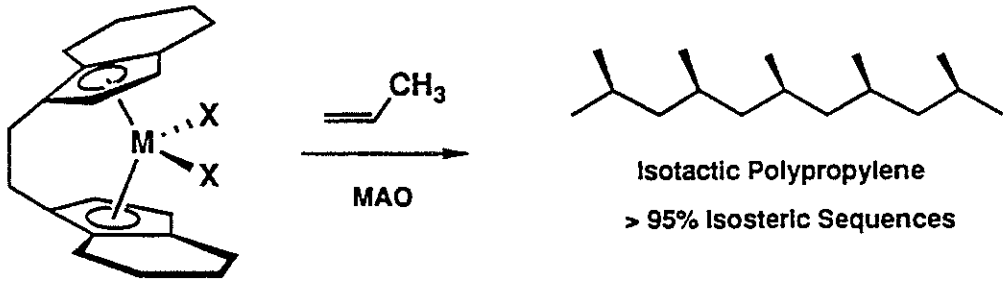

1988 Ewen

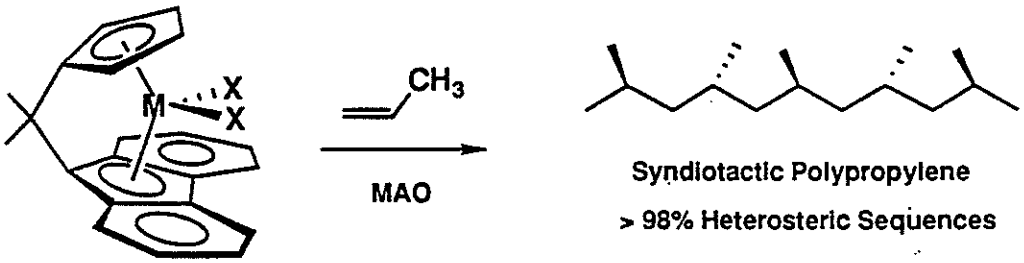

1991 Ewen

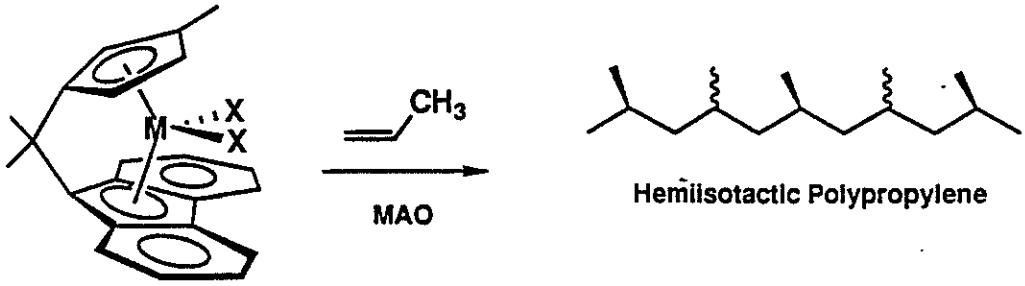

Polymer Microstructure - ^{13}C NMR Spectrum

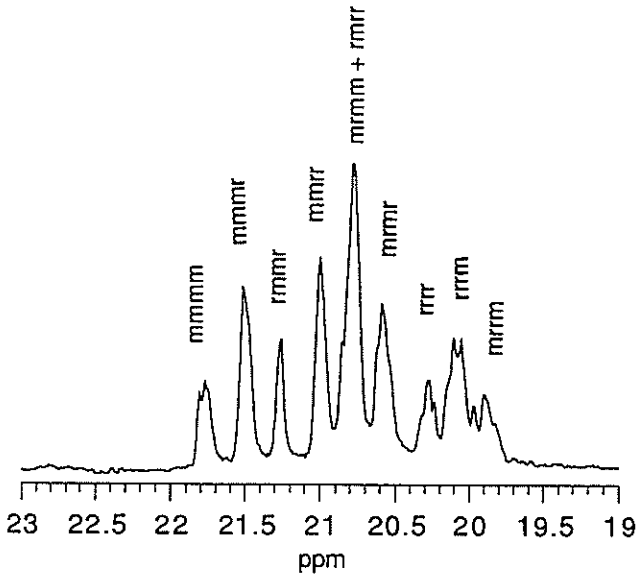

Atactic PP

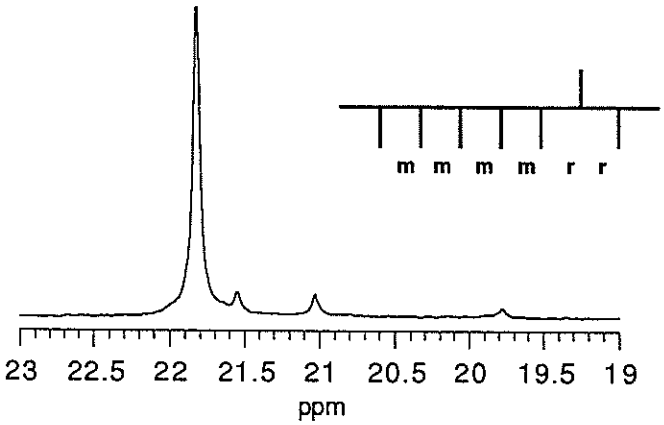

Isotactic PP

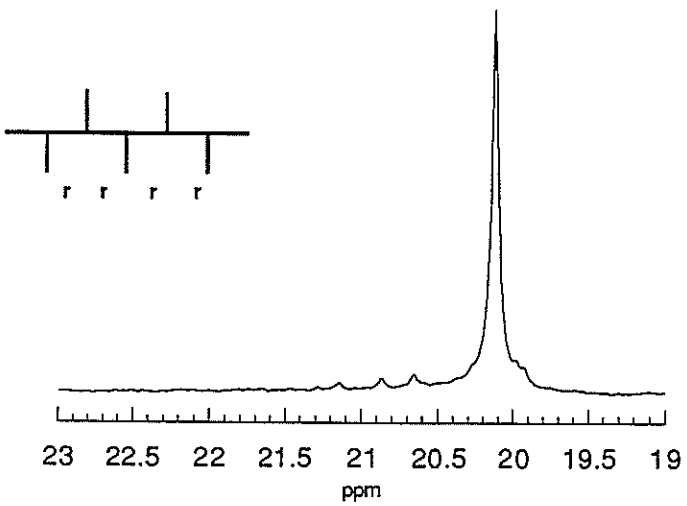

syndiotactic PP

Elastomeric Polypropylene: Initial Discovery

Natta: U. S. Patent **3,175,999**, Mar. 30, 1965, to Montecatini

Chim. e Ind, **1957**, 39, 275

Catalysts: $TiCl_4$ / $AlEt_3$ at 145°C

$VOCl_3$ / $AlEt_3$

- polymer fractionated by boiling solvent extraction: acetone, ether, heptane
- heptane-soluble, isopropyl ether insoluble fraction had elastomeric properties
- elastomeric properties interpreted in terms of stereoblock structure

THERMOPLASTIC ELASTOMERS

MORPHOLOGY:

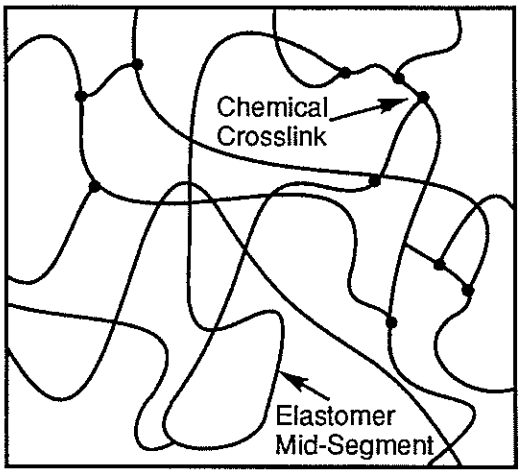

Thermoset Elastomer
(Chemical Crosslinks)

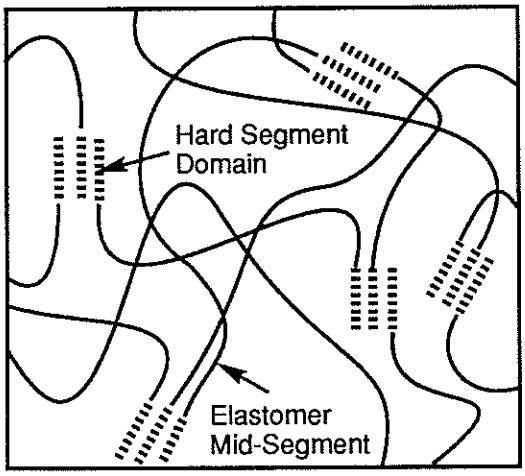

Thermoplastic Elastomer
(Physical Crosslinks)

BLOCK ARRANGEMENTS:

1. 

STYRENE-BUTADIENE-STYRENE

2. 

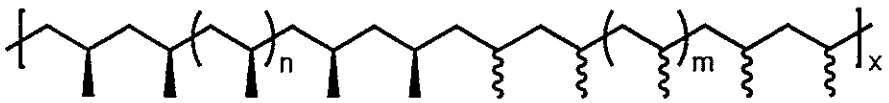

ISOTACTIC-ATACTIC STEREOBLOCK POLYPROPYLENE

DuPont Elastomeric Polypropylene

Collette and Tullock (Macromolecules, **1989**, *22*, 3851)
US Patent **4,335,225** (1982)

$$R_4M + Al_2O_3 \longrightarrow \text{CATALYST FOR OLEFIN POLYMERIZATION}$$

R = 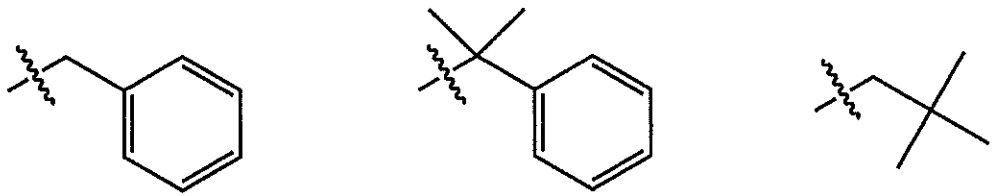

M = Ti, Zr, Hf

Representation of Catalyst:

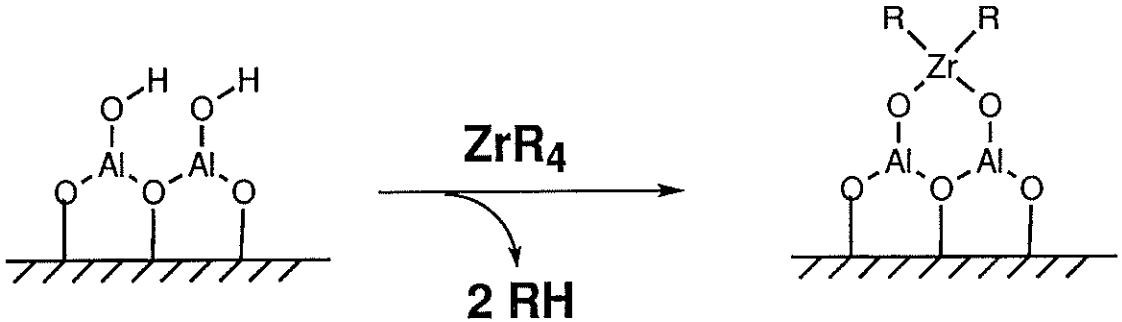

Stereoblock Polypropylene

Chien JACS (1990) 2030, (1991) 8569

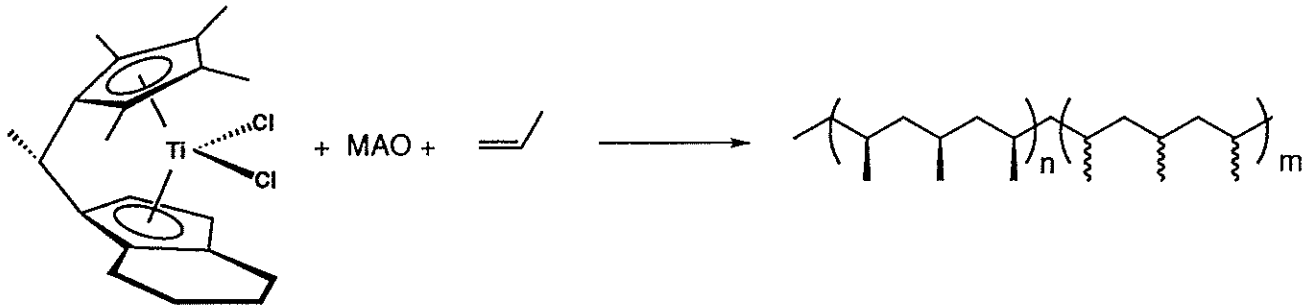

"Two Site" Mechanism Proposed (Coleman and Fox J Chem Phys (1963) 1065)

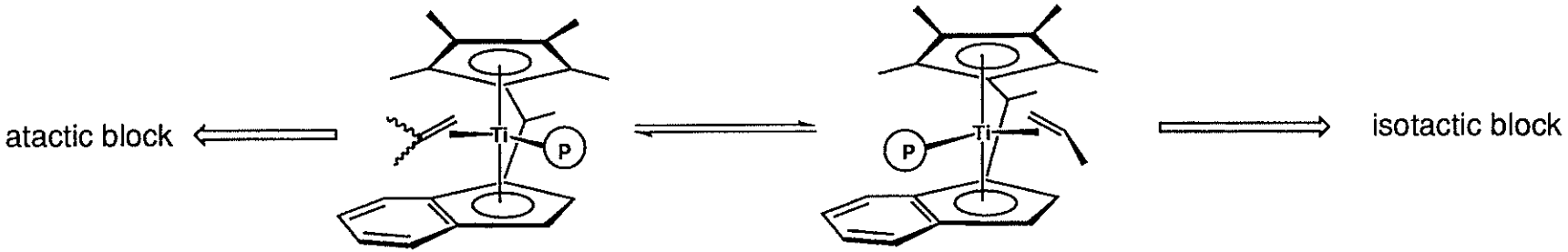

A STRATEGY FOR THE SYNTHESIS OF ATACTIC-ISOTACTIC STEREOBLOCK POLYPROPYLENE

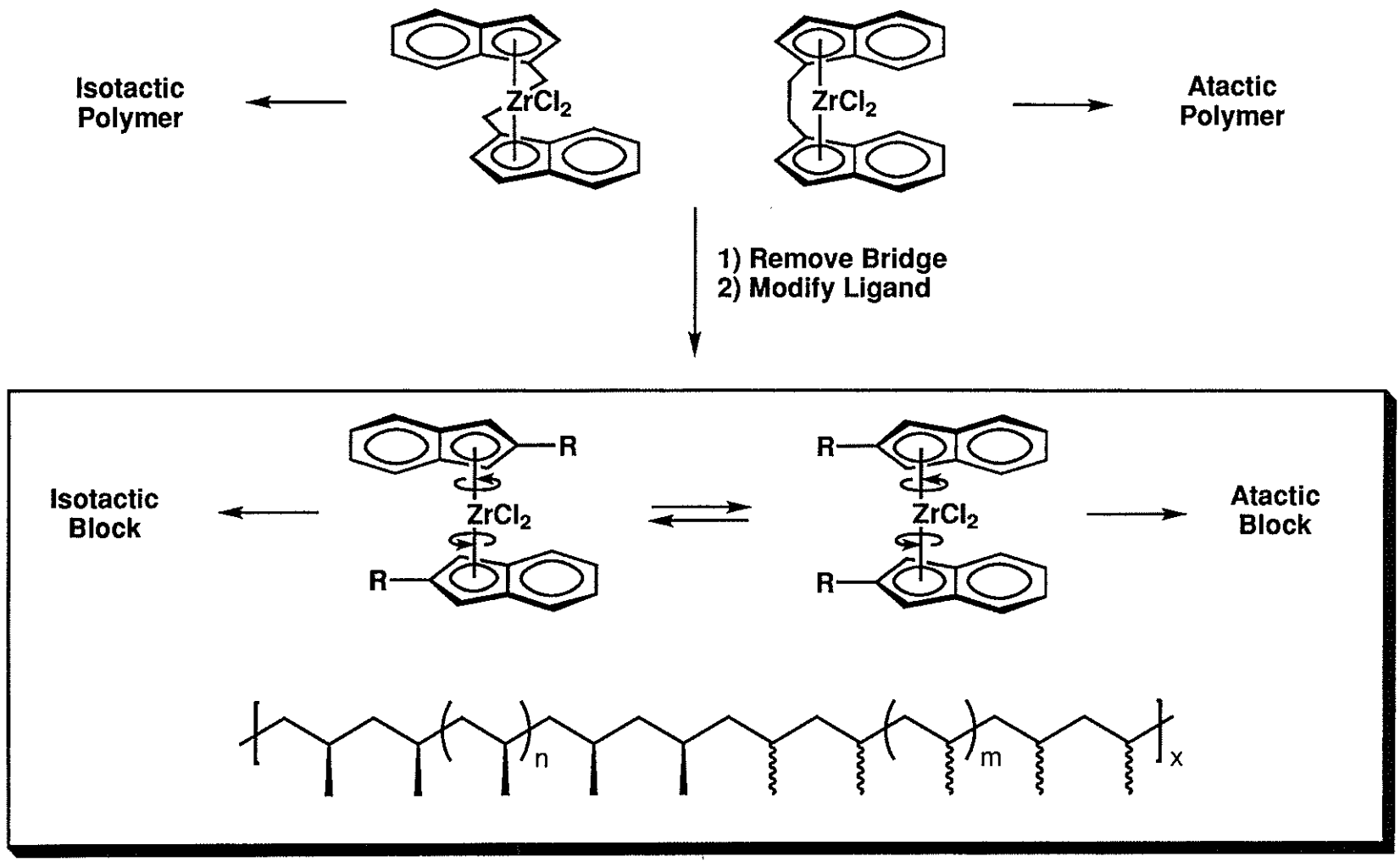

PREPARATION BIS(2-PHENYLINDENYL)ZIRCONIUM DICHLORIDE

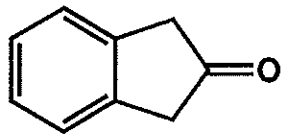

1) PhMgBr
2) $-H_2O$

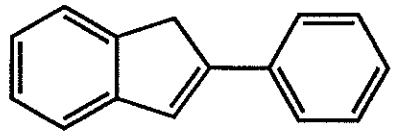

(64% YIELD)

1) BuLi
2) 0.5 $ZrCl_4$

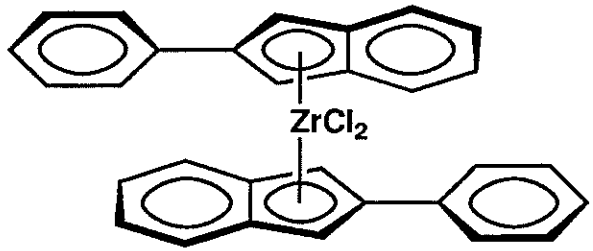

$(2PhInd)_2ZrCl_2$
Yellow-Orange Plates
(82% YIELD)

INITIAL PROPYLENE POLYMERIZATION RESULTS

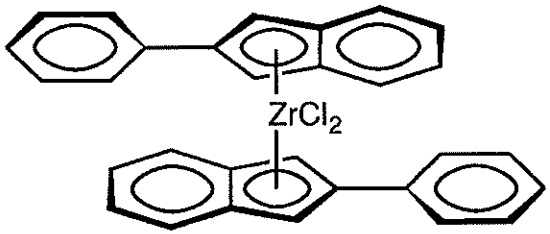

Experiment	Pressure (psig)	Productivity[b] (x 10-5)	M_w[c] (x 10-3)	M_w / M_n
GWC-4-93	5	2.7	213	1.5
GWC-4-95	25	6.2	395	1.9
GWC-4-97	50	10.4	540	1.7
GWC-4-99	75	17.3	604	1.8

[a] [Zr] = 5.5 x 10^{-5} M, [Al]/[Zr] = 1000, T = 0 °C; [b] g PP / mol Zr · h; [c] by GPC vs. polystyrene

STRESS-STRAIN CURVE

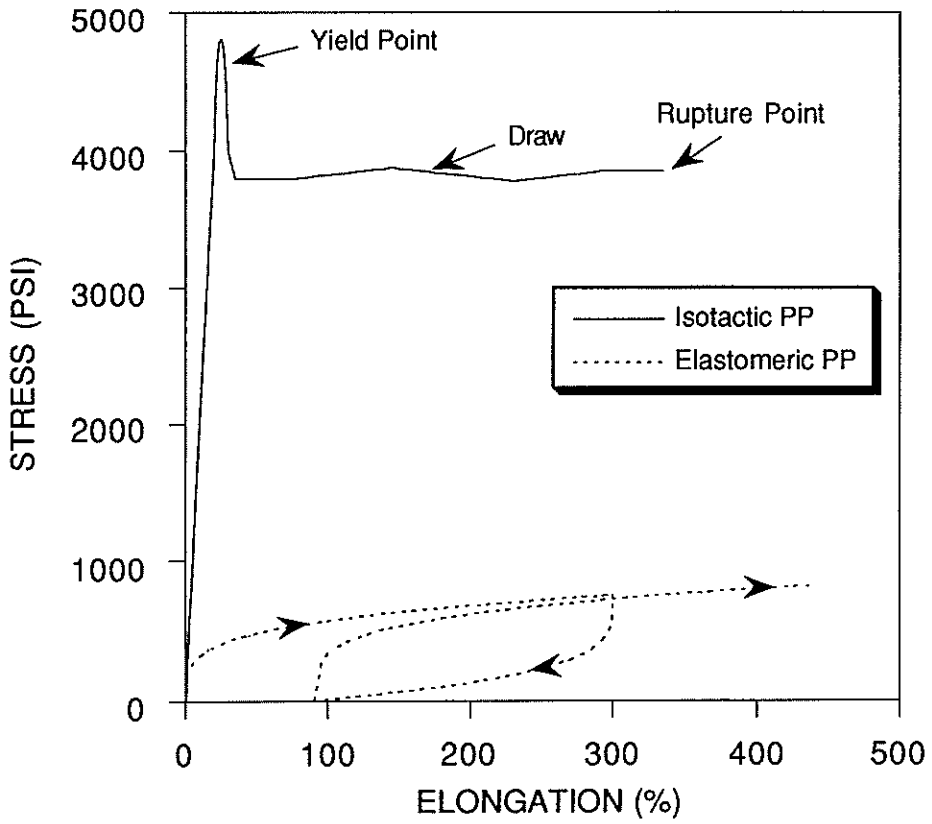

STRESS-STRAIN CURVE OF POLYPROPYLENE MADE AT -25°C

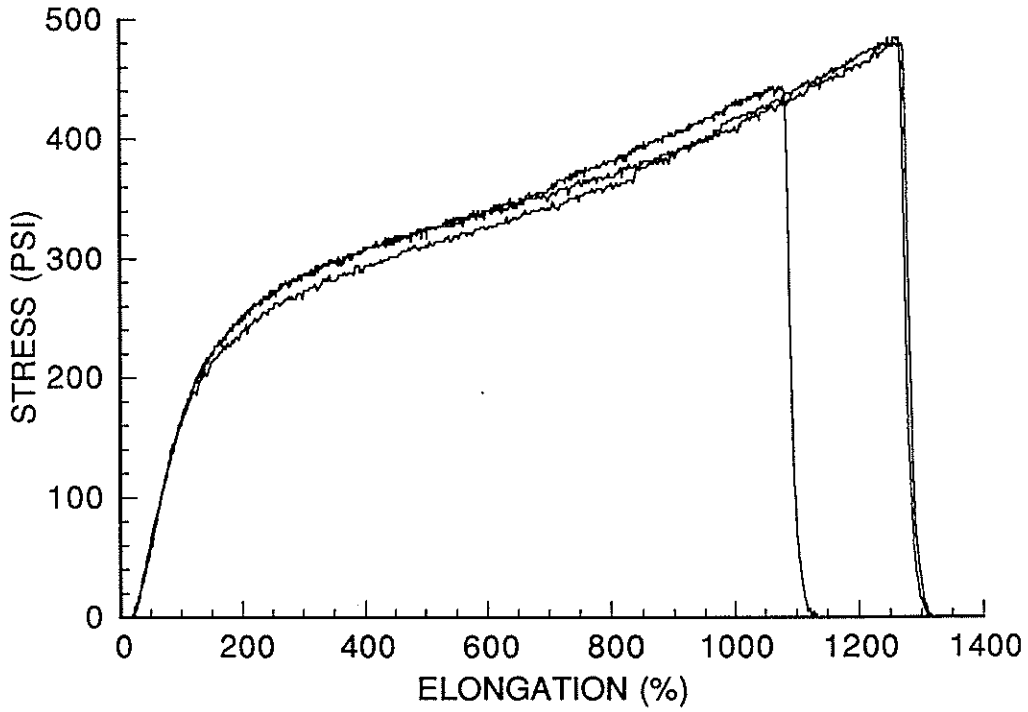

COMPARISON OF PHYSICAL PROPERTIES:

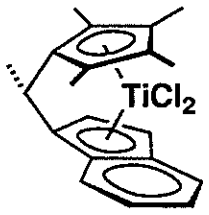

/ MAO

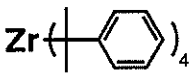

/ Al_2O_3

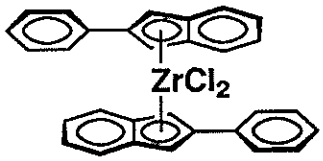

/ MAO

PHYSICAL PROPERTY	CHIEN	DUPONT	WAYMOUTH
TENSILE STRENGTH (psi)	1750	891	462 / 467
ELONGATION (%)	1300	875	1210 / 2550
MODULUS (psi)	nd	nd	246 / 201
TENSILE SET (%)	24	119	44 / 32

POLYMER MICROSTRUCTURE - ^{13}C NMR SPECTRUM

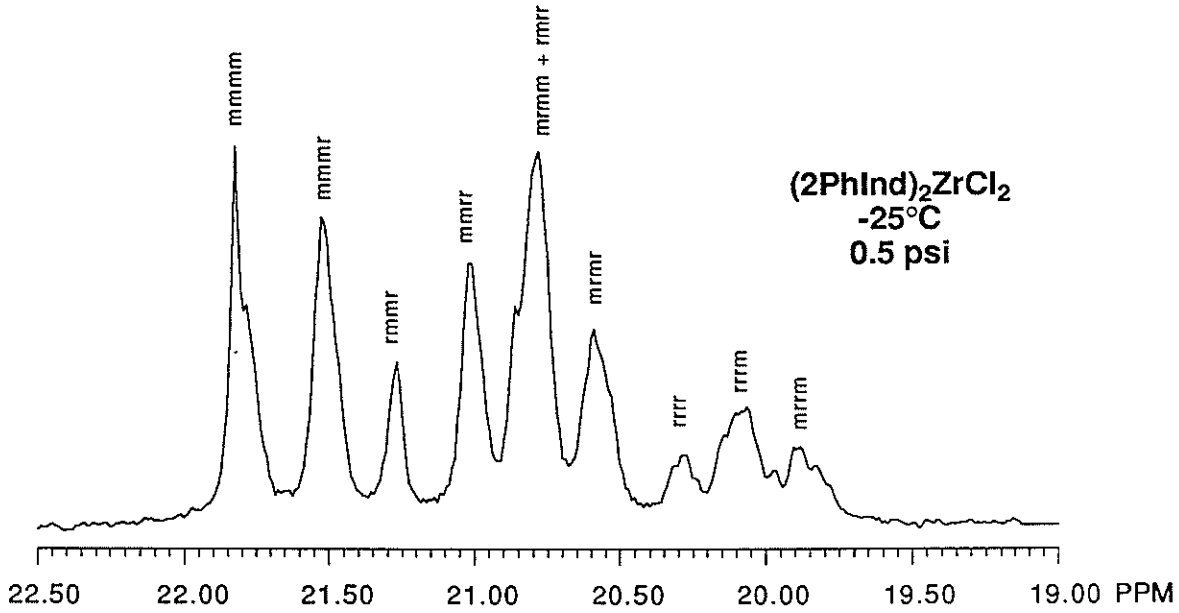

MODEL (CHUJO Polym. J. (1983) 15 859):

Two-Site Model (Mixed Enantiomorphic Site / Bernoullian)

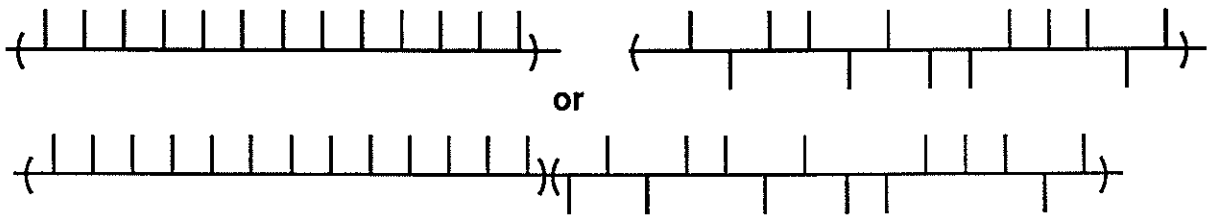

Appropriate for Block polymers if phase boundaries are negligible.

Isotactic Enantiomorphic Site Control, α	Atactic Chain-End Control, $\sigma = P_m$
ω = % Units	1 - ω = % Units

$\omega = 9\%$
$\alpha = 0.92$
$\sigma = 0.56$

Table. Analysis of Pentad Distributions of PP15 Using Statistical Models Based on the Mechanism of Stereochemical Control.

Pentad	*Obsvd*[a]	*Enantiomor. Site*	*Bernoullian*	*1st Order Markov*	*2nd Order Markov*	*Concurrent Model - (Chujo)*	*Consecutive Model - (Cheng)*
mmmm	25.8	23.0	25.0	24.8	25.1	25.6	25.6
mmmr	15.5	16.3	20.7	18.4	17.2	15.2	15.6
rmmr	4.4	3.6	4.3	3.4	3.0	4.7	4.0
mmrr	11.6	16.3	8.6	9.1	11.4	11.0	10.7
mrmm+ rmrr	20.4	14.4	24.3	19.4	19.3	19.9	19.8
mrmr	7.8	7.2	8.6	5.9	7.8	9.3	8.8
rrrr	1.4	3.6	0.7	1.3	0.8	2.3	2.9
mrrr	8.3	7.2	3.5	4.5	4.7	6.5	7.6
mrrm	4.8	8.2	4.3	4.0	7.1	5.5	5.0
WF[b]		12.6	10.4	4.0	2.3	0.61	0.34
Parameters		$\alpha = 0.74$	$P_m = 0.71$	$P_{mm}=0.73$ $P_{rm}=0.64$	$P_{mmm} = 0.74$ $P_{rmm} = 0.60$ $P_{mrm} = 0.51$ $P_{rrm} = 0.75$ $P_{rrm} = 0.75$	$W_E = 0.21$ $P_m = 0.59$ $\alpha = 0.95$	$W_E = 0.33$ $P_m = 0.54$ $\alpha = 0.99$ $B_E = 9.1$ $B_B = 18.7$

[a] Determined by quantitative ^{13}C NMR spectroscopy, with Lorentzian peak fitting. [b] Weighted Fit = $(\Sigma\ I_o(I_o-I_c)^2)/100$, I_o = Observed intensity, I_c = Calculated intensity.

NUMBER OF ISOTACTIC BLOCKS PER CHAIN

THE FORMATION OF A PHYSICALLY CROSSLINKED NETWORK IS CRITICALLY DEPENDENT UPON THE PRESENCE OF TWO OF MORE SEGMENTS PER CHAIN THAT ARE CAPABLE OF COCRYSTALLIZATION WITH OTHER CHAINS.

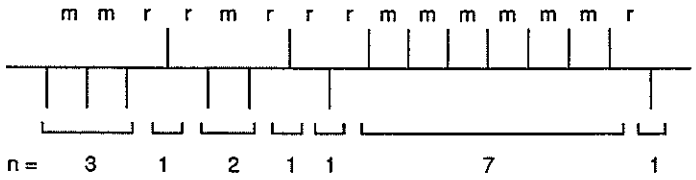

The probability of an isotactic block of length n:

$$P_i(n) = Prm^{(n-1)}r = W_E[(\alpha)^n(1-\alpha)^2 + (\alpha)^2(1-\alpha)^n] + W_B[(P_m)^{n-1}(1-P_m)^2]$$

The number of isotactic blocks of length n per polymer chain:

$$N_i(n) = P_i(n)DP$$

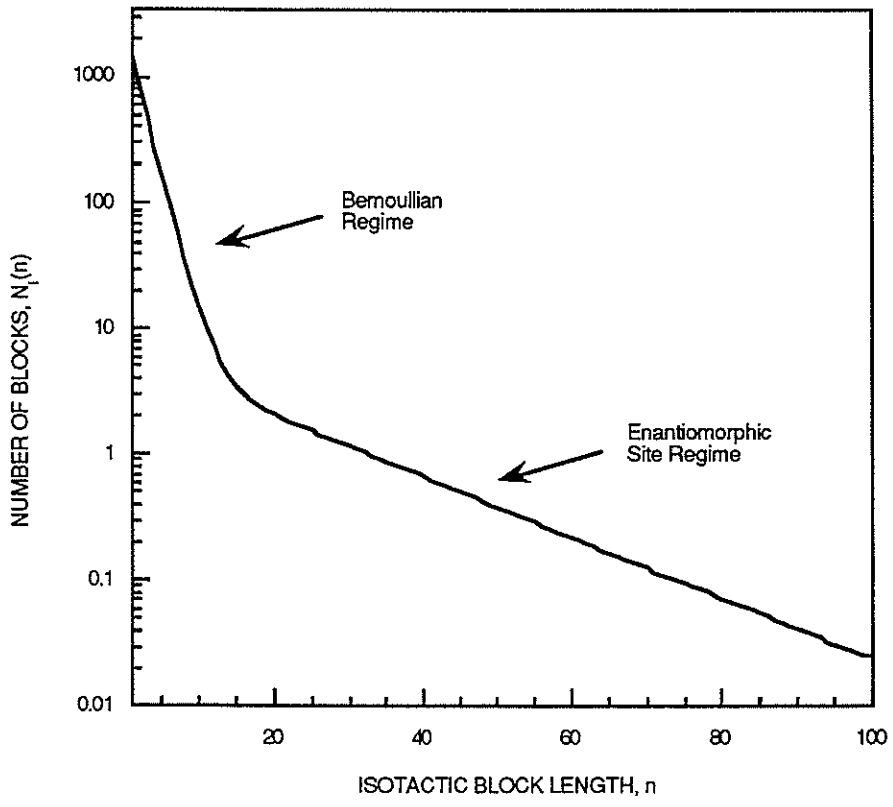

Table 5.14. Number of Isotactic Blocks of Length n per Chain of PP15.[a]

Block Length, n	N_i	*Block Length, n*	N_i
1	1430.9	13	5.4
2	794.2	14	4.3
3	469.2	15	3.5
4	279.4	16	3.0
5	167.2	17	2.7
6	100.6	18	2.4
7	61.1	19	2.3
8	37.7	20	2.1
9	23.7	21	2.0
10	15.4	22	1.8
11	10.3	23	1.7
12	7.3	24	1.6

[a] [mmmm] = 25.8, W_E = 0.21, α = 0.95, P_m = 0.59, DP = 10,060.

X-TAL STRUCTURE CONTAINS 2 ROTAMERS!

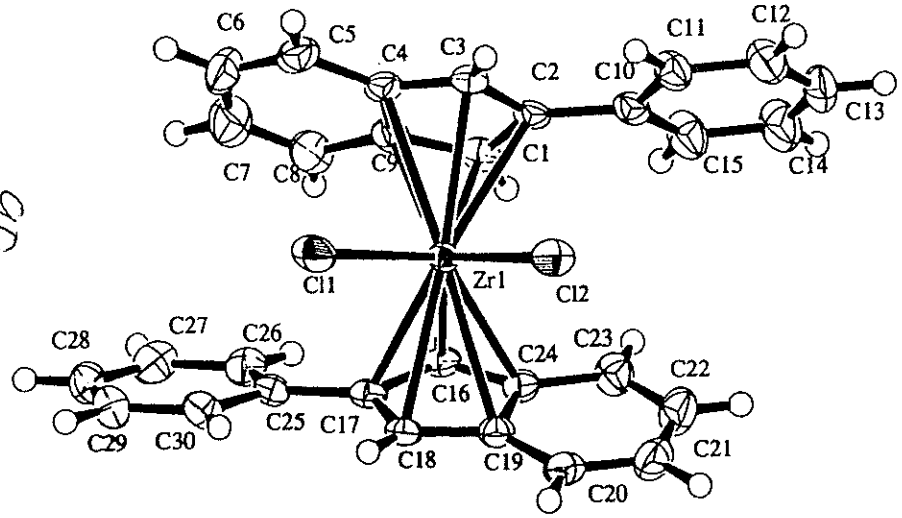

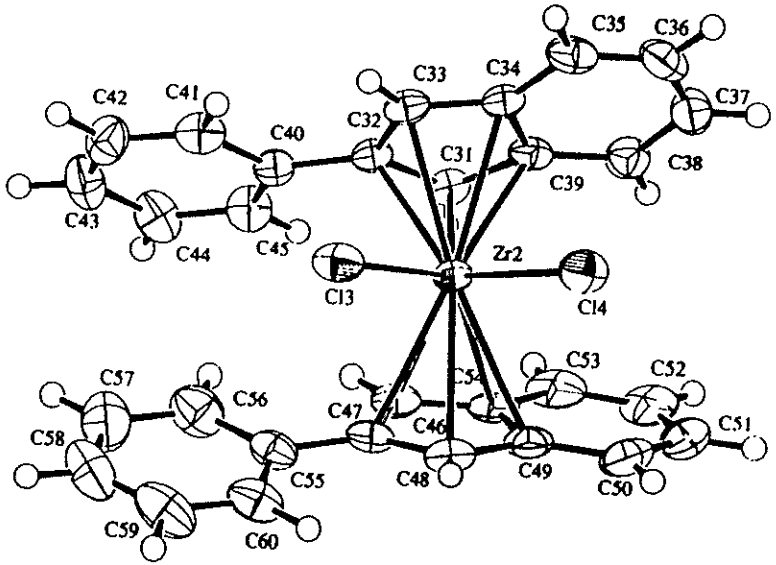

RAC **- LIKE ISOMER**

MESO **- LIKE ISOMER**

TORSIONAL ANGLES OF PHENYL GROUPS ~ 12°

Multistate Mechanism for Ionic Polymerization

Coleman and Fox J. Chem. Phys. 1963 38, 1065

$$\text{isotactic block} \xleftarrow{k_1} E_1 \rightleftharpoons E_2 \xrightarrow{k_2} \text{atactic block}$$

$$E_1^n \xrightarrow{\lambda_a} E_2^n$$

$$E_2^n \xrightarrow{\lambda_b} E_1^n$$

$$E_1^n + M \xrightarrow{k_{1,i}} E_1^{n+1}$$

$$E_1^n + M \xrightarrow{k_{1,s}} E_1^{n+1}$$

$$E_2^n + M \xrightarrow{k_{2,i}} E_2^{n+1}$$

$$E_2^n + M \xrightarrow{k_{2,s}} E_2^{n+1}$$

Model: no monomer concentration dependence on [m] or [r]:

$$p_1\{I\} = \phi_1\alpha_1 + \phi_2\alpha_2 = [m]$$

However, isotactic block lengths depend on monomer concentration:

$$\mu\{I\} = \frac{\phi_1\alpha_1 + \phi_2\alpha_2}{\phi_1\alpha_1(1-\alpha_1) + \phi_2\alpha_2(1-\alpha_2) + \dfrac{\lambda_b\phi_1(\alpha_1 - \alpha_2)}{k_1[(\lambda_a/k_1\phi_1 + [M]]}}$$

EFFECT OF PROPENE PRESSURE ON MICROSTRUCTURE

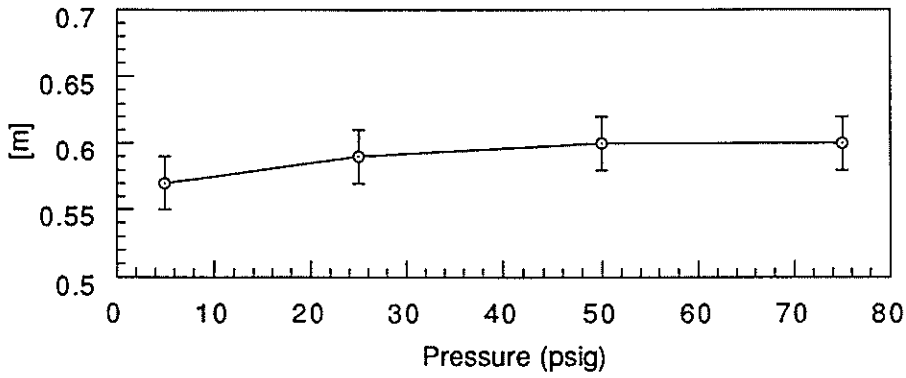

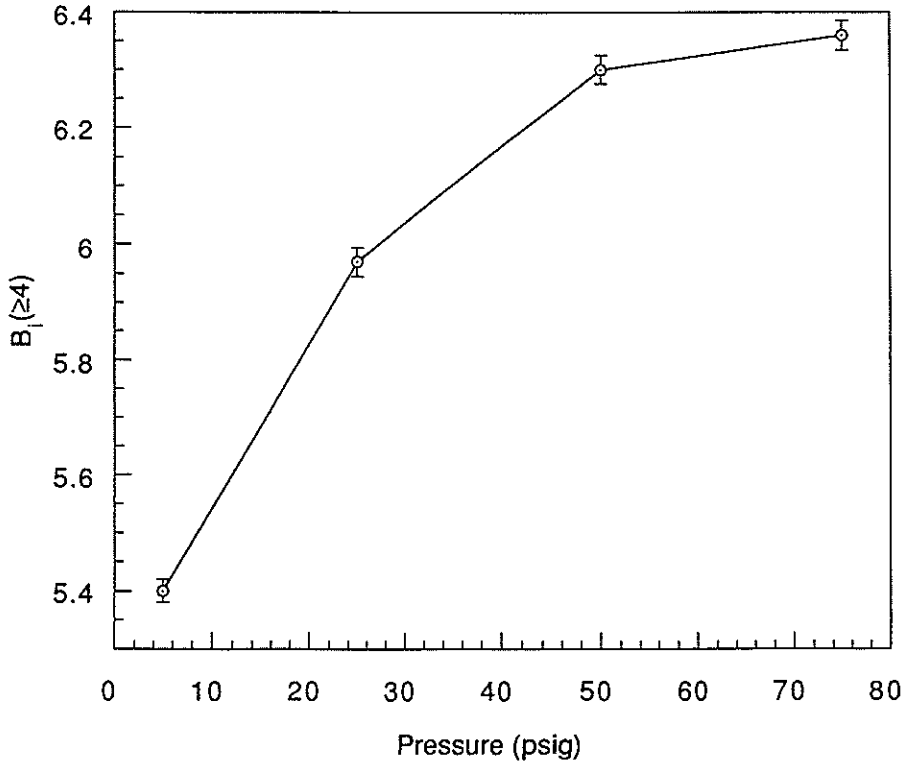

MECHANISM OF STEREOBLOCK FORMATION

Effect of Temperature on Microstructure

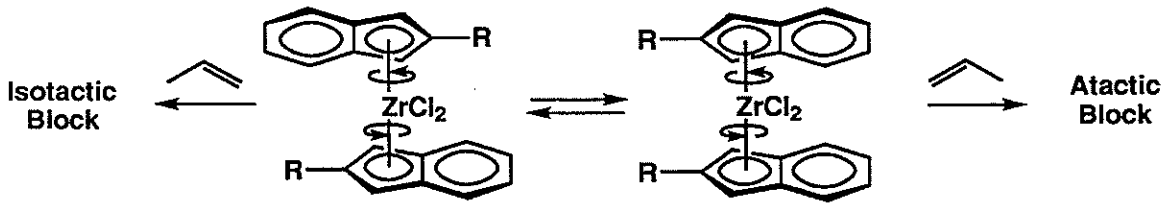

$$\text{Block Size } \alpha \frac{\text{Propagation Rate}}{\text{Ligand Isomerization Rate}}$$

$$\langle B_i \rangle (\geq 4) = 4 + 2[mmmm]/[mmmr]$$

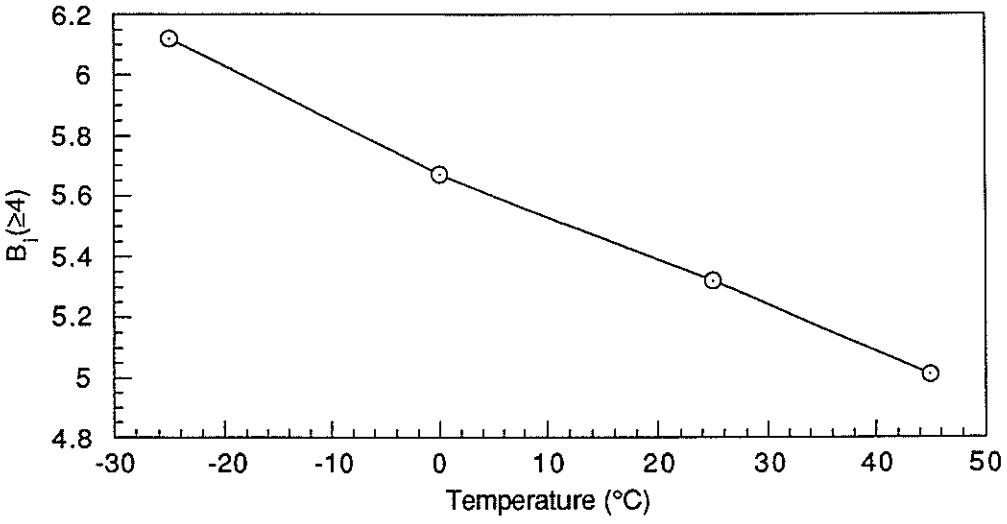

PREPARATION OF (EB2PhI)$ZrCl_2$

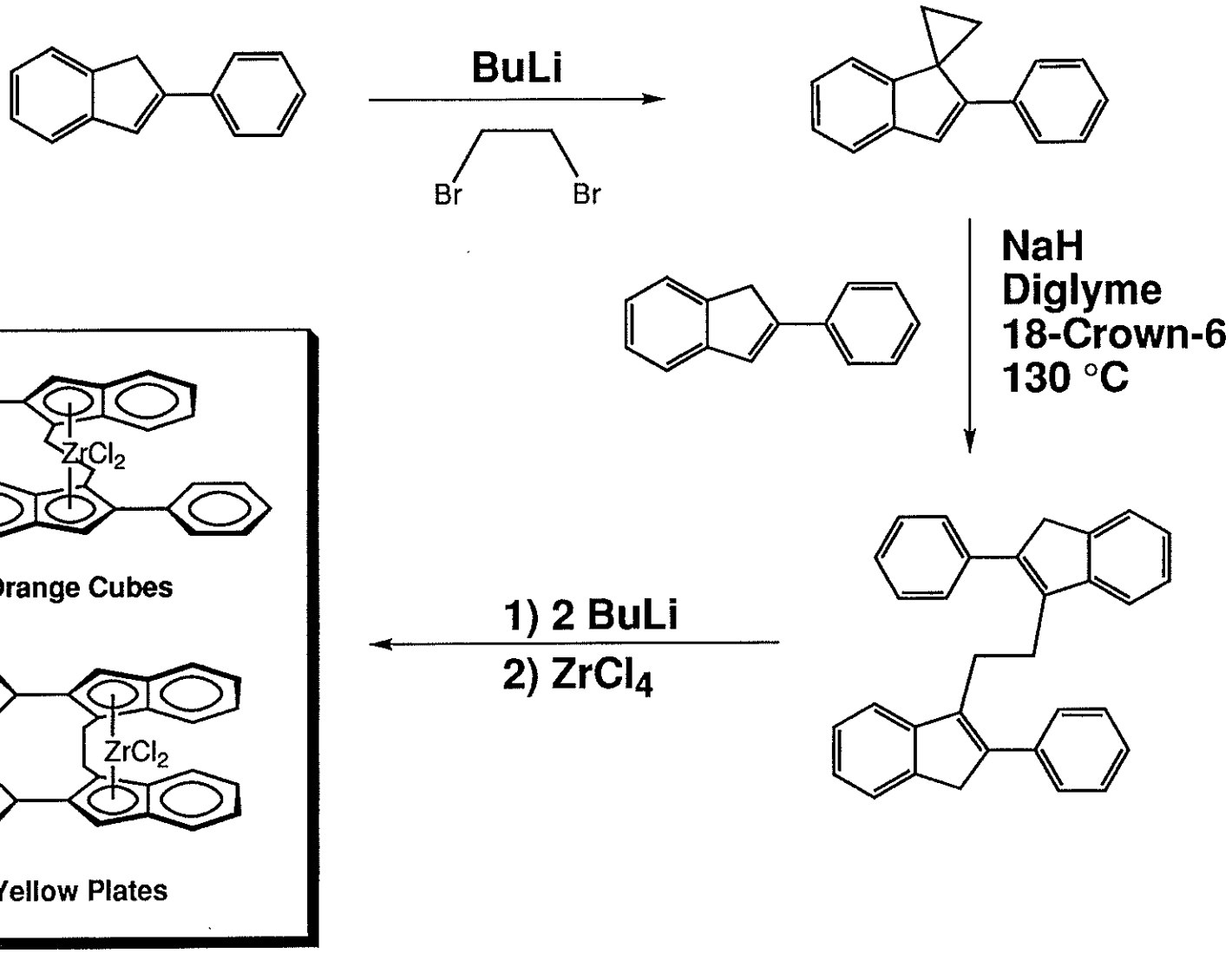

STEREOSPECIFICITY OF ETHYLENE-BRIDGED COMPOUND

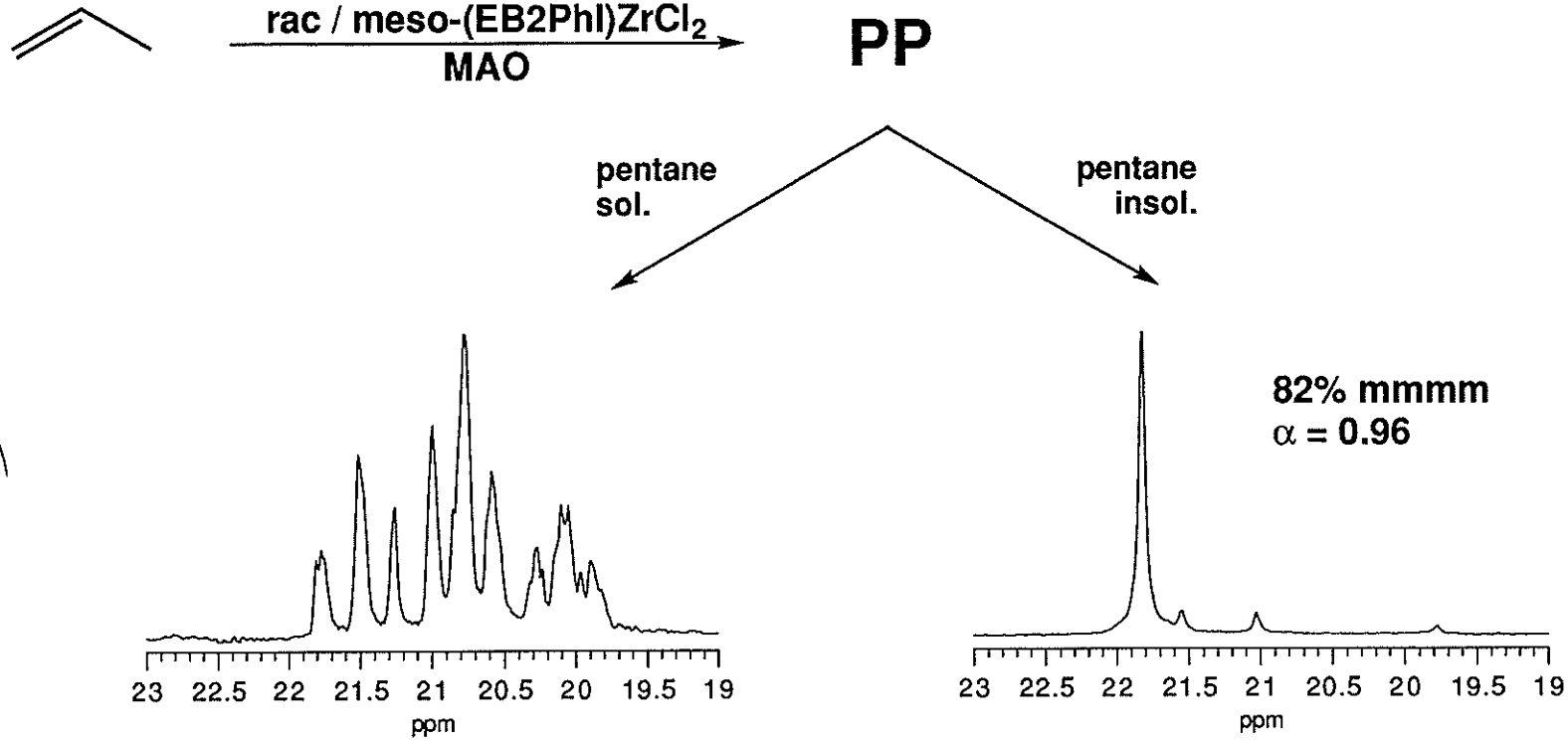

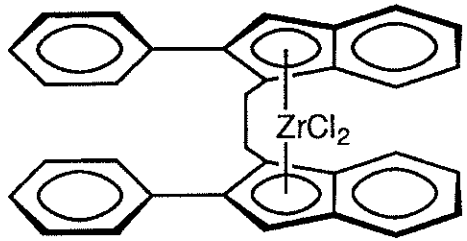

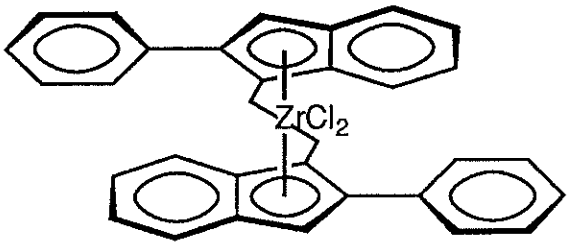

Fractionation of Polypropylenes

$(2\text{-PhInd})_2ZrCl_2$ 1 atm, -25°C

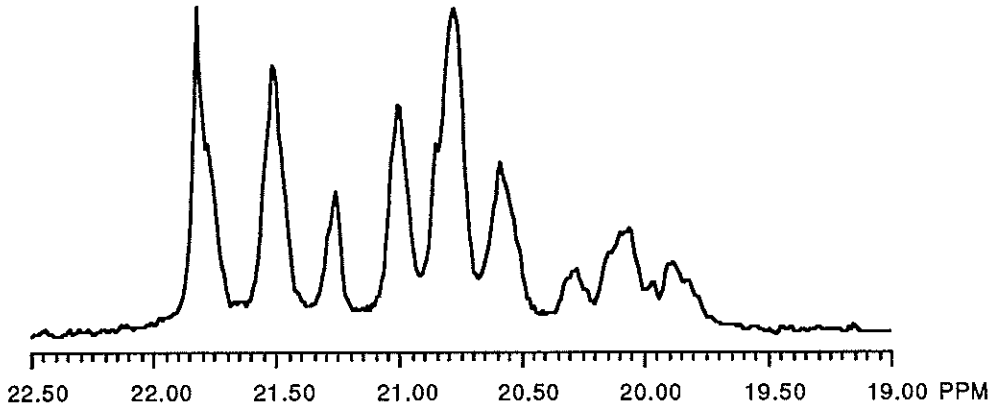

96

RAW POLYMER

[mmmm] = 16.1

M_w = 457,000; M_w/M_n = 2.2

Et_2O soluble (80%)

Et_2O insoluble (20%)

[mmmm] = 13.5

M_w = 451,000
M_w/M_n = 2.1

[mmmm] = 28.0

M_w = 484,000
M_w/M_n = 2.0

FRACTIONATION OF POLYPROPYLENES

WHY ARE THESE MATERIALS FRACTIONABLE ?

I. MULTIPLE SITES

- fractionable by solvent extraction
- broad molecular weight distribution
- different fractions should have different M_w

II. DISTRIBUTION OF BLOCK LENGTHS; SINGLE SITES

- fractionable by solvent extraction
- narrow molecular weight distribution
- different fractions should have similar M_w
- Press. dependence on block lengths, extractable fractions
- % of insoluble material should depend on minimum isotactic sequence length that can crystallize

BLOCK POLYMER SYNTHESIS

1. LIVING POLYMERIZATION CATALYSTS

◦ **Styrene-Butadiene-Styrene (Kraton^{TM})**

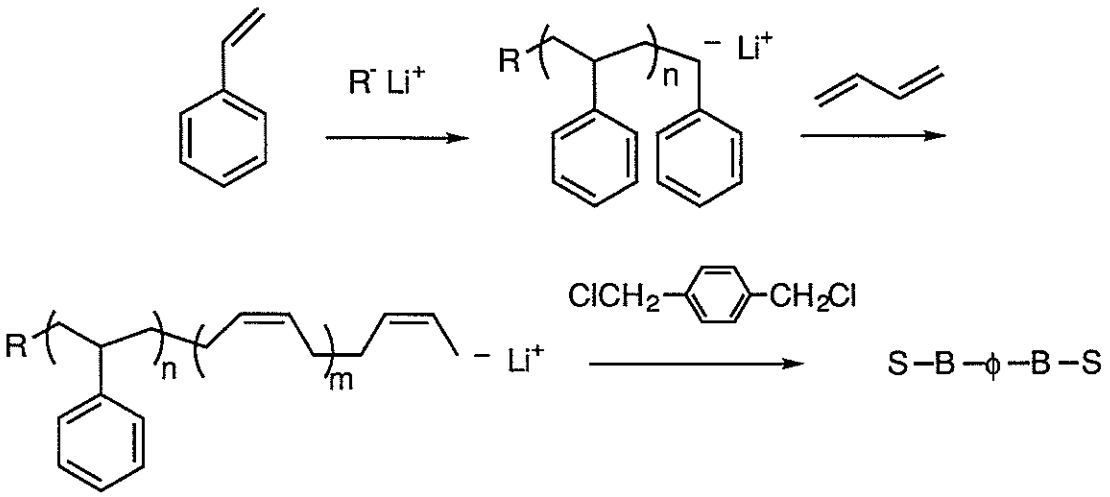

2. STEP-GROWTH POLYMERIZATION

◦ **Polyester-Polyurethanes (Lycra^{TM})**

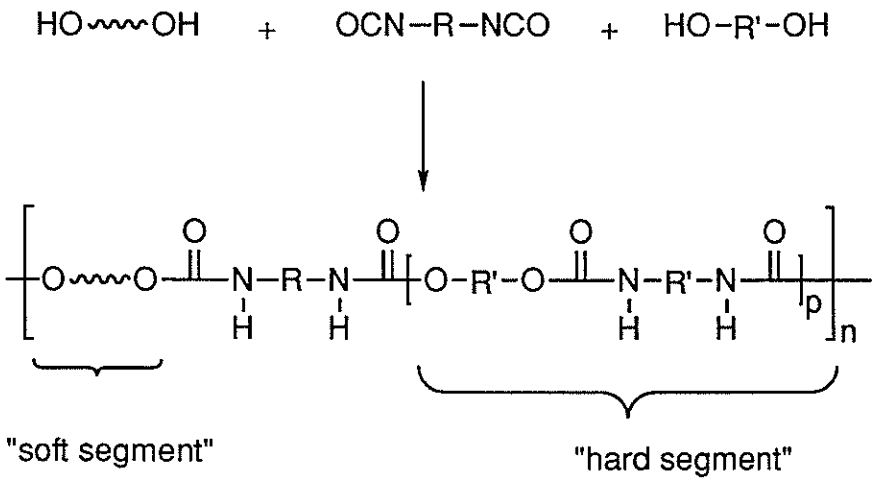

Modified 2-Phenyl Indene Catalyst Precursors

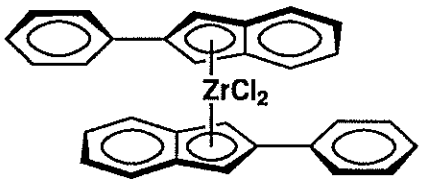

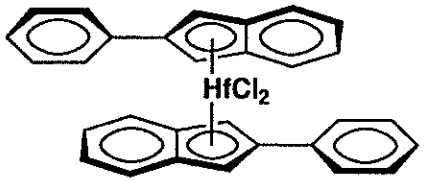

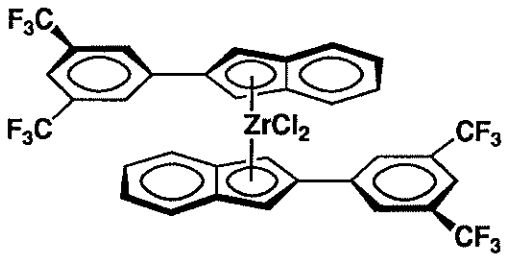

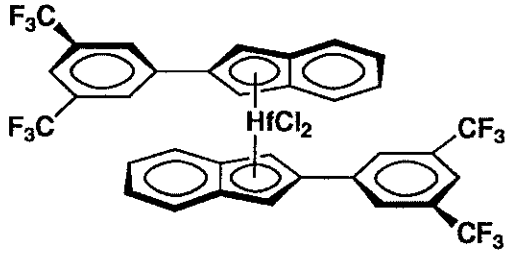

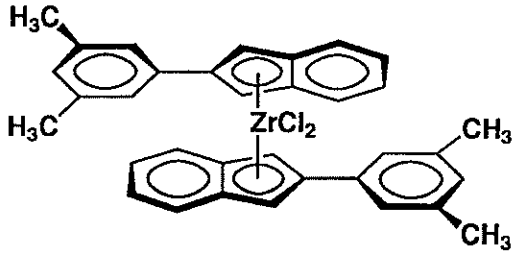

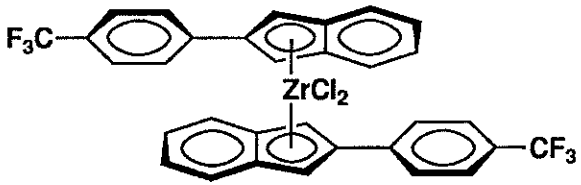

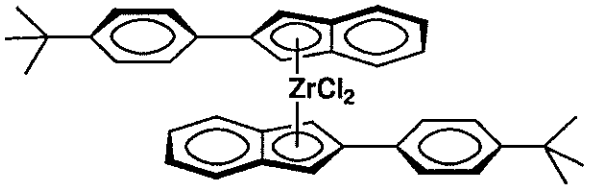

Pressure Dependence at 25°C

$(2\text{-}(3,5\text{-}(CF_3)_2C_6H_3)Ind)_2ZrCl_2$ vs $(2\text{-}PhInd)_2ZrCl_2$

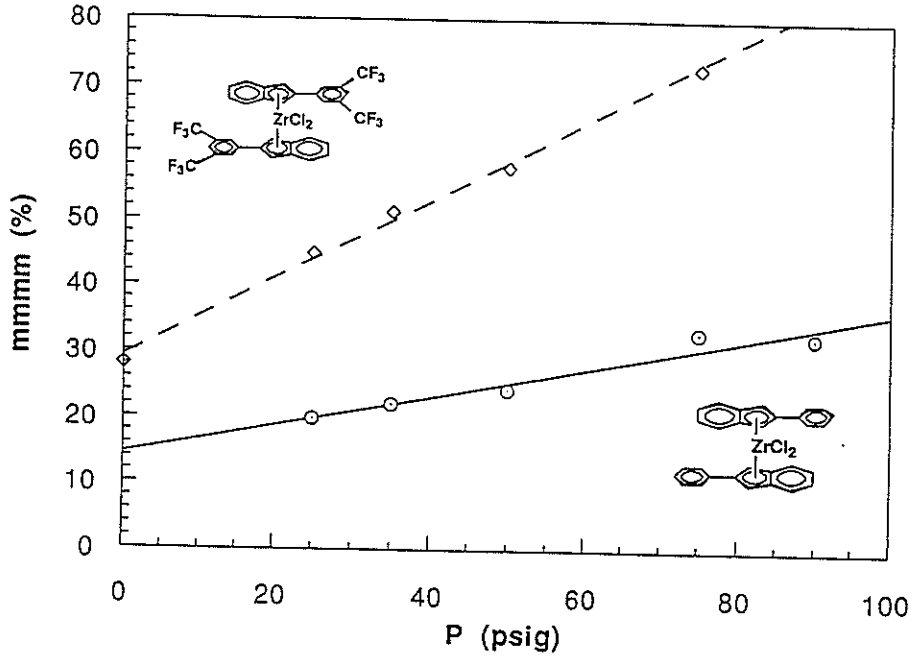

Pressure Dependence at 25°C

$(2\text{-}(3,5\text{-}(CH_3)_2C_6H_3)Ind)_2ZrCl_2$ vs $(2\text{-}PhInd)_2ZrCl_2$

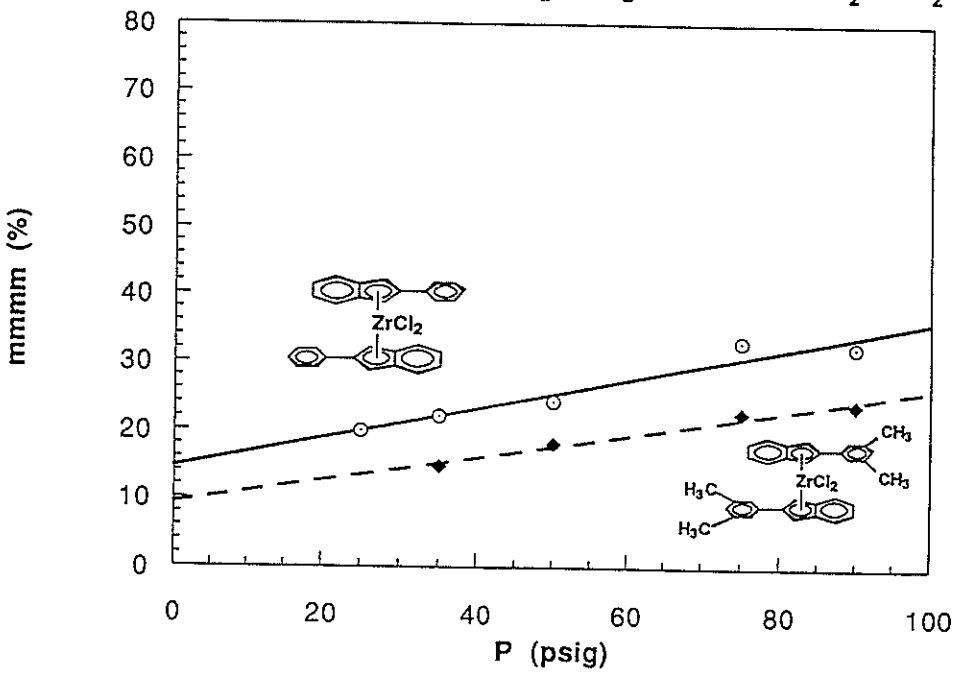

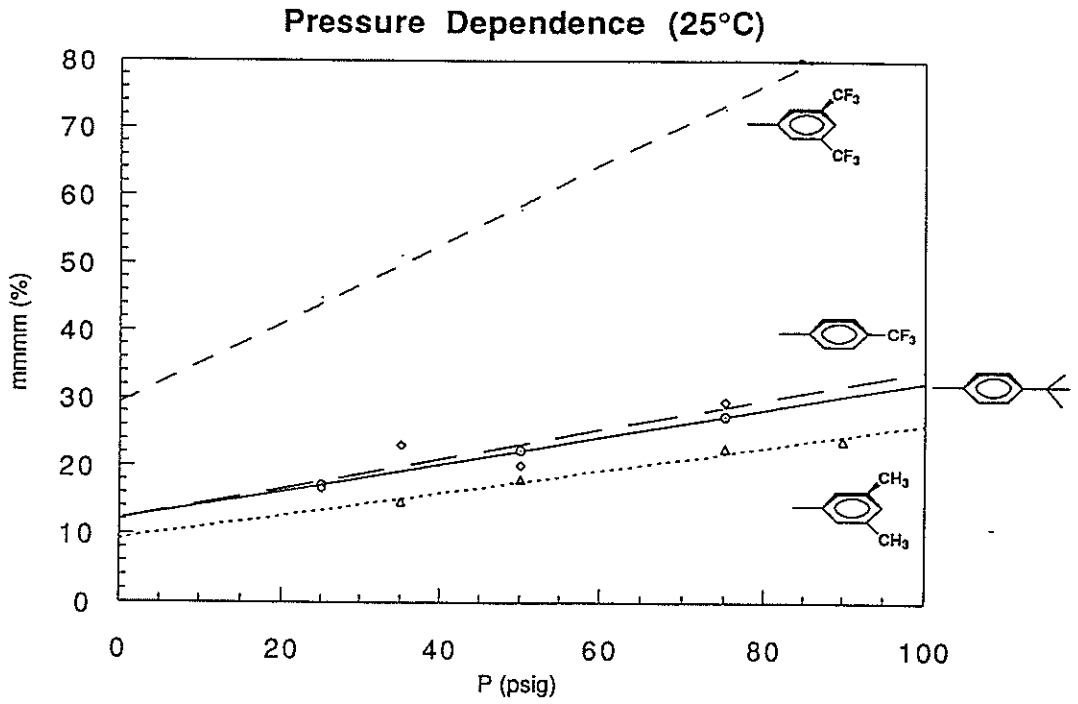

COMPARISON OF PHYSICAL PROPERTIES:

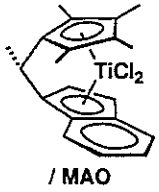

/ MAO

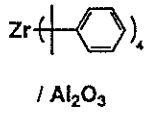

/ Al_2O_3

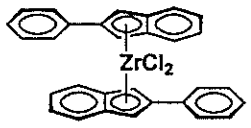

/ MAO

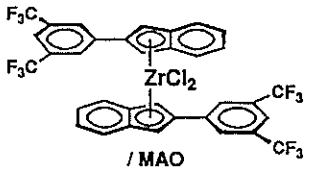

/ MAO

PHYSICAL PROPERTY	CHIEN	DUPONT	WAYMOUTH	WAYMOUTH
TENSILE STRENGTH (psi)	1750	891	462 / 467	5040
ELONGATION (%)	1300	875	1210 / 2550	100
MODULUS (psi)	nd	nd	246 / 201	12,390
TENSILE SET (%)	24	93	44 / 32	197

Polypropylene Microstructures

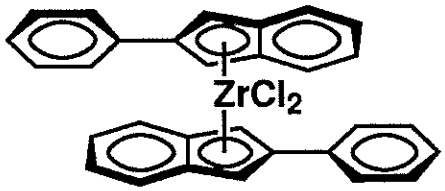

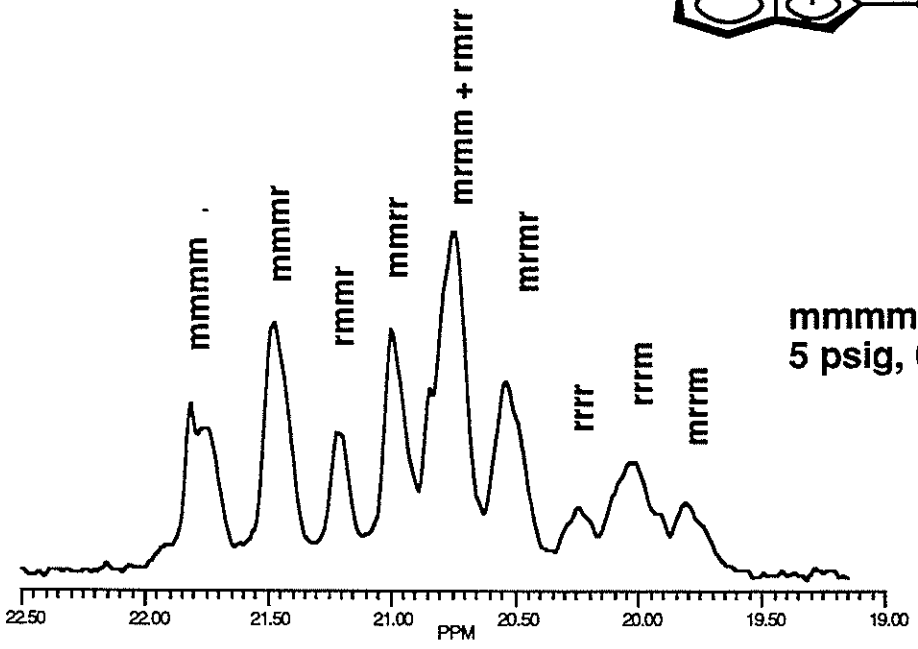

mmmm = 11%
5 psig, 0°C

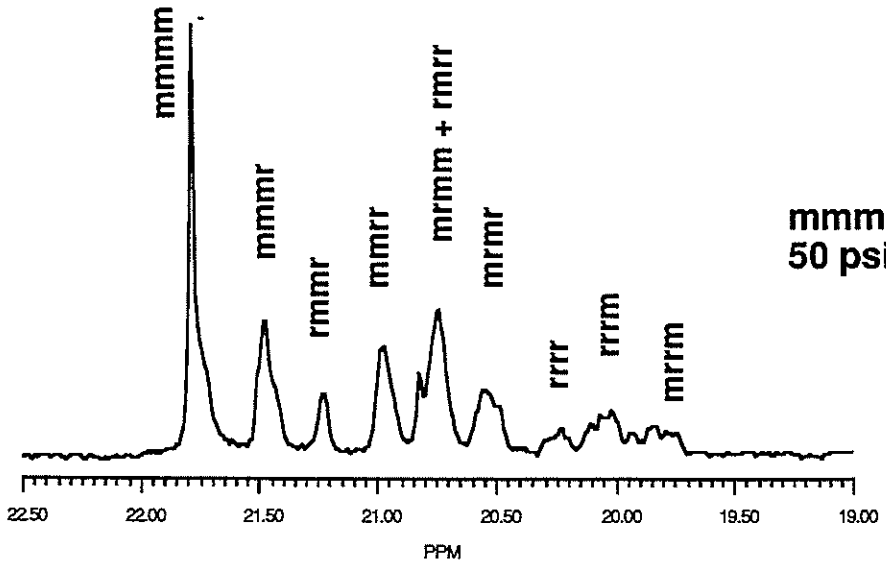

mmmm = 28.1
50 psig, -25°C

Polypropylene Microstructures

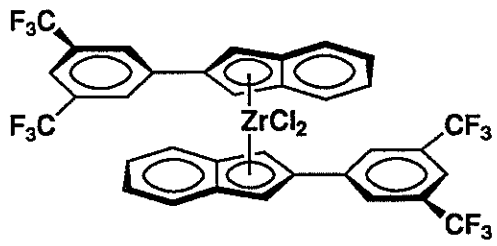

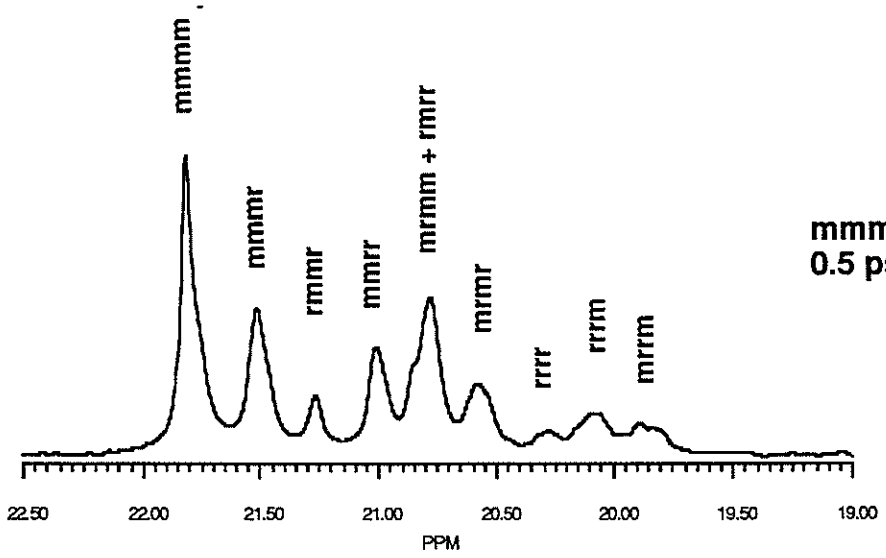

mmmm = 28%
0.5 psig, 25°C

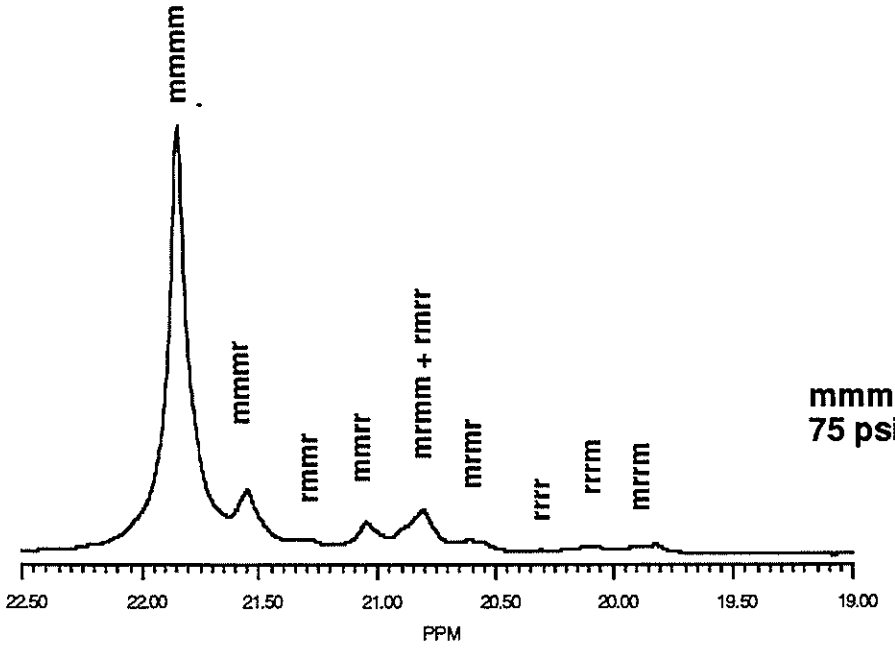

mmmm = 68%
75 psig, 25°C

New Pd(II)- and Ni(II)-Based Catalysts for Polymerization of Ethylene and α-Olefins

Lynda K. Johnson, Christopher M. Killian and Maurice Brookhart

Department of Chemistry
University of North Carolina at Chapel Hill
Chapel Hill, NC 27599-3290

Olefin Polymerizations Using Early Metal Catalysts

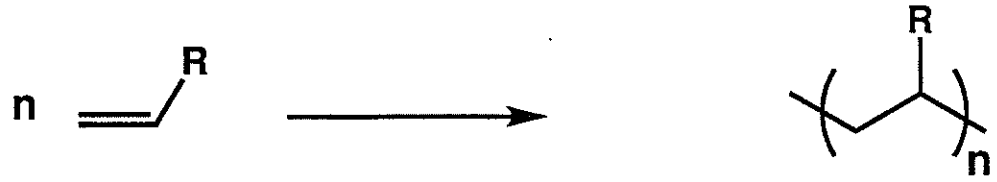

Ziegler-Natta Systems

1. $TiCl_3$ / $AlEt_2Cl$ ($AlEt_3$)

2. $TiCl_3$ / $AlEt_2Cl$ / Lewis Base

3. $TiCl_4$ / $MgCl_2$ / Lewis Base / $AlEt_2Cl$

Supported Catalysts

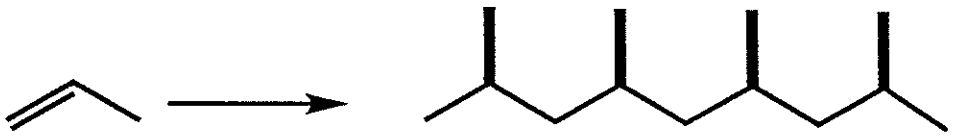

highly isotactic

"Single-Site" Homogeneous Metallocene-Based Catalysts

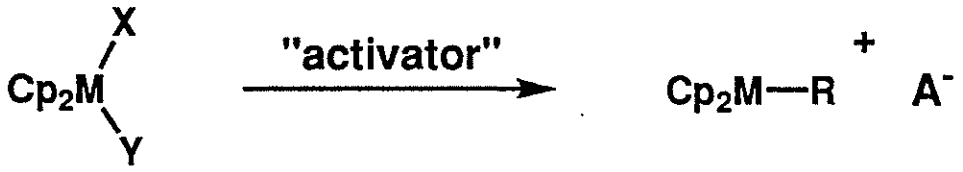

X,Y = halide, alkyl

M = early metal or lanthanide
d^0 or d^0f^n

A^- = noncoordinating counterion

Examples of Activators

- Methylaluminoxane (Sinn, Kaminsky)

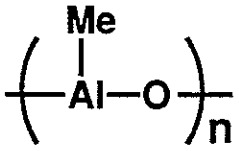

MAO •10^3 fold excess used

- Lewis or Bronsted Acids based on fluorinated aryl borates (Turner, Jordan, Marks, ...)

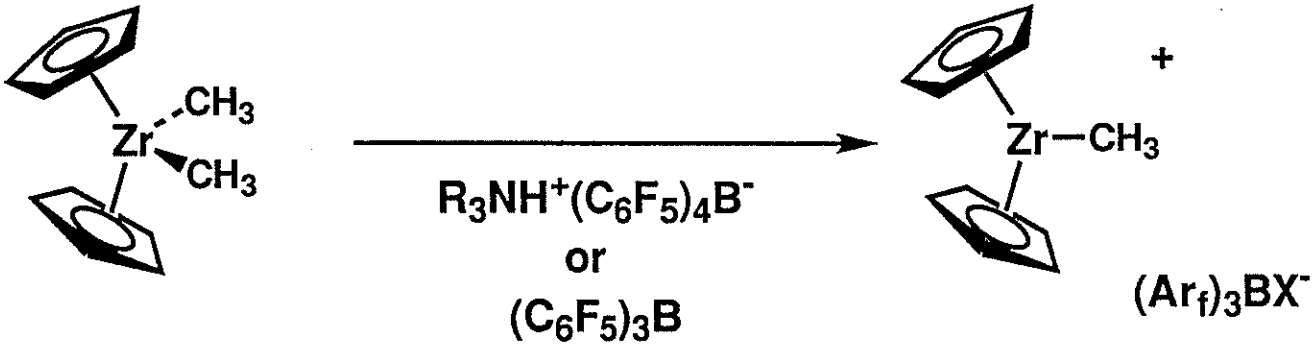

"Single-Site" Catalysts

- Modification of ligand structures allows control of:

  - activity
  - molecular weight, molecular weight distribution
  - microstructure / regiochemistry
  - comonomer incorporation

Polypropylene

Brintzinger, Ewen

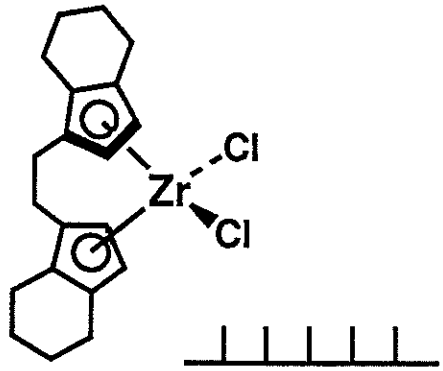

Isotactic

Bercaw

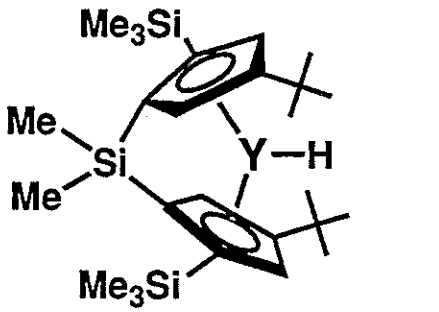

Isotactic

Ewen

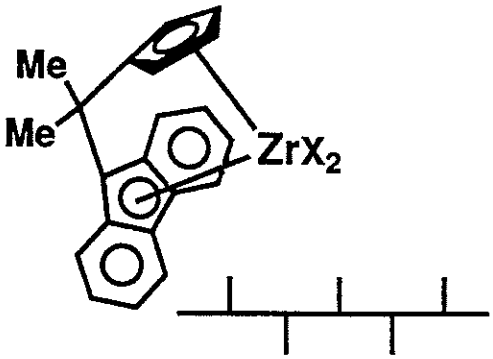

Syndiotactic

Waymouth

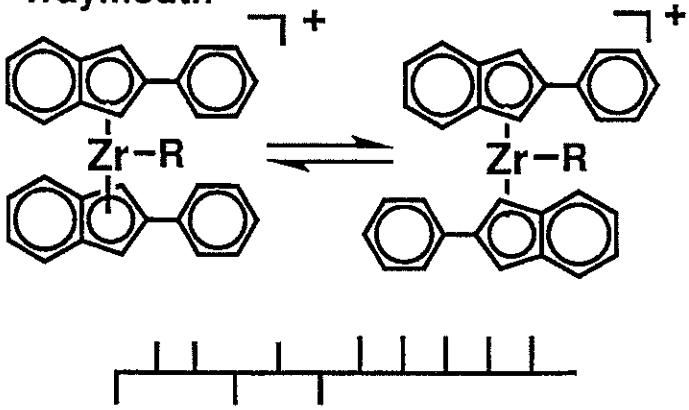

Stereoblock (thermoplastic elastomer)

Polyethylene

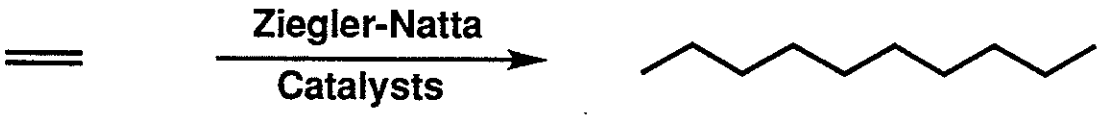

linear, semicrystalline

T_m = 133-138 °C

High Density
Polyethylene (HDPE)

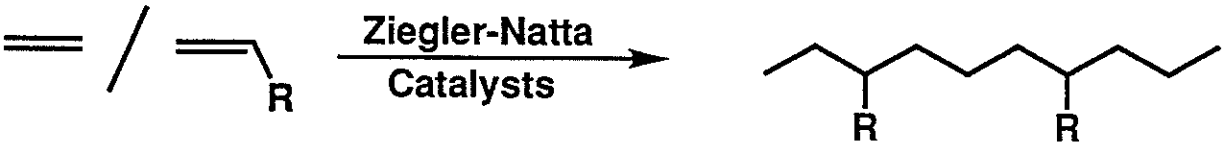

1- 10% comonomer incorporation

T_m = 115-130 °C

Linear Low Density
Polyethylene (LLDPE)

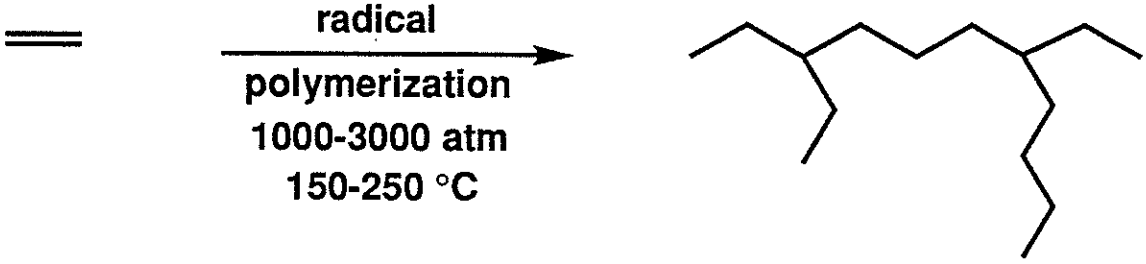

T_m = 105-115 °C

Low Density
Polyethylene (LDPE)

Late Metal Catalysts

Advantages

- Less oxophilic, more functional group tolerant

Disadvantages

- Reduced activities
- β-Elimination competitive with insertion

Brookhart

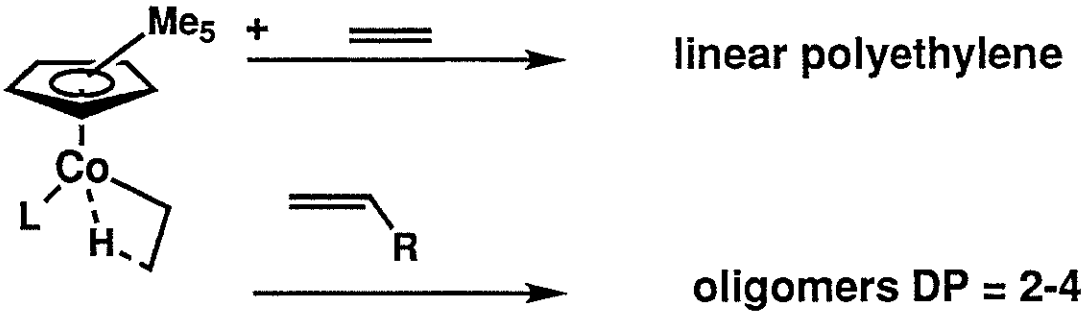

Wilke

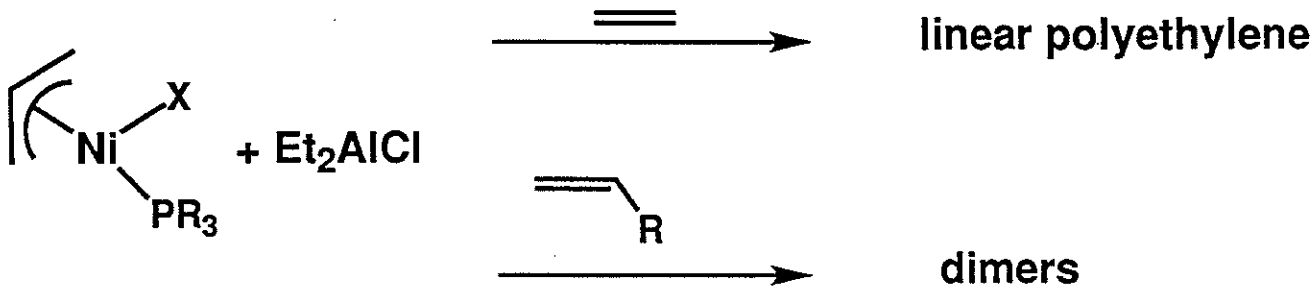

R = t-butyl

Nickel-Catalyzed Oligomerization and Polymerization of Olefins

Shell Higher Olefin Process (SHOP)

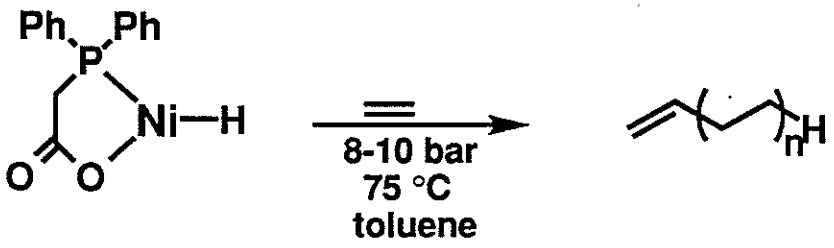

n = 1 - 20

Peuckert, M.; Keim, W. *Organometallics* **1983**, *2*, 594.

Dupont

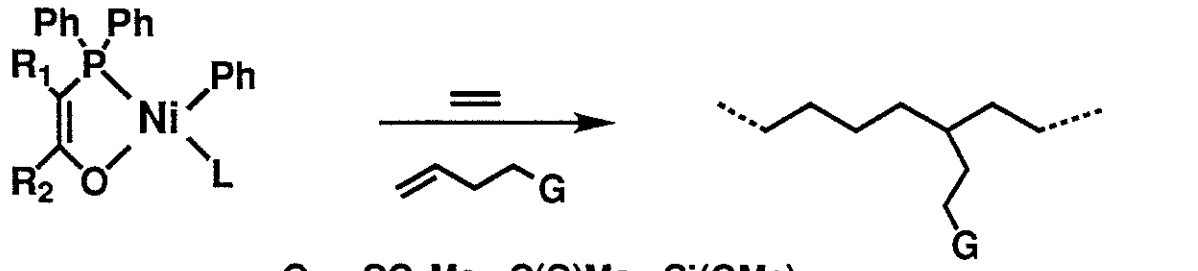

G = -CO_2Me, -C(O)Me, -Si(OMe)$_3$

- low % incorporation of functionalized comonomer

Klabunde, U.; Ittel, S.D. *J. Mol. Cat.* **1987**,*41*, 123.

Möhring and Fink

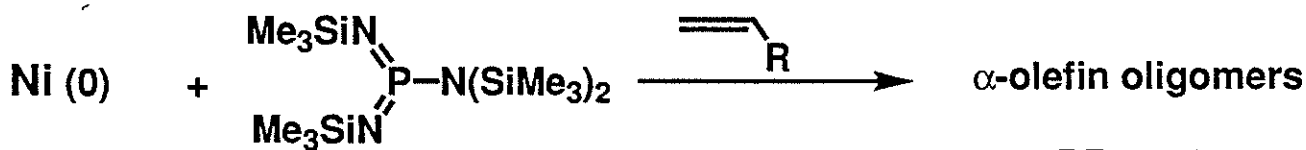

R = Et, Bu, Hex

DP = 8-24

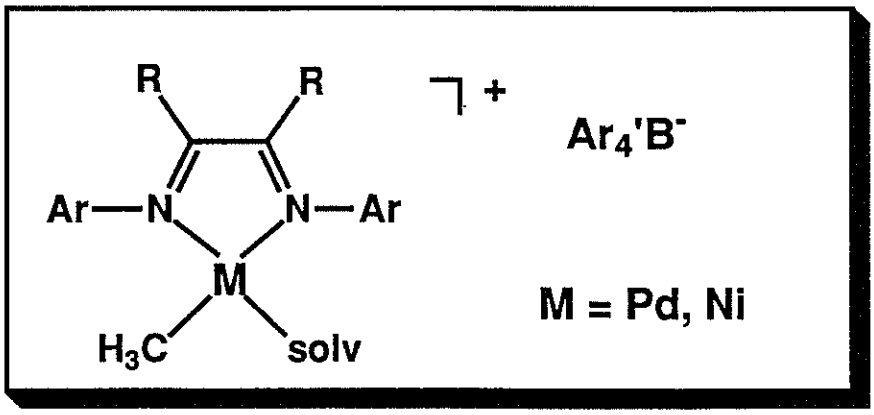

New Class Of Late Metal Catalysts For:

- Polymerization of ethylene to polyethylene
  - unique and variable microstructures
  - activities approach Ziegler-Natta activities

- Polymerization of α-olefins to high molar mass polymers

- Polymerization of 1,2-disubstituted olefins and cyclic olefins

- Copolymerizations of ethylene and methyl acrylate

Well-Defined Initiators

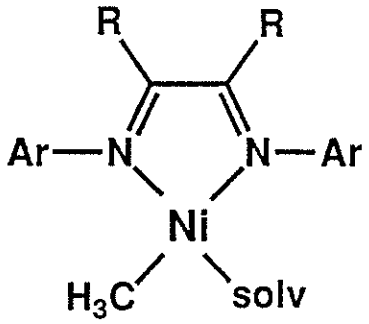

$\neg$ + $Ar_4'B^-$

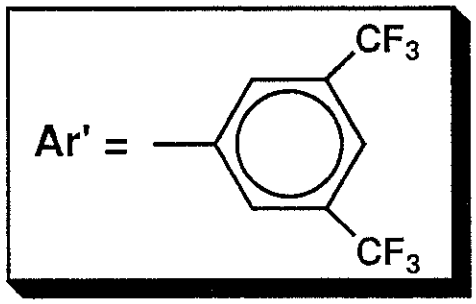

Examples of Diimine Ligands Employed

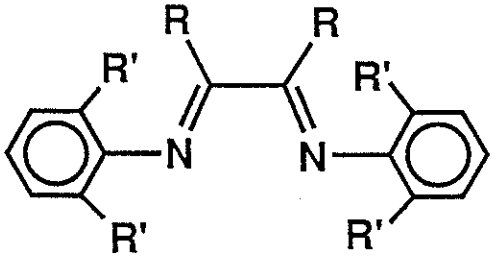

Backbones (R) =

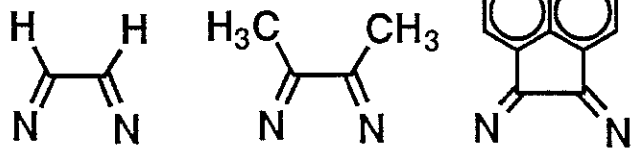

Ortho substituents (R') = $-CH_3$, $-CH(CH_3)_2$

Synthesis of Pd (II)- Based Initiators

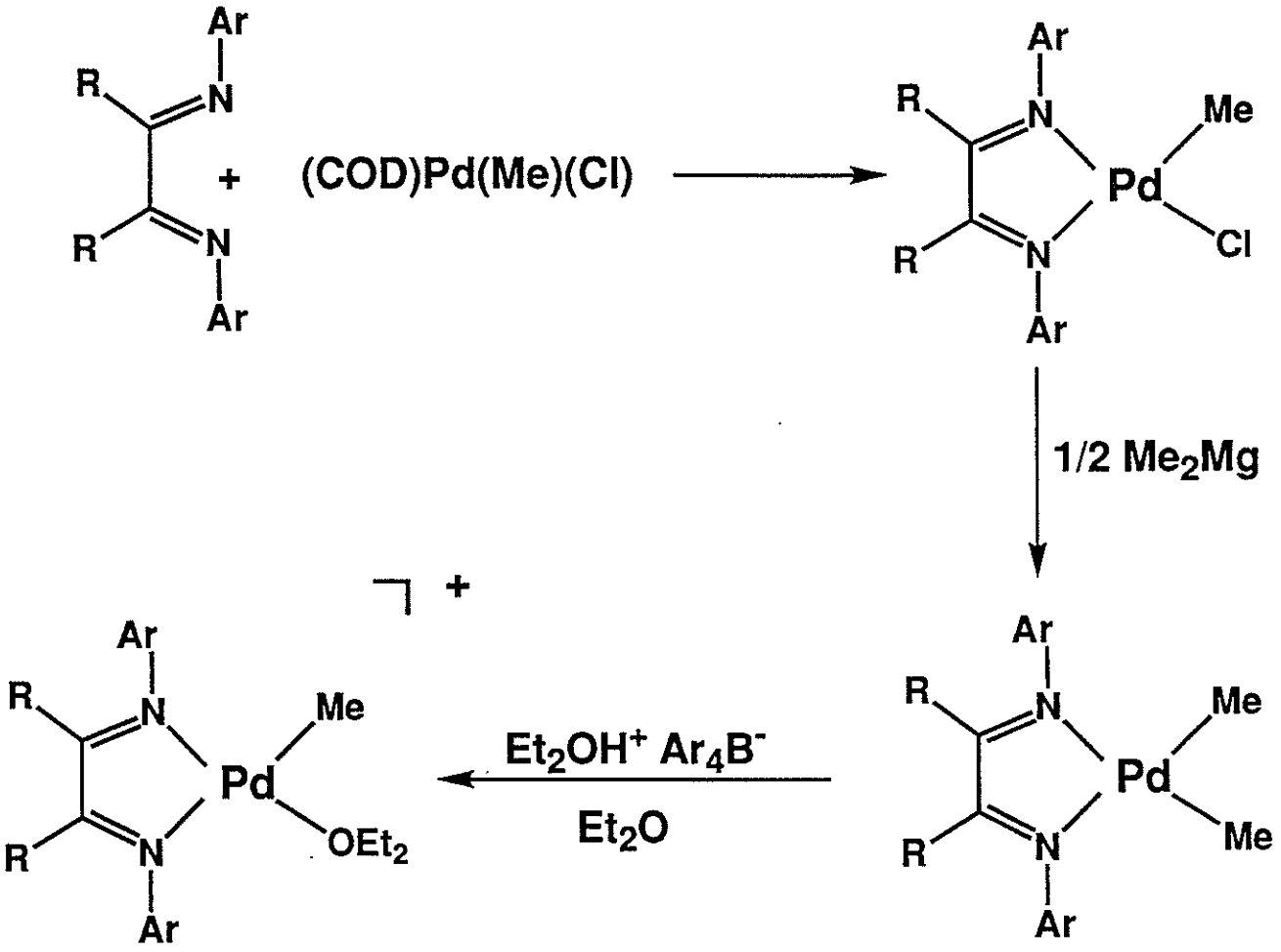

Synthesis of Pd (II)-Based Initiators

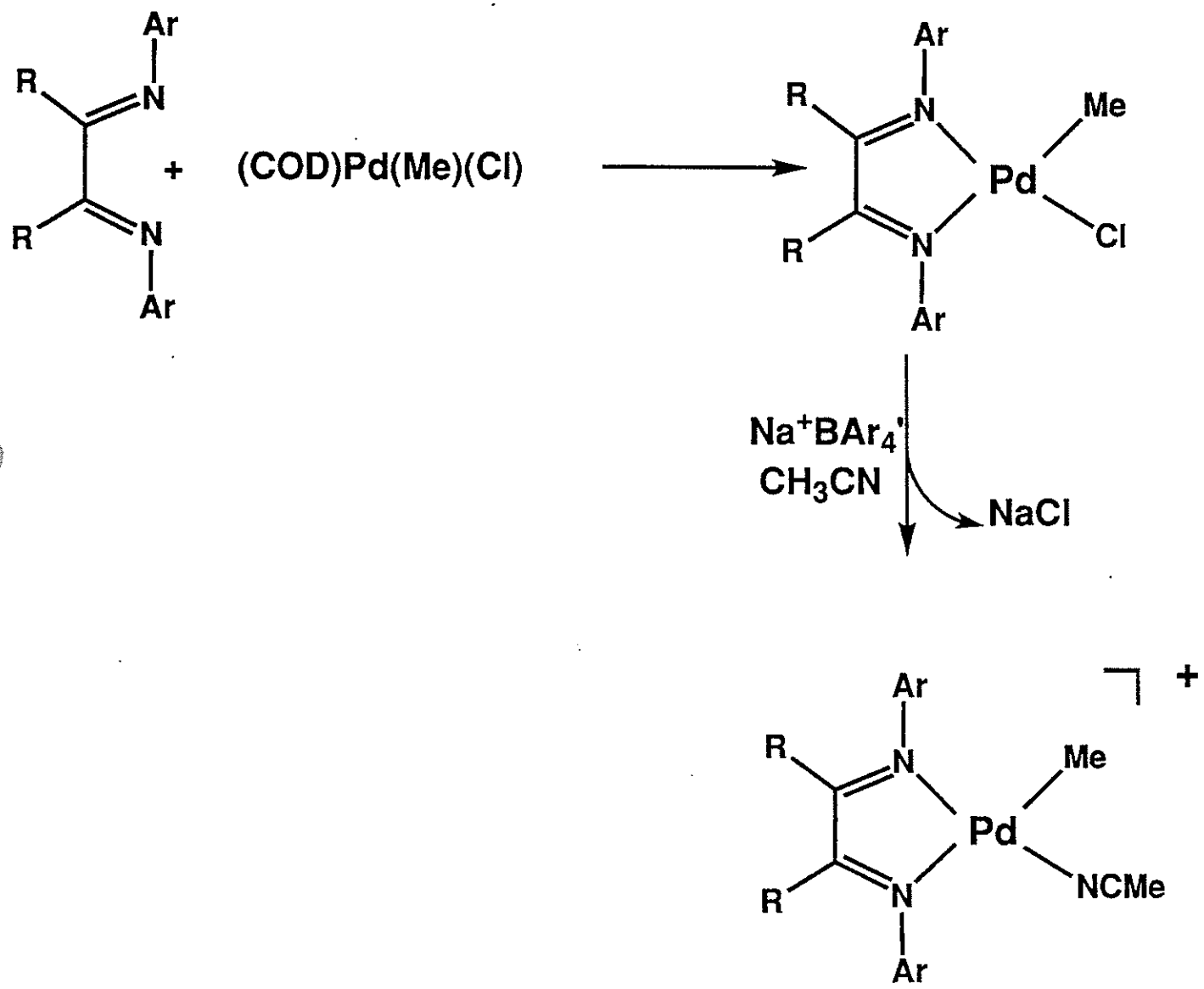

Stability of Initiators

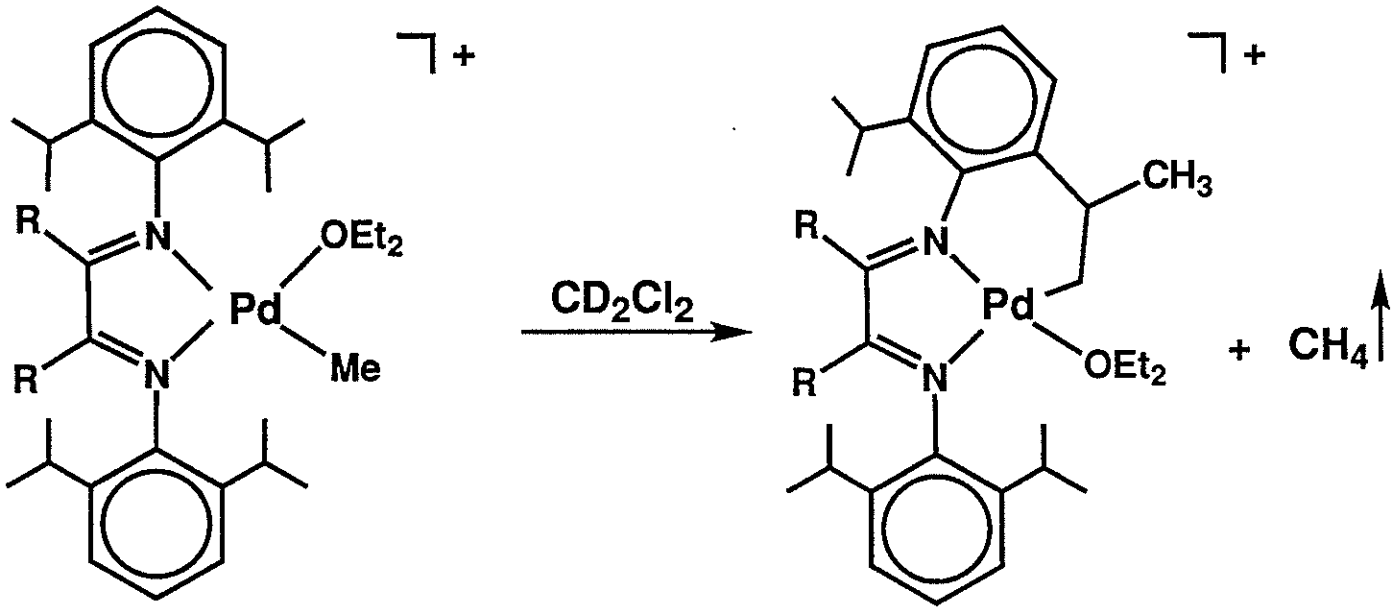

(more stable)	R = CH_3	25 °C	$t_{1/2}$ ca. 30 min
	R = H	25 °C	$t_{1/2}$ < 5 min

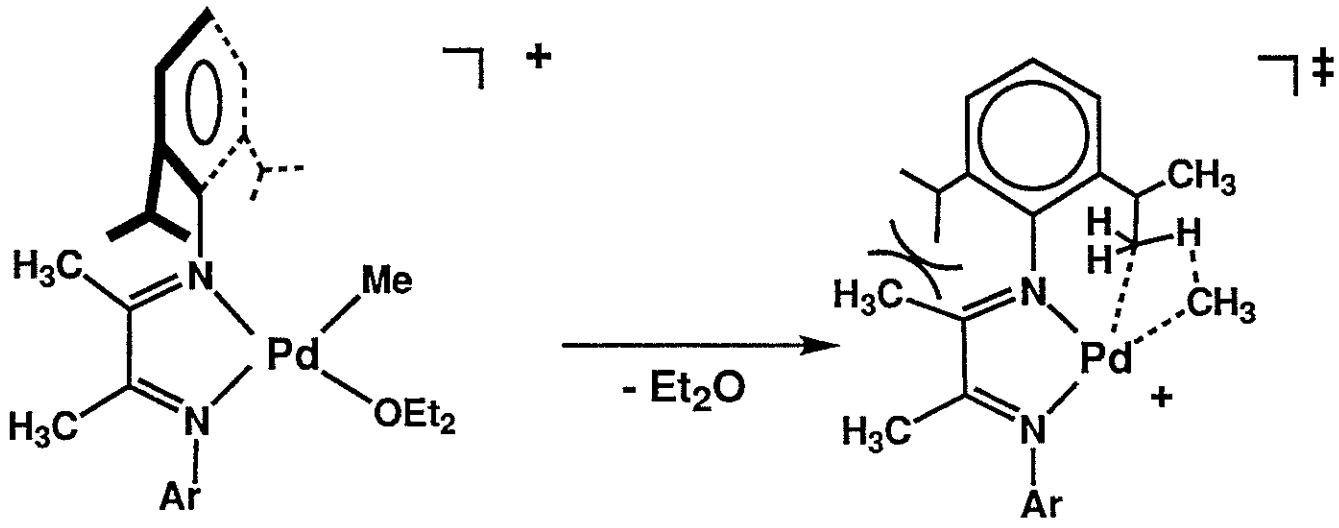

σ-bond metathesis?

Ethylene Polymerization

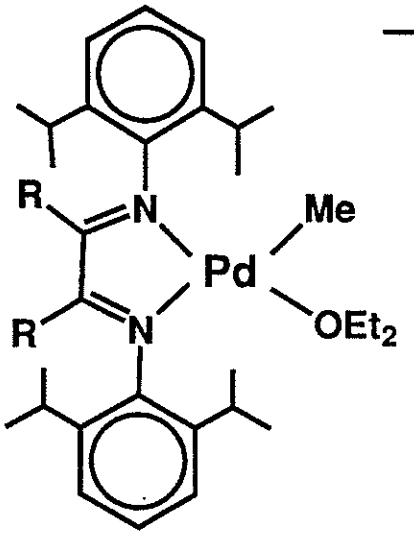

CH_2Cl_2

1 atm C_2H_4
25 °C

polyethylene

		time	total TO	$\bar{M}_w$	$\bar{M}_n$	$\bar{M}_w/\bar{M}_n$
1)	R = H	24 h	3500	18,000	6,000	3.0
2)	R = CH_3	17 h	16,000	112,000	29,000	3.9
3)	R = CH_3 (28 atm)	29 h	55,000	407,000	177,000	2.3

Polymer Microstructure

- Amorphous, Highly Branched Polymer (^{13}C, ^{1}H NMR)

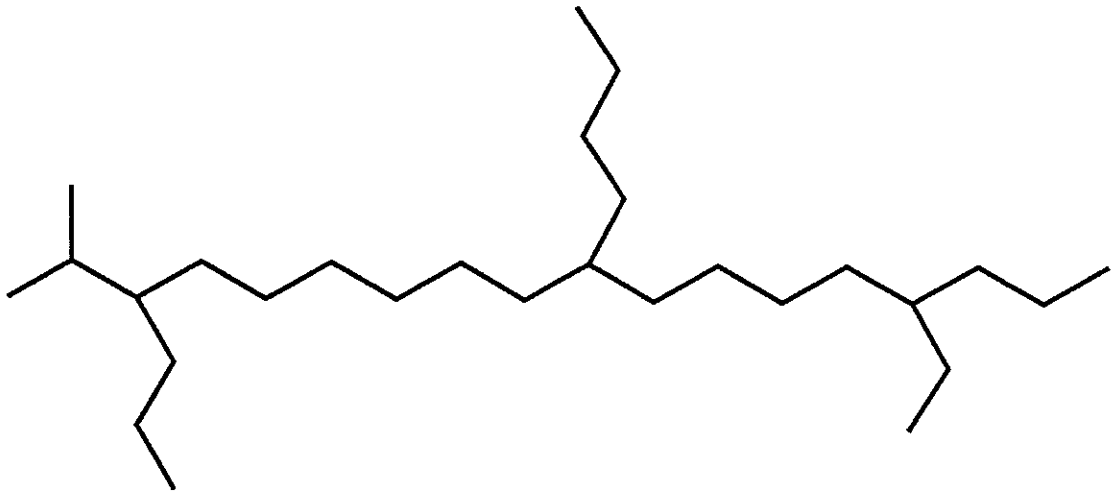

^{1}H: $-\overset{|}{\underset{|}{C}}H$, $-CH_2-$ vs $-CH_3$ yields branches / 1000 carbons

1) 116 branches / 1000 C T_g = -85 °C

2) 103 branches / 1000 C T_g = -68 °C

3) 97 branches / 1000C T_g = -66 °C

^{1}H, ^{13}C NMR Studies

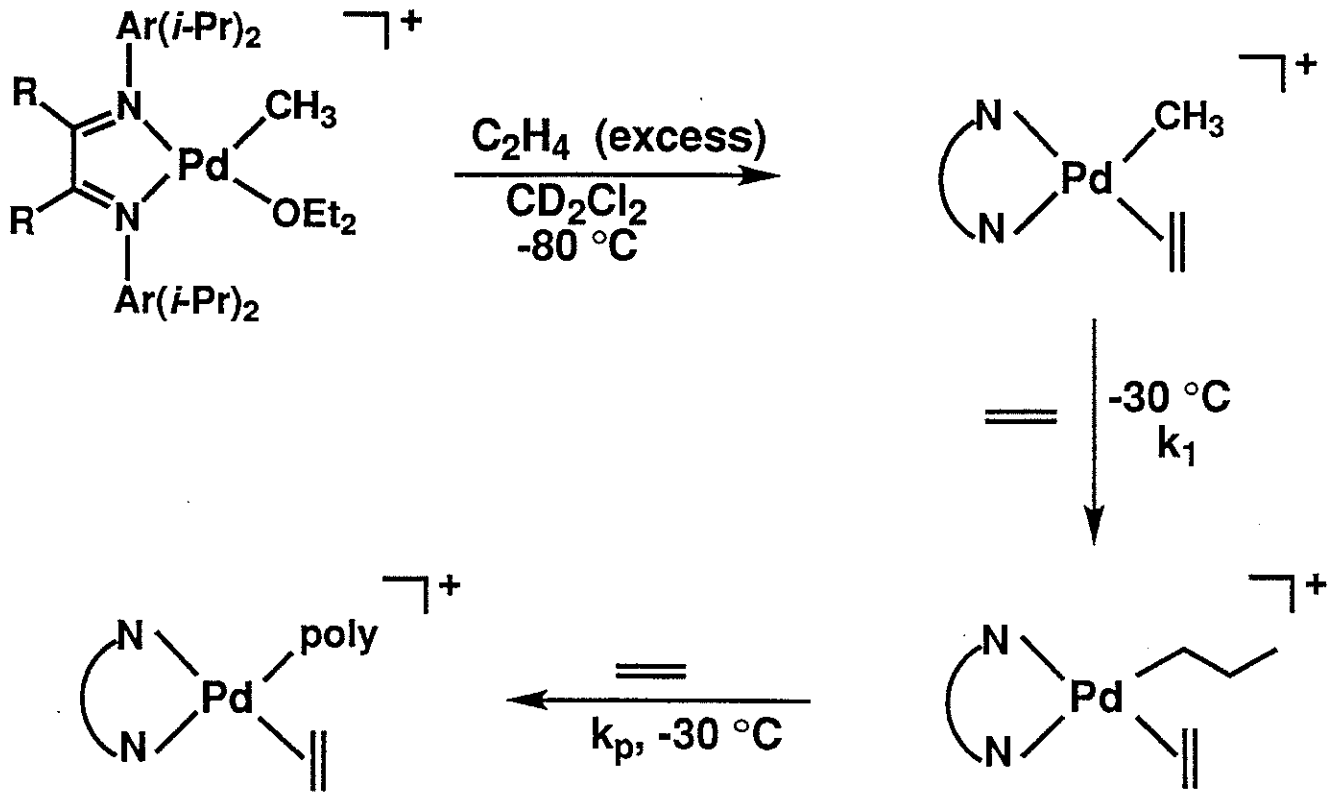

R = - H	$k_1 = 1.9 \times 10^{-3}$ sec^{-1}	$\Delta G^{\ddagger} = 17.2$ kcal/mol
	$k_p = 1.7 \times 10^{-3}$ sec^{-1}	$\Delta G^{\ddagger} = 17.3$ kcal/mol
R = -CH_3	$k_1 = 8.8 \times 10^{-4}$ sec^{-1}	$\Delta G^{\ddagger} = 17.8$ kcal/mol
	$k_p = 3.4 \times 10^{-3}$ sec^{-1}	$\Delta G^{\ddagger} = 16.9$ kcal/mol

- Catalyst resting state = alkyl ethylene complex
- Chain growth zero order in ethylene

NMR Studies

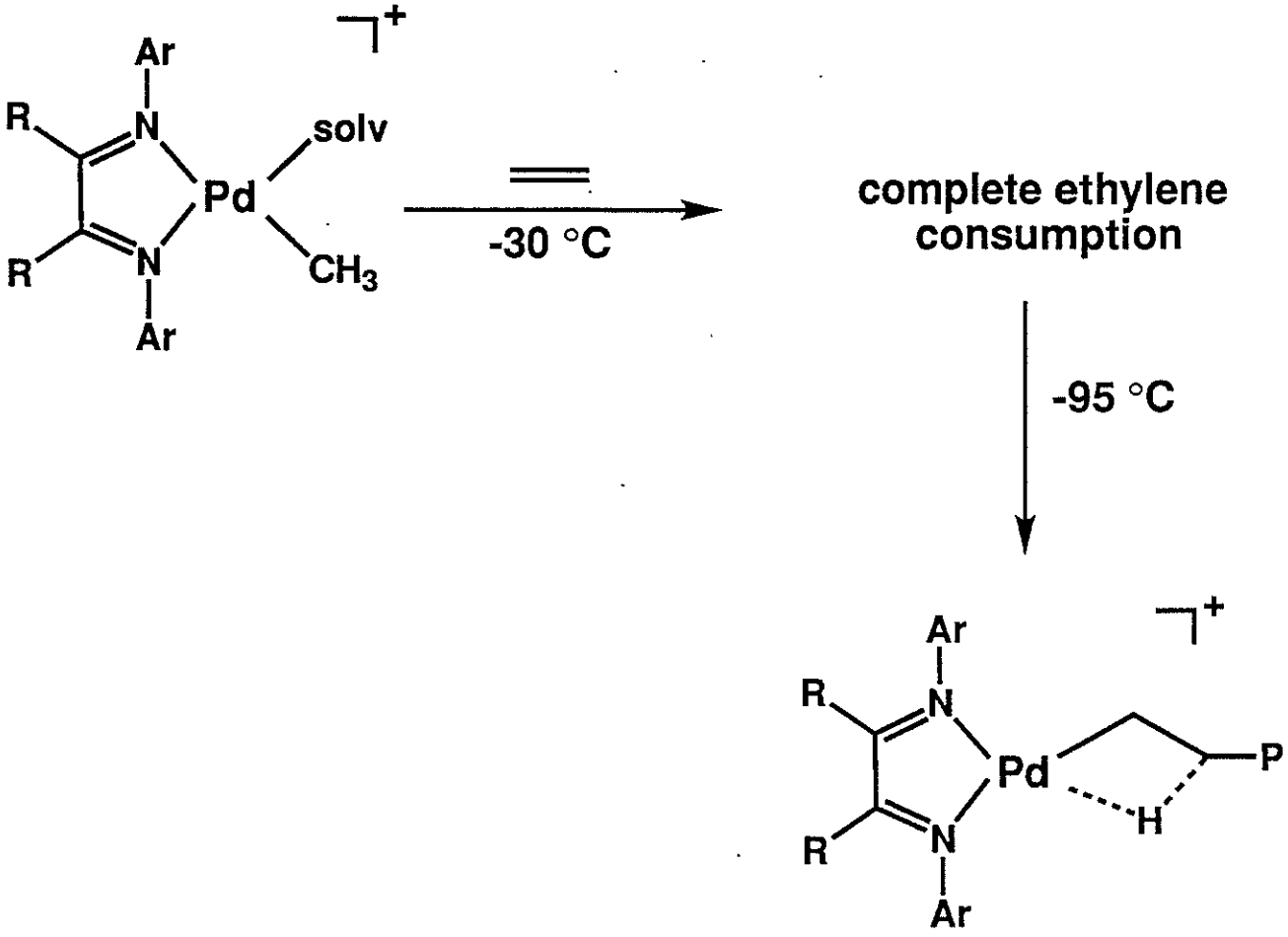

R = $-CH_3$	-8.4 ppm (br)
R = -H	-7.2 to -7.5 (br) -8.0 to -8.5 (br)

Proposed Mechanistic Model

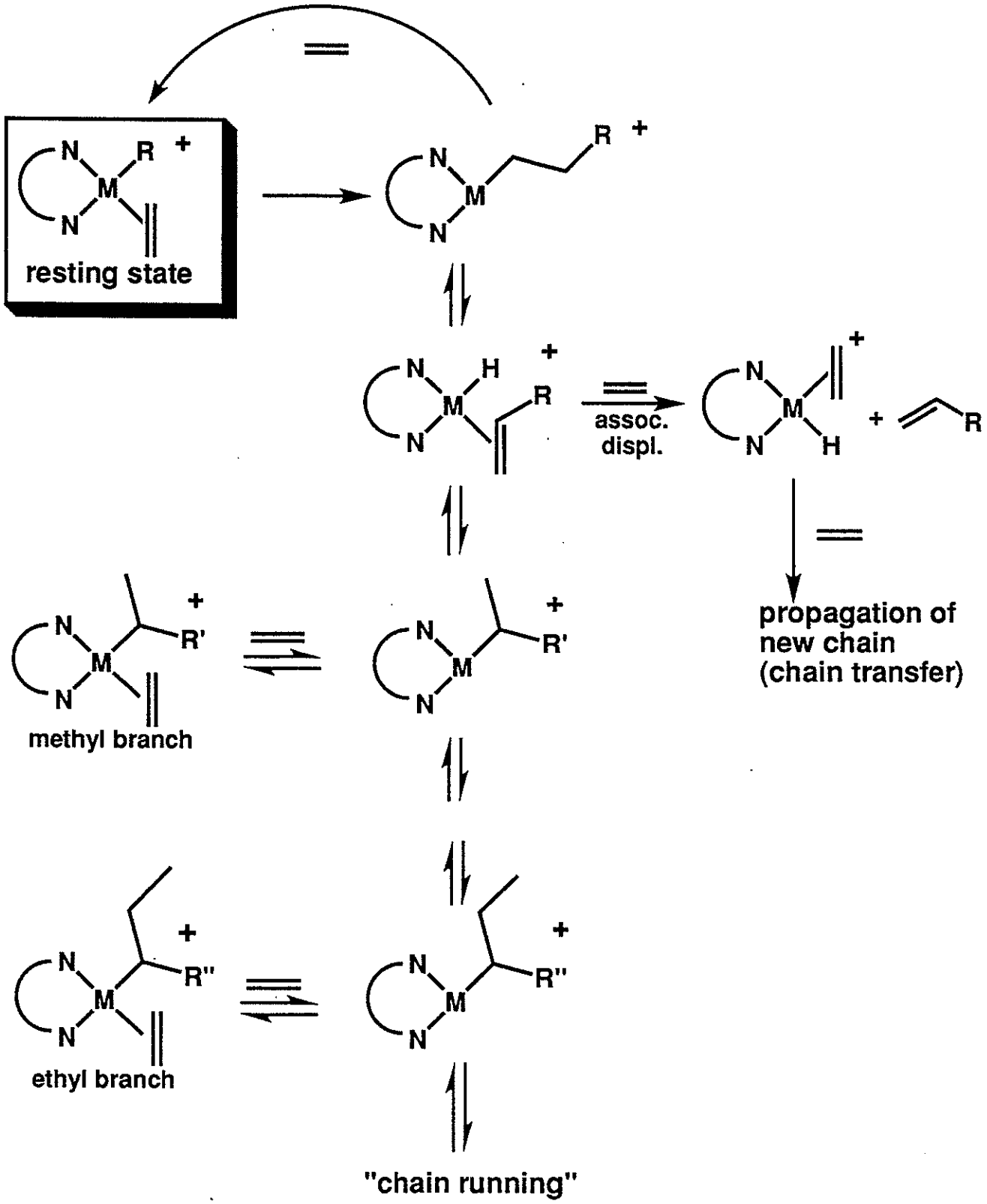

Chain Transfer Rate Controlled by <u>Associative Exchange</u>

- **Key to large k_p/k_t - Retard associative exchange by sterically blocking axial positions in d^8 square planar complexes**

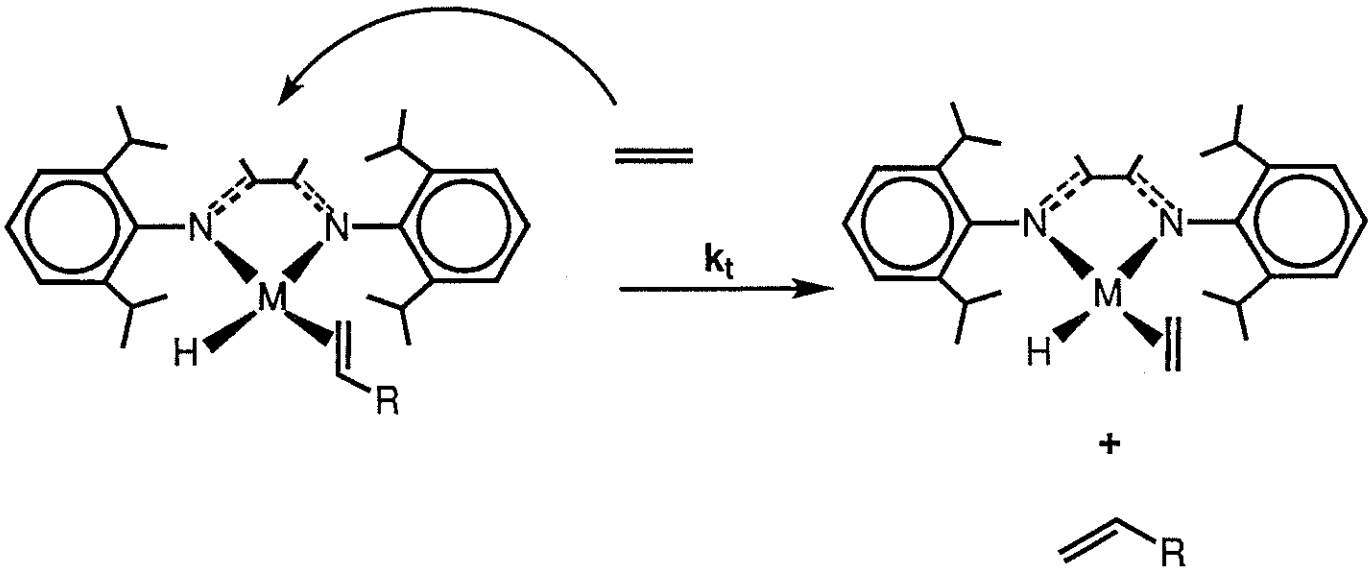

Models for Associative Exchange Rates

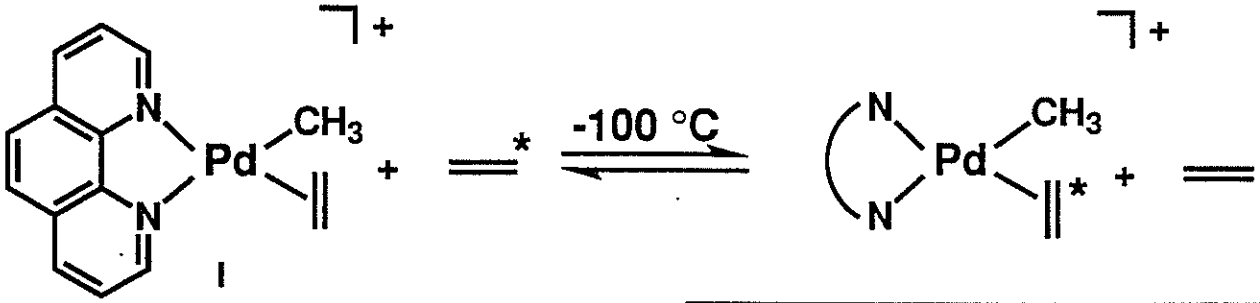

I

too fast to measure at -100 °C

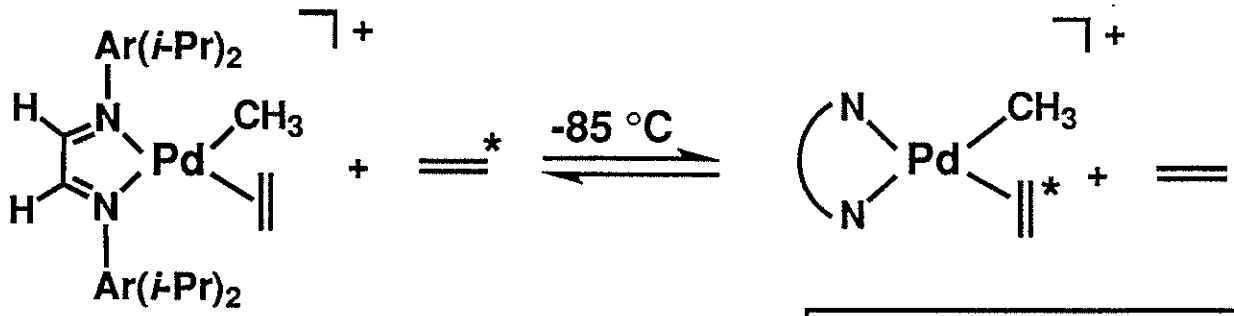

II

k = 8100 L mol^{-1}sec^{-1}

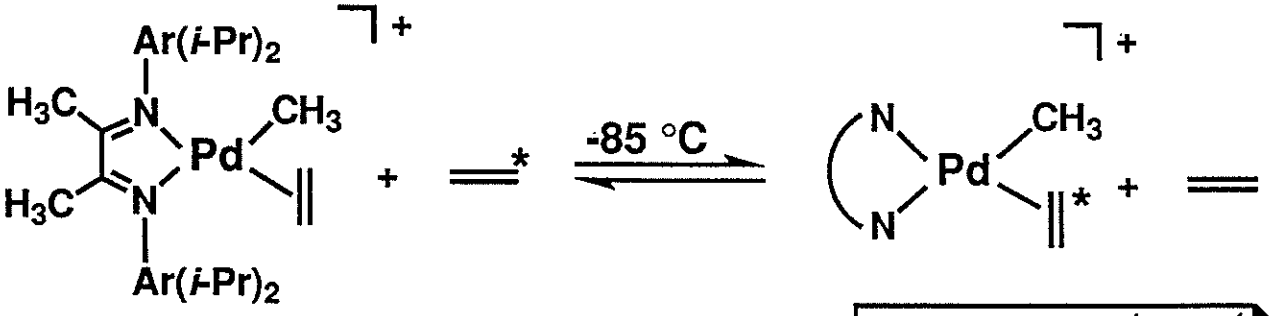

III

k = 45 L mol^{-1}sec^{-1}

II $\longrightarrow$ $\bar{M}_n$ = 6,000

III $\longrightarrow$ $\bar{M}_n$ = 29,000

Pd (II) Polymerization of α-Olefins

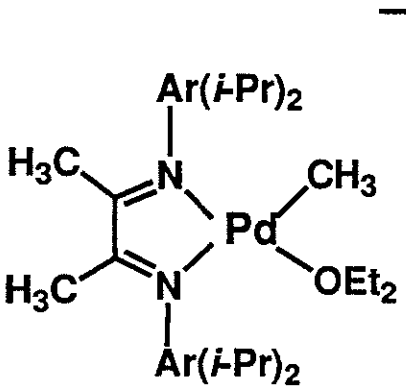

(1 atm)
CH_2Cl_2
25 °C
16 h

polypropylene (amorphous)

TO = 11,000

$\bar{M}_n$ = 15,000

$\bar{M}_w$ = 66,000

T_g = -43 °C

213 branches / 1000 C

1,2
insertions

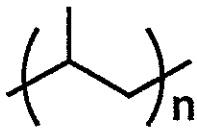

333 branches / 1000 C

(observed: 213)

Implies " Chain Straightening"

Pd (II) Polymerization of α-Olefins

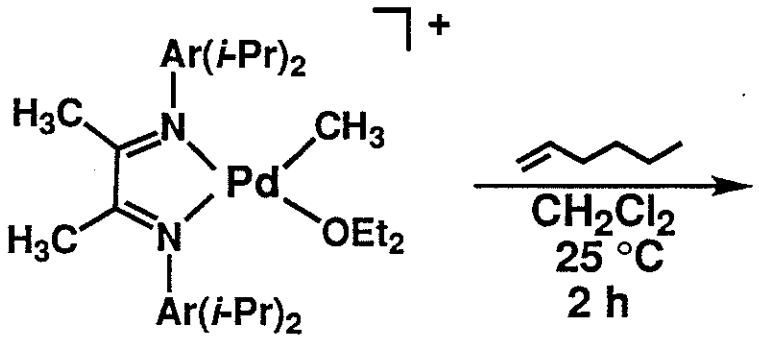

poly-1-hexene

TO = 1,300

$\bar{M}_n$ = 31,000

$\bar{M}_w$ = 77,000

T_g = -42 °C

88 branches / 1000 C

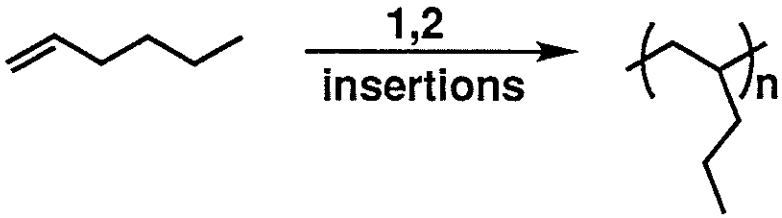

167 branches / 1000 C

(observed: 88)

Implies " Chain Straightening"

^{1}H, ^{13}C NMR Studies

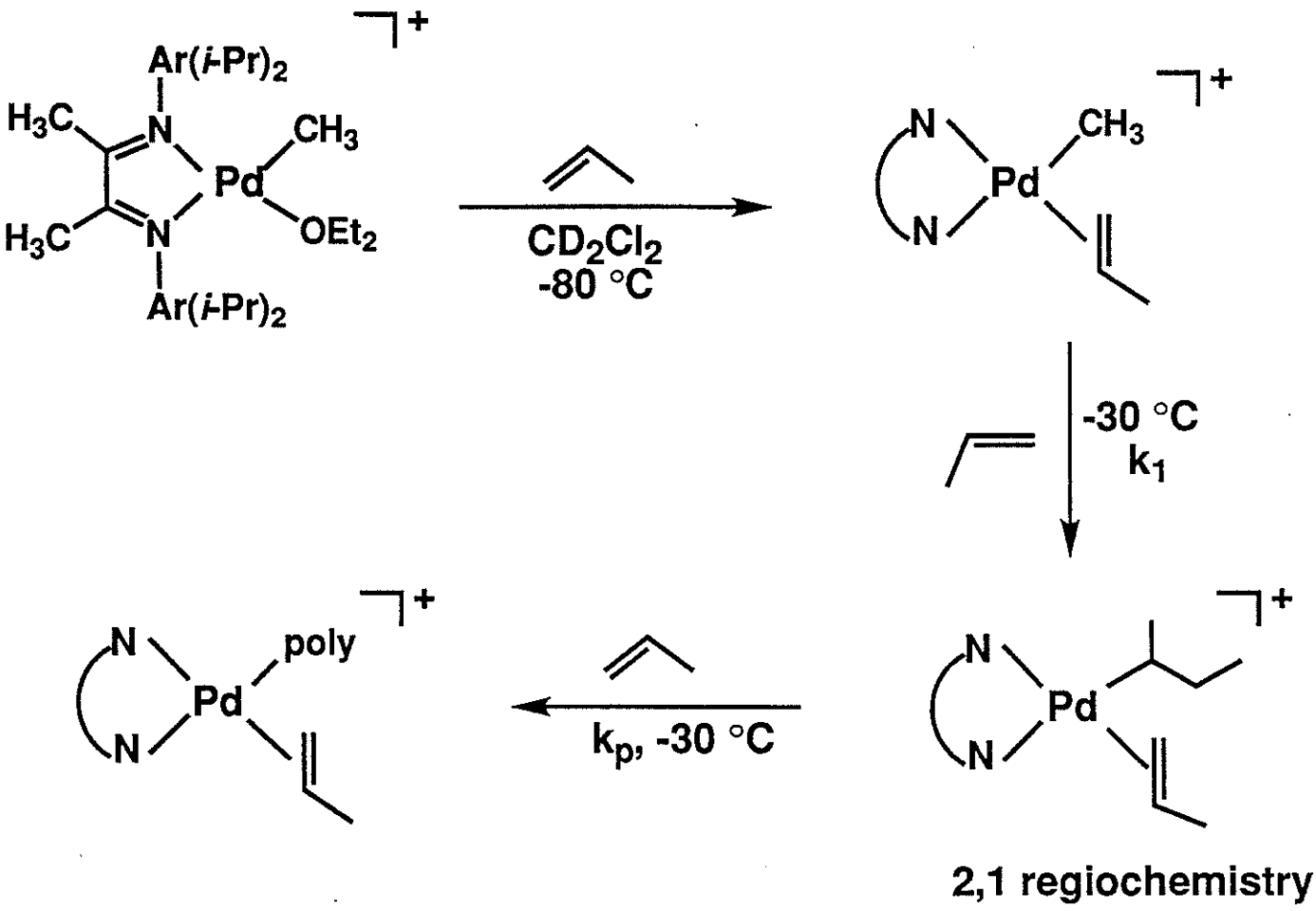

2,1 regiochemistry

$k_1 = 5.4 \times 10^{-4}$ sec^{-1} $\Delta G^{\ddagger} = 17.8$ kcal/mol, -30 °C

$k_p = 1.2 \times 10^{-3}$ sec^{-1} $\Delta G^{\ddagger} = 17.4$ kcal/mol, -30 °C

- Catalyst resting state = alkyl propylene complex
- Chain growth zero order in propylene
- 2,1 insertions predominate

Chain Straightening Mechanism

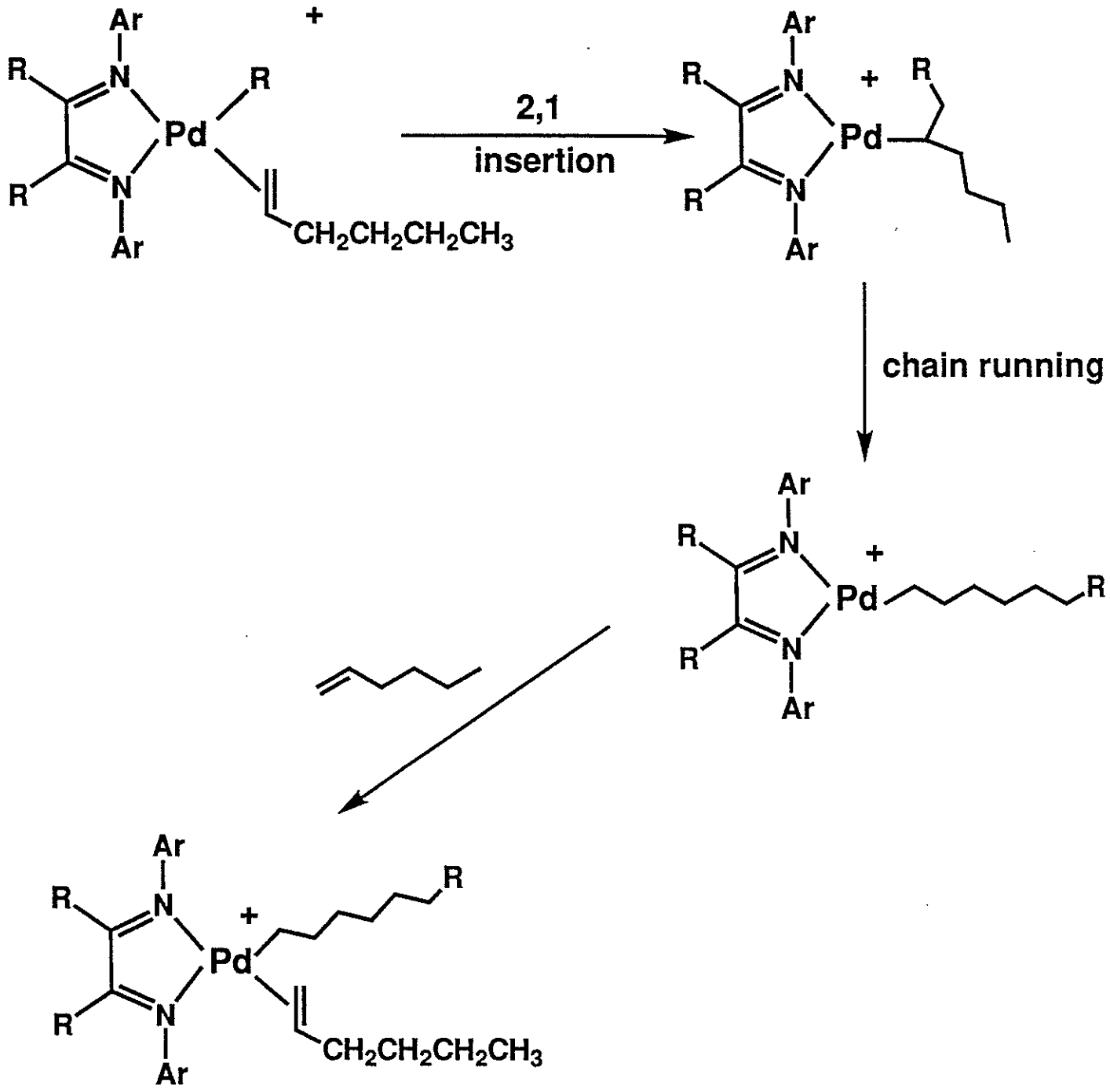

Ni (II)- Ethylene Polymerization

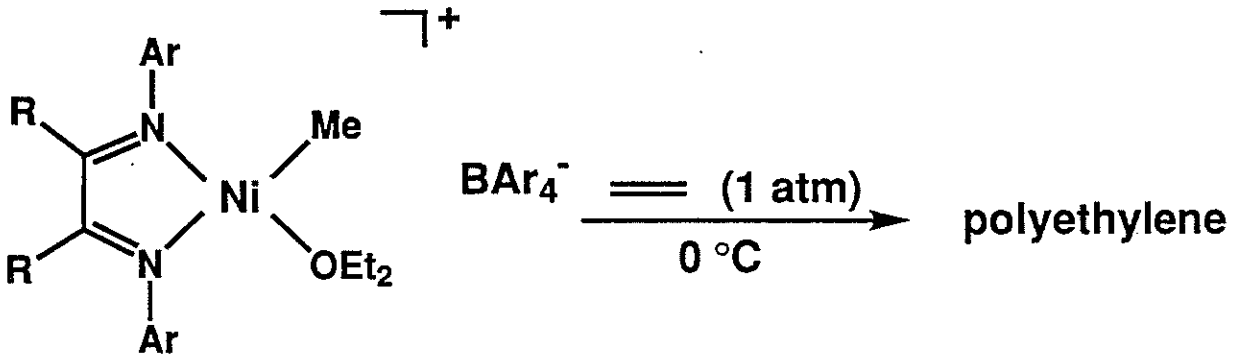

MAO Activated

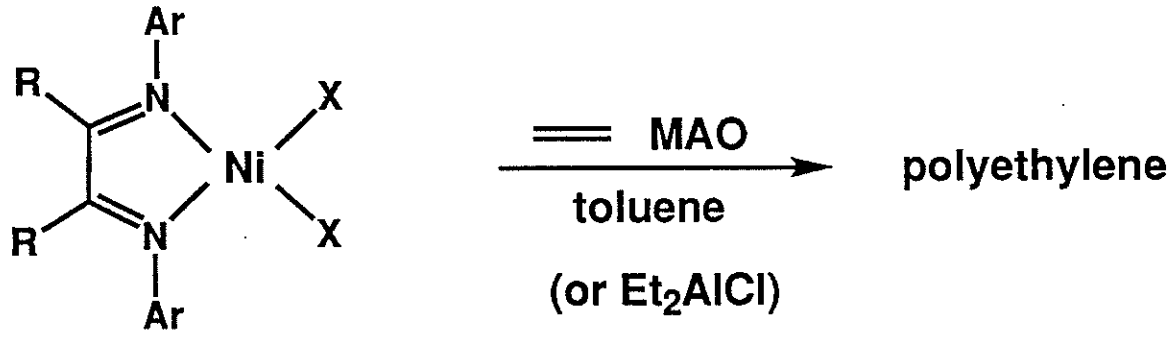

Activities (MAO Activated in toluene, 25 °C)

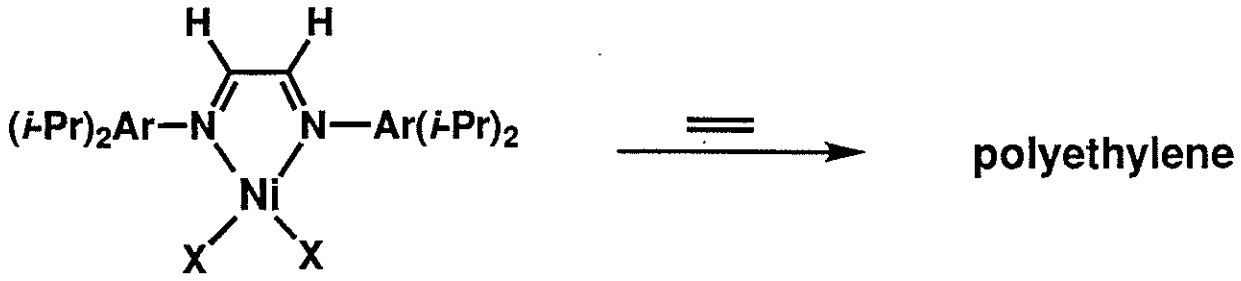

solvent volume	$P_{(C_2H_4)}$	moles cat x 10^6	TOF
100 mL	1 atm	1.7	4 x 10^5/h

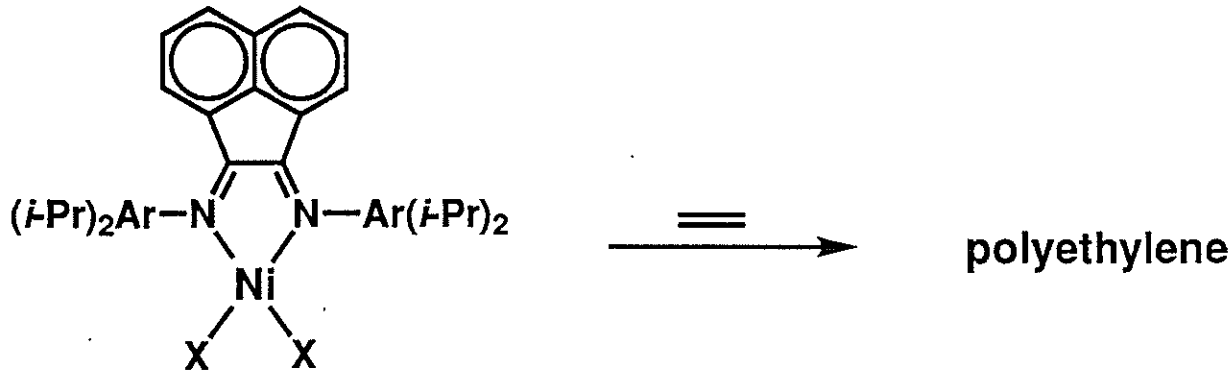

solvent volume	$P_{(C_2H_4)}$	moles cat x 10^6	TOF
200 mL	15 atm	0.8	2 x 10^6/h
200 mL	30 atm	0.8	2 x 10^6/h
200 mL	40 atm	0.8	2 x 10^6/h

Pressure Effects

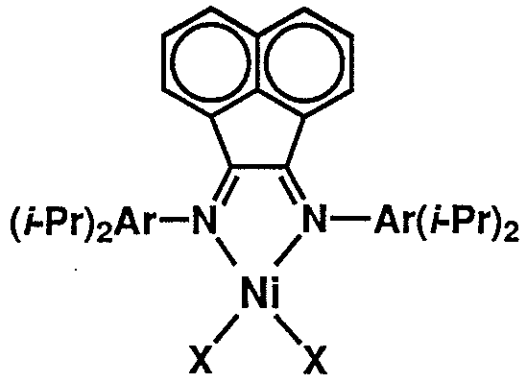

toluene
MAO, 0 °C

1 atm C_2H_4

4 atm C_2H_4

2.2 g PE	2.1 g PE
$\bar{M}_n$ = 650,000	$\bar{M}_n$ = 610,000
T_m = 112 °C	T_m = 122 °C
24 branches/1000 C	5 branches/1000 C

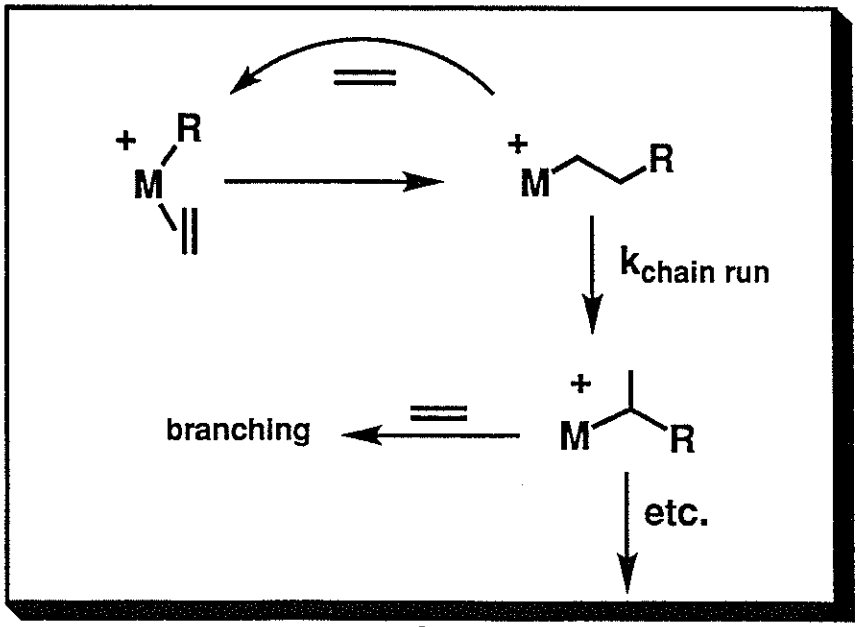

Temperature Effects

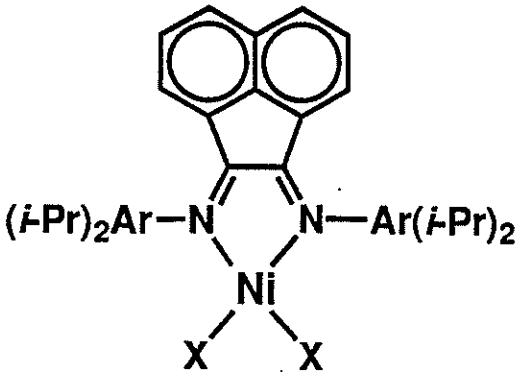

1 atm C_2H_4 | toluene MAO

0 °C

25 °C

2.2 g PE

$\bar{M}_n$ = 650,000

T_m = 112 °C

24 branches/1000 C

1.8 g PE

$\bar{M}_n$ = 190,000

T_m = 39 °C, T_g = -46 °C

71 branches/1000 C

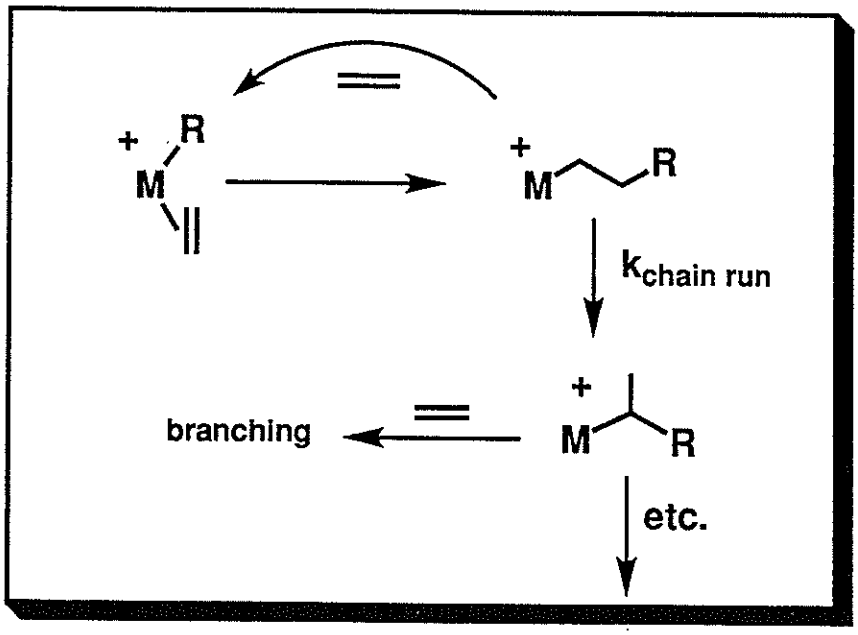

Effect of Ortho- Substituents (MAO Activated in toluene, 0 °C)

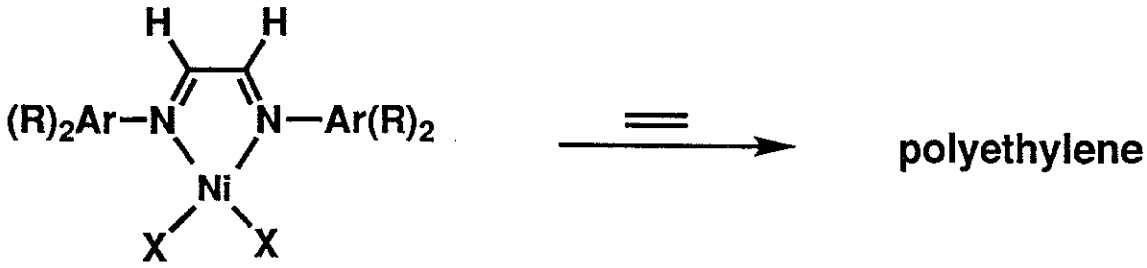

	$\bar{M}_n$	$\bar{M}_w/\bar{M}_n$	T_m	branches/1000 C
R = *o* - *i*-Pr	110,000	2.7	129 °C	7

	$\bar{M}_n$	$\bar{M}_w/\bar{M}_n$	T_m	branches/1000 C
R = *o* - CH_3	43,000	2.5	132 °C	1

Effect of Ortho- Substituents (MAO Activated in toluene, 0 °C)

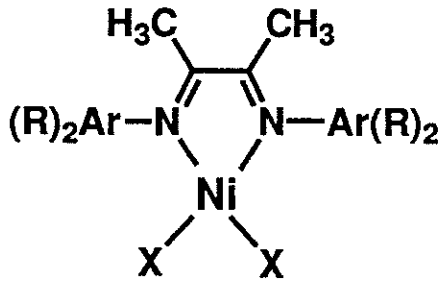

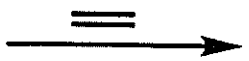

polyethylene

	$\bar{M}_n$	$\bar{M}_w/\bar{M}_n$	T_m	branches/1000 C
R = *o* - *i*-Pr	520,000	1.6	109 °C	48

	$\bar{M}_n$	$\bar{M}_w/\bar{M}_n$	T_m	branches/1000 C
R = *o* - CH_3	170,000	2.6	115 °C	20

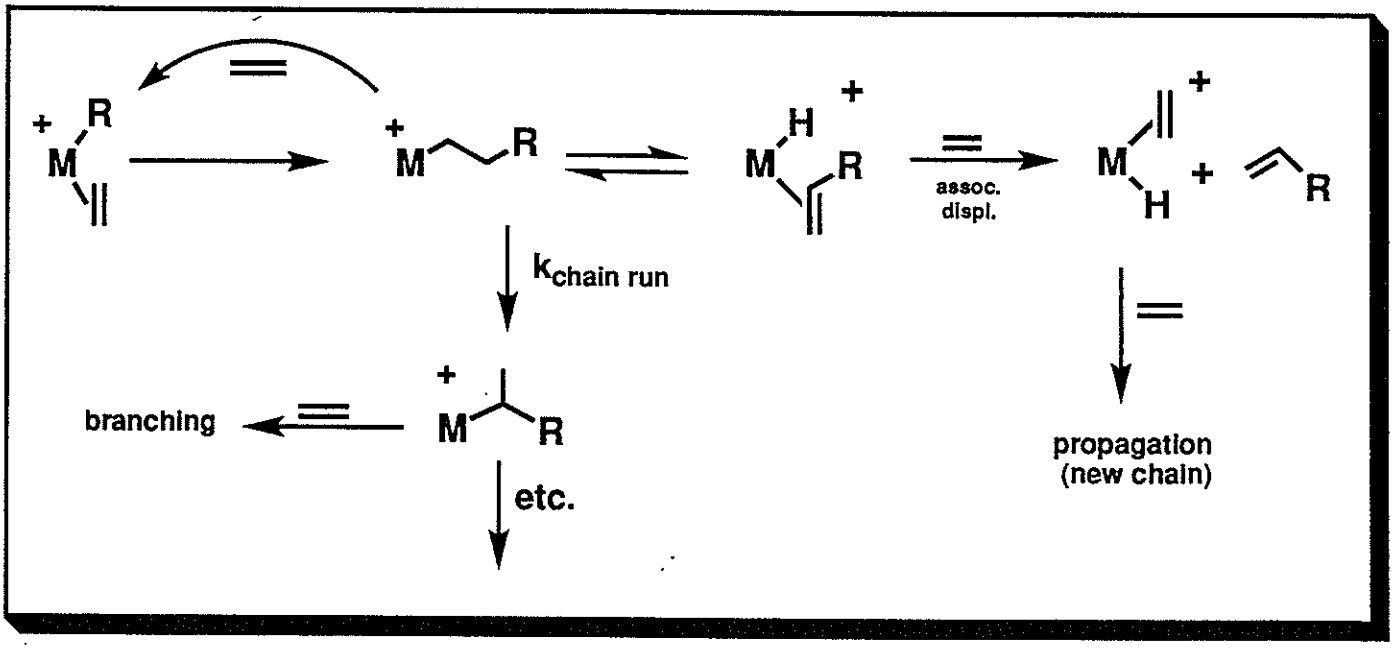

Effect of Backbone Substituents (MAO Activated in toluene, 0 °C)

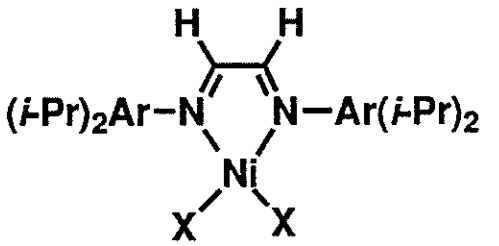

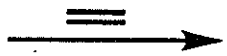

polyethylene

$\bar{M}_n$	$\bar{M}_w/\bar{M}_n$	T_m	branches/1000 C
110,000	2.7	129 °C	7

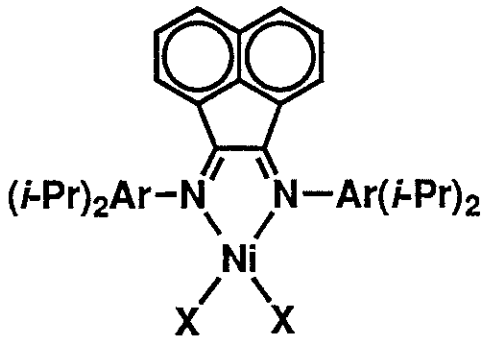

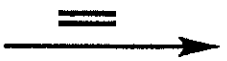

polyethylene

$\bar{M}_n$	$\bar{M}_w/\bar{M}_n$	T_m	branches/1000 C
650,000	2.4	112 °C	24

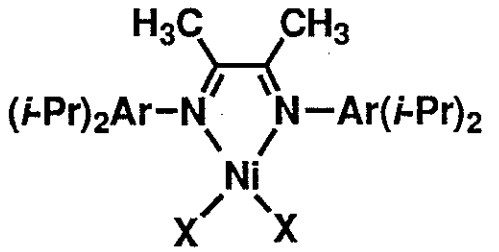

polyethylene

$\bar{M}_n$	$\bar{M}_w/\bar{M}_n$	T_m	branches/1000 C
520,000	1.6	109 °C	48

Ni (II) Polymerization of α-Olefins

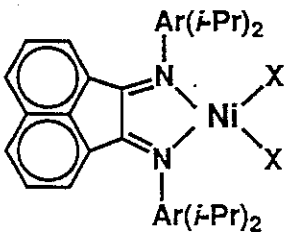

toluene
MAO, 0 °C
2 h

polypropylene
TO = 5,800
$\bar{M}_n$ = 150,000
$\bar{M}_w$ = 240,000
T_g = -20 °C
300 branches / 1000 C

1,2
insertions

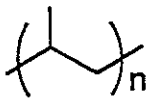

333 branches / 1000 C
(observed: 300)

Ni (II) Polymerization of α-Olefins

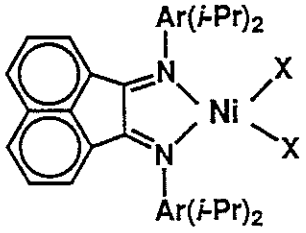

toluene
Et_2AlCl, 0 °C
2 h

poly-1-hexene
TO = 1,500
$\bar{M}_n$ = 140,000
$\bar{M}_w$ = 310,000
T_g = -57 °C
T_m = -20 °C
100 branches / 1000 C

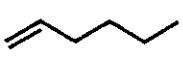

1,2
insertions

167 branches / 1000 C
(observed: 100)

Implies " Chain Straightening"

Summary

- First late metal catalysts to convert α-olefins to high molar mass polymers

- First catalyst systems examined where alkyl olefin complexes definitively established as catalyst resting states

- Polyethylenes variable from highly branched, amorphous to linear, crystalline material by changes in pressure, temperature, and catalyst structures. No comonomers required.

- Activities of Ni(II) systems approach Ziegler-Natta activities-ligands are inexpensive, minimal quantities of Lewis acid activators required.

- First demonstration of metal-based random copolymerization of ethylene and methyl acrylate

Material Design in Poly(Lactic Acid) Systems

M. Spinu, C. Jackson, M. Y. Keating, K. H. Gardner

ACS Symposium on New Organic Chemistry for Polymer Synthesis

Santa Fe, New Mexico - May 22, 1995

Outline

- Background
- New PLA Materials
  - (i) Copolymerization
    - ABA triblocks
    - $(ABA)_n$ multiblocks
    - Stereoblocks
  - (ii) Controlled architecture
  - (iii) Controlled microstructure
  - (iv) Stereocomplex - L/D-PLA blends
- Conclusions

PLA Synthesis

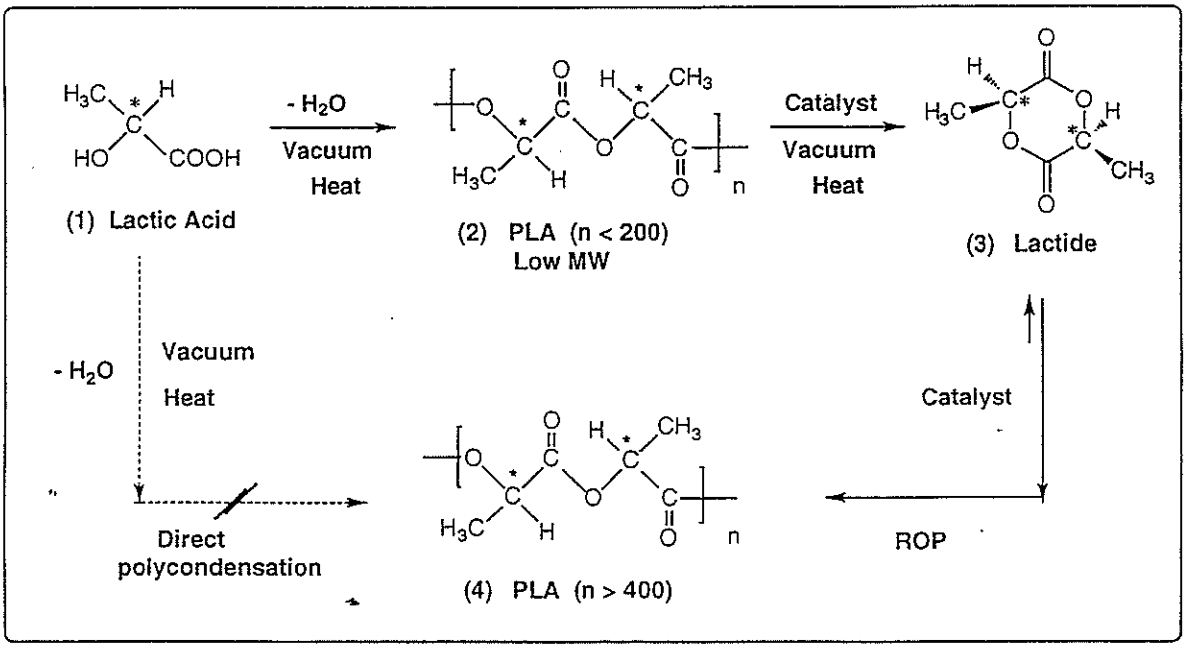

Characteristics of PLA Polymers

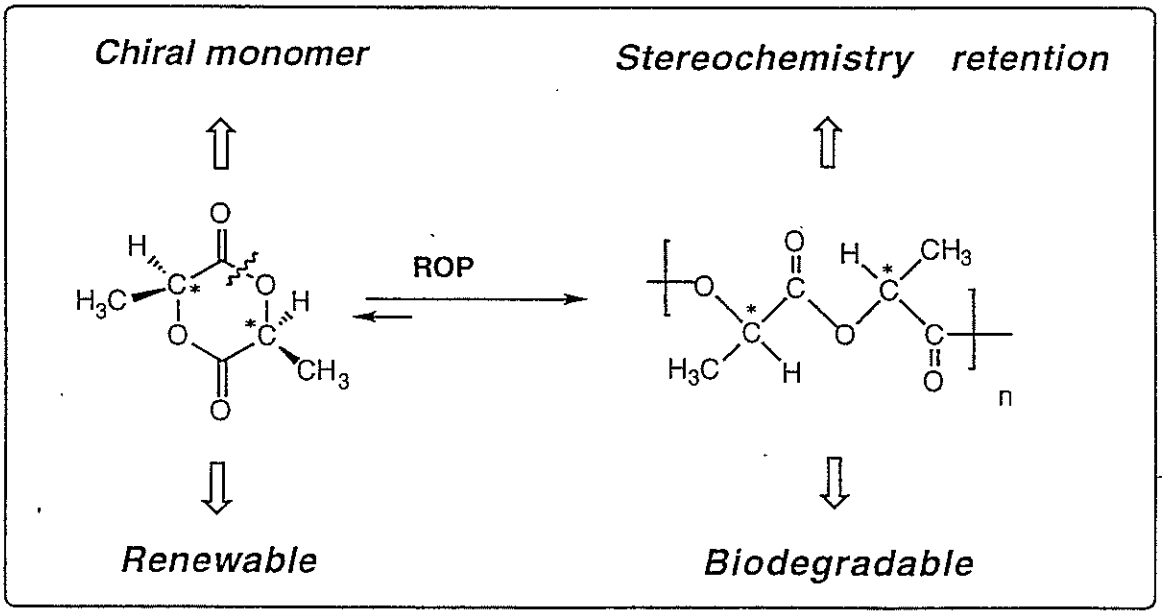

PLA Synthesis

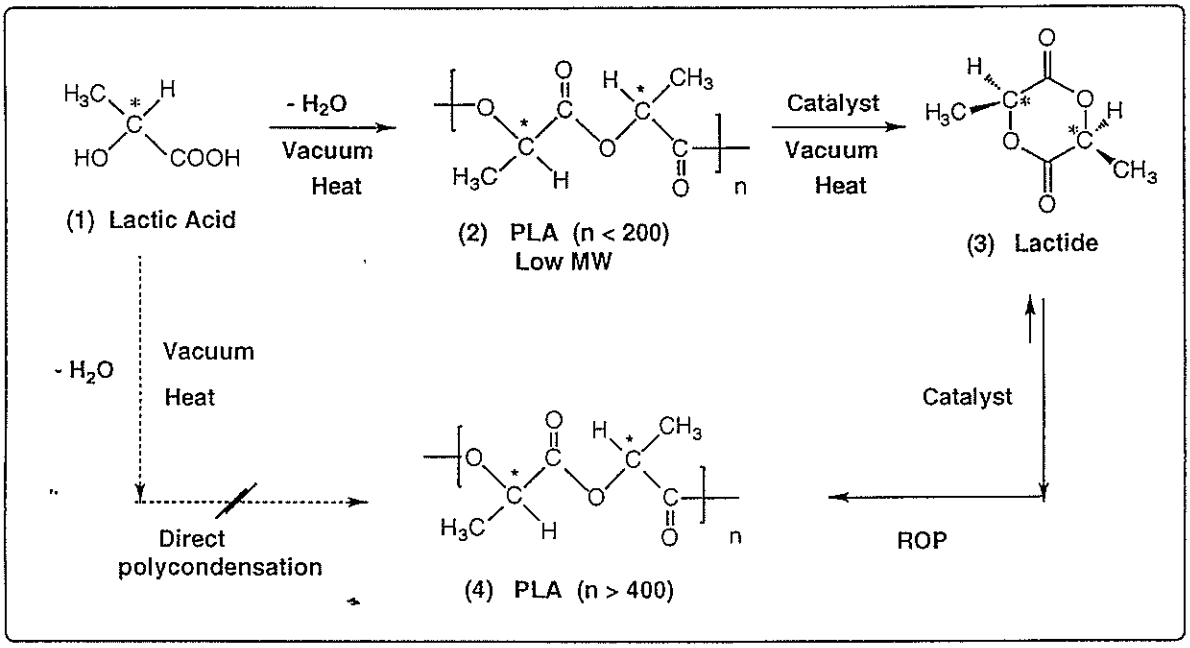

Characteristics of PLA Polymers

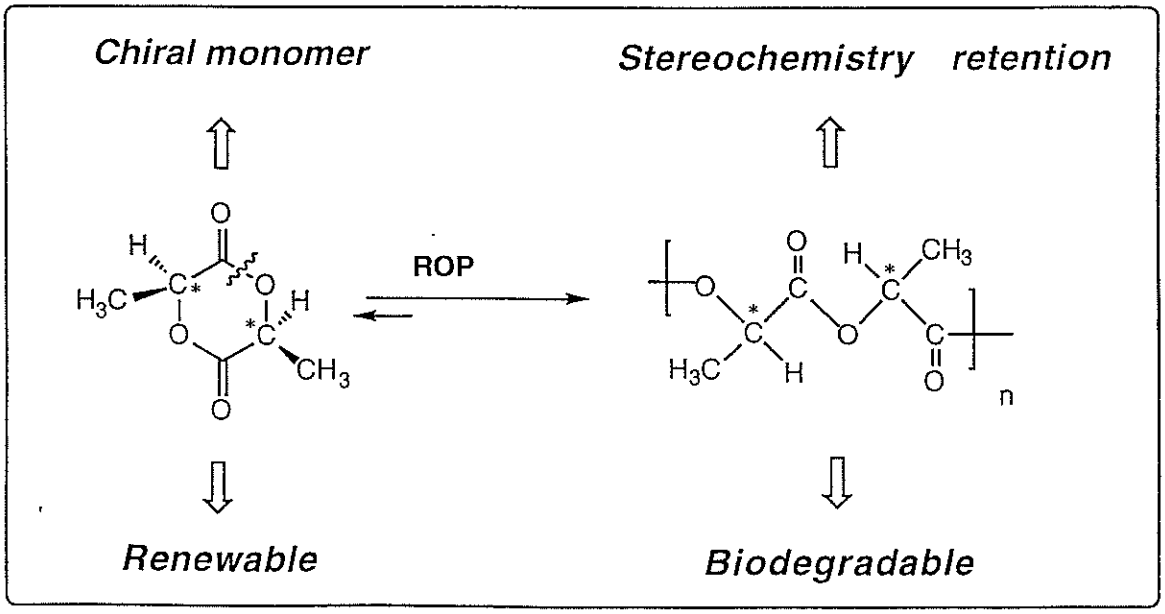

PLA - General Properties

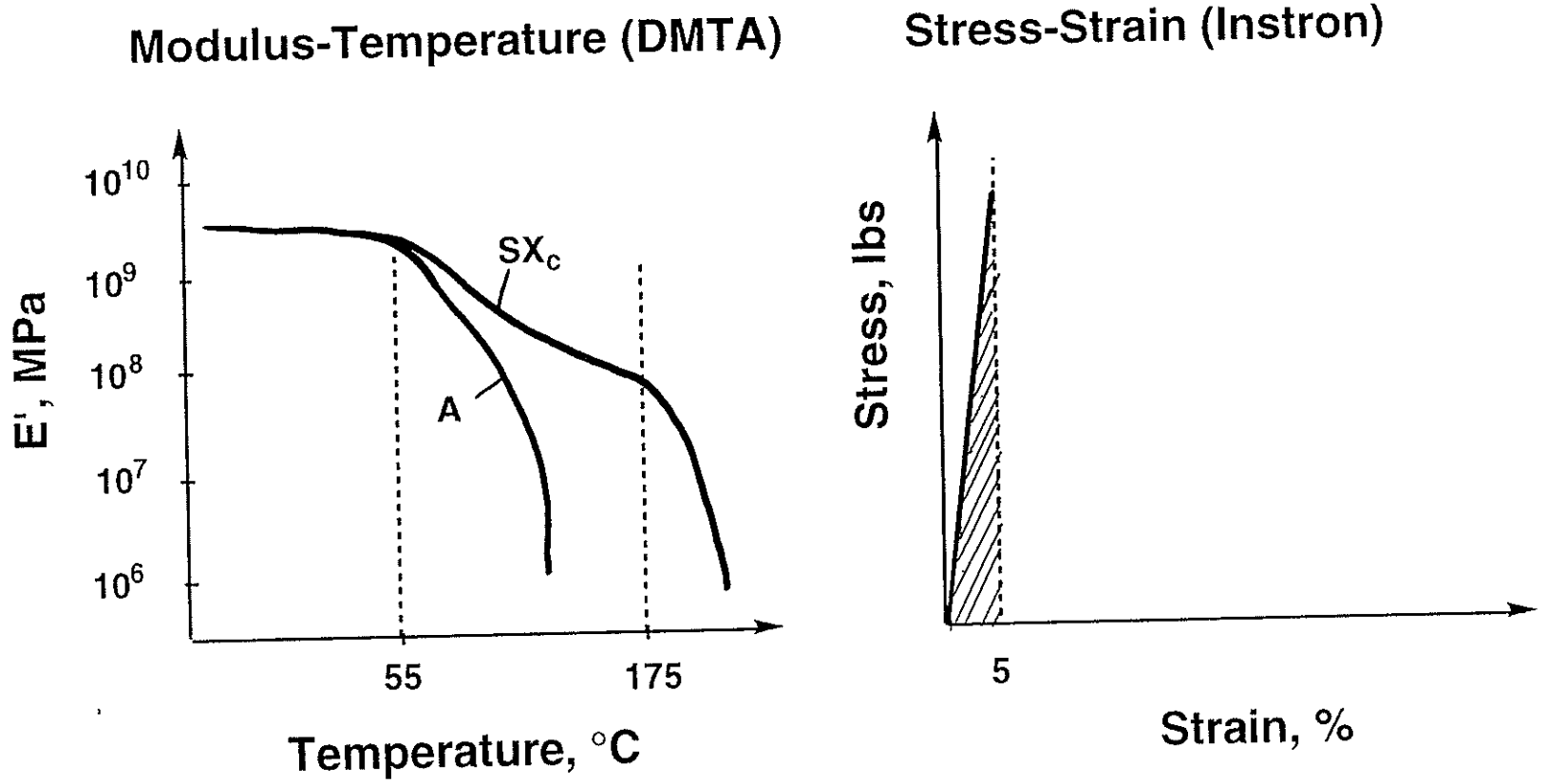

T.S. = 9,000psi (62.1 MPa); I.M. = 300 Kpsi (2.1 GPa); % E = 5%

Research Objectives

- **Diversify polymer properties**

  Hard Plastics ⟷ *Elastomers*

- **Improve processability**
  - lower Tm
  - high degree of crystallinity
  - high crystallization rates

- **Develop economical polymerization processes**

Synthetic Tools

- *Chiral monomer:*

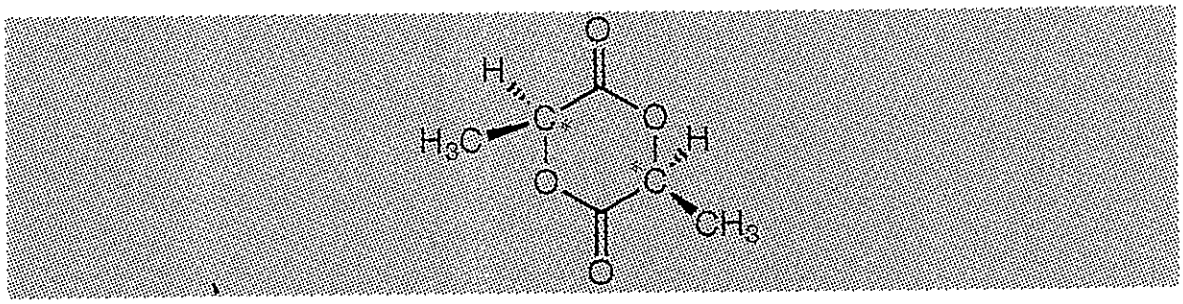

- *Retention of configuration on polymerization*

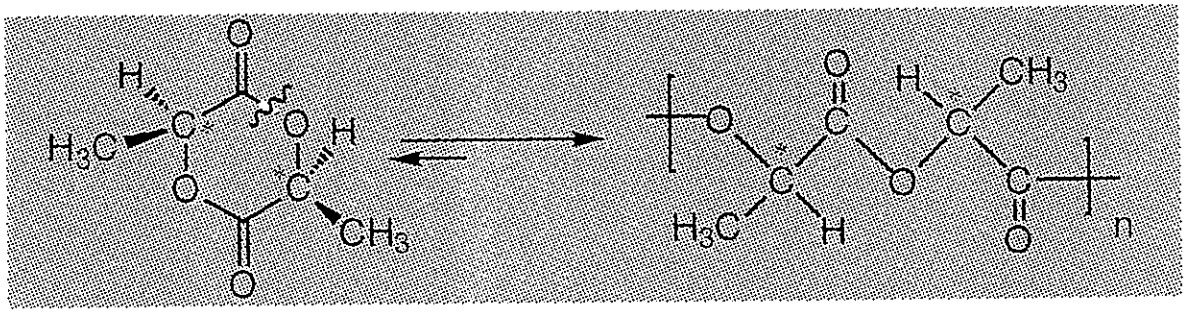

- *"Living" nature of ROP*

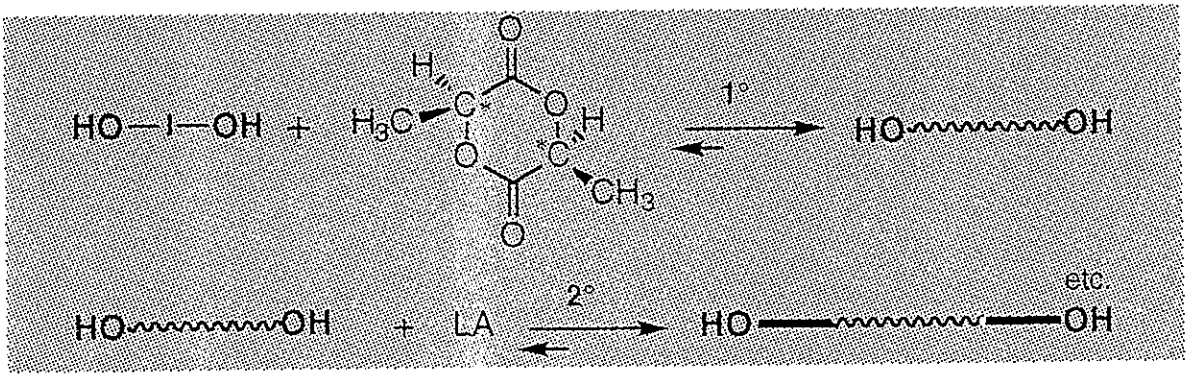

- *No transesterifications*

PLA Block Copolymers

Triblocks

Multiblocks

Stereoblocks

ABA Tri-block Copolymers

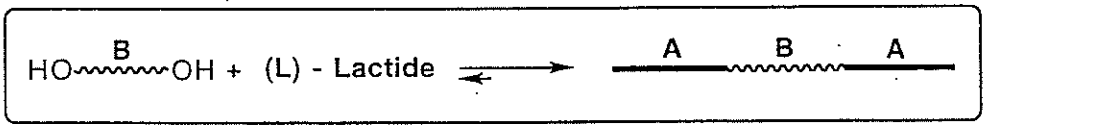

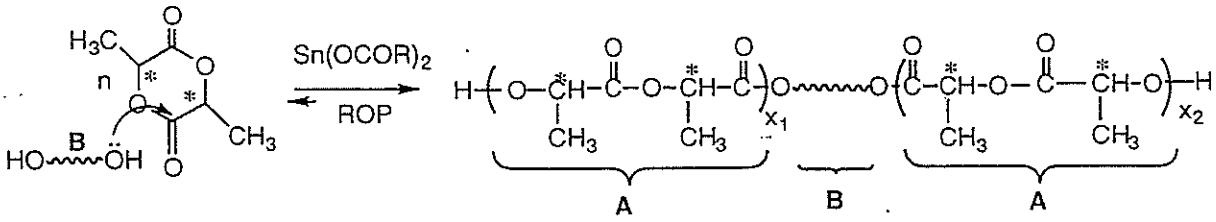

$$\overline{M}_n\ (PLA) = \frac{\text{Grams LA}}{\text{Moles OH}} \dashrightarrow \overline{M}_n\ (ABA) \sim \frac{1}{[B]}$$

⇩

Limited Composition Range

Initial Modulus and % Elongation vs Composition

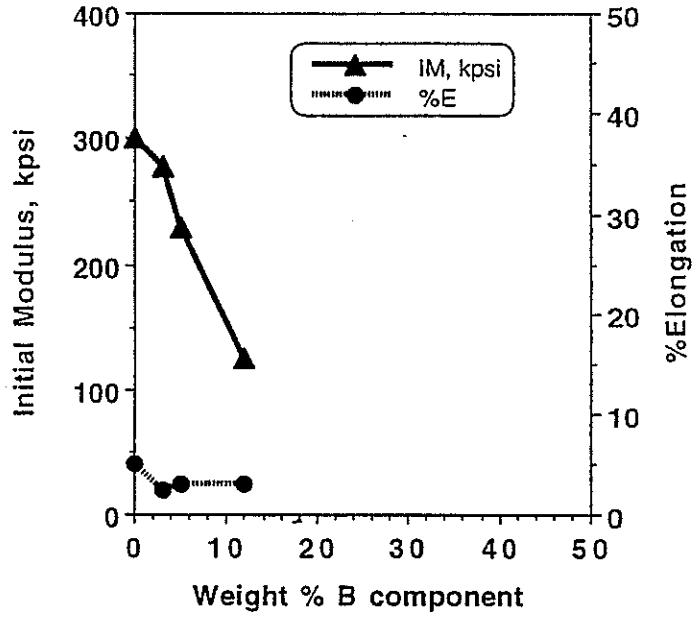

Tensile Strength and % Elongation vs Composition

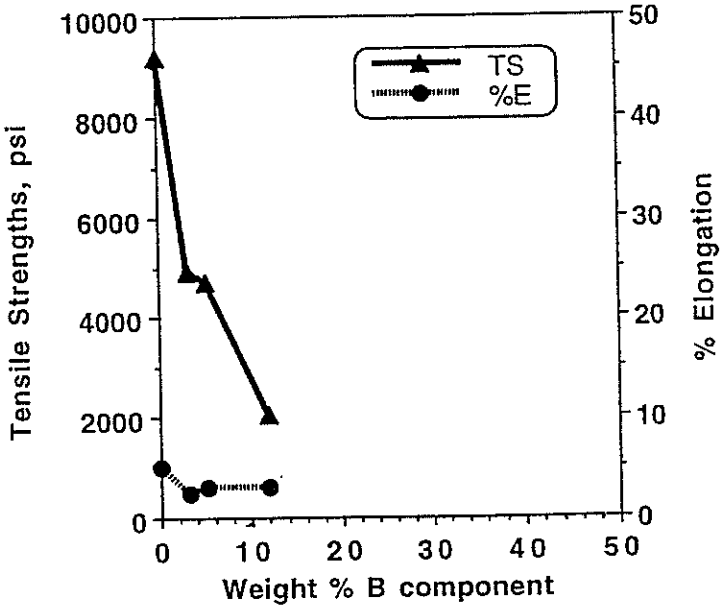

(ABA)n Multi-Block Copolymers

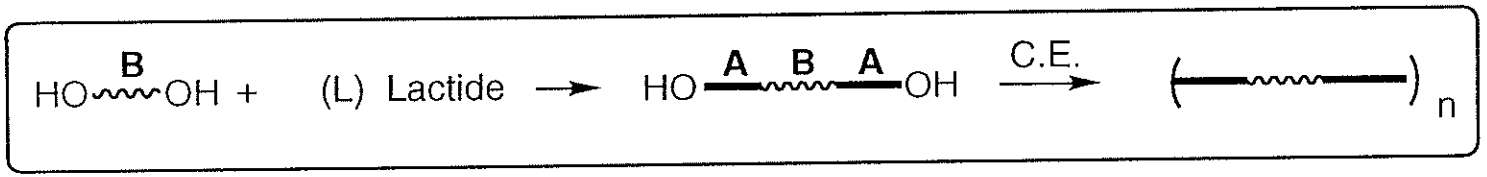

<Mn> ≠ f(composition)

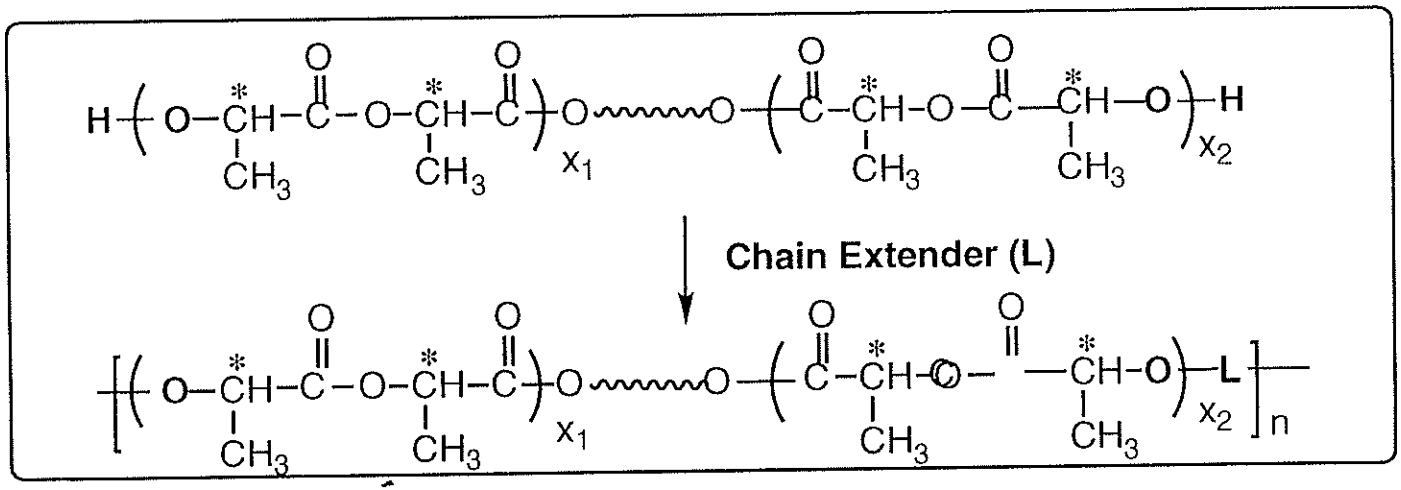

US Patent 5,202,413, M. Spinu (1993)

System Variables

- Chemical composition (A/B)
- Nature of B block
  - Aliphatic polyester
  - Aliphatic polyether
  - Polydimethylsiloxane
- Block length

Initial Modulus and % Elongation vs Composition

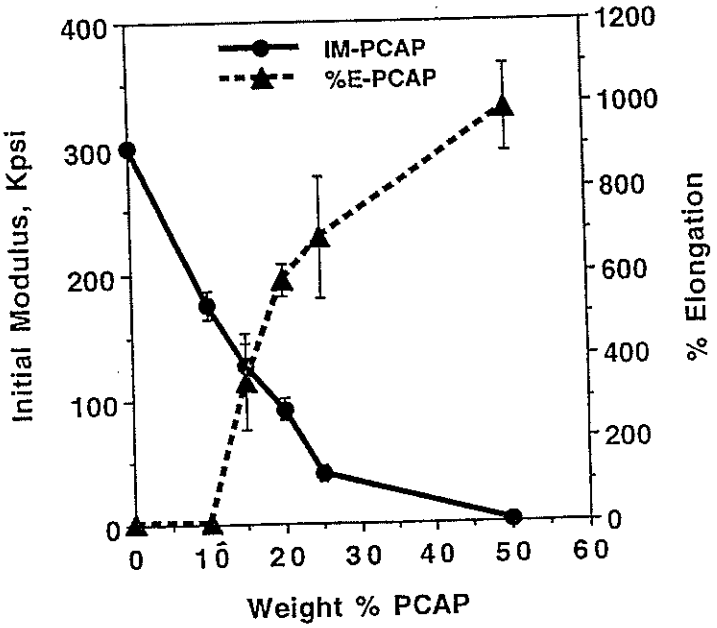

PLA Stereoblocks

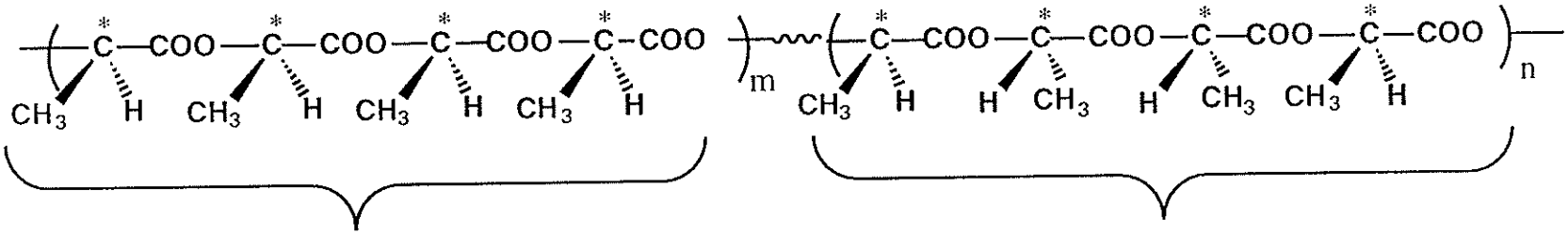

Semicrystalline (SX_c) Amorphous (A)

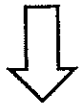

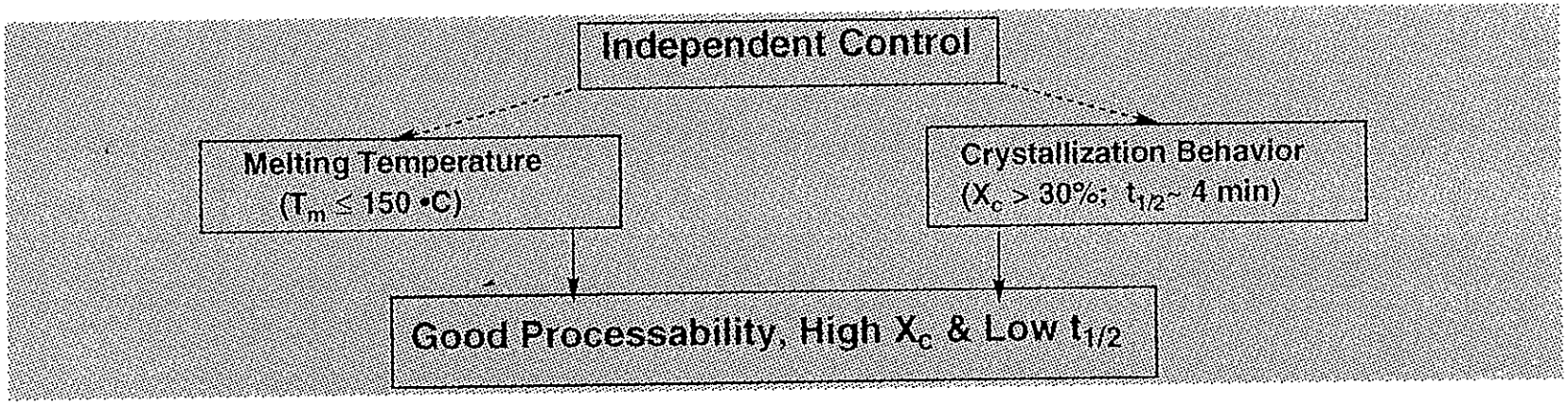

Synthesis of PLA Stereoblocks

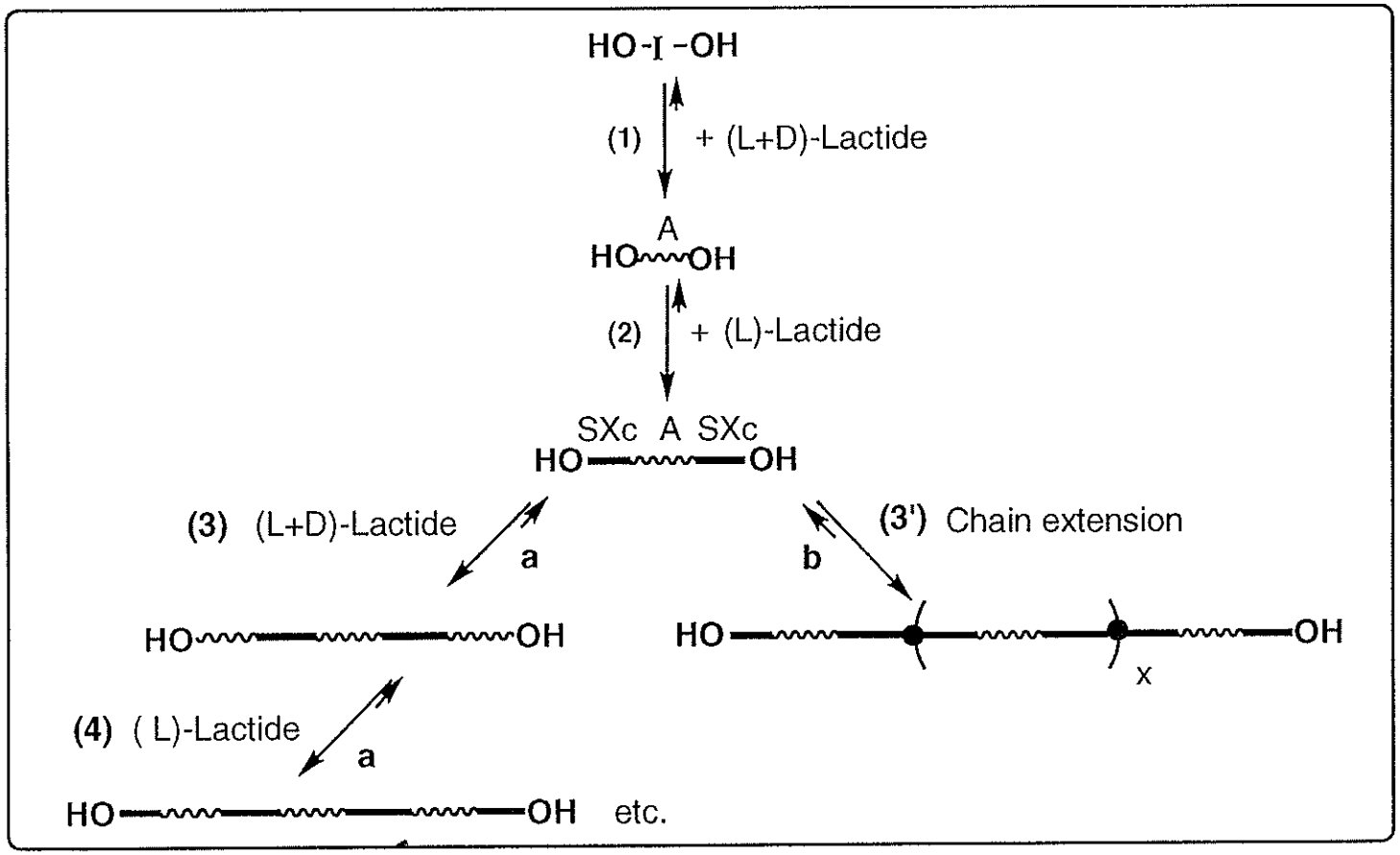

US Patent 5,270,400, M. Spinu (1993); US Patent 5,346,966, M. Spinu (1994)

Tm and t1/2 for PLA Stereoblock Copolymers

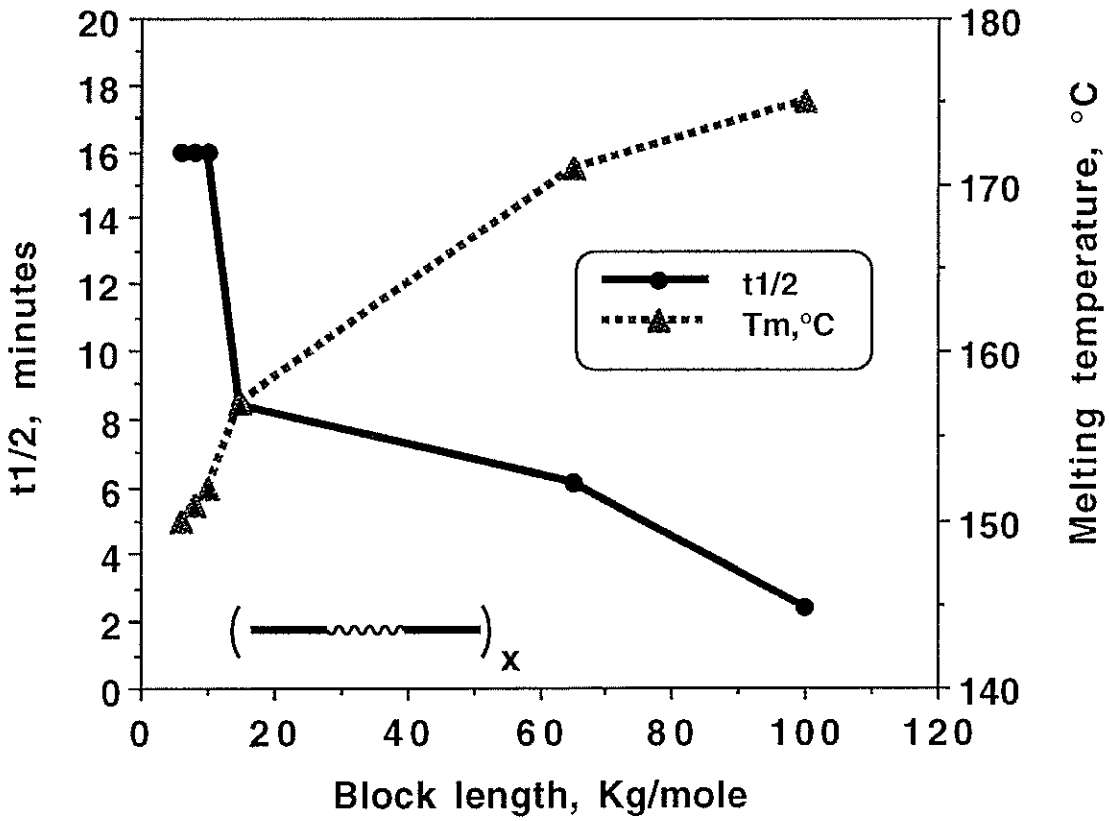

8h1

Typical stress-strain plots
(I) PLA; (II) PLA/PBEA 75/25; (III) PLA/PBEA 50/50

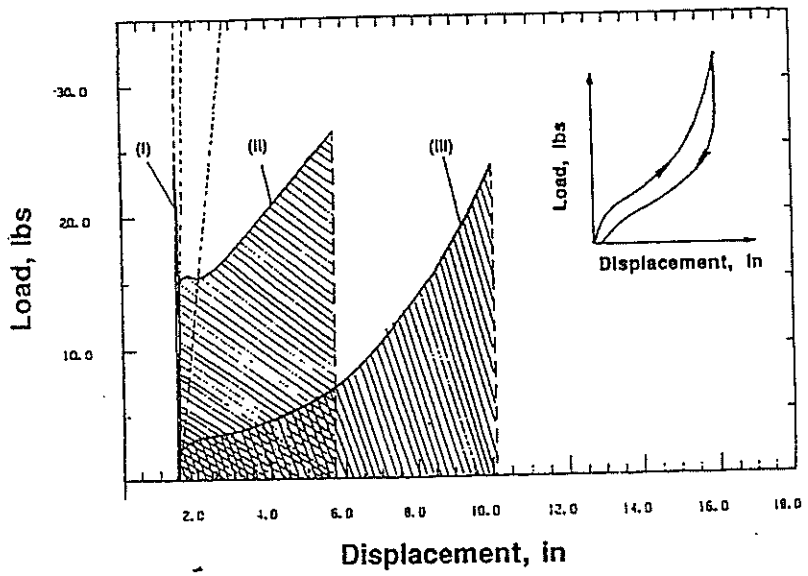

PLA Stars

Controlled Architecture & Microstructure

Synthesis of PLA Stars
(w/Controlled Microstructure)

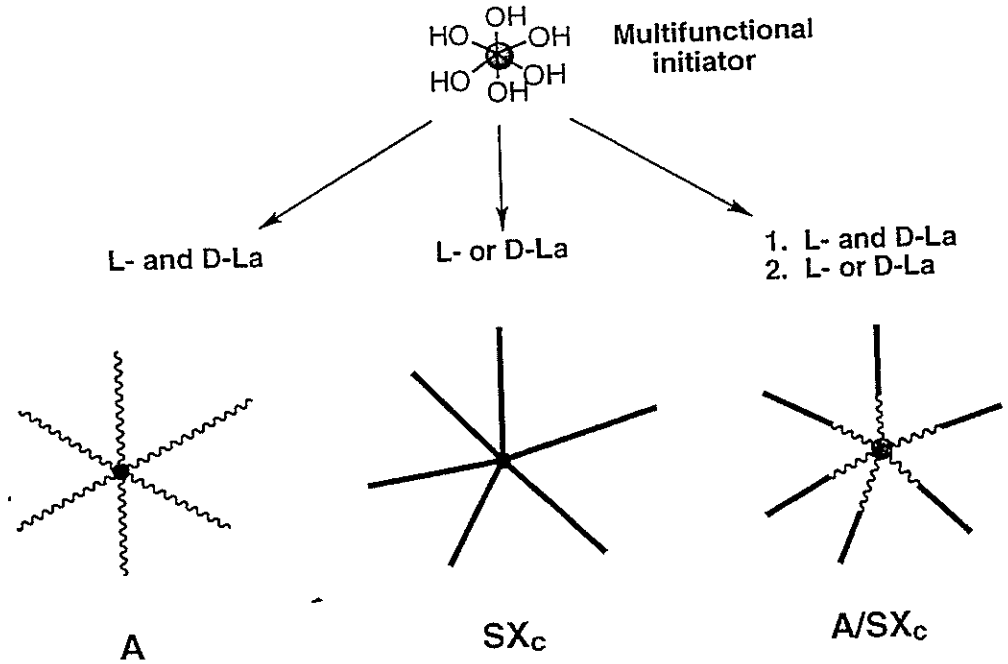

US Patent 5,225,521, M. Spinu (1993).

Star and Linear PLA w/Controlled Microstructure

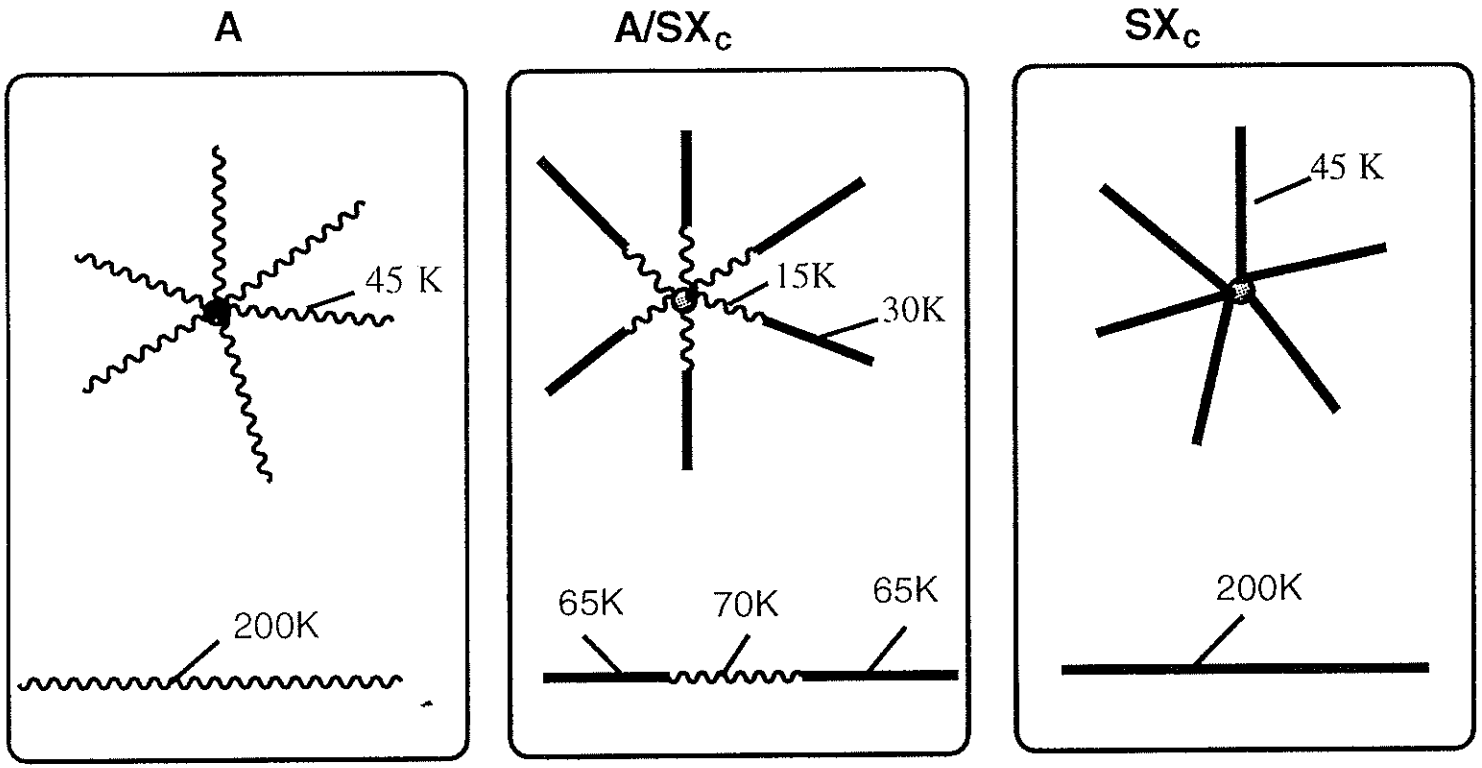

Typical GPC Traces for 6-Arm PLA Stars (a) before and (b) after fractionation

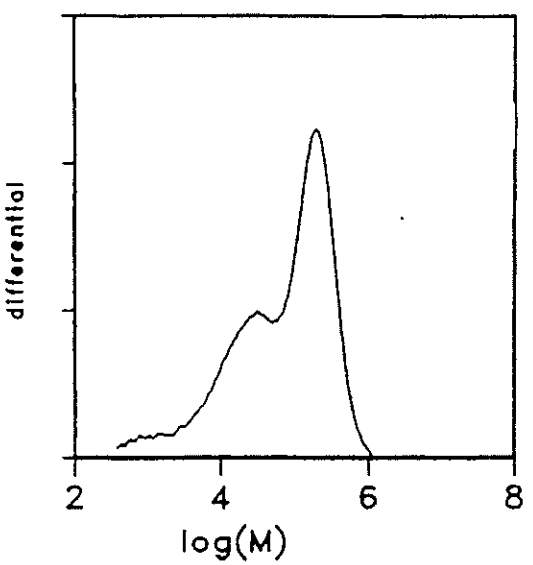

Mw = 146000 Mn = 12000 P/D =12.15
Mz = 299000 Mz` = 454000 Mv = 124000
Mp = 218000 Pm = 26.93 C` = 29.14

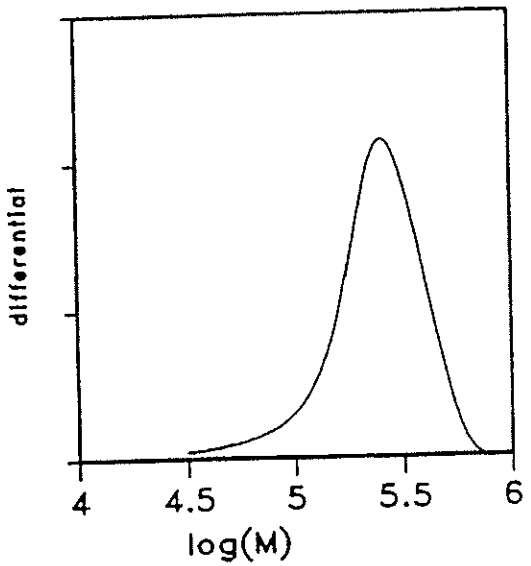

Mw = 270000 Mn = 207000 P/D = 1.30
Mz = 318000 Mz` = 364000 Mv = 263000
Mp = 265000 Pm = 35.35 C` = 35.63

Solution Properties
Mark-Houwink Plots

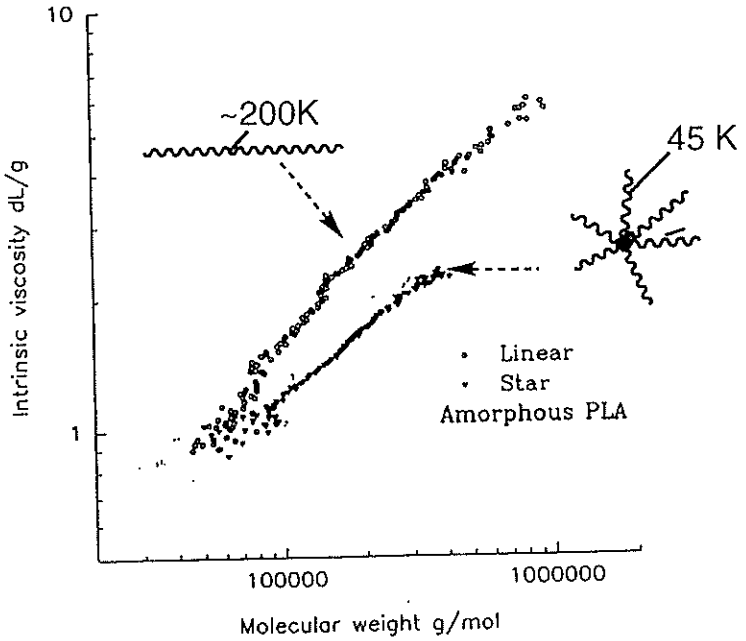

$$g' = \left(\frac{[\eta]_{br}}{[\eta]_l}\right)_M$$

$$g' = g^{\varepsilon}$$

$$g = \left(\frac{\langle R^2_g \rangle_{0,br}}{\langle R^2_g \rangle_{0,l}}\right)_M$$

Number of Arms

	g'	Number of arms, f (Calculated)		
	(Experimental)	ε=0.6	ε=0.7	ε = 1.0
A	0.66	8.8	7.6	5.8
A/SXc	0.70	7.6	6.7	5.2
SXc	0.81	5.2	4.7	3.9

$$g' = g^{\varepsilon} \qquad g = \frac{6f}{(f+1)(f+2)}$$

X-Ray Diffraction Patterns
(A vs A/SXc Stars)

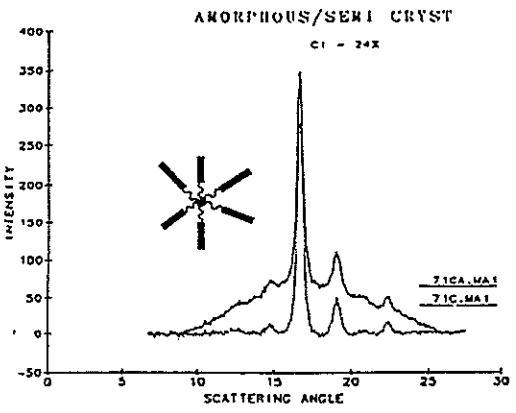

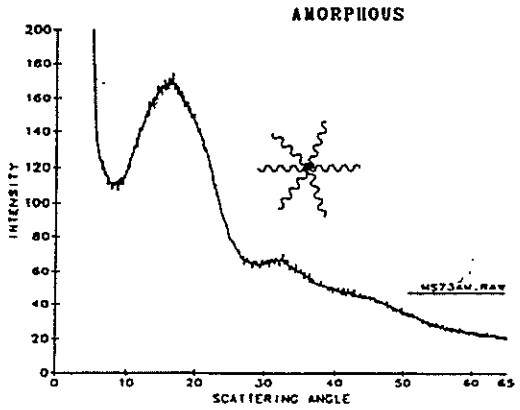

Half Crystallization Time, t1/2
(Star vs Linear PLA)

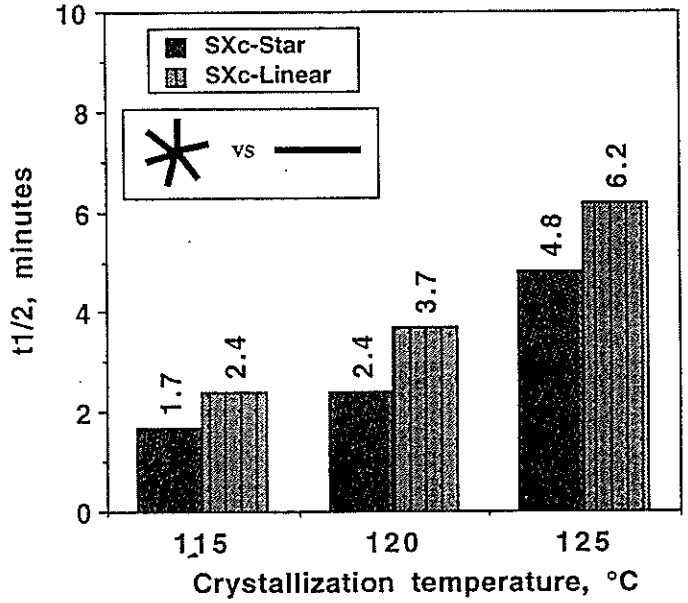

Half Crystallization Time, t1/2
(SXc vs A/SXc PLA stars)

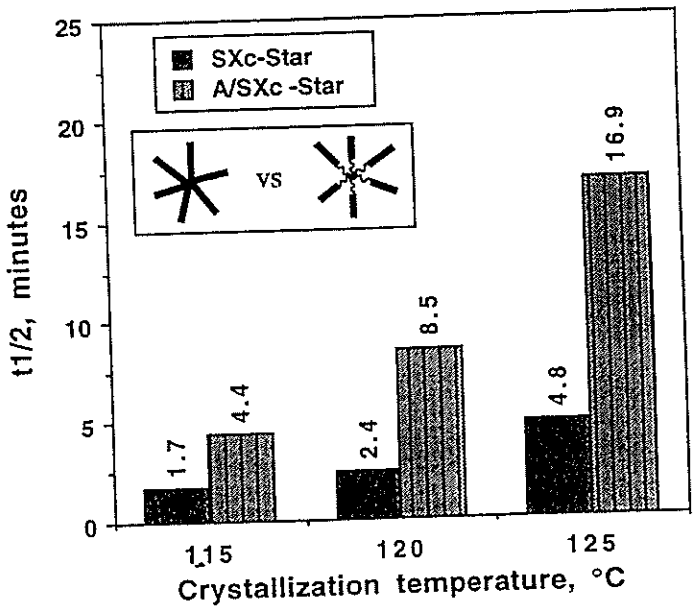

Effect of Polymer Architecture on Melt Rheology

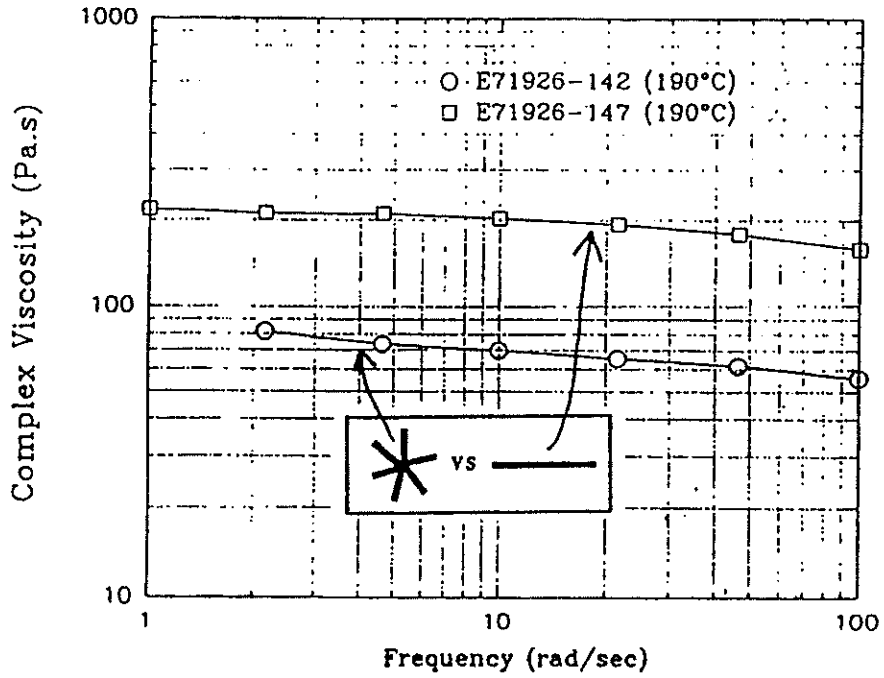

L/D-PLA Stereocomplexes

(PLA Blends)

L/D-PLA Stereocomplex Formation

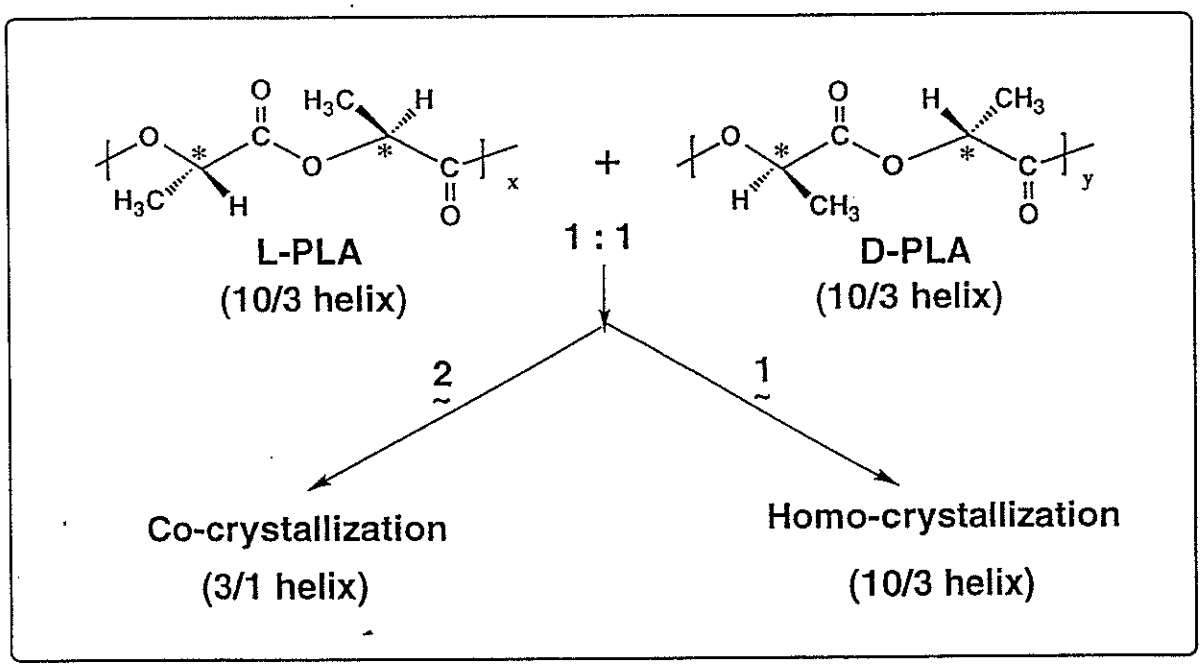

Stereocomplex - Background

1969	*P. De Santis & A. J. Kovacs, Biopolymers, 6, 299.*
1982	*B. Eling, S. Gogolewski, & A. J. Pennings, Polymer, 23, 1587*
1988-1990	*J. Murdoch & G. L. Loomis, Polylactide Compositions US Patents - 4,719,246 - 4,766,182 - 4,800,219 - 4,902,515*
1988	*T. Okihara et al., Bull. Inst. Chem. Res, Kyoto Univ., 66, 271.*
1990	*W. Hoogsteen, A.R. Postema, A.J. Pennings, G.Brinke, and P. Zugenmaier, Macromolecules, 23, 634.*
1991	*T. Okihara et al., J. Makromol. Sci.-Phys., B(30), 119-140.*
1991-1994	*Y. Ikada et al., Macromolecules*

PLA Molecular Conformation

3/1 helix	10/3 helix
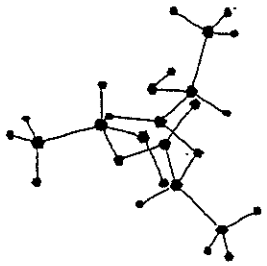	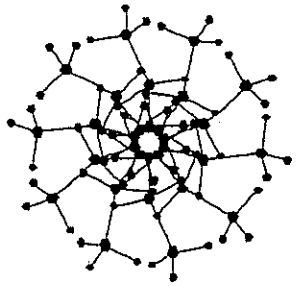
120° rotations/residue $d_{interchain} < 0.4Å$	108° rotations/residue

Preparation of L/D-PLA Stereocomplex

I. Polymer blends

- **Solution blending**
  - Solvent removal
- **Melt blending**
  - Thermal degradation

II. Monomer/Polymer enantiomeric blends

New Stereocomplex Approach

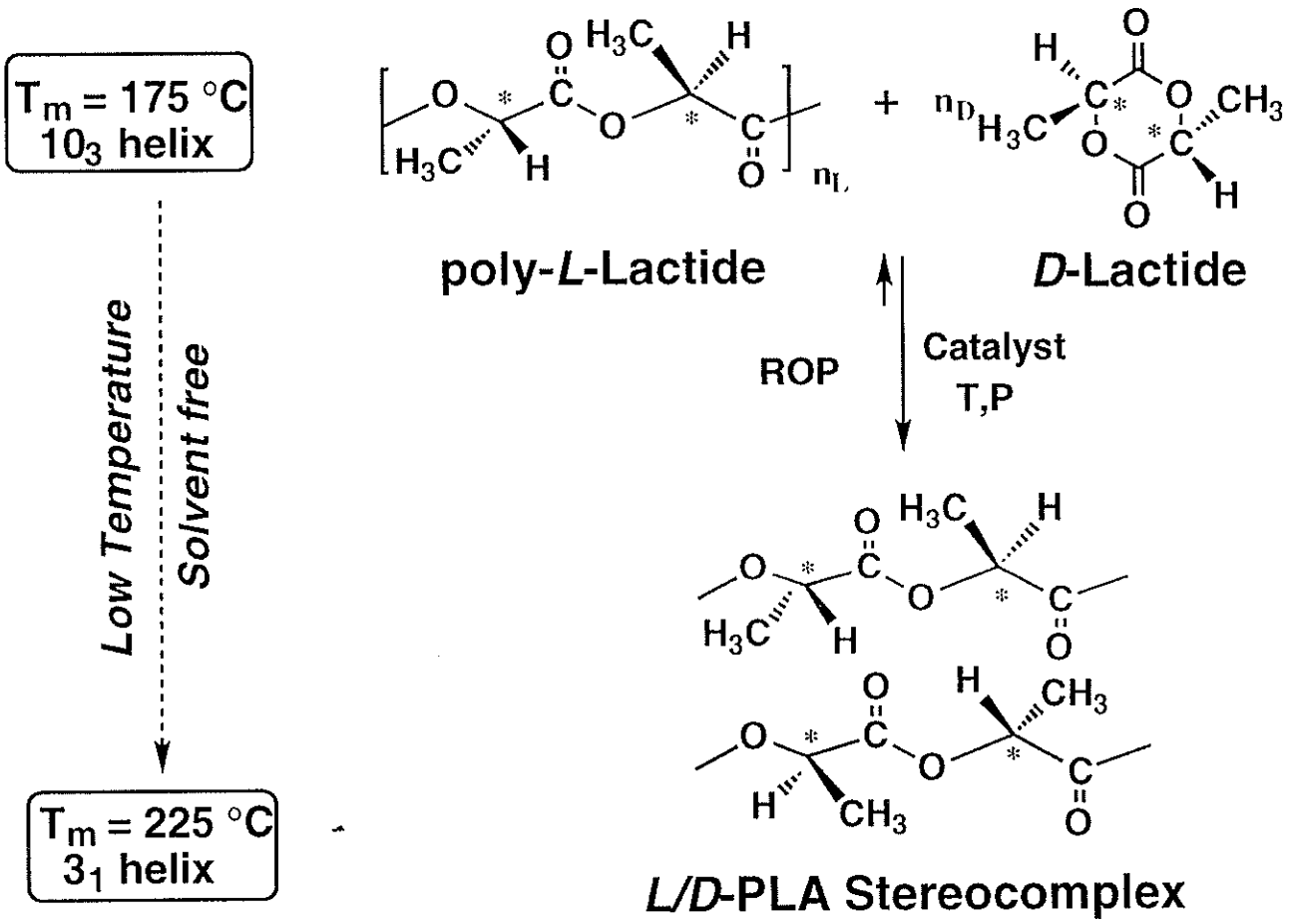

US Patent 5,317,024, M. Spinu (1994)

PVT (Pressure-Volume-Temperature) Experiments

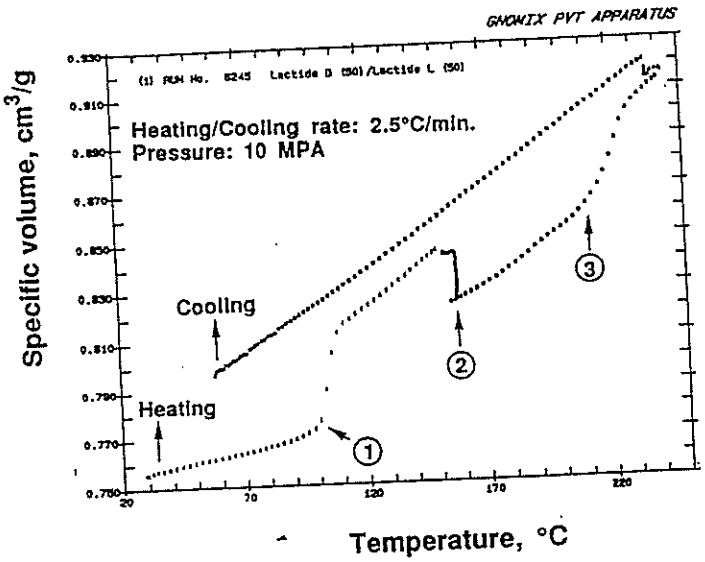

DSC scan for "in situ" generated stereocomplex

(Polymerization: 2.5 hrs @ 170 °C; 500)

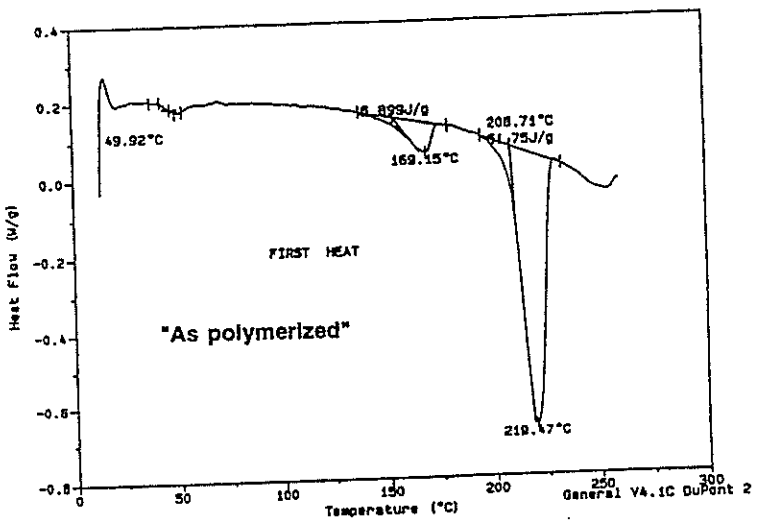

X-ray diffraction patterns

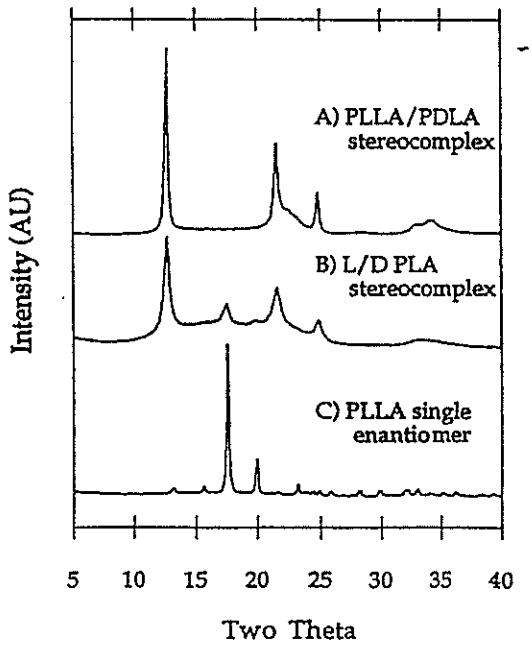

Summary

- *New materials using known characteristic features:*
  - monomer chirality
  - retention of configuration
  - "living" nature of ROP
  - no transesterifications
- *PLA materials with a broad range of properties*
  - Plastics ← → Elastomers
- *PLA with improved processability*
  - lower T_m
  - high X_c and fast $t_{1/2}$
- *Many possible combinations*

Synthesis of Silicone Polymers Via ADMET Polymerization Techniques

K. B. Wagener
University of Florida
Gainesville, FL 32611

RING OPENING VS ACYCLIC DIENE METATHESIS POLYMERIZATION

Ring Opening Metathesis Polymerization

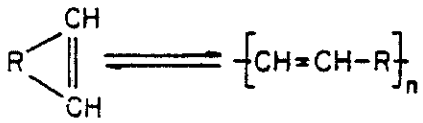

Acyclic Diene Metathesis Polymerization

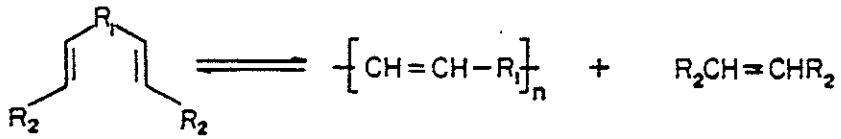

K. J. Ivin, **OLEFIN METATHESIS** (AP 1983)

ADMET DIMERIZATION

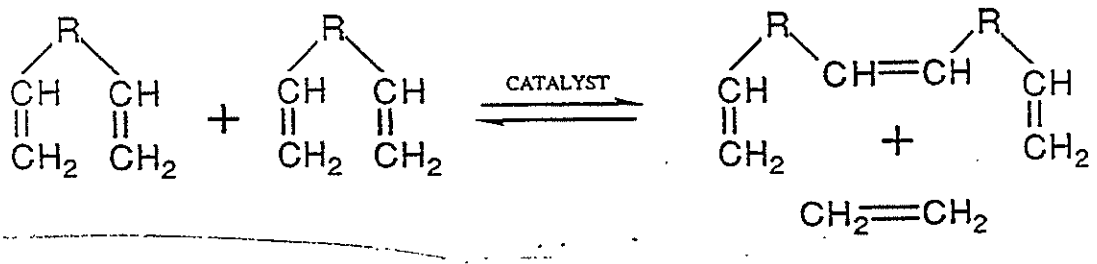

ADMET POLYMERIZATION

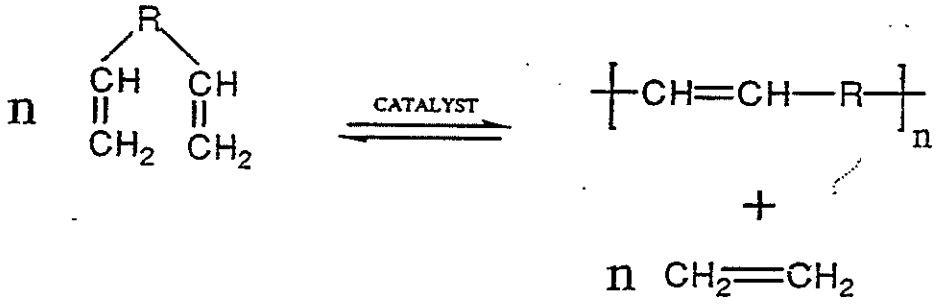

Equilibrium Step Polymerization

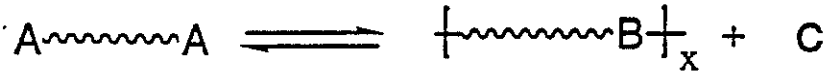

For Example :

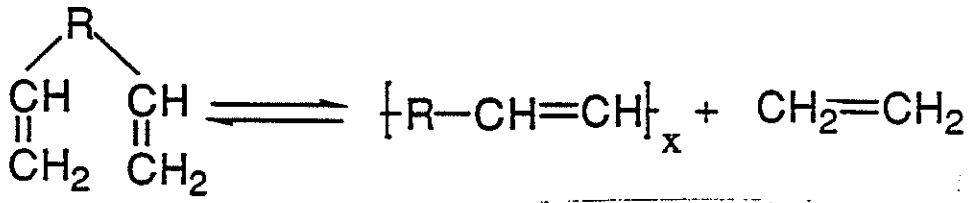

$$\overline{X}_n = \frac{1}{1 - p}$$

p	$\overline{X}_n$
0.8	5
0.9	10
0.95	20
0.99	100
0.995	200

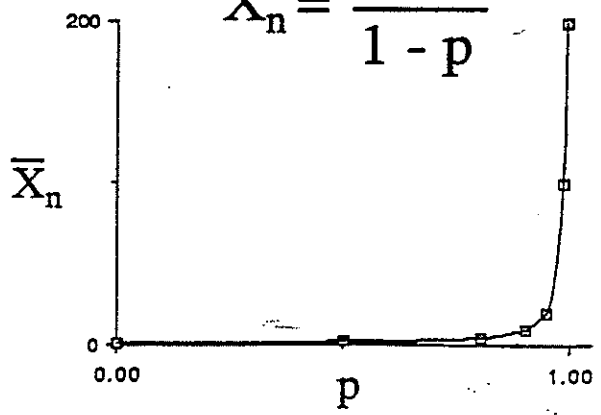

THE KEY TO ADMET CHEMISTRY

-Eliminate Acids in the Catalyst System

The Adverse Effect of Acids:
Vinyl Addition Chemistry Competes with Metathesis

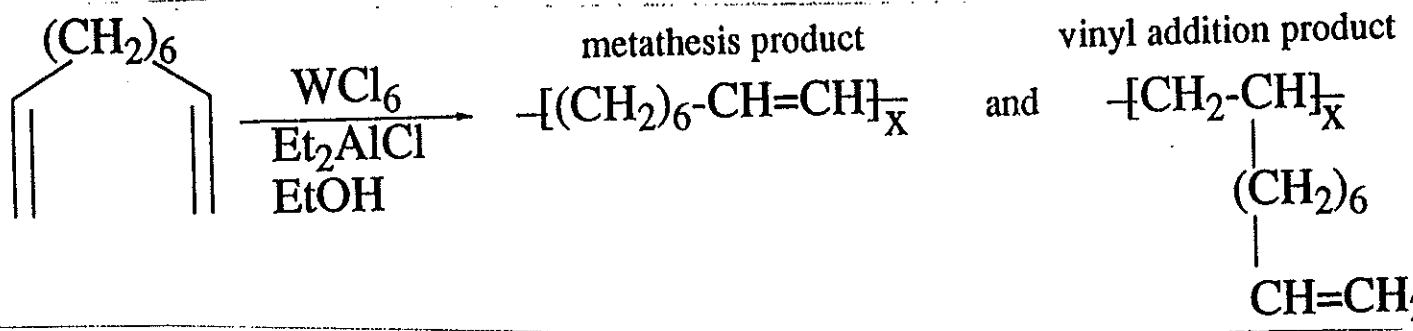

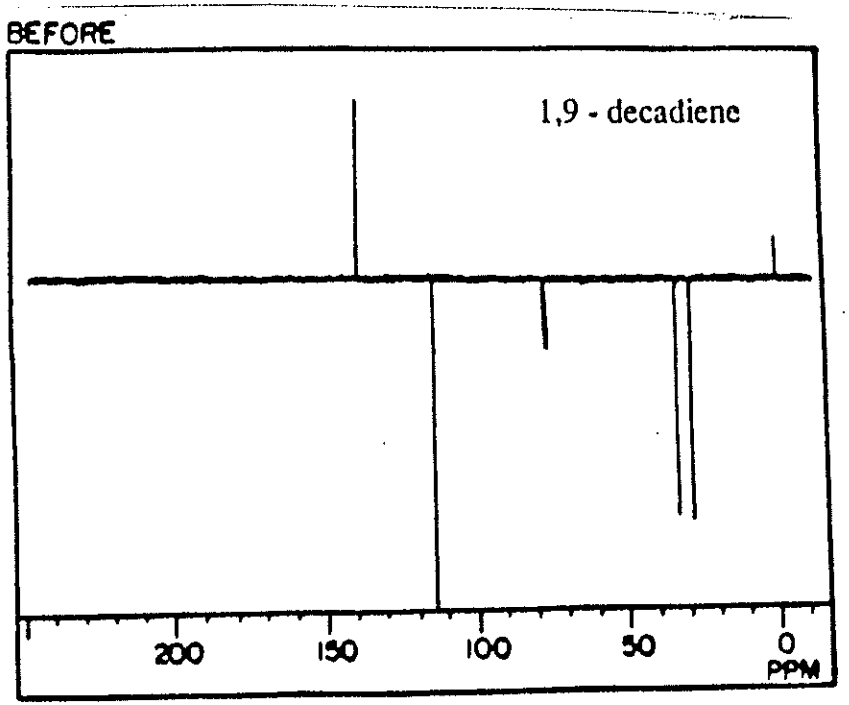

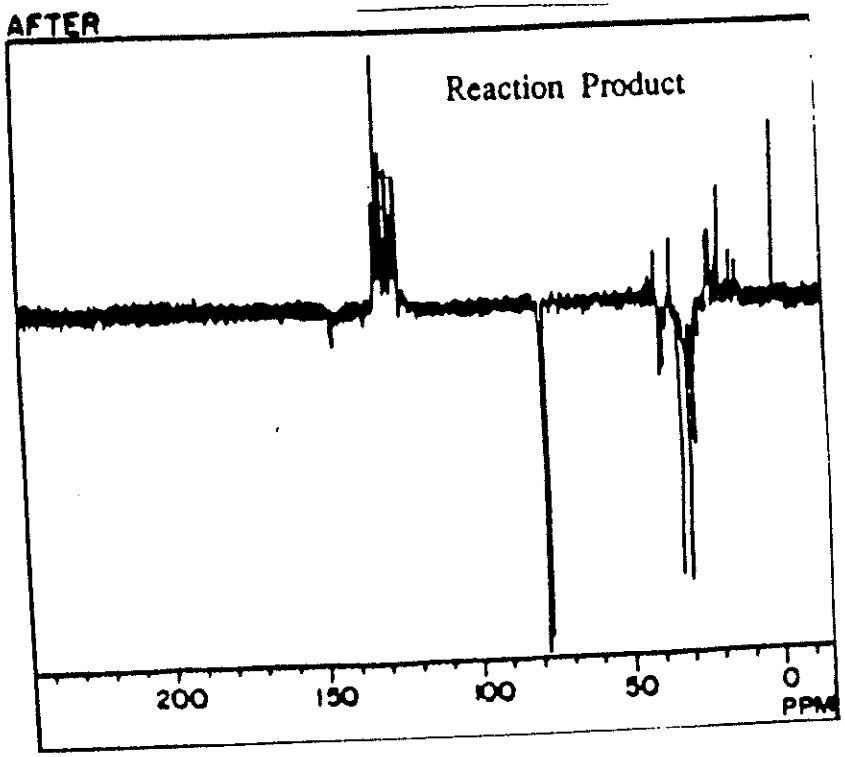

Remove Acids and Only ADMET Chemistry Occurs

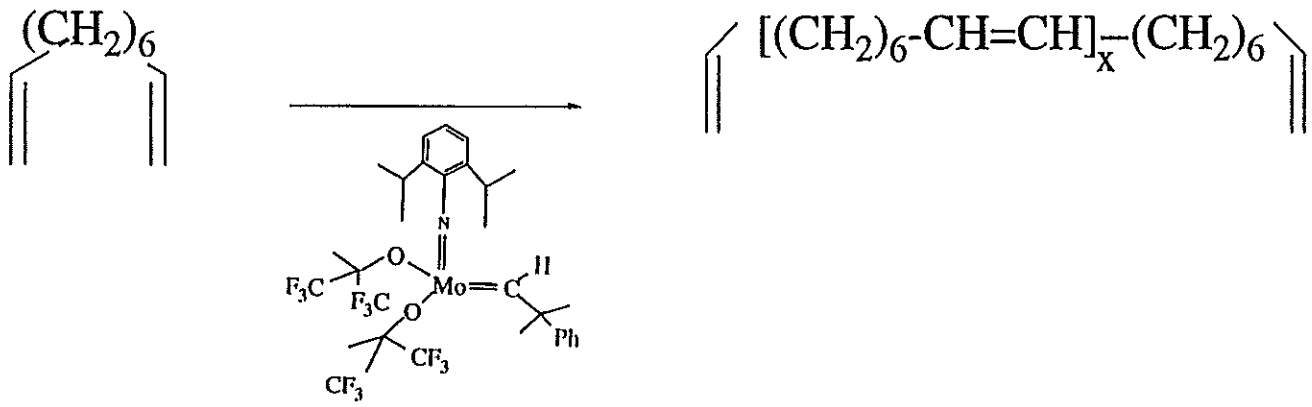

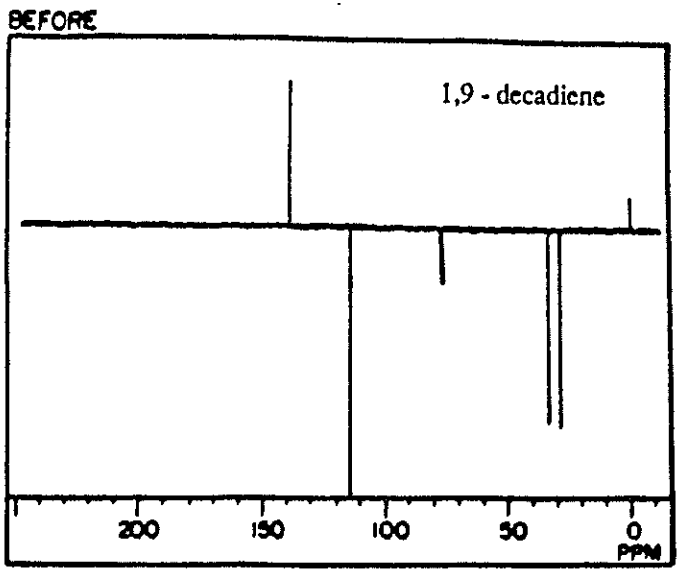

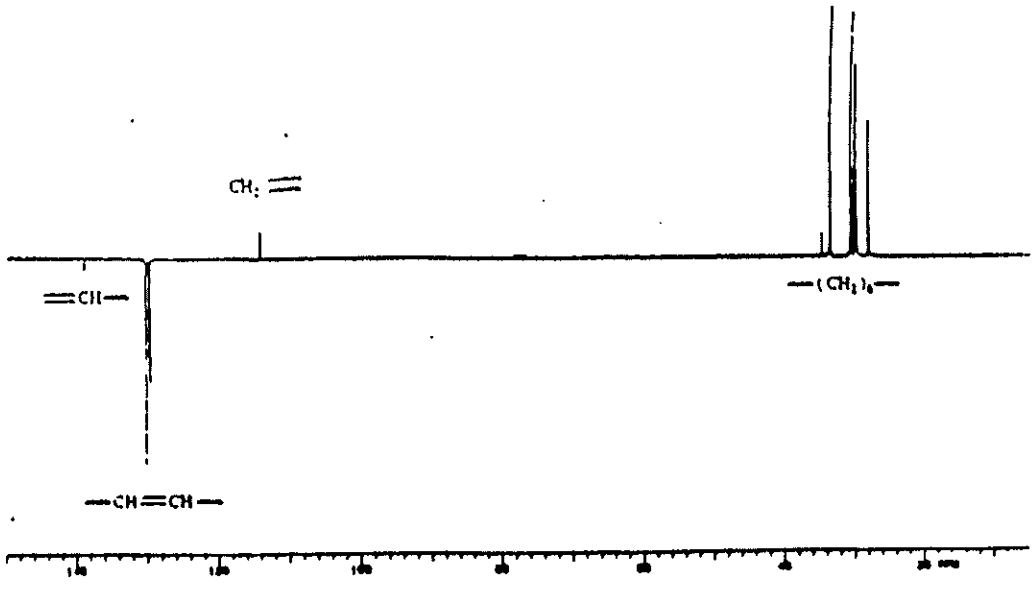

A High Molecular Weight Polymer

	%C	%H
Theory	**87.27**	**12.73**
Experimental	**87.16**	**12.68**

IV = 0.95 dl / gram

Conversion = 99+%

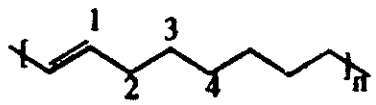

C_1 (cis) = 129.8 C_2 (cis) = 27.3 C_3 = 29.8

C_1 (trans) = 130.4 C_2 (trans) = 32.7 C_4 = 29.1

Solvent = 128

^{13}C NMR of 92% trans Polyoctenamer formed by Acyclic Diene Metathesis Polymerization

Wagener, Boncella, and Nel, **Macromolecules**, 24, 2649 (1991).

ADMET POLYMERIZATION CYCLE

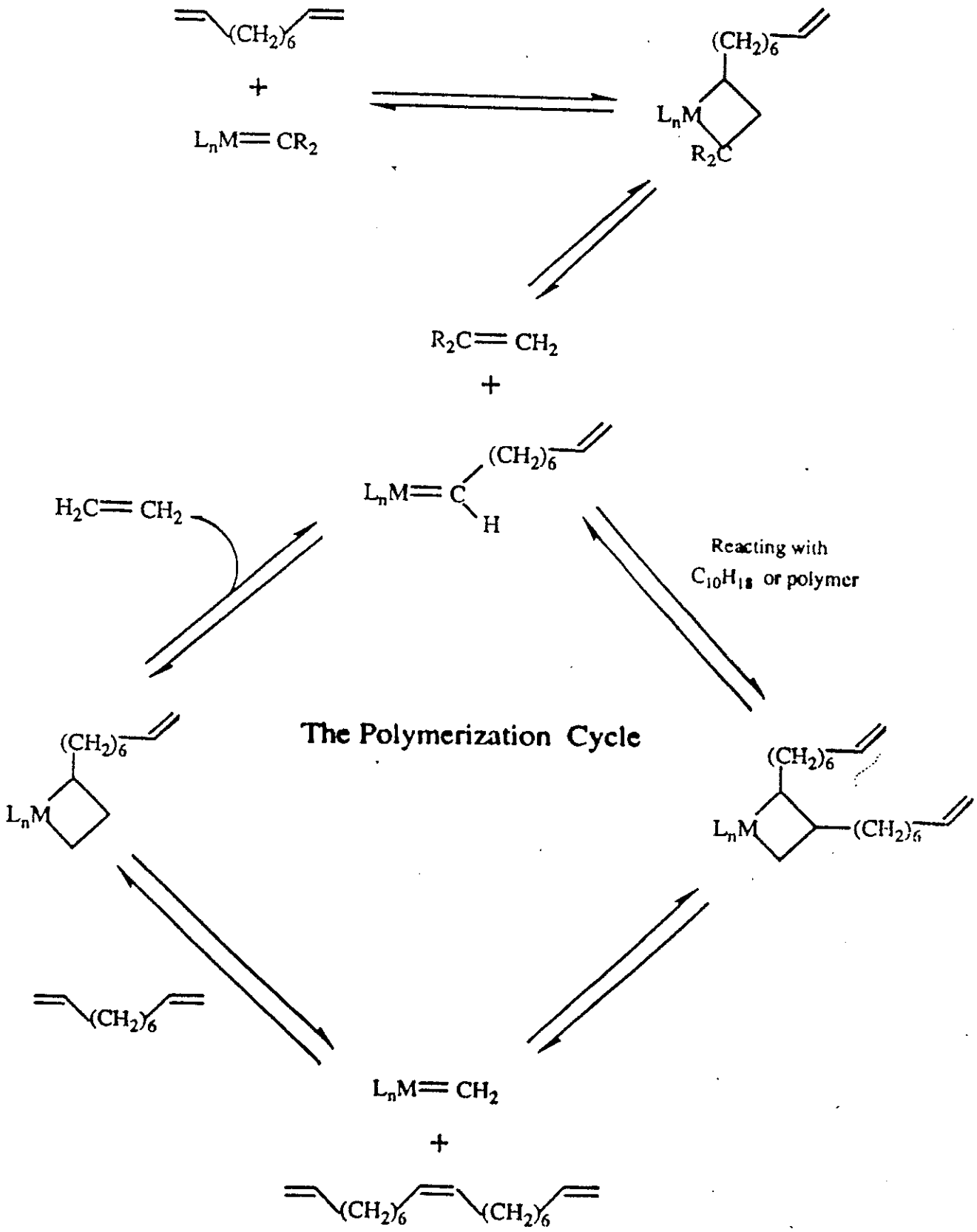

Wagener, Boncella, and Nel, **Macromolecules**, 24, 2649 (1991).

167

Heteroatom Functionality and the Negative Neighboring Group Effect

Proper "spacing" between the functional group and the metathesis olefin permits ADMET chemistry to occur.

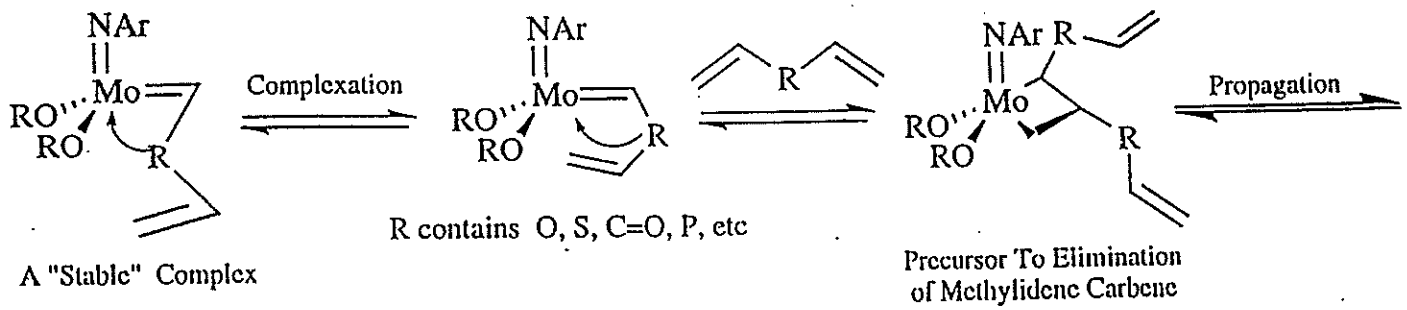

A "Stable" Complex

R contains O, S, C=O, P, etc

Precursor To Elimination of Methylidene Carbene

How the Negative Neighboring Group Effect Works

ADMET
Structure and Reactivity of Ether Containing Dienes (Brezezinska)

The Negative Neighboring Group Effect

Monomer	Reactivity? (YES or NO)
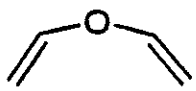	**NO**
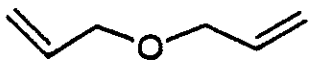	**NO**
	**Sluggish**
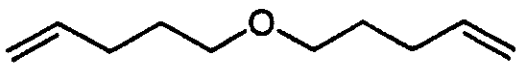	**YES**
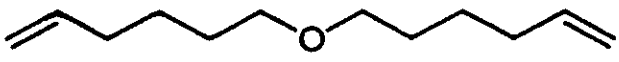	**YES**

Brzezinska and Wagener, *Macromolecules*, **24**, 5273 (1991).

Wagener, Brzezinska and Bauch, *Die Makromol. Chemie*, **13**, 75 (1992).

Keeping the Negative Neighboring Group Effect In Mind, Functional Groups That Can Be Tolerated Include:

Ethers

Esters

Ketones

Carbonates

Aromatic Amines

Imides

Thioethers

Monomer to Polymer

^{13}C NMR Bis(4-pentenyl)sulfide

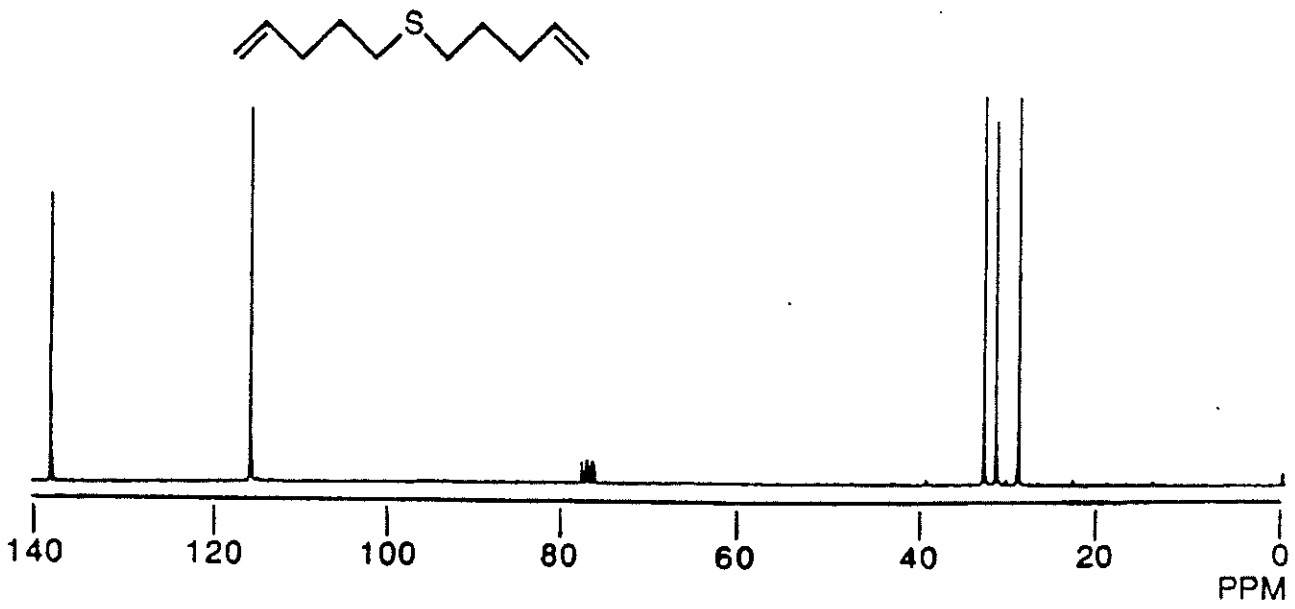

^{13}C NMR "Crude" Polymer

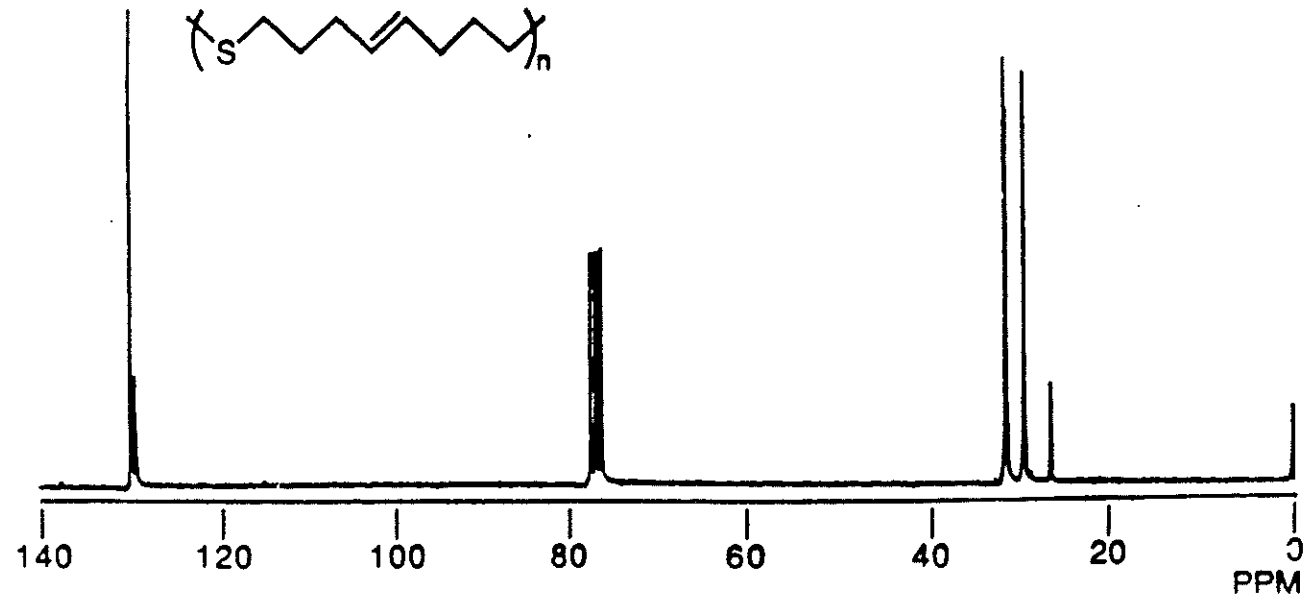

John O'Gara, Jason Portmess, & K. B. Wagener, **Macromolecules**, 26, 2837 (1993).

CARBOSILANES

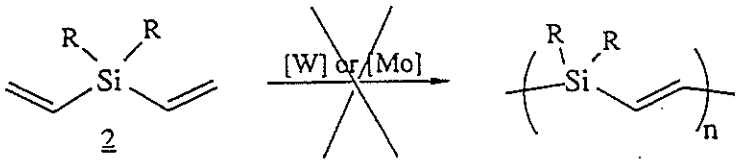

2

Divinylsilane resistance to ADMET, where R = Me (2) or Ph.

Figure 7

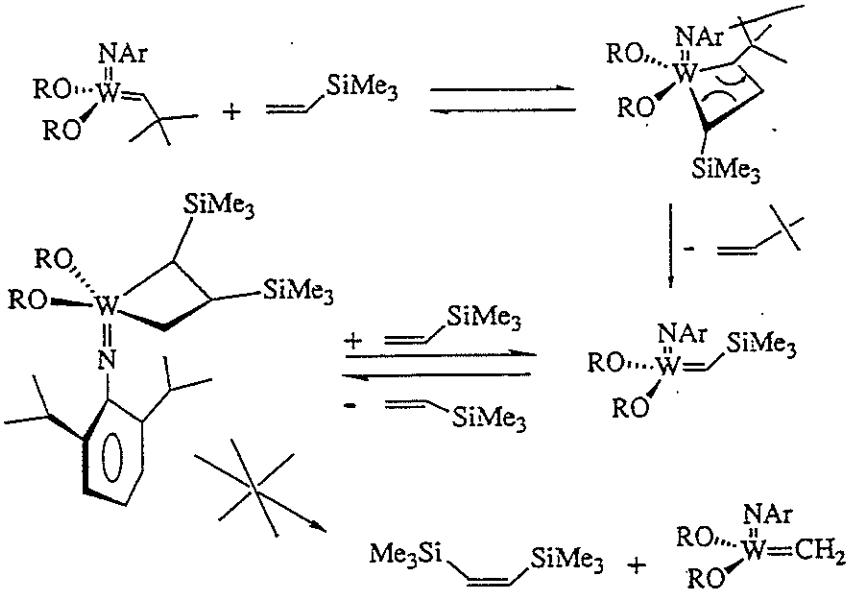

Schrock's VinylTMS Study (R=CMe(CF3)2).

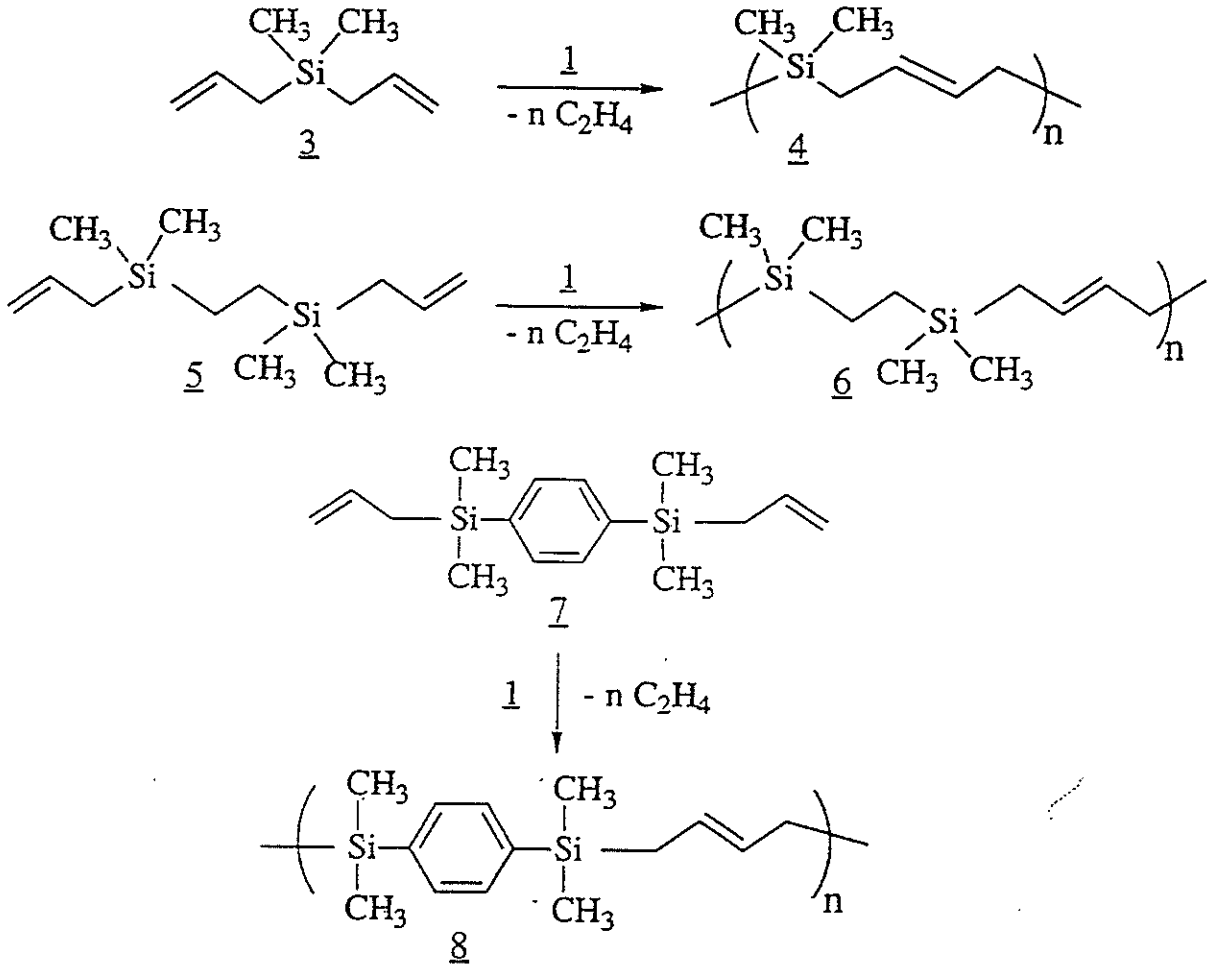

Polycarbo(dimethyl)silanes produced by acyclic diene metathesis (ADMET) polymerization of bis(allyl)carbosilanes.

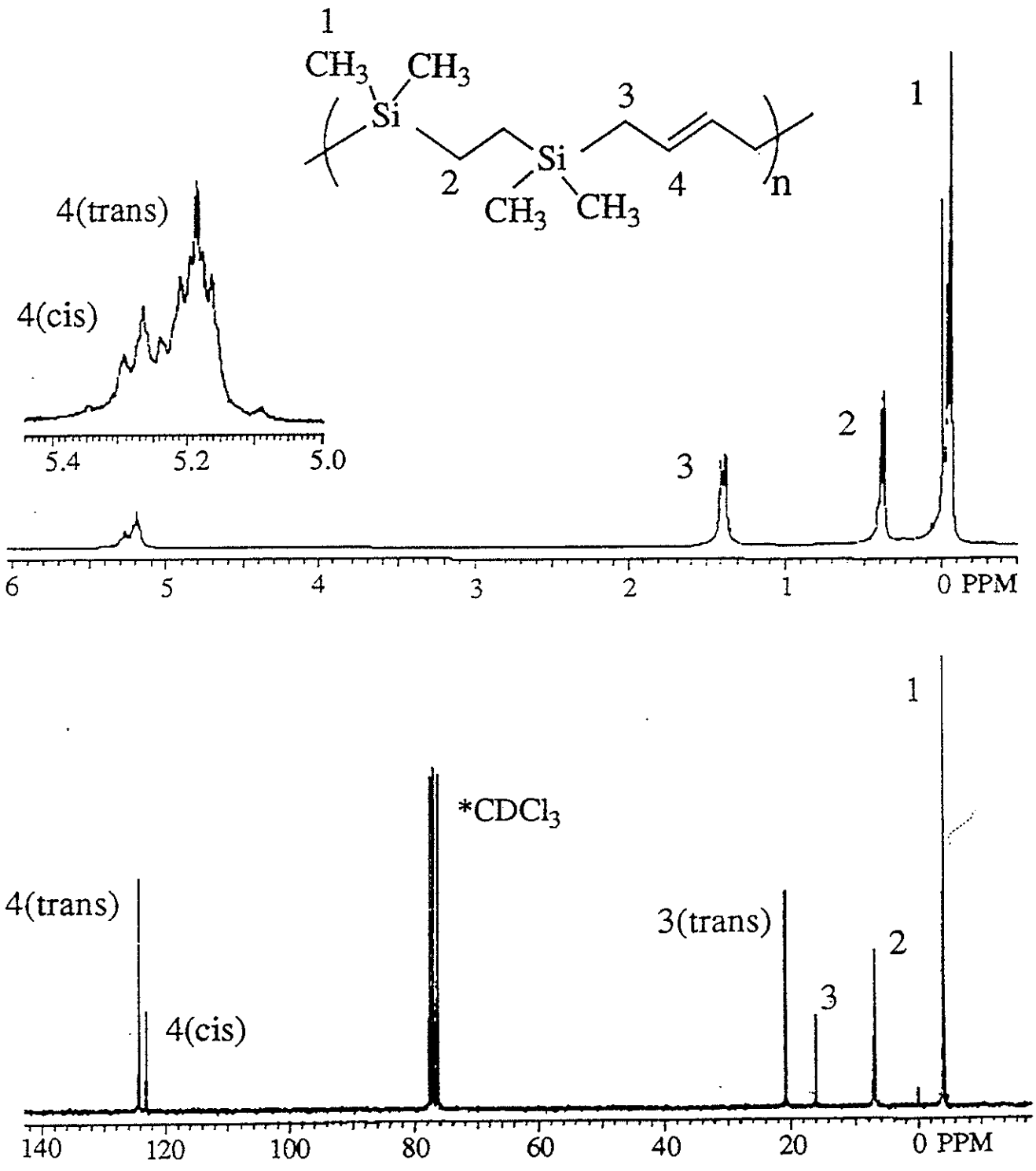

200-MHz ^{1}H and 50-MHz ^{13}C NMR spectra of high molecular weight 73 % *trans* polymer 6 final reaction mixture.

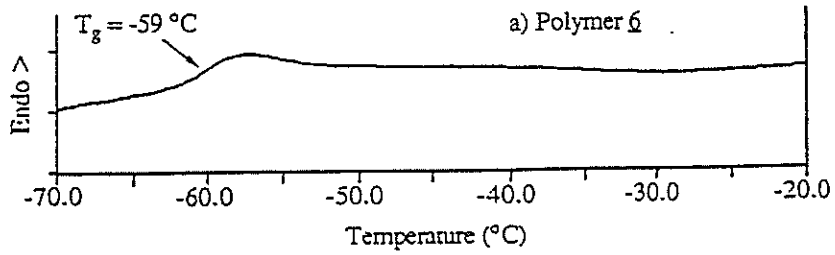

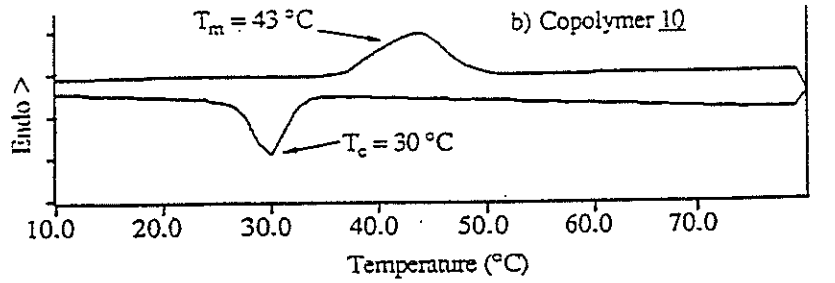

Differential scanning calorimetry (DSC) thermogram of a) polymer 6 at (10 °C/min) and b) copolymer 10 (10 °C/min).

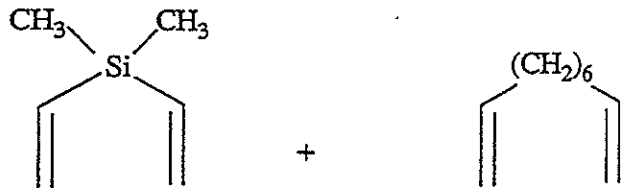

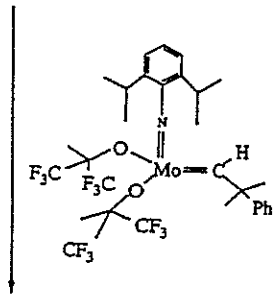

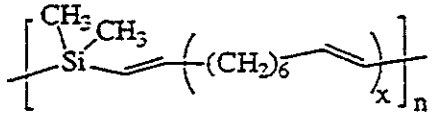

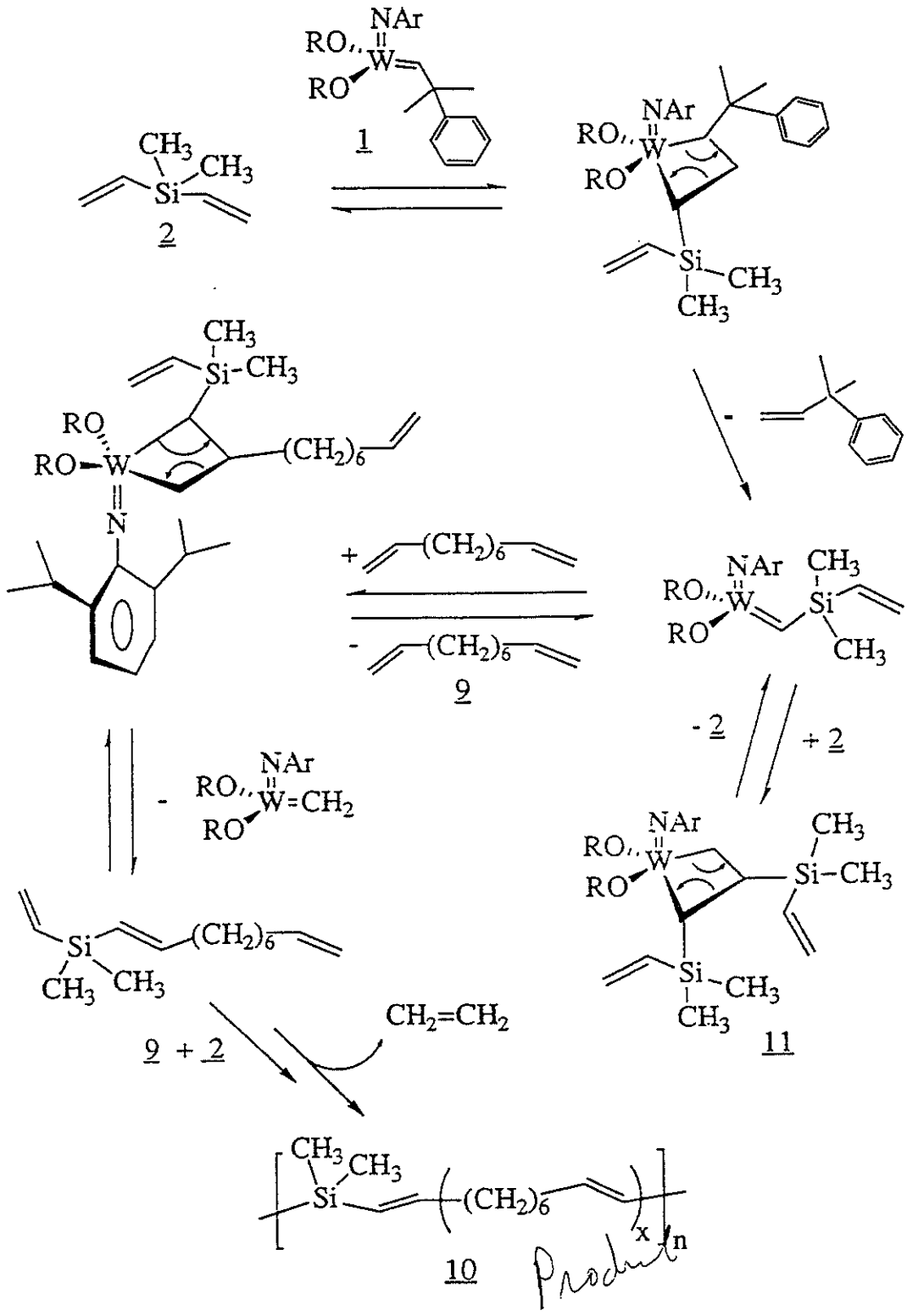

Monomer specific copolymerization of dimethyldivinylsilane (2) and 1,9-decadiene (9) (R = $CMe(CF_3)_2$).

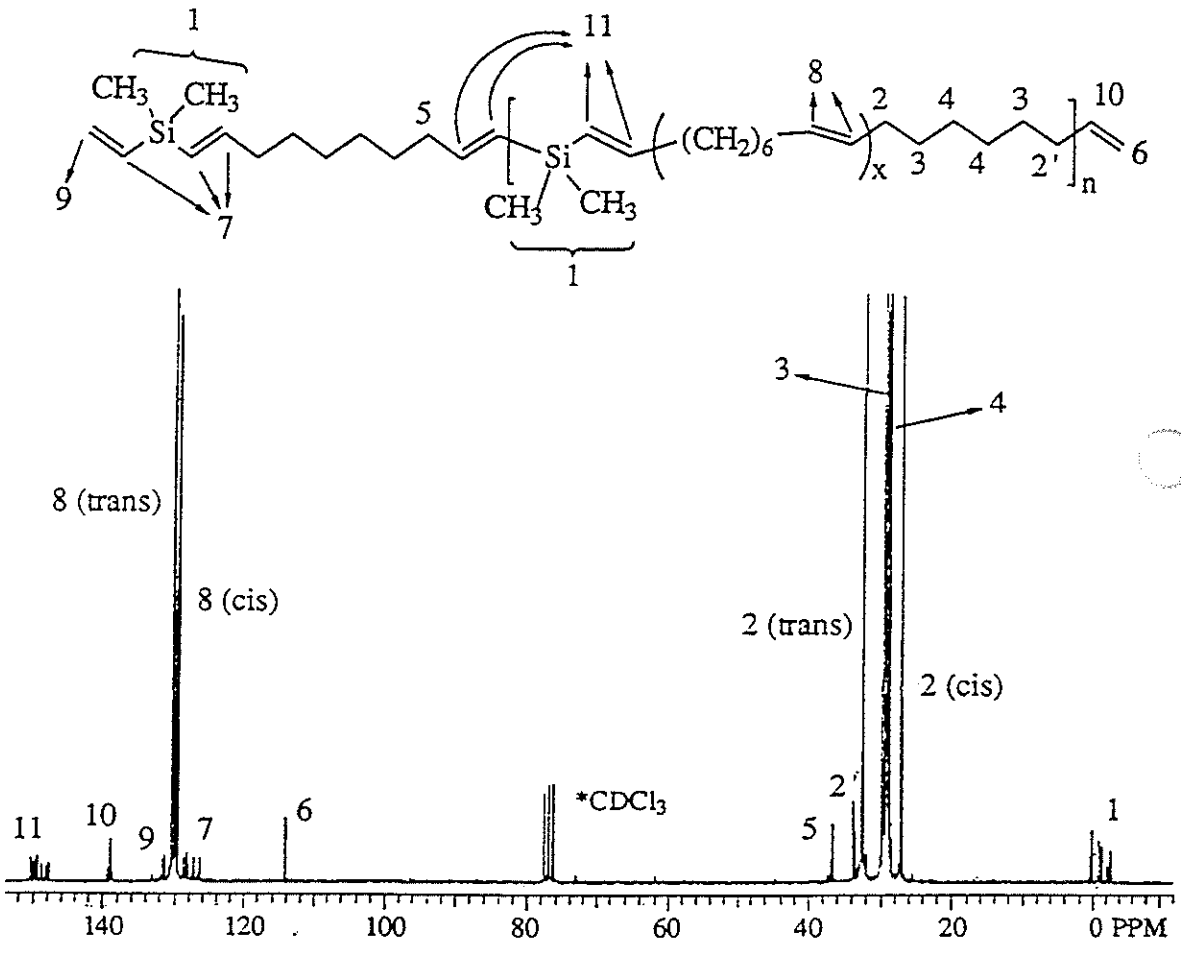

Quantitative 50 MHz ^{13}C NMR spectra for copolymer 10.

CARBOSILOXANES

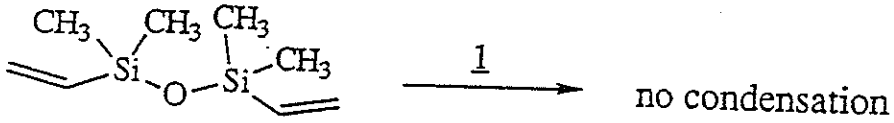

Bis(vinyl)tetramethyldisiloxane fails to polymerize via ADMET.

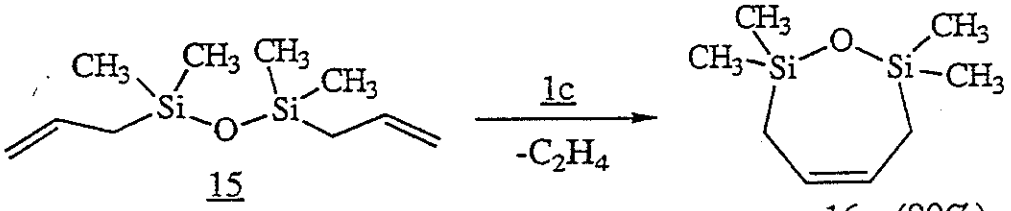

Exculsive metathesis cyclization condensation of bis(allyl)disiloxane.

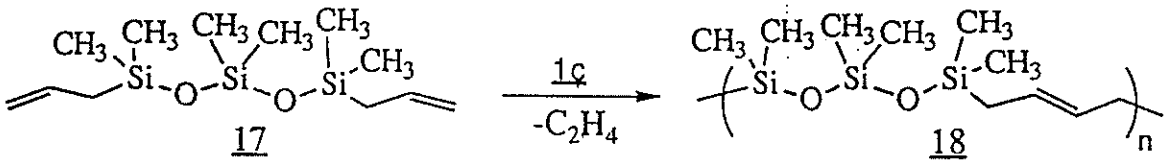

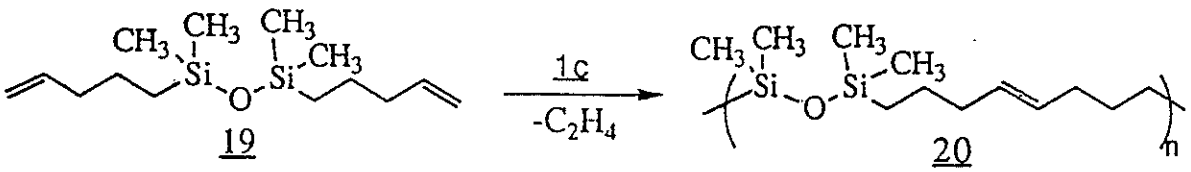

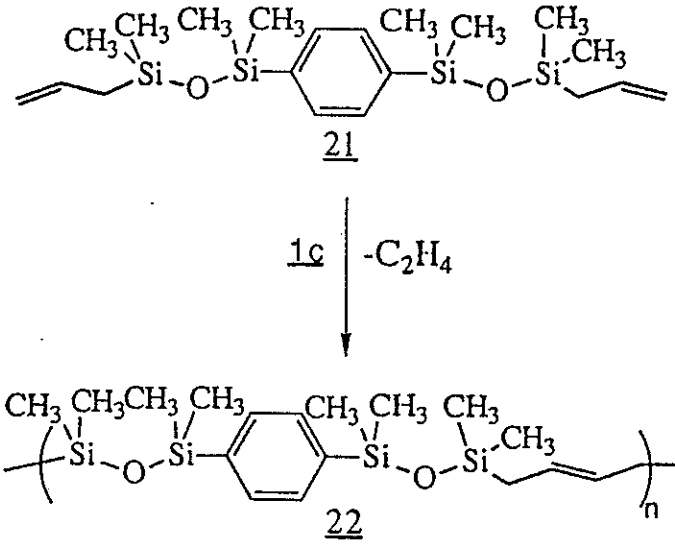

ADMET polymerization of carbosiloxadienes.

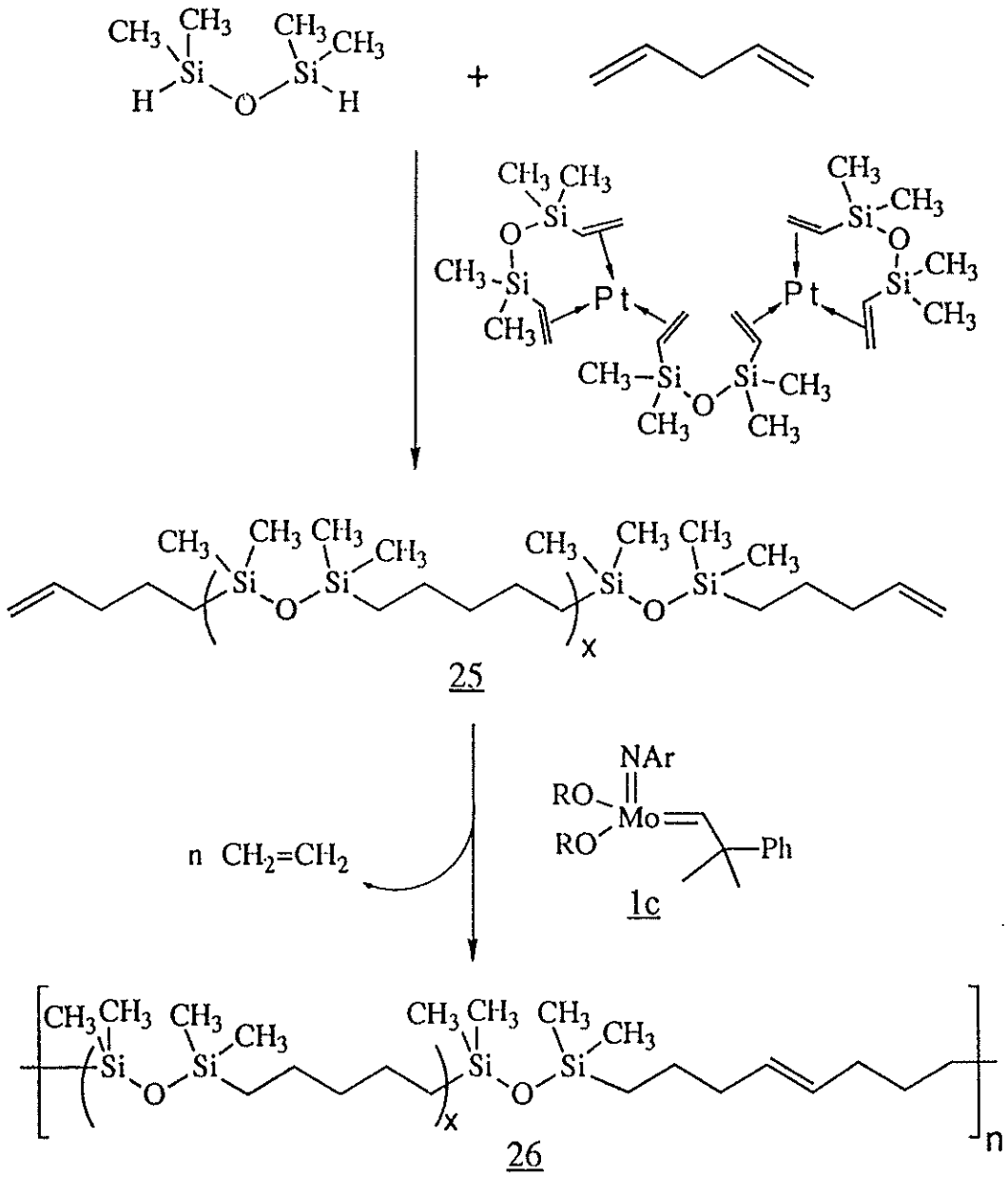

25

1c

26

Synthesis of α,ω-telechelomer 25 and resulting polymer 26.

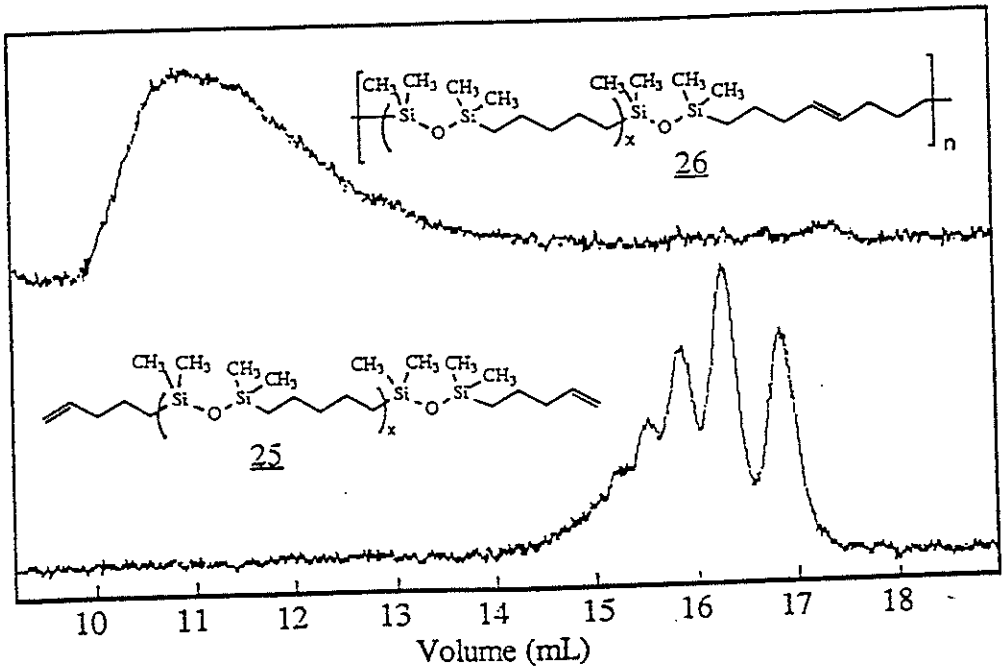

Gel permeation chromatography (GPC) of α,ω-telechelomer 25 and resulting polymer 26.

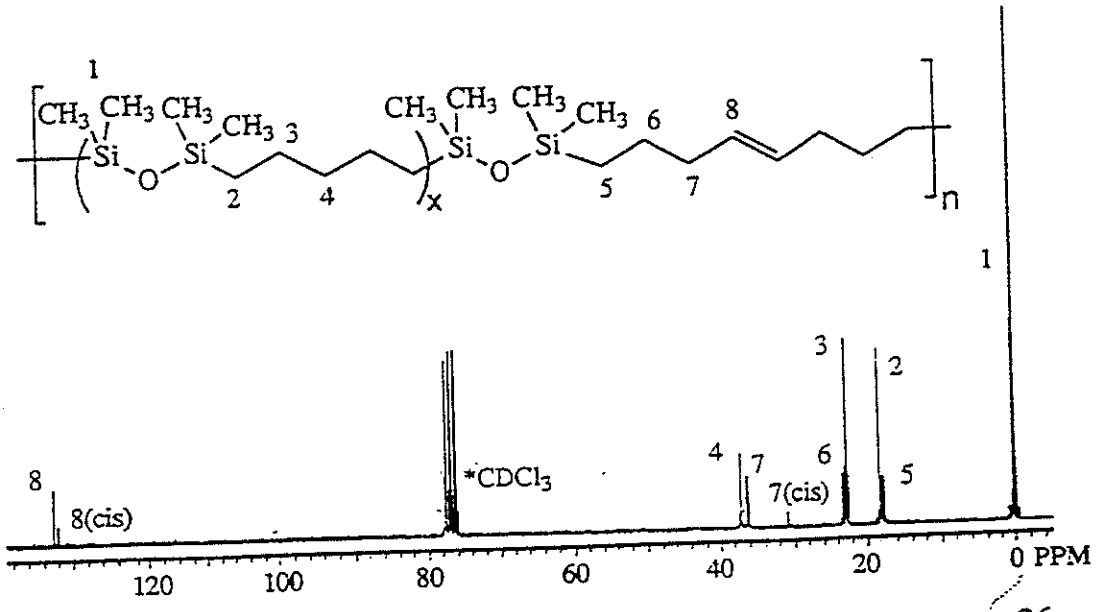

Quantitative 50 MHz ^{13}C NMR spectrum of polymer 26.

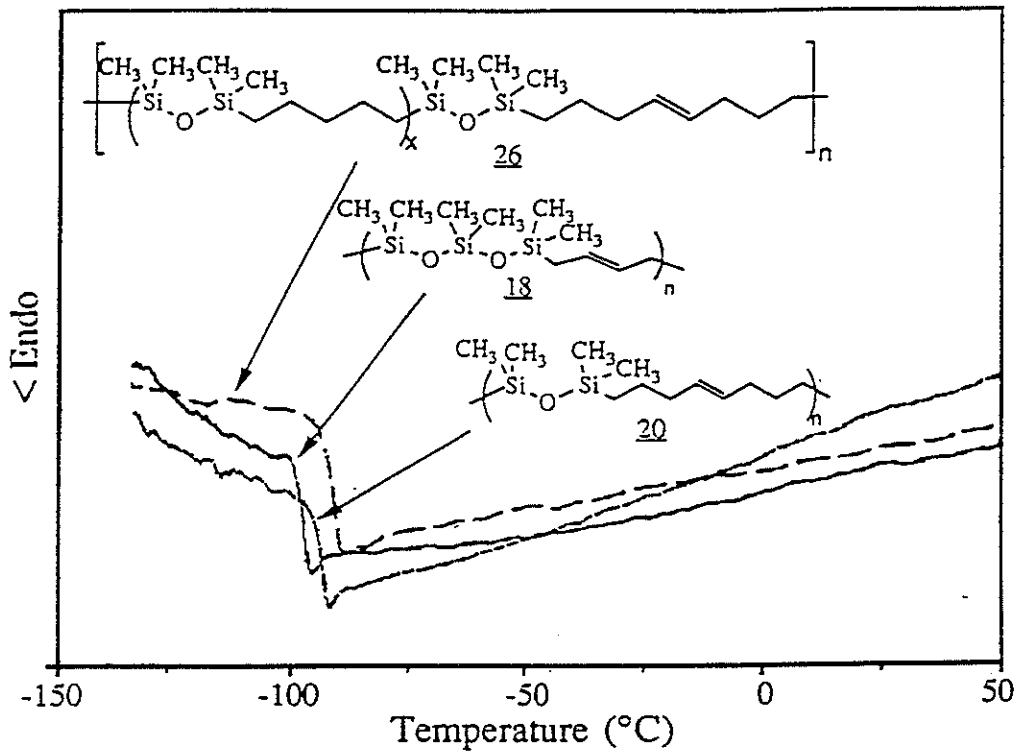

Differential scanning calorimetry (DSC) of polymers 18, 20, and 26: scan rate 10 °C/min.

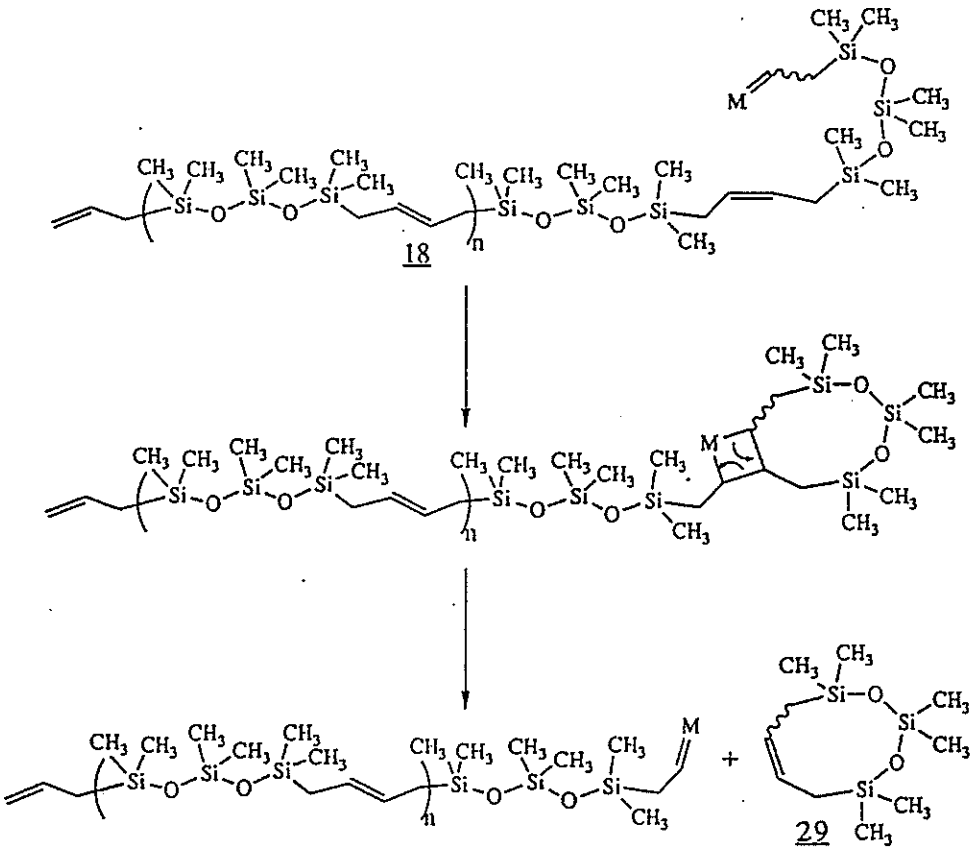

Back biting mechanism for formation of cyclic dimer 29 from polymer 18. M = Mo(N-2,6-C_6H_3-*i*-Pr_2)[OCMe(CF_3)$_2$]$_2$.

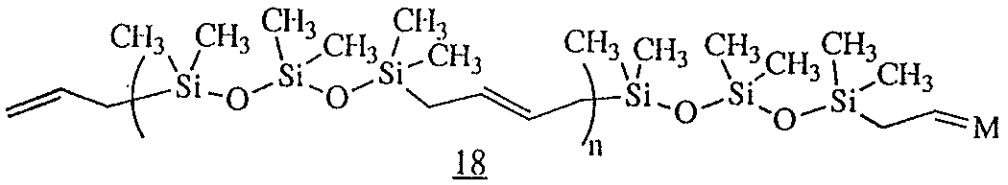

18

Bulk
Vacuum
5 hours
7 mol% 29
(80% 29a)

Benzene solution
Argon
5 minutes
36 mol% 29
(>99% 29a)

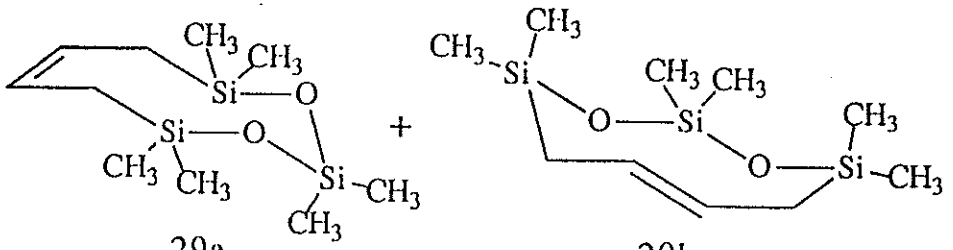

29a + 29b

Preparation of *cis* (29a) and *trans* (29b) cyclic back biting product 29 from polymer 18. M = Mo(N-2,6-C_6H_3-*i*-Pr_2)[OCMe(CF_3)$_2$]$_2$.

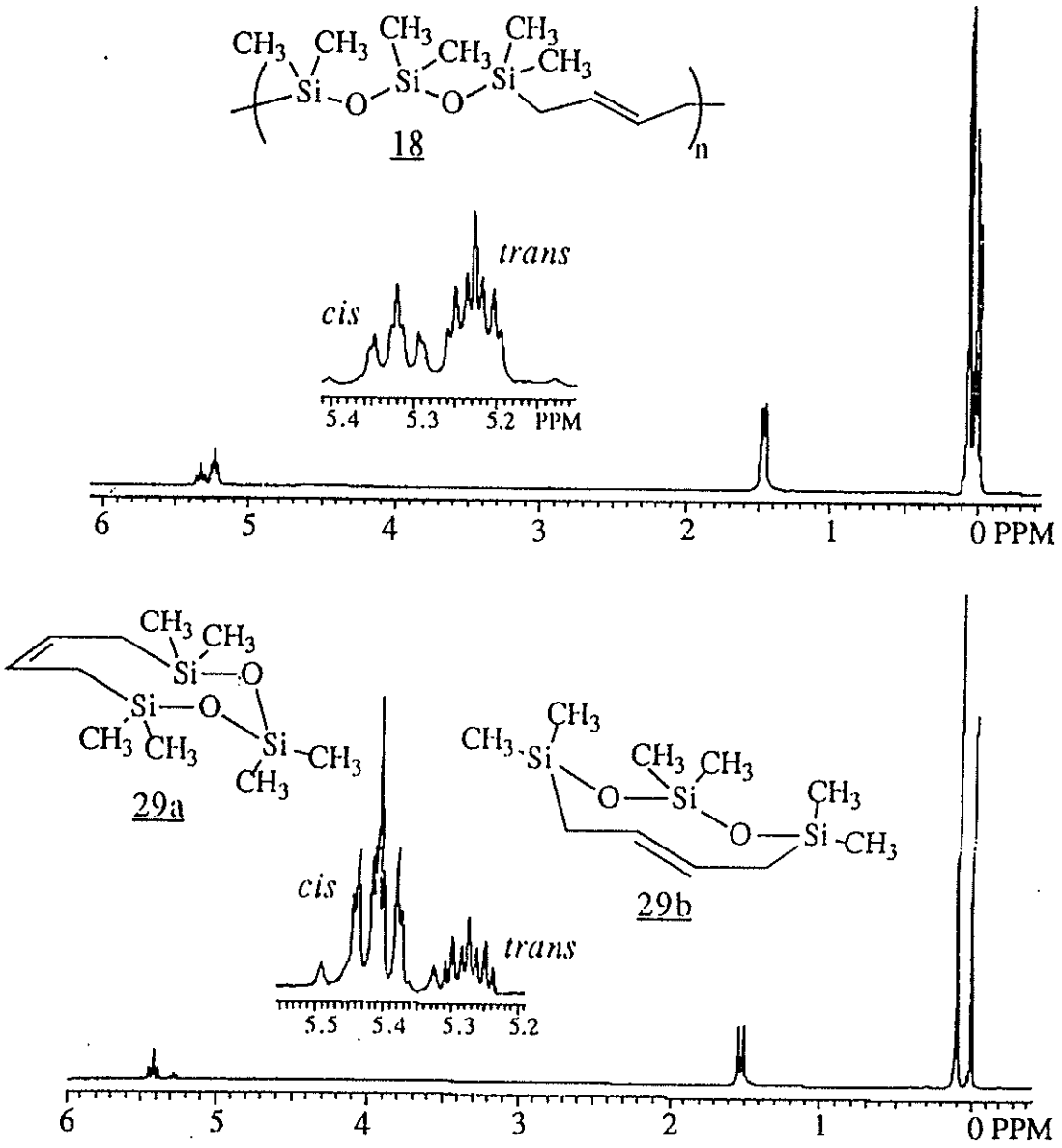

200 MHz ^{1}H NMR spectra of cyclic 65 % *trans* polymer 18 and isomeric mixture of byproduct 29.

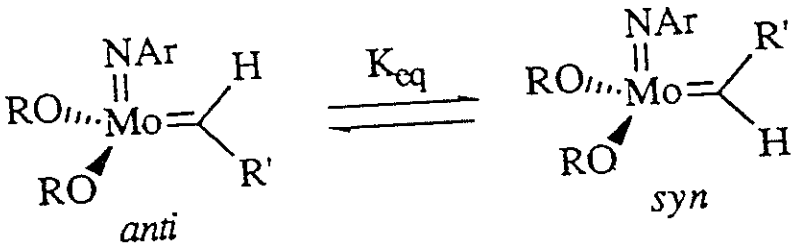

Anti and *syn* rotamers for a molybdenum alkylidene.

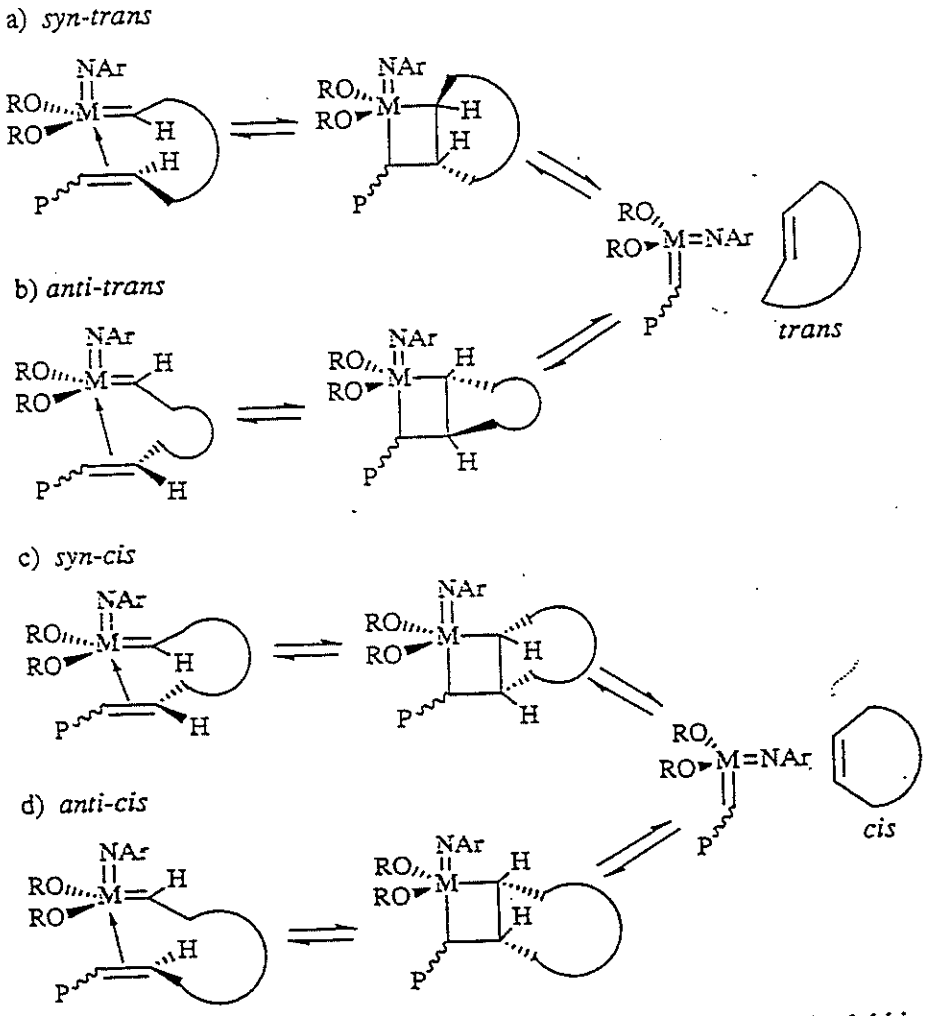

Generalized geometries for intermediates participating in back biting reactions, where M = Mo, R = $CMe(CF_3)_2$ and P = Polymer.

Sigma-Pi Conductive Hybrid Silicon Polymers

Monomer Synthesis – p–bromostyrenes

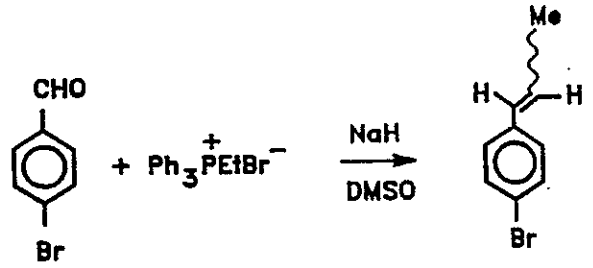

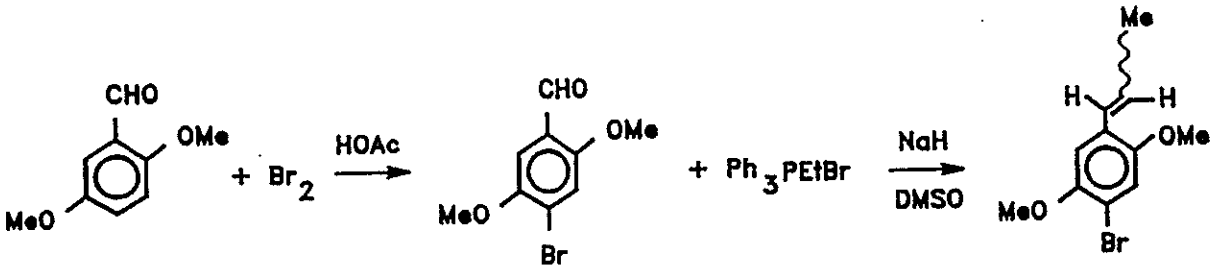

Miller 3-30-95

Oligosilanes

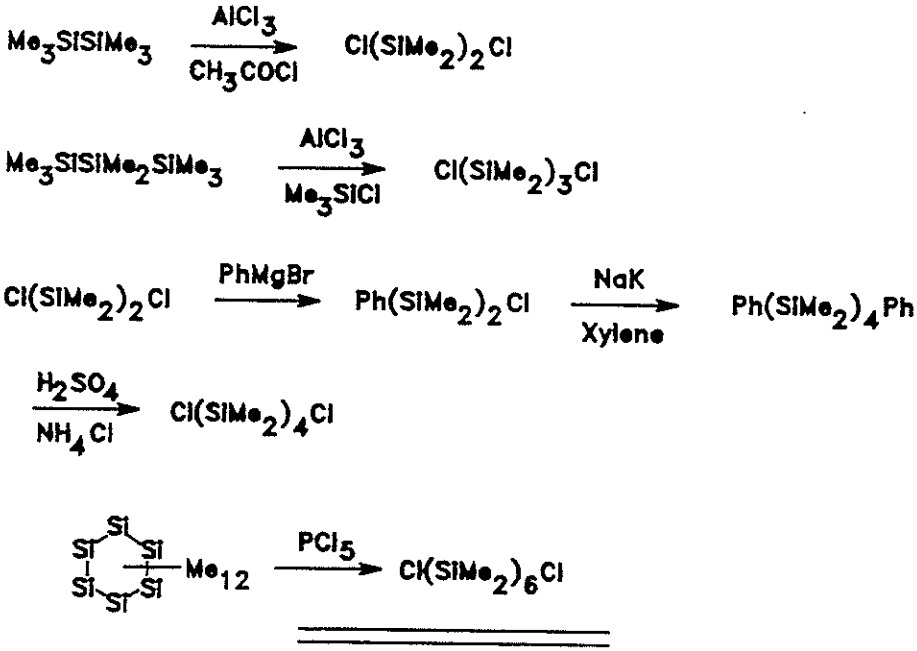

$\sigma-\pi$ Monomers

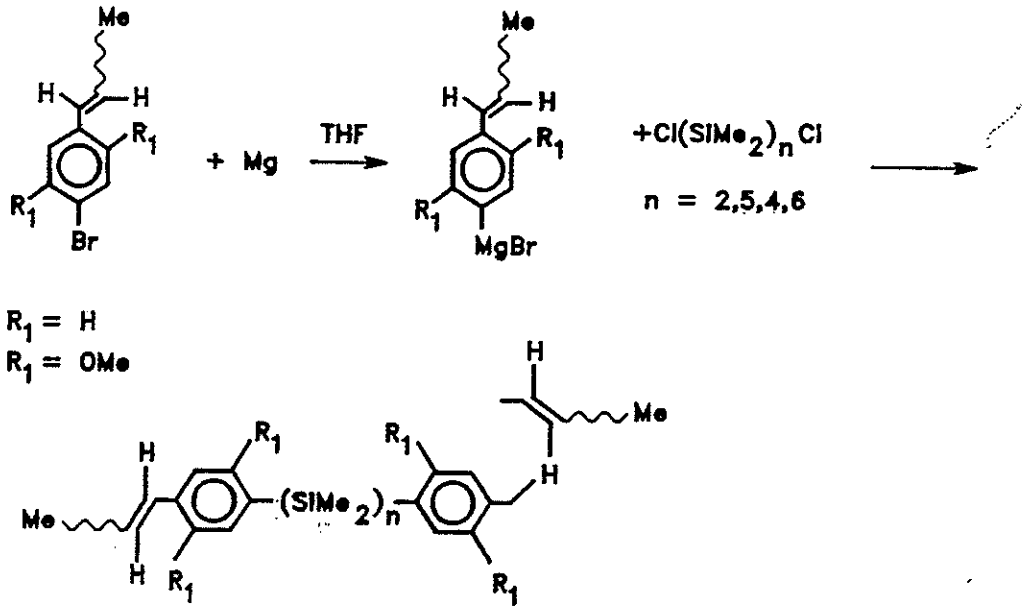

Miller 3-30-95

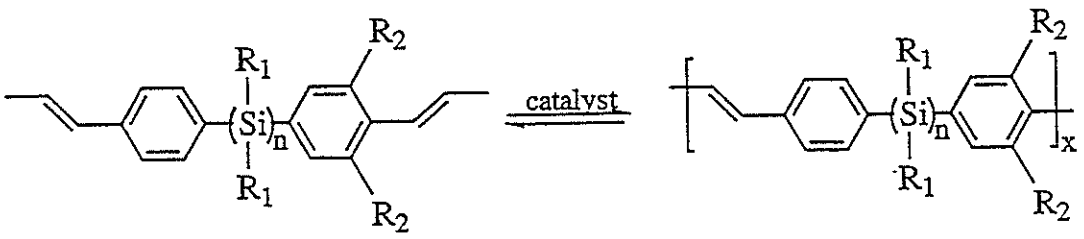

A σ–π Conjugated Hybrid
Polymer System

Silicon Polymers Possessing the Reactive Si-Cl Bond

(Analogous to dichloropolyphosphazenes)

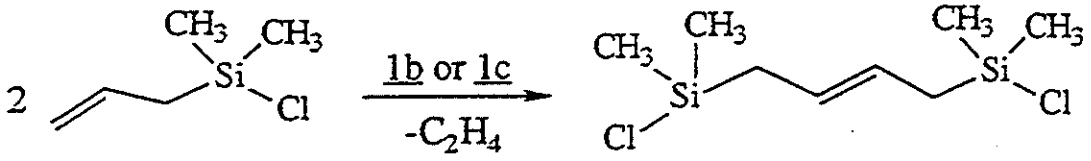

13 1b : 88% (66% *trans*)
1c : 91% (59% *trans*)

ADMET of reactive silicon functionalities.

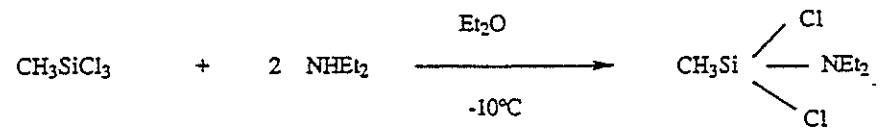

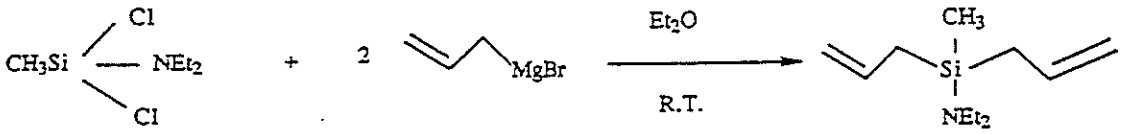

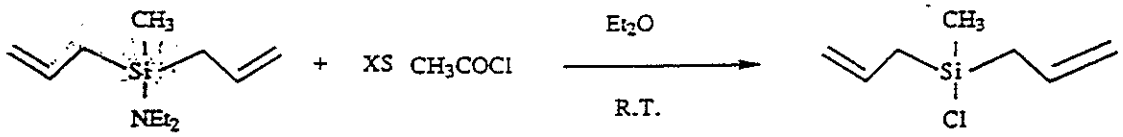

Issleib,K. Kuhne, U. Kreck, F., Phosphorus and Sulfur, 21, 367, 1985.

Burns,G., Barton, T., Journal of the American Chemical Society, 105, 2006, 1983.

ADMET OLIGOMERIZATION

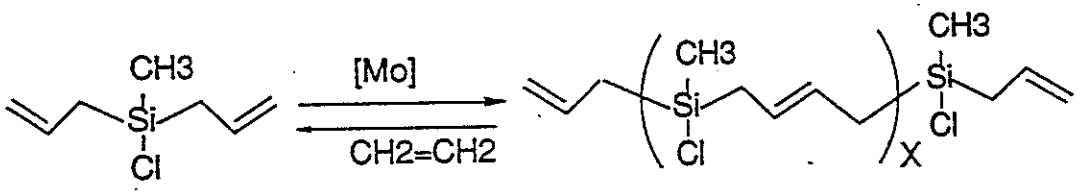

OBSERVATIONS:

Immediate bubbling

Increase in viscosity

Presence of internal olefin

Presence of 5-membered cyclic

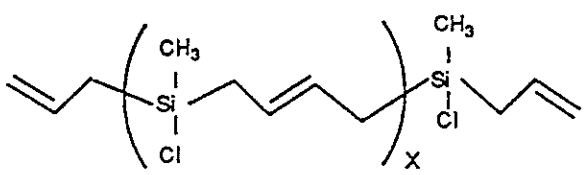
CH3
Si
Cl
X
CH3
Si
Cl

7
6
5
4
3
2
1
0
ppm

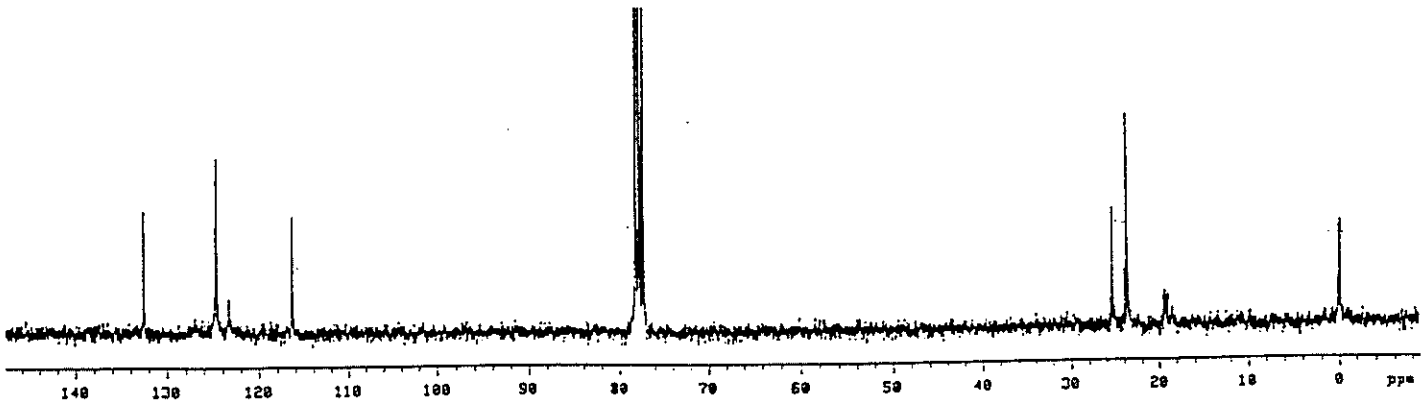
140
130
120
110
100
90
80
70
60
50
40
30
20
10
0
ppm

POLYPHOSPHAZENE CHEMISTRY

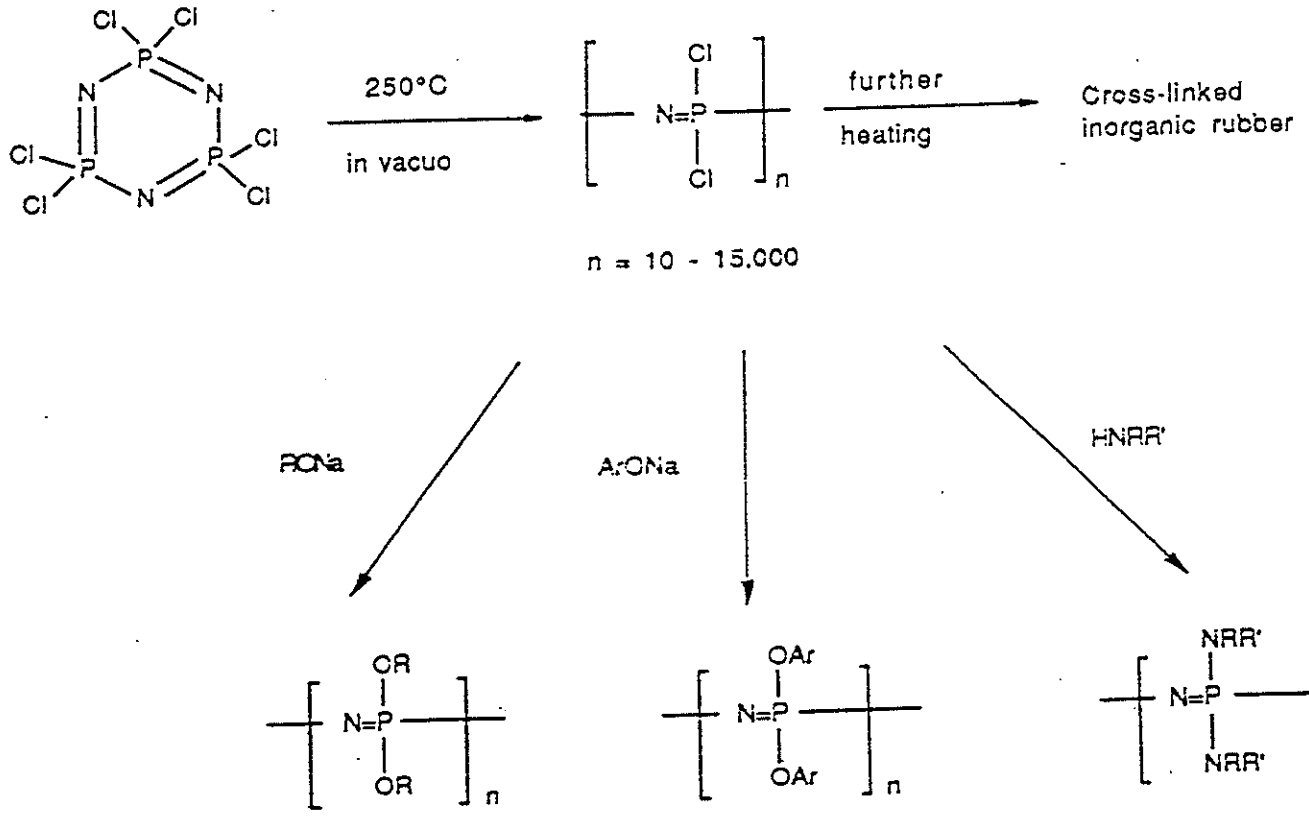

Preliminary Preparation of Carbo(dichloro)siladienes

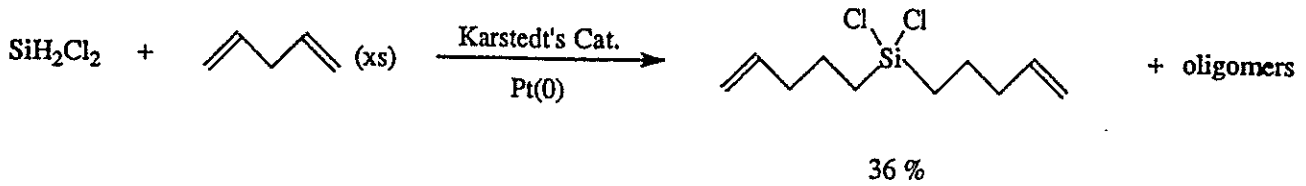

190

Synthesis of Polycarbo(dichloro)silanes

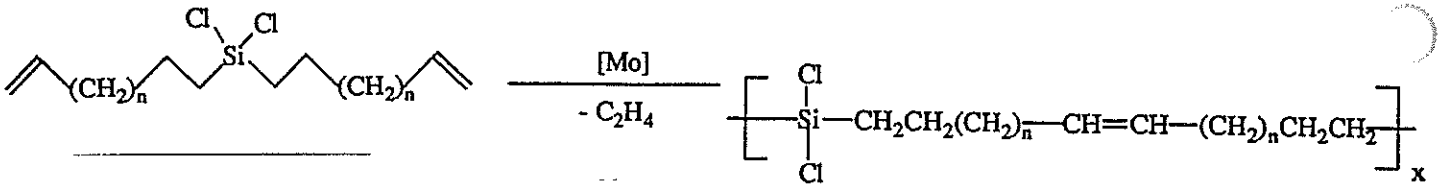

Characterization Data Of Chloro Functionalized Carbosilane Monomer and Polymer

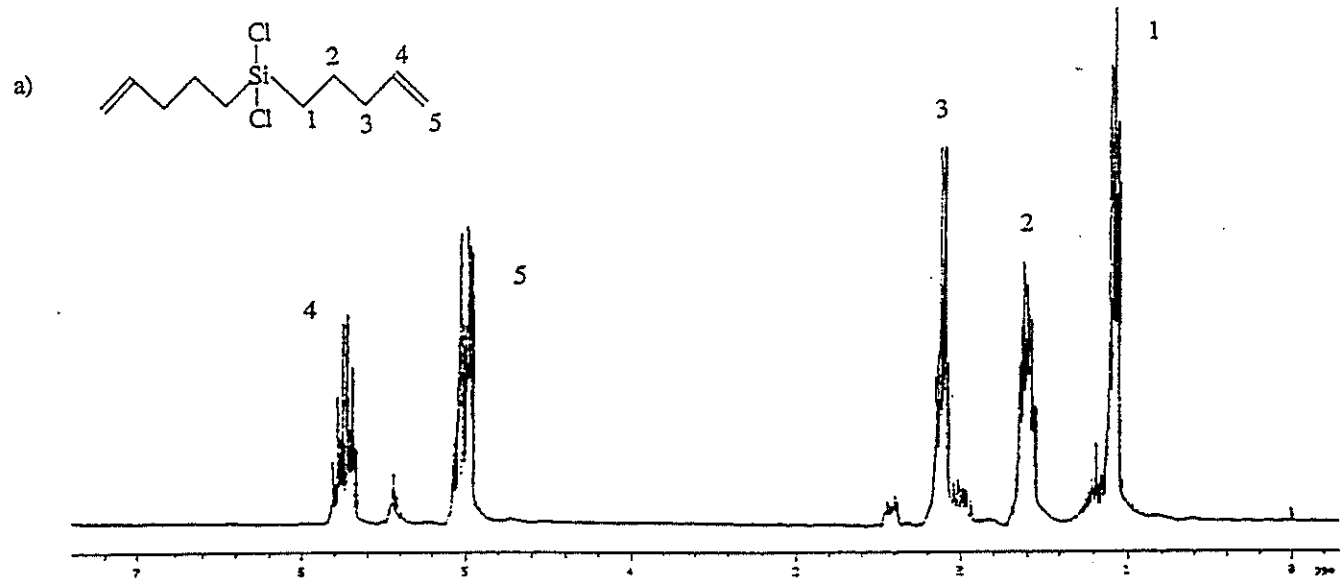

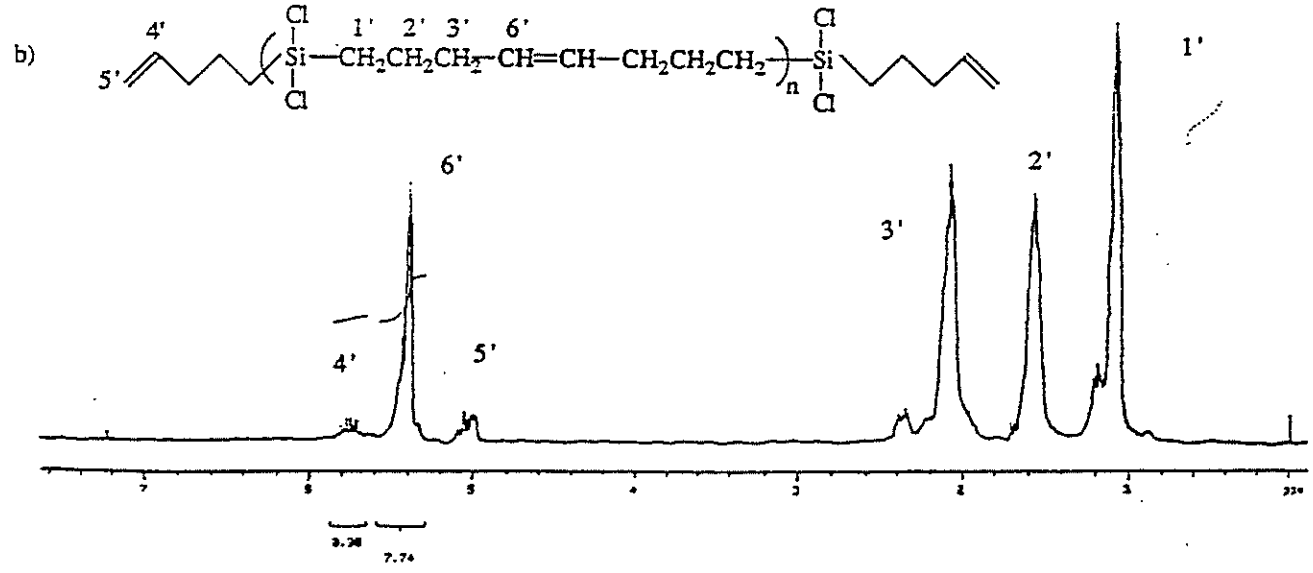

^{1}H NMR Spectra for a) Bis(5-pentenyl)dichlorosilane Monomer and b) Poly(1,1-dichloro-1-sila-5-nonenylene) Polymer

OPPORTUNITY: Carbosilane Analogs of Polyphosphazenes

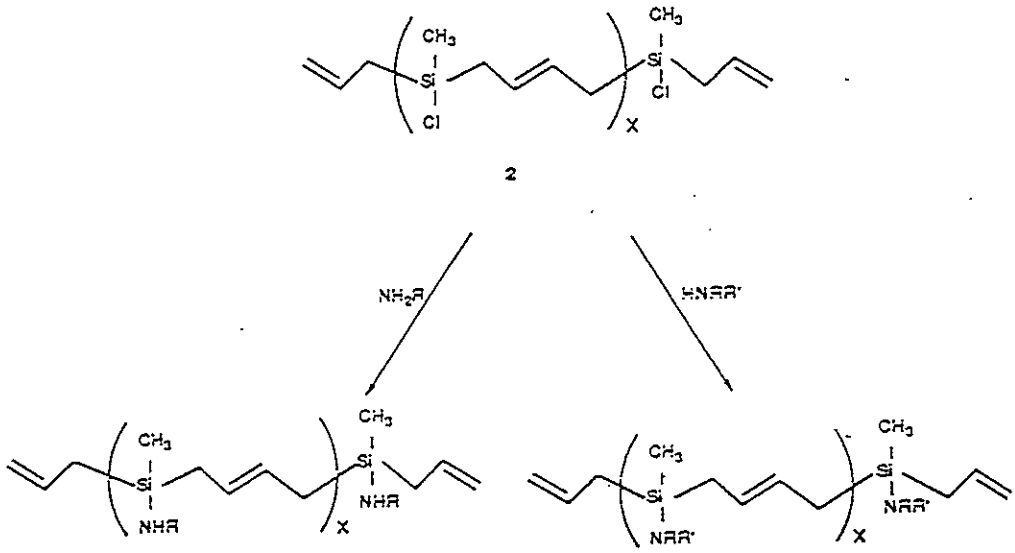

Summary Statements

- ADMET is room temperature polycondensation chemistry, best done in the bulk state.
- The catalysts available for ADMET reactions are beginning to broaden in scope.
- Functionality does not pose a problem given sufficient spacing between the metathesizing olefin and the functional group.
- Aromatic and aliphatic carbosilane polymers are easily accessible by ADMET chemistry, if proper attention is paid to steric and the electronic effects.
- The same holds true for carbosiloxane polymers.
- The silicon-chlorine bond is inert to ADMET chemistry.
- Chlorofunctionalized ADMET oligomers have been synthesized, structures which may be further reacted in a manner reminiscent of dichloropolyphosphazene chemistry.

SYNTHESIS OF POLYMERS WITH CATALYTIC LOCI

Molecular Inclusion Thereof

G. R. NEWKOME, G. R. BAKER and C. N. MOOREFIELD

Center for Molecular Design & Recognition

Department of Chemistry

University of South Florida

Tampa, Florida 33620-5250 USA

1. INTRODUCTION

Since Vögtle's initial cascade synthesis in 1978 [1], the preparation and study of dendritic (cascade) macromolecules has been a rapidly expanding field of polymer chemistry. Numerous researchers have developed procedures to create unique dendritic polymers and are beginning to define the potential applications for these molecules [2]. The inner "void" regions offer the possibility for molecular inclusion or recognition, which may provide access to water soluble catalysts as well as drug and molecular delivery systems.

Our foray into the "molecular forest" began with a desire to mimic at the molecular level the branching pattern of trees. Professor Tomlinson [3] published a thorough description of the architectural design of trees derived from his studies of the rain forests of South America. The Leeuwenberg model represented the ideal topological model for "molecular trees" with branches emanating from quaternary carbons and providing a one-to-three branch multiplicity (i.e., a repetitive synthesis would give molecular structures with a simple mathematical progression of $1 \rightarrow 3 \rightarrow 9 \rightarrow 27 \ldots$). Within this general concept, there remains unlimited variations regarding branch composition, length, and functionality.

2. CASCADE MACROMOLECULES

2.1 BRANCHES WITH AMIDE LINKAGES

From the beginning, our synthetic strategies have employed prebranched "building blocks" each consisting of a central quaternary carbon possessing a single "reactive" functionality and three "protected" (or differentiated) functions. The preparation of the [27]-Arborol is shown in Scheme 1 [4]. Retardation of the chemical reactivity of the neopentyl core necessitated the incorporation of spacer groups, added multiple steps to the synthesis, and ultimately hindered the addition of further branching. The preparation of "2-D" [5,6] and "4-D" [7,8] arborols via similar methods are shown in Schemes 2 and 3.

Bishomotris (BHT) was prepared [9] (Scheme 4) to replace tris(hydroxymethyl)aminomethane (tris) in these reaction schemes; the additional methylenes should circumvent the steric hinderance imposed by neopentyl structure of tris. The use of BHT gave only traces of transesterified material instead of the desired amide formation. This result supports a cyclic intermediate in the proposed mechanism (Figure 1) for the amidation of esters under these conditions [6].

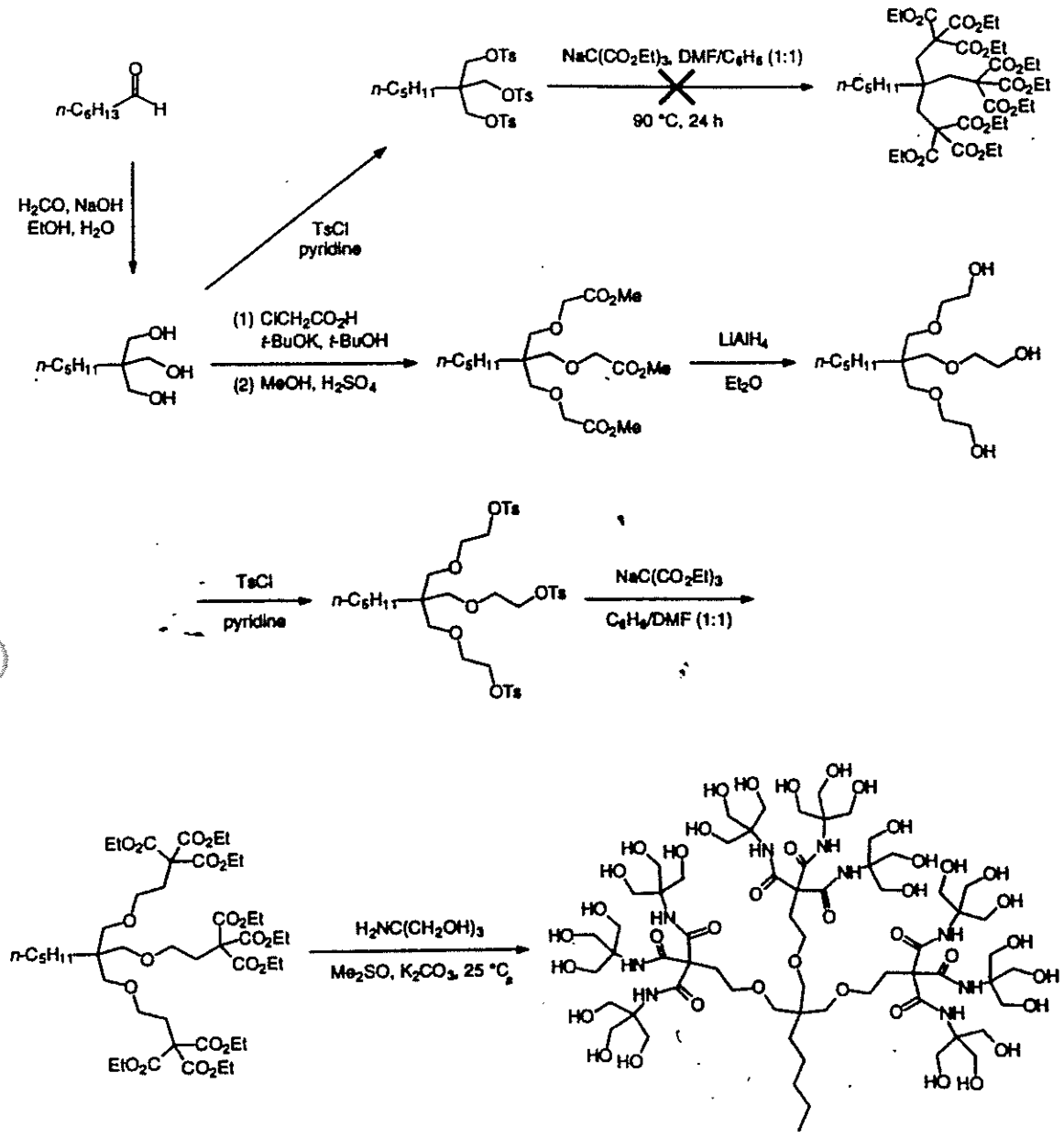

Scheme 1. Preparation of [27]-Arborol.

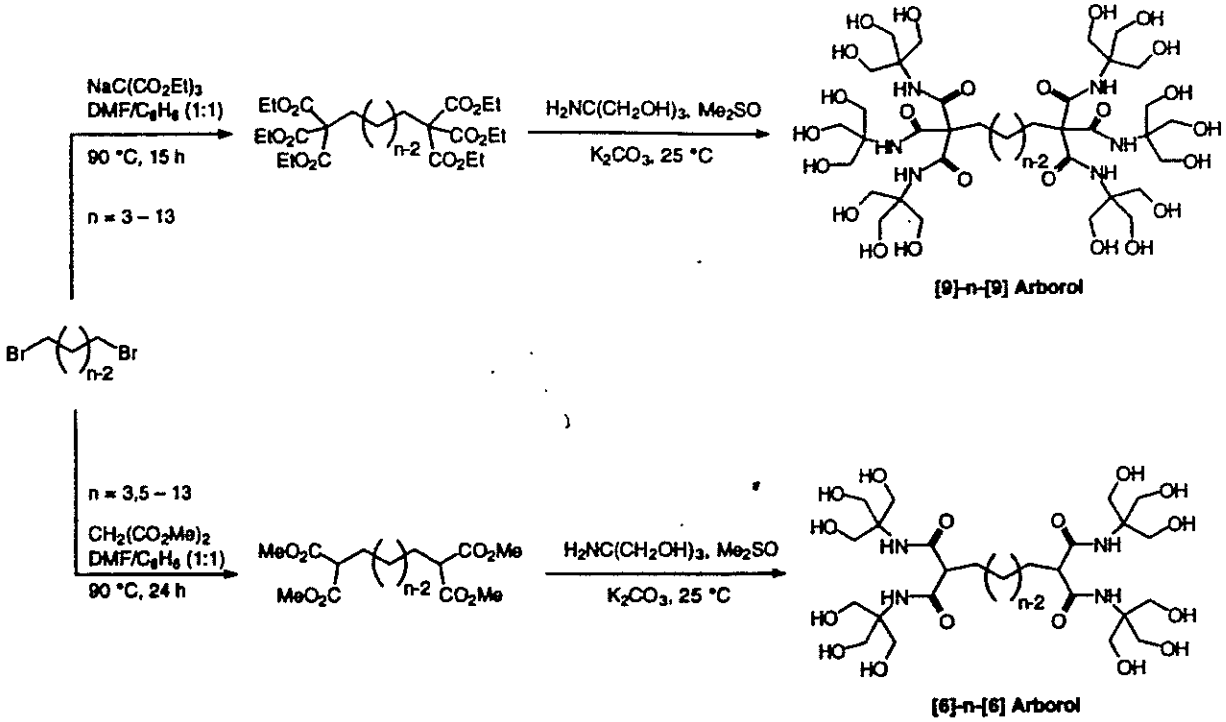

Scheme 2. Preparation of 2-Directional Arborols.

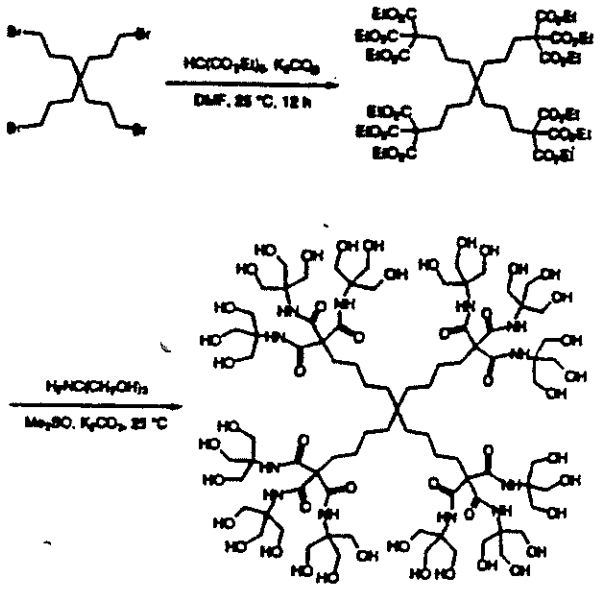

Scheme 3. Preparation of a 4-Directional Arborol.

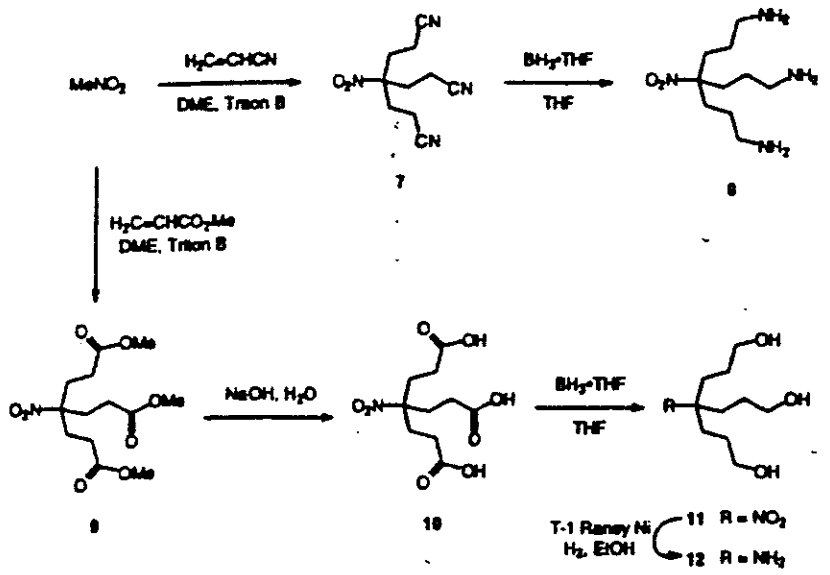

Scheme 4. Synthesis of Bishomotris (BHT).

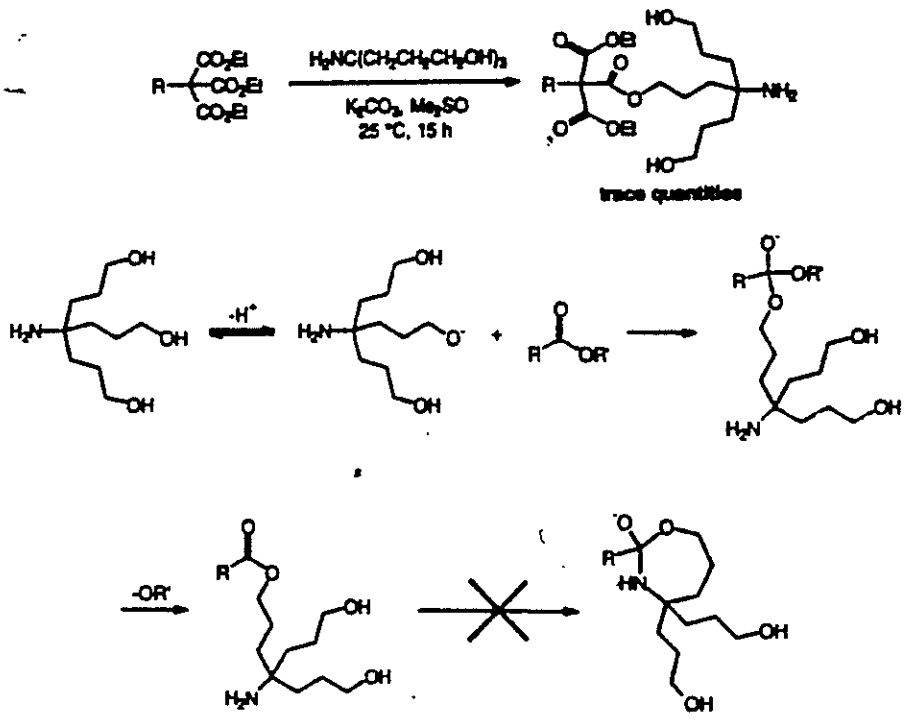

Figure 1. Proposed Mechanism for the Reaction of BHT with an Ester.

These experiences focused our thought process toward the use of protecting groups and functional group differentiation. A building block possessing a pendant amine and three esters would facilitate the amidation of a carboxylic acid via peptide coupling conditions; subsequent ester hydrolysis would yield three acid moieties that could be coupled with additional aminotriester to give larger, more branched macromolecules. The Michael addition of $MeNO_2$ into acrylic esters and subsequent reduction of the nitro to an amine seemed a feasible route into the desired building block. For simple alkyl esters, reduction of the pendant nitro moiety results in lactam formation. This undesirable process was readily avoided by the use of *tert*-butyl esters (Scheme 5) [10].

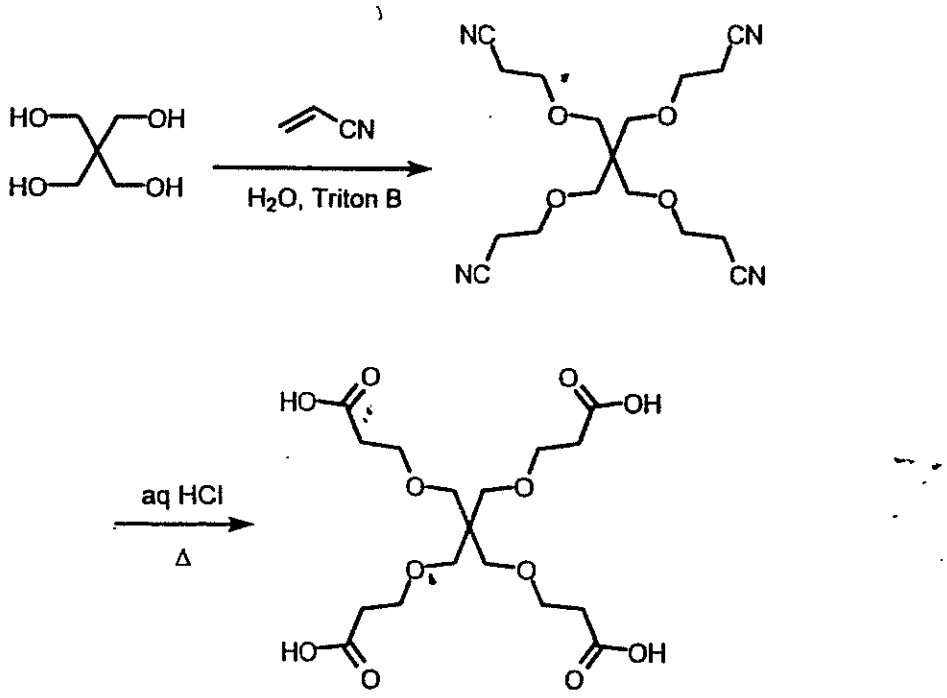

Scheme 5. Synthesis of Di-*tert*-butyl 4-Amino-4-[2-(*tert*-butoxycarbonyl)-ethyl]-1,7-heptanedioate.

An easily accessible tetraacid initiator core was prepared (Scheme 6) via Michael addition of pentaerythritol to acrylonitrile and subsequent hydrolysis with HCl [11]. Amide formation under traditional peptide coupling conditions gave the dodecaester; hydrolysis with formic acid gave the corresponding dodecaacid (Scheme 7). Synthesis of the second generation 36-acid is shown in Scheme 8 [12]; further repetition of these two steps gave the first six generations of the *Z*-Cascade:methane[4]:(3-oxo-6-oxa-2-azaheptylidyne):(3-oxo-2-azapentylidyne)$^{G-1}$:propanoic acid [13] (Figure 2).

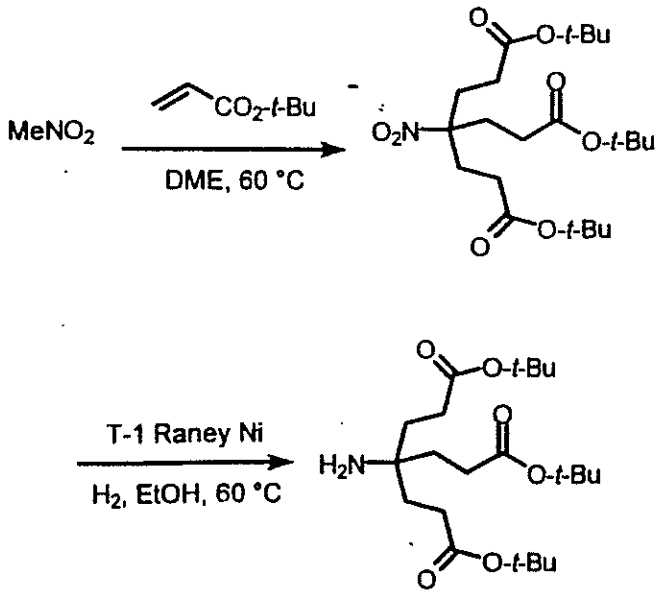

Scheme 6. Preparation of a Tetraacid Initiator Core.

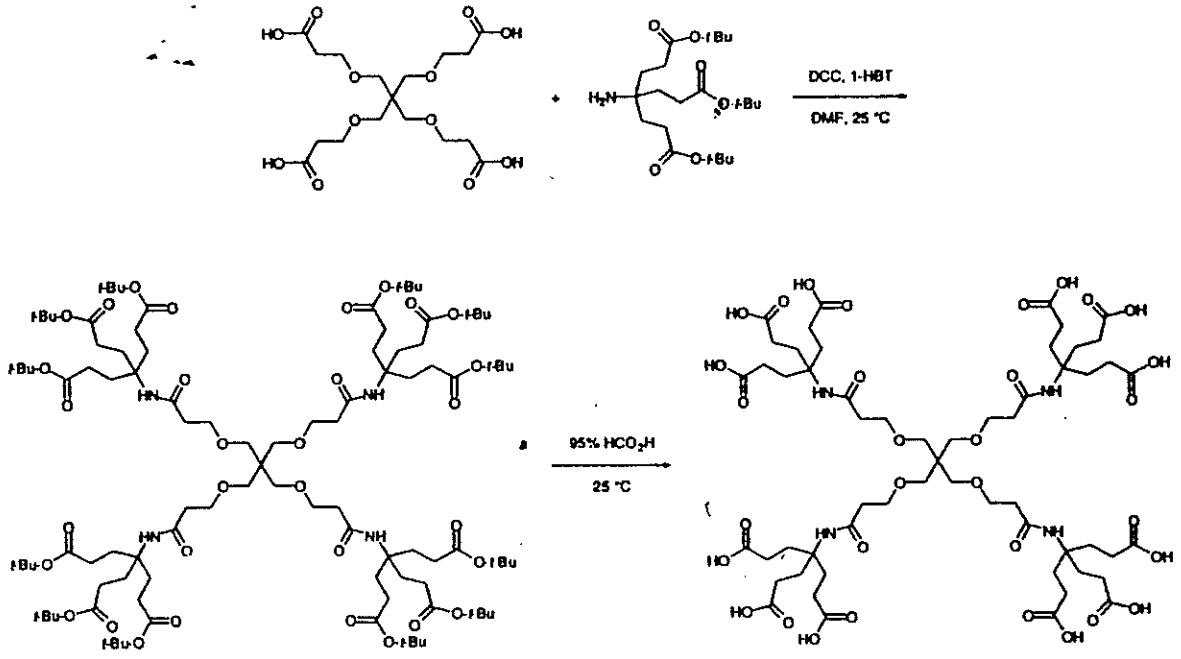

Scheme 7. Synthesis of the 12-Cascade:Acid.

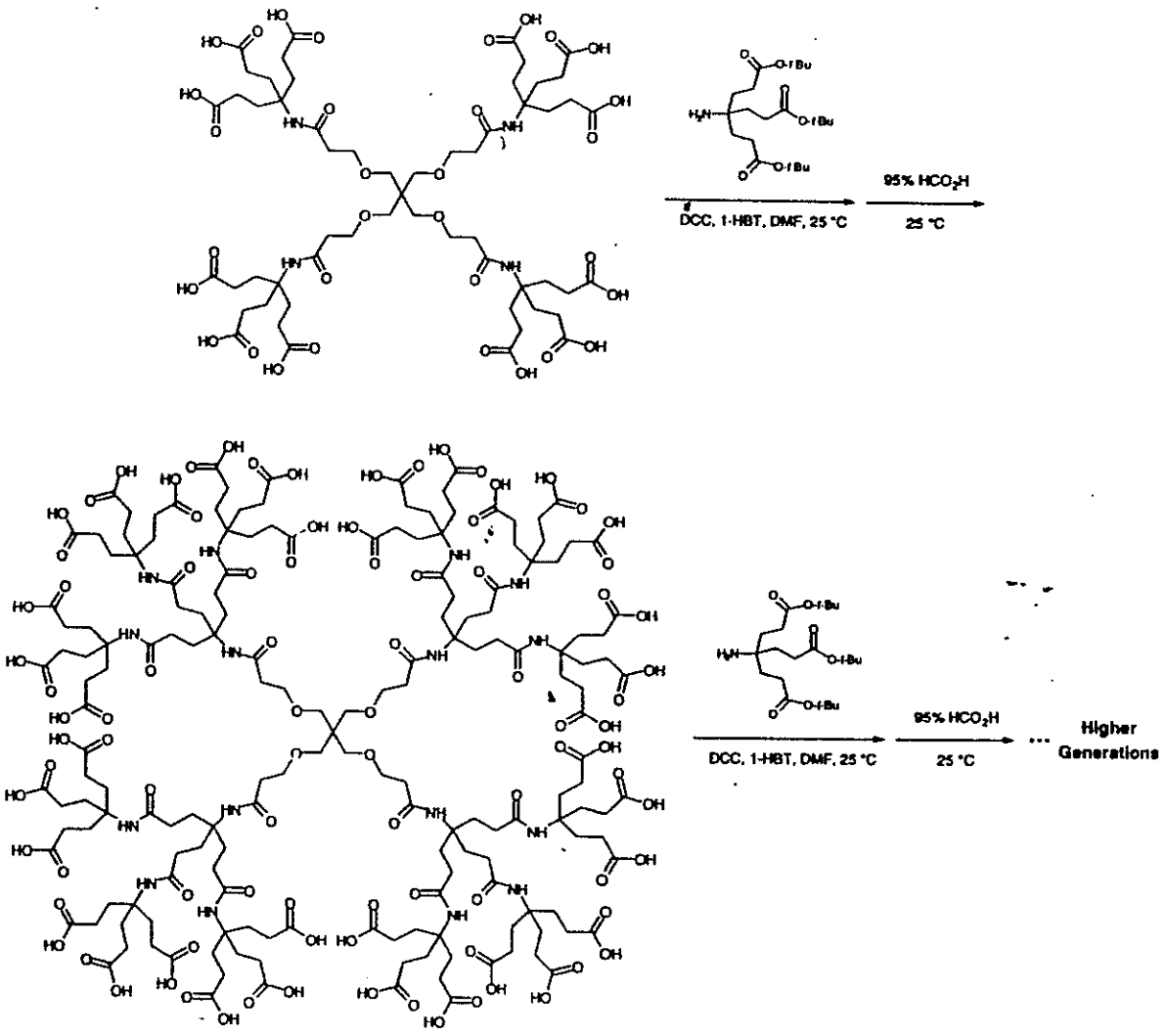

Scheme 8. Iterative Synthesis of Higher Generation Polyamido Cascades.

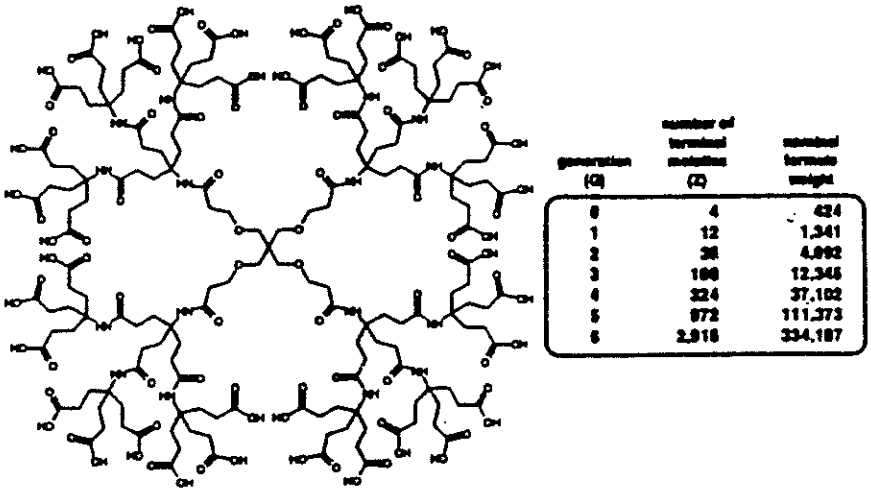

generation (G)	number of terminal molecules (Z)	molecular formula weight
0	4	424
1	12	1,341
2	36	4,992
3	108	12,345
4	324	37,102
5	972	111,373
6	2,916	334,187

Figure 2. Molecular Weight versus Generation for the Polyamido Cascades.

Size exclusion chromatography (SEC) provided verification of the monodispersity and formula weight of the third generation 108-acid [12]. Interestingly, the elution volume exhibited a marked dependence upon the pH of the sample solution. This apparent size change was attributed to expansion (or contraction) of the molecule as the terminal acid moieties were deprotonated (or protonated). Further evidence for this '*smart*' phenomena [14] was obtained by determination of the hydrodynamic radii for the first five generations of this cascade family via diffusion ordered spectroscopy (DOSY NMR) [12].

Ionization of the terminal acid moieties was presumed responsible for the pH dependence of the hydrodynamic radius; incorporation of other terminal functionalities facilitated control of this '*smart*' behavior. Thus, the first three generations of the related alcohol- and amine-terminated cascades were prepared via a modular approach [15]. The required building blocks were synthesized as shown in Scheme 9 and 10. Amide formation with the tetraacid initiator core and the appropriate building block via peptide coupling conditions gave the dodecaalcohol (Scheme 11) or dodecaamine (Scheme 12). Similar reactions with the first or second generation polyacids gave the second and third generation members of each family, respectively. As expected, the amine-terminated cascades exhibited pH-size behavior opposite to that observed for the acid-terminated cascades, and the alcohols showed no change in hydrodynamic radius as a function of pH (Figure 3) [15].

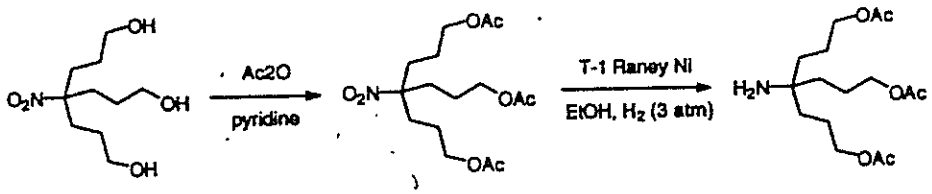

Scheme 9. Preparation of the Alcohol-Terminated Modular Building Block.

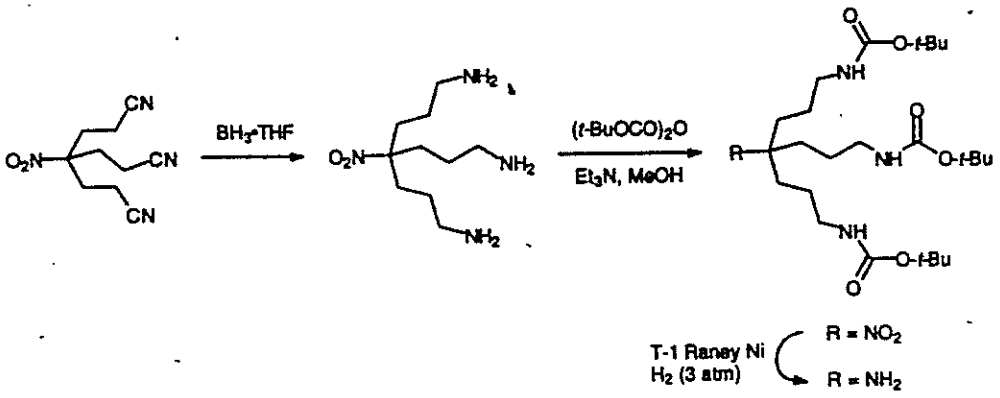

Scheme 10. Preparation of the Amine-Terminated Modular Building Block.

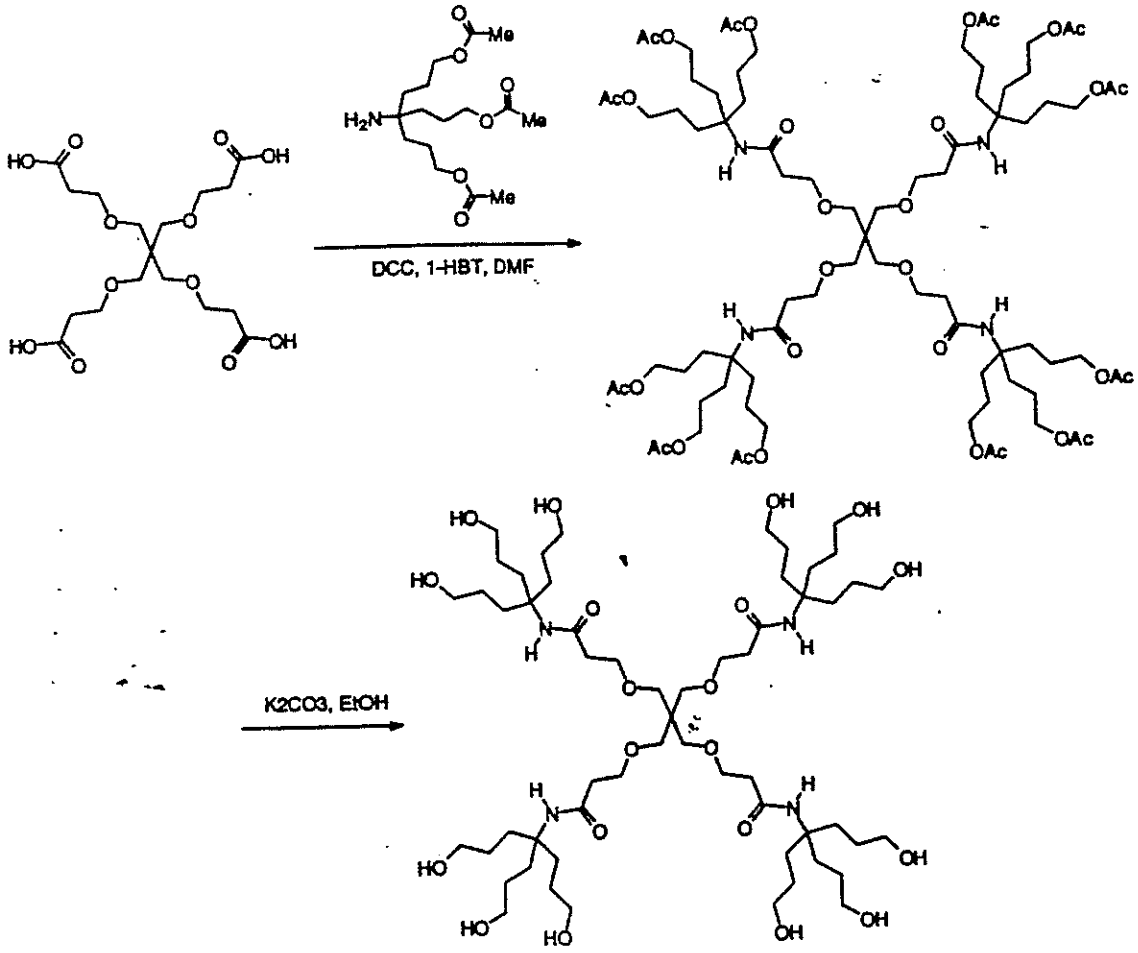

Scheme 11. Synthesis of the 12-Cascade:Alcohol.

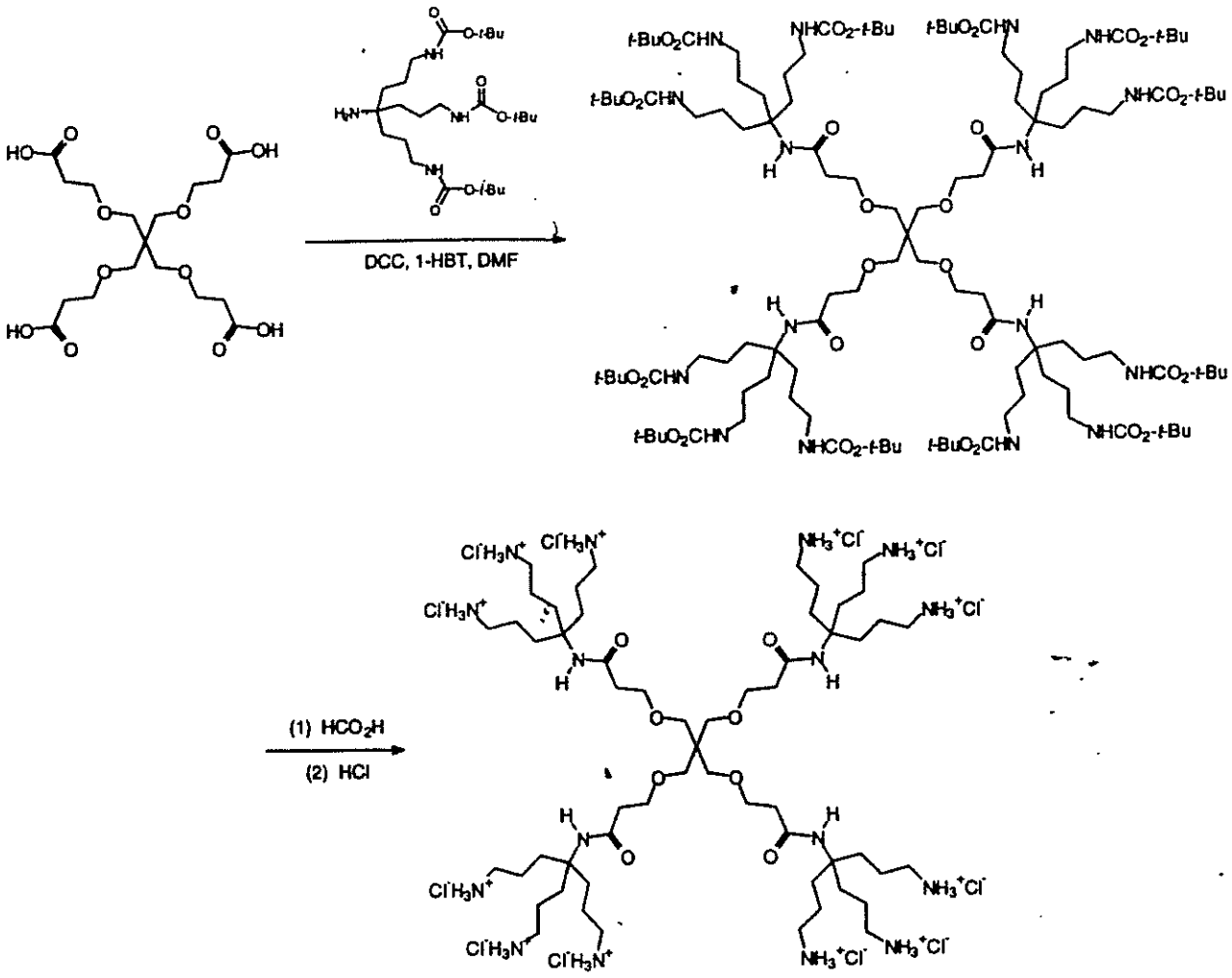

Scheme 12. Synthesis of the 12-Cascade:Amine.

Generation (G)	Number of Terminal Groups (Z)	Formula Weight	[Cascade] (mM)	D (cm^2s^{-1}) / Hydrodynamic Radius (Å)		
				Acidic pH	Neutral pH	Basic pH
1	12	1,341	1.00	2.41×10^{-6} 8.24	1.62×10^{-6} 12.3	1.68×10^{-6} 11.8
2	36	4,092	1.00	1.74×10^{-6} 11.4	1.15×10^{-6} 17.3	1.26×10^{-6} 15.8
3	108	12,345	1.00	1.15×10^{-6} 17.3	8.32×10^{-7} 23.9	9.09×10^{-7} 21.9
4	324	37,102	0.97	8.79×10^{-7} 22.6	6.01×10^{-7} 33.1	6.87×10^{-7} 28.9
5	972	111,373	0.34	7.83×10^{-7} 25.4	5.35×10^{-7} 37.1	6.17×10^{-7} 32.3

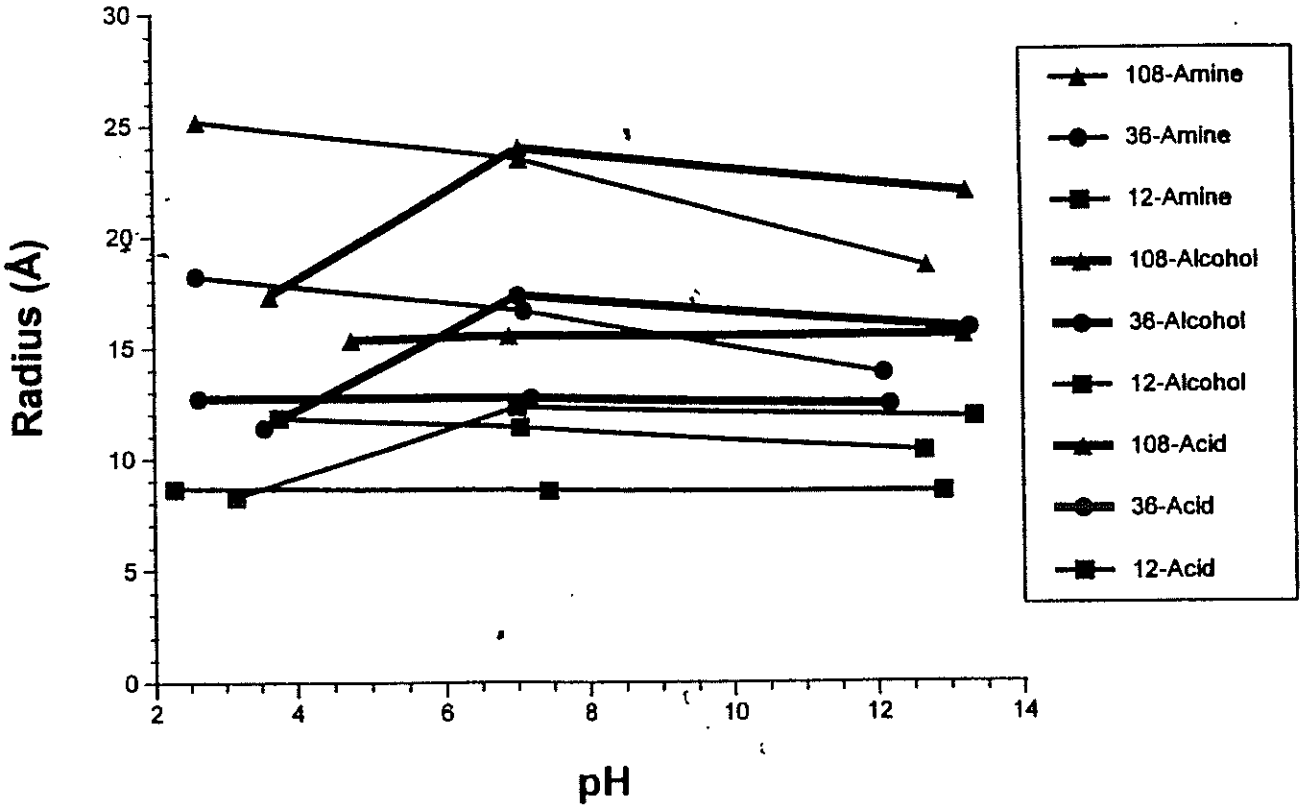

Figure 3. Hydrodynamic Radius as a Function of pH for the Polyamido Cascades.

2.2. *HYDROCARBON BRANCHES*

Synthesis of a tetraalkylmethane building block possessing a reactive functionality on one alkyl group and suitably protected functions on the three remaining alkyl moieties opened an avenue to a dendritic macromolecule with polar surface (terminal) groups and an entirely hydrocarbon interior. One possible synthon was prepared from the nitrotriol precursor to BHT. The alcohol groups were protected as benzyl ethers, followed by substitution of a cyanoethyl group for the tertiary nitro moiety via the method of Ono16 (Scheme 13); further chemical manipulation afforded terminal alkyne (Scheme 14) [17].

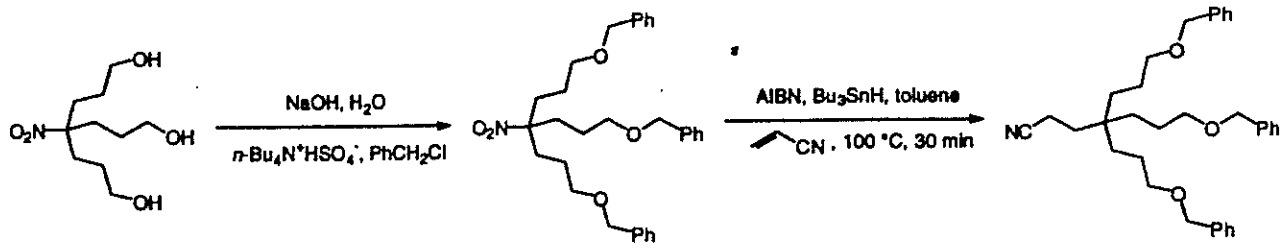

Scheme 13. Cyanoethylation of the Nitrotriether.

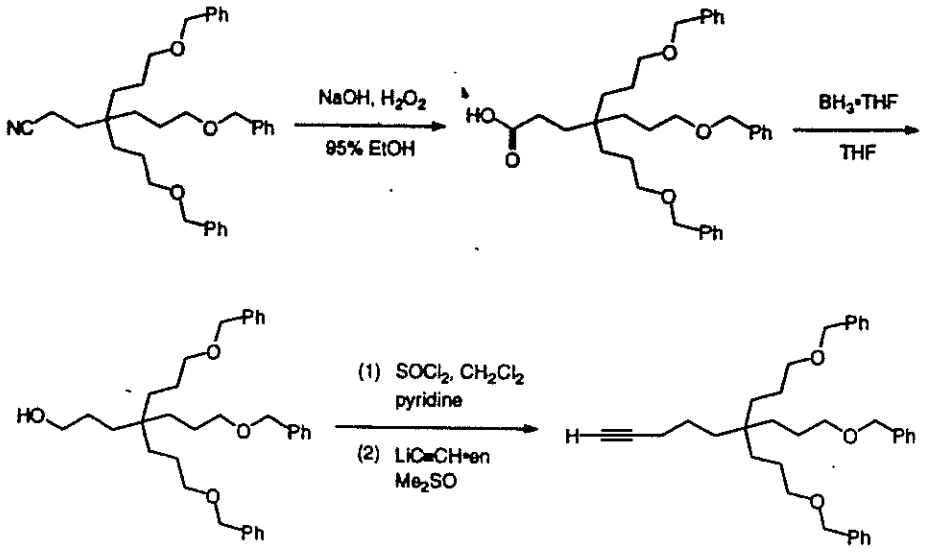

Scheme 14. Synthesis of the Alkyne Building Block.

Scheme 15 illustrates several routes to 4,4-bis(3-bromopropyl)-1,7-dibromoheptane; the shortest reported preparation arose from conversion of the nitrotriol (Scheme 16) [8]. Successful first tier construction was effected via addition of four equivalents of the alkynide of the building block to the tetrabromide initiator core and subsequent catalytic reduction of the benzyl ethers with concomitant reduction of the internal alkynes (Scheme 17) [17]. Conversion of the terminal alcohols to bromides and repetition of the alkylation-reduction steps afforded the second generation 36-Micellanol™ cascade (Scheme 18) [17]. Water solubility of this polyol was enhanced by oxidation with $RuO_2/NaIO_4$ to afford the corresponding 36-Micellanoic Acid™ cascade {36-Cascade:methane[4]:(nonylidyne)2:propanoic Acid; Figure 4} [17].

UV studies of guest molecules traditionally used to ascertain micelle properties (e.g., phenol blue, pinacyanol chloride, naphthalene, and chlortetracycline) and fluorescence lifetime decay experiments of diphenylhexatriene confirmed the micellar behavior of the NMe_4^+ salt of 36-Micellanoic Acid™ cascade[18]. Electron microscopy was used to determine the monodispersity, size, and absence of intermolecular aggregation.

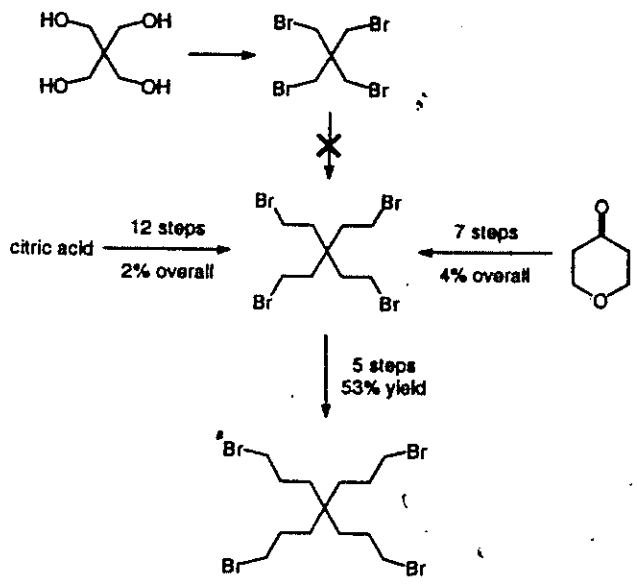

Scheme 15. Possible Routes to 4,4-Bis(3-bromopropyl)-1,7-dibromoheptane.

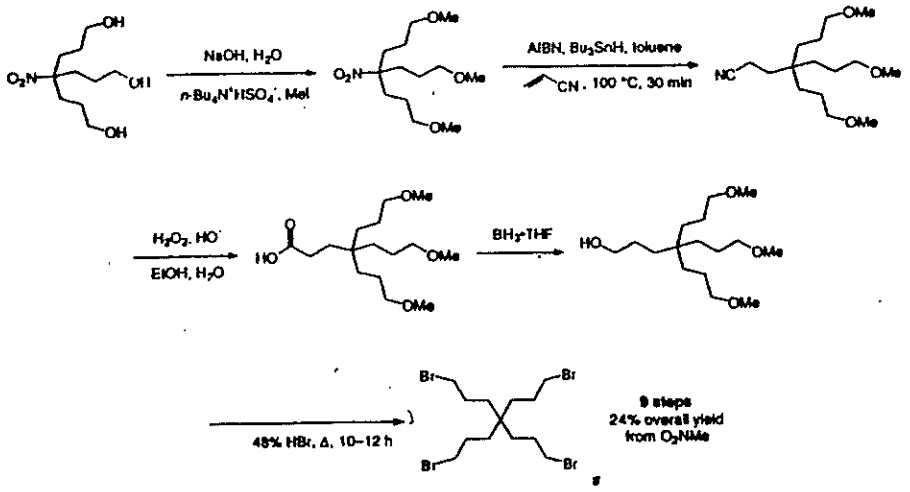

Scheme 16. Improved Synthesis of 4,4-Bis(3-bromopropyl)-1,7-dibromoheptane.

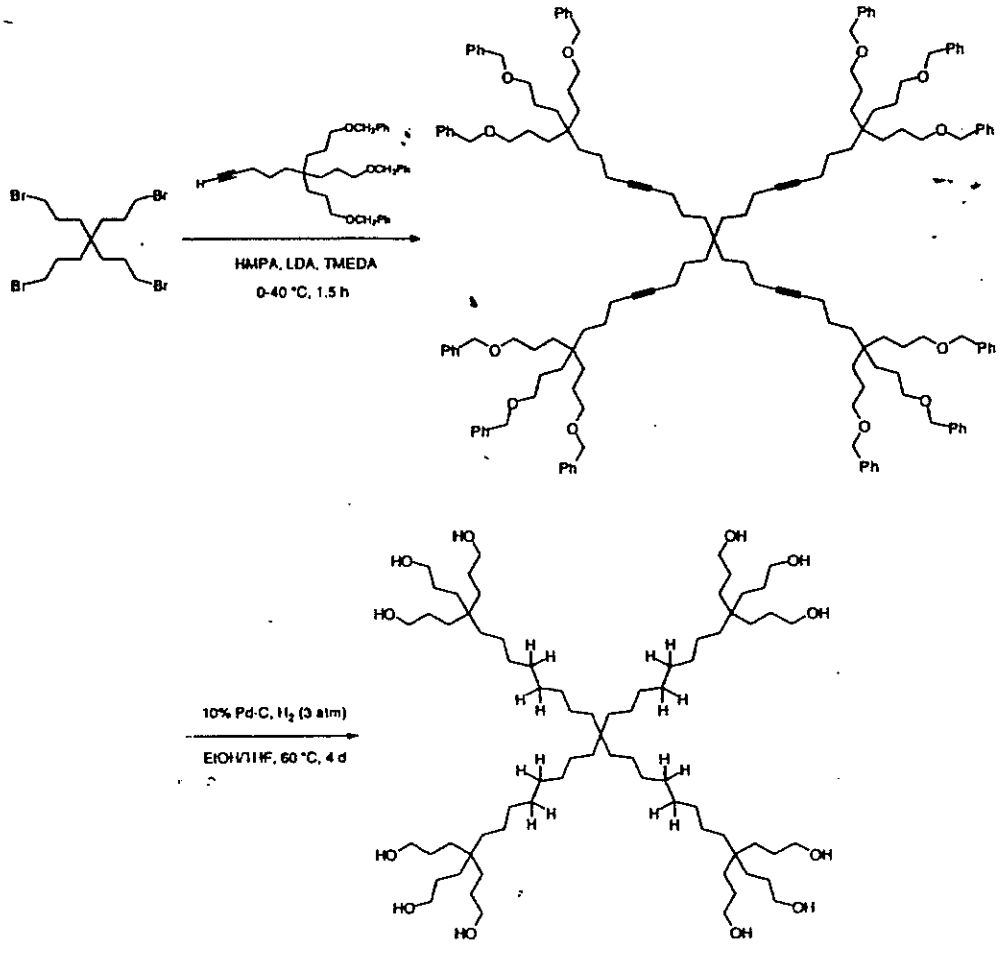

Scheme 17. Preparation of the 12-Micellane™ Alcohol .

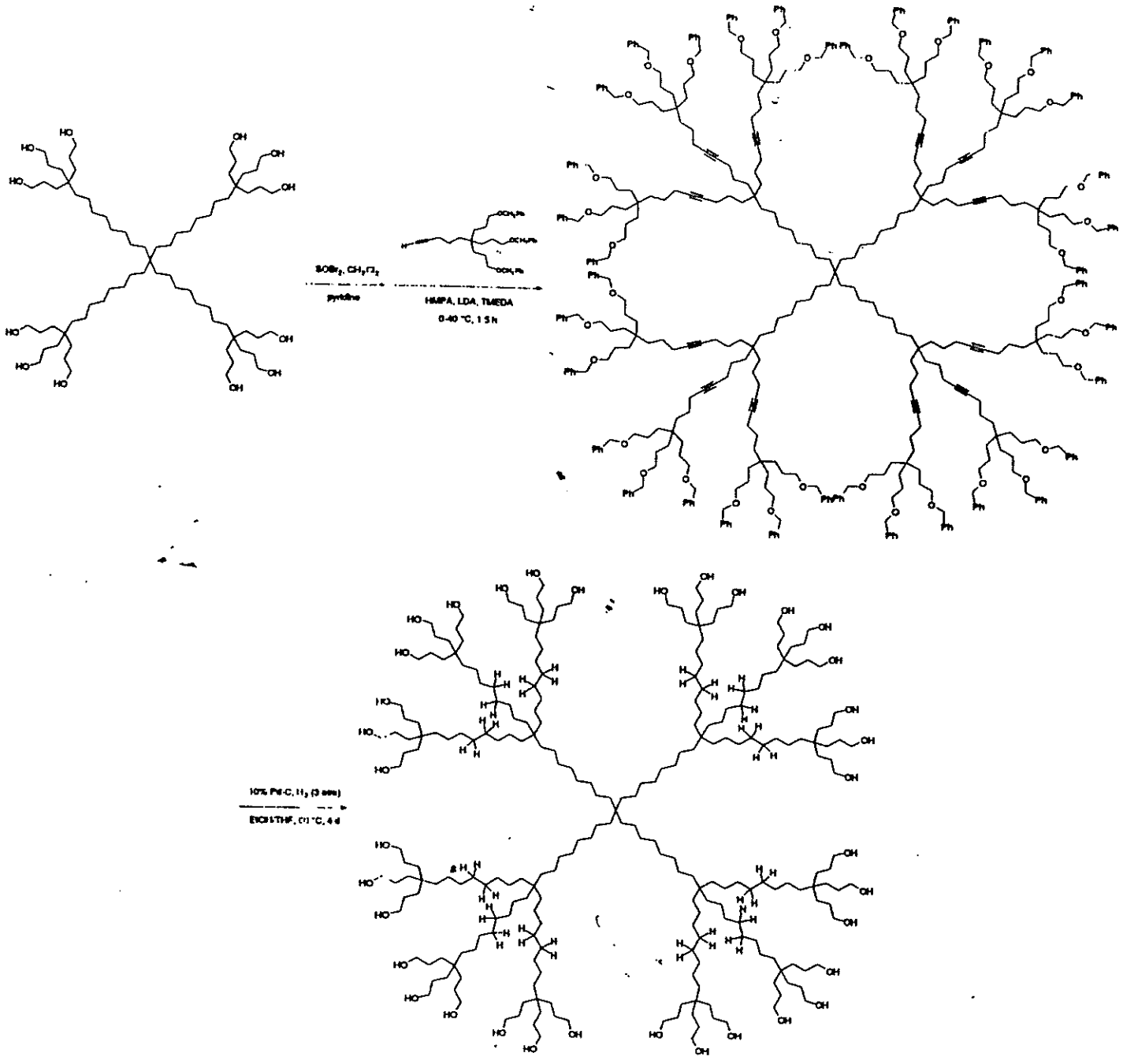

Scheme 18. Preparation of the 36-Micellane™ Alcohol .

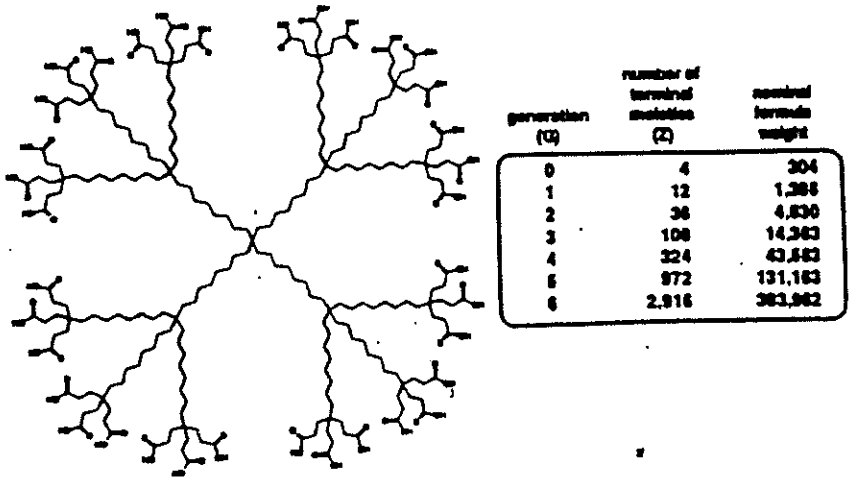

generation (G)	number of terminal methine (Z)	nominal formula weight
0	4	304
1	12	1,288
2	36	4,856
3	108	14,363
4	324	43,583
5	972	131,183
6	2,916	393,962

Figure 4. Molecular Weight versus Generation for the Micellanoic Acid™ Cascades.

3. SUPRAMOLECULAR CHEMISTRY WITHIN DENDRITIC MOLECULES

The relative ease of *heterogeneous* catalytic reduction of the internal alkynes (Schemes 17 and 18) and the interior 'void' regions within the lipophilic interior of the Micellane™ cascades has motivated our use of these molecules as 'molecular scaffolding' for the attachment of chemically active species. Initial studies have been directed toward chemical modification of the internal alkynes of the polybenzyl ether precursor to the Micellanoic Acid cascades; the incorporated functionalities are symmetrically located equidistant from the initiator core.

3.1. METALLOIDOMICELLANE™ CASCADES

Treatment of the second generation dodeaalkyne with acetonitrile activated decaborane ($B_{10}H_{14}$) gave an essentially quantitative yield of the dodeca-*o*-carborane. Catalytic reduction to remove the benzyl ether protecting groups gave the polyol. The limited water solubility of this polyol was enhanced via treatment with chlorosulfonic acid to give the polysulfate (Scheme 19) [19].

3.2. METALLOMICELLANE™ CASCADES

Polybenzyl ether terminated hydrocarbon based cascades possessing internal alkyne moieties have also been employed to attach metal species such as Co via reaction with $Co_2(CO)_8$. Other cascade macromolecules internally functionalized with diamine ligands are currently being examined for inclusic of metals such as Cu, Pt, and Pd.

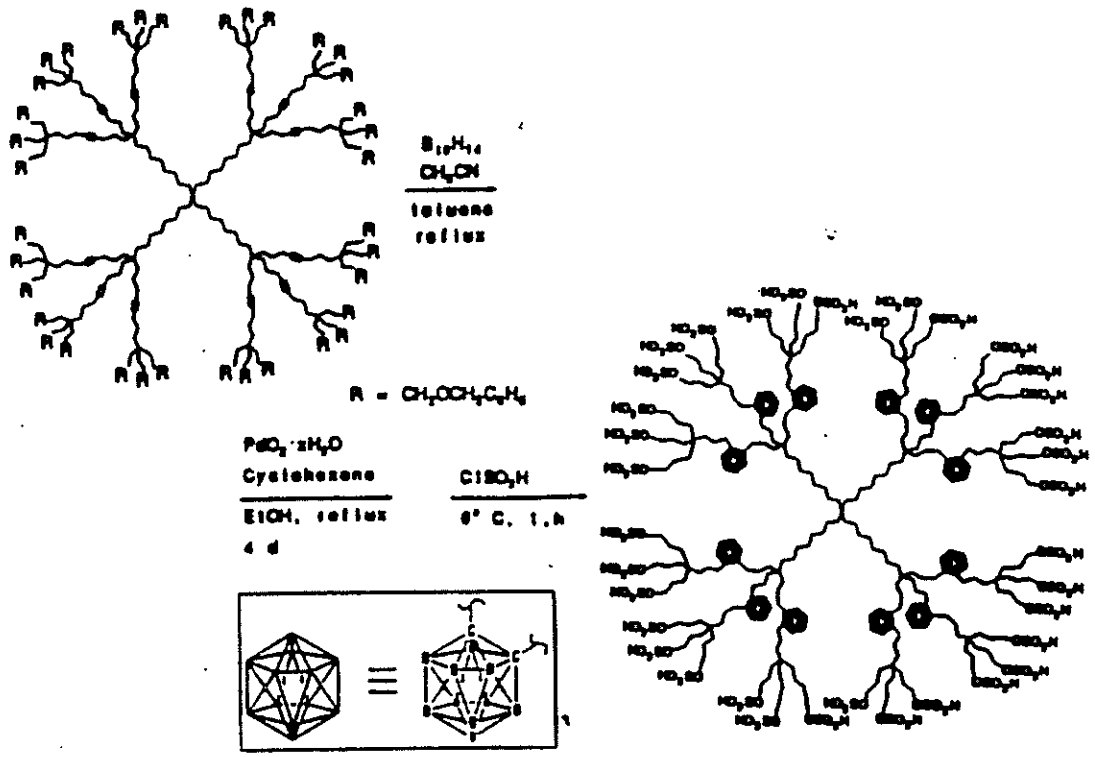

Scheme 19. Synthesis of a Sulfate-Terminated 36-MetalloidoMicellane™ Cascade.

Metallomicellane™ macromolecules have also been prepared that utilize chelation of Ru^{+2} building block connectivity. Reaction of BHT with 4'-chloroterpyridine gave an amine building block that was coupled with the tetraacid described earlier to give a dodecaterpy cascade (Scheme 20) [20]. A Ru^{+3} containing building block was prepared (Scheme 21) and coupled to the dodecaterpy cascade with concomitant reduction to give a metallocascade as shown in Scheme 22 [20].

Figure 5 is a graphical depiction of the utilization of our newest terpyridine building blocks (Scheme 23) for the construction of dendritic complexes. These studies on small "oligomers" will ultimately lead to the construction of well-defined dendritic networks.

Figures 6 and 7 show the cyclic voltammagrams obtained for the Ru containing dendrimers.

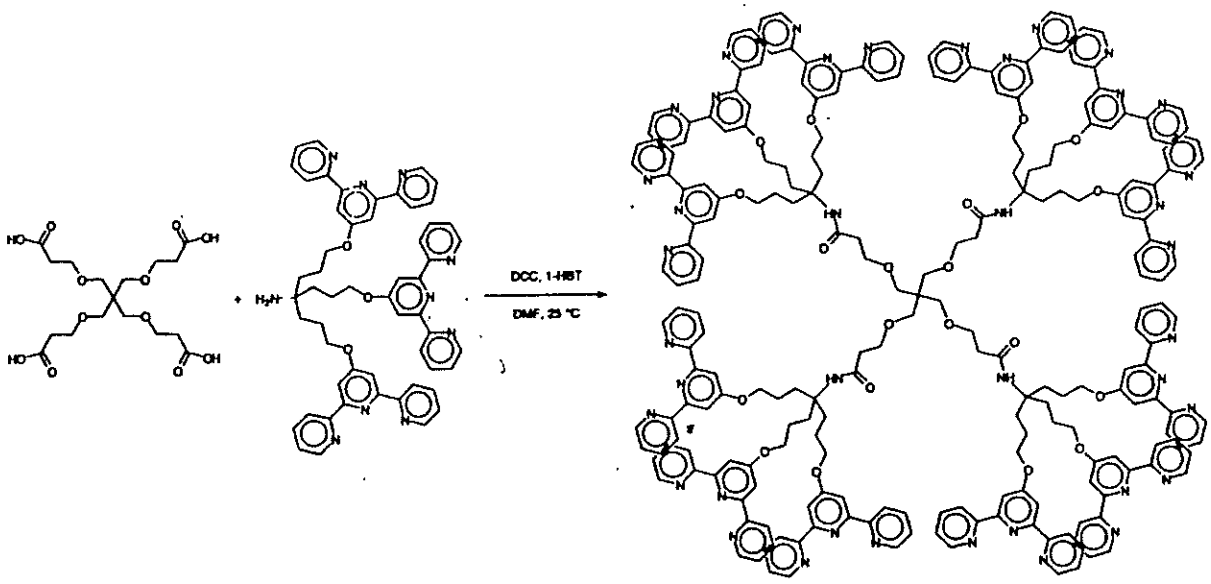

Scheme 20. Synthesis of a Terpyridine-Terminated Cascade.

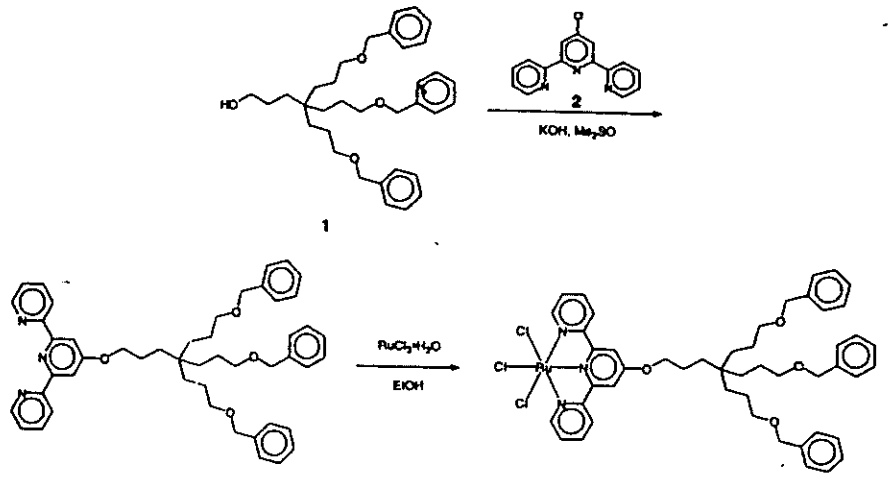

Scheme 21. Preparation of a $RuCl_3$-tpy Building Block.

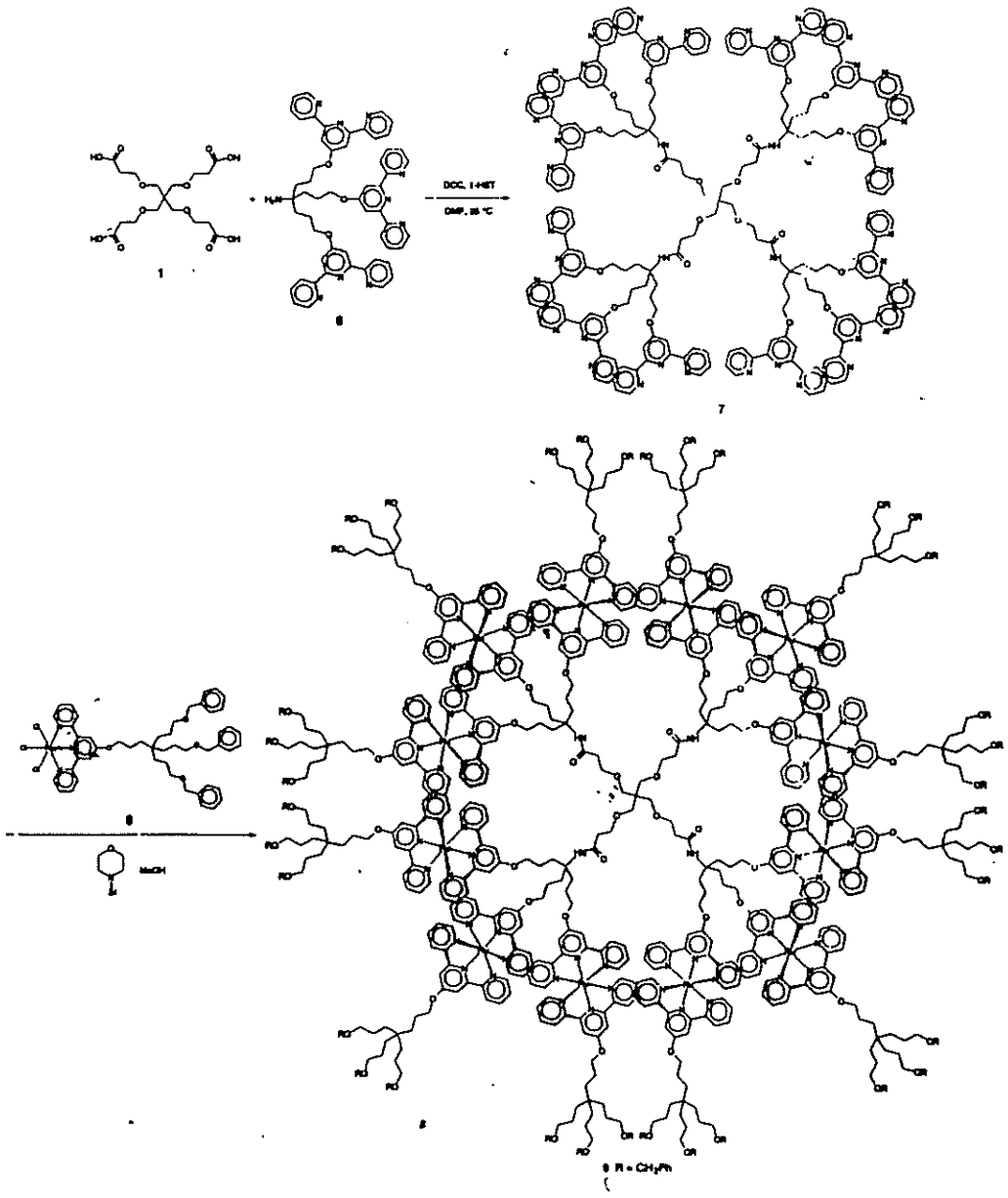

Scheme 22. Synthesis of a Ru^{+2}-Linked MetalloMicellane™ Cascade.

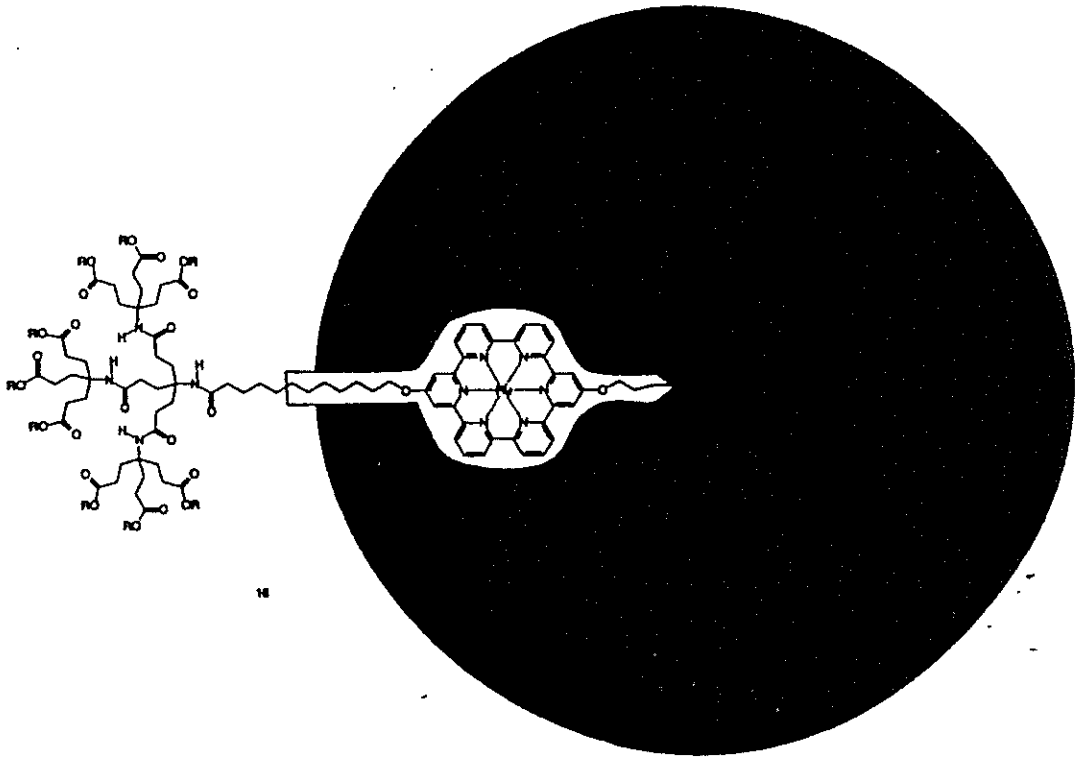

Figure 5. Beginnings of a Dendritic Network

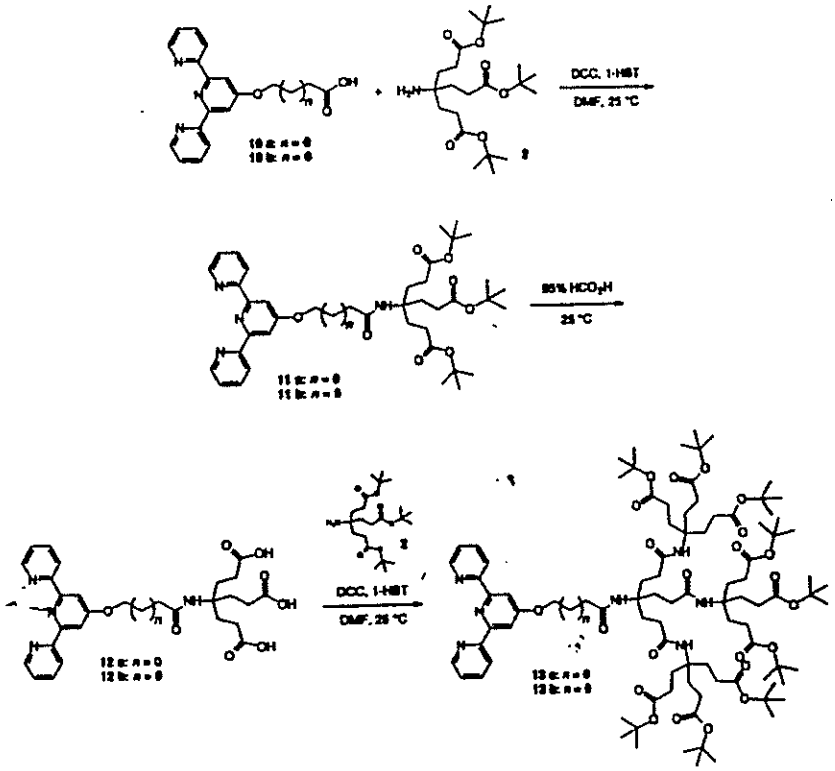

Scheme 23. Preparation of Terpyridine Dendrimer Building Blocks

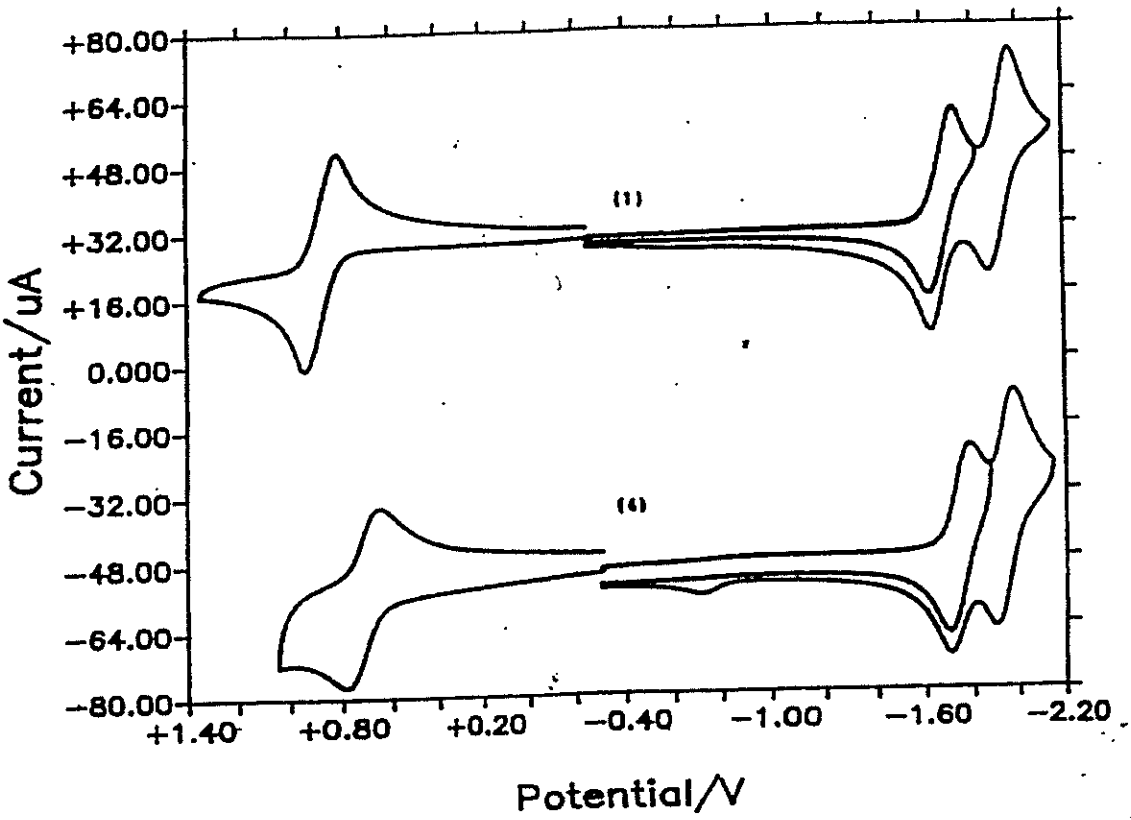

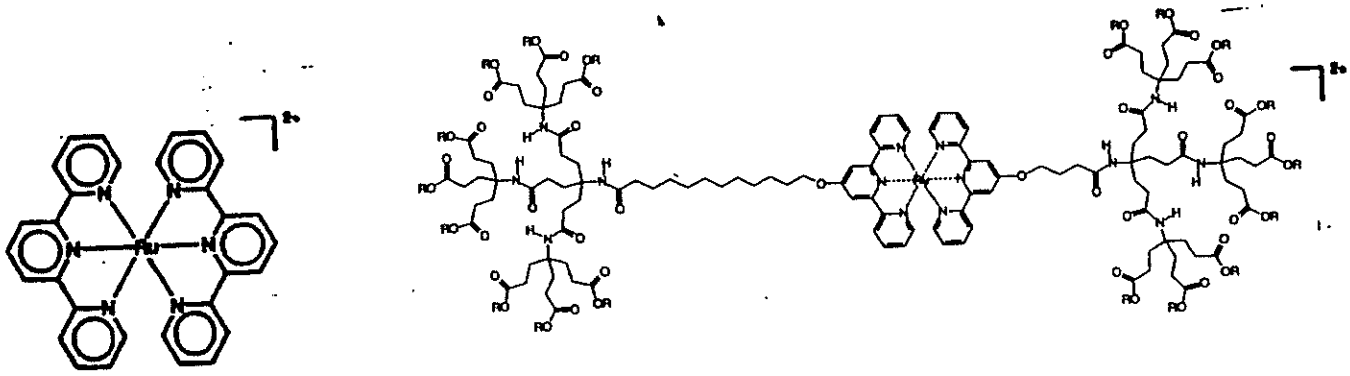

Figure 6. Cyclic Voltammagram

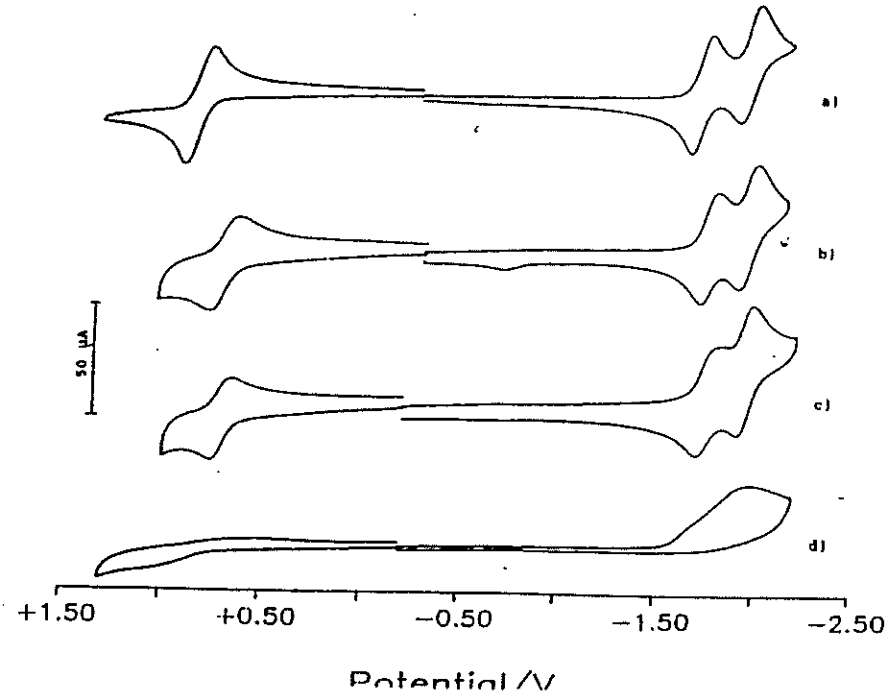

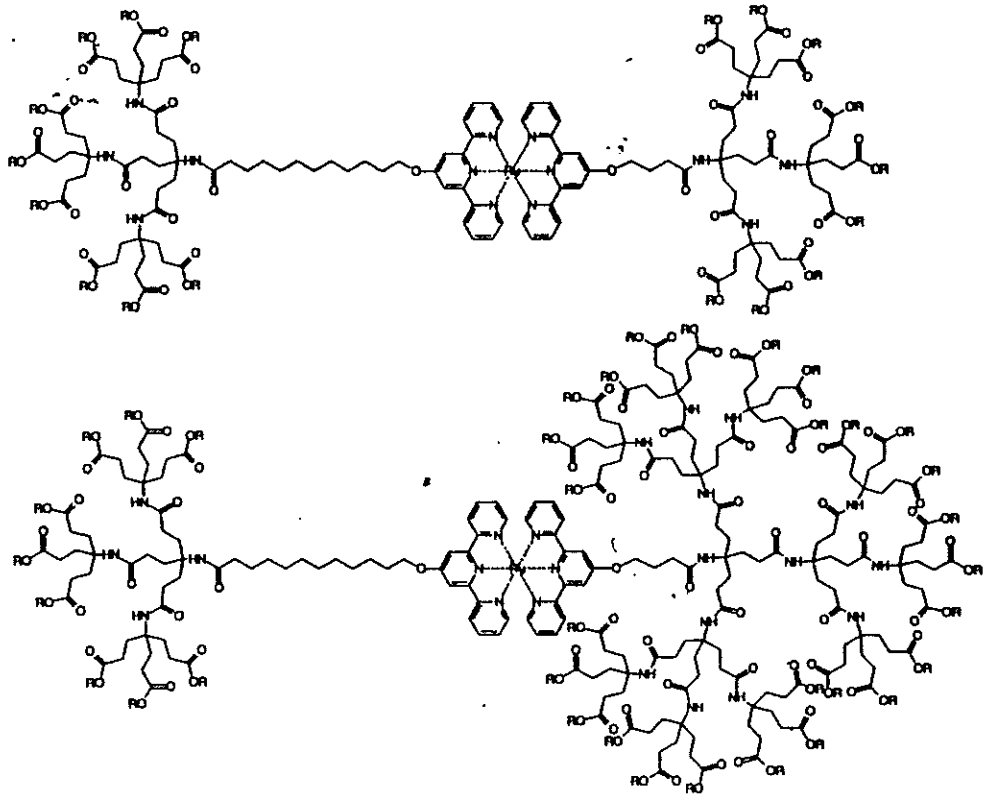

Figure 7. Cyclic Voltammagram

4. MOLECULAR RECOGNITION

Introduction of molecular recognition sites along the dendritic infrastructure will impart specificity toward included guest molecules. We have readily incorporated several H-bonding and ligating moieties into our cascade macromolecules via a straightforward, high-dilution synthesis of functionalized building blocks (Scheme 24 and 25). The preparation of a 2,6-diaminopyridine containing cascade molecule is shown in Scheme 26 and 27. The diaminopyridine moiety forms relatively strong H-bonded interactions with imide containing substrates [e.g., barbituric acids (Figure 8) and uracils].

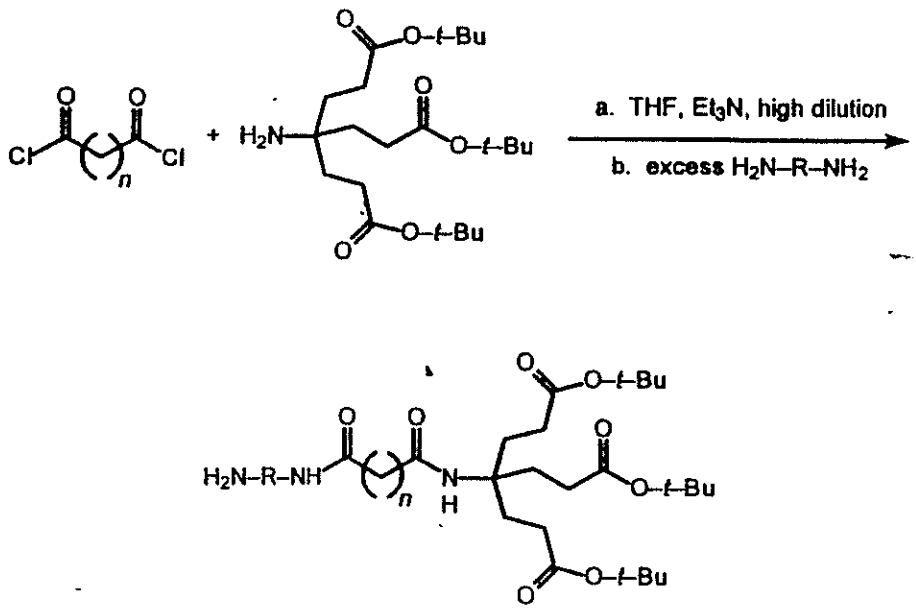

Scheme 24. General High Dilution Building Block Preparation

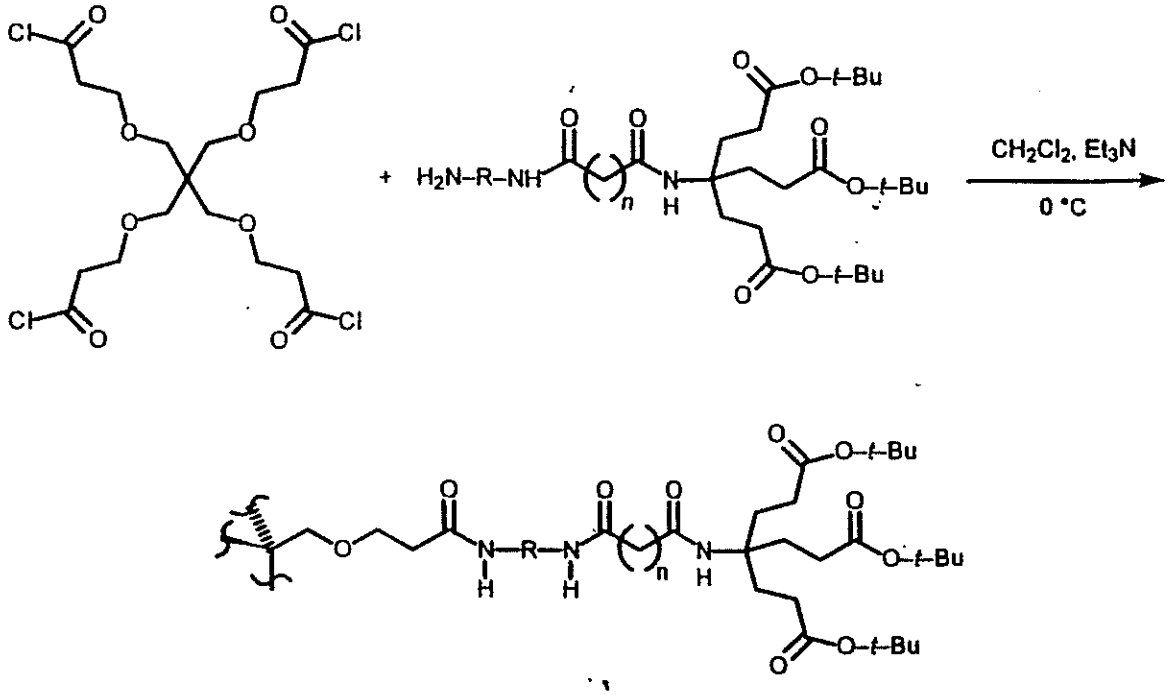

Scheme 25. General Casacde Molecule Synthesis with Functionalized Building Blocks

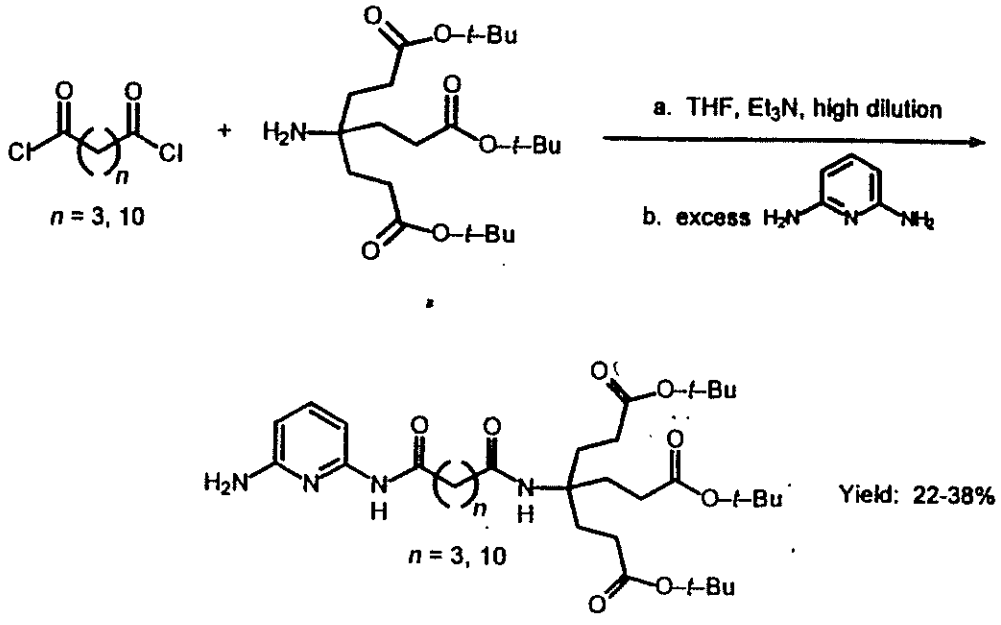

Scheme 26. Preparation of a Diaminopyridine Containing Building Block

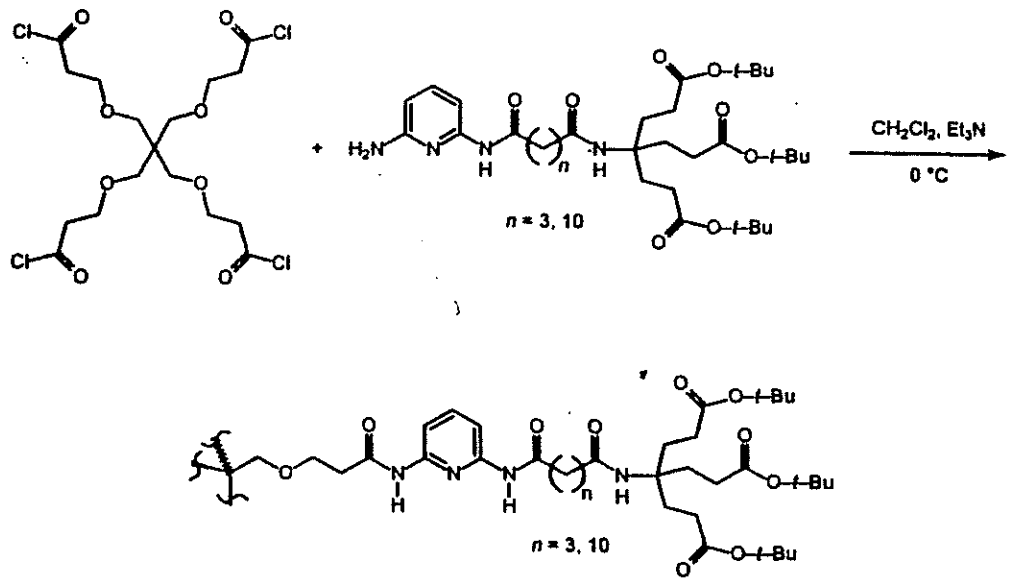

Scheme 27. Synthesis of the First Generation Diaminopyridine Containing Cascade Molecule

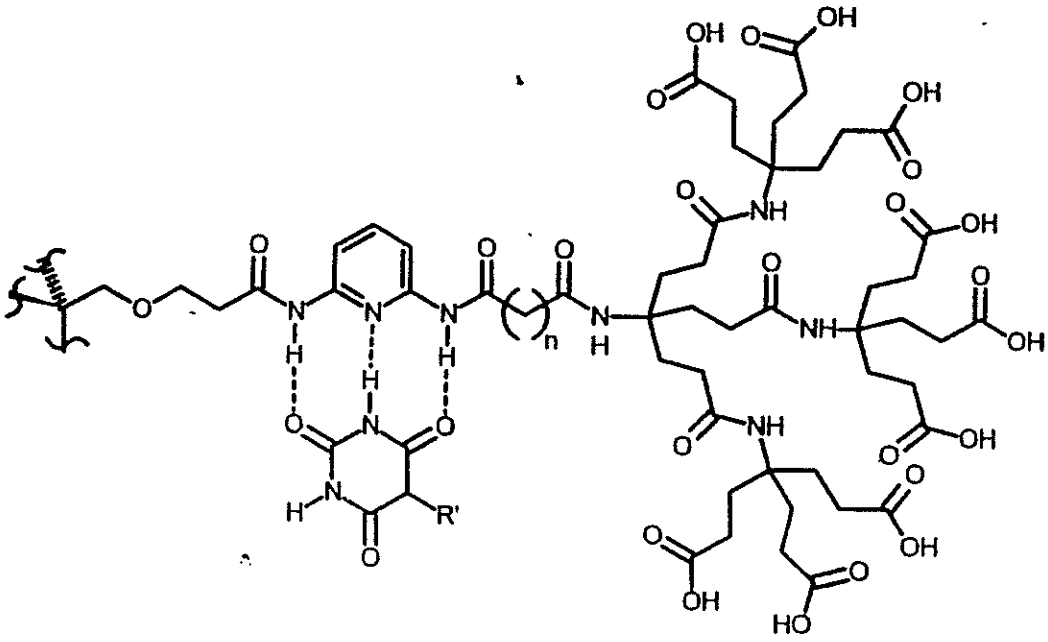

Figure 8. *H*-Bonding Complex with Barbituric Acid

5. METAL COMPLEXES

The three component, high dilution process shown above (Scheme 24) has also been used for the introduction of ligands into the cascade interior. A building block derived from *N,N'*-bis(3-aminopropyl)piperazine was prepared (Scheme 28) and subsequently used to prepare a dendrimer possessing 4 piperazines and 12 surface carboxylic acids (Scheme 29). Alternatively, the same building block may be coupled with larger acid terminated cascade molecules (e.g., Scheme 30: 12 piperazines and 36 surface carboxylic acids). Formation of the $CuBr_2$ complex proceeds smoothly (Scheme 31). Coordination by the piperazine nitrogens (as opposed to the carboxylic acids) is clearly seen by comparison of the ^{13}C NMR spectra of the two dendrimers (Figures 9 and 10).

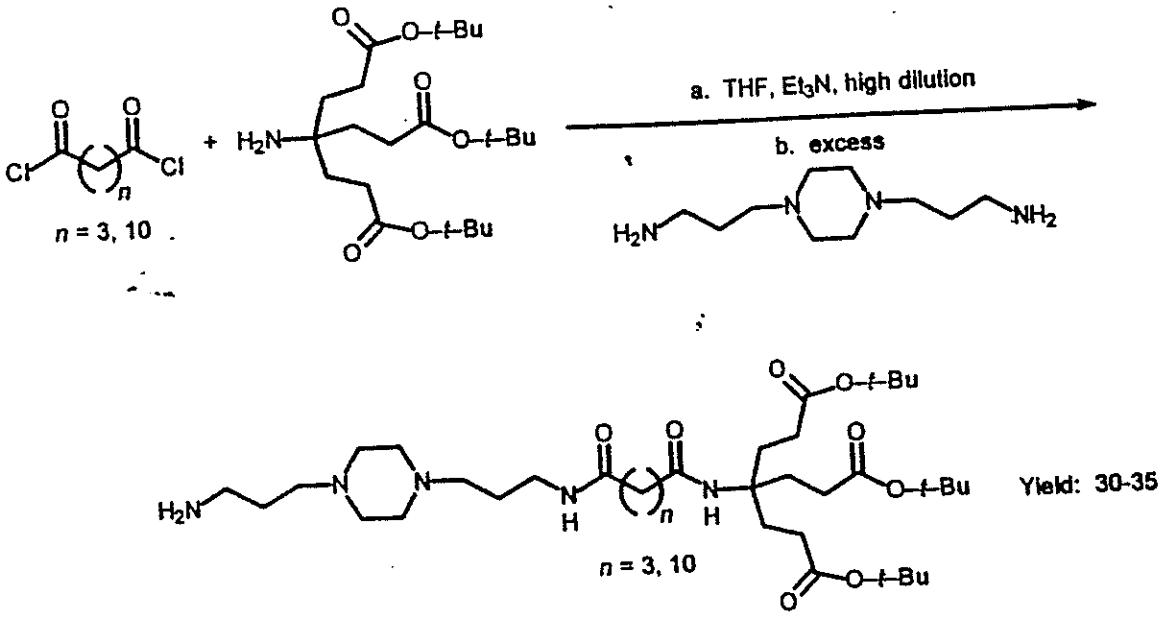

Scheme 28. Preparation of a Piperazine Containing Building Block

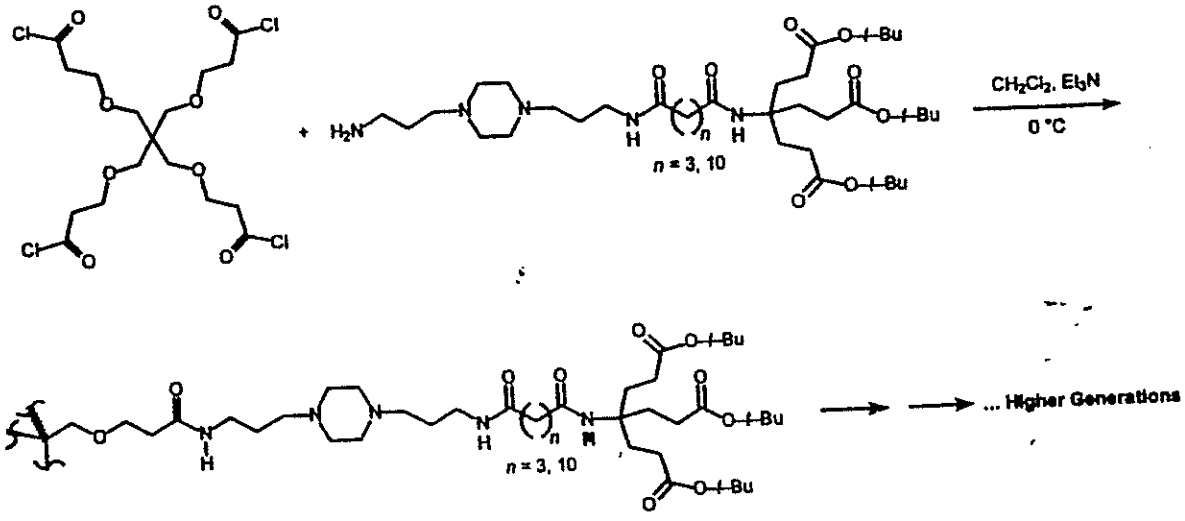

Scheme 29. Preparation of the First Generation Piperazine Containing Cascade Molecule

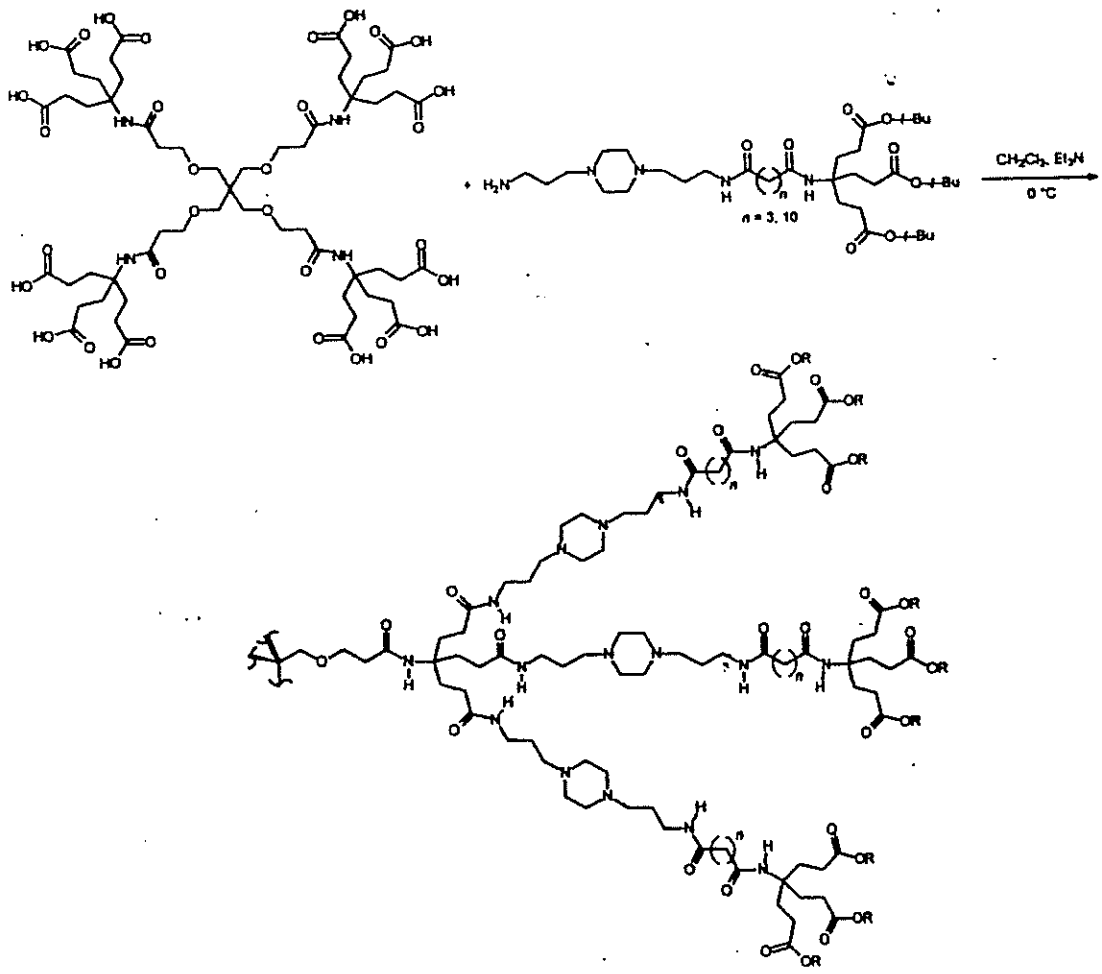

Scheme 30. Synthesis of a Second Generation Piperazine Containing Cascade Molecule

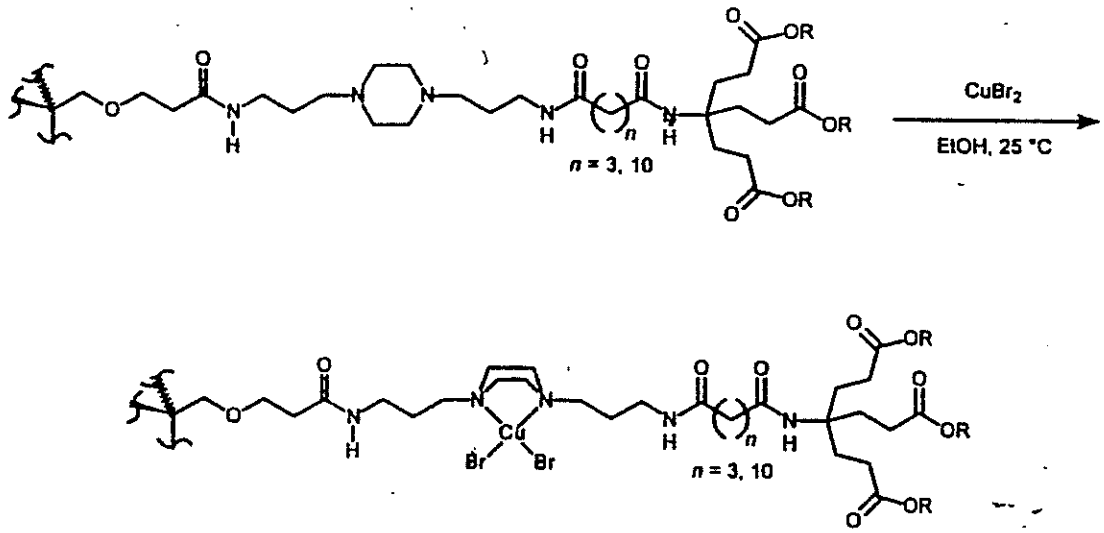

Scheme 31. Formation of the Piperazine Dendrimer-$CuBr_2$ Complex

$CuBr_2$

EtOH, 25 °C

OR

plex

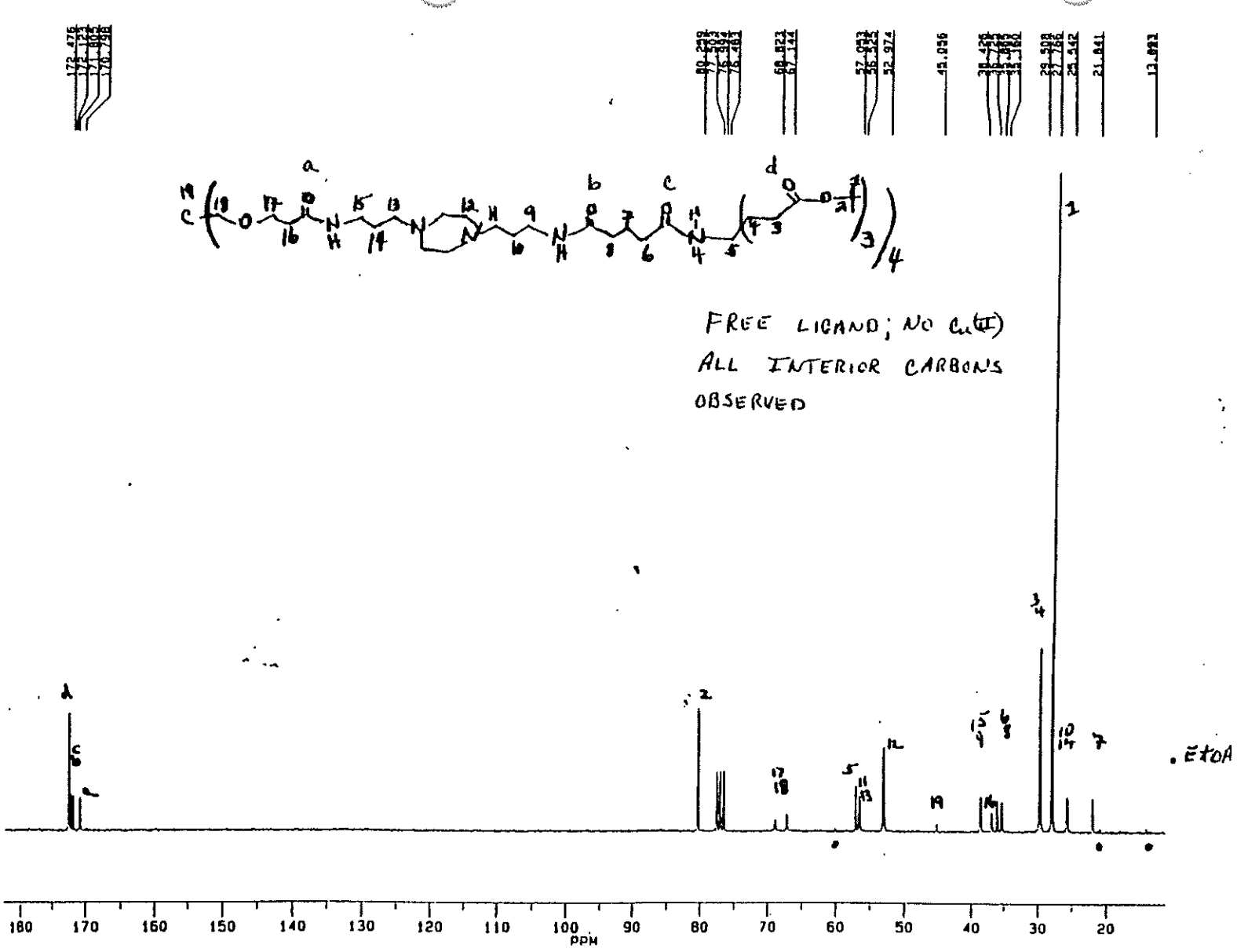

Figure 9. ^{13}C NMR Spectrum of the Piperazine Containing Cascade Molecule

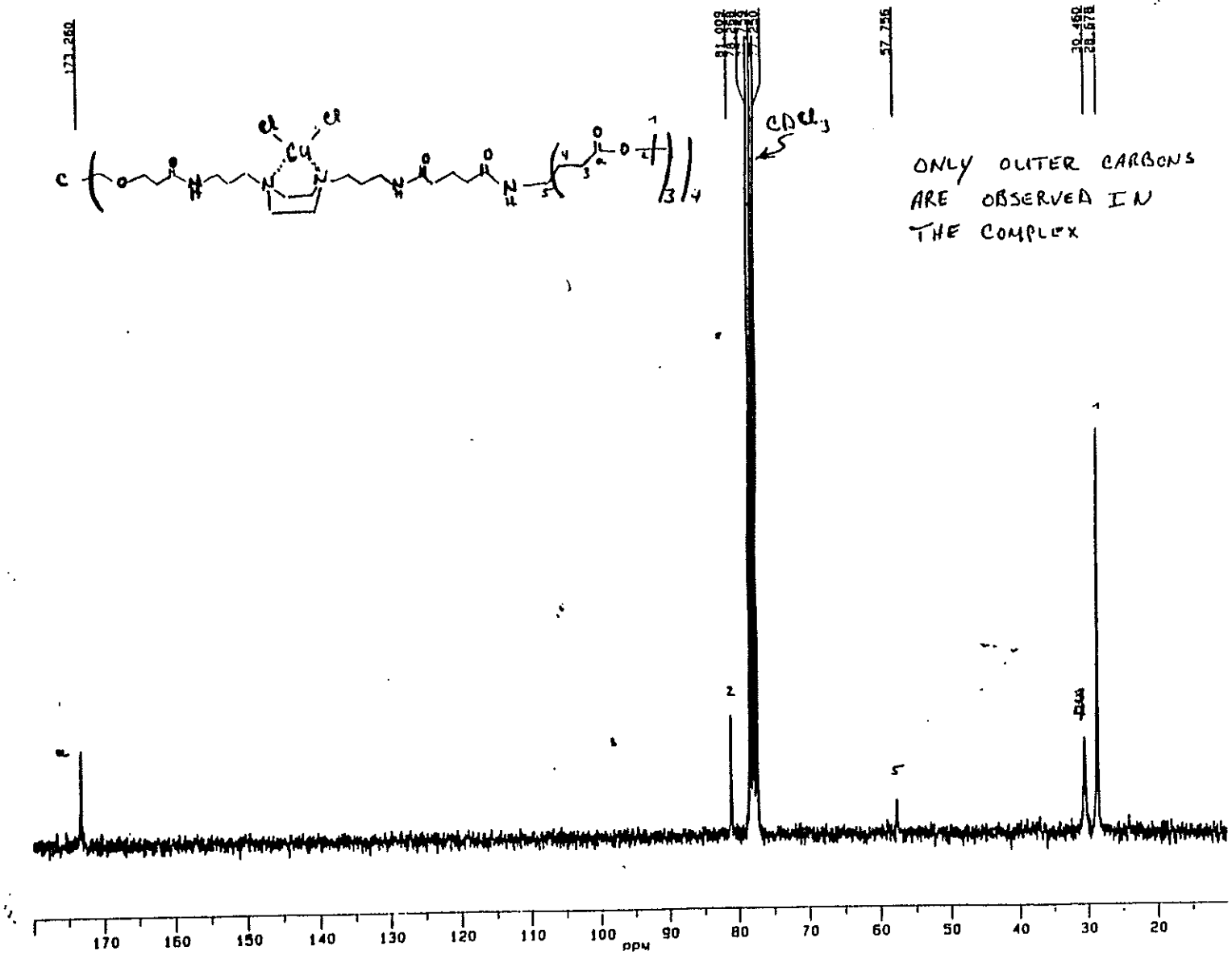

Figure 10. ^{13}C NMR Spectrum of the Piperazine-$CuBr_2$ Complex.

6. ACKNOWLEDGMENT

This work was supported in part by the National Science Foundation (DMR 86-00929, 89-06792, 92-17331), the Army Research Office (DAAH04-93-G-0448), and the Petroleum Research Fund, administered by the American Chemical Society. We also thank the National Science Foundation for the acquisition of a superconducting FT-NMR (DMR 92-08925).

7. REFERENCES

1. Buhleier, E., Wehner, W., and Vögtle, F. (1978) *Synthesis*, 155-158.
2. Moorefield, C.N. and Newkome, G.R. (1994) Cascade Macromolecules, in G.R. Newkome (ed), *Advances in Dendritic Macromolecules*, JAI Press, Greenwich, Conn., Vol. 1., Chapter 1.
3. Hallé, F., Oldeman, R.A.A., and Tomlinson, P.B. (1982) *Tropical Trees and Forests: An Architectural Analysis*, Springer-Verlag, Berlin.
4. Newkome, G.R., Gupta, V.K., Baker, G.R., and Yao, Z.-Q. (1985) *J. Org. Chem.* **50**, 2003.
5. Newkome, G.R., Baker, G.R., Saunders, M.J., Russo, P.S., Gupta, V.K., Yao, Z.-Q., Miller, J.E., and Bouillon, K. (1986) *J. Chem. Soc., Chem. Gommun.*, 752.
6. Newkome, G.R., Baker, G.R., Arai, S., Saunders, M.J., Russo, P.S., Theriot, K.J., Moorefield, C.N., Miller, J.E., Lieux, T.R., Murray, M.E., Phillips, B., and Pascal, L. (1990) *J. Am. Chem. Soc.* **112**, 8458.
7. Newkome, G.R. and Arai, S. (1987) Four-Directional Arborols, ORGN 66, 193rd National Meeting of the American Chemical Society, Denver, CO.
8. Newkome, G.R., Arai, S., Fronczek, F.R., Moorefield, C.N., Lin, X., and Weis, C.D. (1993) *J. Org. Chem.* **58**, 898.
9. Newkome, G.R., Moorefield, C.N., and Theriot, K.J. (1988) *J. Org. Chem.* **53**, 5552.
10. Newkome, G.R., Behera, R.K., Moorefield, C.N., and Baker, G.R. (1991) *J. Org. Chem.* **56**, 7162.
11. Newkome, G.R. and Lin, X. (1991) *Macromolecules* **24**, 1443.
12. Newkome, G.R., Young, J.K., Baker, G.R., Potter, R.L., Audoly, L., Cooper, D., Weis, C.D., Morris, K., and Johnson, C.S., Jr. (1993) *Macromolecules* **26**, 2394.
13. Cascade Nomenclature: Newkome, G.R., Baker, G.R., Young, J.K., and Traynham, J.G. (1993) *J. Polym. Sci., Part A: Polymer Chem.* **31**, 641.
14. Reneker, D.H., Mattice, W.L., Quirk, R.P., and Kim, S.J. (1992) *Smart Mater. Struct.* **1**, 84. Kuhn, W., Hargity, B., Katchaisky, A., and Eisenberg, H. (1950) *Nature* **165**, 514. Siegel, R.A. and Firestone, B.A. (1988) *Macromolecules* **21**, 3254.
15. Young, J.K., Baker, G.R., Newkome, G.R., Morris, K.F., and Johnson, C.S., Jr. (1994) *Macromolecules* **27**, in press.

16. Ono, N.; Miyake, H.; Tamura, R.; Kaji, A. *Tetrahedron Lett.* **1981**, *22*(18), 1705-1708.

17. Newkome, G.R., Moorefield, C.N., Baker, G.R., Johnson, A.L., and Behera, R.K. (1991) *Angew. Chem.* **103**, 1991; (1991) *Angew. Chem., Int. Ed. Engl.* **30**, 1176.

18. Newkome, G.R., Moorefield, C.N., Baker, G.R., Saunders, M.J., and Grossman, S.H. (1991) *Angew. Chem.* **103**, 1207; (1991) *Angew. Chem., Int. Ed. Engl.* **30**, 1178.

19. Newkome, G.R., Moorefield, C.N., Keith, J.M., Baker, G.R., and Escamilla, G.H. (1994) *Angew. Chem.* **106**, in press.

20. Newkome, G.R., Cardullo, F., Constable, E.C., Moorefield, C.N., and Thompson, A.M.W.C. (1993) *J. Chem. Soc., Chem. Commun.*, 925-927.

The Key to the Synthesis of Organic Nanoarchitectures - Repetitive Nonlinear Growth Schemes

Jeffrey S. Moore
University of Illinois

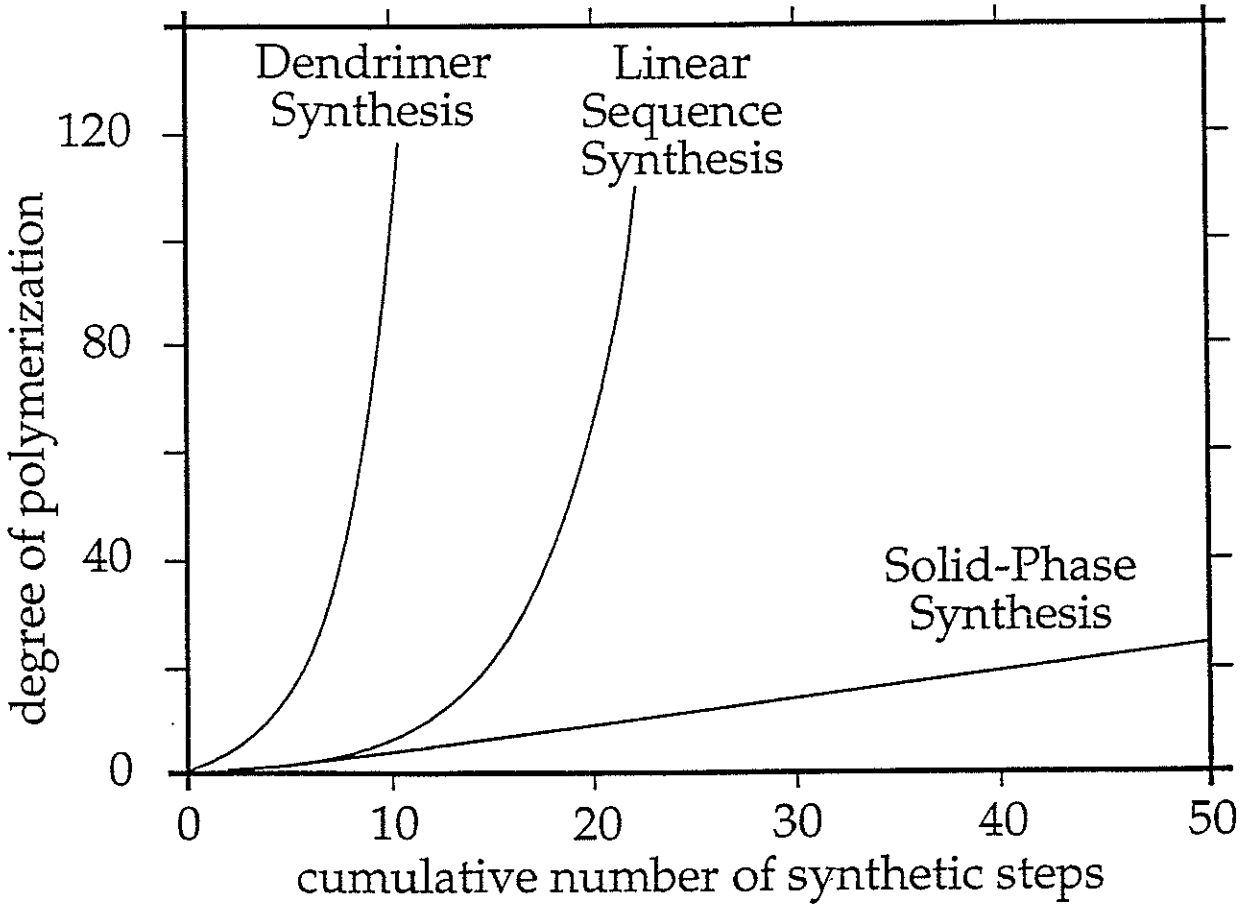

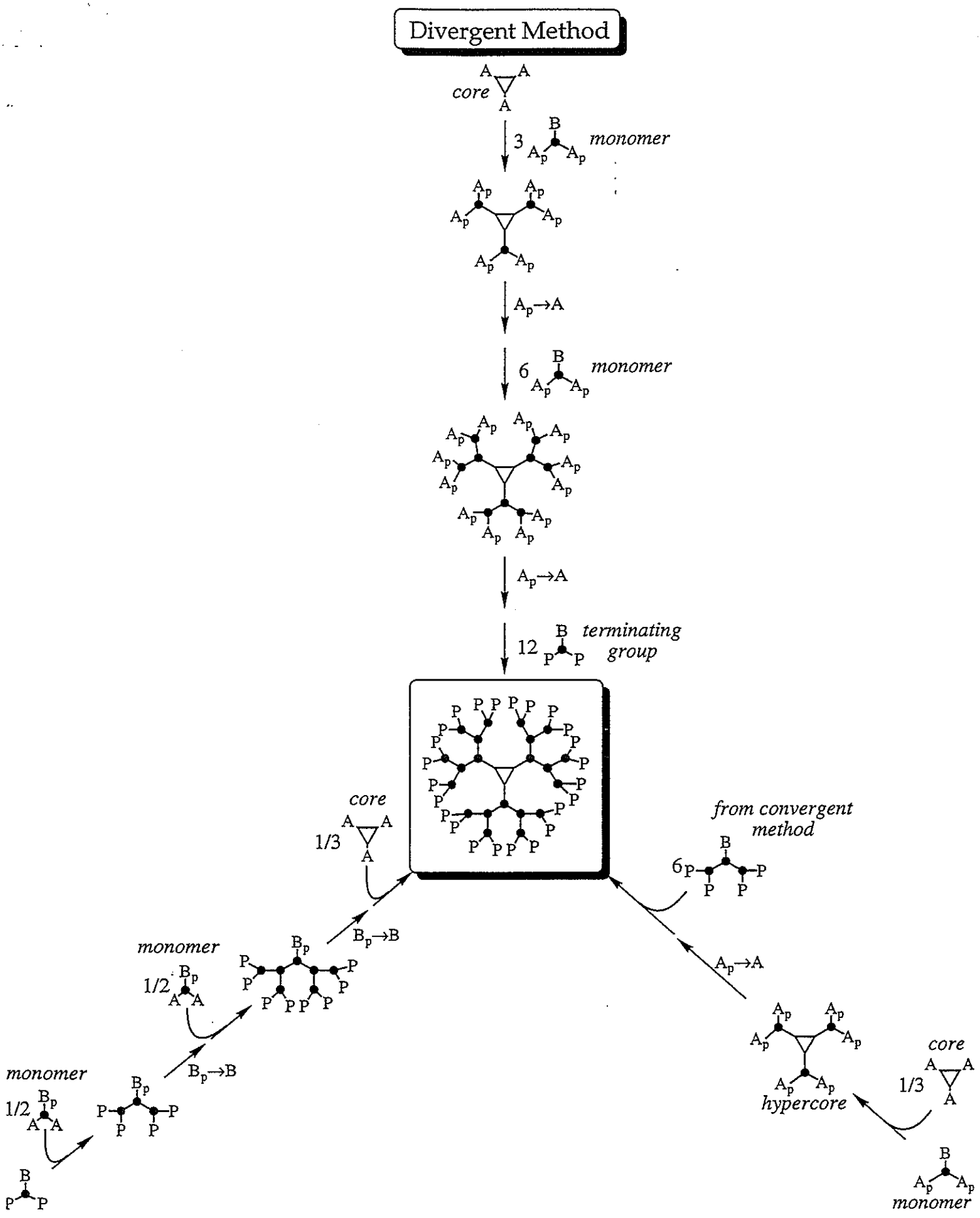
Divergent Method
core
3
monomer
$A_p \rightarrow A$
6
monomer
$A_p \rightarrow A$
12
terminating group
core
1/3
from convergent method
6
monomer
1/2
$B_p \rightarrow B$
$B_p \rightarrow B$
$A_p \rightarrow A$
core
1/3
hypercore
monomer
1/2
monomer
Convergent Method
Double-Stage Method

A Repetitive Method for Synthesizing Oligomeric Sequences

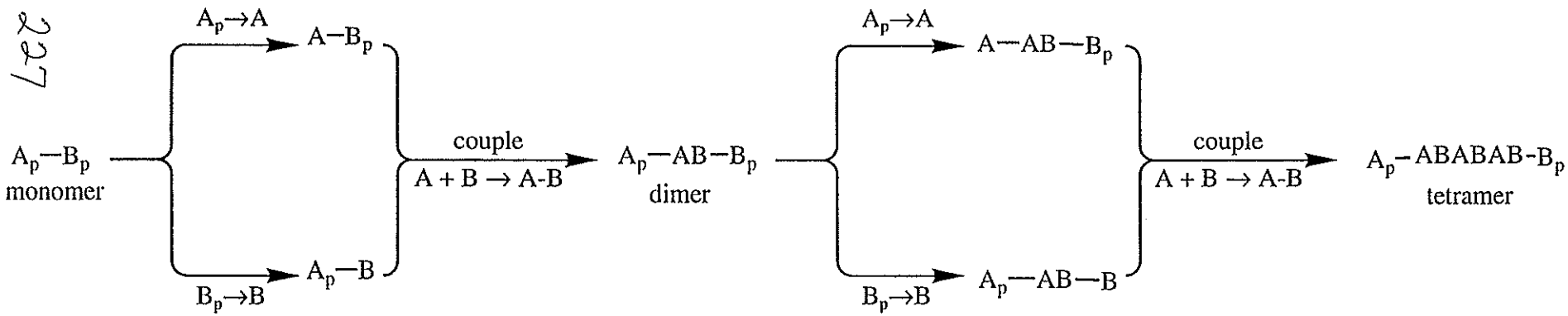

number of monomers ~ 2^n

Phenylacetylene Monomer Protocol

Geometric Considerations

Phenylacetylene "valence angles"

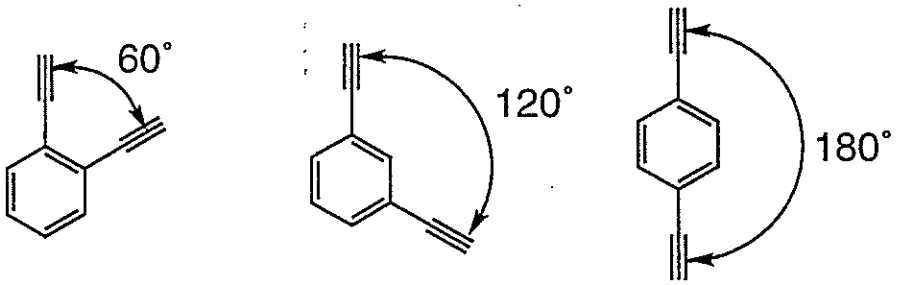

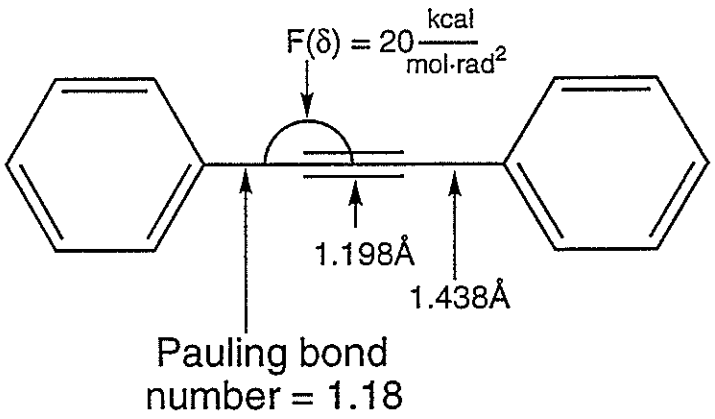

Conformational Considerations

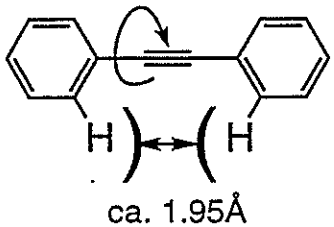

Ito et al. *J. Phys. Chem.* **1984**, *88*, 1711-16

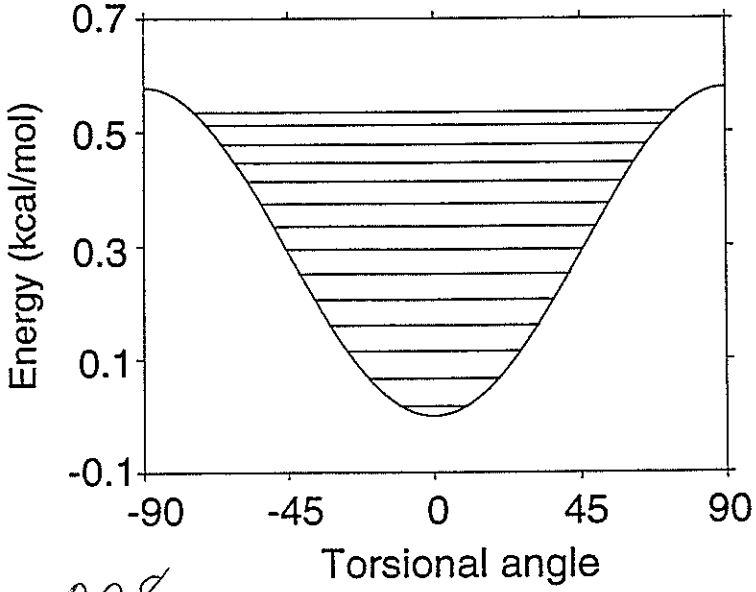

the repetitive chemistry

A + B → A-B

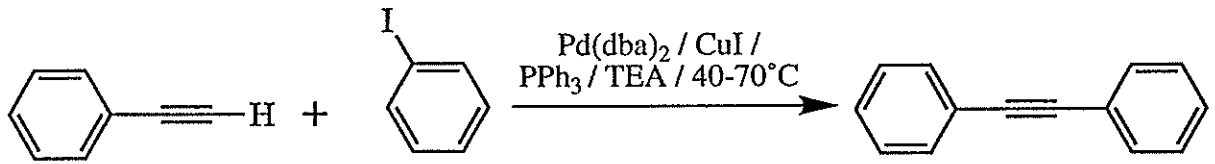

~98%

$A_p \rightarrow A$

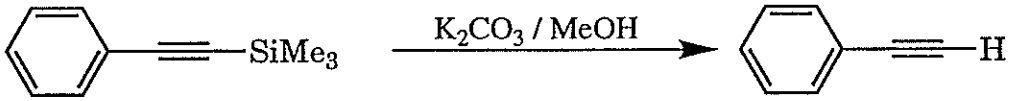

$B_p \rightarrow B$

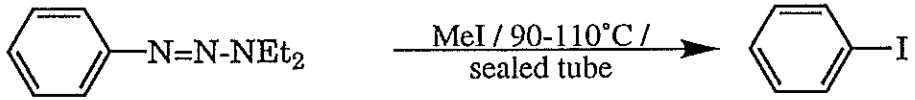

A side reaction

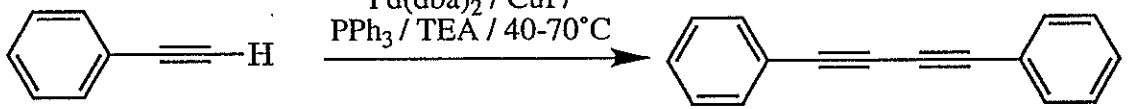

≤2%

A Modular Approach to Supermolecule Building Blocks

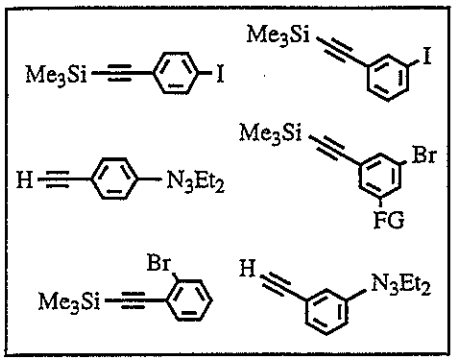

monomer pool

sequence synthesis

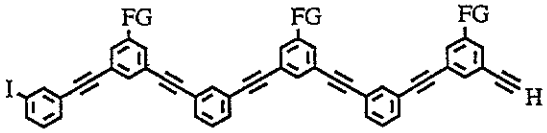

sequence specific oligomer

cyclization

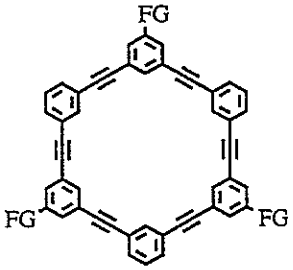

supramolecular ordering

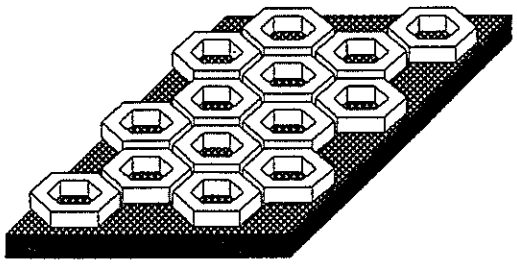

monolayers

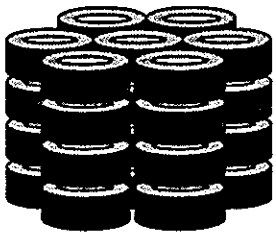

liquid crystals

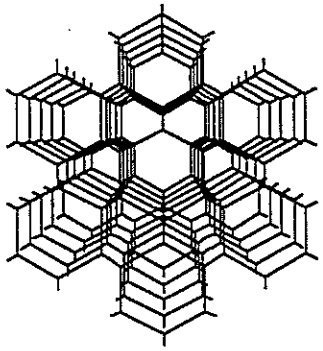

porous crystals

Hypothetical Supramolecular Networks Based on Supermolecule Building Blocks

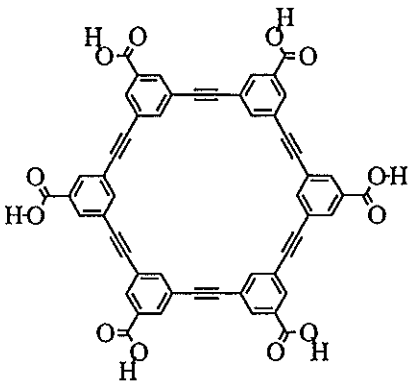

crystallization

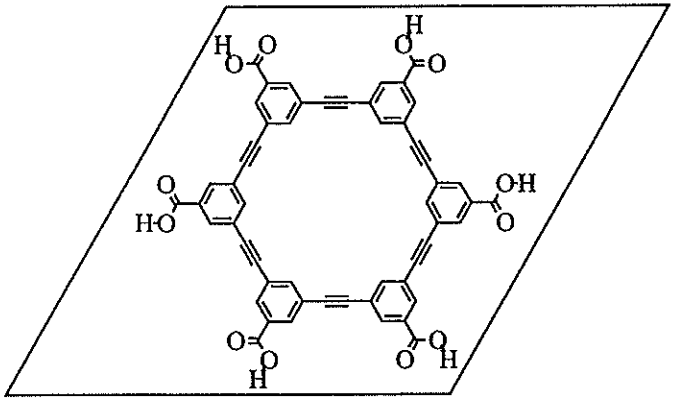

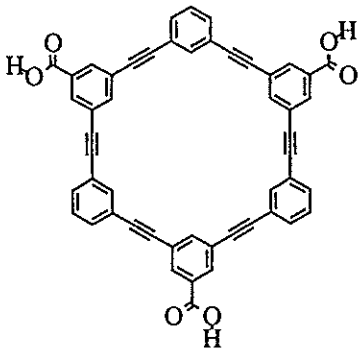

crystallization

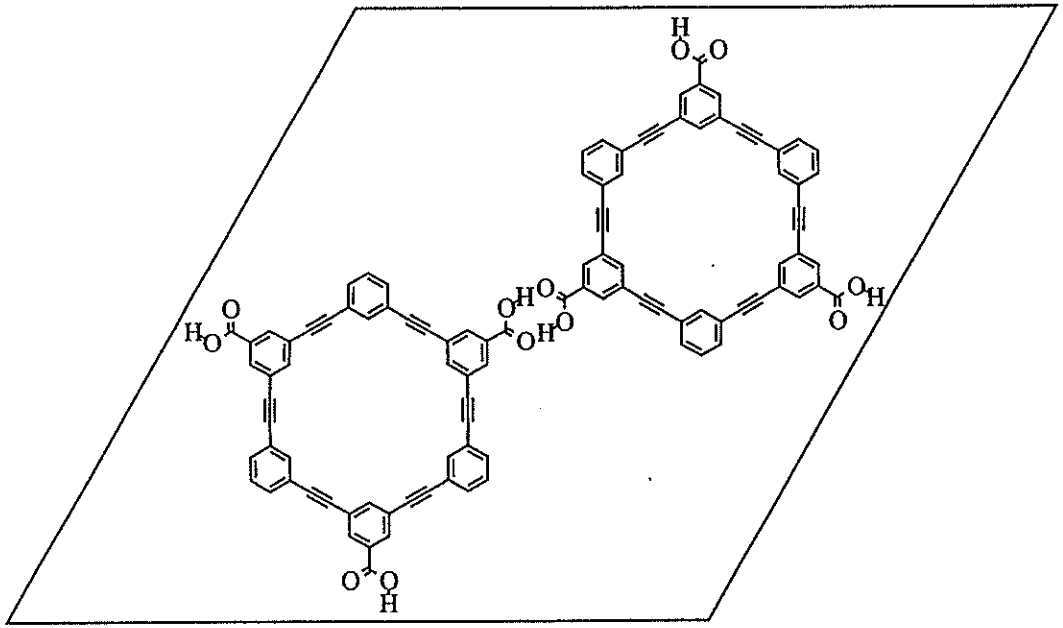

Triazene Formation Using an *N*-Alkylated Aminomethylated Polystyrene

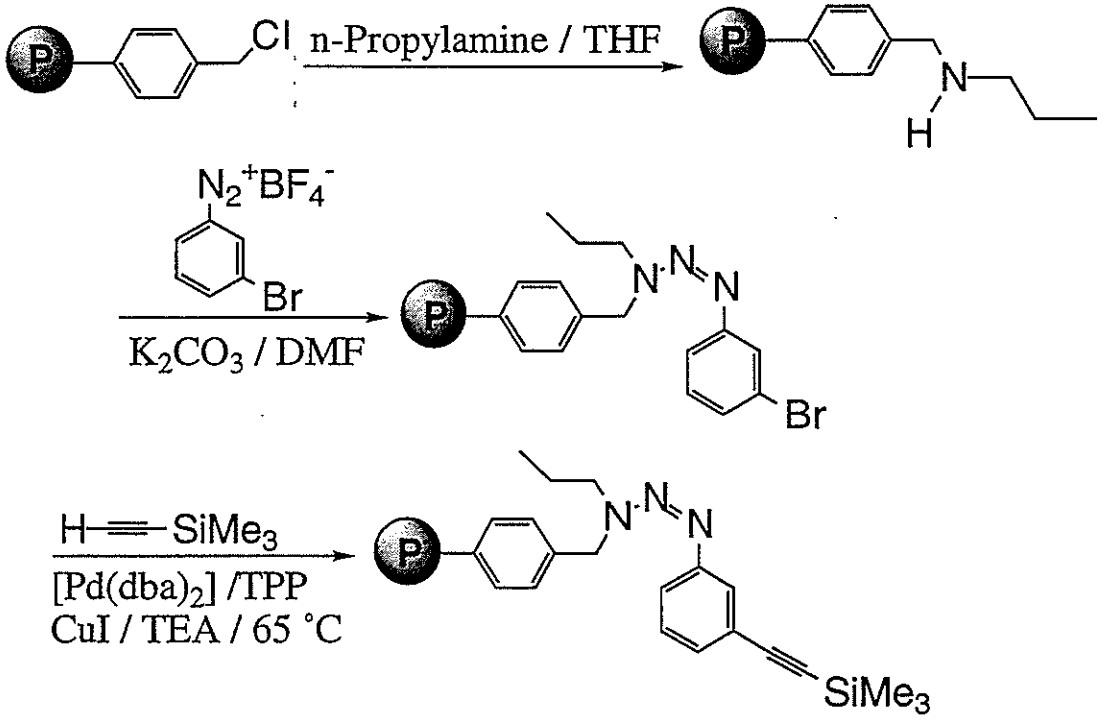

SOLID PHASE REPETITIVE SYNTHESIS OF PHENYLACETYLENE OLIGOMERS

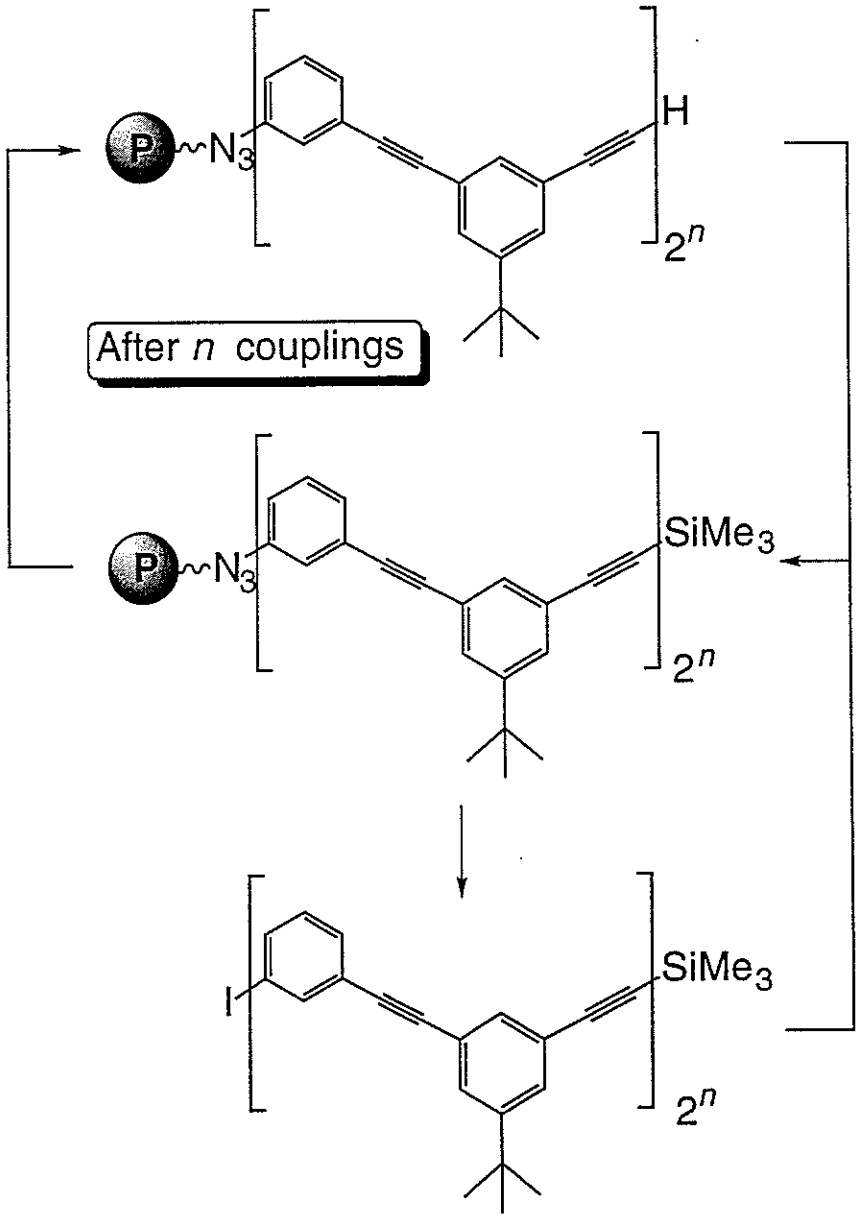

P ≡ Polystyrene, 200-400 Mesh,
1% Crosslinked with Divinylbenzene

Monitoring Polymer Supported Phenylacetylene Reactions

Infrared Spectra

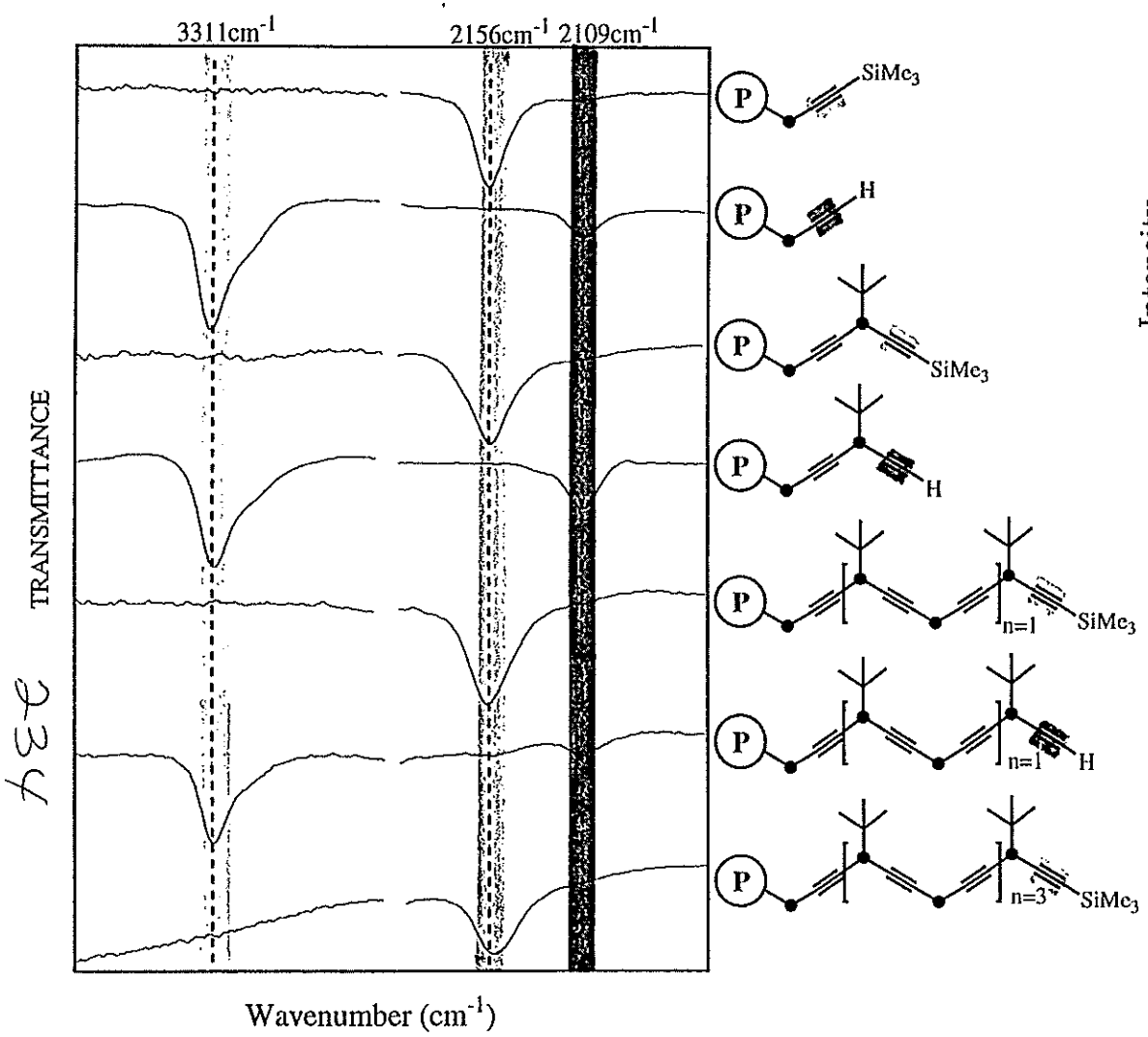

Size Exclusion Chromatographs

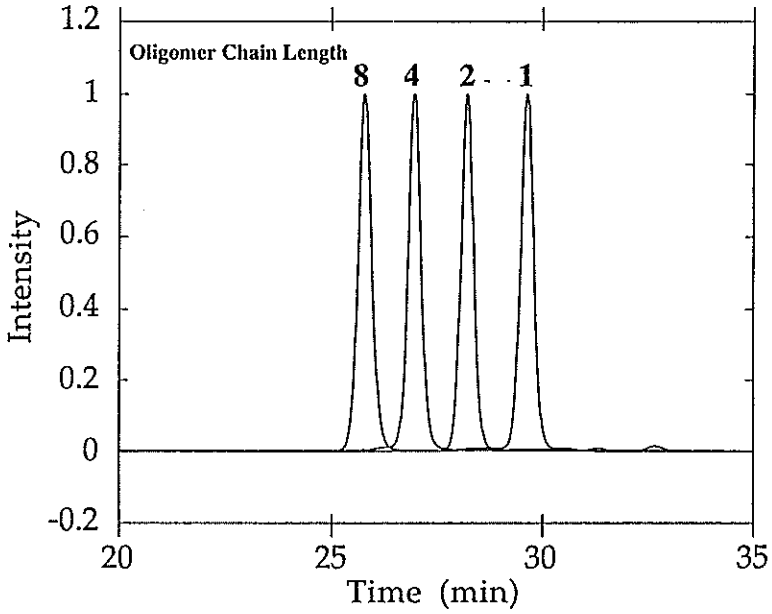

Structure Key

= 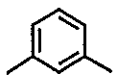

= 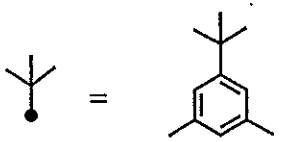

P = Polystyrene, 200-400 Mesh,
1% Crosslinked with Divinylbenzene

Synthesis of Polyaromatic Macrocycles

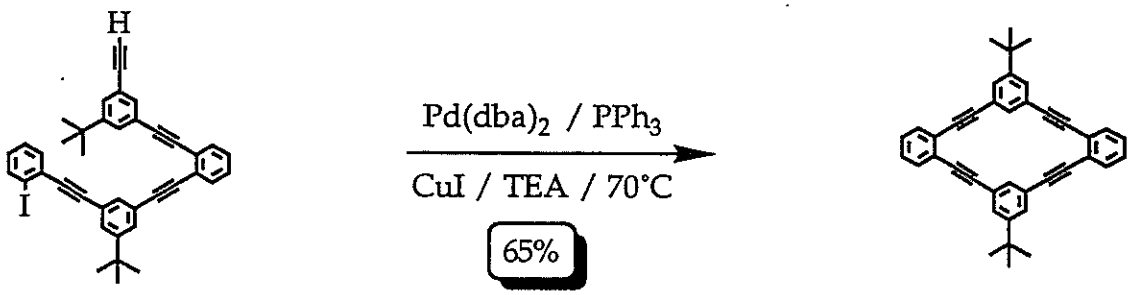

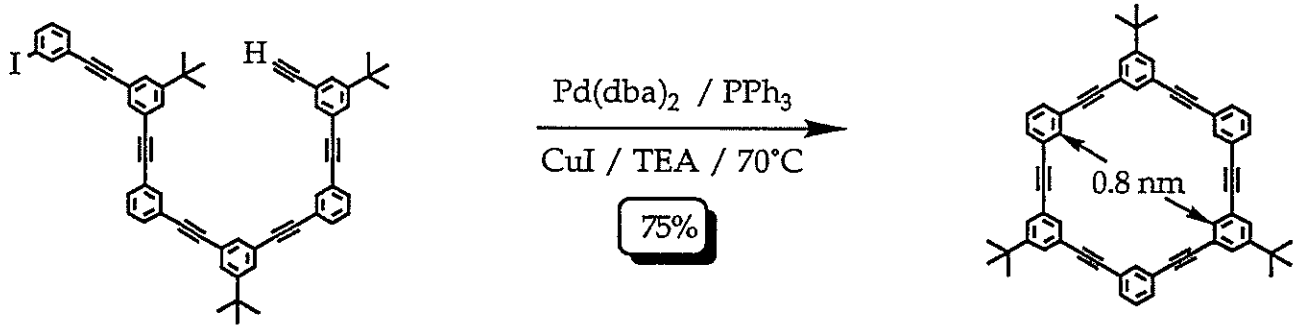

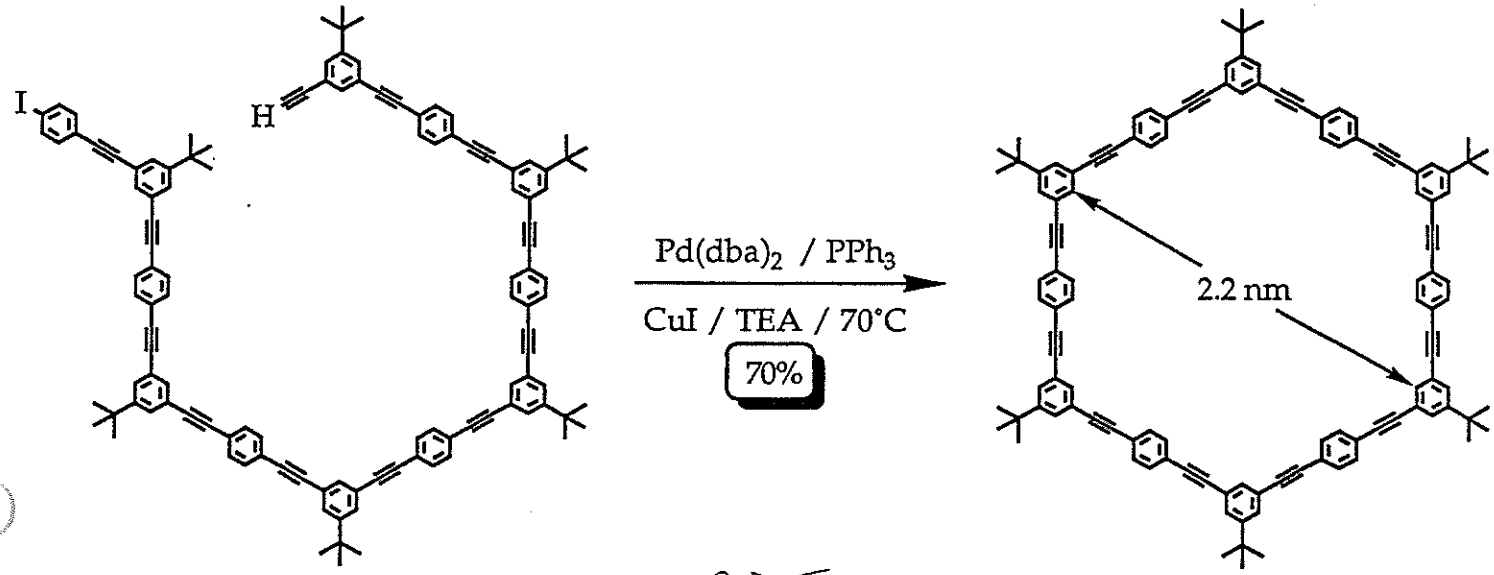

Double Cyclization Gives Macrobicycles

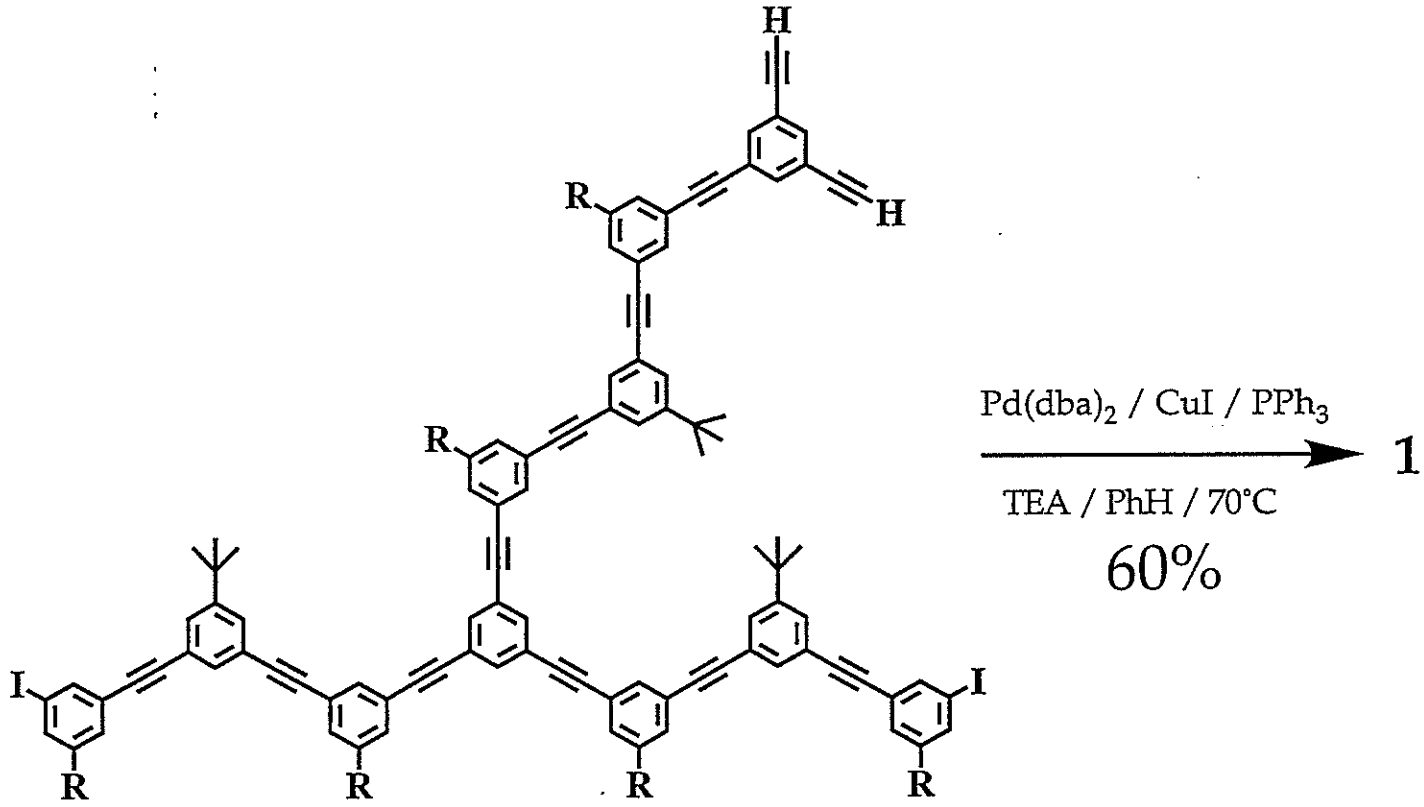

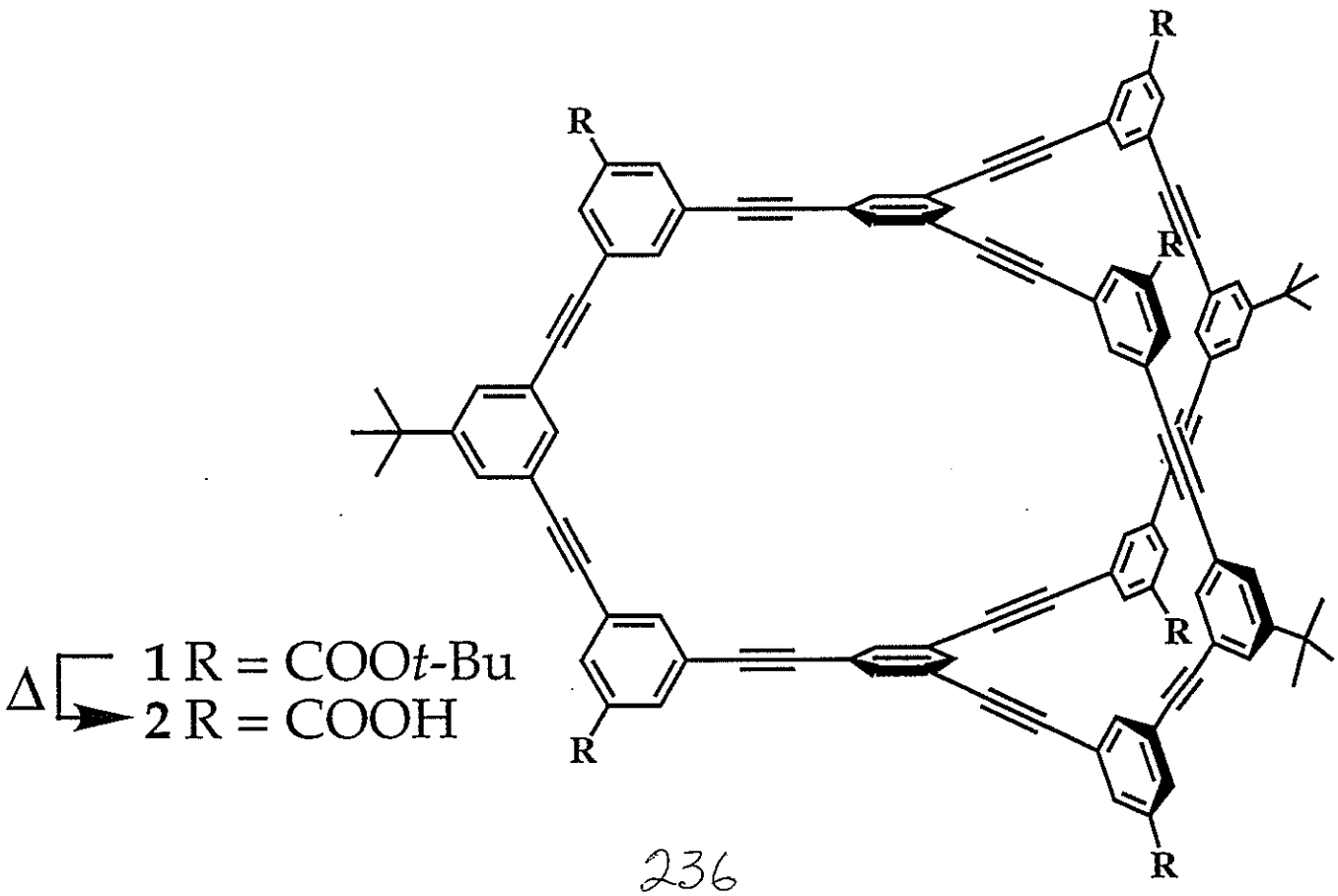

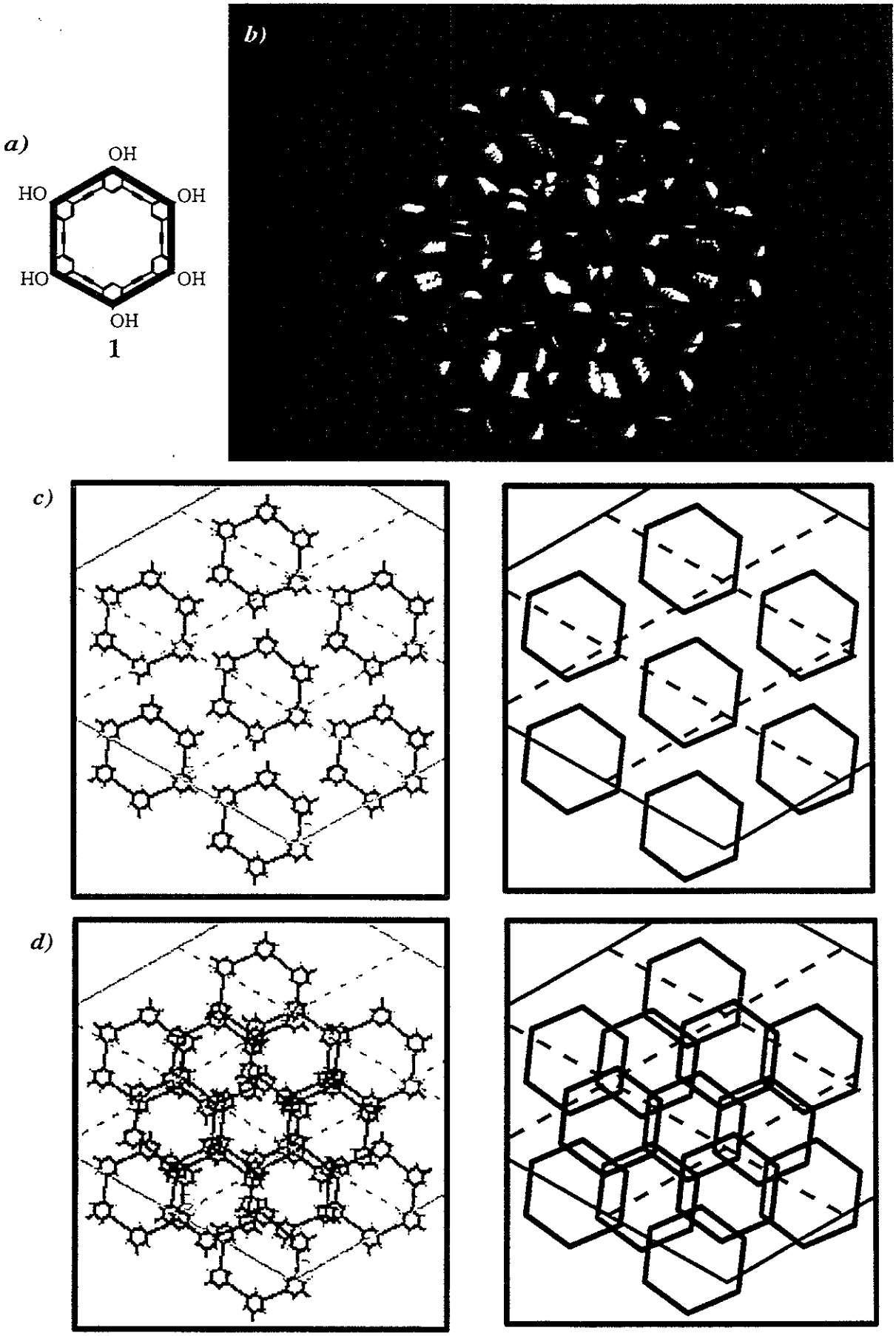

Figure 3. (a) Chemical structure of 1 superimposed with its hexagonal polygon representation, (b) X–ray structure of 1 shown as its space filling model, (c) packing diagram of a single hydrogen–bonded layer, (d) packing diagram of three layers. The central hexagon in (c) has a total of 12 nearest neighbors (6 in same plane (red hexagons), 3 in upper plane (blue hexagons), and 3 in the lower plane (green hexagons)).

SEC

Figure 4. (a) Chemical structure of 2 superimposed with its trigonal prismatic representation, (b) X–ray structure of 2 shown as its space–filling model, (c) packing diagram viewed along the c axis. The central molecule in (c) has 6 nearest neighbors in the same plane (colored blue) and 3 nearest neighbors in each of the two adjacent planes (colored red) making a total of 12 nearest neighbors. Note that hydrogen atoms have been omitted.

a)

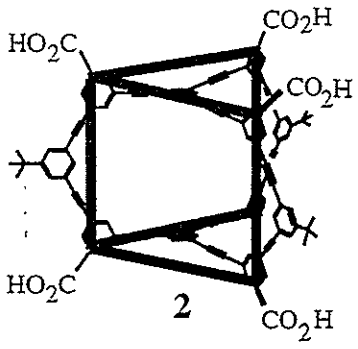

b)

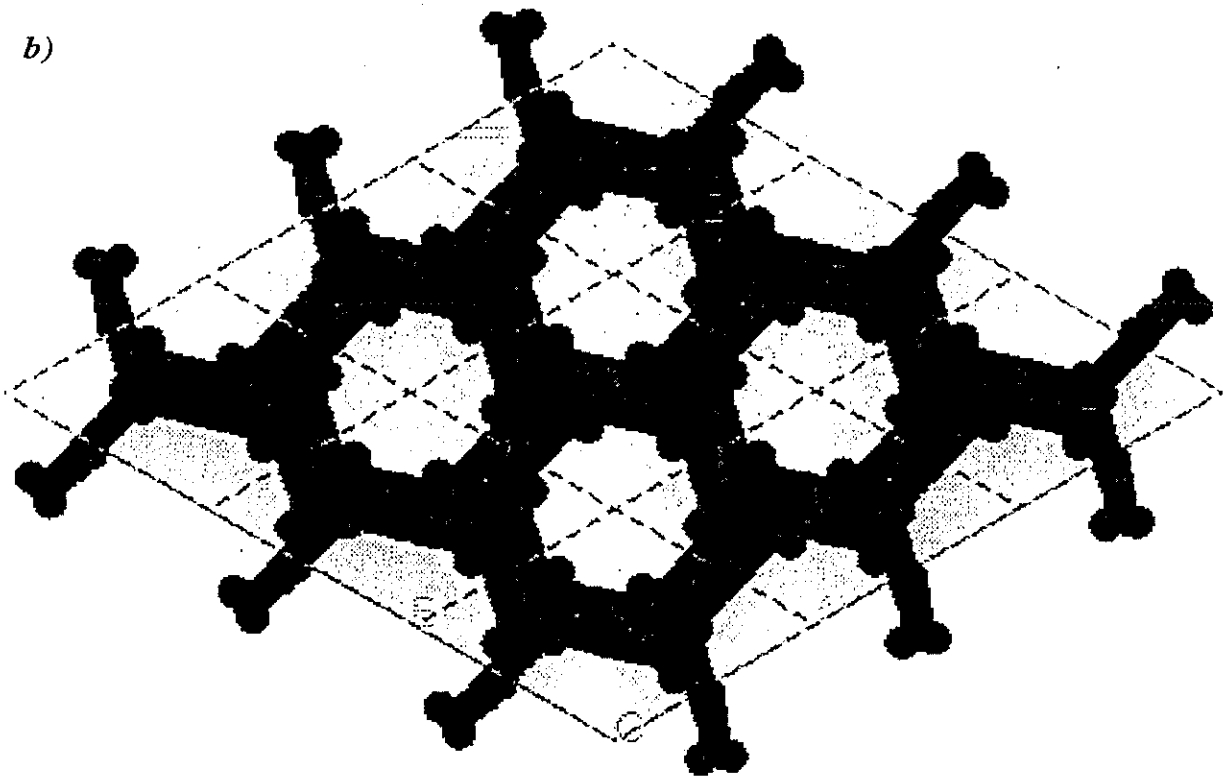

c)

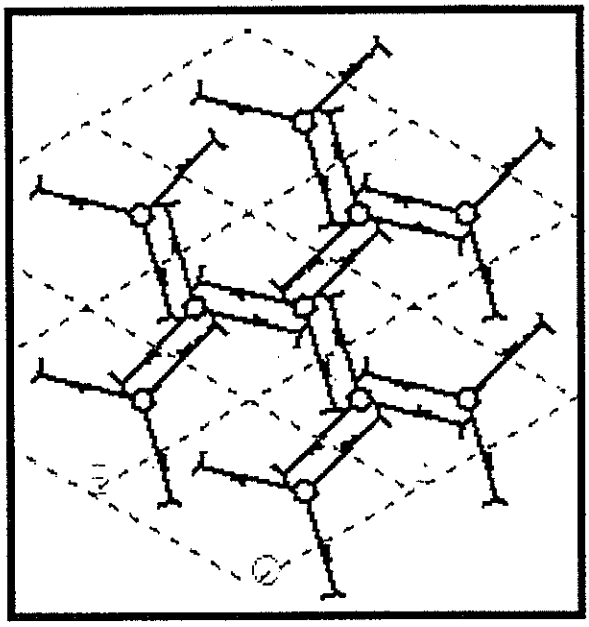

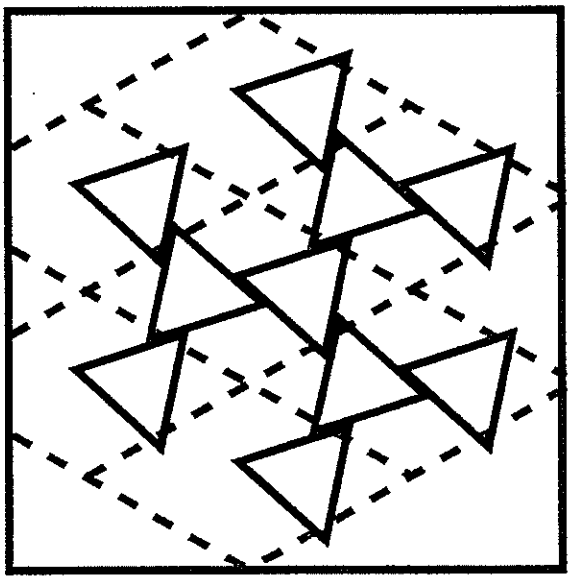

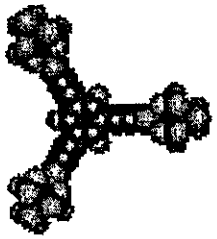

D–4

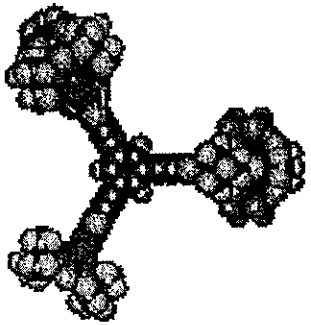

D–10

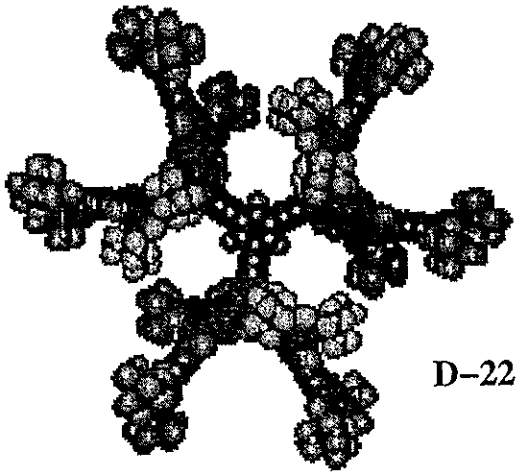

D–22

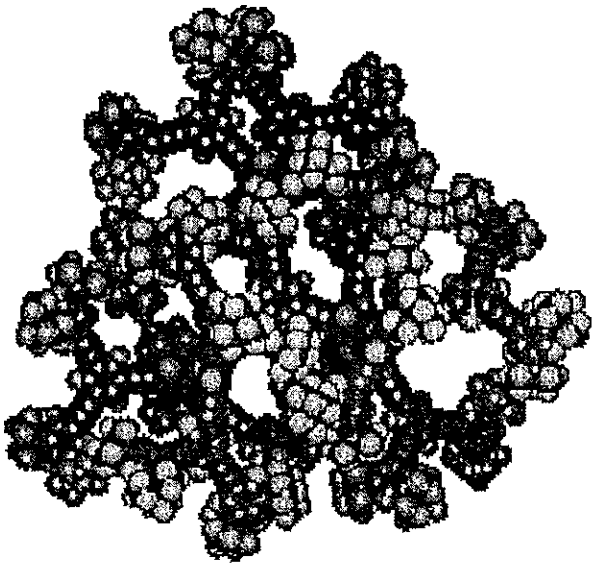

D–46

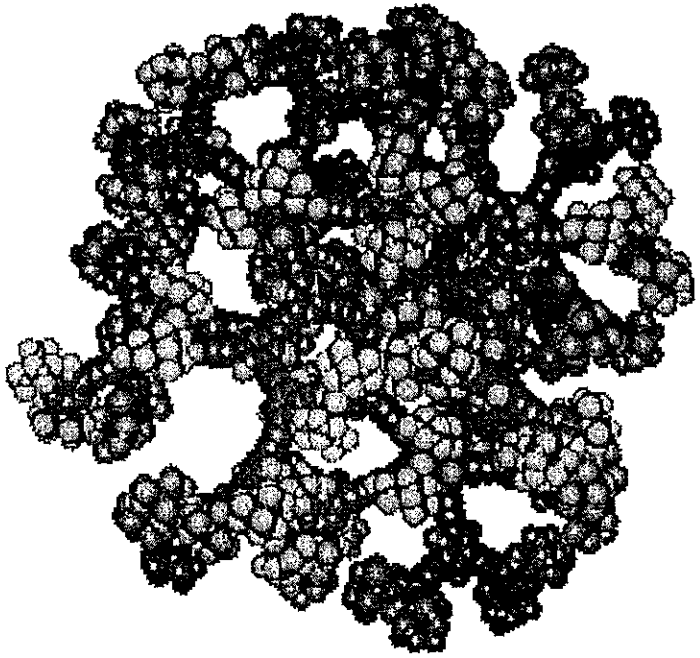

D–94

Two Schemes to Prepare Phenylacetylene Monodendrons

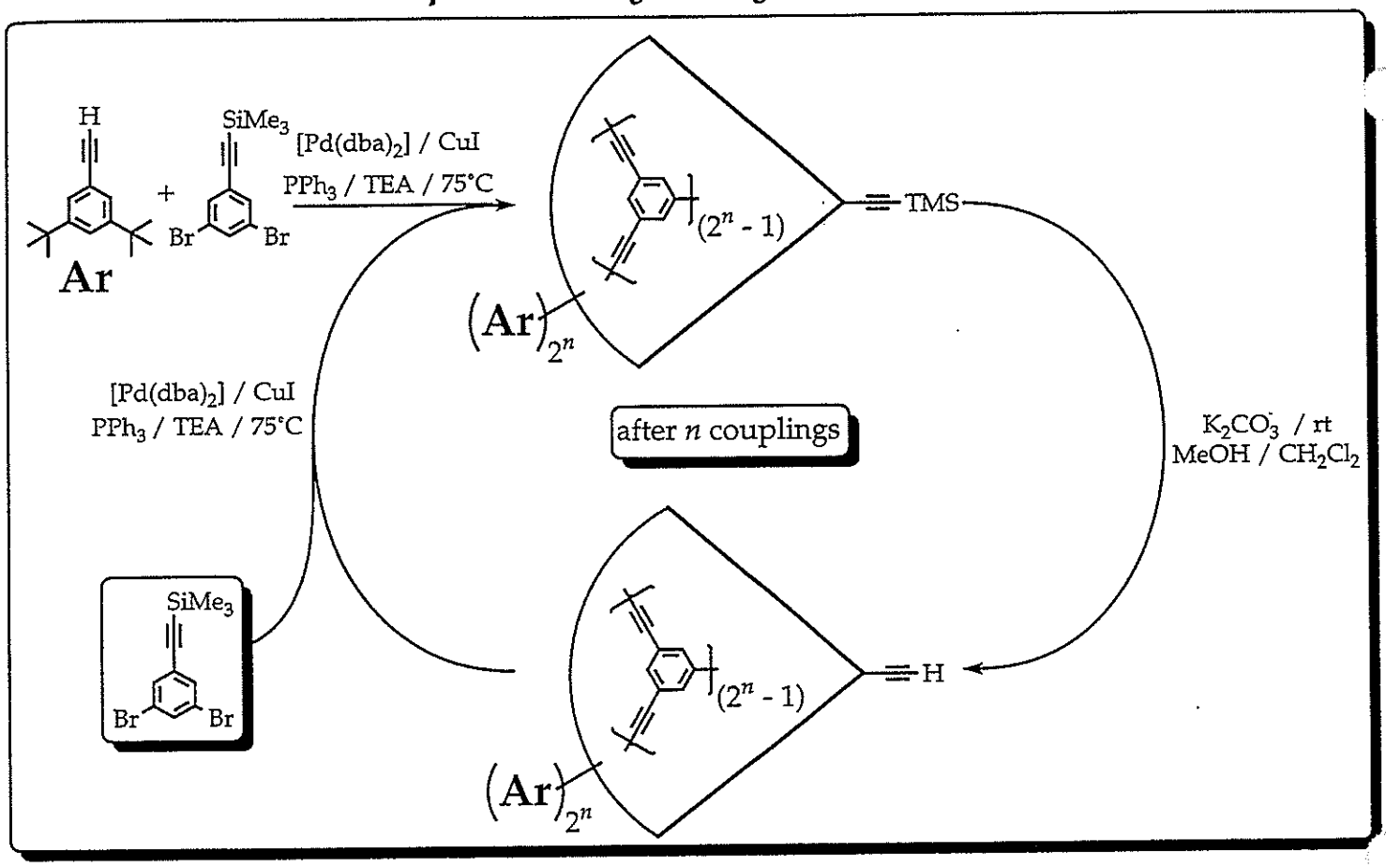

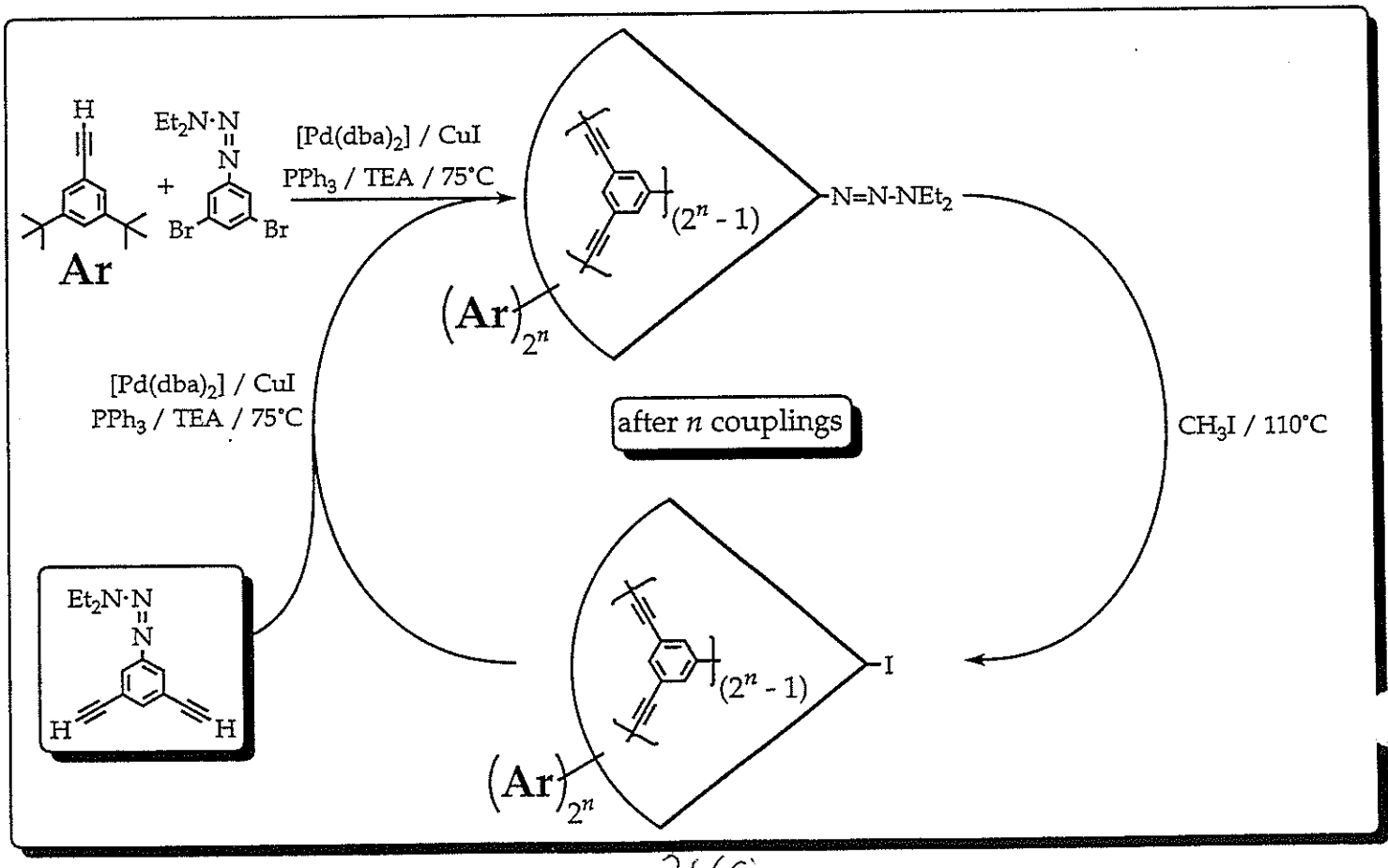

Subtle changes in chemistry can have significant consequences on monodendron yields

monodendron	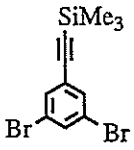 scheme	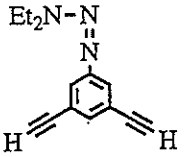 scheme
3-mer	93	88
7-mer	80	82
15-mer	51	84
31-mer	27	81
63-mer	0	85

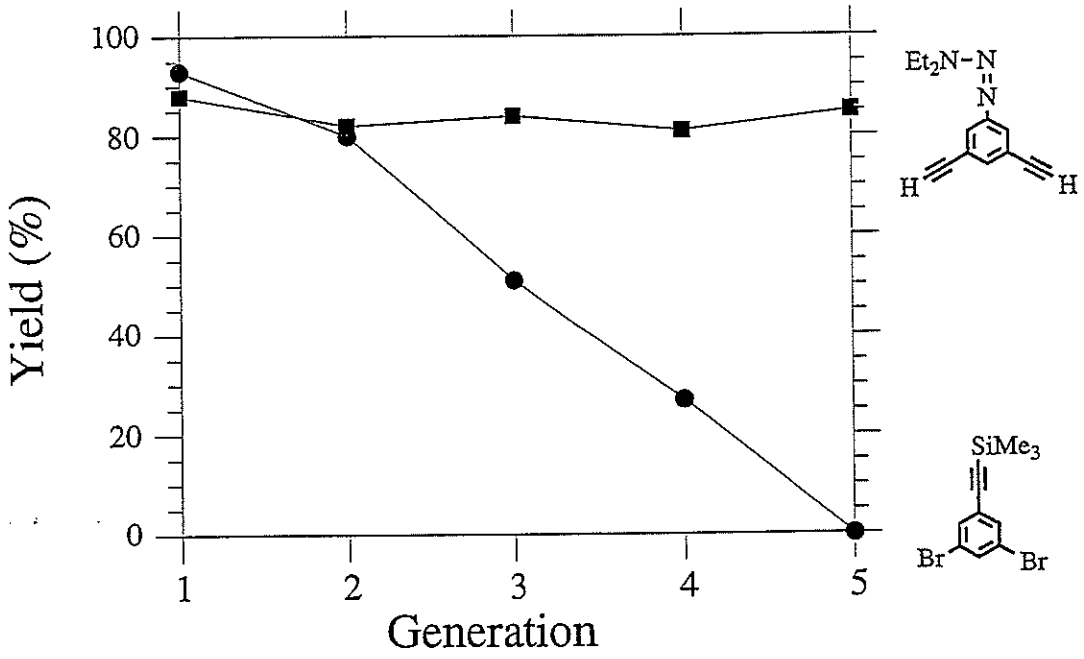

A Solid Phase Convergent Synthesis Simplifies Purification

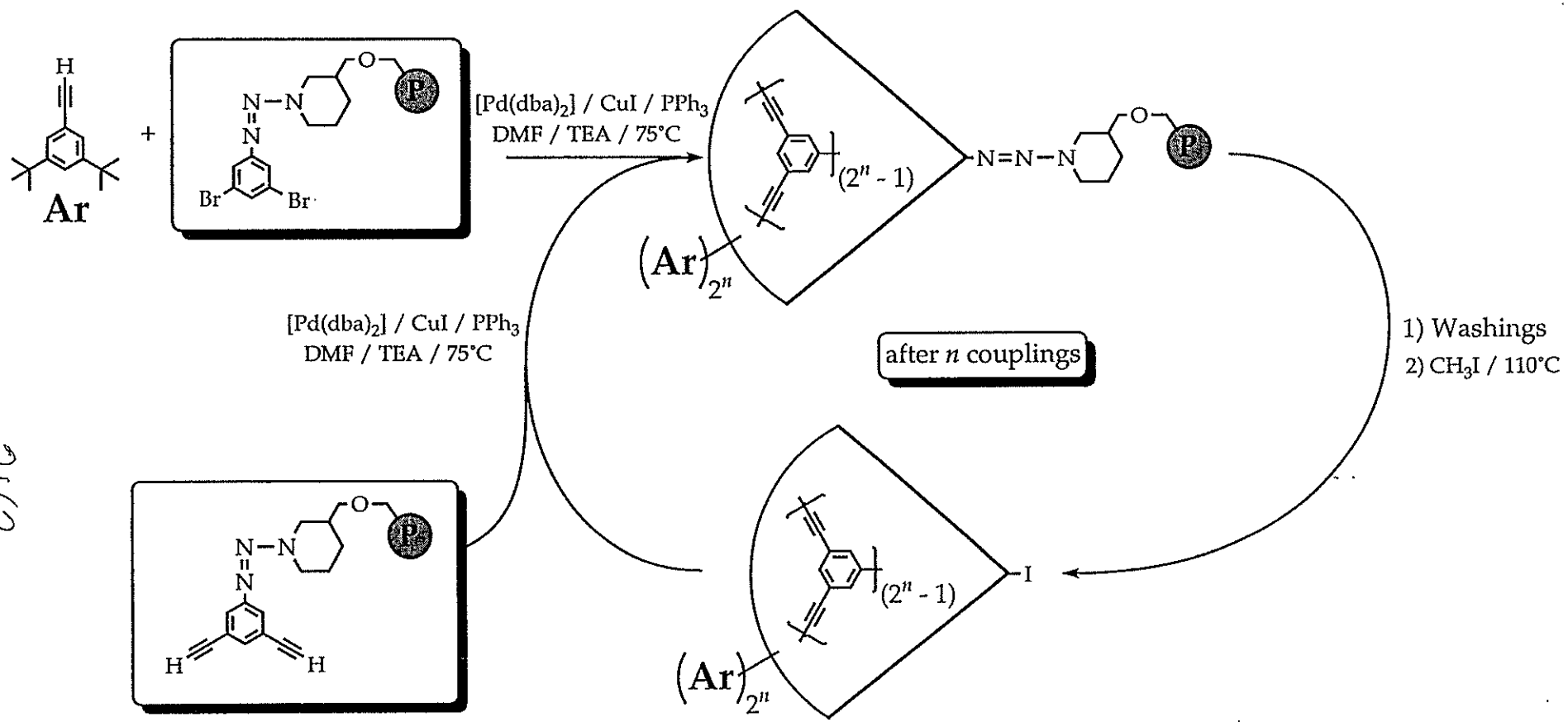

242

Solid Phase Chemistry Can be Monitored by Infrared Spectroscopy

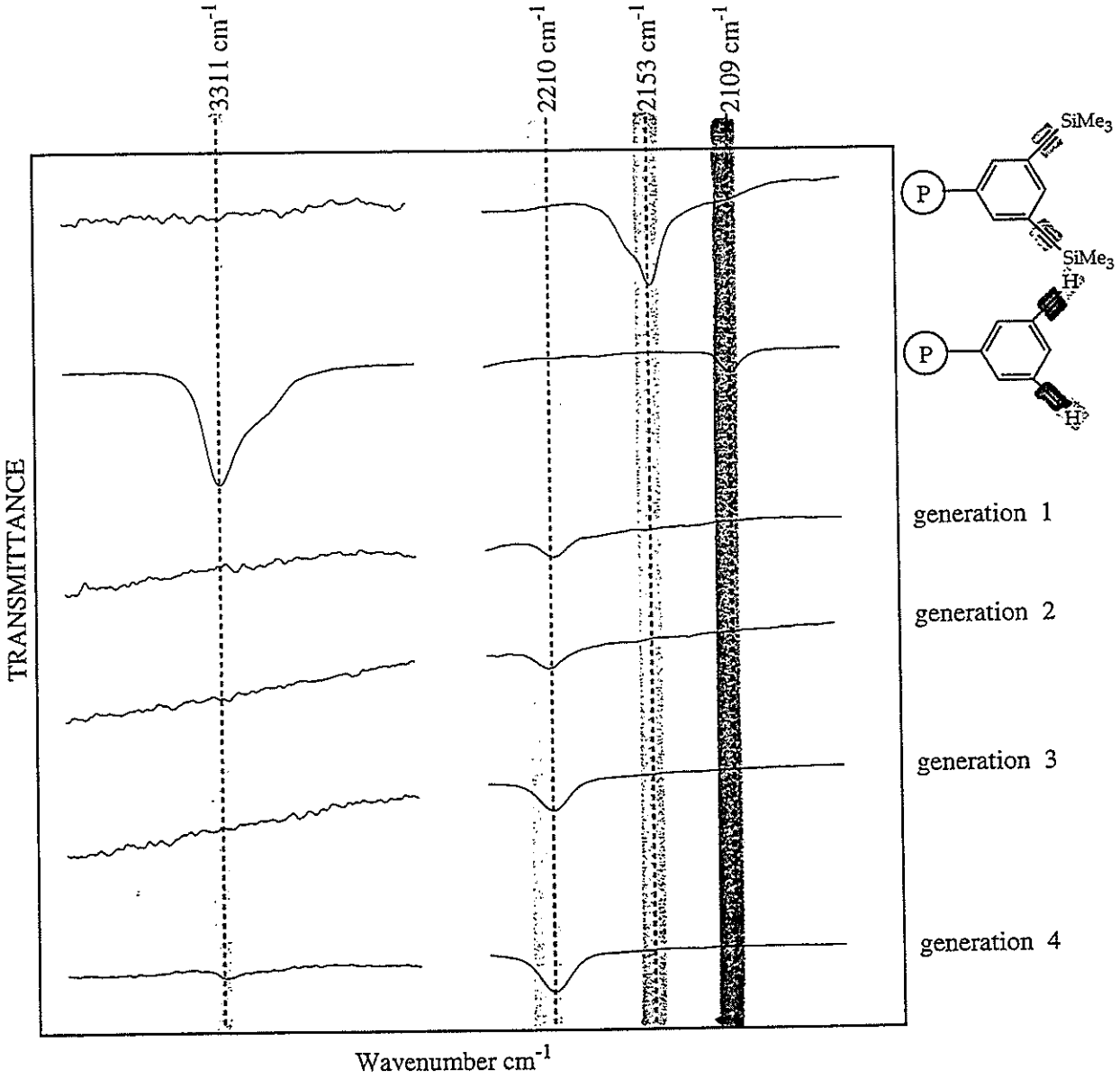

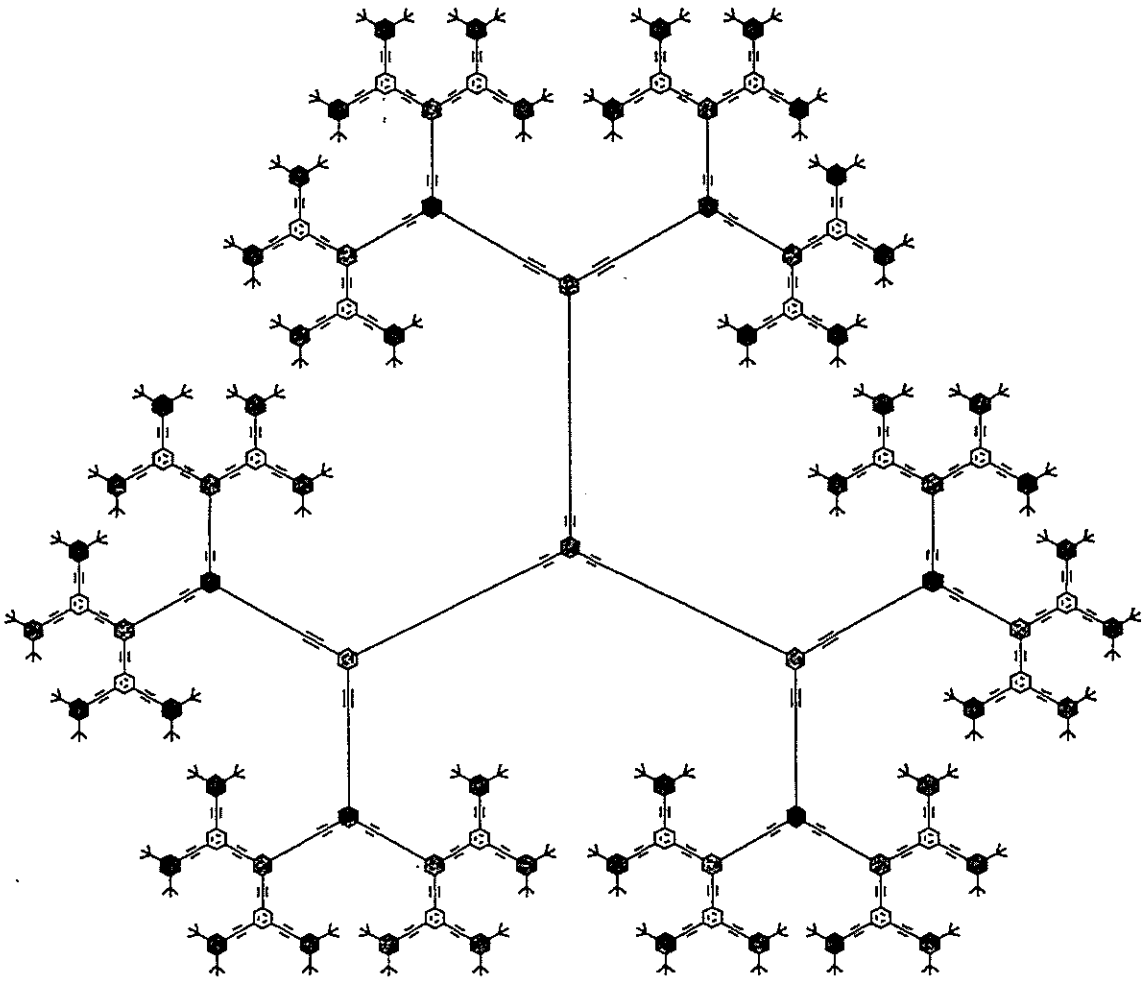

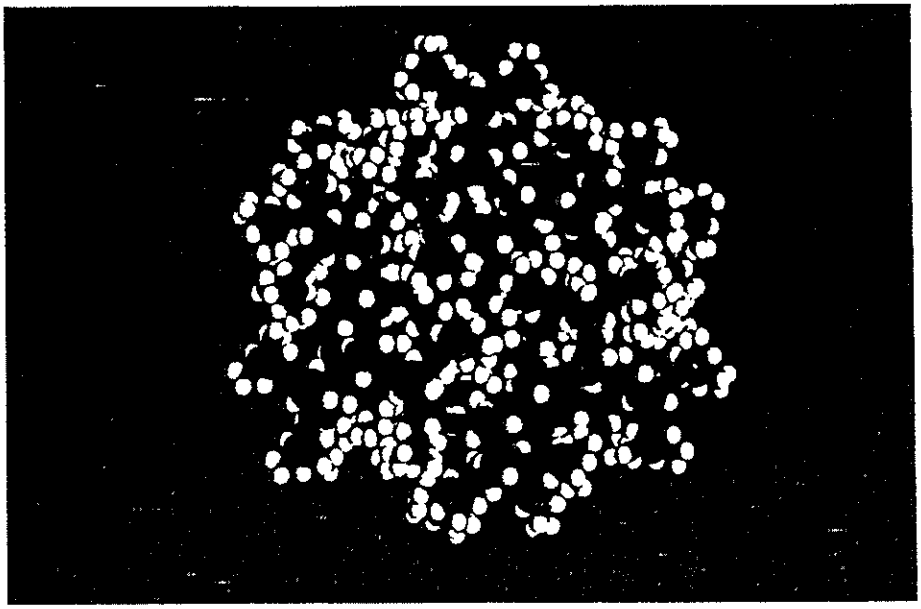

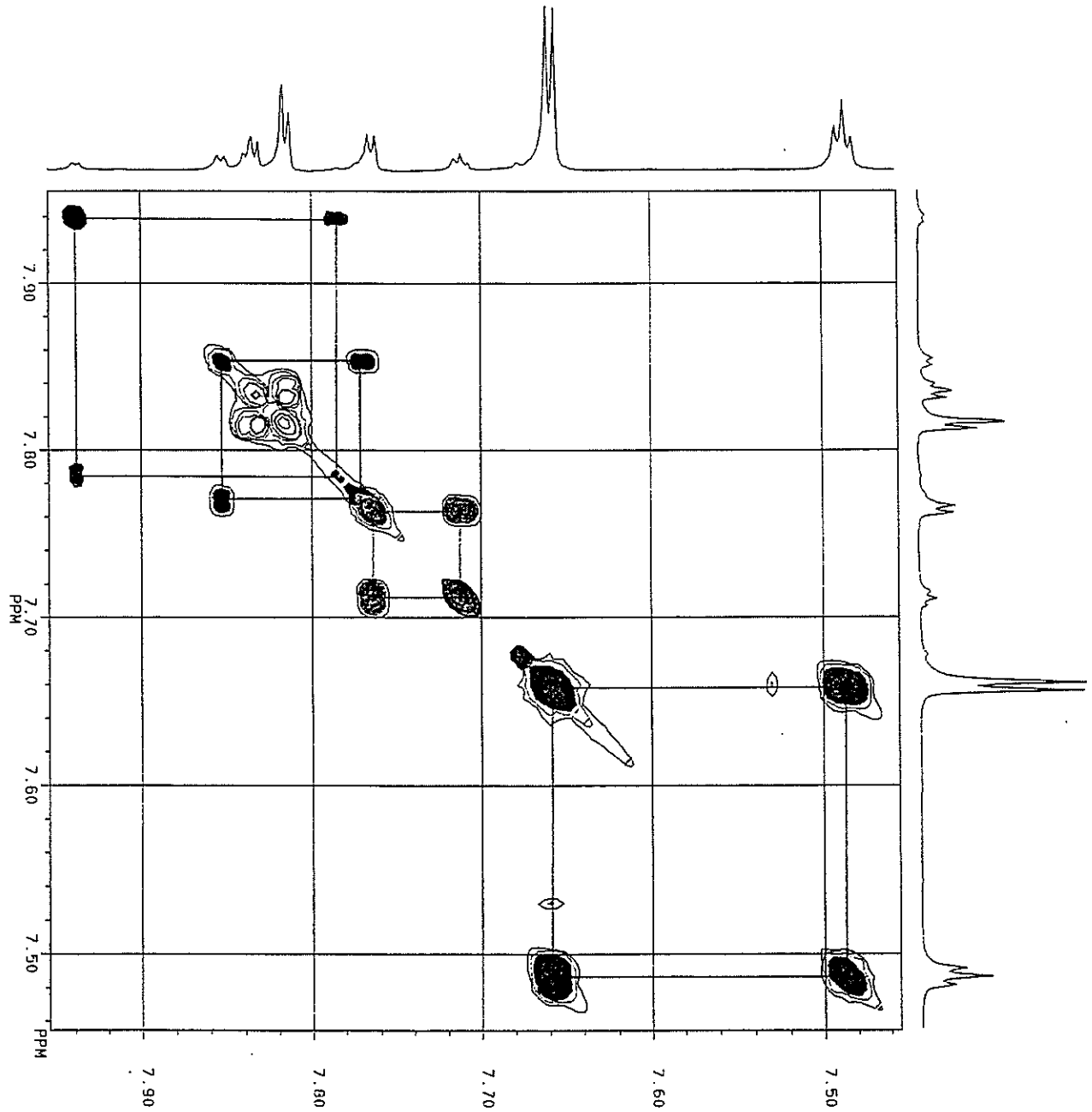
7.90
7.80
7.70
7.60
7.50
PPM
7.90
7.80
7.70
7.60
7.50
PPM

Mass Spectrometric Analysis of D-94

(In collaboration with Charles Wilkins, UC Riverside)

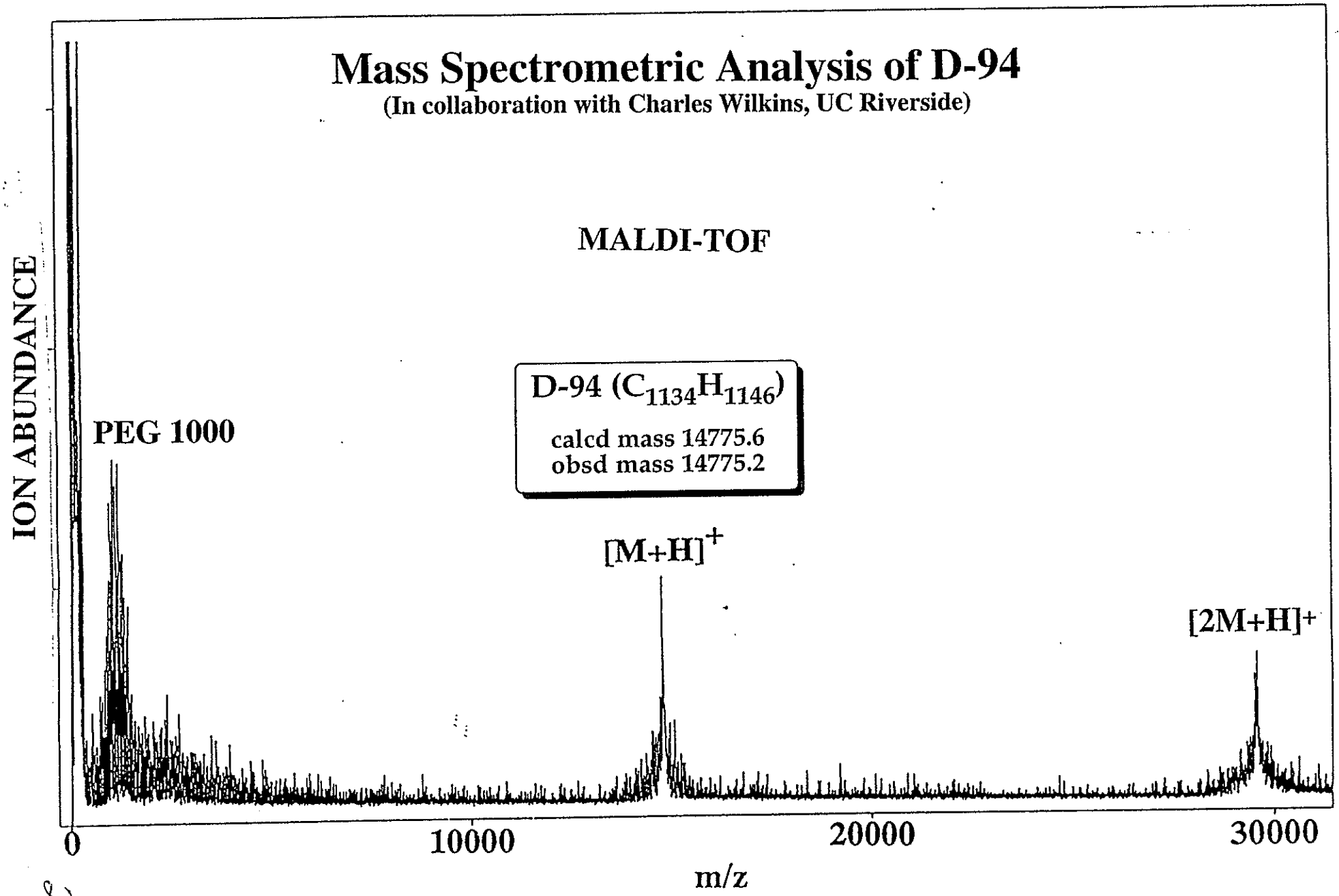

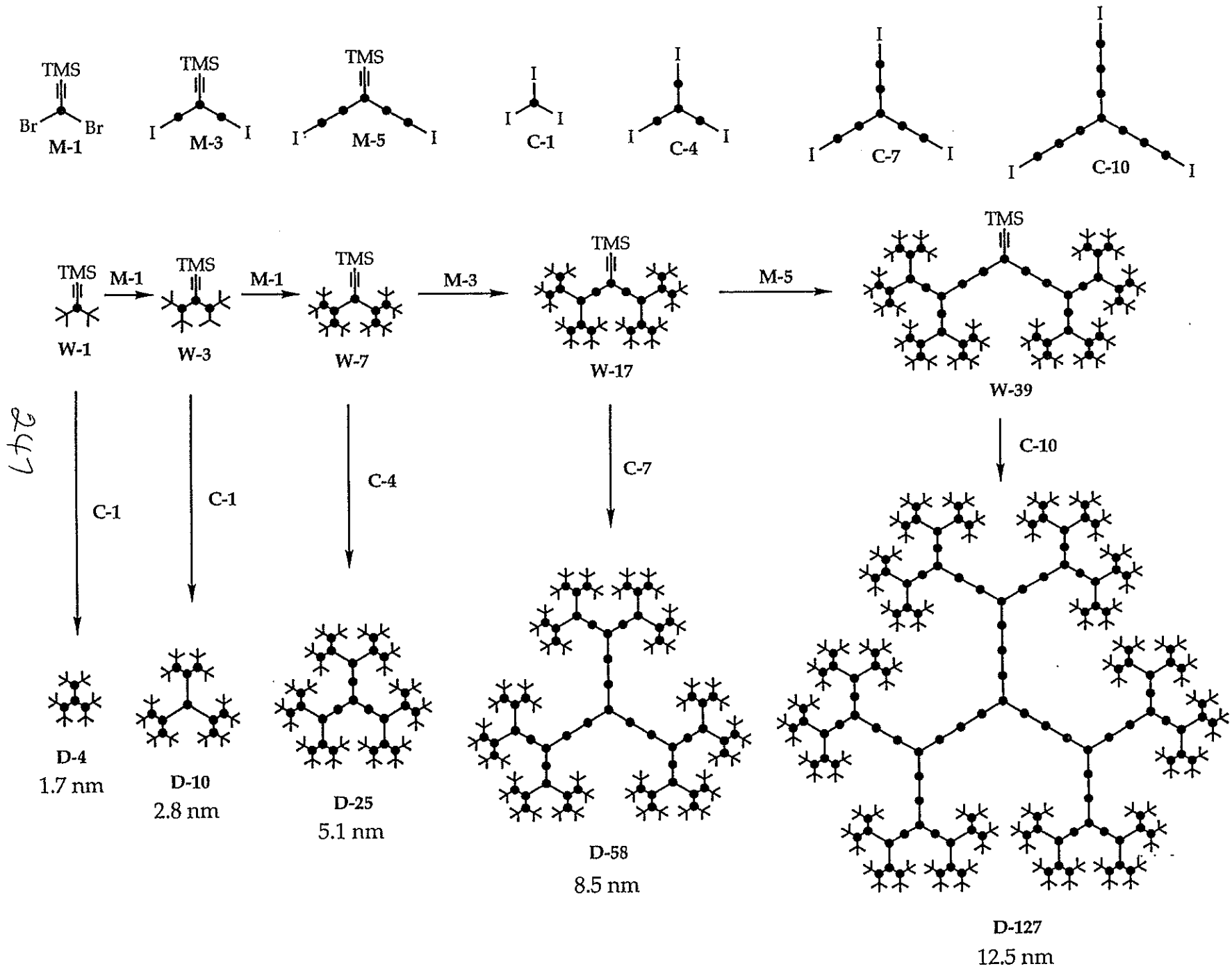
TMS
Br
Br
M-1
TMS
I
I
M-3
TMS
I
I
M-5
I
I
C-1
I
I
C-4
I
I
C-7
I
I
C-10
TMS
W-1
M-1
TMS
W-3
M-1
TMS
W-7
M-3
TMS
W-17
M-5
TMS
W-39
C-1
C-1
C-4
C-7
C-10
D-4
1.7 nm
D-10
2.8 nm
D-25
5.1 nm
D-58
8.5 nm
D-127
12.5 nm

Double Exponential Dendrimer Growth

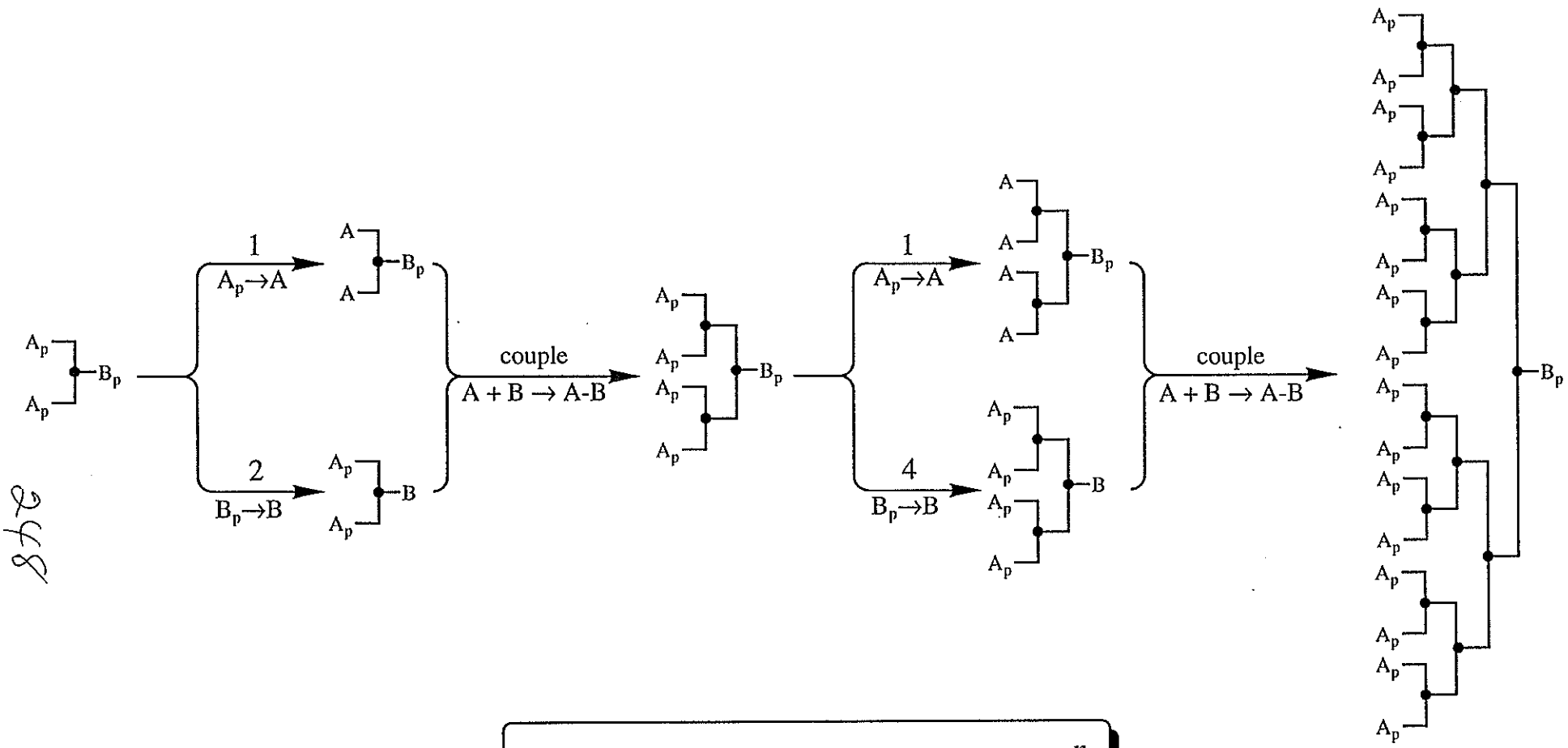

number of monomers ~ 2^{2^n}

Double Exponential Dendrimer Growth Rate

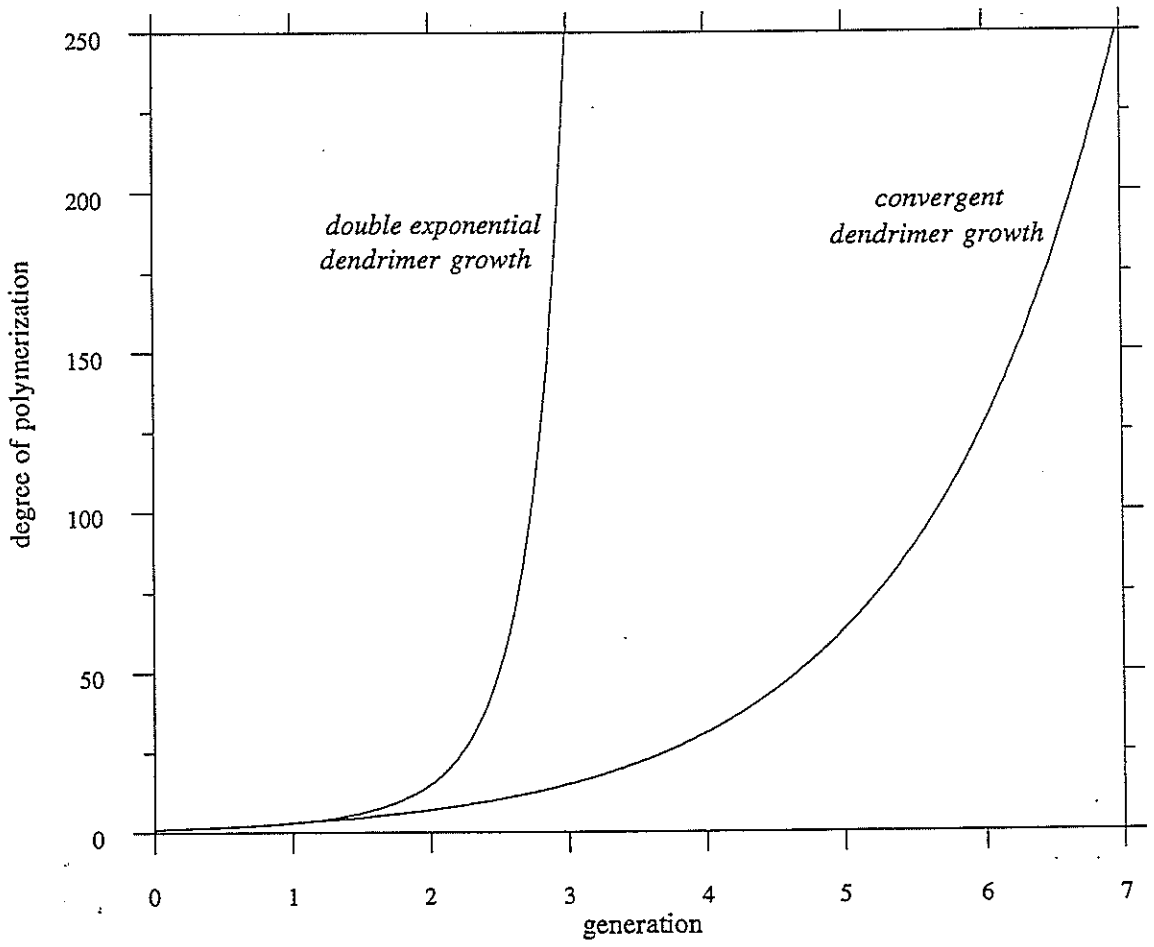

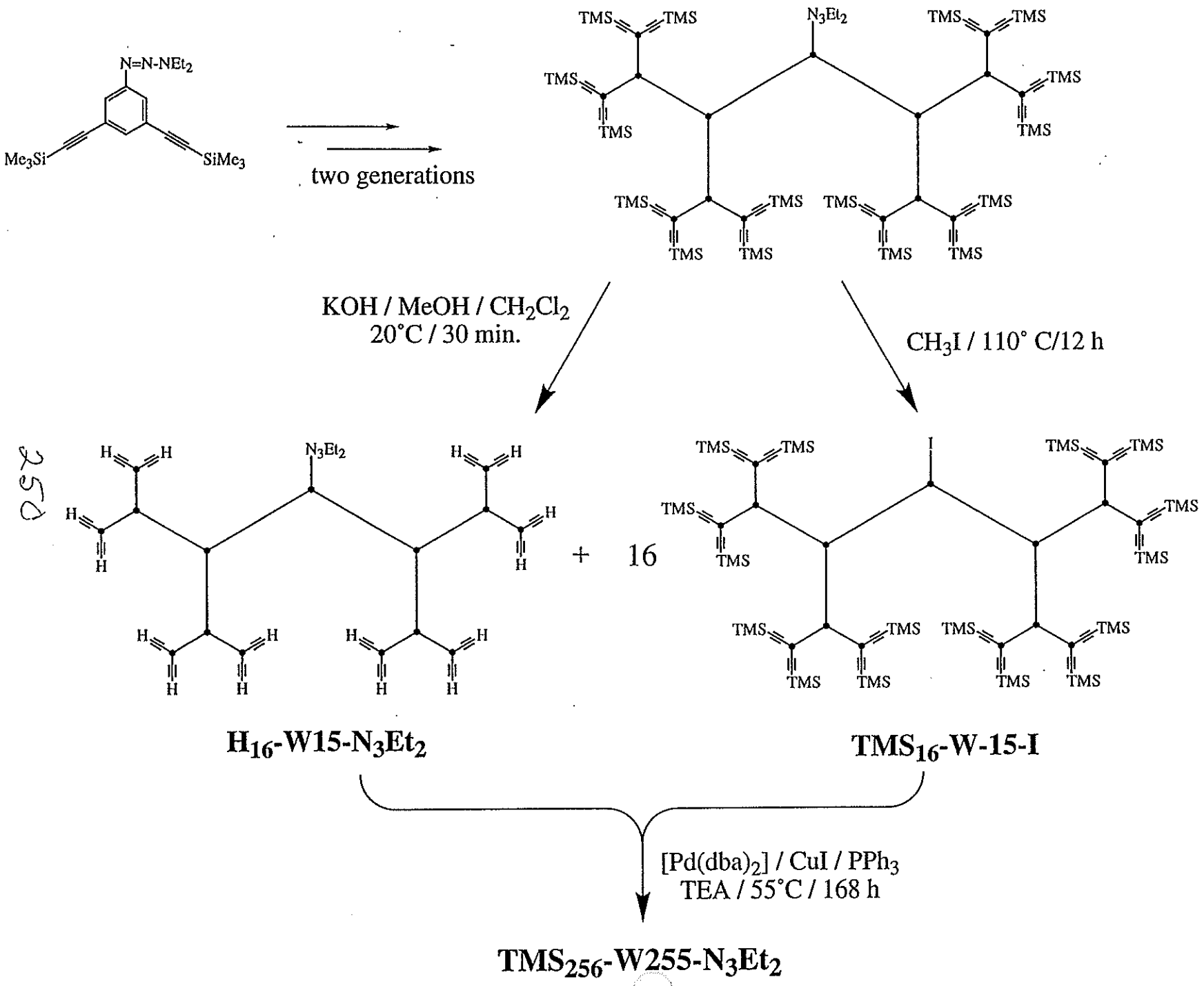
N=N-NEt2
Me3Si
SiMe3
two generations
N3Et2
TMS
KOH / MeOH / CH2Cl2
20°C / 30 min.
CH3I / 110° C/12 h
H
+ 16
I
H16-W15-N3Et2
TMS16-W-15-I
[Pd(dba)2] / CuI / PPh3
TEA / 55°C / 168 h
TMS256-W255-N3Et2

SEC Gives the Appearance of a Single High MW Product

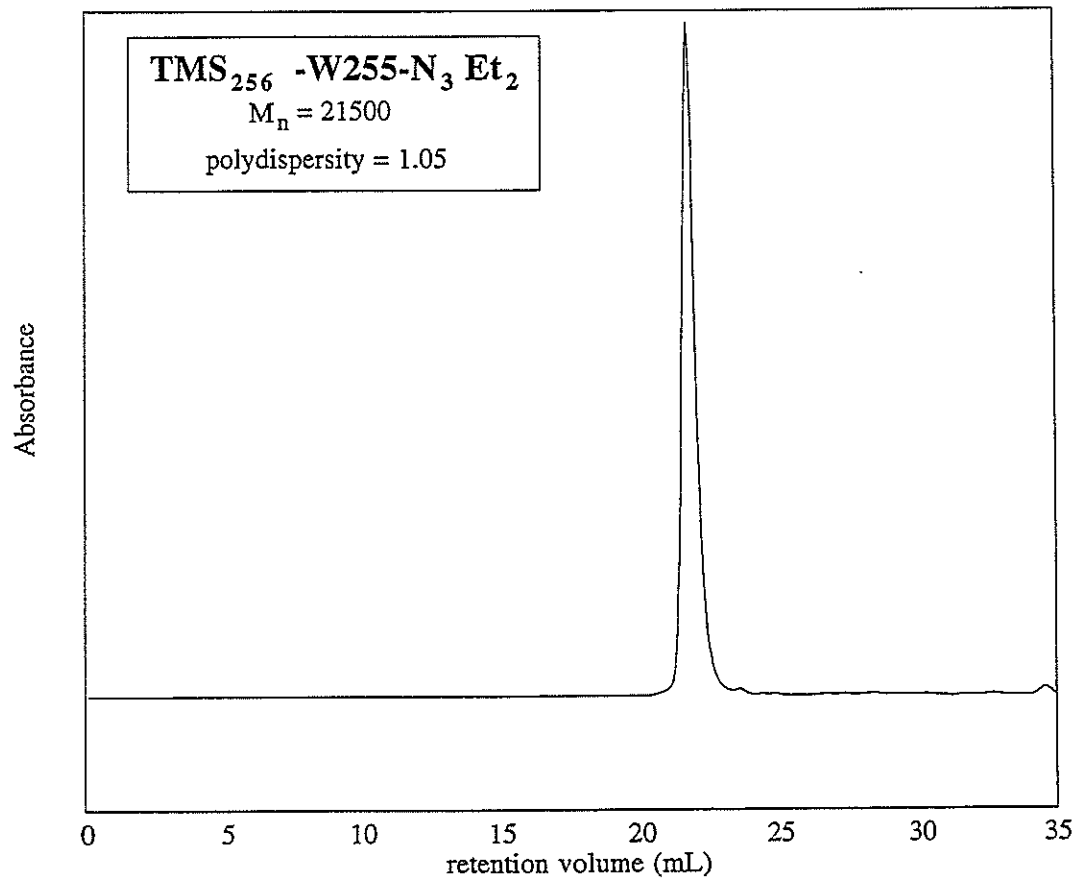

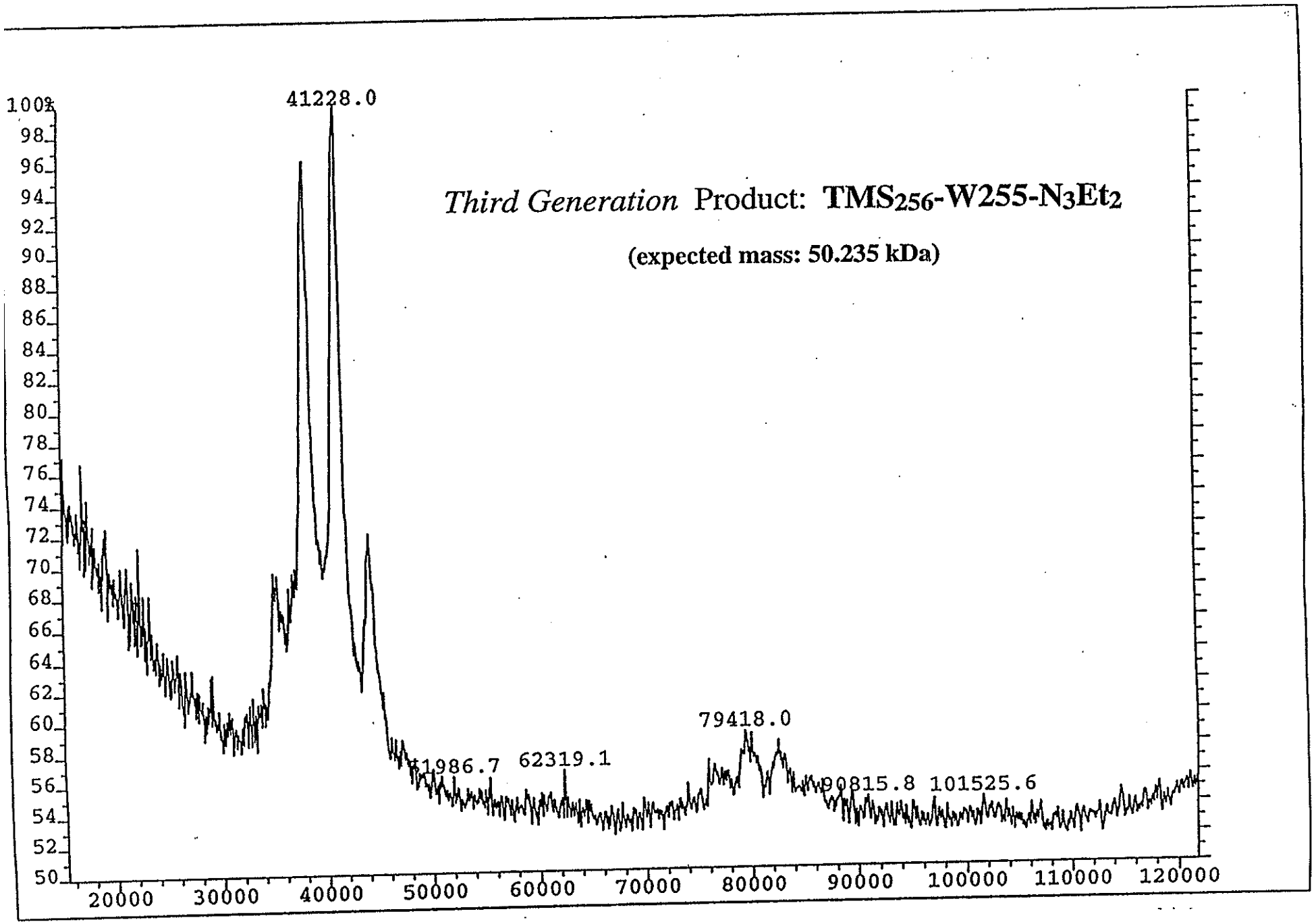
41228.0
Third Generation Product: **TMS256-W255-N3Et2**
(expected mass: 50.235 kDa)
100%
98
96
94
92
90
88
86
84
82
80
78
76
74
72
70
68
66
64
62
60
58
56
54
52
50
41986.7
62319.1
79418.0
90815.8
101525.6
20000
30000
40000
50000
60000
70000
80000
90000
100000
110000
120000

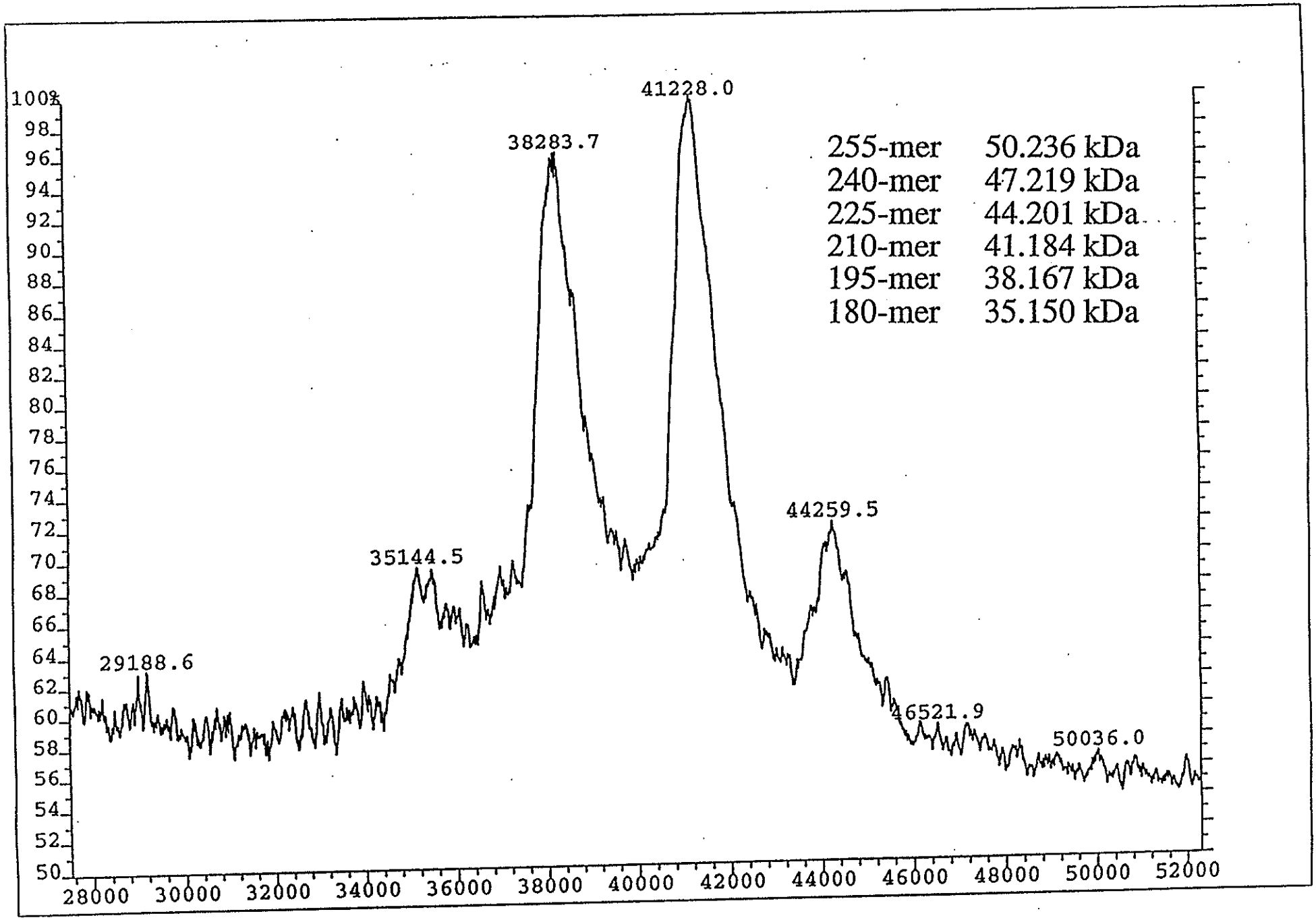
41228.0
38283.7
35144.5
29188.6
44259.5
46521.9
50036.0
255-mer 50.236 kDa
240-mer 47.219 kDa
225-mer 44.201 kDa
210-mer 41.184 kDa
195-mer 38.167 kDa
180-mer 35.150 kDa
100%
98
96
94
92
90
88
86
84
82
80
78
76
74
72
70
68
66
64
62
60
58
56
54
52
50
28000
30000
32000
34000
36000
38000
40000
42000
44000
46000
48000
50000
52000

Incomplete Coupling Would GiveThese Products

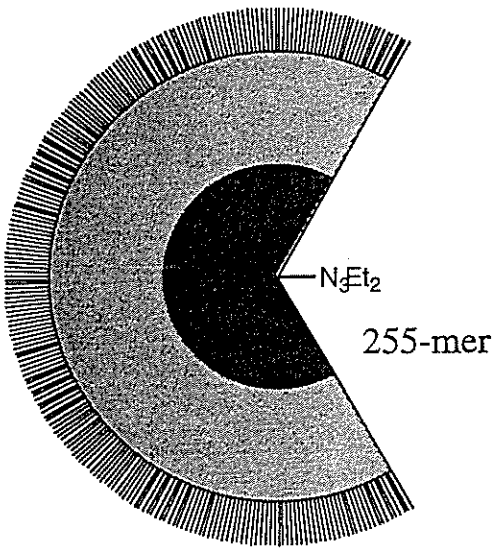

255-mer

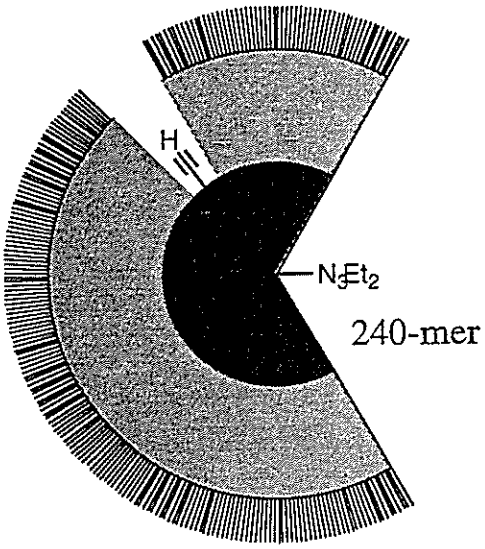

240-mer

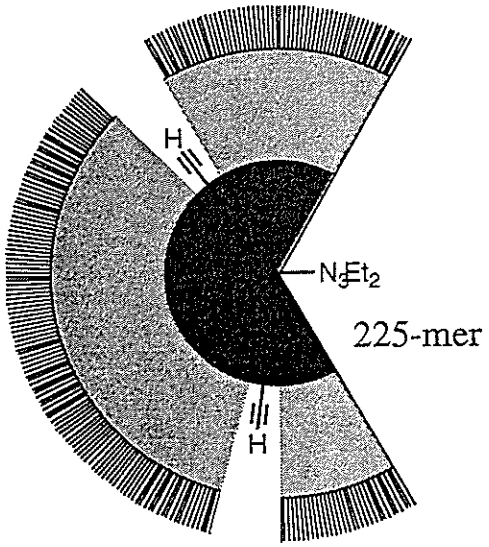

225-mer

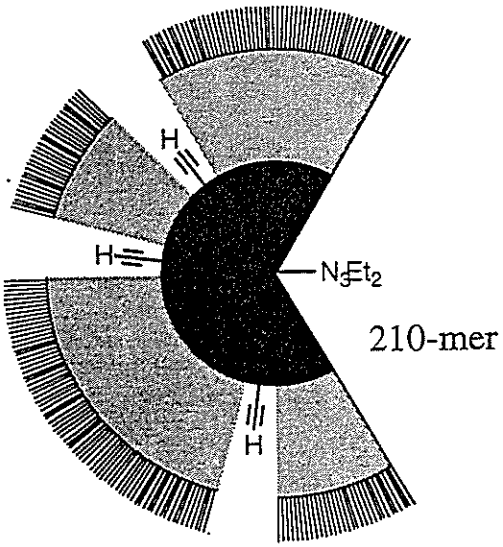

210-mer

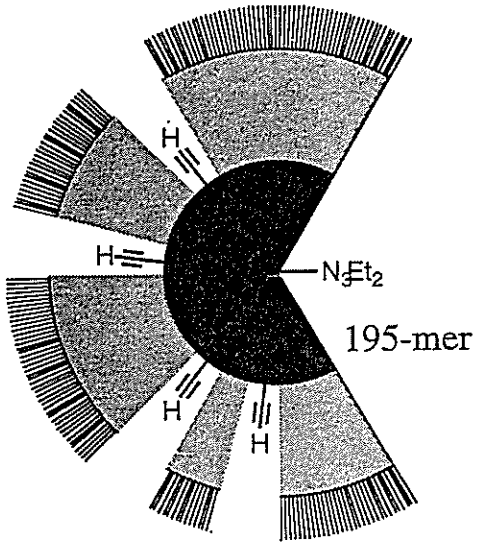

195-mer

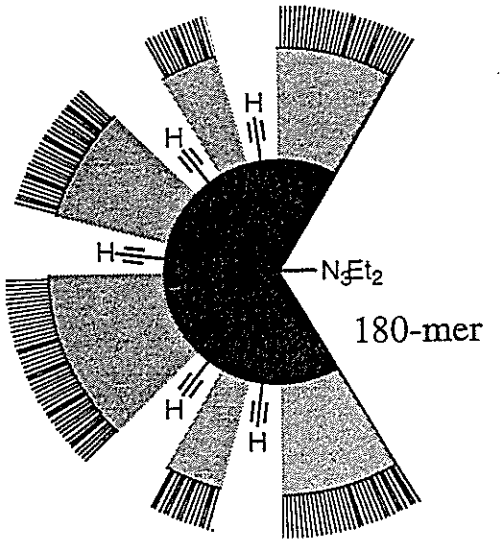

180-mer

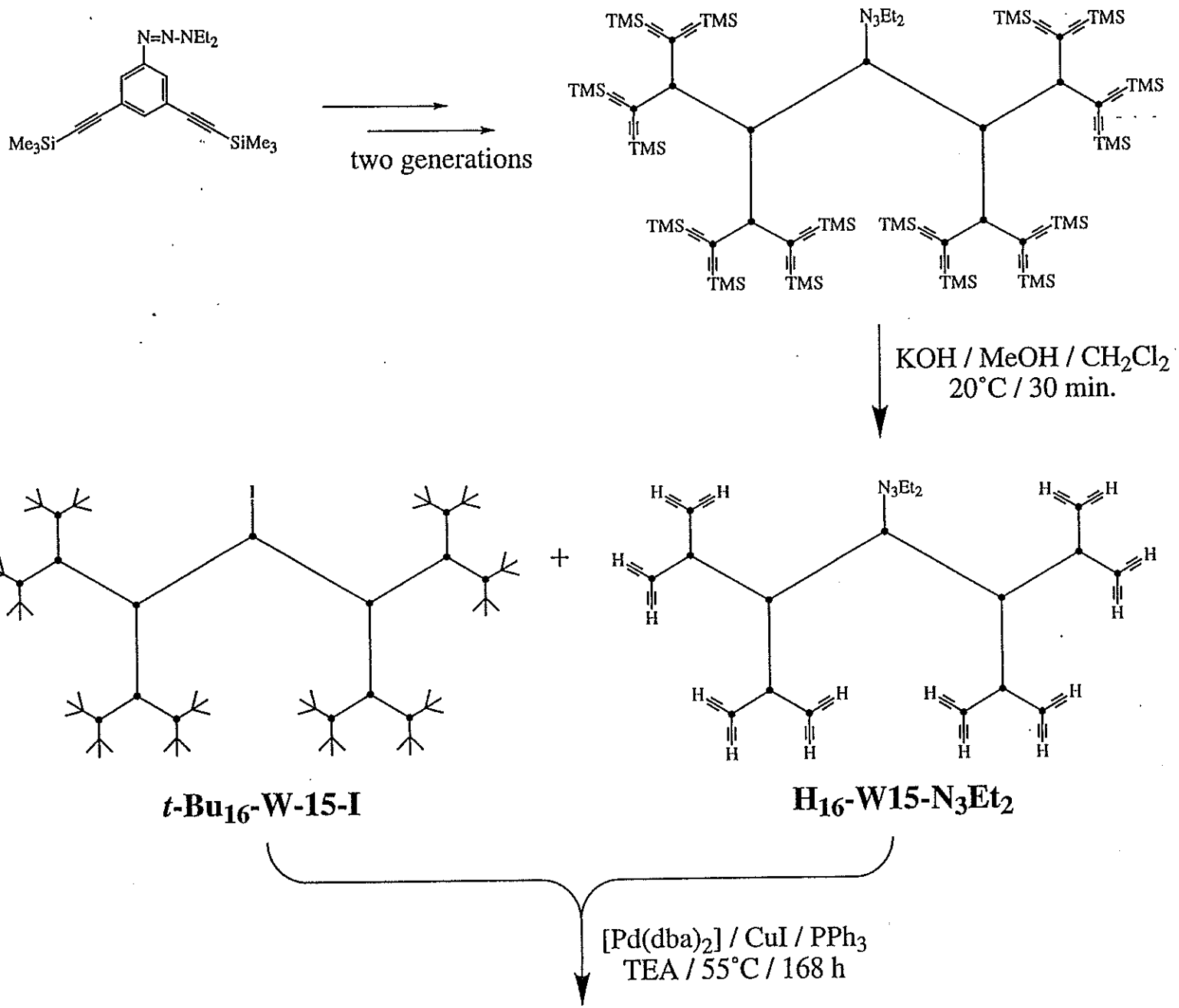
N=N-NEt2
Me3Si
SiMe3
two generations
TMS
N3Et2
KOH / MeOH / CH2Cl2
20°C / 30 min.
16
255
I
H
t-Bu16-W-15-I
H16-W15-N3Et2
[Pd(dba)2] / CuI / PPh3
TEA / 55°C / 168 h
t-Bu256-W255-N3Et2

The Dendritic Topology is Unique: Convergent and Divergent Paths

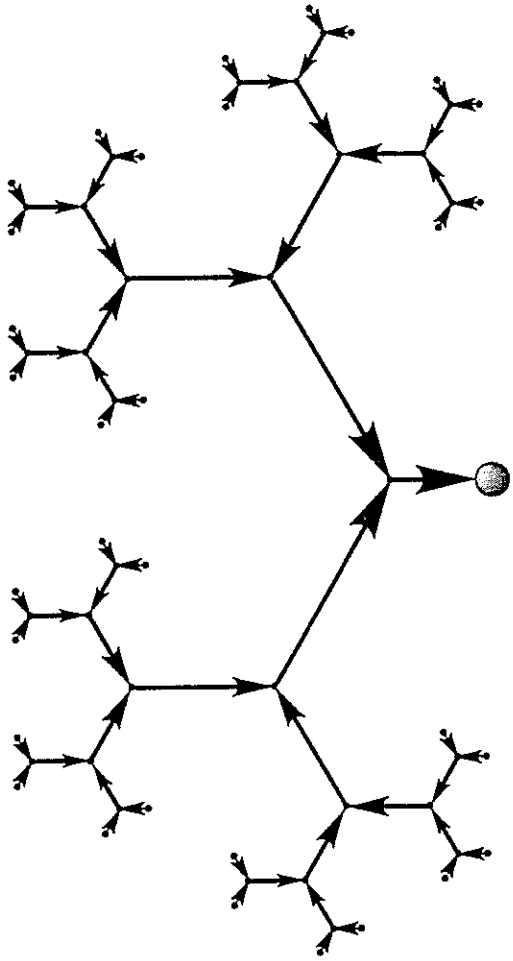

converging paths

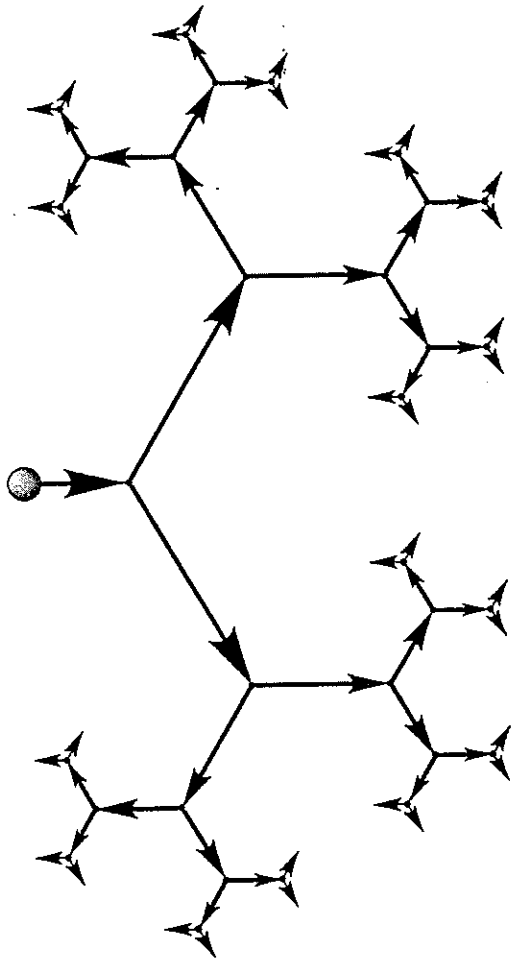

diverging paths

ELECTROLUMINESCENT THIN FILMS BASED ON DENDRITIC MACROMOLECULES

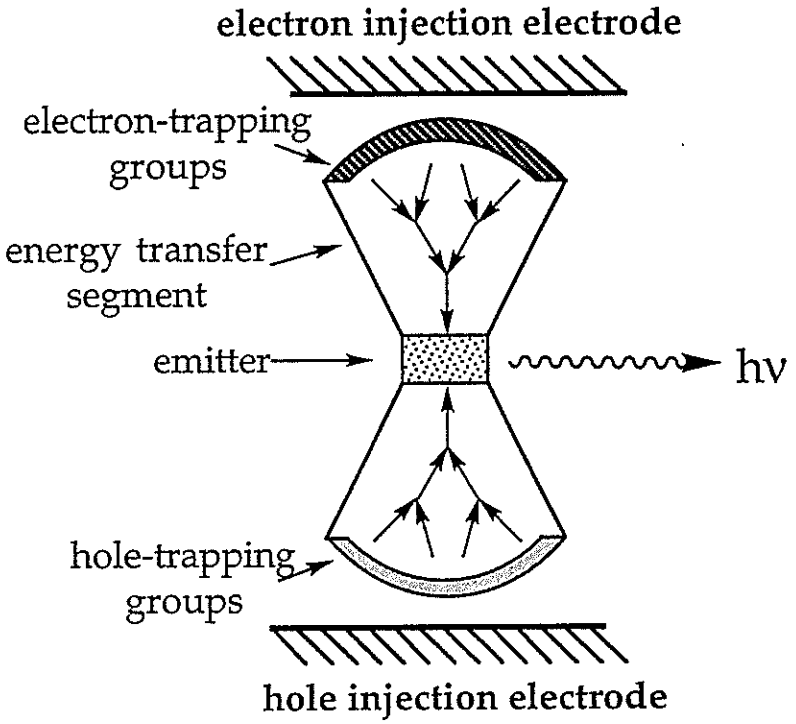

Potential Features:

- modular design and construction
  - charge trapping groups
  - convergent energy transfer
  - luminescent core
  - oriented by self-assembly
- single component device
- monolayer device?

Unknown Issues:

- thin film formation / quality
- charge trapping and recombination
- energy transfer efficiency
- solid state quantum yield

Convergent and Directional Energy Transfer in a Dendritic Macromolecule

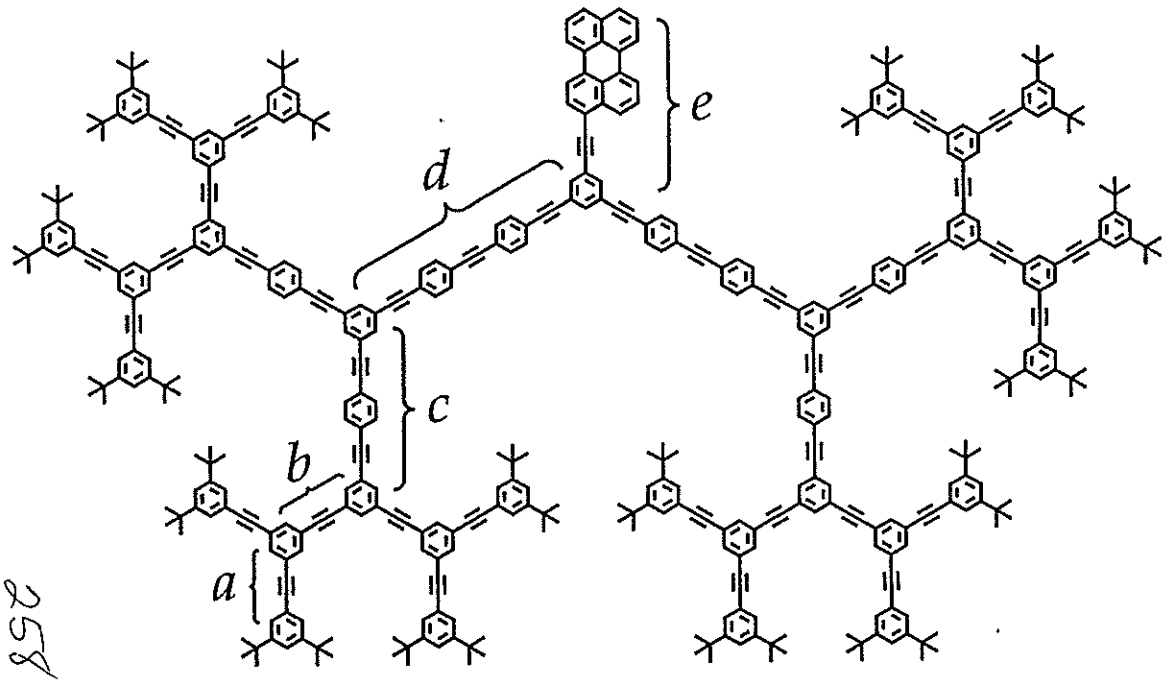

to be represented as:

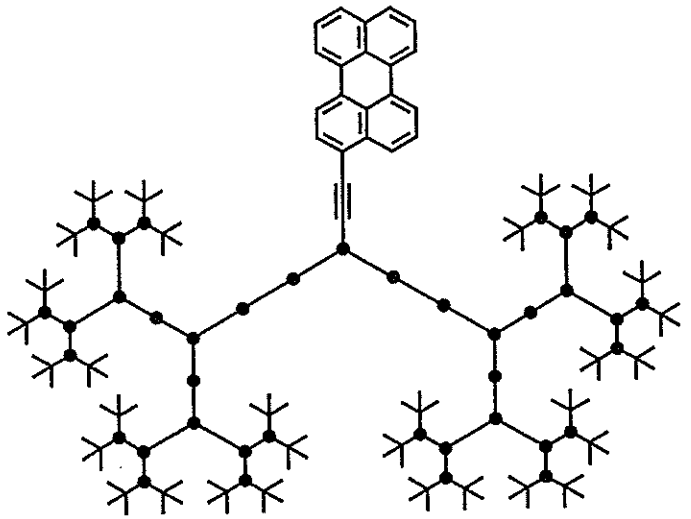

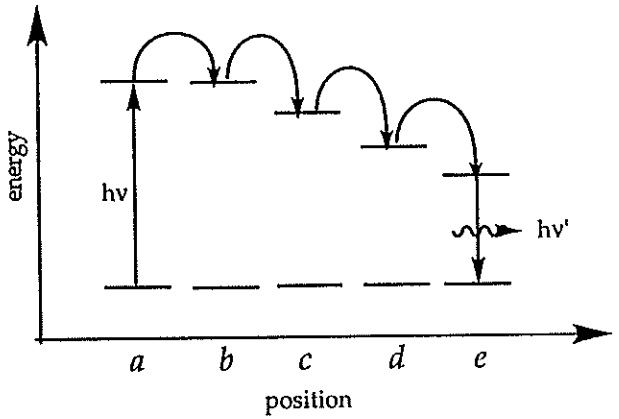

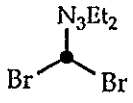

M-1a

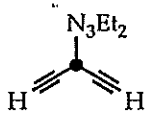

M-1

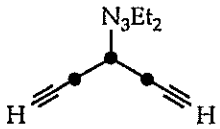

M-3

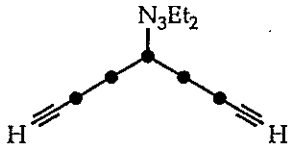

M-5

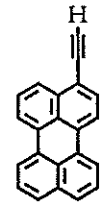

1-ethynylperylene

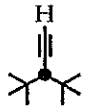

W-1-H

M-1a

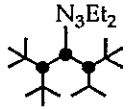

W-3-N_3Et_2

M-1

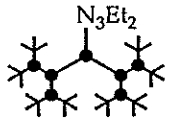

W-7-N_3Et_2

M-3

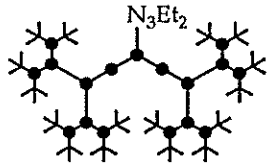

W-17-N_3Et_2

M-5

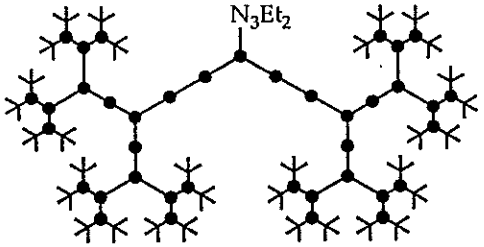

W-39-N_3Et_2

1-ethynylperylene

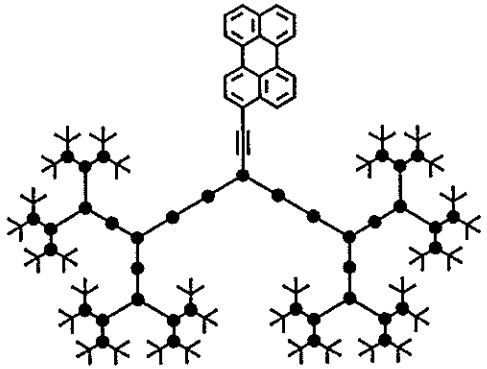

W-39 perylene

259

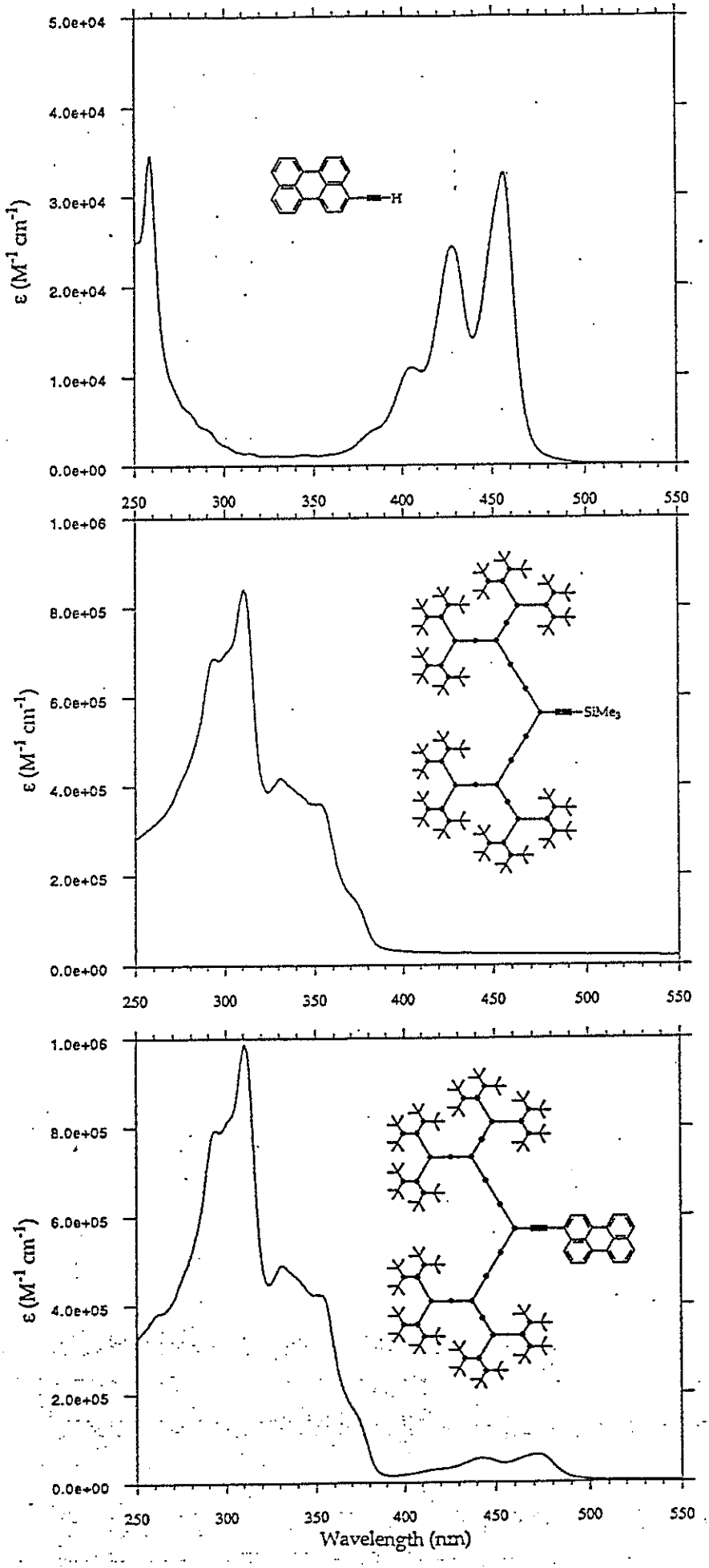
5.0e+04
4.0e+04
3.0e+04
2.0e+04
1.0e+04
0.0e+00
ε (M⁻¹ cm⁻¹)
H
250
300
350
400
450
500
550
1.0e+06
8.0e+05
6.0e+05
4.0e+05
2.0e+05
0.0e+00
ε (M⁻¹ cm⁻¹)
SiMe3
250
300
350
400
450
500
550
1.0e+06
8.0e+05
6.0e+05
4.0e+05
2.0e+05
0.0e+00
ε (M⁻¹ cm⁻¹)
250
300
350
400
450
500
550
Wavelength (nm)

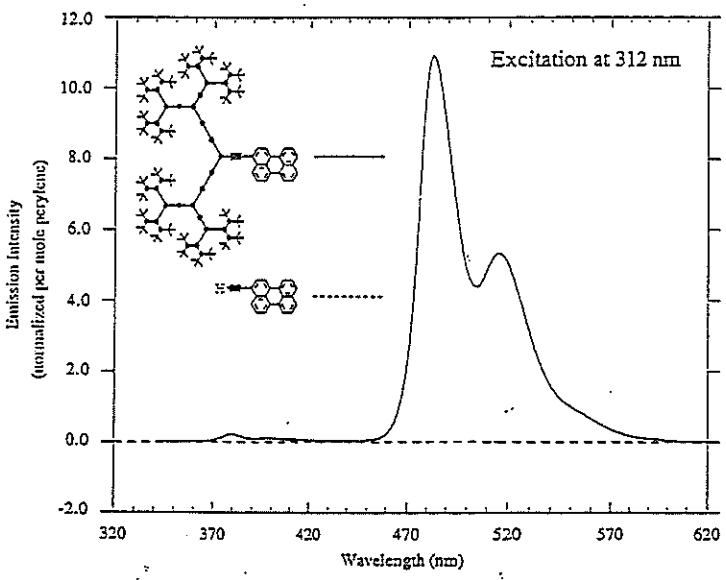

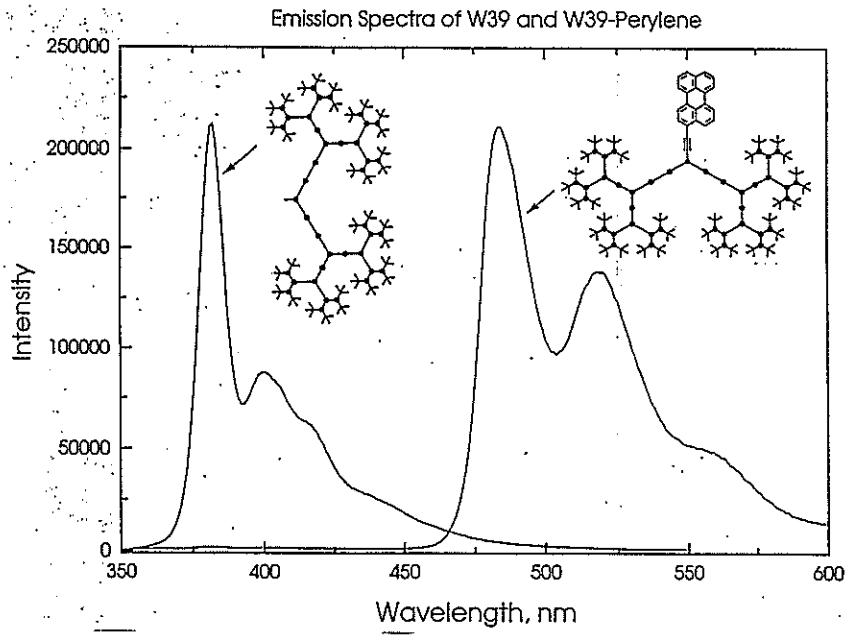

Energy Transfer Efficiency ~ 98%

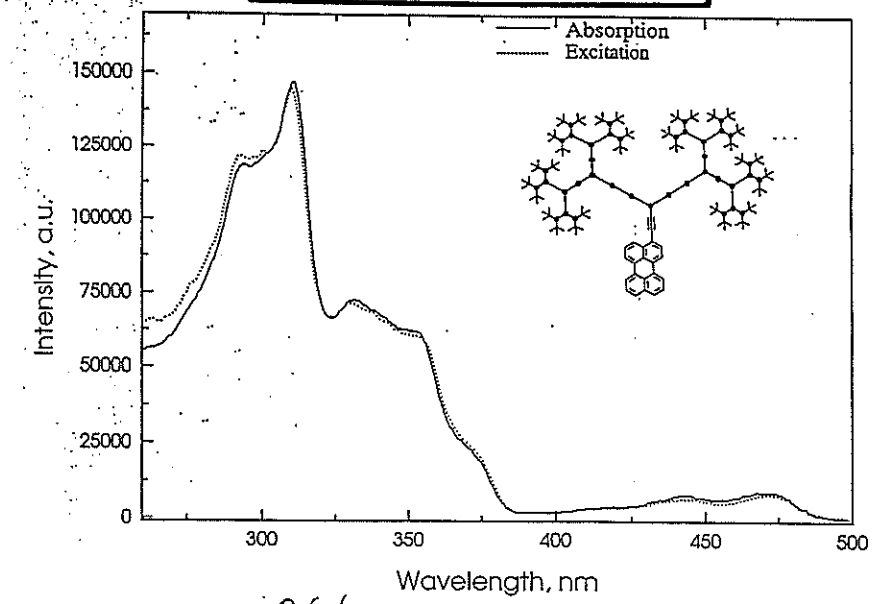

Photophysics Summary

	λ_{max}^{em} (nm)	Φ_{fl}	τ (ns)
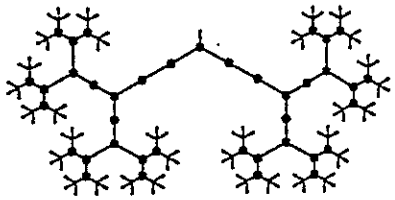	382, 400	0.74	0.24
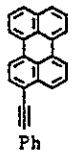	480, 511	0.48	2.3
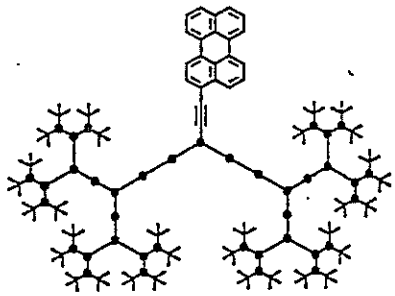	482, 515	0.87	2.1

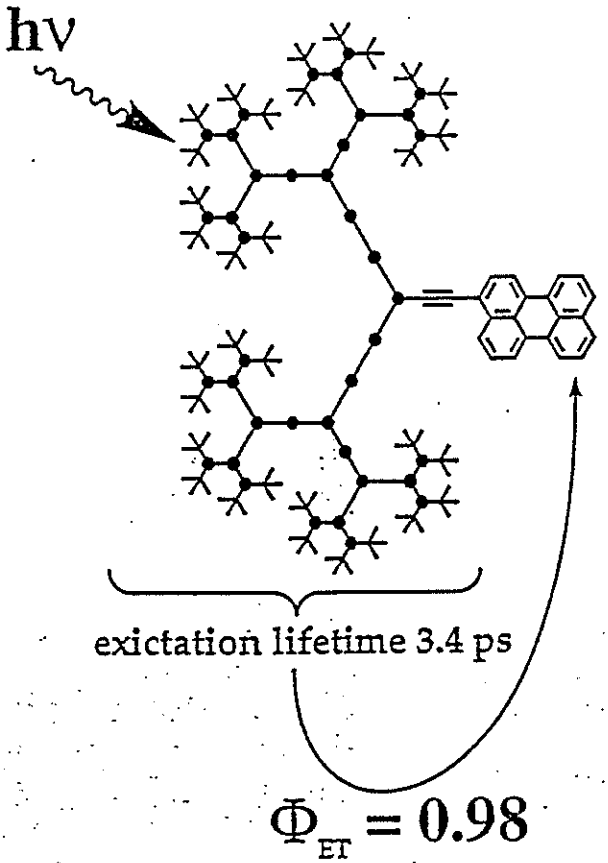

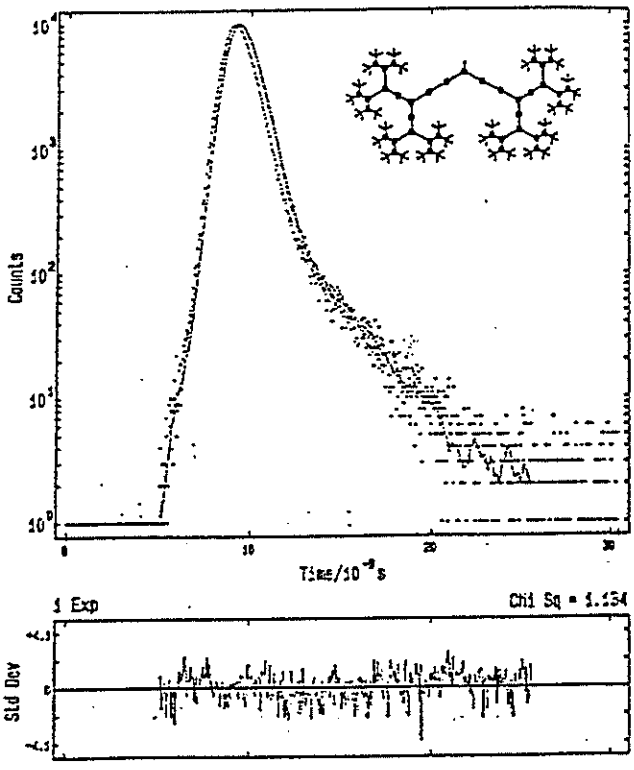

Defect-Free Thin Films Are Produced From 3rd Generation and Higher Dendrimers (spin-coated from THF)

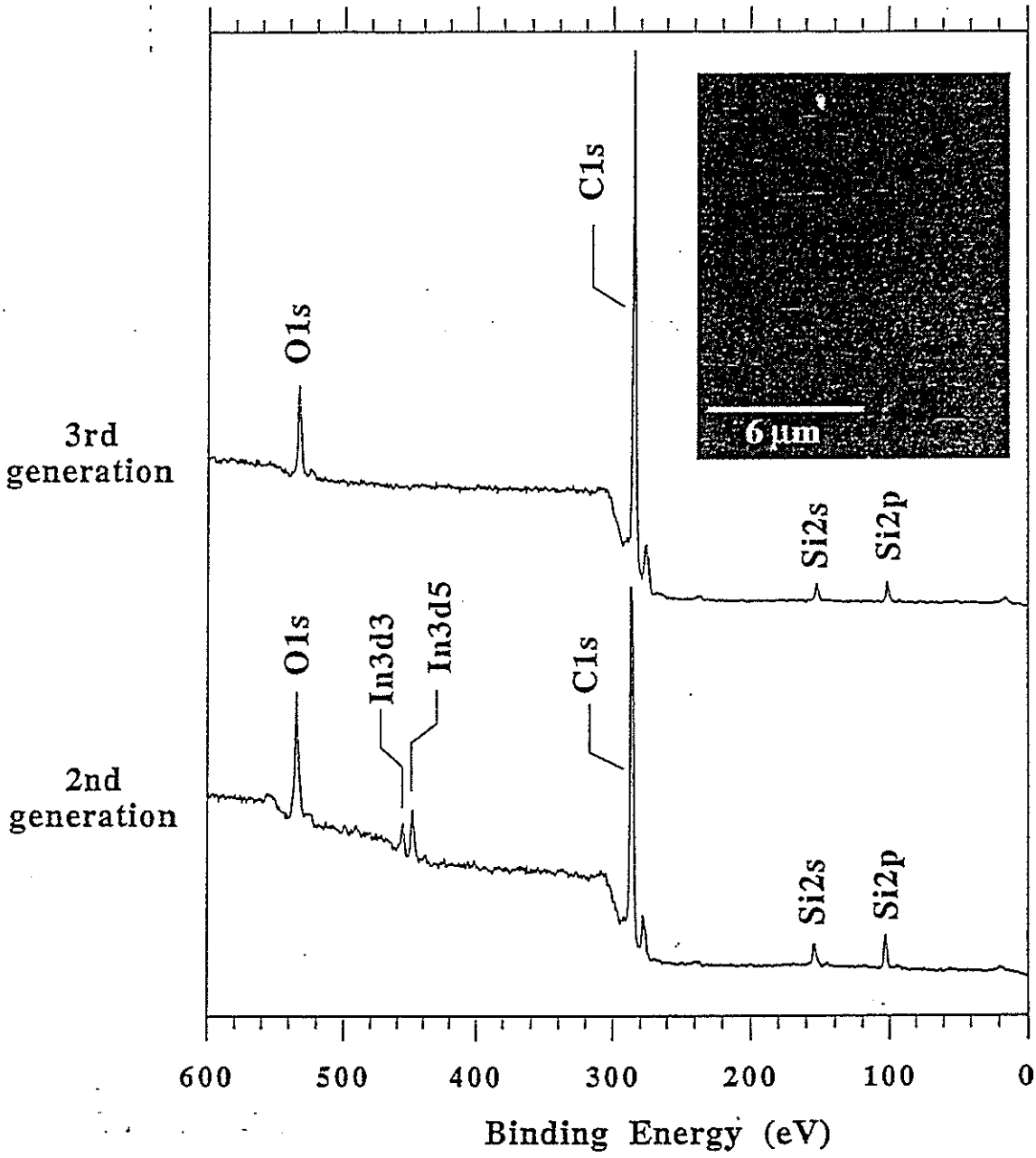

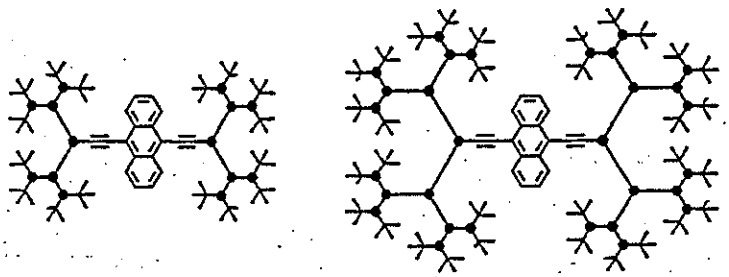

2nd generation 3rd generation

Excimer Formation Observed in Solid Films

(Solid State Photoluminescence Reduced by Self-Quenching)

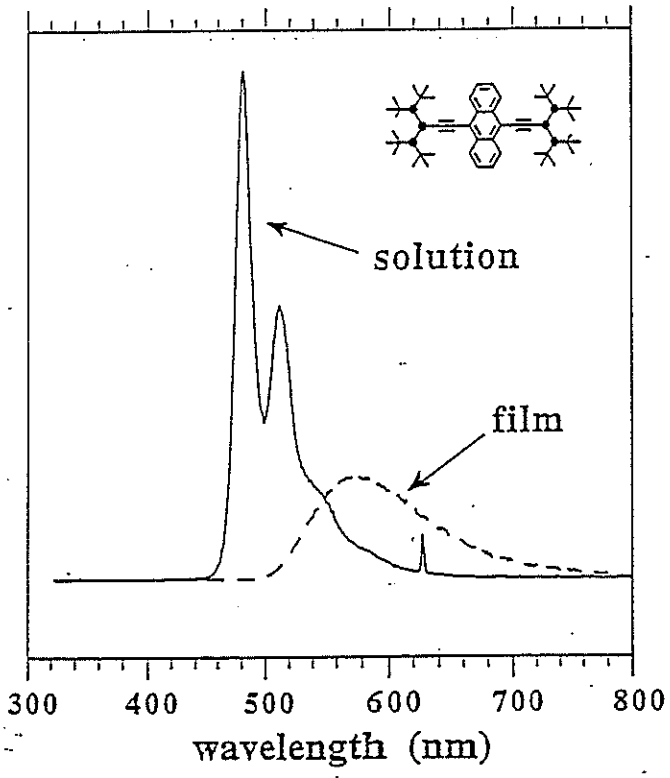

Solid State Photoluminescence vs. Generation

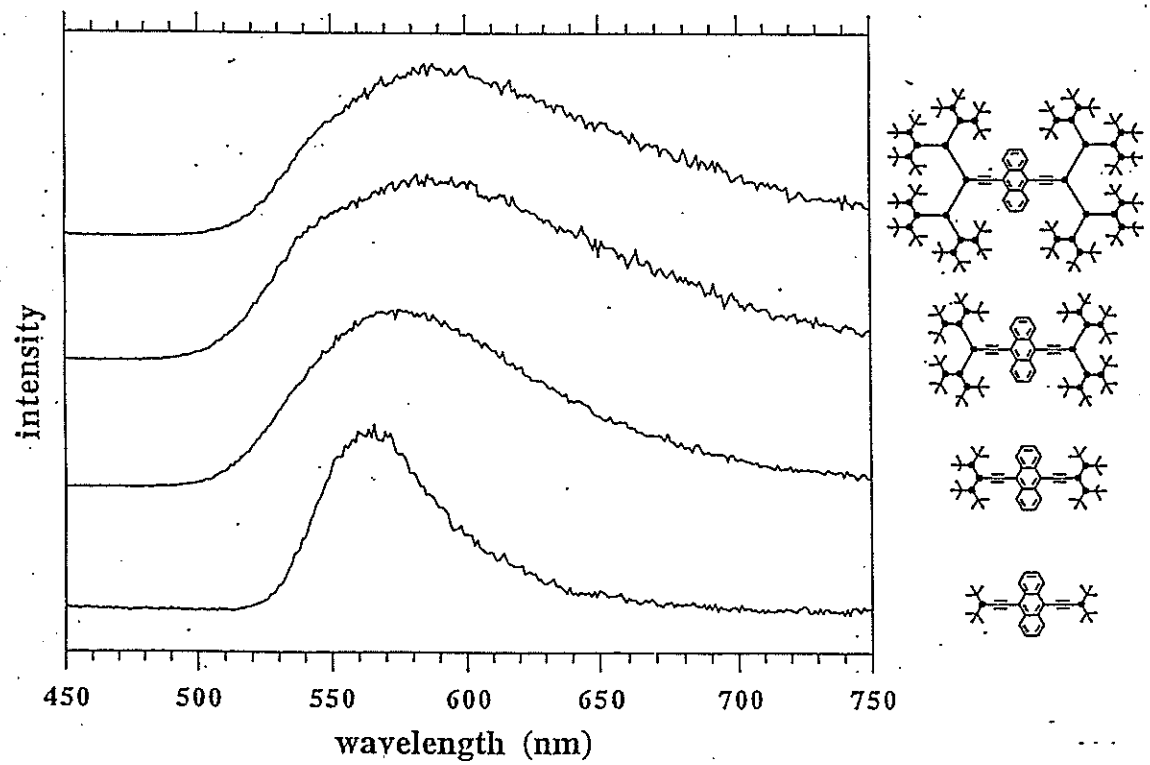

Solid State Dilution Studies Show that Luminophor Does Not Form Exciplex with Phenylacetylene Dendrimer

Films of mixture: 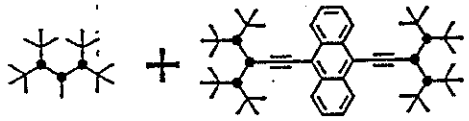

Phenylacetylene : Anthracene
42:1

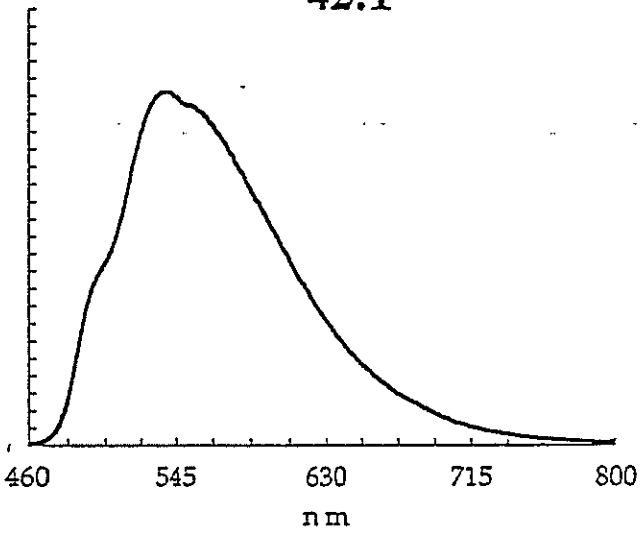

Phenylacetylene : Anthracene
69:1

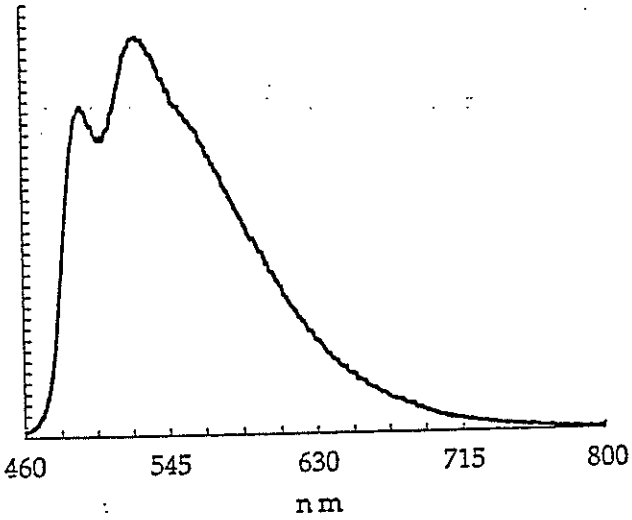

Phenylacetylene : Anthracene
84:1

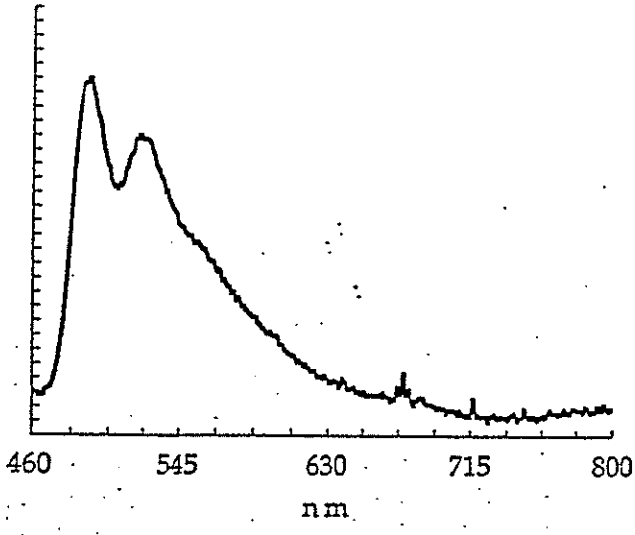

Phenylacetylene : Anthracene
96:1

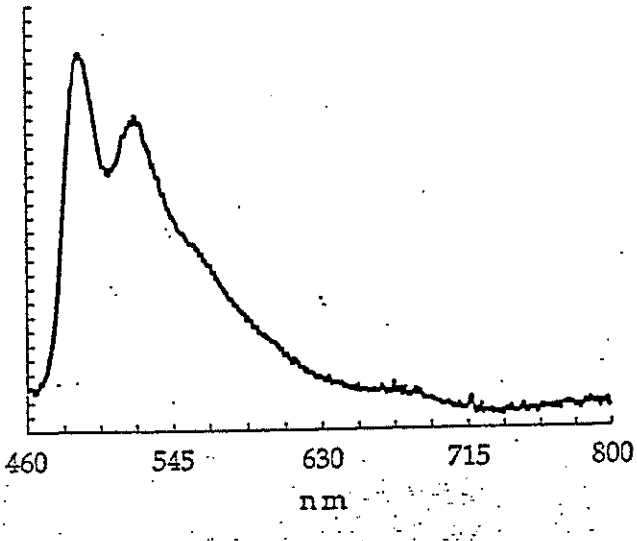

ARBORESCENT GRAFT POLYMERS AND COPOLYMERS: SYNTHESIS AND PROPERTIES

Mario Gauthier, Institute for Polymer Research, University of Waterloo, Waterloo, ON N2L 3G1, Canada

Lecture notes

Slide 1 - Title page

Slide 2 - Outline

Slide 3 - General characteristics of arborescent graft polymers

AGPs are prepared by successive anionic grafting reactions. A linear polymer backbone is first functionalized to introduce grafting sites, which are coupled with living anions to produce a comb (generation G=0) structure. If the side chains can be functionalized in the same manner, the grafting process can be repeated, leading to subsequent generations G=1, 2, etc. The approach used provides extensive control over the structure of the molecules. The branching density can be varied by controlling the degree of substitution of the backbone polymer. The molecular weight of the chains grafted in each reaction cycle is also controllable. The chemical functionality of the molecules can be controlled by introducing functional groups throughout the structure, or specifically at the chain ends. Using these parameters, it is possible to obtain branched polymers with a wide range of molecular weights and branching functionalities, while maintaining a low apparent polydispersity. Although AGPs in their simplest form are styrene-based, it will be shown that the basic method can also be extended to include other monomers.

Slide 4 - Advantages / disadvantages

The method used to prepare AGPs results in a diffuse layer growth process. This is because the grafting sites are randomly distributed on the backbone polymer, rather than strictly at the chain ends like in dendritic systems. This results in distinct advantages and disadvantages when AGPs and dendritic polymers are compared. **Advantages:** As mentioned previously, extensive control is gained over the structure of the polymers. The molecular weight of the polymers increases very rapidly for successive generations, because the building blocks used are linear polymer chains, rather than small molecules. The homopolymers can be easily functionalized through electrophilic substitution reactions, since they are styrene-based. Random distribution of grafting sites has a distinct advantage in that side reactions leading to a lower grafting efficiency also take place randomly over the molecular structure. The overall shape of the molecules is thus unaffected. **Disadvantages:** The introduction of grafting sites relies on electrophilic substitution; the method is therefore limited to aromatic vinyl monomers. As discussed later, the importance of this problem can be minimized, and copolymers containing a large proportion of a different monomer can also be prepared. The apparent polydispersity of AGPs is much lower than that of hyperbranched polymers (M_w/M_n

= 1.5-2 typically), but still higher than for dendrimers, for which polydispersities below 1.01 have been reported. The surface of AGPs is also expected to be less well defined than that of dendrimers, because of the diffuse layer growth process.

PREPARATION OF STYRENE HOMOPOLYMERS

Slide 5 - Introduction of grafting sites

Two types of grafting sites have been used to prepare styrene-based AGPs, chloromethyl and acetyl functionalities. Both reactions can be carried out under conditions preventing intermolecular cross-linking, leaving the molecular weight distribution (MWD) of the polymers unaffected. The choice of reaction conditions (catalyst, solvent, polymer concentration) are critical in determining the success of the reaction.

Slide 6 - Grafting

Chloromethyl functionalities are preferred for the grafting reaction, because of their high grafting efficiency under optimal conditions, reaching over 95%. This simplifies the purification of the graft polymer, since the removal of only a minor amount of ungrafted side chains is required. The graft polymers are prepared by titrating the living anions, capped with 1,1-diphenylethylene, with the chloromethylated backbone polymer at -30°C. Capping is a major factor increasing the efficiency of the coupling reaction, since it minimizes the occurrence of side reactions involving metal-halogen exchange, as described in *Macromolecules* **1991**, *24*, 4548. Subsequent generations are prepared by repetition of the functionalization and grafting cycles in the same manner. Grafting on acetyl functionalities is also possible, although less efficient, resulting in the deactivation of around 35% of the living anions.

CHARACTERIZATION OF HOMOPOLYMERS

Slide 7 - Gel permeation chromatography

The example given here is for a series of graft polymers with a branch molecular weight around 5000 g/mol for each generation. Characterization of the branches was possible was removing a sample of the living anions from the reactor prior to the grafting process. The branches have a low polydispersity, as expected for anionic polymerization. The graft polymers can also be characterized by GPC, although only apparent molecular weight and polydispersity values are obtained, since the calculations are normally based on a linear polystyrene standards calibration curve. The low polydispersities obtained for each generation nevertheless show that a relatively narrow MWD is maintained at each step. The apparent molecular weights determined for the branched polymers are expected to be strongly underestimated, because of the very compact structure of AGPs. No GPC data could be obtained for the generation G=4 polymers, which were systematically retained on the different columns tested.

Slide 8 - Light scattering - Dilute solutions

Static light scattering allows the measurement of absolute weight-average molecular weights, which are shown to increase in an approximately geometric fashion for successive generations. The branching functionalities f_w reported are the number of branches grafted in each of the reactions. They were calculated from

$$f_w = \frac{\overline{M}_w(G) - \overline{M}_w(G-1)}{\overline{M}_w(br)}$$

where $\overline{M}_w(G)$ and $\overline{M}_w(G\text{-}1)$ are the weight-average molecular weights of generation G and of the previous generation, respectively, and $\overline{M}_w(br)$ is the weight-average molecular weight of the branches grafted in generation G. The branching functionality of the polymers also increases for successive generations.

Slide 9 - Scaling behaviour

One way to obtain information about the structure of the polymers prepared is to look at the relation between certain parameters (e.g., the second virial coefficient A_2, the radius of gyration R_g and the translational diffusion coefficient D_z) and $\overline{M}_w$. The scaling relation between the parameters mentioned and the molecular weight is an exponential function, the value of the exponent (a, b or c) in the relation being structure-sensitive. The exponent is obtained as the slope of a log-log plot, as illustrated here for the diffusion coefficients. The three series of data given are for arborescent polymers with branch molecular weights of either 5000 g/mol (hollow circles), 10000 g/mol (solid circles) or 20000 g/mol (inverted triangles). All three data series have essentially the same slope, which is -0.34 overall. The table underneath gives the exponent values expected for random coils (formed by linear chains in solution) and for hard spheres. Obviously, the arborescent polymers behave like hard spheres in dilute solution. The same conclusions can be drawn by examining the exponents obtained for A_2 and R_g, although the errors in the measurements are larger in these cases.

Slide 10 - Dilute solution viscosity

The intrinsic viscosities obtained are compared for two series of polymers with comparable branching functionalities, one with 5000 g/mol branches, the other one with 30000 g/mol branches for each generation. A good solvent (toluene) and a poor solvent for polystyrene (cyclohexane) was used for each of the polymer series. As in the previous cases, the intrinsic viscosity is an exponential function of the molecular weight for linear polymers. For hard spheres, however, $[\eta]$ should be independent of $\overline{M}_w$, i.e. a flat line should be obtained on a $[\eta]$ - $\overline{M}_w$ plot. This is easy to understand looking at the Einstein equation (given at the bottom) in the limit of infinite dilution (N_A = Avogadro's number). Since the ratio M/V_H represents the density of the spheres, the limiting value of η_{sp}/c, i.e. $[\eta]$ should remain constant as long as the density of the spheres remains constant. This is essentially the case for each of the two series of polymers investigated. The density of the spheres actually seems to increase slightly for the upper generations, since $[\eta]$ decreases slightly. Another interesting observation concerns the difference in $[\eta]$ between toluene and cyclohexane

solutions in each of the two series. There is little change in [η] in the 5K series, implying that the molecules have a very rigid structure and undergo little expansion in a good solvent. The difference is much more significant in the 30K series, implying that the molecules are much more expanded in toluene than in cyclohexane. These results confirm that it is possible to tailor the solution behavior of AGPs by varying the structure of the polymers.

Slide 11 - Light scattering - Semidilute solutions

Dilute solutions normally measure the properties of individual, non-interacting molecules. Useful information on intermolecular interactions can be gained when the molecules are forced to overlap, i.e., in the semidilute concentration range (typically 1-15 % w/v). One of the methods suggested to characterize the repulsive forces between molecules under these conditions is the so-called osmotic modulus. It can be shown that the osmotic modulus corresponds experimentally to the ratio M_w/M_{app} of the molecular weight at infinite dilution to the apparent molecular weight determined at a finite concentration c. The osmotic modulus is expressed as a function of a scaling parameter X which is proportional to concentration for a given polymer sample. In the example given, the solid line and the dotted line correspond to theories for random coils and for hard spheres, respectively. Both types of behaviors have been verified experimentally, using linear polymers and globular proteins. The data points provided are for three generations of arborescent polymers with branches of 5000 g/mol. It can be seen that the behavior of the G=0 (comb) polymer (hollow circles) somewhat resembles linear chains, while the G=1 and G=2 polymers (solid circles and inverted triangles, respectively) are closer to hard spheres. None of the polymers investigated fall directly on the curve for hard spheres, however. This is easy to understand by recalling the structure postulated for AGPs (slide 12). The inner portion of the molecules should have a rigid, impenetrable structure, resulting from a high segmental density. The outer layer, on the other hand, should be more diffuse and flexible, allowing limited interpenetration of the molecules.

Slide 12 - Reminder - Structure of G=1 polymer

Slide 13 - COPOLYMERS WITH A MAJOR COMONOMER COMPONENT

The basic grafting reaction relies on electrophilic substitution on aromatic rings for the preparation of successive generations. This does not, however, preclude the preparation of highly branched polymers containing a different type of monomer unit in the last generation. By adjusting the relative amounts of core polymer, the number of grafting sites and the molecular weight of the grafted chains, it is possible to prepare graft polymers in which the polystyrene core accounts for a very small fraction of the total mass. These polymers should, therefore, behave essentially like highly branched polymers of the comonomer. This approach was illustrated by preparing a copolymer where polyisoprene is the major component.

Slide 14 - Preparation of polyisoprene copolymer

The approach used is very similar to the preparation of the styrene homopolymers. In this case, however, living chains of the second monomer type are prepared, and are titrated with a chloromethylated backbone polymer.

Slide 15 - Characterization of copolymer

The results obtained so far by this technique are very encouraging. The GPC diagrams obtained show that the polyisoprenyl anions were grafted on the chloromethylated backbone in 75% yield, and the resulting polymer had a narrow apparent polydispersity. Ungrafted material was easily removed by precipitation fractionation.

Slide 16 - NMR

The fractionated graft copolymer was analyzed by ^{1}H-NMR, to confirm the presence of a large polyisoprene component (80% by weight), and hence the success of the reaction. The polyisoprene chains have a microstructure including different isomers, because the polymerization was carried out in THF. The cis-1,4- isomer, preferred for elastomeric applications, could be prepared as easily using hexanes in the isoprene polymerization, followed by addition of THF prior to grafting.

Slide 17 - COPOLYMERS WITH A CORE-SHELL MORPHOLOGY

Copolymers including a lower amount of comonomer preferentially on the outside of the molecules can be prepared by a variation of the basic technique. These molecules are particularly interesting when a hydrophilic component such as poly(ethylene oxide) is incorporated in the shell, leading to micelle-like character. Amphiphilic block copolymers are commonly used to mimic micelles, but suffer from a number of limitations. The micellar structures obtained typically have a bimodal size distribution, because larger aggregates are formed in addition to desolvated single molecules. Block copolymer micelles are also susceptible to aggregation and/or coagulation when subjected to flow or solvency conditions are changed. The highly branched structures should greatly minimize the occurrence of these problems.

Slide 18 - Preparation of functionalized core

The synthetic scheme used is similar to the preparation of homopolymers, except for the last core generation, where a bifunctional initiator (6-lithiohexyl acetaldehyde acetal) is used. The preparation of a G=1 functionalized core is given for illustration purposes. The bifunctional initiator results in protected hydroxyl functionalities being introduced at or near the surface of the highly branched core. It should be noted that the same approach can be used to prepare arborescent polymers carrying functional groups at the surface, providing control over the surface chemistry of the polymers.

Slide 19 - Addition of poly(ethylene oxide) shell

The acetal functionalities are hydrolyzed under mildly acidic conditions, and then titrated with a potassium naphthalide solution, to give the potassium alcoholate. A poly(ethylene oxide) shell is thus grown directly on the core when ethylene oxide monomer is added. The thickness of the hydrophilic shell is easily varied by controlling the amount of ethylene oxide added in the reaction.

Slide 20 - Reaction on a G=1 core

First attempts at growing the hydrophilic shell as described led to a large increase in the apparent polydispersity of the products, as determined by GPC analysis. The appearance of a large shoulder at low elution volumes implies the occurrence of cross-linking reactions.

Slide 21 - Cross-linking side reactions

Side reactions were linked to the presence of residual chloromethyl groups, resulting from incomplete grafting reactions in the preparation of the core. The cross-linking mechanism suggested involves formation of highly reactive benzylpotassium functionalities through metal-halogen exchange, followed by coupling with an unreacted chloromethyl functionality. Intermolecular reactions lead to dimer and multimer formation, as illustrated.

Slide 22 - Elimination of residual chloromethyl groups: Metal-halogen exchange

To test the hypothesis suggested, residual chloromethyl sites were destroyed by exhaustive metal-halogen exchange under controlled conditions. The polymer in THF was equilibrated with a large excess of n-butyllithium, and hydrolyzed to convert benzyllithium functionalities to methyl groups.

Slide 23 - Addition of shell on treated core

Following the metal-halogen exchange reaction, the core was used in the shell growth process. The resulting polymer, containing 30% poly(ethylene oxide) by weight, was initially characterized by GPC in pure THF. The considerably lower apparent polydispersity obtained confirms the cross-linking mechanism suggested. The asymmetry of the peak, which displays a shoulder at low elution volumes, could be due to association between core-shell polymer molecules. The problem was even more obvious when core-shell polymers with a higher poly(ethylene oxide) content (70% w/w) were prepared and analyzed. More detailed GPC studies were undertaken to determine the origin of the peak broadening effects observed.

Slide 24 - GPC analysis of core-shell polymers

A mixture of THF with 4% acetic acid v/v was used as the mobile phase in a first series of measurements of core-shell polymers with 30% and 70% poly(ethylene oxide) by weight, respectively. The peak obtained for the 30% copolymer is symmetrical, and is characterized by a low apparent polydispersity $\bar{M}_w/\bar{M}_n = 1.09$, compared to 1.20 obtained for the same polymer in pure THF. The peak broadening observed in THF was therefore due to association, rather than cross-linking. The copolymer with a higher poly(ethylene oxide) content, on the other hand, gives a shoulder at high elution volumes in the THF/acetic acid mixture, which could be due to adsorption of the polymer on the polystyrene beads of the GPC column. To prevent this, the measurements were repeated using N,N-dimethylformamide as the mobile phase. In this case, a low apparent polydispersity was obtained for the sample containing 70% poly(ethylene oxide), but a shoulder appeared in the 30% sample. It should be noted that the horizontal line displayed in both figures represents

the range over which the calibration curve is linear. This shows that all samples analyzed were in the linear portion of the calibration curves. Therefore, none of the effects reported can be attributed to peak distortion because the maximum exclusion volume of the column is reached.

Slide 25 - Characterization of the core-shell polymers

GPC analysis shows that the core-shell polymers prepared have a low apparent polydispersity, but the analysis conditions must be carefully selected, depending on the composition of the copolymers analyzed. The solubility behaviour of the copolymers strongly supports a core-shell morphology. Redispersion of the G=1 solid polymer in water is possible, although the dispersion is turbid, resulting from partial aggregation of the molecules. When a 2-5% solution of the core-shell polymer in THF is dropped in water, however, a clear solution is obtained. This presumably corresponds to a molecularly dispersed state, or else involving minimal aggregation. Dispersion of the molecules in water would of course be impossible if the hydrophobic polystyrene core was not covered by a poly(ethylene oxide) shell, acting as a stabilizing layer. A last confirmation of the success of the reaction can be found in the hydrodynamic radii determined by dynamic light scattering. The values reported in the table compare the radii determined in THF for the hydroxyl-functionalized core and for the core-shell molecules based on a G=1 core and a G=4 core. The hydrodynamic radius increased after growth of the shell in all cases, and the increase was higher when a larger amount of poly(ethylene oxide) was incorporated.

CONCLUSIONS

Slide 26 - Synthesis

Slide 27 - Properties

Slide 28 - Future developments

Slide 29 - Acknowledgements

ARBORESCENT GRAFT POLYMERS AND COPOLYMERS: SYNTHESIS AND PROPERTIES

Mario Gauthier

Institute for Polymer Research
Department of Chemistry
University of Waterloo
Waterloo, ON N2L 3G1

273

OUTLINE

1. General characteristics of arborescent polymers

2. Preparation of styrene homopolymers

   Characterization

   Solution properties

3. Copolymers with a major comonomer component

   Characterization

4. Copolymers with a core-shell morphology

   Characterization and properties

5. Conclusions

6. Future developments

7. Acknowledgements

GENERAL CHARACTERISTICS OF AGP's

- Successive grafting reactions

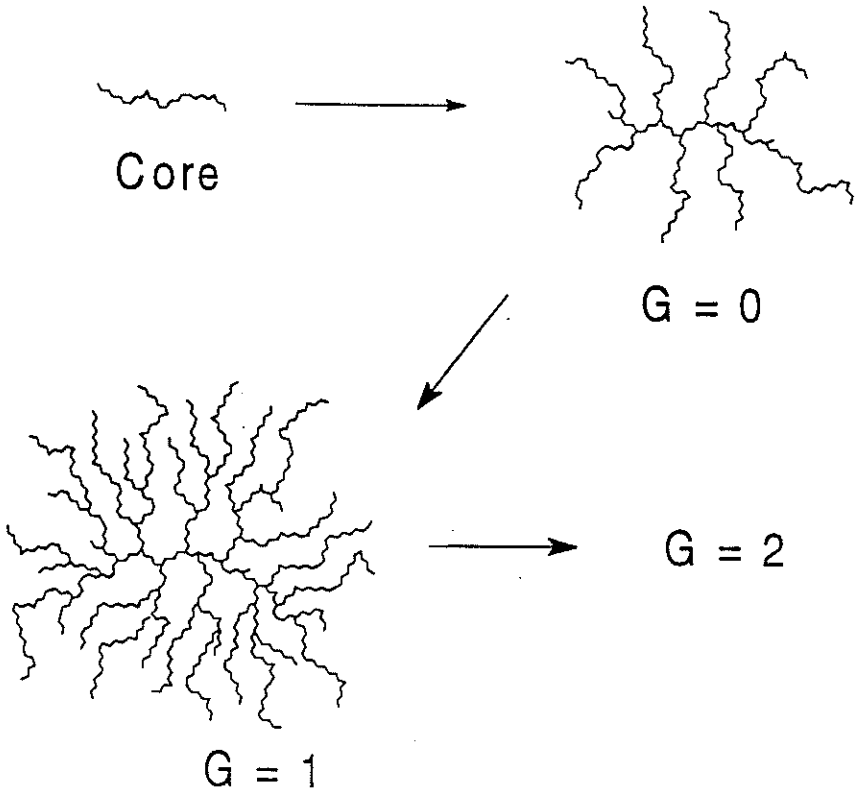

- Control over branching density

  branch molecular weight

  chemical functionality

- Mol. weights $\bar{M}_w = 5 \cdot 10^4 - 5 \cdot 10^8$ g/mol, $(\bar{M}_w/\bar{M}_n)_{app} = 1.1\text{-}1.2$
- Branching functionalities $f = 10 - 10^4$

ADVANTAGES / DISADVANTAGES

- Diffuse layer growth

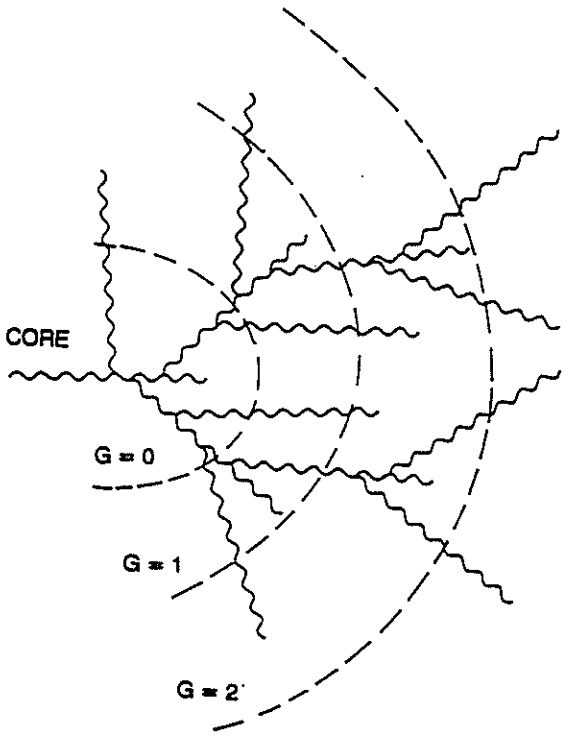

- Control over the structure
- Functionalization possible (polystyrene)
- Fast increase in molecular weight, branching functionality
- Insensitive to side reactions

- Grafting site introduction requires electrophilic substitution
- Apparent $\bar{M}_w/\bar{M}_n$ = 1.1-1.2 > dendrimers
- Surface not as well-defined as dendrimers

PREPARATION OF STYRENE HOMOPOLYMERS

Gauthier, M.; Möller, M. *Macromolecules* **1991**, *24*, 4548.

INTRODUCTION OF GRAFTING SITES

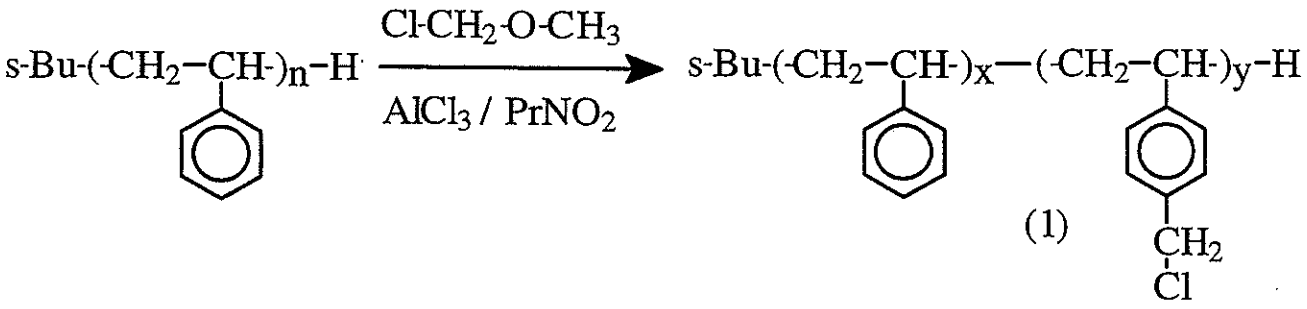

(1)

OR

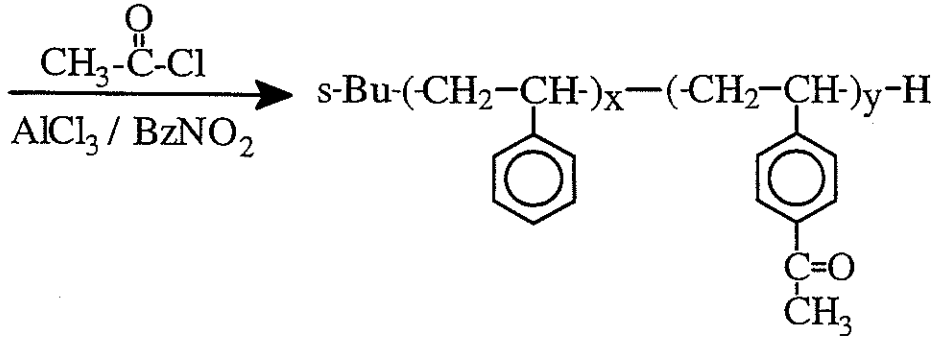

277

GRAFTING

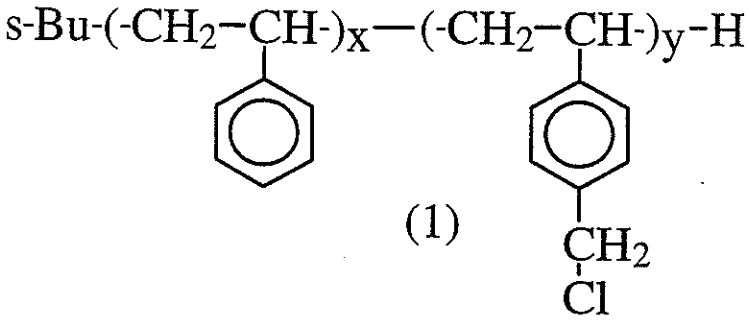

(1)

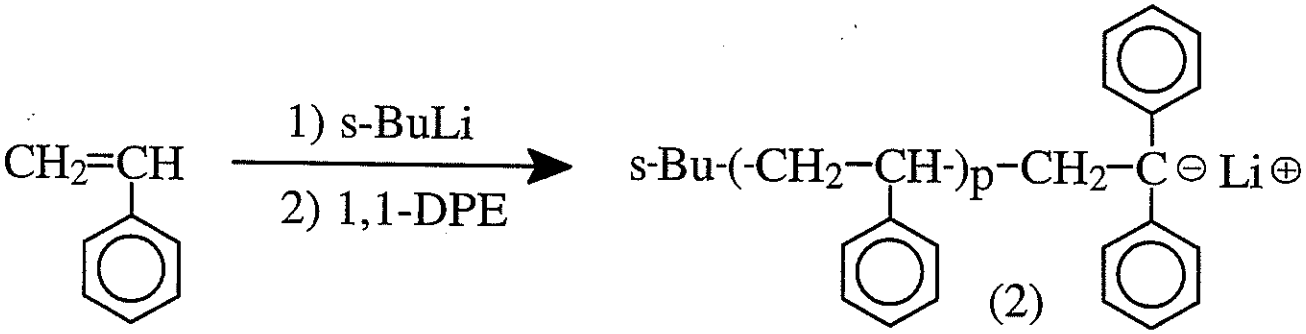

(2)

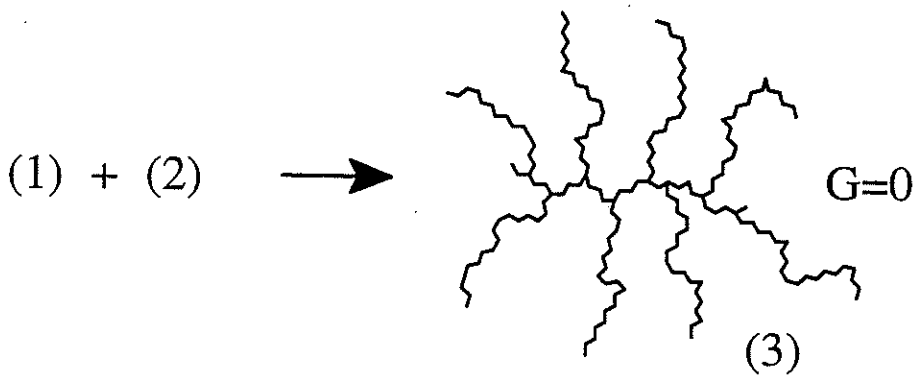

(3)

Grafting efficiency

> 95% ($ClCH_2$-)

≈ 65% (CH_3CO-)

CHARACTERIZATION OF HOMOPOLYMERS

GEL PERMEATION CHROMATOGRAPHY

Generation	Branches		Graft polymers	
	$\bar{M}_w$(br) /g·mol^{-1}	PDI (br)	$\bar{M}_w$ /g·mol^{-1}	PDI
Core	$4.7 \cdot 10^3$	1.08	-----	-----
0	$4.4 \cdot 10^3$	1.03	$4.2 \cdot 10^4$	1.06
1	$4.7 \cdot 10^3$	1.03	$1.4 \cdot 10^5$	1.07
2	$4.4 \cdot 10^3$	1.04	$3.6 \cdot 10^5$	1.20
3	$4.6 \cdot 10^3$	1.05	$5.1 \cdot 10^5$	1.15
4	$5.3 \cdot 10^3$	1.08	-----	-----

- Low apparent PDI
- Molecular weights underestimated!

LIGHT SCATTERING - DILUTE SOLUTIONS

Generation	$\bar{M}_w$(LS) /g·mol^{-1}	f_w
0	$6.7 \cdot 10^4$	14
1	$8.7 \cdot 10^5$	170
2	$1.3 \cdot 10^7$	2800
3	$8.8 \cdot 10^7$	16000
4	$2.3 \cdot 10^8$	27000

- Absolute molecular weight $\bar{M}_w$
- Geometric increase in $\bar{M}_w$
- Uniform growth for successive generations

SCALING BEHAVIOR

Gauthier, M.; Möller, M.; Burchard, W. *Macromol. Symp.* **1994**, *77*, 43.

$$A_2 = k_1 \bar{M}_w^{\,a} \qquad R_g = k_2 \bar{M}_w^{\,b} \qquad D_z = k_3 \bar{M}_w^{\,c}$$

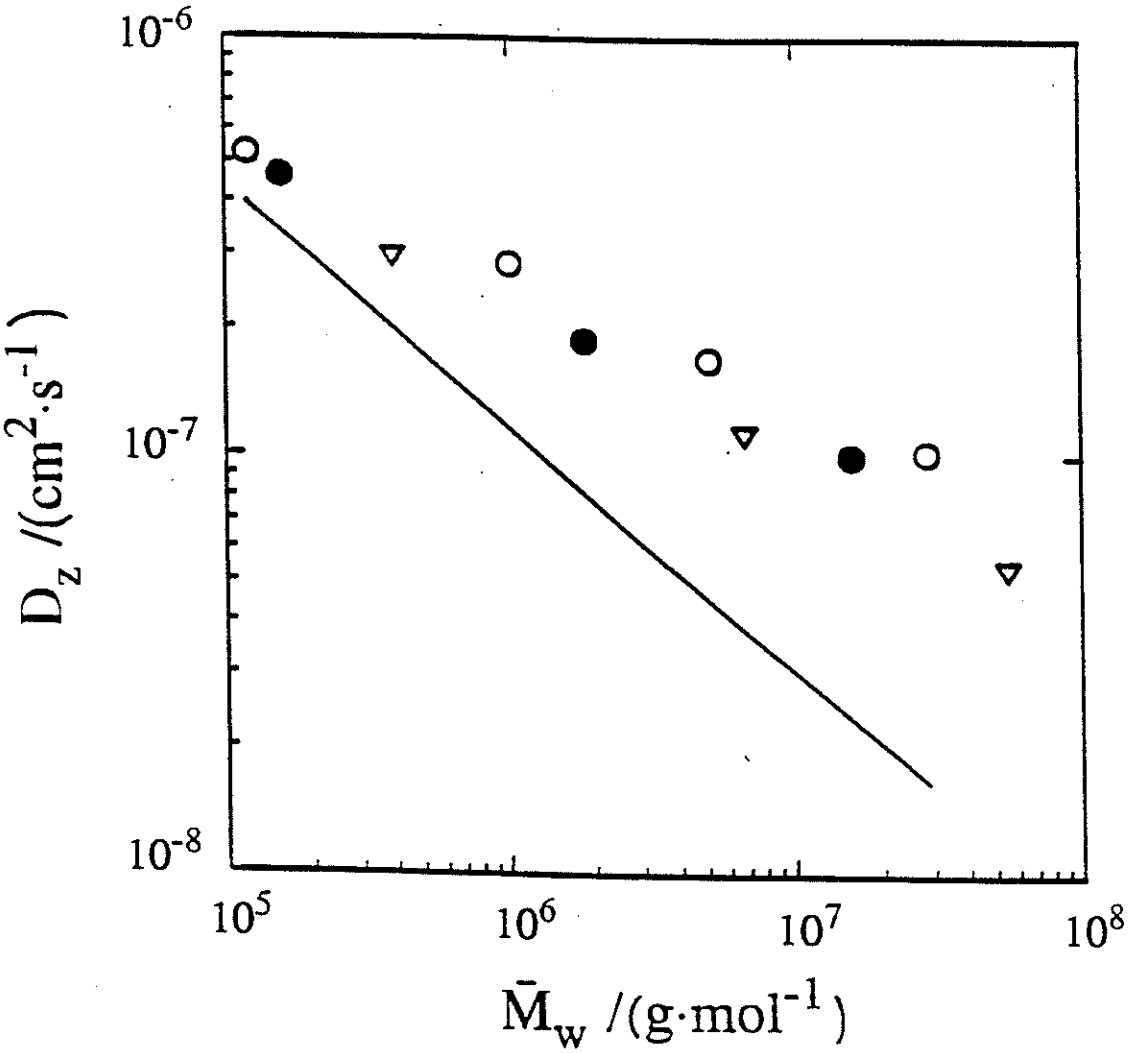

Parameter	Coils	Hard spheres	Graft polymers
D_z	-0,6	-0,33	-0,34
R_g	0,6	0,33	0,2
A_2	-0,2	-1	-0,9

DILUTE SOLUTION VISCOSITY

Gauthier, M.; Li, W.; Tichagwa, L. *Polym. Prepr.* **1995**, *36(2)*.

- 5K branches, ca. 10 branches/backbone chain

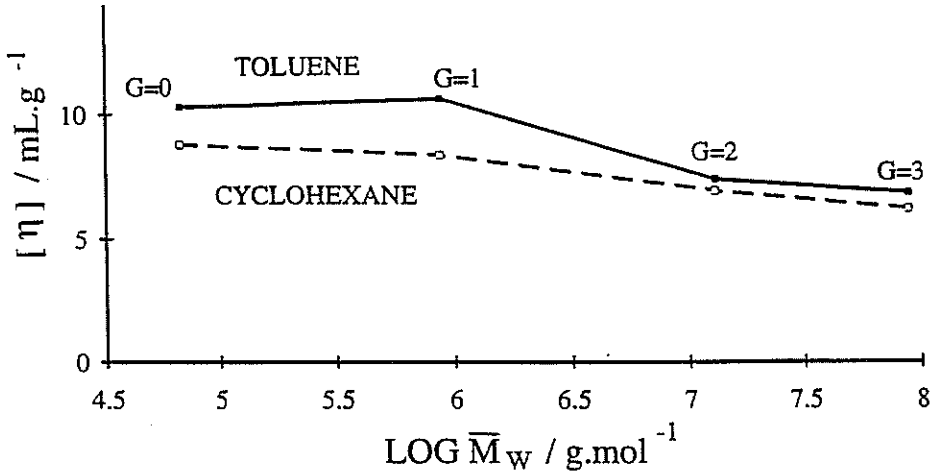

- 30K branches, ca. 10 branches/backbone chain

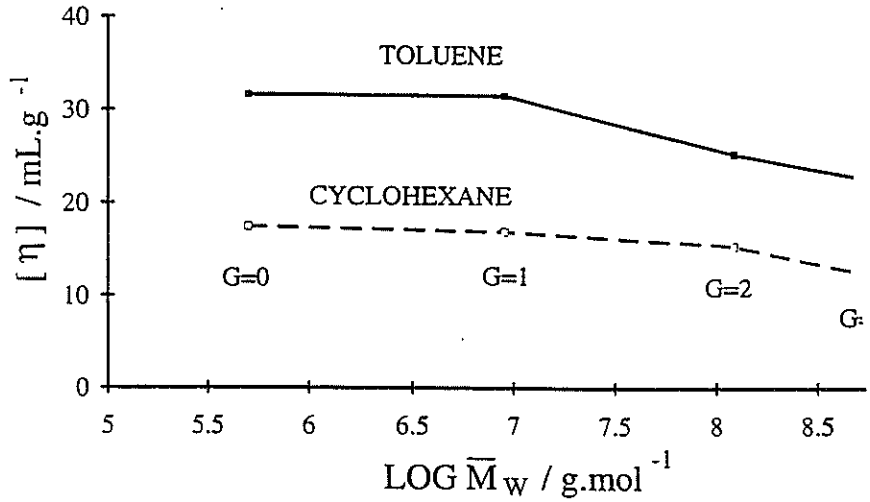

$$\frac{\eta_{sp}}{c} = \frac{5}{2} N_A \frac{V_H}{M}$$

∴ Hard-sphere behavior

281

LIGHT SCATTERING - SEMIDILUTE SOLUTIONS

Gauthier, M.; Möller, M.; Burchard, W. *Macromol. Symp.* **1994**, *77*, 43.

- Osmotic modulus

$$\frac{\overline{M}_w}{RT}\frac{\partial \pi}{\partial c} = \frac{\overline{M}_w}{\overline{M}_{app}}$$

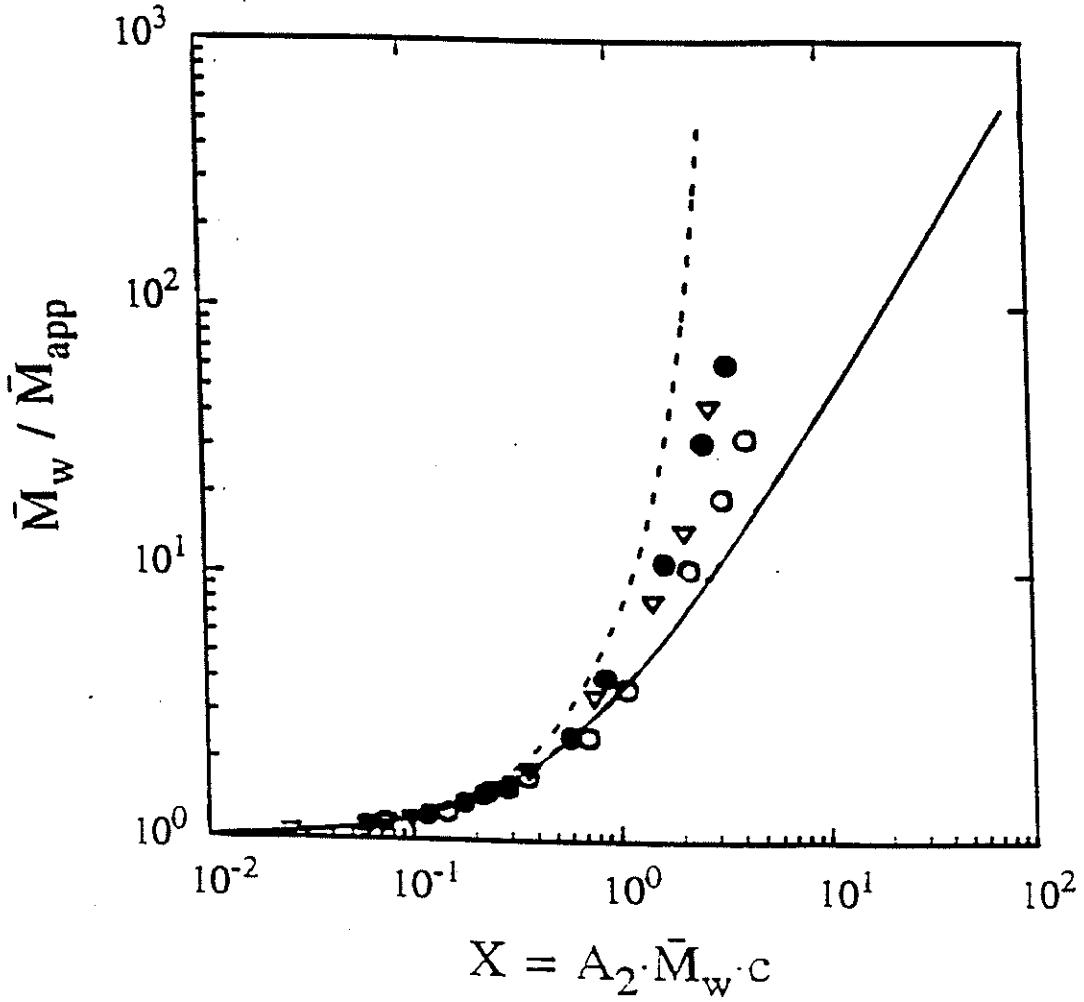

∴ Limited interpenetration at higher concentrations

(consistent with diffuse layer growth)

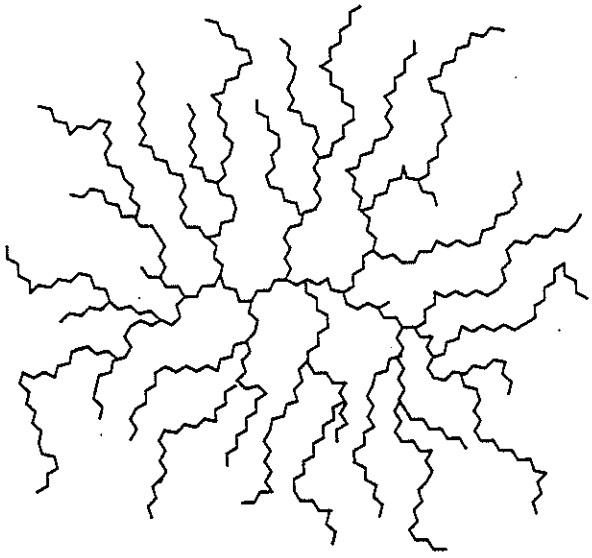

COPOLYMERS WITH A MAJOR COMONOMER COMPONENT

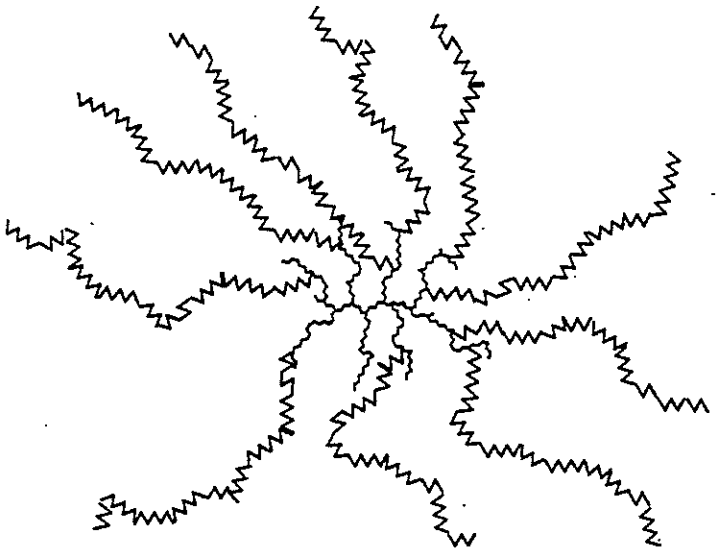

- High branching functionalities
- 80% to over 95% comonomer by weight

PREPARATION OF POLYISOPRENE COPOLYMER

Kee, R.A.; Gauthier, M. *Polym. Prepr.* **1995**, *36(2)*.

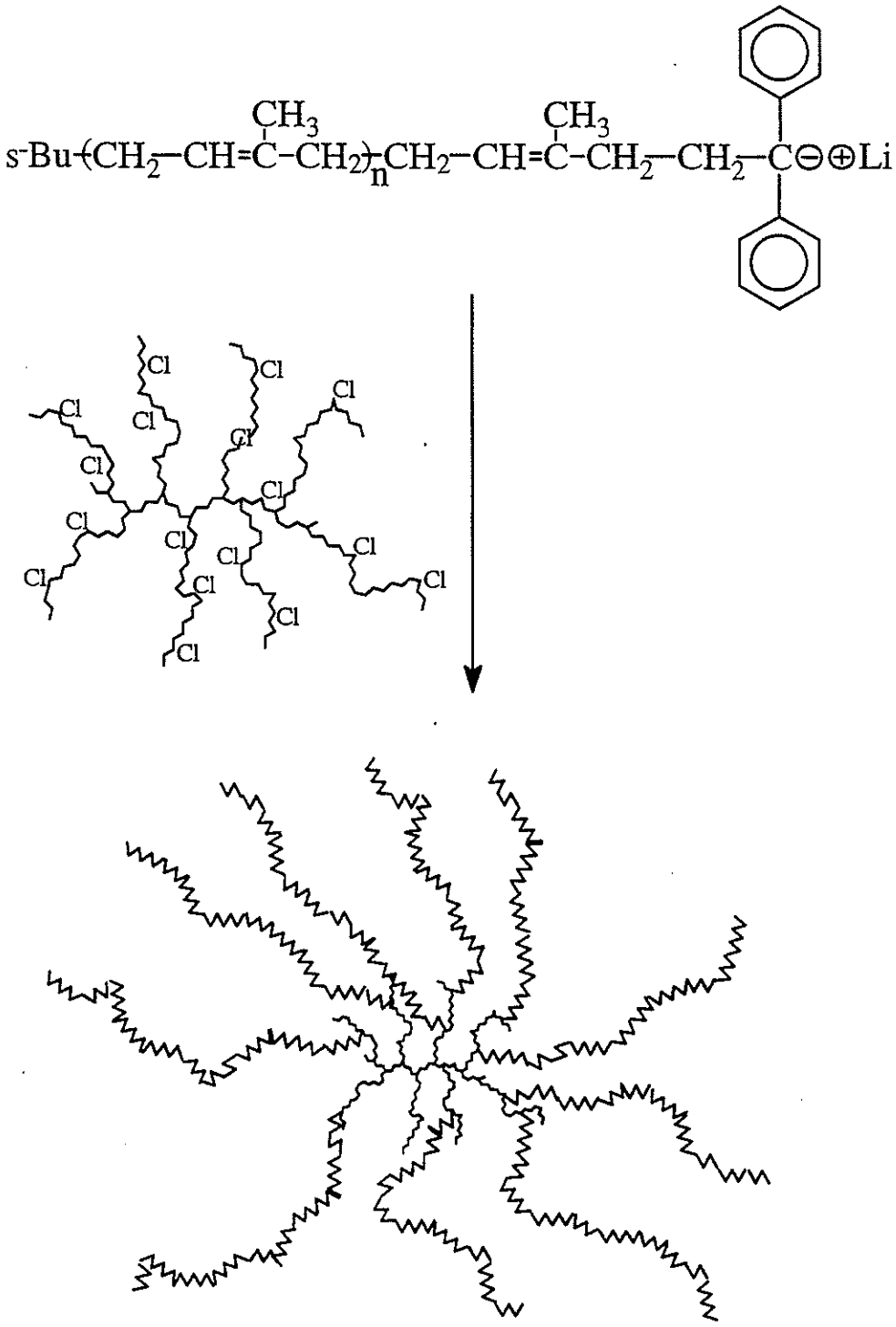

CHARACTERIZATION OF COPOLYMER

- GPC

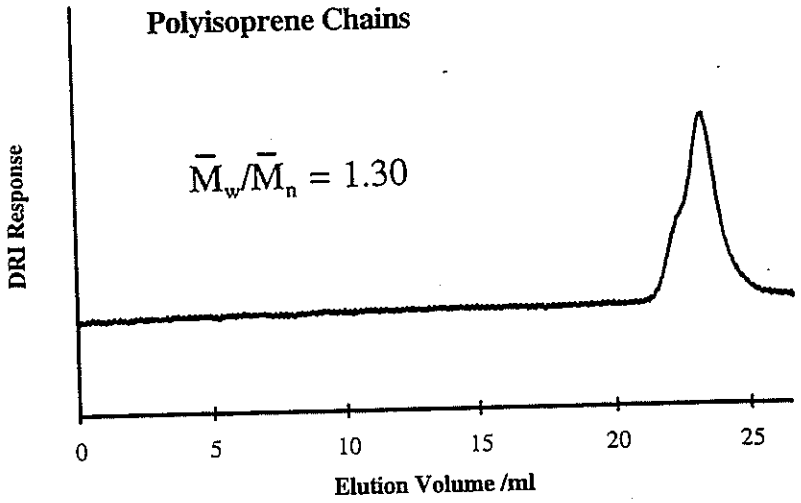

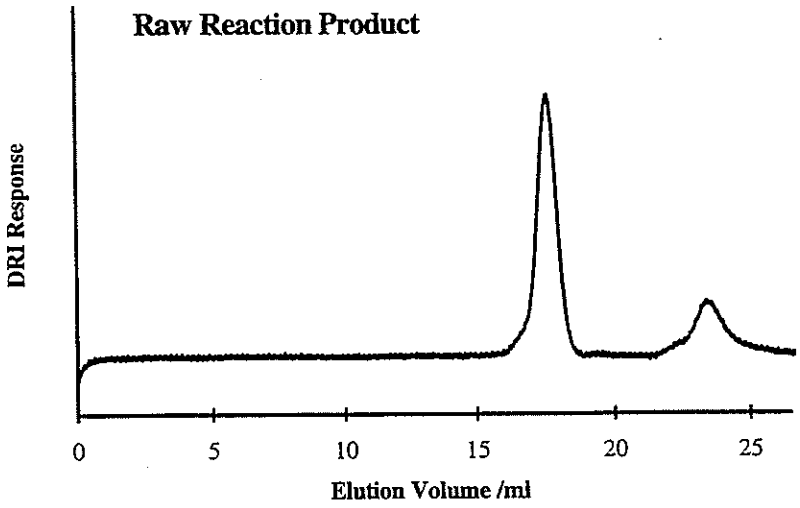

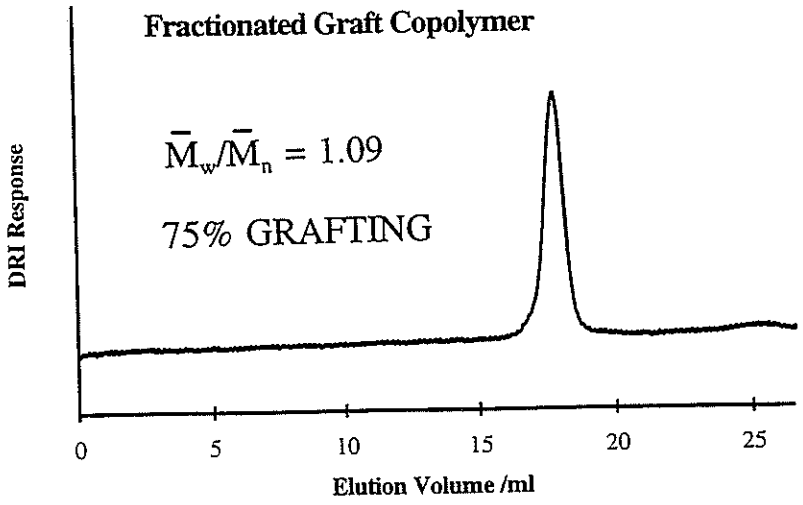

285

- NMR

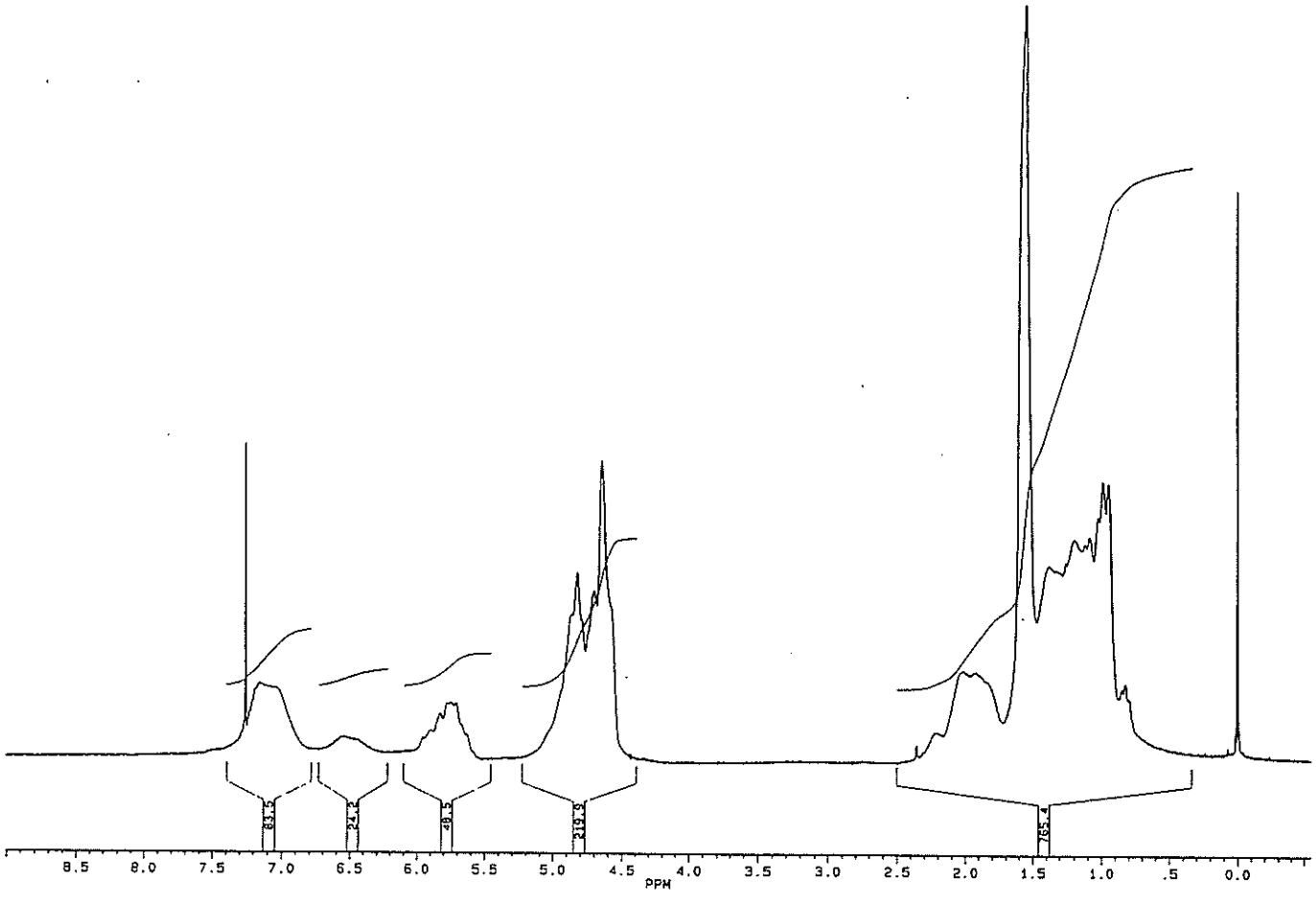

- 80% PIP by weight
- Mixed microstructure (polymerization in THF)

286

COPOLYMERS WITH A CORE-SHELL MORPHOLOGY

Gauthier, M.; Tichagwa, L.; Li, W. *Polym. Prepr.* **1994**, *35(2)*, 482.

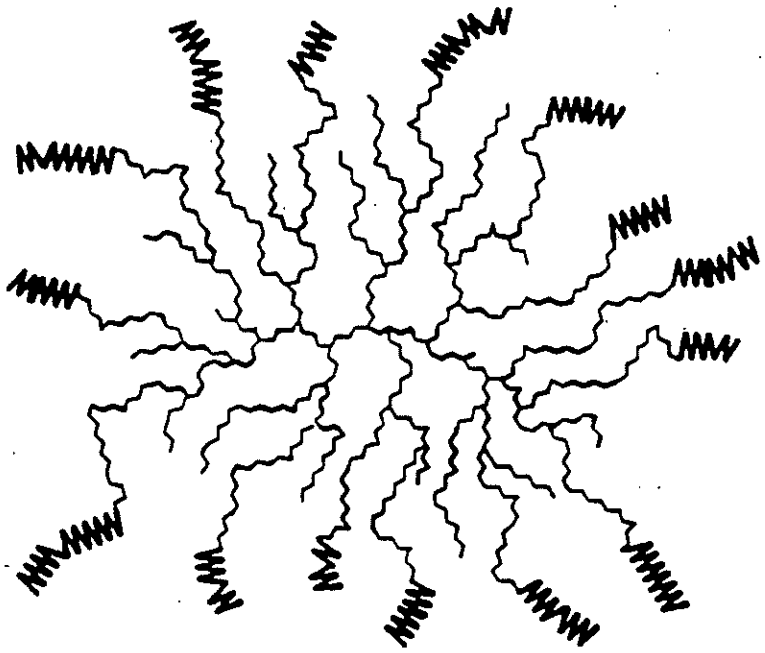

- Polystyrene core / poly(ethylene oxide) shell
- Monomolecular micelles

PREPARATION OF FUNCTIONALIZED CORE

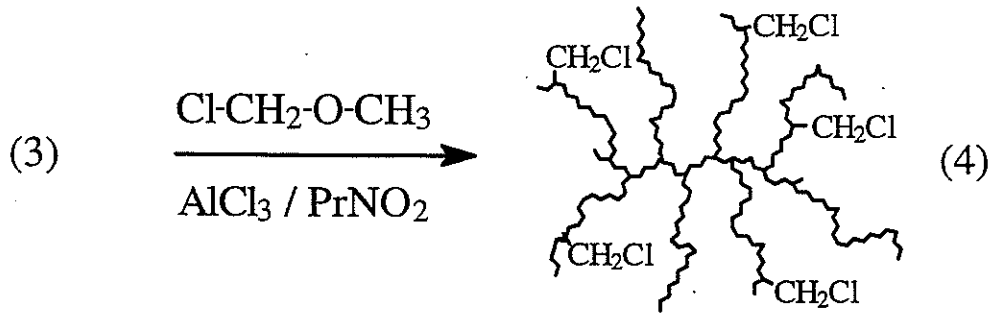

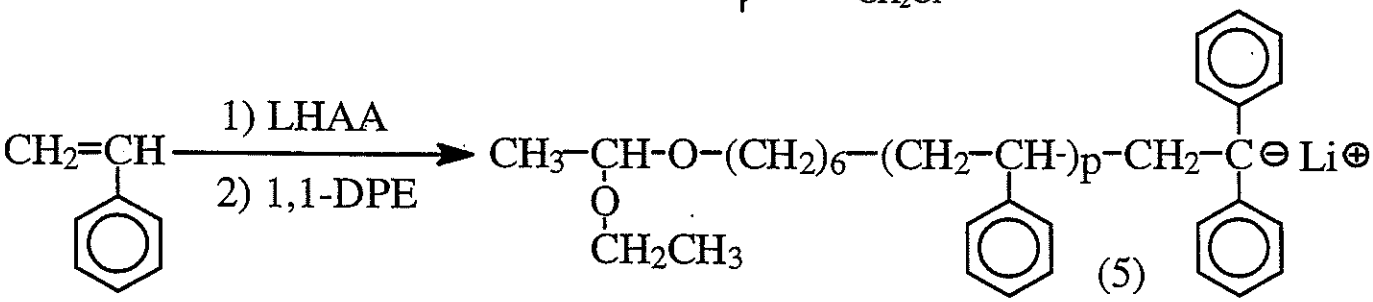

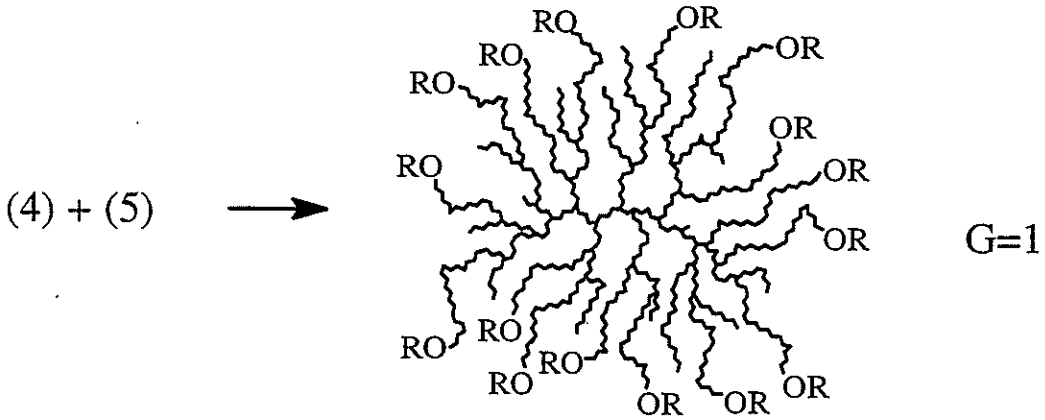

LHAA = CH_3–CH-O-$(CH_2)_6$⊖Li⊕
O
CH_2CH_3

2-88

ADDITION OF POLY(ETHYLENE OXIDE) SHELL

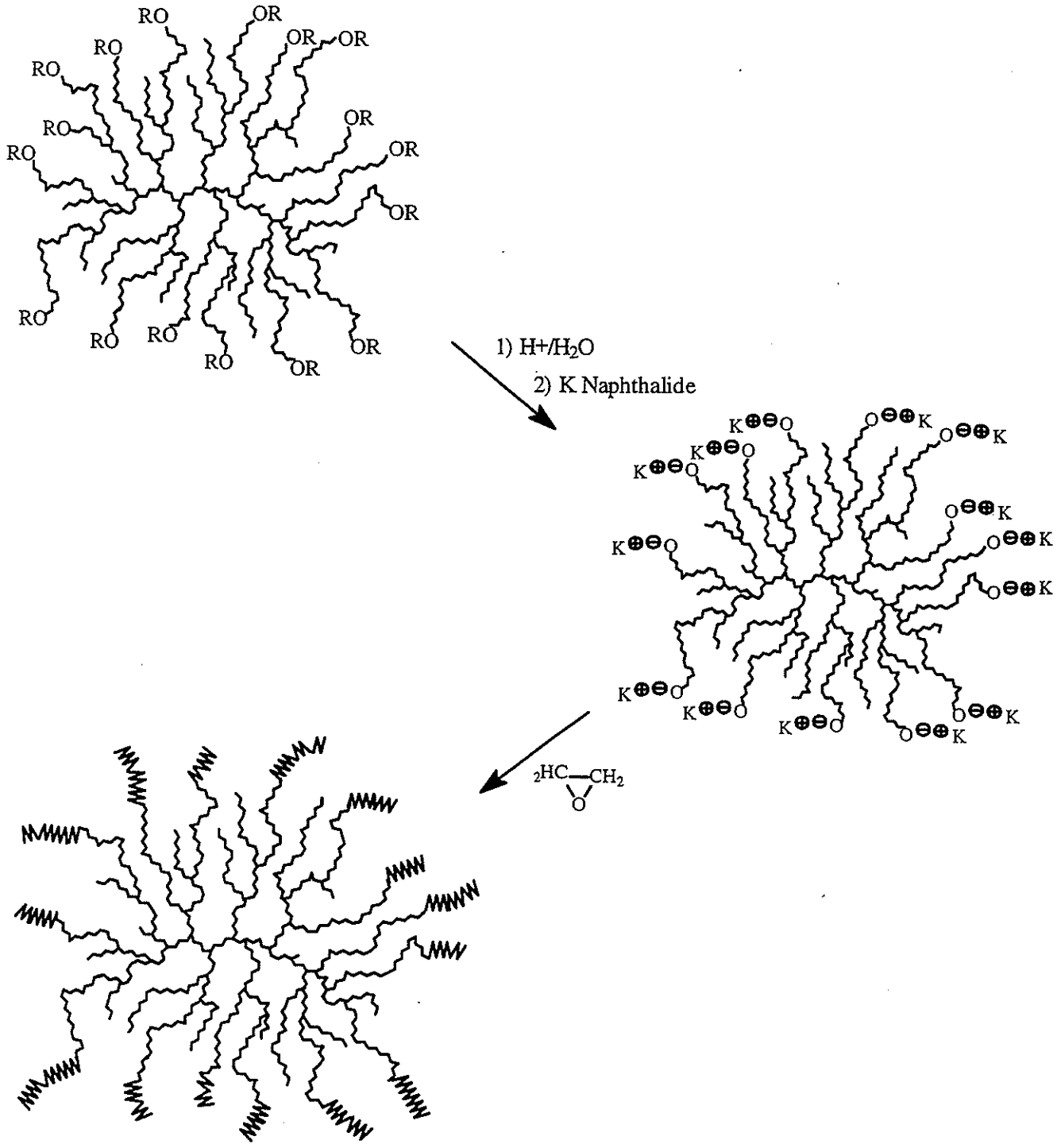

289

REACTION ON A G=1 CORE

- GPC

Hydroxyl-functionalized core

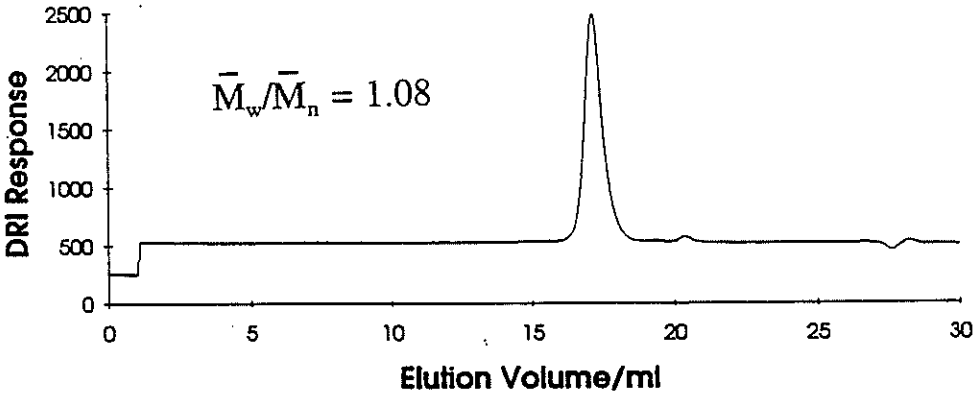

Core-shell polymer

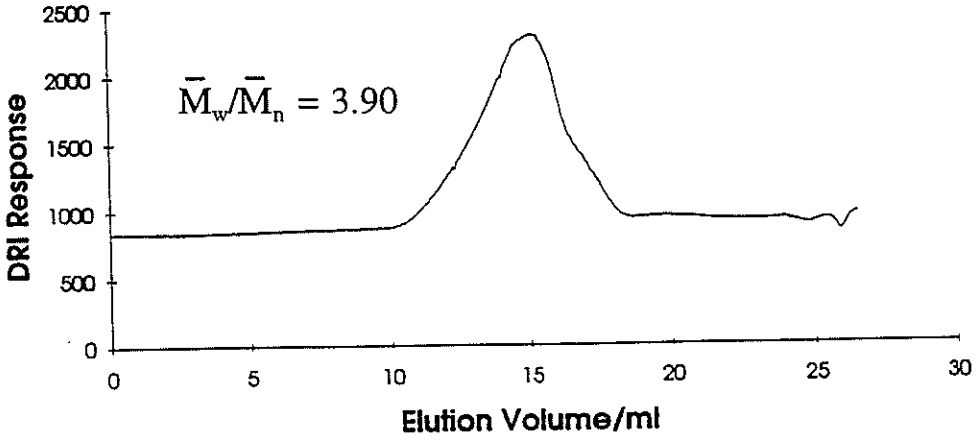

CROSS-LINKING SIDE REACTION

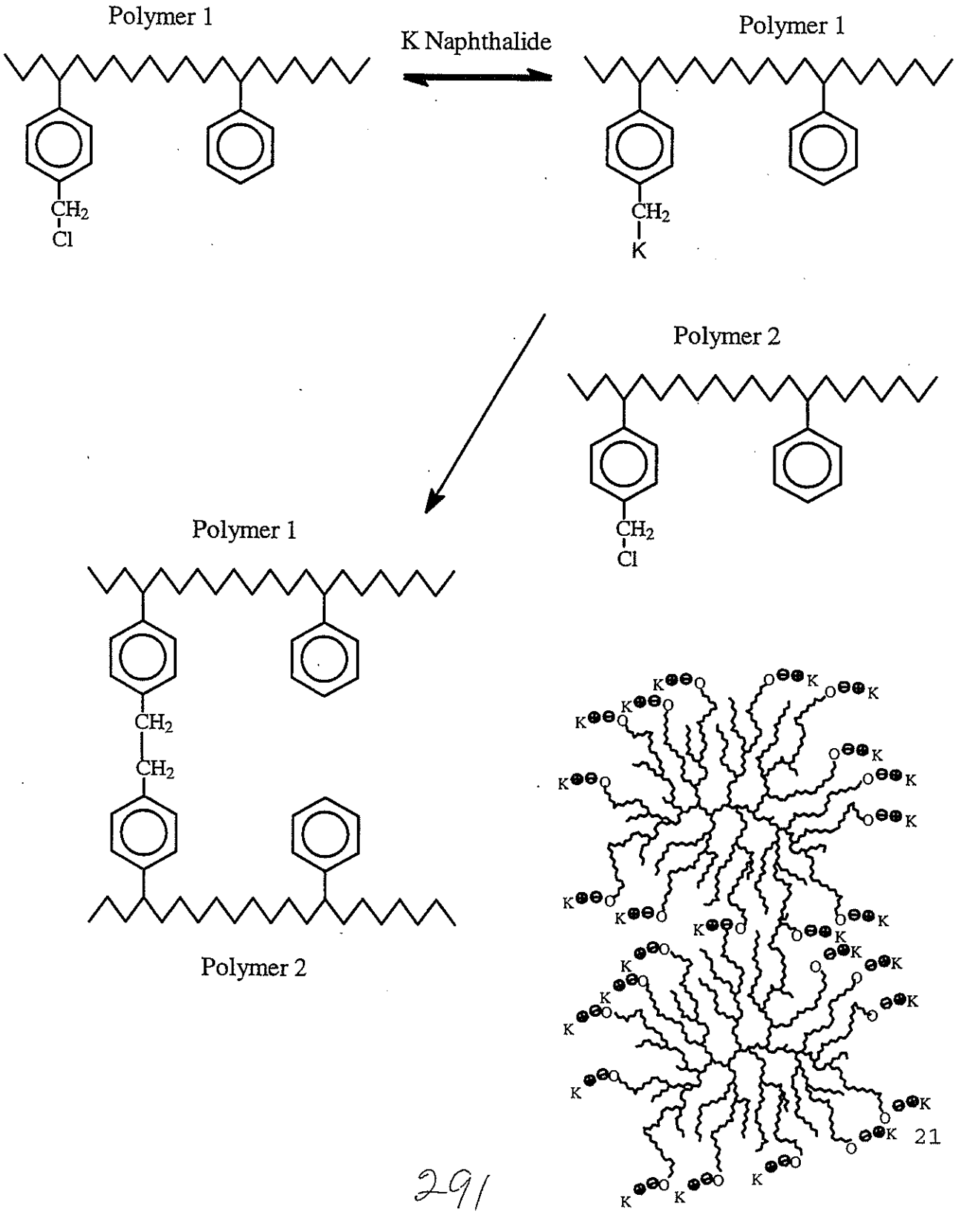

291

ELIMINATION OF RESIDUAL CHLOROMETHYL GROUPS: METAL-HALOGEN EXCHANGE

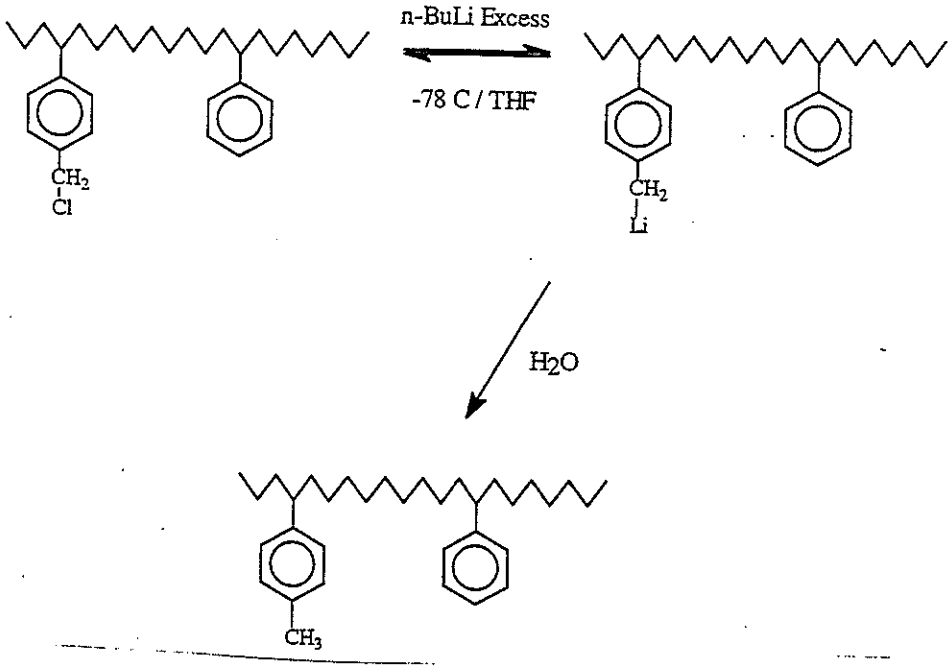

ADDITION OF SHELL ON TREATED CORE

- GPC

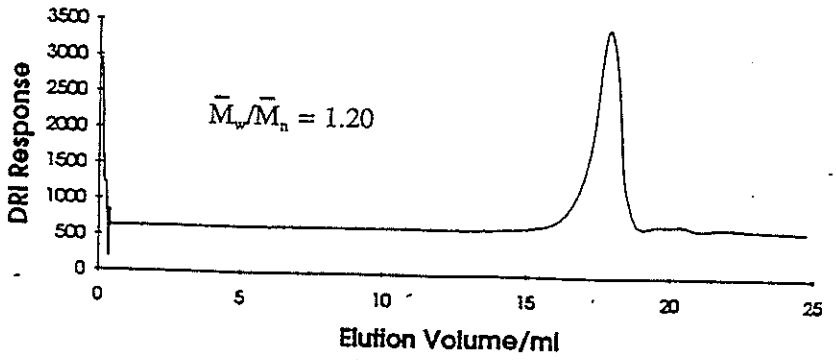

- Pure THF as eluent
- Shoulder at low elution volume - association?

GPC ANALYSIS OF CORE-SHELL POLYMERS

- THF + 4% Acetic acid

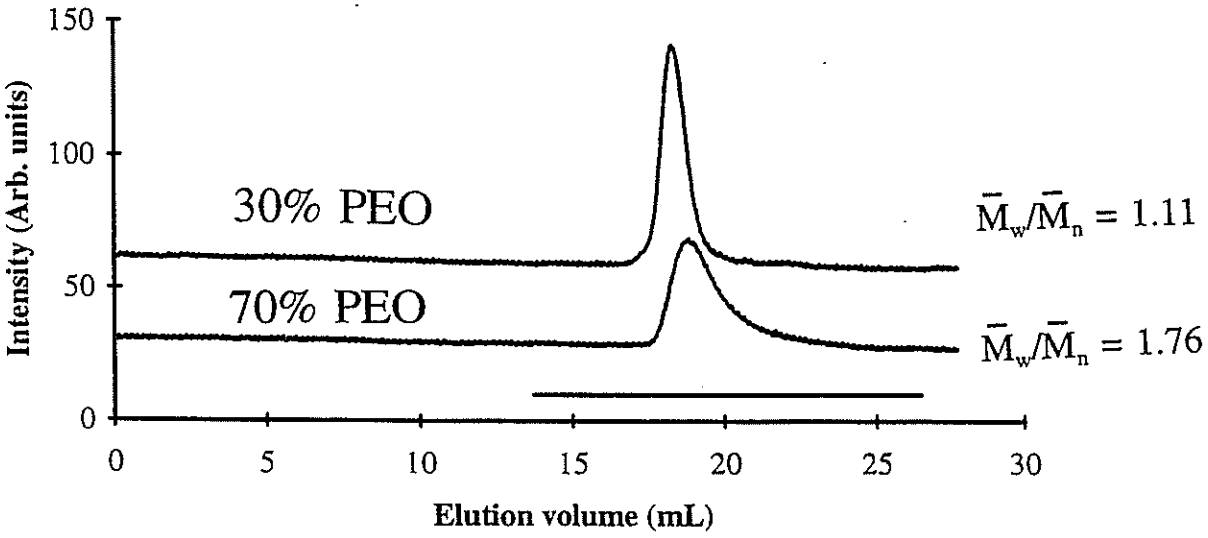

- N,N-Dimethylformamide

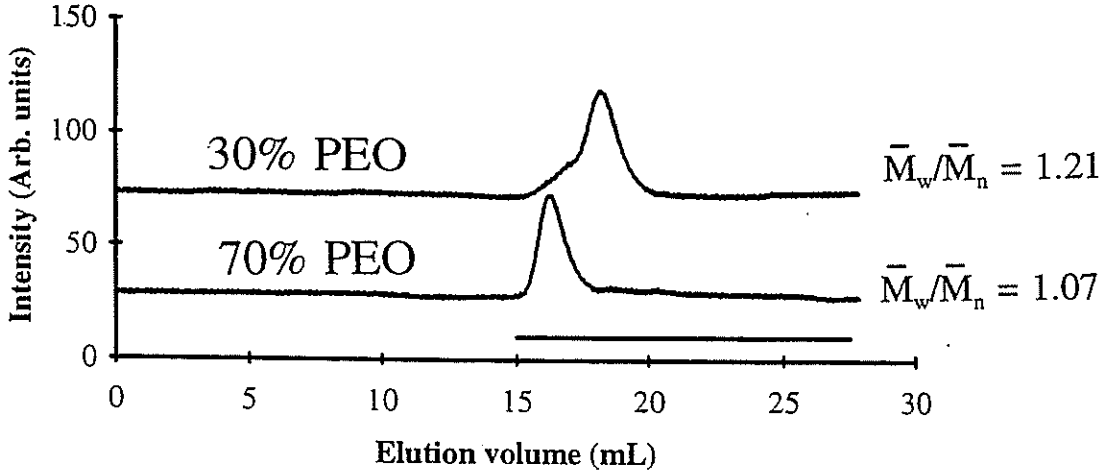

CHARACTERIZATION OF CORE-SHELL COPOLYMERS

- GPC: low apparent polydispersity index
- FT-IR: can vary PEO content (30%, 70% by weight)
- Solubility behavior

  Turbid solution when redispersed from solid state

  Desolubilization easy, clear solution obtained

  Consistent with core-shell morphology, PEO-rich shell

- Dynamic light scattering: R_h

Sample	R_h (nm)
G=1 core	$12._9$
G=1 core-shell, 30% PEO	$16._8$
G=1 core-shell, 70% PEO	$23._3$
G=4 core	$63._7$
G=4 core-shell, 30% PEO	$66._0$

CONCLUSIONS

SYNTHESIS

- Highly branched homopolymers and copolymers can be prepared by successive grafting reactions.
- The polymers have well-defined side chains randomly distributed on the polymer backbone.
- The size of the grafted chains and the branching density can be controlled for each generation.
- A wide range of molecular weights and branching functionalities are accessible.
- Core-shell polymers and surface-functionalized polymers can be prepared by a variation of the basic technique.
- Shell thickness can be accurately controlled in these systems.

PROPERTIES

- Molecular weights increasing geometrically for successive generations, apparent polydispersity $(\bar{M}_w/\bar{M}_n)_{app}$ = 1.1-1.2.
- Dilute solution properties corresponding to hard-sphere behavior.
- Some interpenetration is possible in the semi-dilute range.
- Intrinsic viscosity independent of molecular weight, dominated by molecular weight of side chains.
- Core-shell polymers have micelle-like character.

FUTURE DEVELOPMENTS

- Perfection of grafting reaction using acetyl sites
- Generalization to other monomers (methacrylates, siloxanes)
- Morphological and physical properties investigations of core-shell polymers
- Solubilization / extraction of hydrophobic molecules
- Multilayered core-shell structures
- Highly branched polyelectrolytes

ACKNOWLEDGEMENTS

Prof. Martin Möller

Lilian Tichagwa

Randy Frank

Peter Frank

Dr. Wenguang Li

Sun Gao

Andrew Kee

NSERC

OCMR

STARBURST DENDRIMERS

Synthesis of Precise Macromolecular Architecture

D. A. Tomalia

STARBURST DENDRIMERS

Building a New Nanoscopic Chemistry Set

Donald A. Tomalia
Michigan Molecular Institute

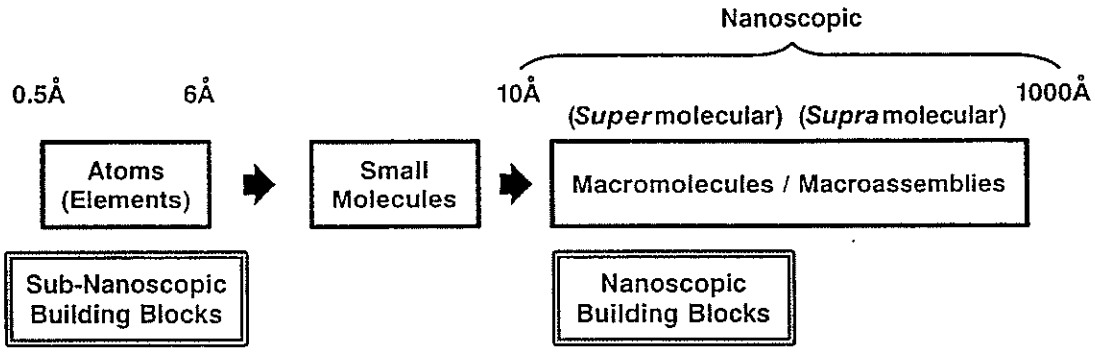

NANOSCOPIC TECHNOLOGY

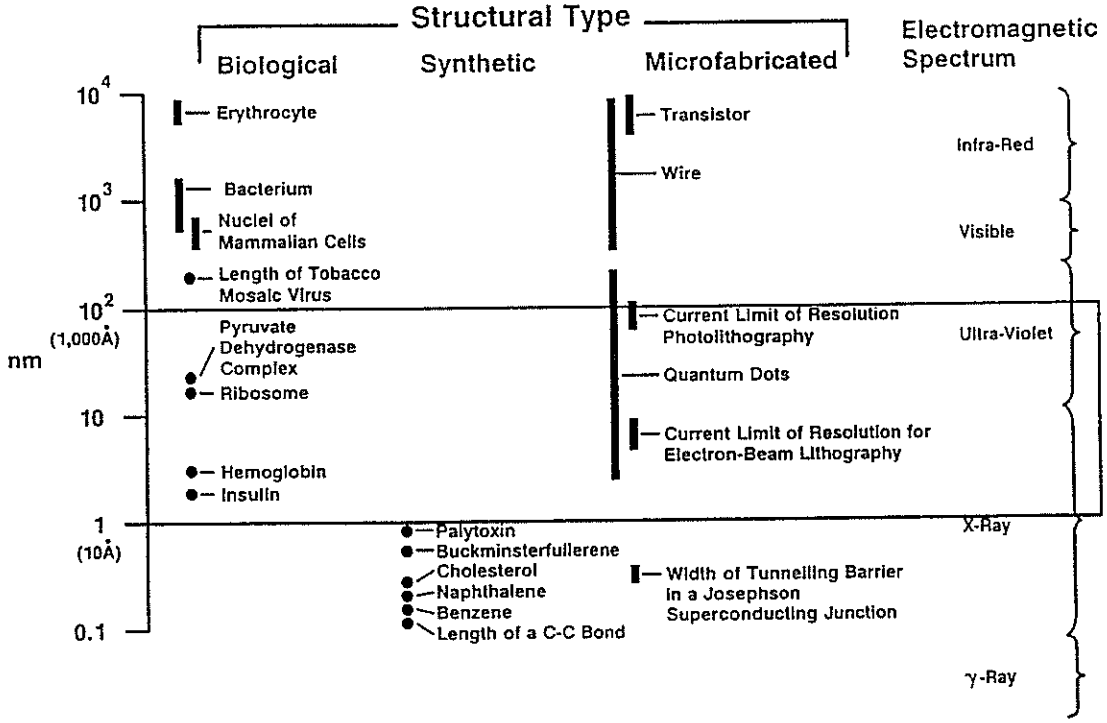

DIMENSIONAL HIERARCHY OF ORGANIC MATTER (MOLECULAR EVOLUTION)

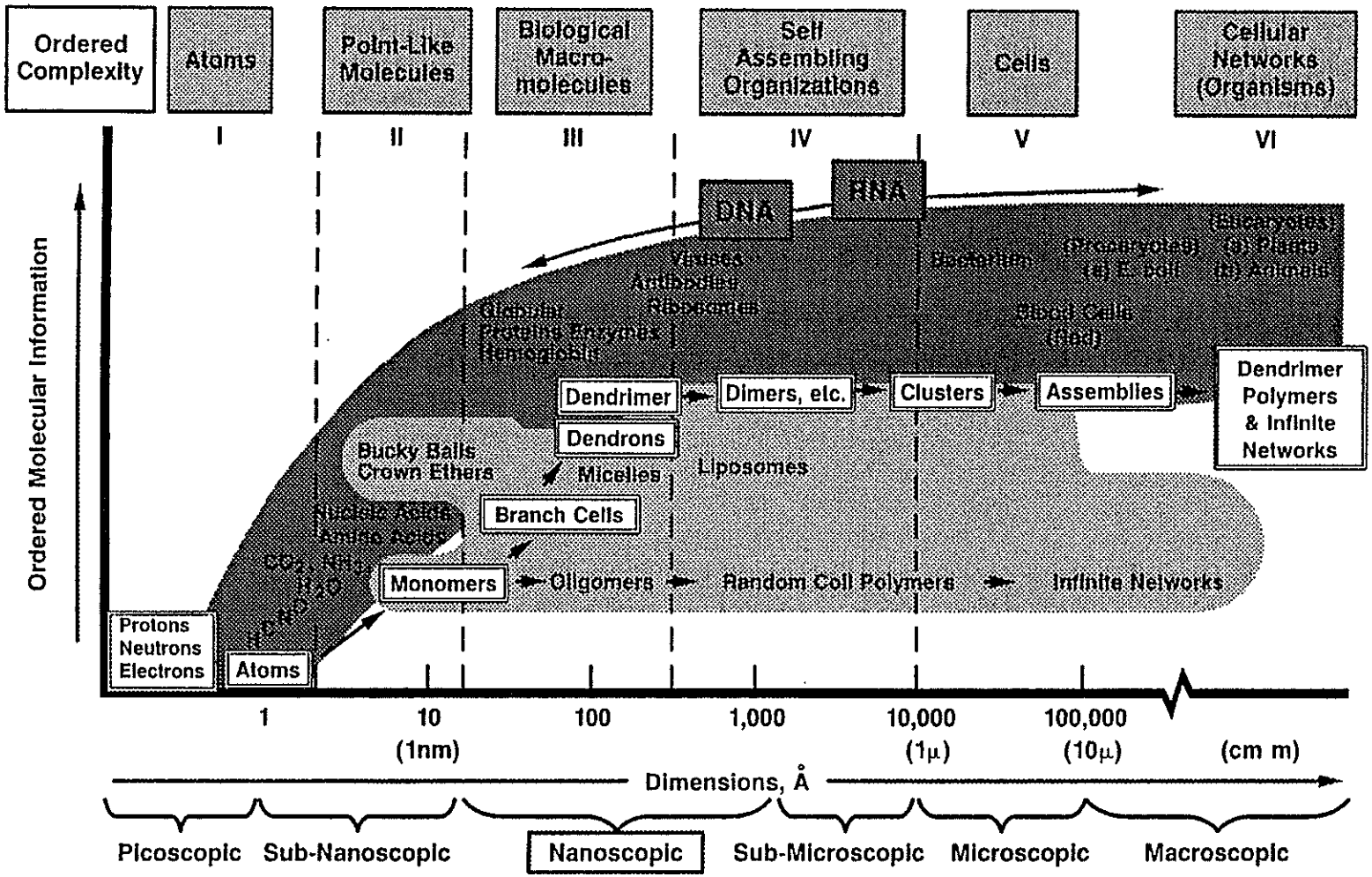

DIMENSIONAL HIERARCHY OF ORGANIC MATTER (NATURAL MOLECULAR EVOLUTION)

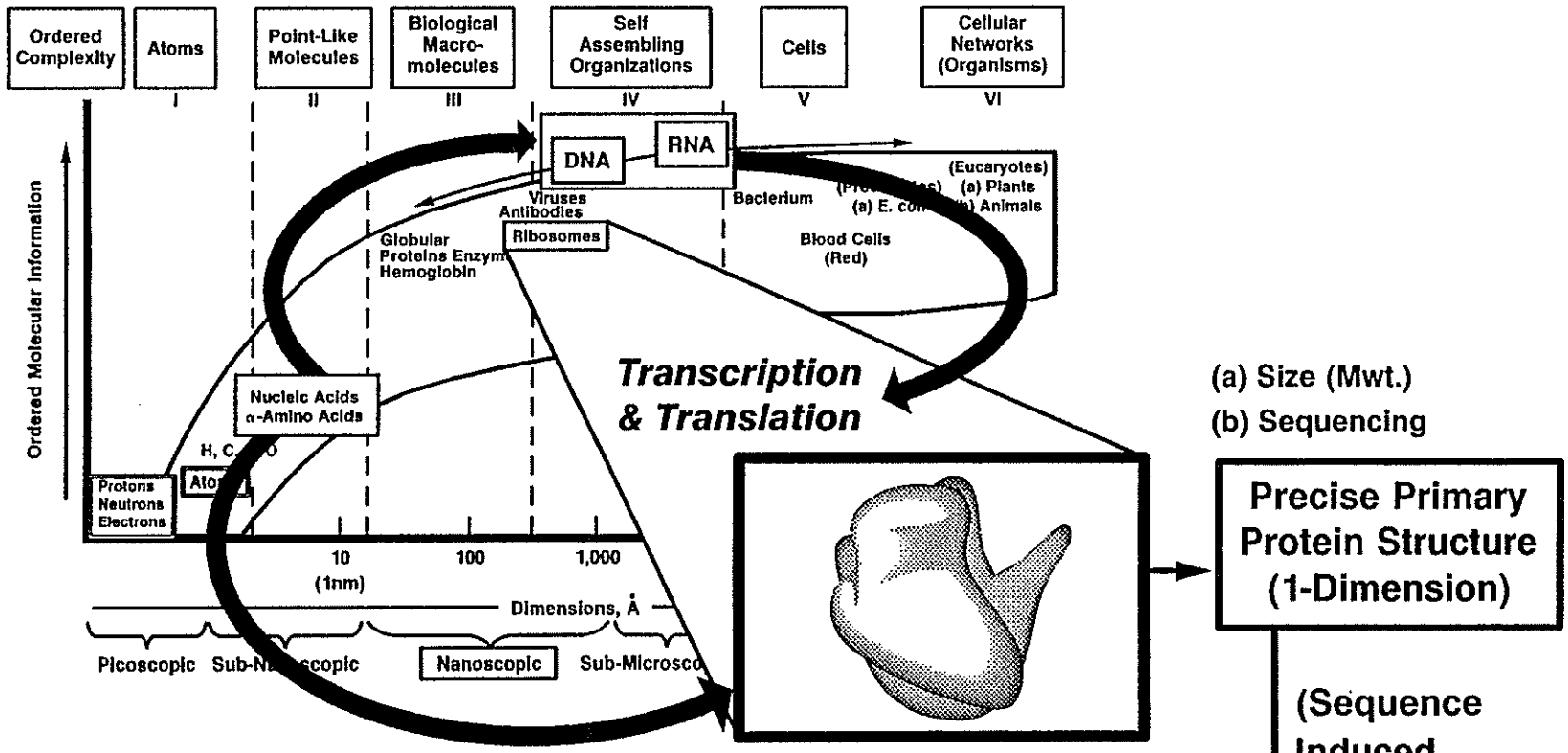

Critical Molecular Design Parameters (CMDP's)

(a) Size (b) Shape
(c) Surface Chemistry
(d) Flexibility (e) Topology

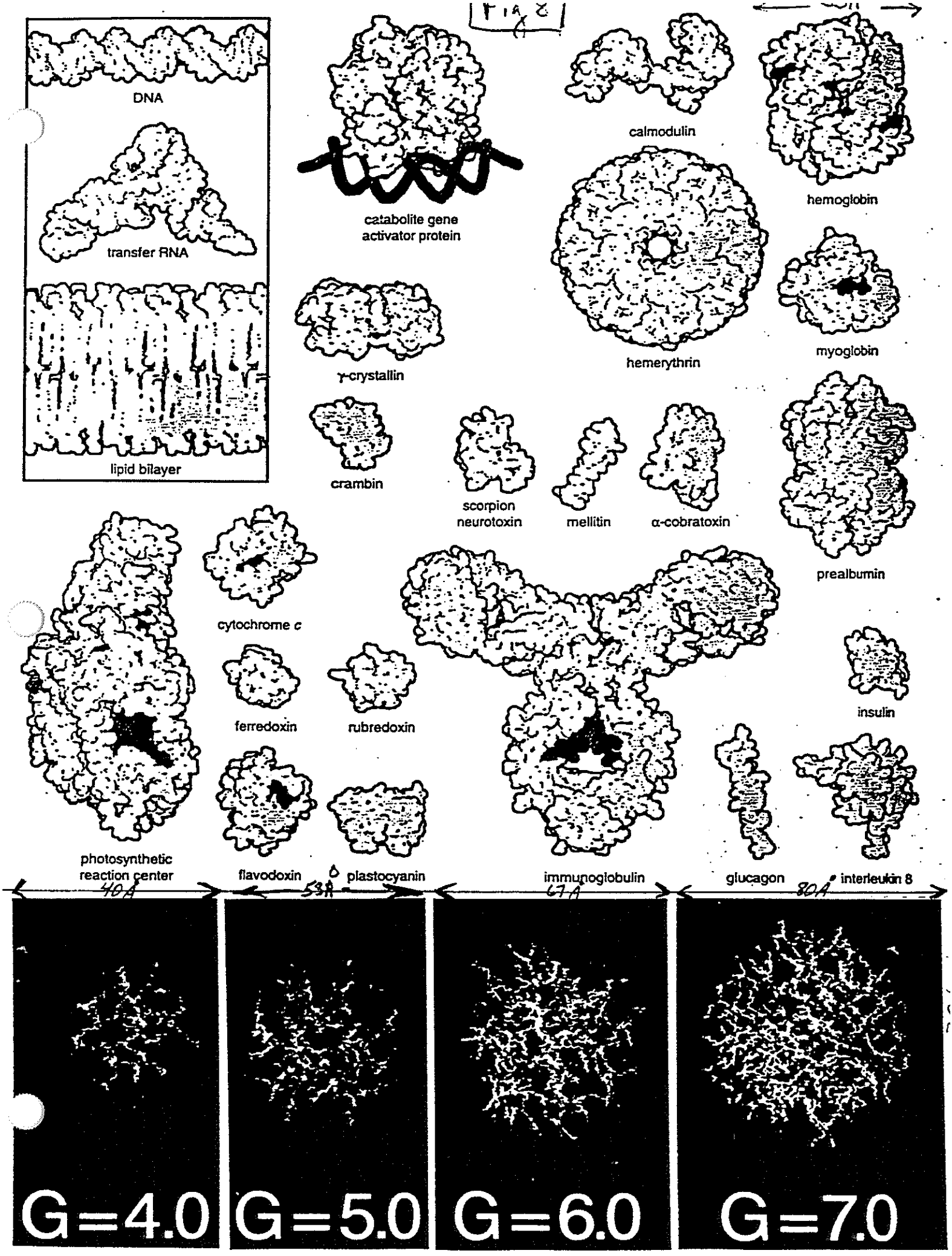
DNA
transfer RNA
lipid bilayer
catabolite gene activator protein
calmodulin
hemoglobin
hemerythrin
myoglobin
γ-crystallin
crambin
scorpion neurotoxin
mellitin
α-cobratoxin
prealbumin
cytochrome c
ferredoxin
rubredoxin
insulin
photosynthetic reaction center
flavodoxin
plastocyanin
immunoglobulin
glucagon
interleukin 8
40Å
53Å
67Å
80Å
G=4.0
G=5.0
G=6.0
G=7.0

BIOLOGICAL HIERARCHY

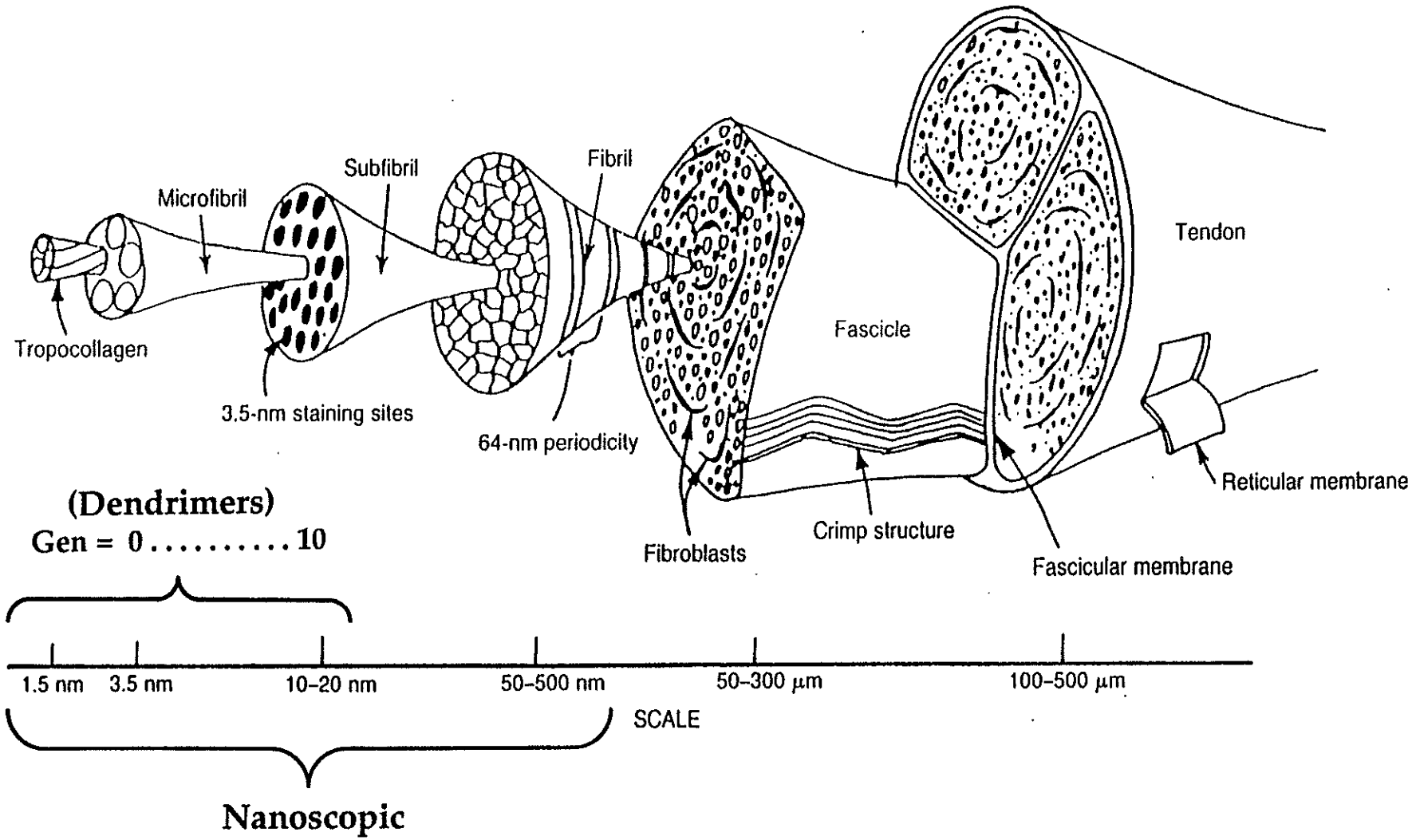

Hierarchical organization of tendon has six levels from the molecular to the macroscopic scales.
Eric Baer, et al.

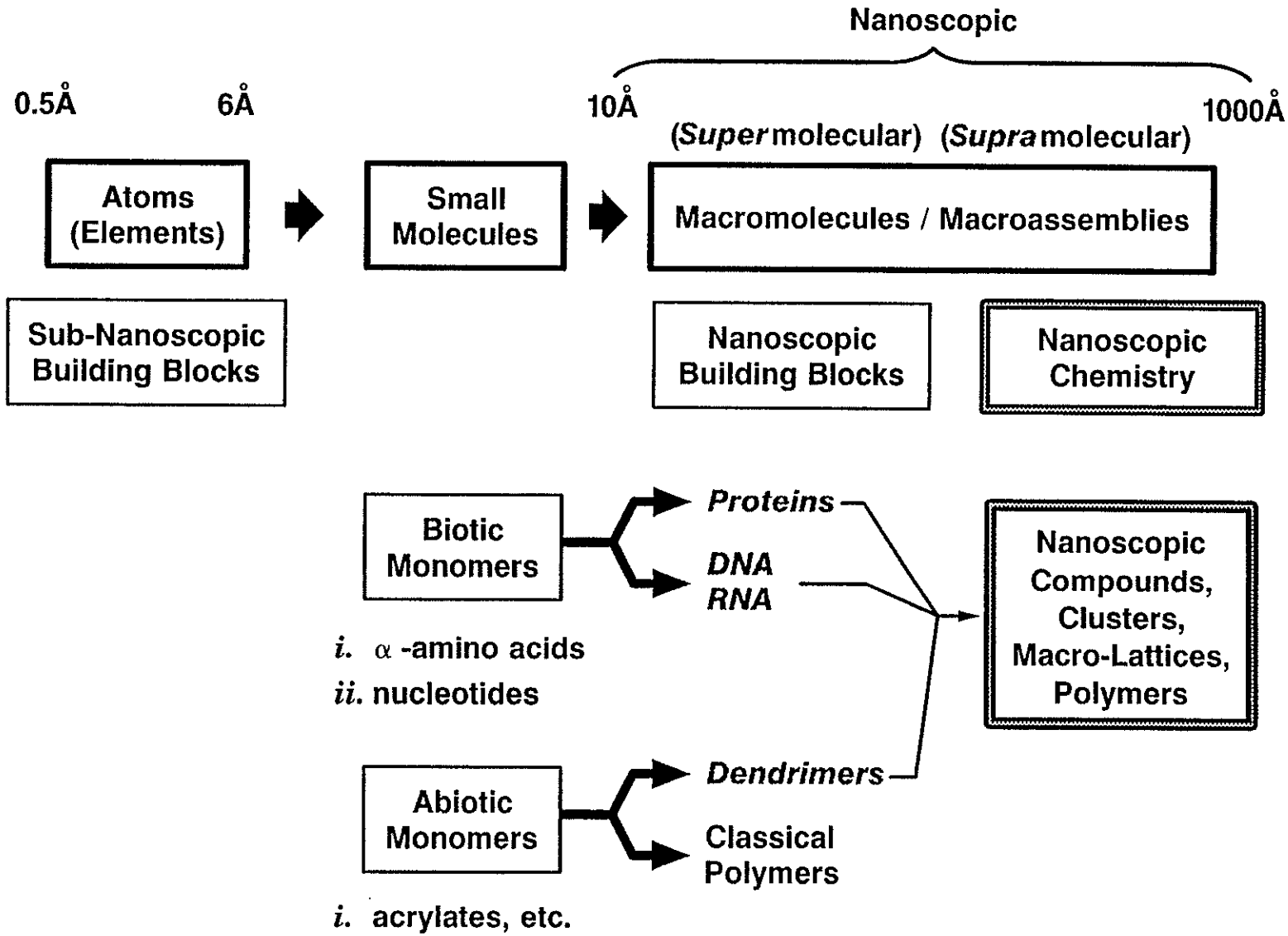
Nanoscopic
0.5Å
6Å
10Å
1000Å
(*Super*molecular)
(*Supra*molecular)
Atoms (Elements)
Small Molecules
Macromolecules / Macroassemblies
Sub-Nanoscopic Building Blocks
Nanoscopic Building Blocks
Nanoscopic Chemistry
Biotic Monomers
Proteins
DNA
RNA
i. α -amino acids
ii. nucleotides
Nanoscopic Compounds, Clusters, Macro-Lattices, Polymers
Abiotic Monomers
Dendrimers
Classical Polymers
i. acrylates, etc.

MAJOR MACROMOLECULAR ARCHITECTURES

I	II	III	IV
Linear	**Cross-Linked**	**Branched**	**Dendritic**
 Flexible Coil	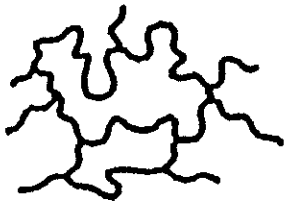 Lightly Cross-Linked	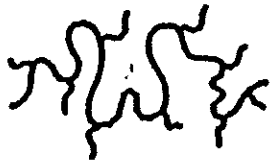 Random Short Branches	(a) 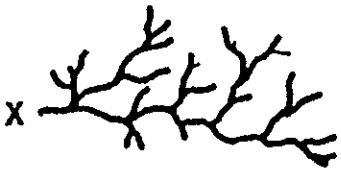 Random Hyperbranched
 Rigid Rod	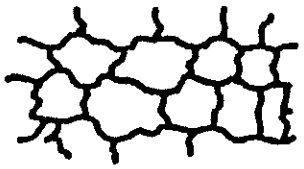 Densely Cross-Linked	 Random Long Branches	(b) 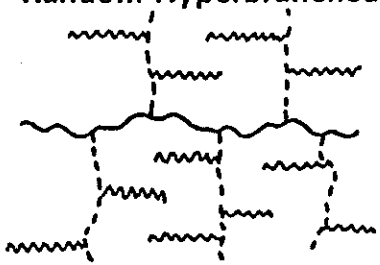 Controlled Hyperbranched (Comb-burst™)
 Cyclic (Closed Linear)		 Regular Comb-Branched	
 Polyrotaxane	 Interpenetrating Networks	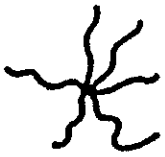 Regular Star-Branched	(c) 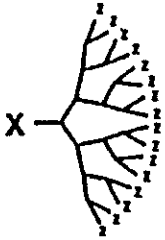 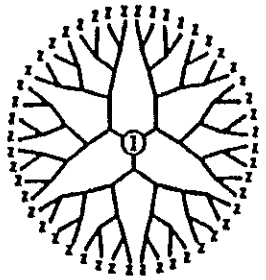 Regular Dendrons (Starburst®) Dendrimers
1930's -	1940's -	1960's -	1980's -

304

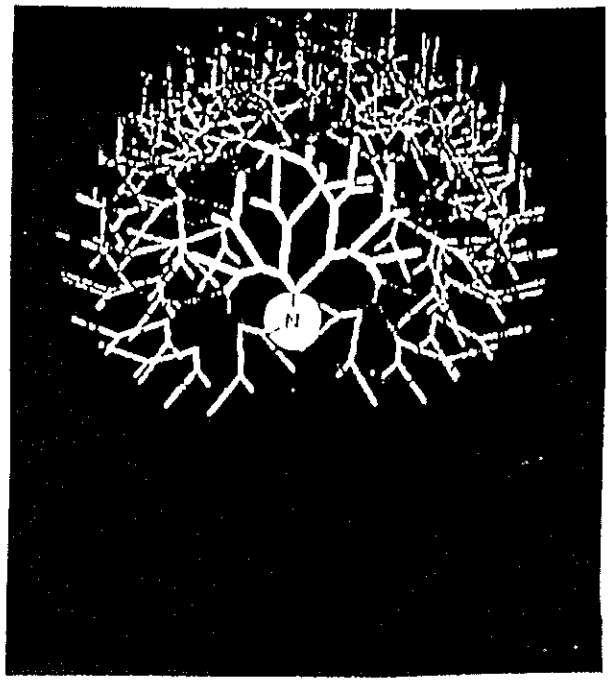

Figure 3a

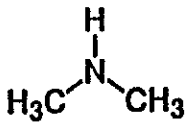

Core

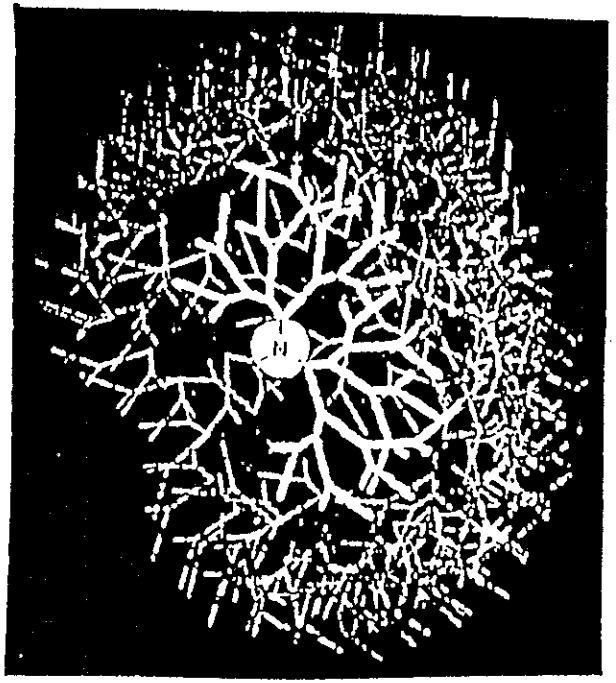

Figure 3b

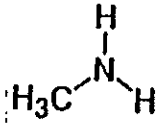

Core

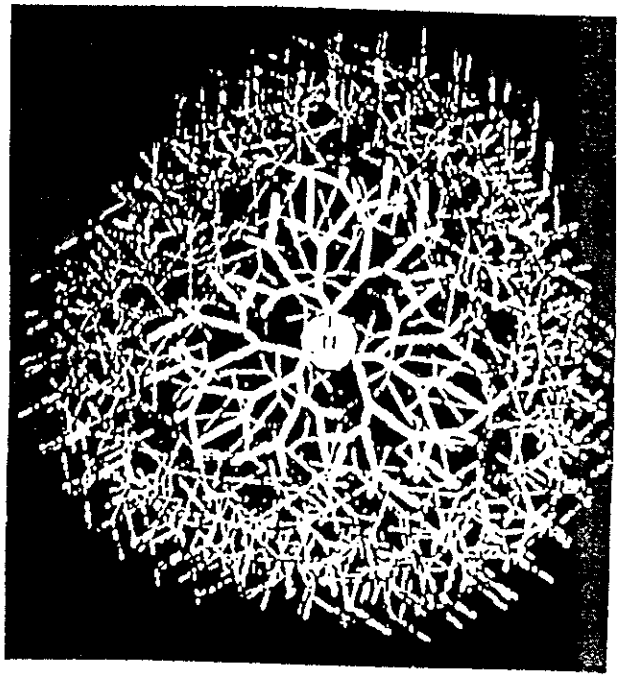

Figure 3c

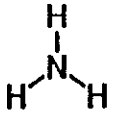

Core

305

306

Generation: 9.0 (PAMAM)

Surface: $NH_3^{\oplus}\,{}^{\ominus}CO_2$ - Polystyrene

Stain: RuO_4 (vapor); 40 min

Magnification: 150,000X (1mm ≡ 71A°)

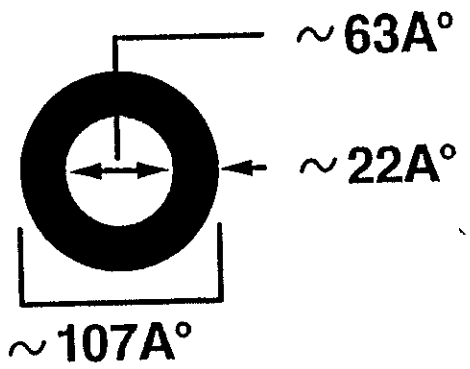

100nm

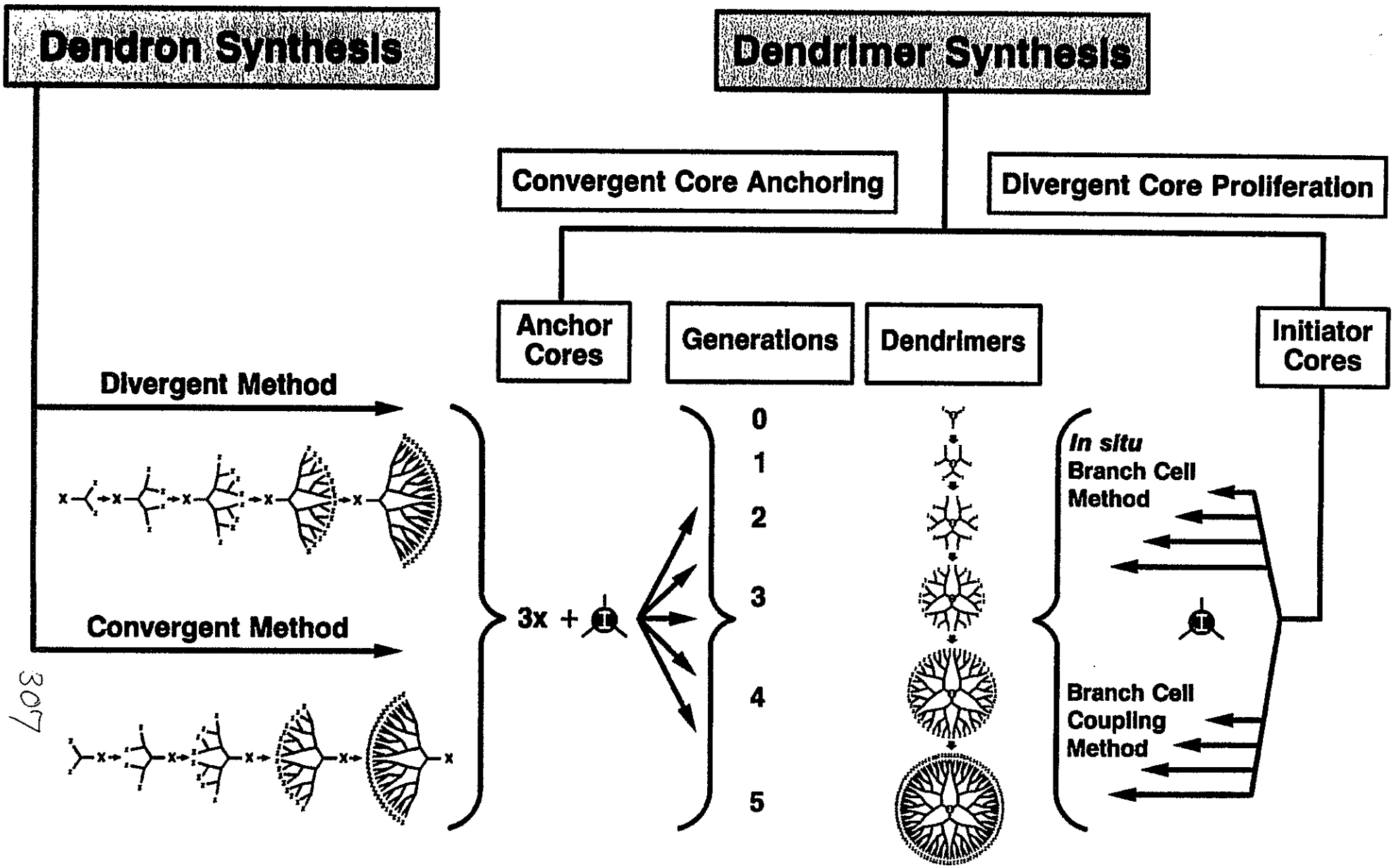
Dendron Synthesis
Dendrimer Synthesis
Convergent Core Anchoring
Divergent Core Proliferation
Anchor Cores
Generations
Dendrimers
Initiator Cores
Divergent Method
Convergent Method
3x +
0
1
2
3
4
5
In situ
Branch Cell
Method
Branch Cell
Coupling
Method

TIME SEQUENCED MONOMER SELF ORGANIZATION AROUND ⓘ TO GIVE A DENDRIMER; GEN. = 4.0, $N_c = 3$, $N_b = 2$

- DP = $\boxed{N_{RU}} = N_c \left[\frac{N_b^{G+1} - 1}{N_b - 1} \right]$
- • $\boxed{MW} = M_c + N_c \left[M_{RU} \left(\frac{N_b^{G+1} - 1}{N_b - 1} \right) + M_c N_b^{G+1} \right]$
- • • $\boxed{\text{Valency}}\ (Z) = N_c N_b^{G}$

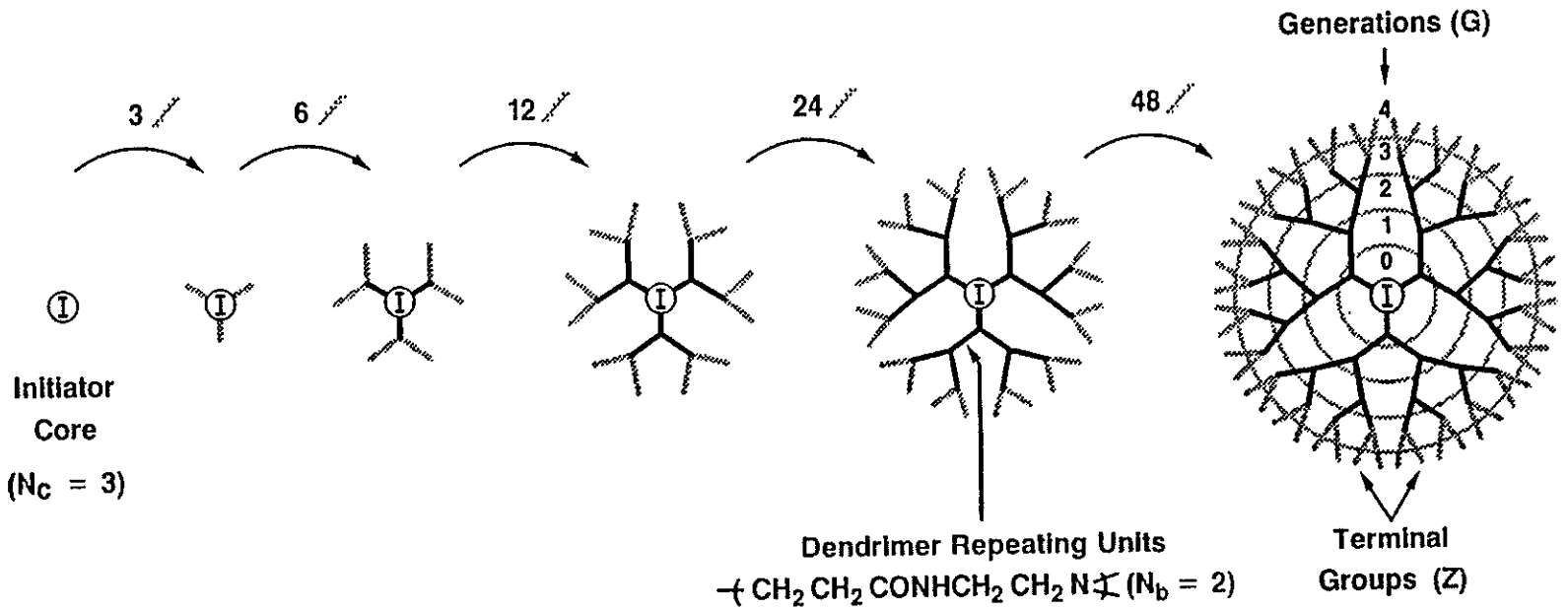

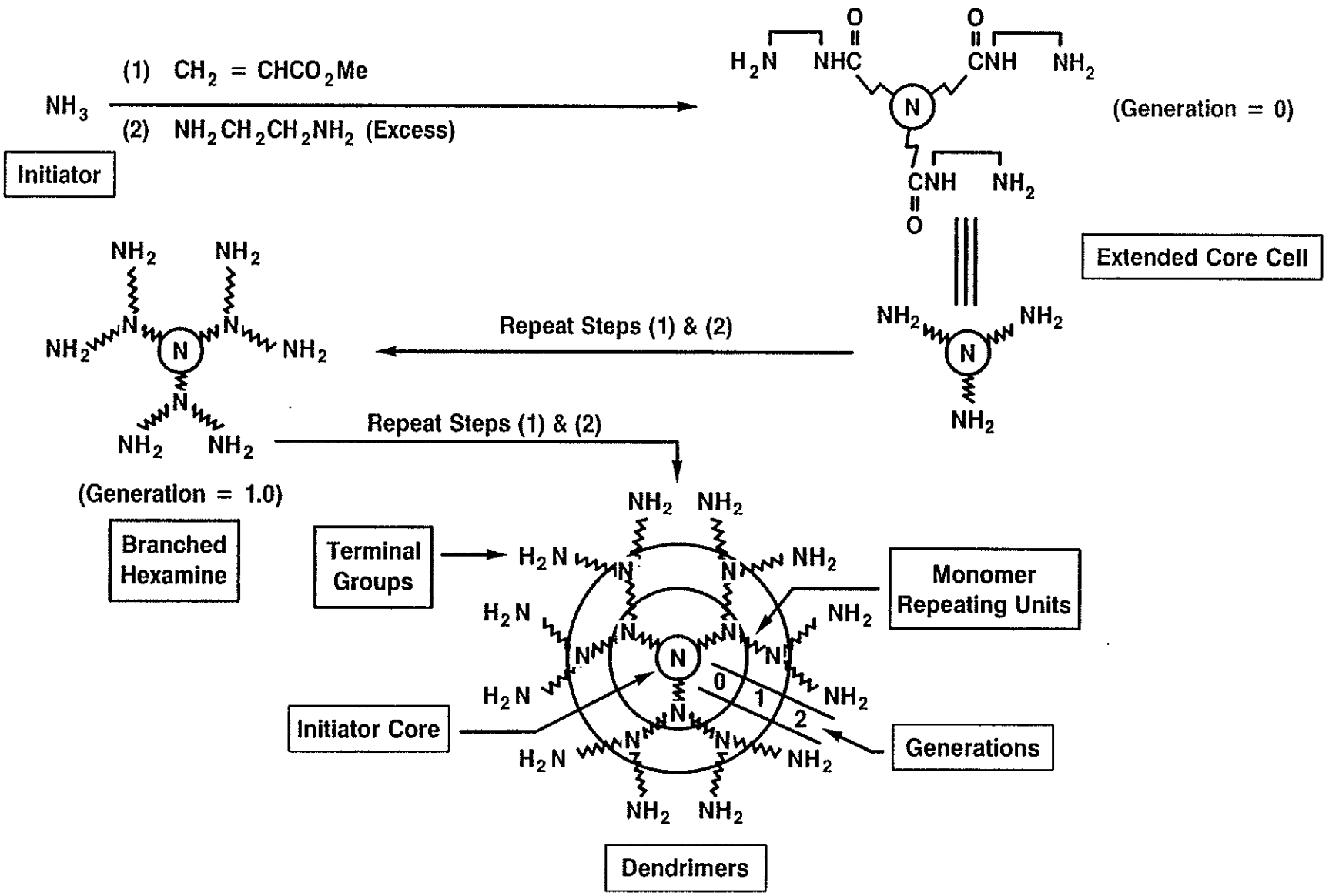
(1) $CH_2 = CHCO_2Me$
NH_3
(2) $NH_2CH_2CH_2NH_2$ (Excess)
Initiator
(Generation = 0)
Extended Core Cell
Repeat Steps (1) & (2)
Repeat Steps (1) & (2)
(Generation = 1.0)
Branched Hexamine
Terminal Groups
Monomer Repeating Units
Initiator Core
Generations
0
1
2
Dendrimers

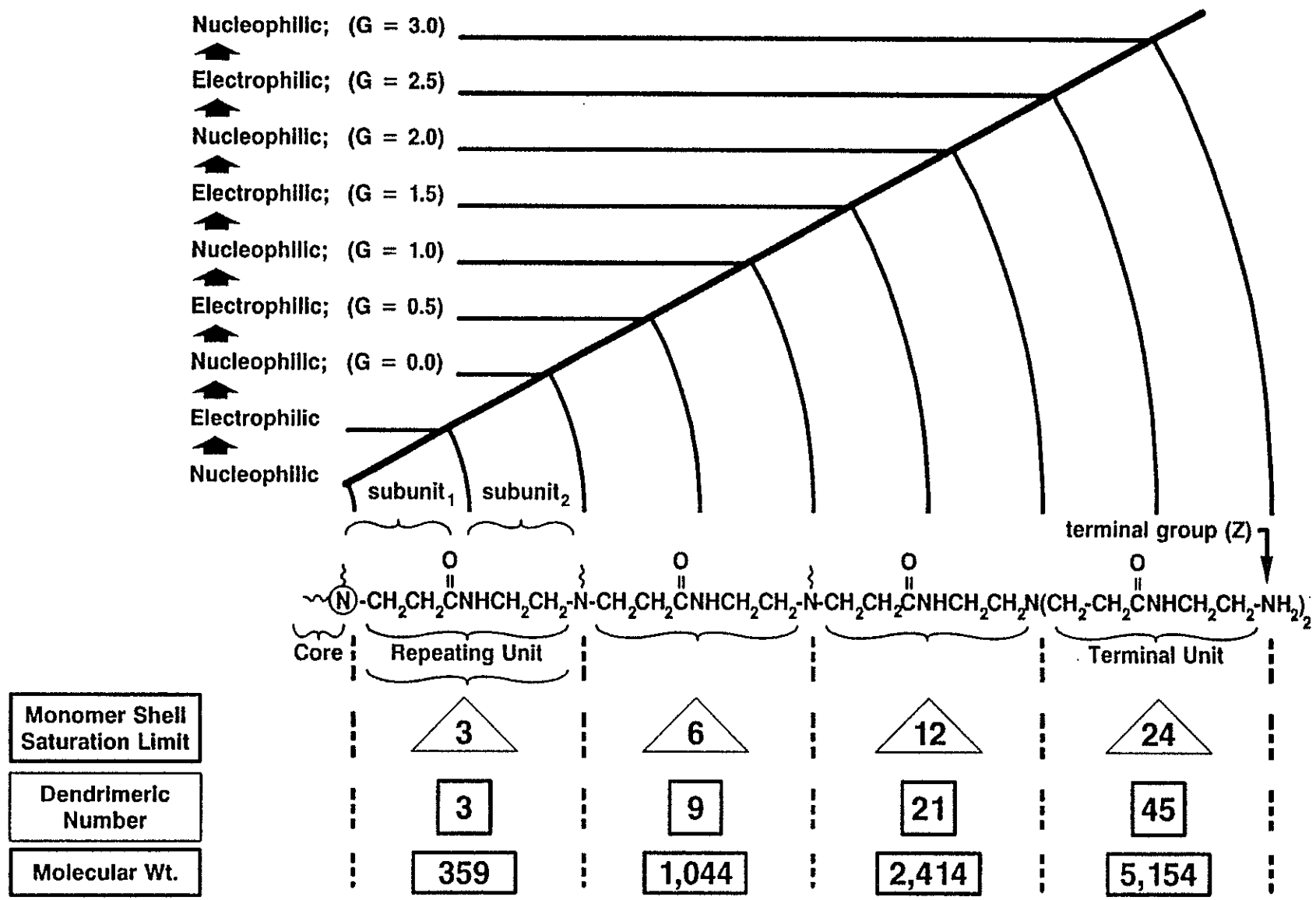
Nucleophilic; (G = 3.0)
Electrophilic; (G = 2.5)
Nucleophilic; (G = 2.0)
Electrophilic; (G = 1.5)
Nucleophilic; (G = 1.0)
Electrophilic; (G = 0.5)
Nucleophilic; (G = 0.0)
Electrophilic
Nucleophilic
subunit1
subunit2
terminal group (Z)
Core
Repeating Unit
Terminal Unit
Monomer Shell Saturation Limit
Dendrimeric Number
Molecular Wt.
3
6
12
24
3
9
21
45
359
1,044
2,414
5,154

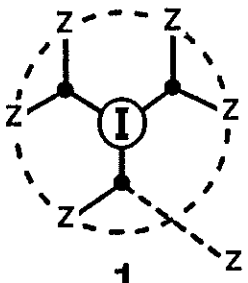

1

Branch Defective Dendrimer

MWt. - 114 amu

(ideal)

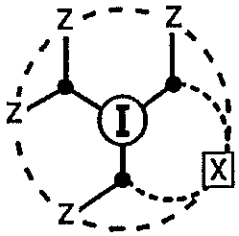

2

Intra **- Dendrimer Looped**

MWt. - 60 amu

(ideal)

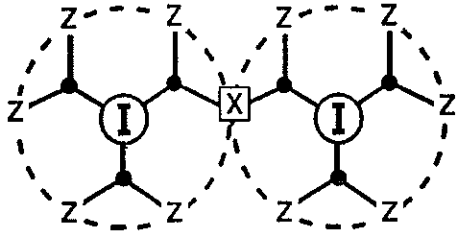

3

Inter **- Dendrimer Bridged**

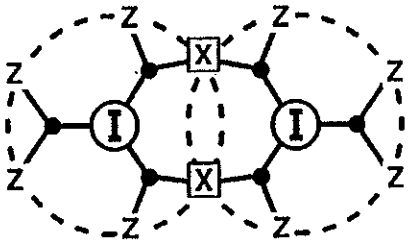

4

Inter **- Dendrimer Looped**

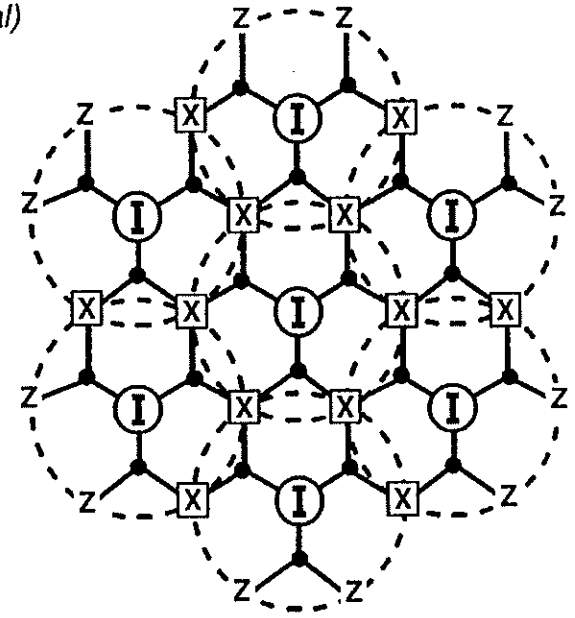

5

Dendrimer Cluster (Bridged / Looped)

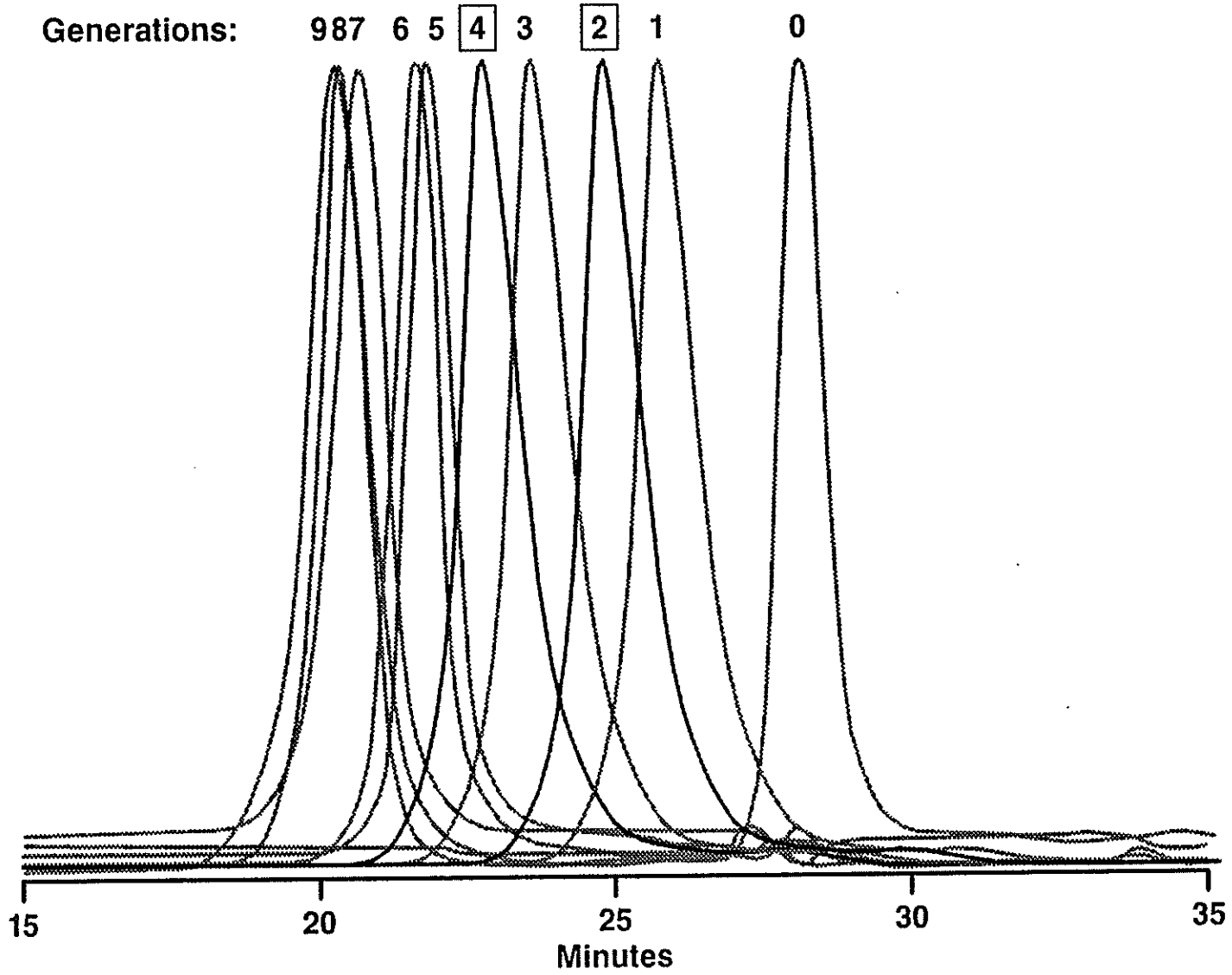
Generations:
9 8 7
6
5
4
3
2
1
0
15
20
25
30
35
Minutes

GEL ELECTROPHORESIS

Starburst (PAMAM) - Half Generations

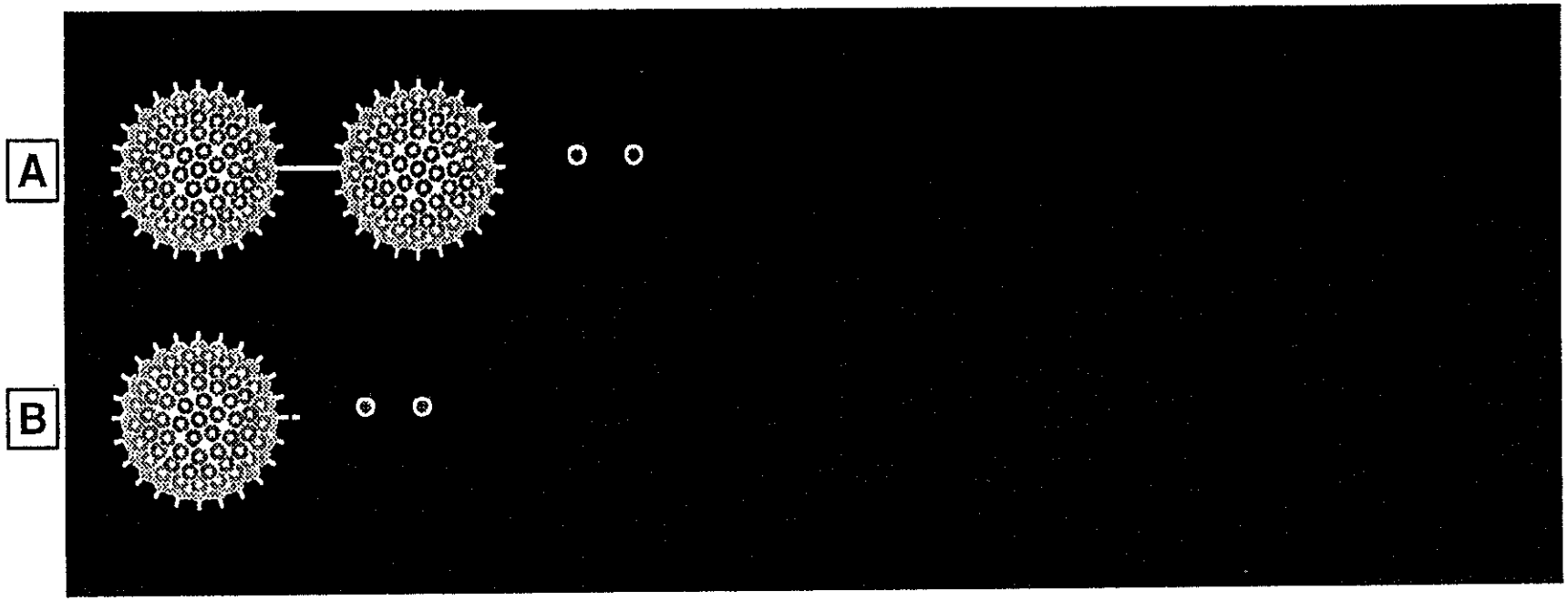

313

STARBURST™(PAMAM) - GENERATION = 2

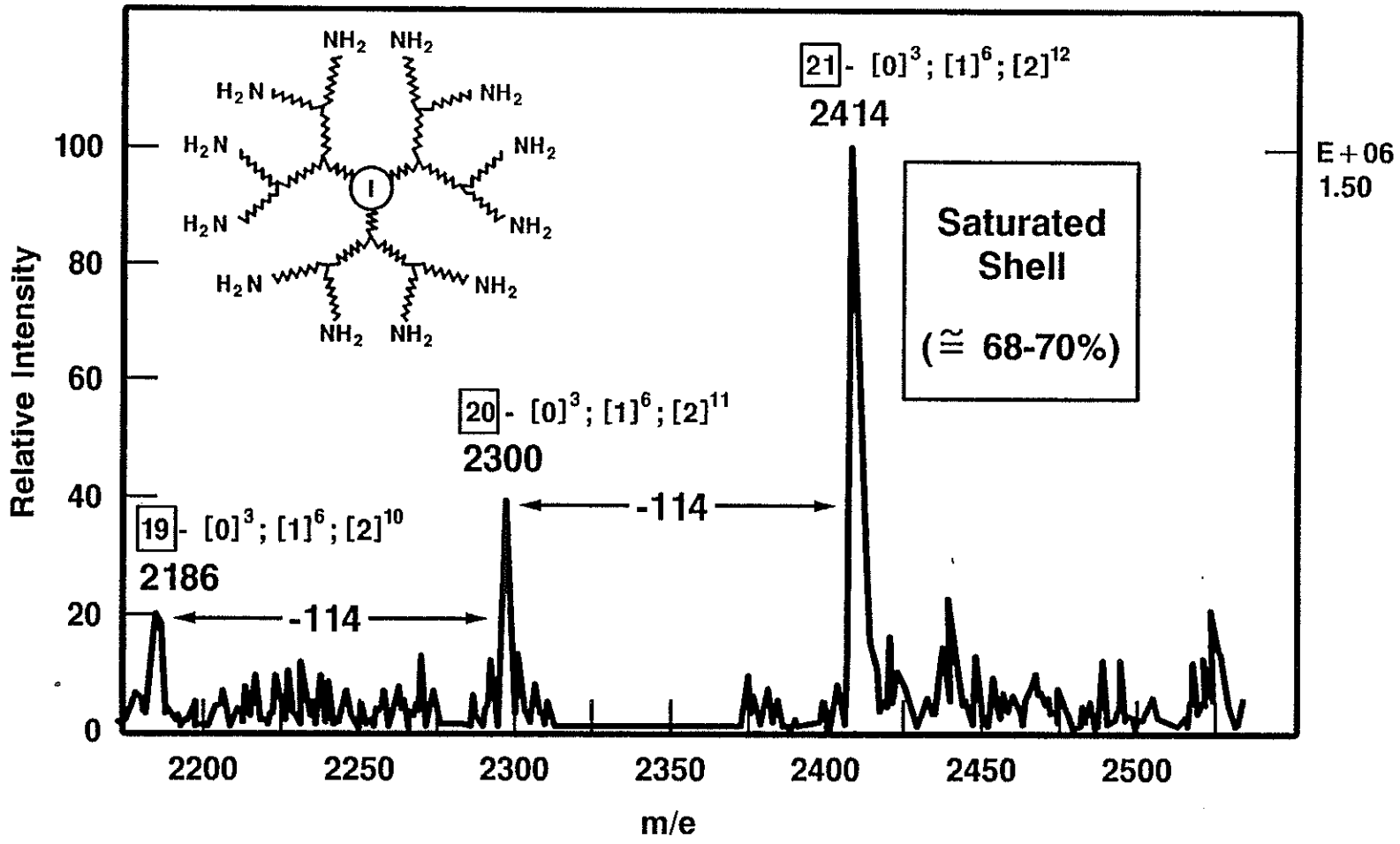

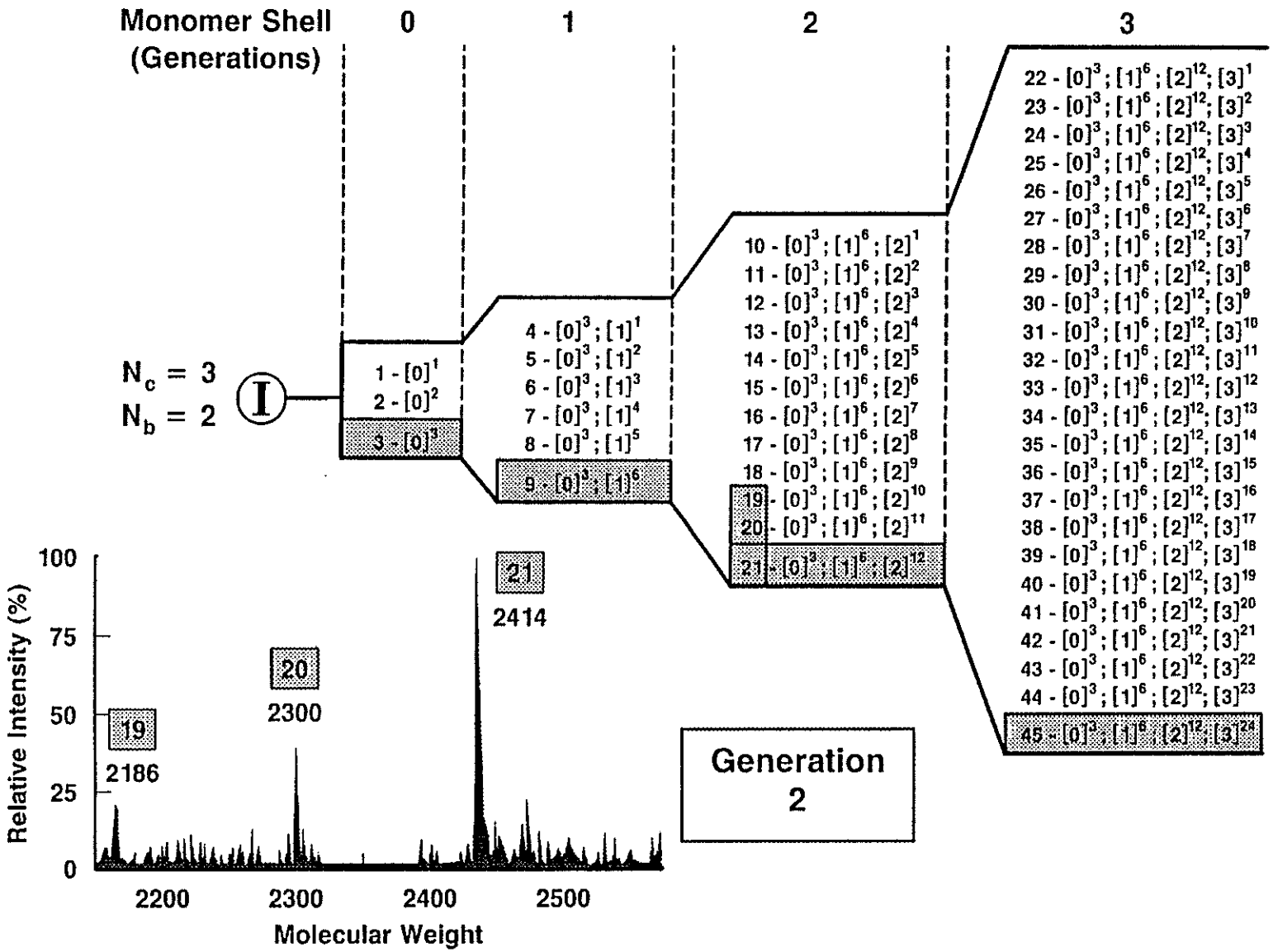
Monomer Shell (Generations)
0
1
2
3
$N_c = 3$
$N_b = 2$
I
1 - $[0]^1$
2 - $[0]^2$
3 - $[0]^3$
4 - $[0]^3$; $[1]^1$
5 - $[0]^3$; $[1]^2$
6 - $[0]^3$; $[1]^3$
7 - $[0]^3$; $[1]^4$
8 - $[0]^3$; $[1]^5$
9 - $[0]^3$; $[1]^6$
10 - $[0]^3$; $[1]^6$; $[2]^1$
11 - $[0]^3$; $[1]^6$; $[2]^2$
12 - $[0]^3$; $[1]^6$; $[2]^3$
13 - $[0]^3$; $[1]^6$; $[2]^4$
14 - $[0]^3$; $[1]^6$; $[2]^5$
15 - $[0]^3$; $[1]^6$; $[2]^6$
16 - $[0]^3$; $[1]^6$; $[2]^7$
17 - $[0]^3$; $[1]^6$; $[2]^8$
18 - $[0]^3$; $[1]^6$; $[2]^9$
19 - $[0]^3$; $[1]^6$; $[2]^{10}$
20 - $[0]^3$; $[1]^6$; $[2]^{11}$
21 - $[0]^3$; $[1]^6$; $[2]^{12}$
22 - $[0]^3$; $[1]^6$; $[2]^{12}$; $[3]^1$
23 - $[0]^3$; $[1]^6$; $[2]^{12}$; $[3]^2$
24 - $[0]^3$; $[1]^6$; $[2]^{12}$; $[3]^3$
25 - $[0]^3$; $[1]^6$; $[2]^{12}$; $[3]^4$
26 - $[0]^3$; $[1]^6$; $[2]^{12}$; $[3]^5$
27 - $[0]^3$; $[1]^6$; $[2]^{12}$; $[3]^6$
28 - $[0]^3$; $[1]^6$; $[2]^{12}$; $[3]^7$
29 - $[0]^3$; $[1]^6$; $[2]^{12}$; $[3]^8$
30 - $[0]^3$; $[1]^6$; $[2]^{12}$; $[3]^9$
31 - $[0]^3$; $[1]^6$; $[2]^{12}$; $[3]^{10}$
32 - $[0]^3$; $[1]^6$; $[2]^{12}$; $[3]^{11}$
33 - $[0]^3$; $[1]^6$; $[2]^{12}$; $[3]^{12}$
34 - $[0]^3$; $[1]^6$; $[2]^{12}$; $[3]^{13}$
35 - $[0]^3$; $[1]^6$; $[2]^{12}$; $[3]^{14}$
36 - $[0]^3$; $[1]^6$; $[2]^{12}$; $[3]^{15}$
37 - $[0]^3$; $[1]^6$; $[2]^{12}$; $[3]^{16}$
38 - $[0]^3$; $[1]^6$; $[2]^{12}$; $[3]^{17}$
39 - $[0]^3$; $[1]^6$; $[2]^{12}$; $[3]^{18}$
40 - $[0]^3$; $[1]^6$; $[2]^{12}$; $[3]^{19}$
41 - $[0]^3$; $[1]^6$; $[2]^{12}$; $[3]^{20}$
42 - $[0]^3$; $[1]^6$; $[2]^{12}$; $[3]^{21}$
43 - $[0]^3$; $[1]^6$; $[2]^{12}$; $[3]^{22}$
44 - $[0]^3$; $[1]^6$; $[2]^{12}$; $[3]^{23}$
45 - $[0]^3$; $[1]^6$; $[2]^{12}$; $[3]^{24}$
Relative Intensity (%)
100
75
50
25
0
19
2186
20
2300
21
2414
2200
2300
2400
2500
Molecular Weight
Generation 2

Starburst Poly(amidoamine) Dendrimers

	I	G=0 (Core)	G=1.0	G=2.0	G=3.0
M Wt.	17	359	1,043	2,411	5,147
D.P.	—	3	9	21	45
# of terminal groups (z)	—	3	6	12	24

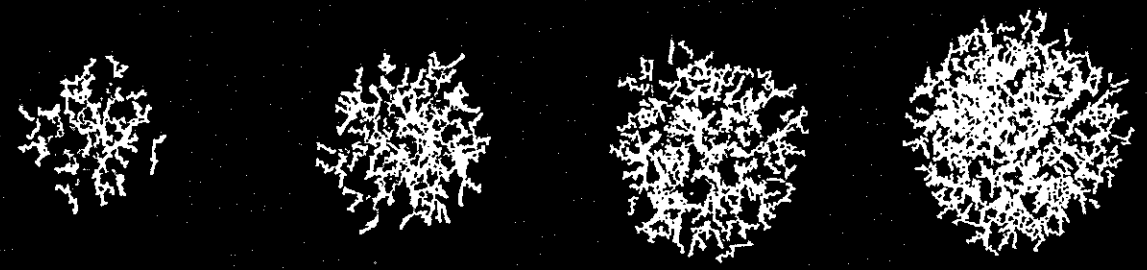

	G=4.0	G=5.0	G=6.0	G=7.0
M Wt.	10,619	21,583	43,451	87,2277
D.P.	93	189	381	765
# of terminal groups (z)	48	96	192	384

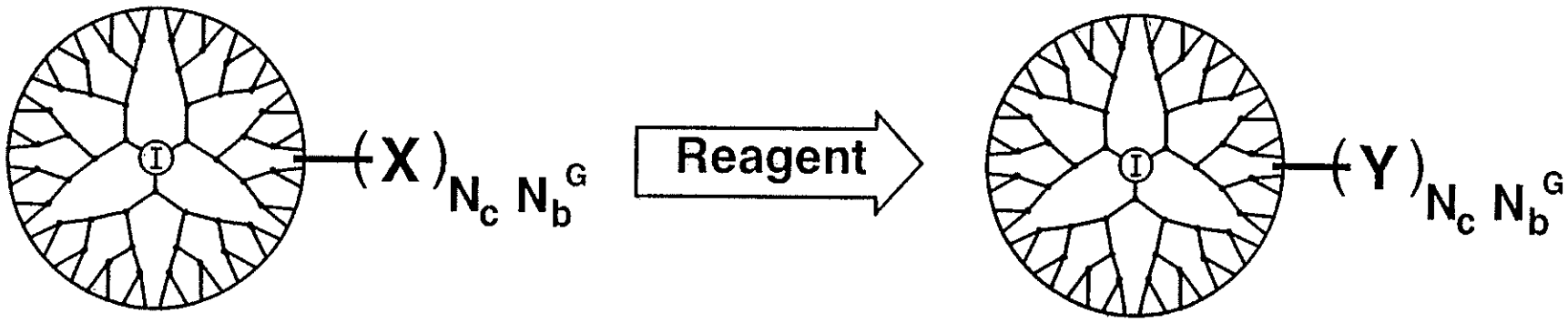
I
(X)
N_c N_b G
Reagent
I
(Y)
N_c N_b G

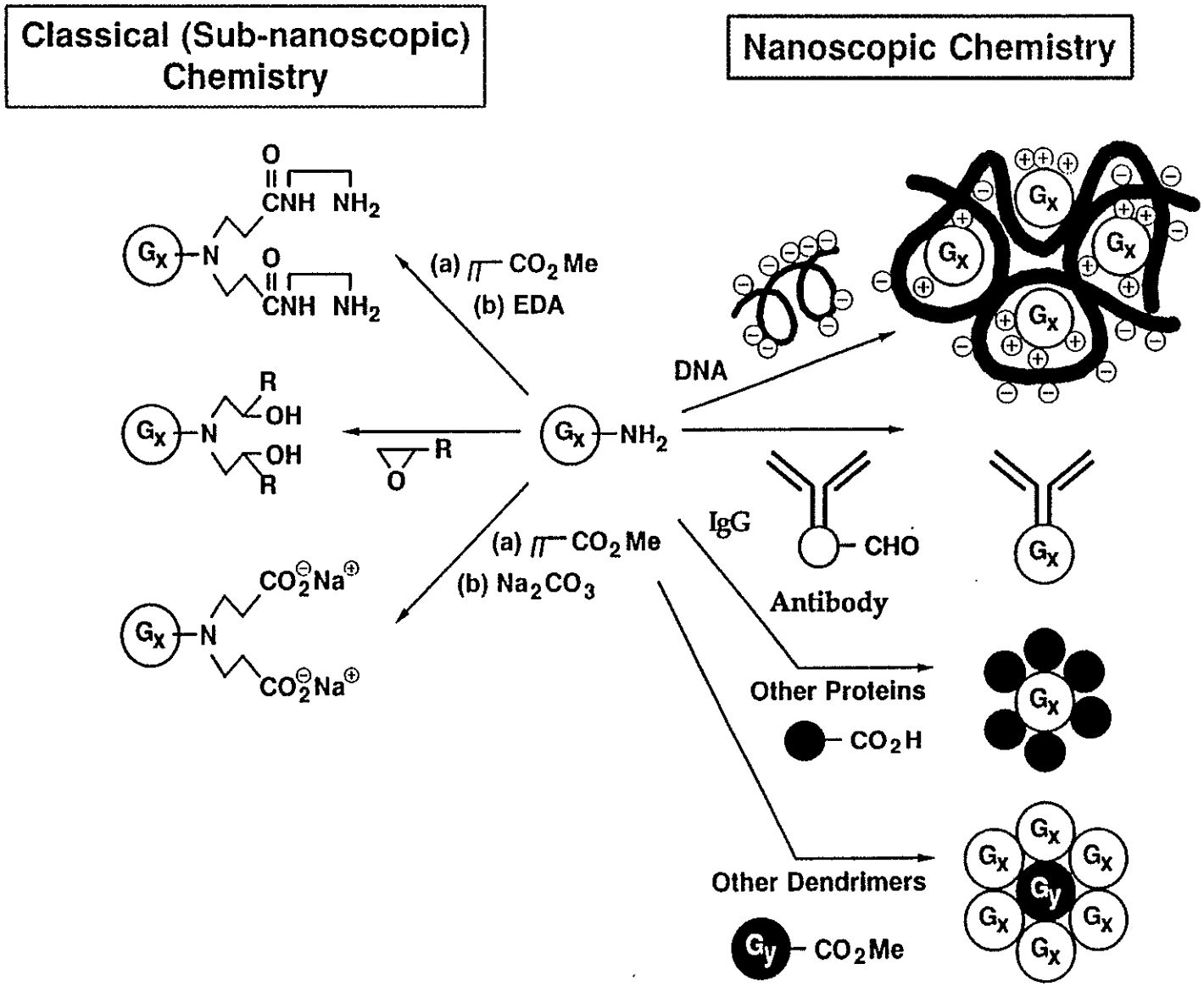
Classical (Sub-nanoscopic) Chemistry
Nanoscopic Chemistry
(a) CO2Me
(b) EDA
DNA
IgG
CHO
Antibody
(a) CO2Me
(b) Na2CO3
Other Proteins
CO2H
Other Dendrimers
CO2Me

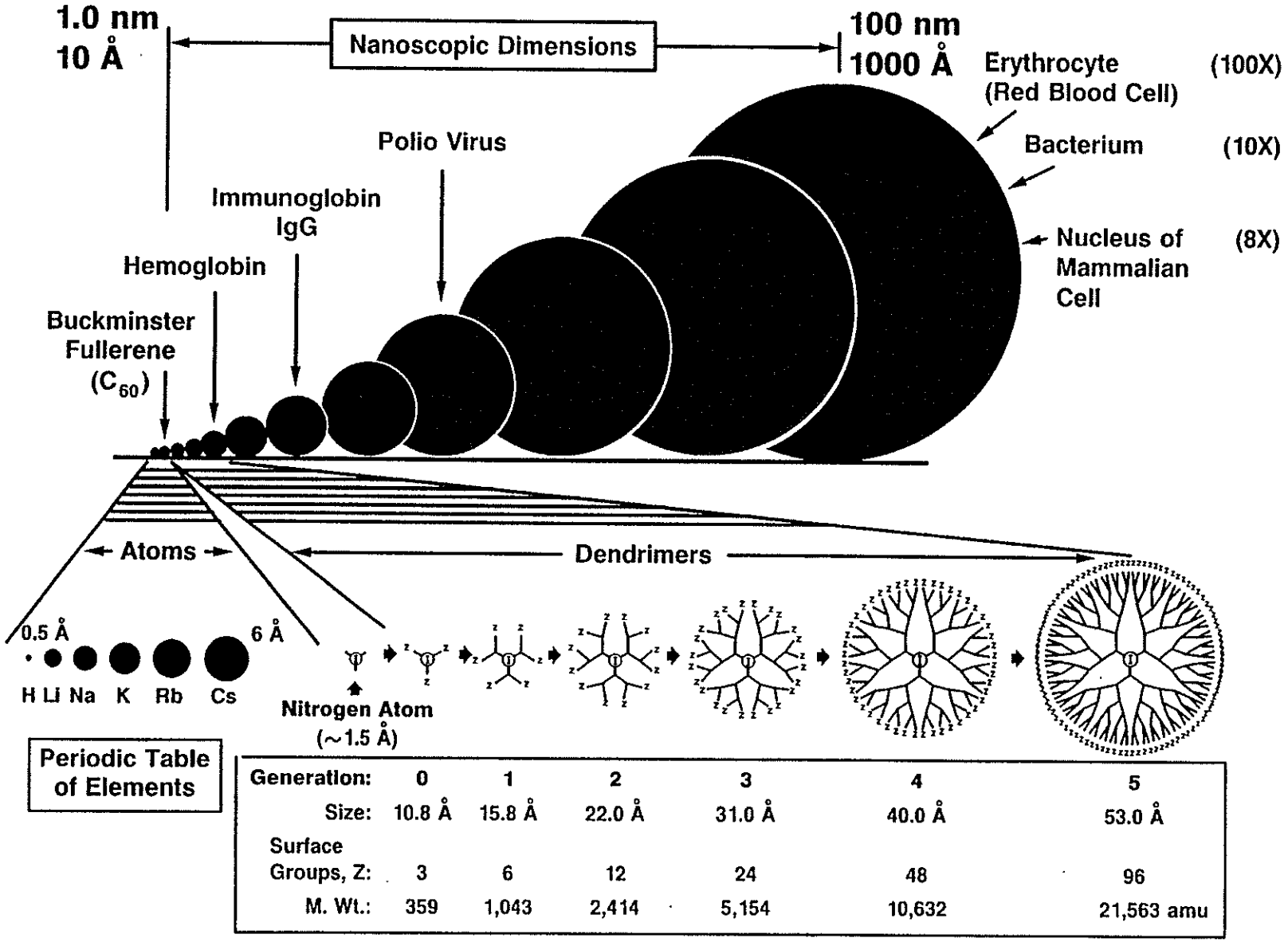

Generation:	0	1	2	3	4	5
Size:	10.8 Å	15.8 Å	22.0 Å	31.0 Å	40.0 Å	53.0 Å
Surface Groups, Z:	3	6	12	24	48	96
M. Wt.:	359	1,043	2,414	5,154	10,632	21,563 amu

The elements, their symbols and weights according to Dalton[6].

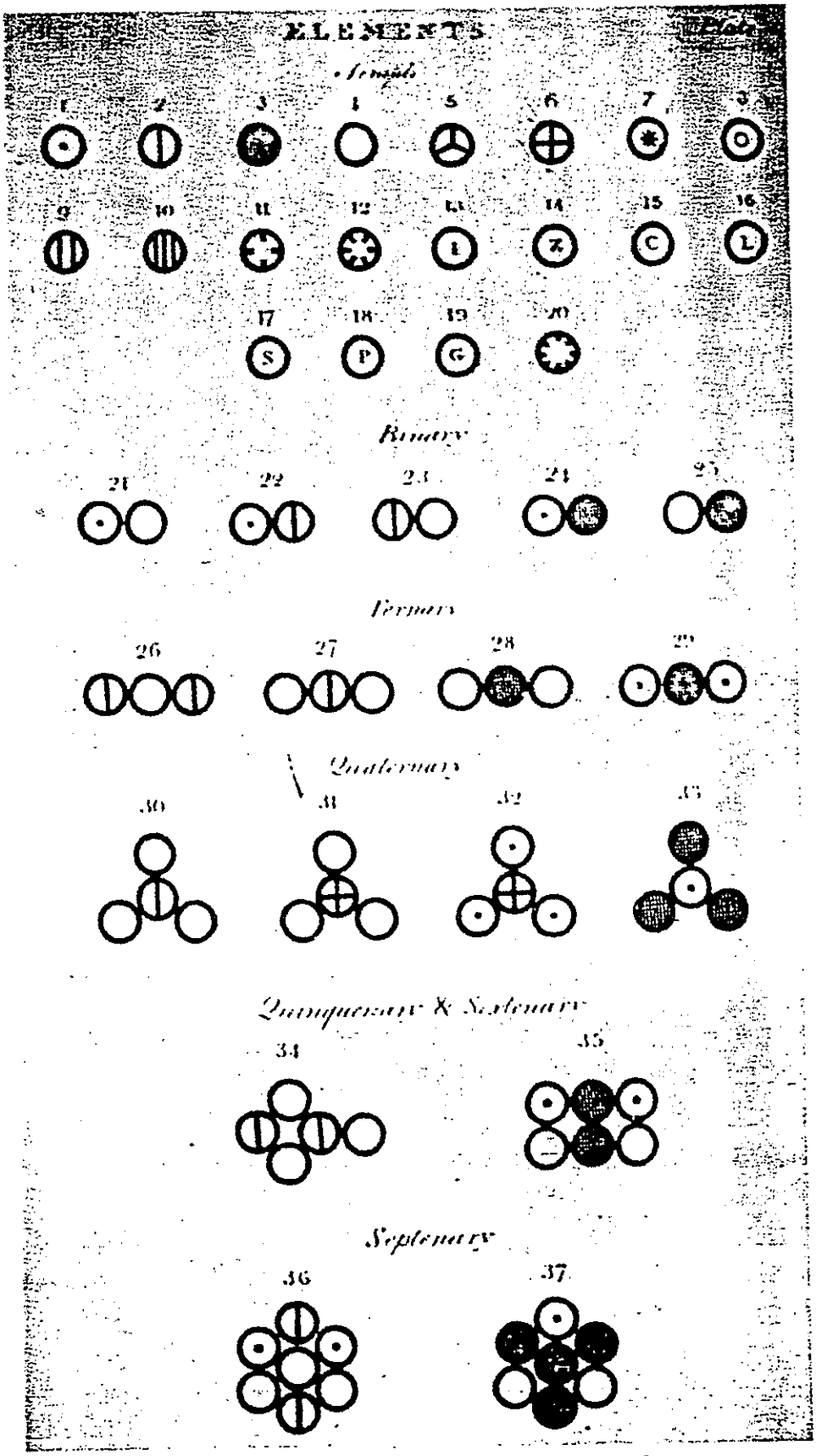

'Compound atoms', according to Dalton[6].

Atom Based (Classical) Chemistry

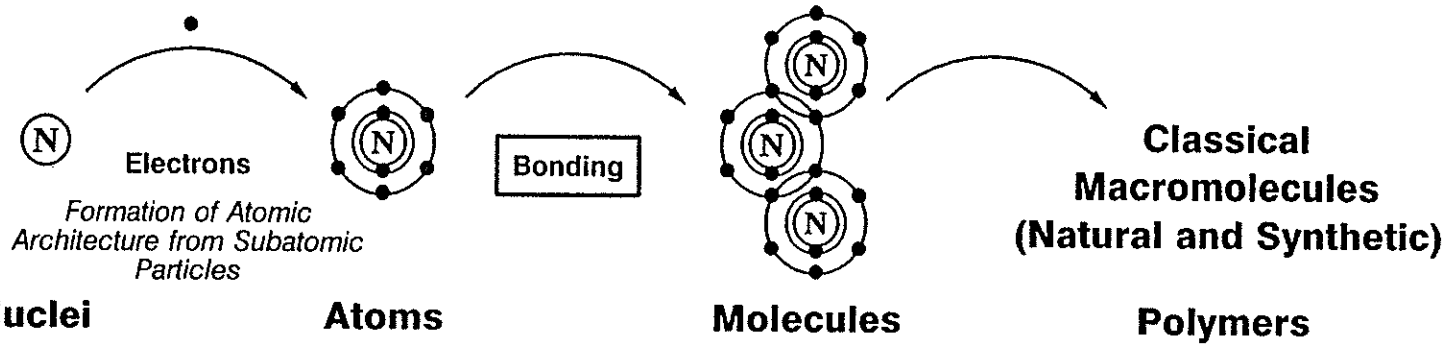

Dendrimer Based (Nanoscopic) Chemistry

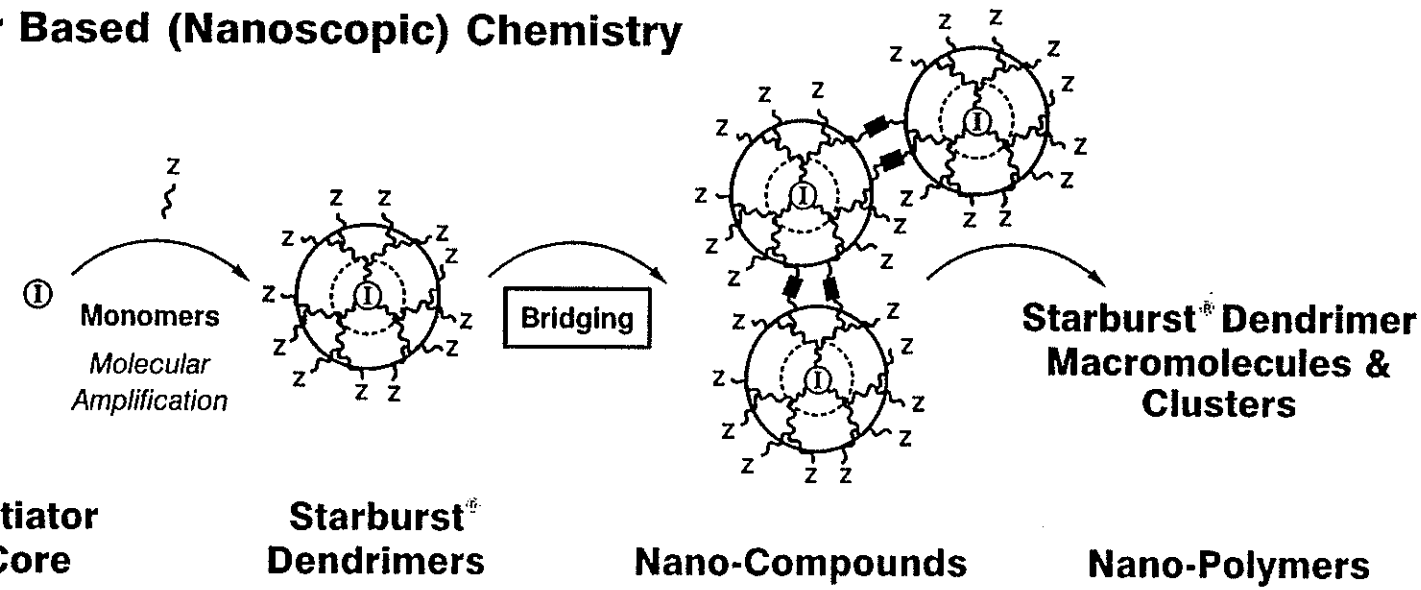

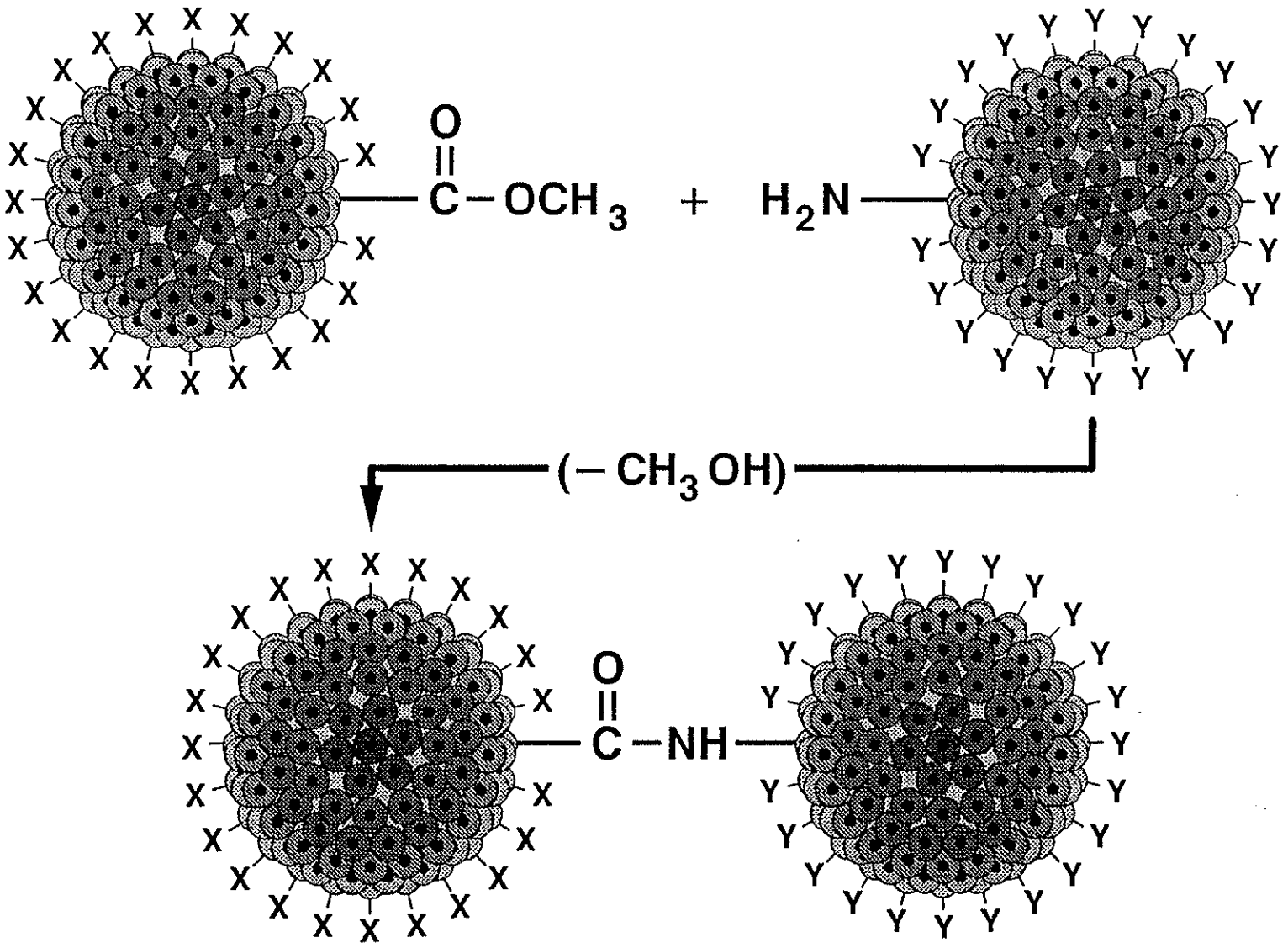
X
Y
O
C – OCH3
+
H2N
(– CH3 OH)
C – NH

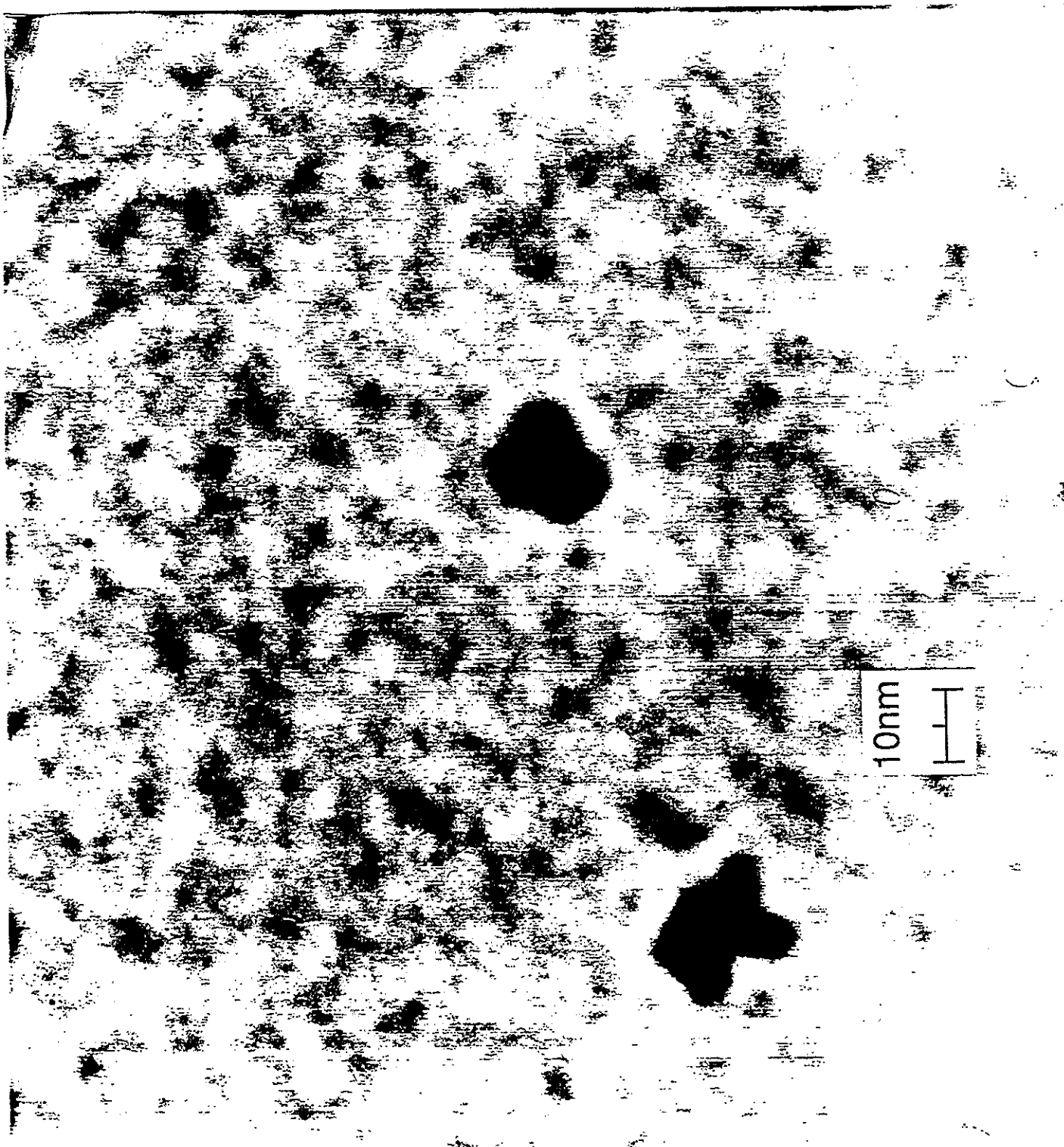
10nm

STARBURST POLYMERS
(Bridged Dendrimers)

(Core EDA; Gen. = 4.5; Z = CO_2Me)

and

(Core EDA; Gen. = 5.0; Z = $-NH_2$)

480,000X

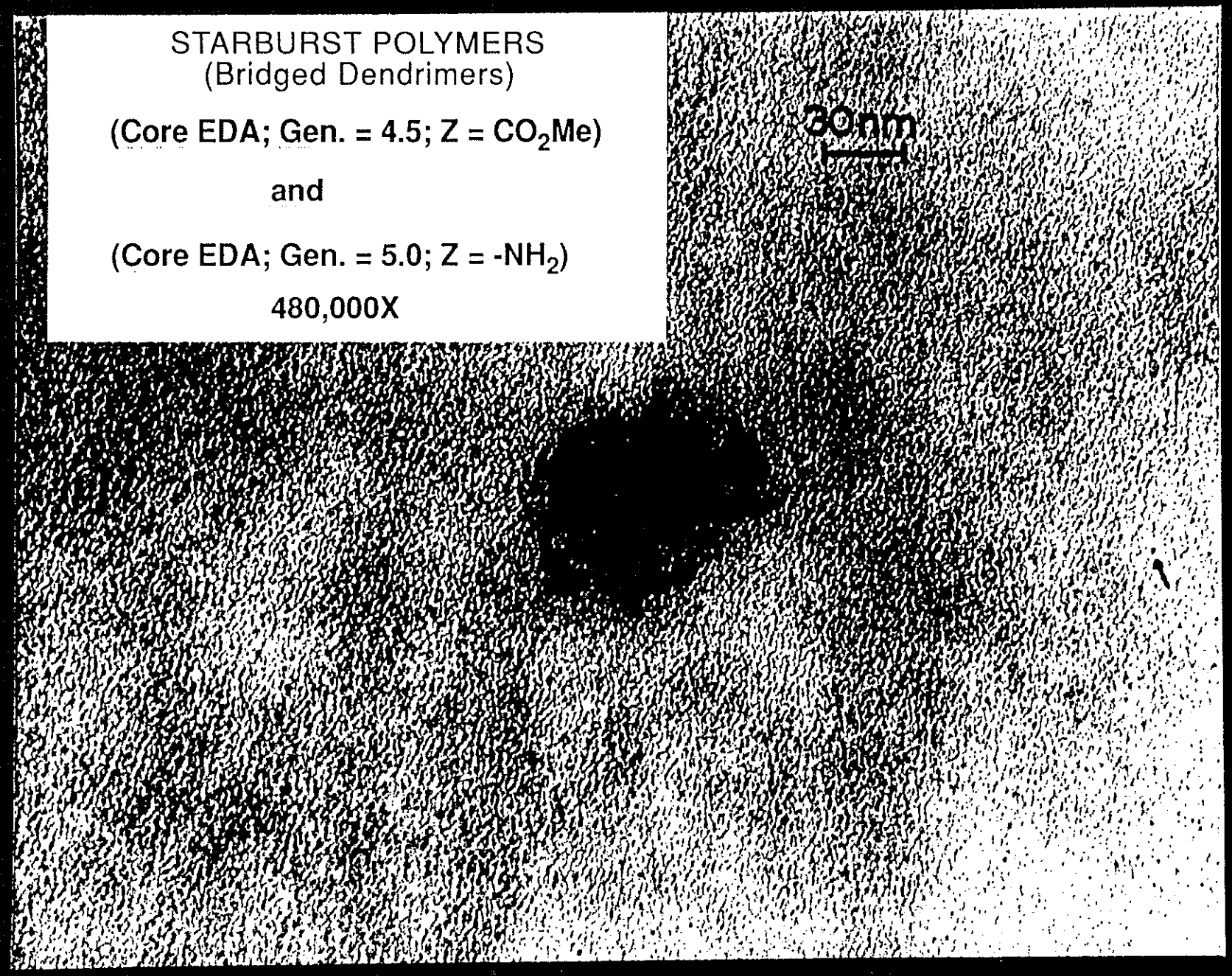

d379.043 *tomalia/9-94*

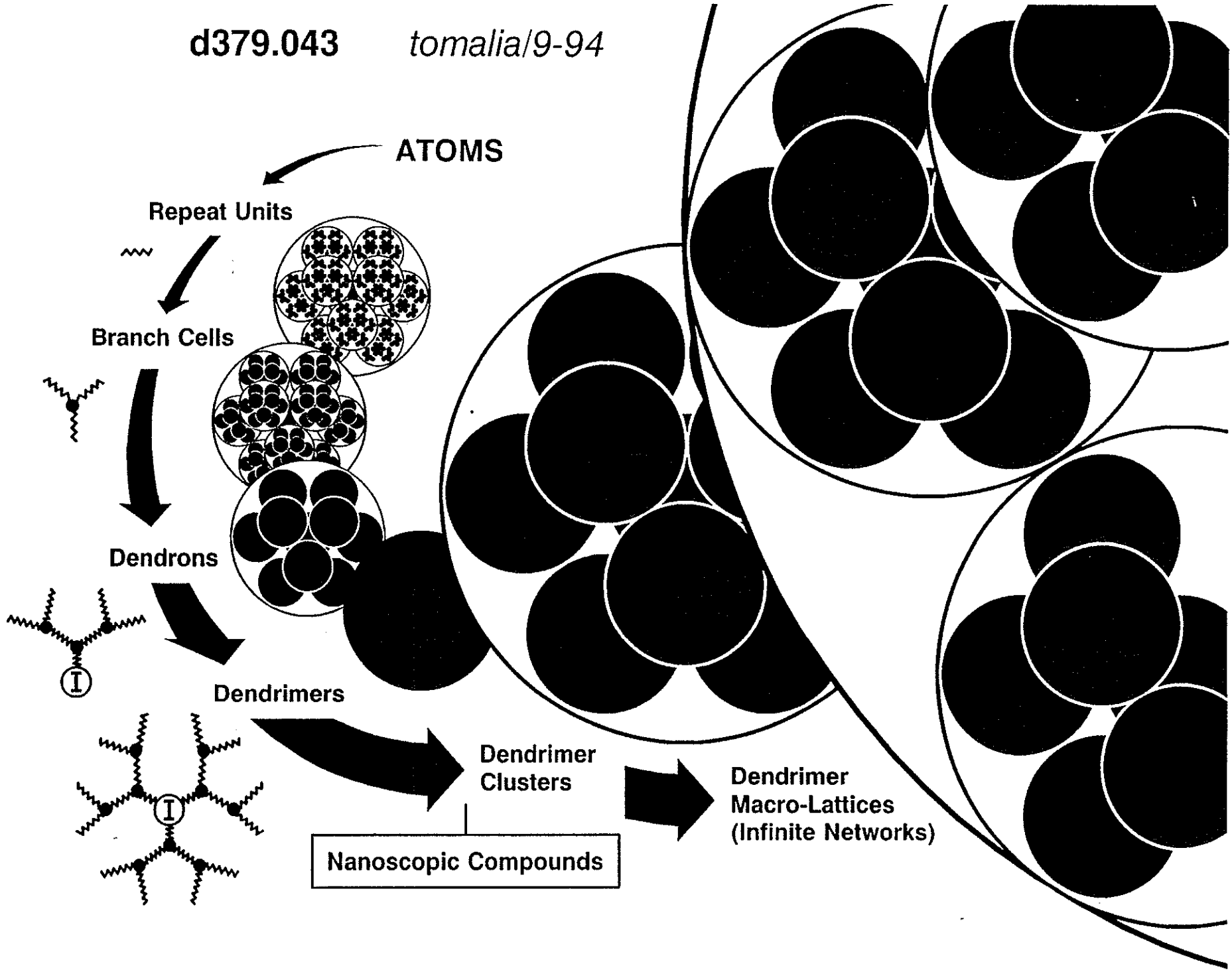

ACKNOWLEDGEMENTS

Nanoscopic Chemistry/Architecture Group

Alicia Asadorian
David Hedstrand
June Klimash
Christoph Rickert
Stephan Sprenger
Ray Yin

Herb Brothers II
Peter Houck
Bart Maxon
Yasmin Sayed-Sweet
Douglas Swanson
Luyin Zhao

Masaaki Fujiwara
Anne Jurek
Linda Nixon
Ralph Spindler
Srinivas Uppuluri

Prof. Harold Blecker (University of Michigan)
Prof. Harold Heine (Bucknell University)
Prof. Harold Hart (Michigan State University)

Technology

STARBURST* dendrimer technology includes all chemical compositions that fall within the STARBURST dendrimer architecture. While polyamidoamine (PAMAM) compositions currently under development are the most widely investigated systems, there are many other demonstrated examples. Polyethyleneimines, polyethers, polyphosphoniums, polysiloxanes, polyamides and polyaryls are among those identified. Copolymeric dendrimers possessing stratified infrastructures have also been demonstrated.

This variety of compositions gives, in addition to the precise size and topology implied by the STARBURST dendrimer architecture, a wide range of stability and reactivity that allows the choice of the most appropriate chemistry for a given application. Thus, very inert systems may be designed for long lifetime materials. Conversely, thermal, photo, or biodegradability may be built into the dendrimers for short term applications. Inquiries for custom materials to fit specific applications are encouraged.

Process

Kilogram quantities of PAMAM *STARBURST* dendrimers are now being produced. A production facility with thousands of pounds per year is in the planning and engineering stages, due on stream in mid-'94.

Patents

The STARBURST dendrimer technology is covered by over twenty U.S. and foreign patents that include the basic compositions and several application areas. Other patents are in prosecution. Licensing and partnership opportunities are available for those who wish to become a part of this emerging field of technology. Please address inquiries, on company letterhead, to:

DENDRITECH INC.

A Subsidiary of Michigan Molecular Institute

3110 SCHUETTE DRIVE • MIDLAND, MICHIGAN 48642
PHONE: (517) 496-2016 • FAX: (517) 496-2051

DENDRITECH

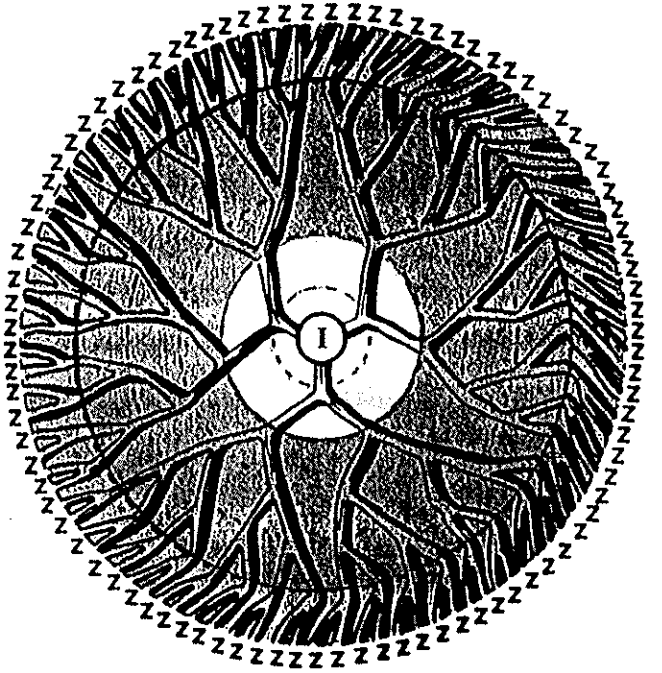

STARBURST

DENDRIMERS

A NEW SYNTHESIS OF POLYMERIC KETONES

Harry W. Gibson

Department of Chemistry

Virginia Polytechnic Institute & State University

Blacksburg, VA 24061

703-231-5902

POLY(ARYLENE ETHER KETONE)S

* A CLASS OF HIGH PERFORMANCE ENGINEERING THERMOPLASTICS:
  - CRYSTALLINITY DUE TO CARBONYL MOIETY;
  - EXCELLENT THERMAL STABILITY & CHEMICAL RESISTIVITY;
  - GOOD MECHANICAL PROPERTIES, ETC.

ELECTROPHILIC ROUTE (FRIEDEL-CRAFTS)

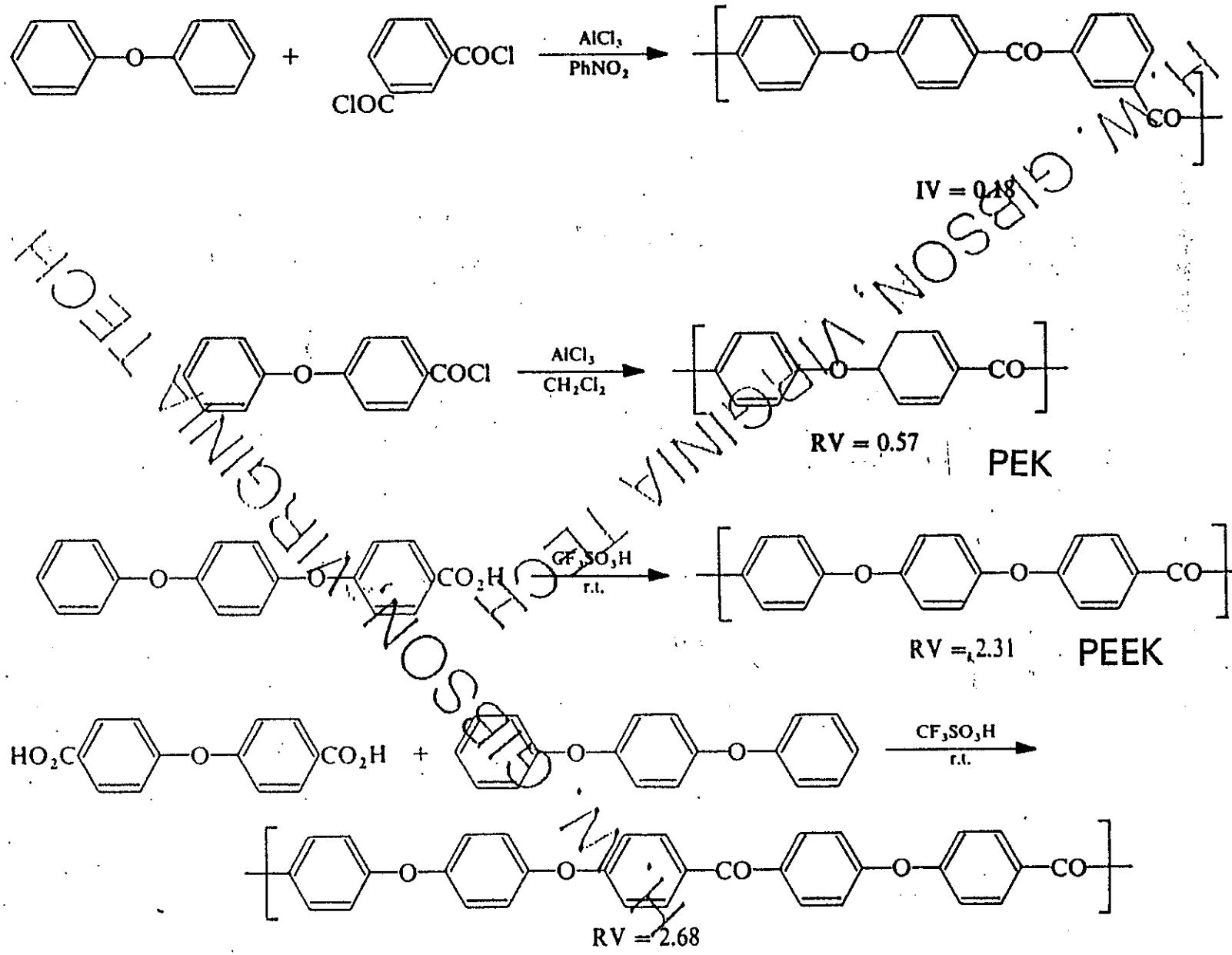

ELECTROPHILIC ROUTE (FRIEDEL-CRAFTS)

PROBLEMS:

1. INSOLUBILITY OF PRODUCTS REQUIRES USE OF LARGE AMOUNTS OF LEWIS ACID CATALYSTS TO ACHIEVE SOLUBILIZATION AND HIGH MW

2. LARGE AMOUNTS OF CATALYSTS FOR DISPOSAL

3. LIMITED NUMBER OF POLYKETONES CAN BE MADE

NUCLEOPHILIC ROUTE (ETHERS OR THIOETHERS)

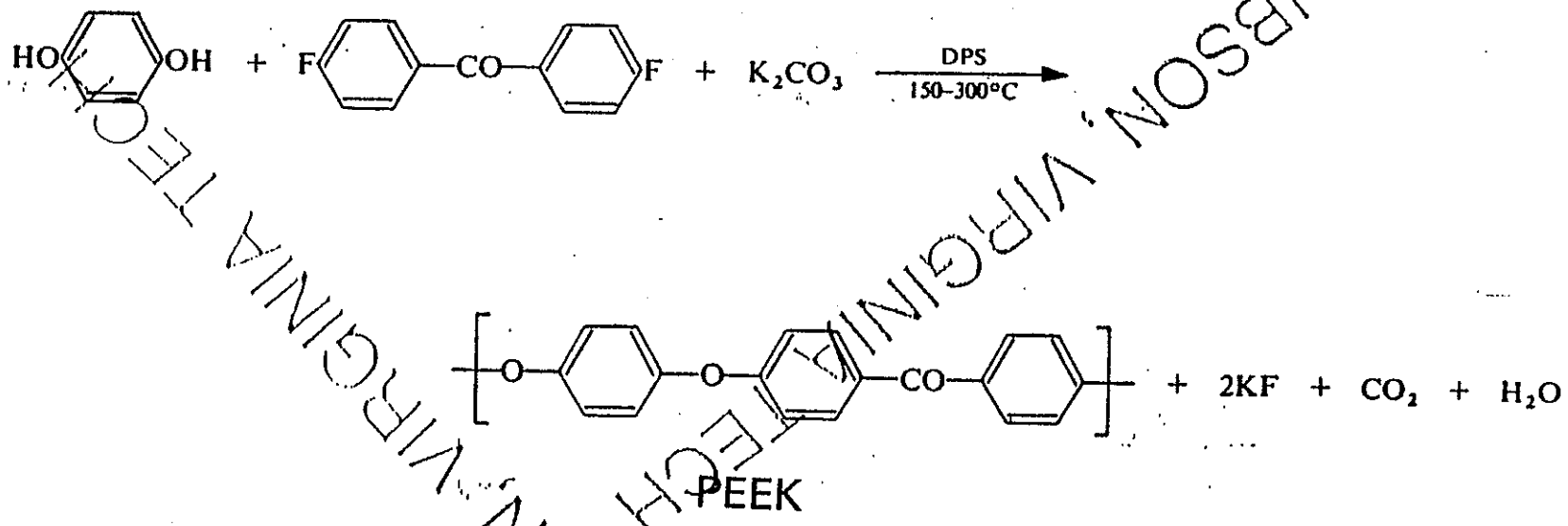

PEEK

NUCLEOPHILIC ROUTE (ETHERS OR THIOETHERS)

PROBLEMS:

1. CRYSTALLINITY OF PRODUCT REQUIRES USE OF HIGH TEMPERATURES IN SYNTHESIS

2. CRYSTALLINITY & HIGH T_M MAKE PROCESSING DIFFICULT

3. CANNOT SYNTHESIZE POLYKETONES WITHOUT ETHER LINKAGES

ALTERNATIVE NUCLEOPHILIC APPROACHES (contd)

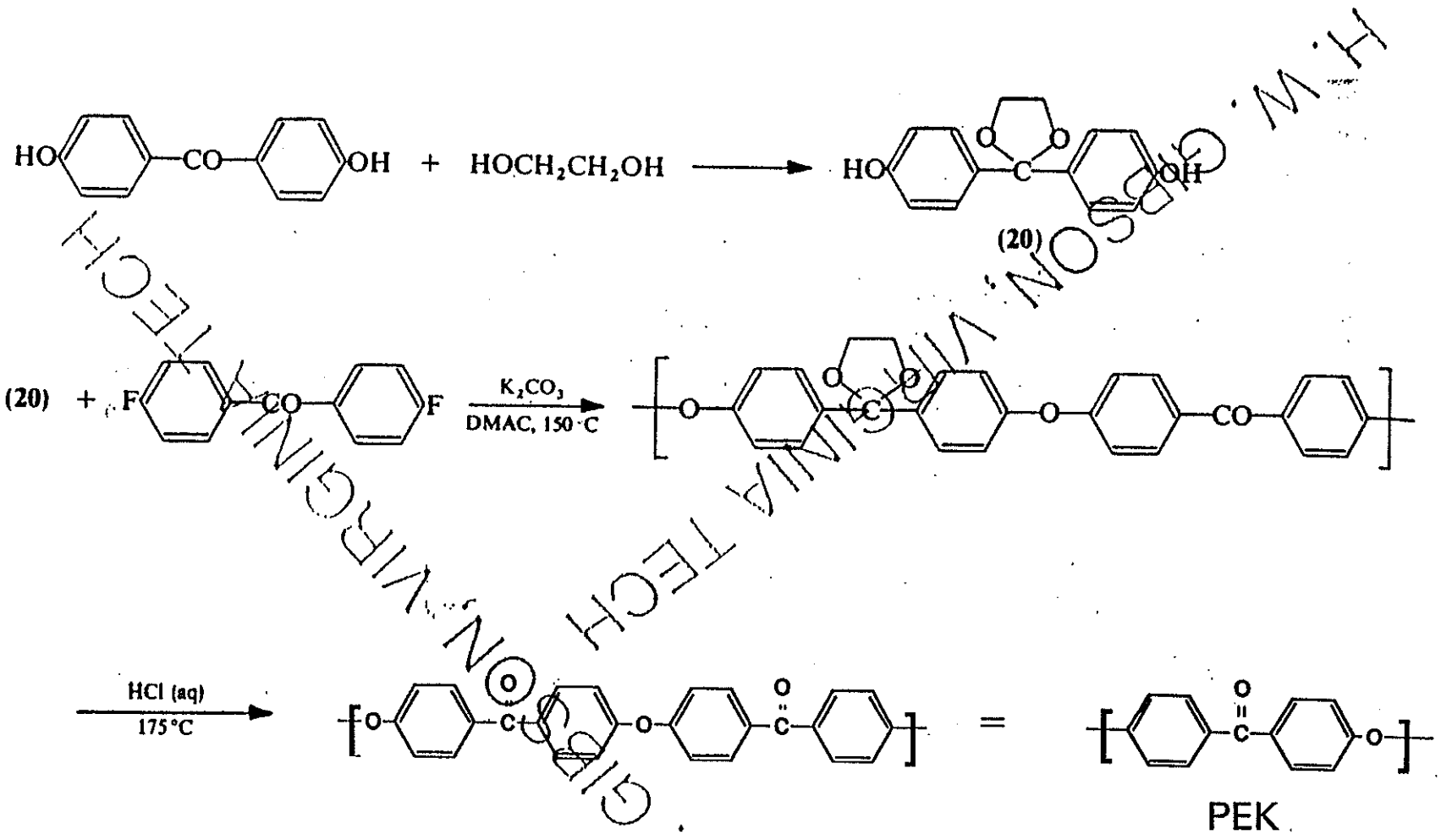

D. R. Kelsey, L. M. Robeson, R. A. Clendinning & C. S. Blackwell, Macromolecules, **1987**, 20, 1204.

ALTERNATIVE NUCLEOPHILIC APPROACHES (contd)

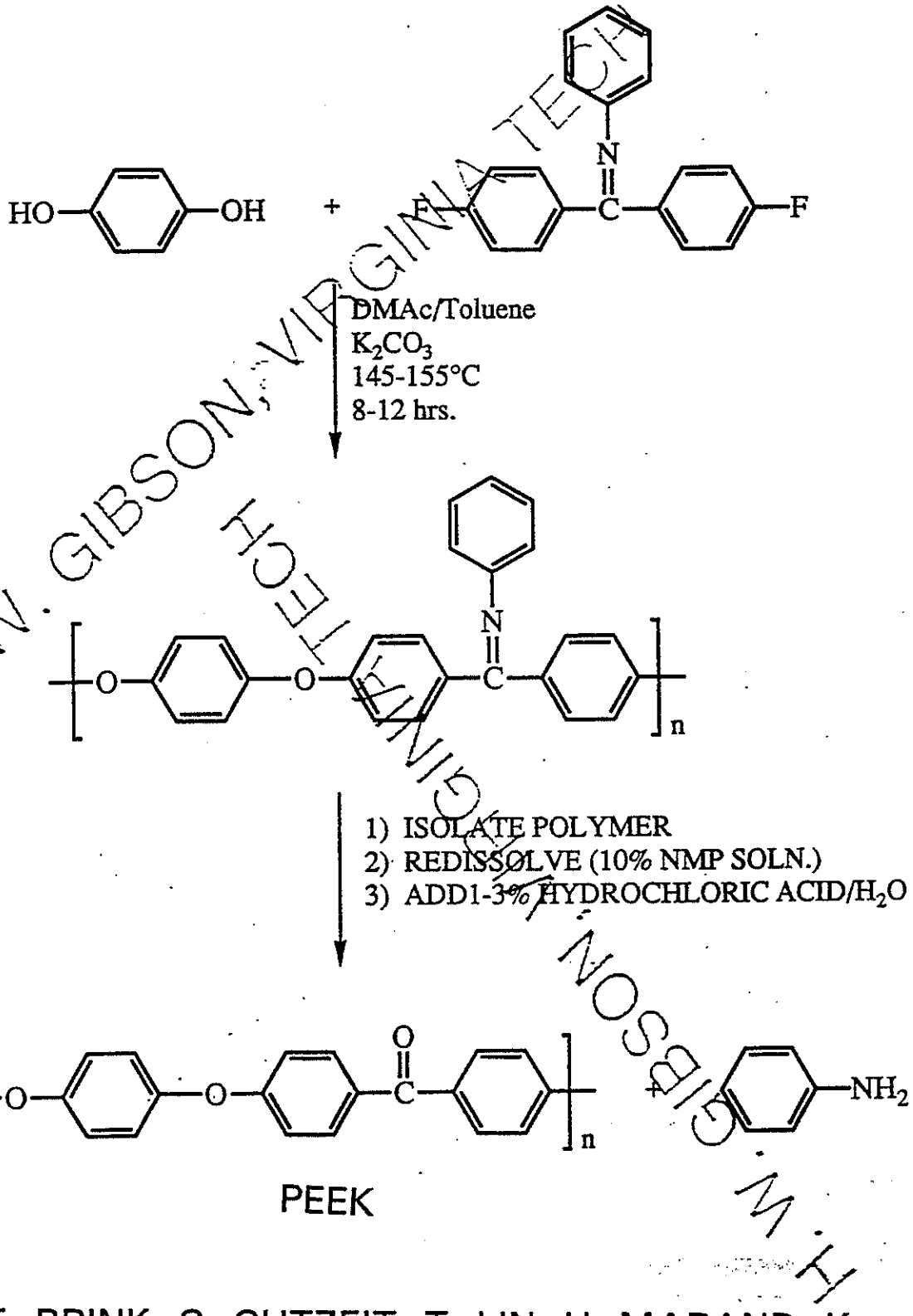

PEEK

A. E. BRINK, S. GUTZEIT, T. LIN, H. MARAND, K. LYON, J. E. MCGRATH & J. S. RIFFLE, POLYM. PREPRINTS, **1992**, 33 (1), 402.

ALTERNATIVE NUCLEOPHILIC APPROACHES (contd)

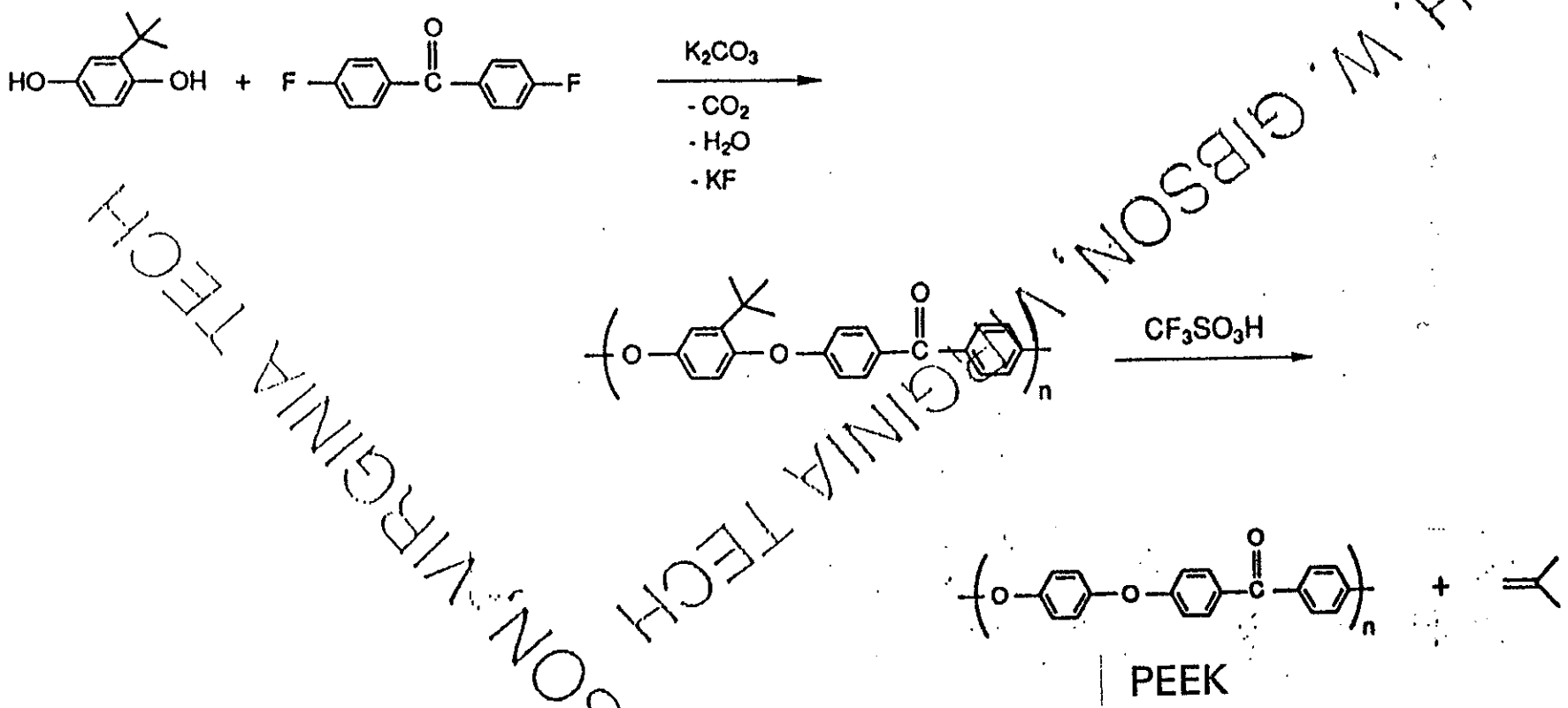

W. Risse & D. Y. Sogah, Macromolecules, **1990**, 23, 4029.

LITERATURE PRECEDENT: MONOFUNCTIONAL AMINONITRILES

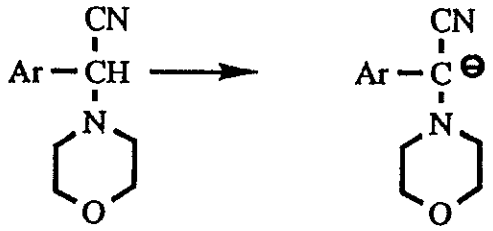

REACTIONS OF AMINONITRILE ANIONS WITH ACTIVATED AROMATICS

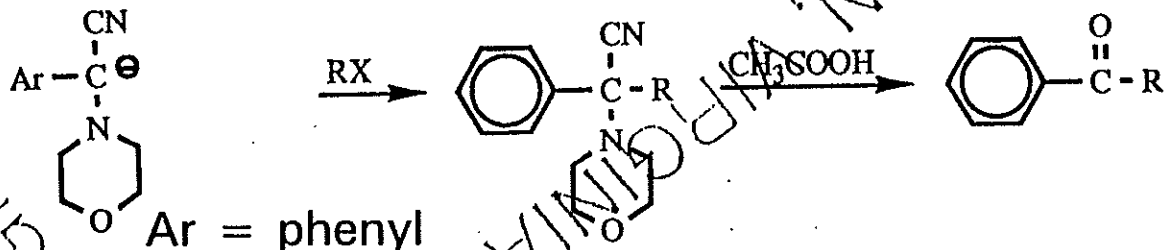

Ar = phenyl

REACTIONS OF AMINONITRILE ANIONS WITH ALKYL HALIDES

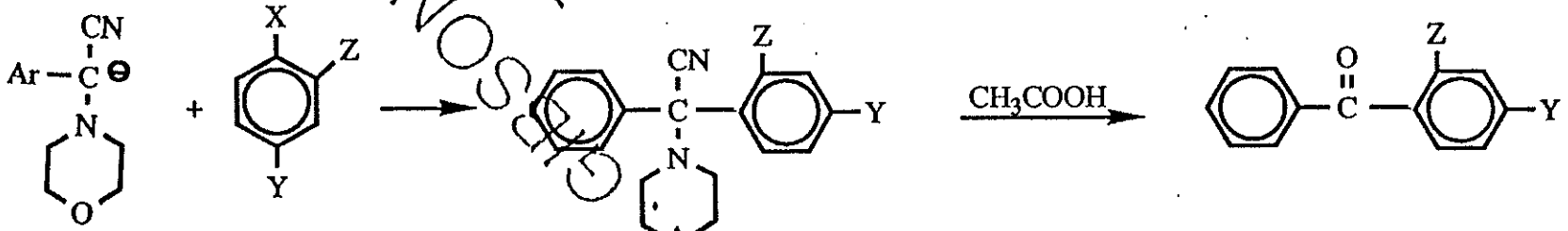

Ar = phenyl

(F. J. McEvoy& J. D. Albright, J. Org. Chem., **1979**, 44, 4597; H. Albrecht, W. Raab & C. Vonderheid, Synthesis, **1979**, 127)

PROF. H. W. GIBSON, STUDENT: JIM YANG

GENERAL SCHEME FOR SYNTHESIS OF POLYKETONES VIA AMINONITRILE'S

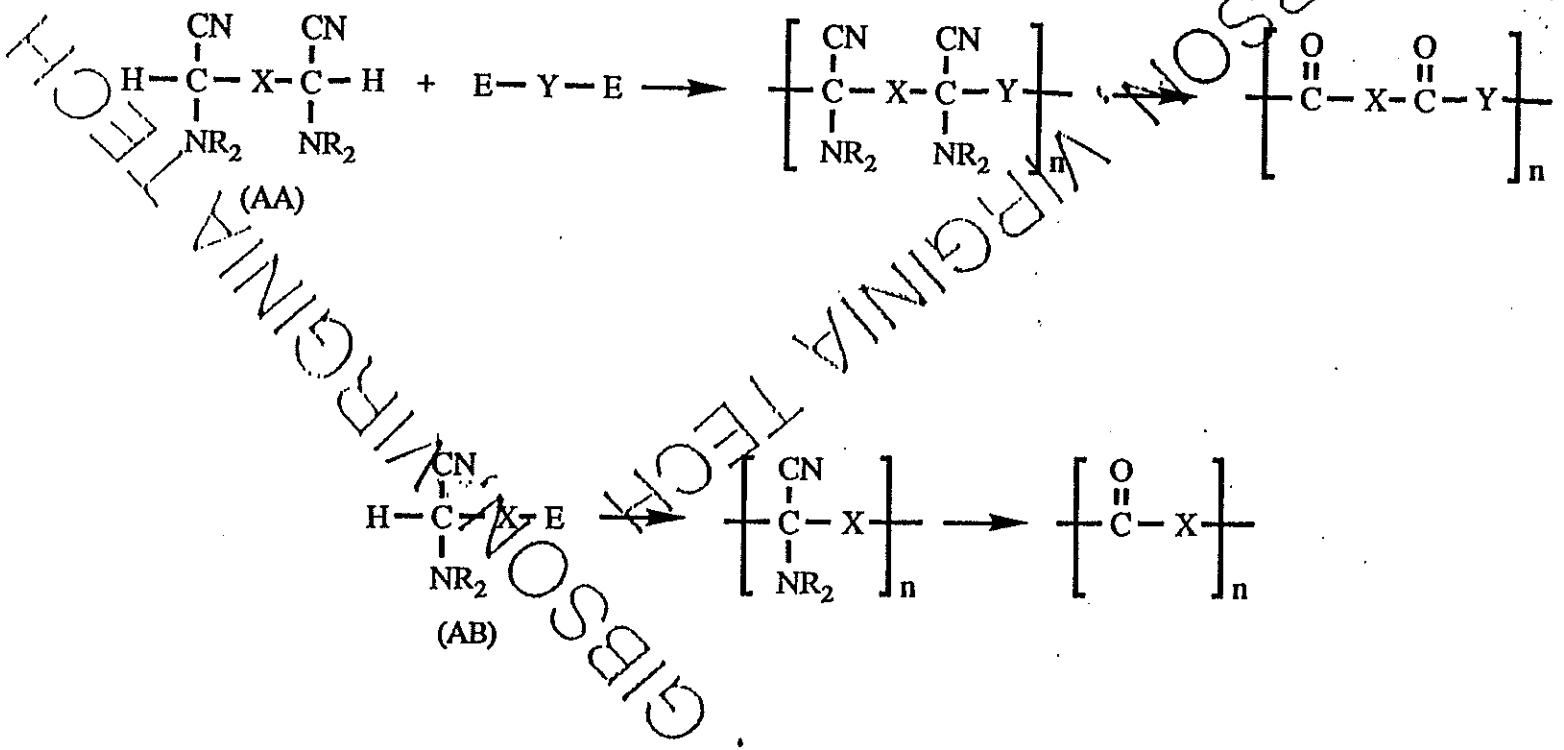

Polyaminonitriles have 1 or 2 stereogenic centers per repeat unit, thus atactic, amorphous, soluble.

OBJECTIVES

1. To synthesize wholly aromatic or mixed aliphatic/aromatic soluble poly(bis-α-aminonitrile)s

2. Hydrolyze these poly(bis-α-aminonitrile)s with aqueous acid to produce high-performance semicrystalline polyketones

WHY?

* PRODUCTION OF ENTIRELY NEW CLASSES OF CRYSTALLINE, HIGH PERFORMANCE POLYKETONES AND POLY(KETONE SULFONE)S WITHOUT ETHER OR THIOETHER LINKAGES

* ENTIRELY NEW ROUTE TO ALIPHATIC POLYKETONES WITH INDEPENDENT CONTROL OF TWO DIFFERENT ALKYLENE GROUPS. CRYSTALLINE, BIODEGRADABLE IN SOME CASES.

* AFFORDS MIXED AROMATIC/ALIPHATIC SYSTEMS. CRYSTALLINE, BIODEGRADABLE IN SOME CASES.

* KNOWN POLY(ETHER KETONE)S ALSO ACCESSIBLE BY THIS CHEMISTRY

* POTENTIAL TO MAKE POWDERS FOR PREPREGS VIA SAME OVERALL PROCESS NOW APPLIED TO OTHER PROTECTED POLY(ETHER KETONES), I.E., ACID HYDROLYSIS

MODEL REACTIONS

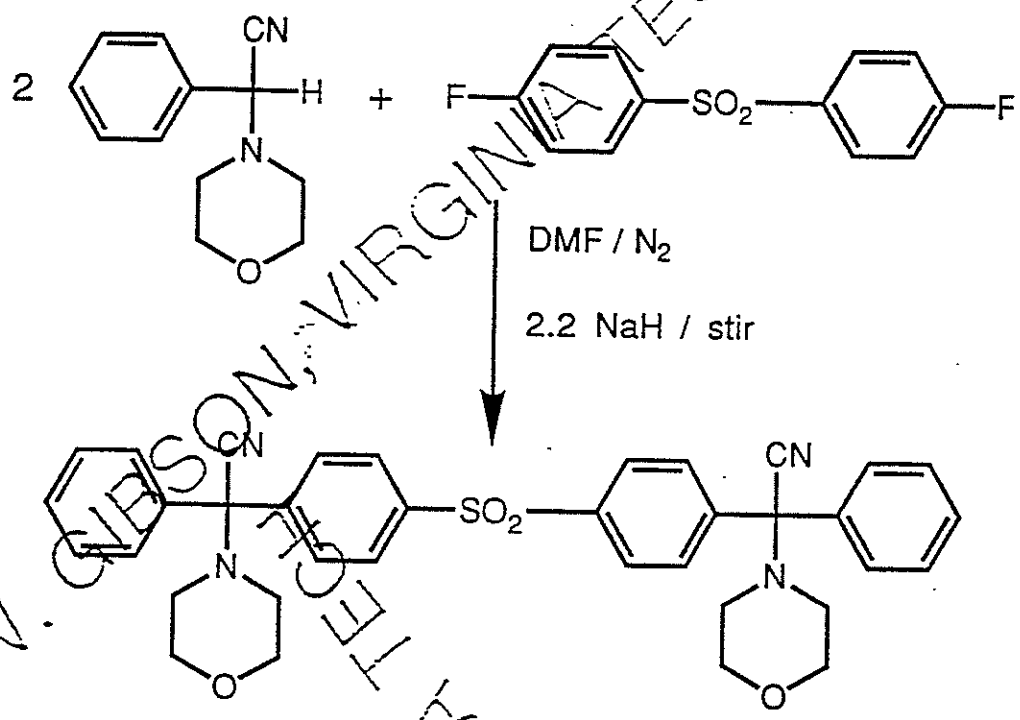

100% YIELD MP 144-220° (2 DIASTEREOMERS)

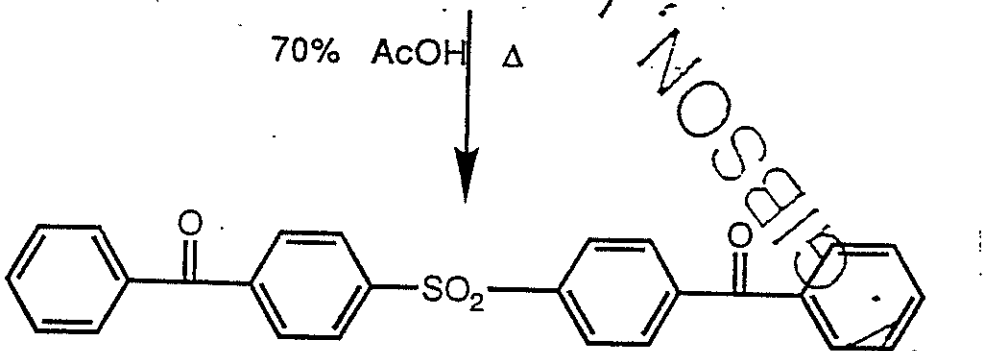

100% YIELD MP 203-4°

A. Pandya, Ph.D. Thesis, VPI&SU, **1992.**

MODEL REACTIONS (CONTD)

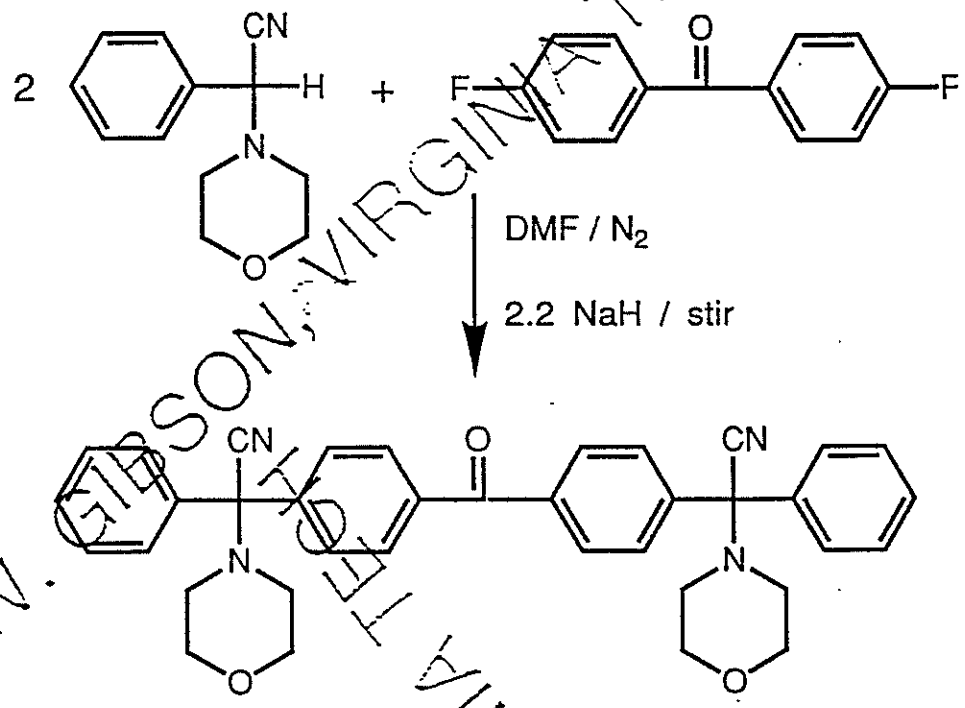

100% YIELD MP 124-142° (2 DIASTEREOMERS)

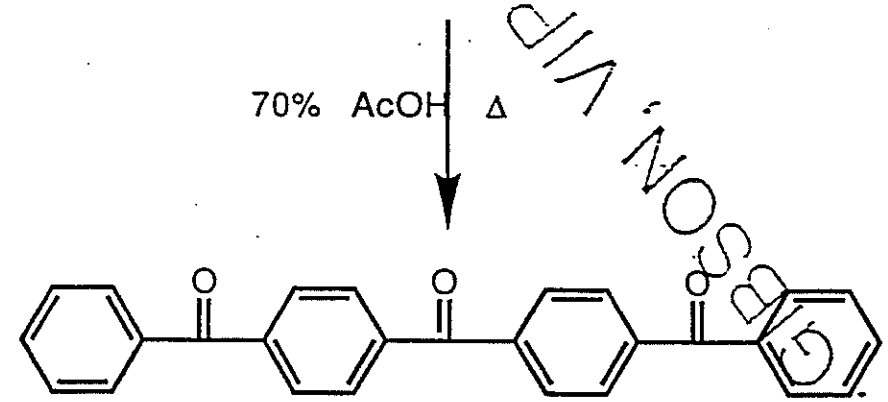

100% YIELD MP 231-2°

A. Pandya, Ph.D. Thesis, VPI&SU, **1992.** 343

Synthesis of bis-α-aminonitrile

Strecker Synthesis

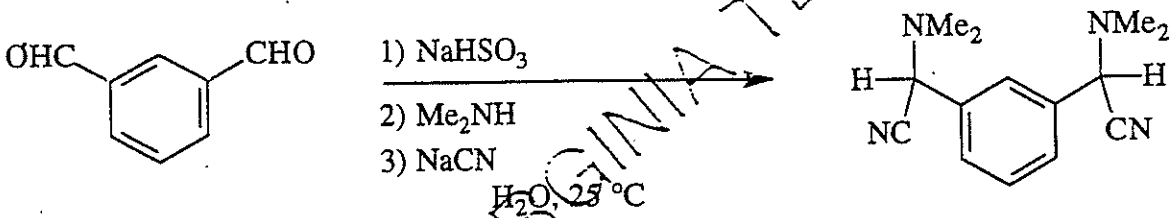

98% Yield
mp 142-144 °C

Characteristics of Strecker-α-aminonitriles

1) α-protons are acidic and can be removed easily with NaH

2) resulting carbanions are excellent nucleophiles

3) amine group can be varied to invoke different solubilities in polymers

4) aliphatic aminonitriles can also be prepared this way

EVIDENCE OF THE VALIDITY OF THE CONCEPT FORMATION OF HIGH POLYMER

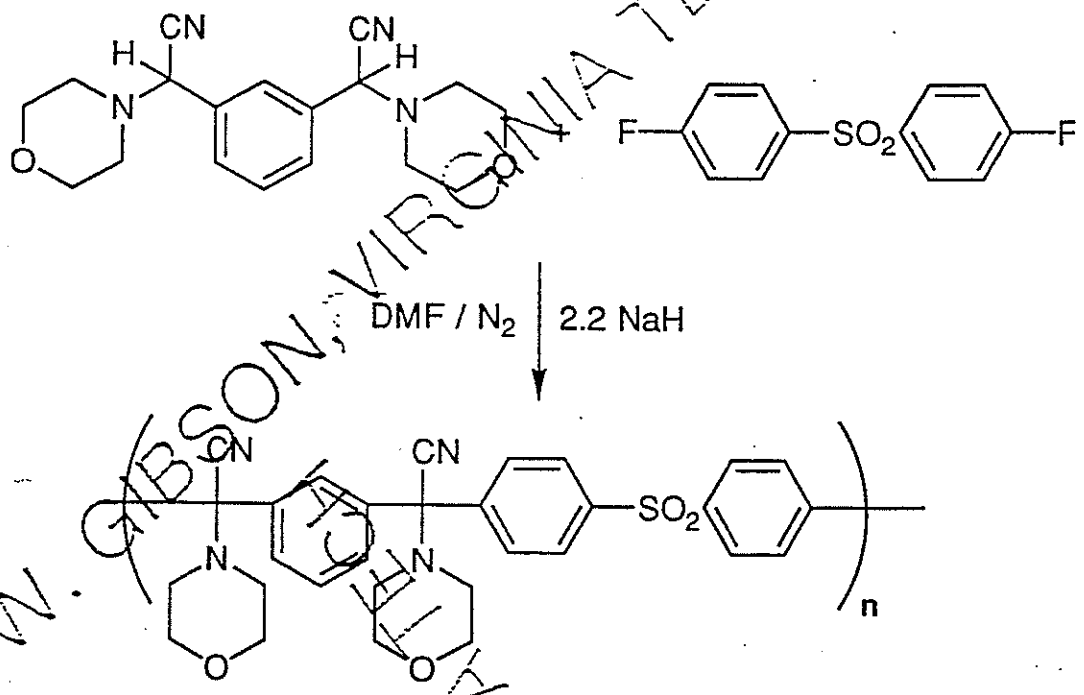

$M_n = 32.3 \times 10^3$, $M_w = 44.0 \times 10^3$ (abs., NMP, 60°)

TGA (10%): 298° SOLUBLE $CHCl_3$, THF, ETC.

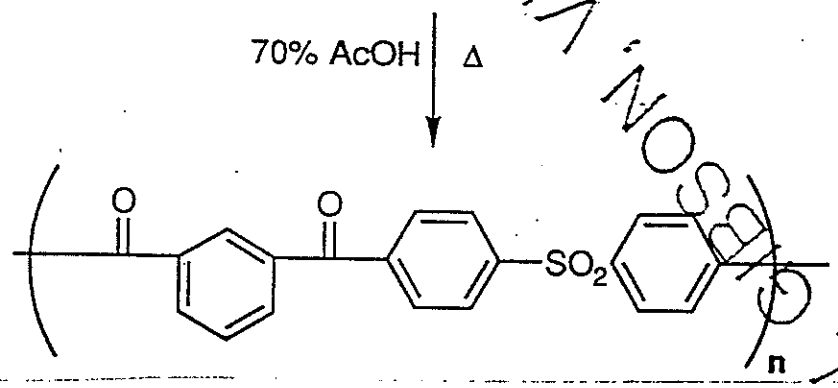

NEW

$M_n = 16.4 \times 10^3$, $M_w = 30.6 \times 10^3$ (abs., NMP, 60°)

TGA (10%): 530°, T_g = 208°C, T_m = 458°C

A. Pandya, J. Yang and H. W. Gibson, Macromolecules, 1994, *27*, 1367.

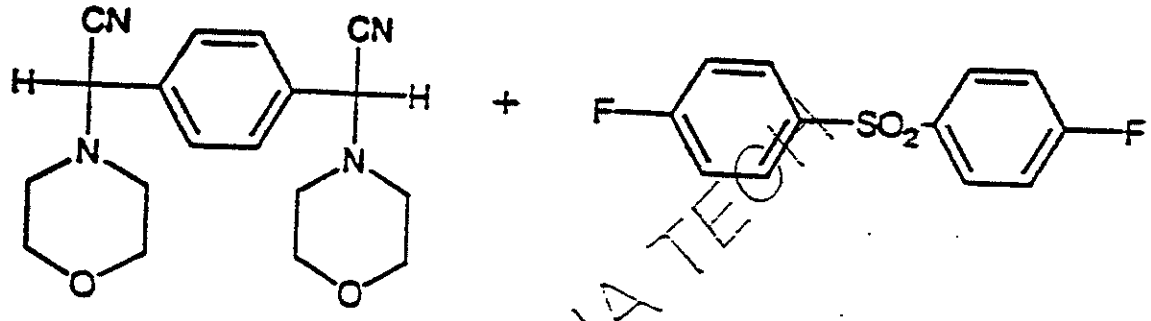

DMF / N_2 / NaH

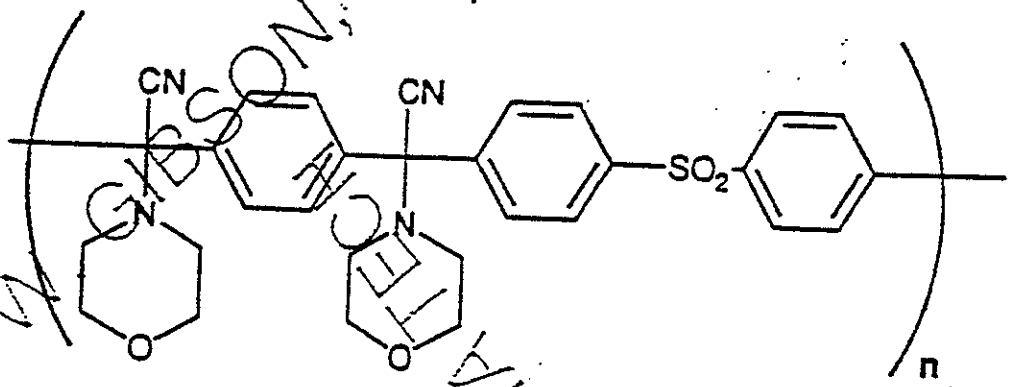

Soluble

M_n = 8.6 K, M_w = 17.2 K

(abs. GPC, NMP, 0.5% LiCl, 60°C)

DSC: no transitions, TGA: 252°C.

30% AcOH / Δ

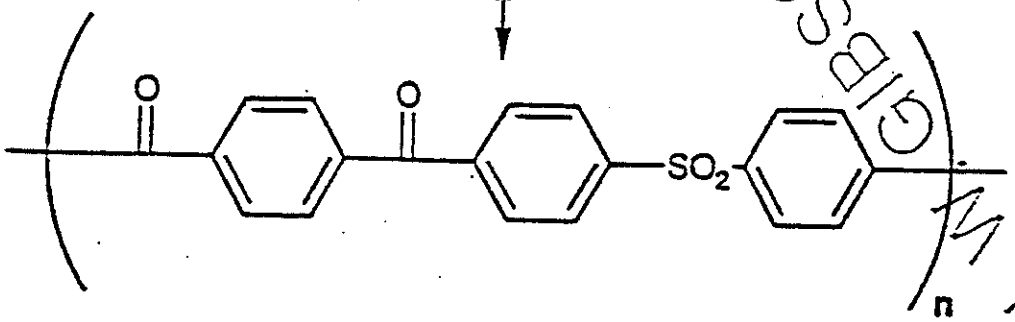

Insoluble

T_g = 228°C, T_m = 414°C (WAXS)

TGA: 493°C (10%)

346

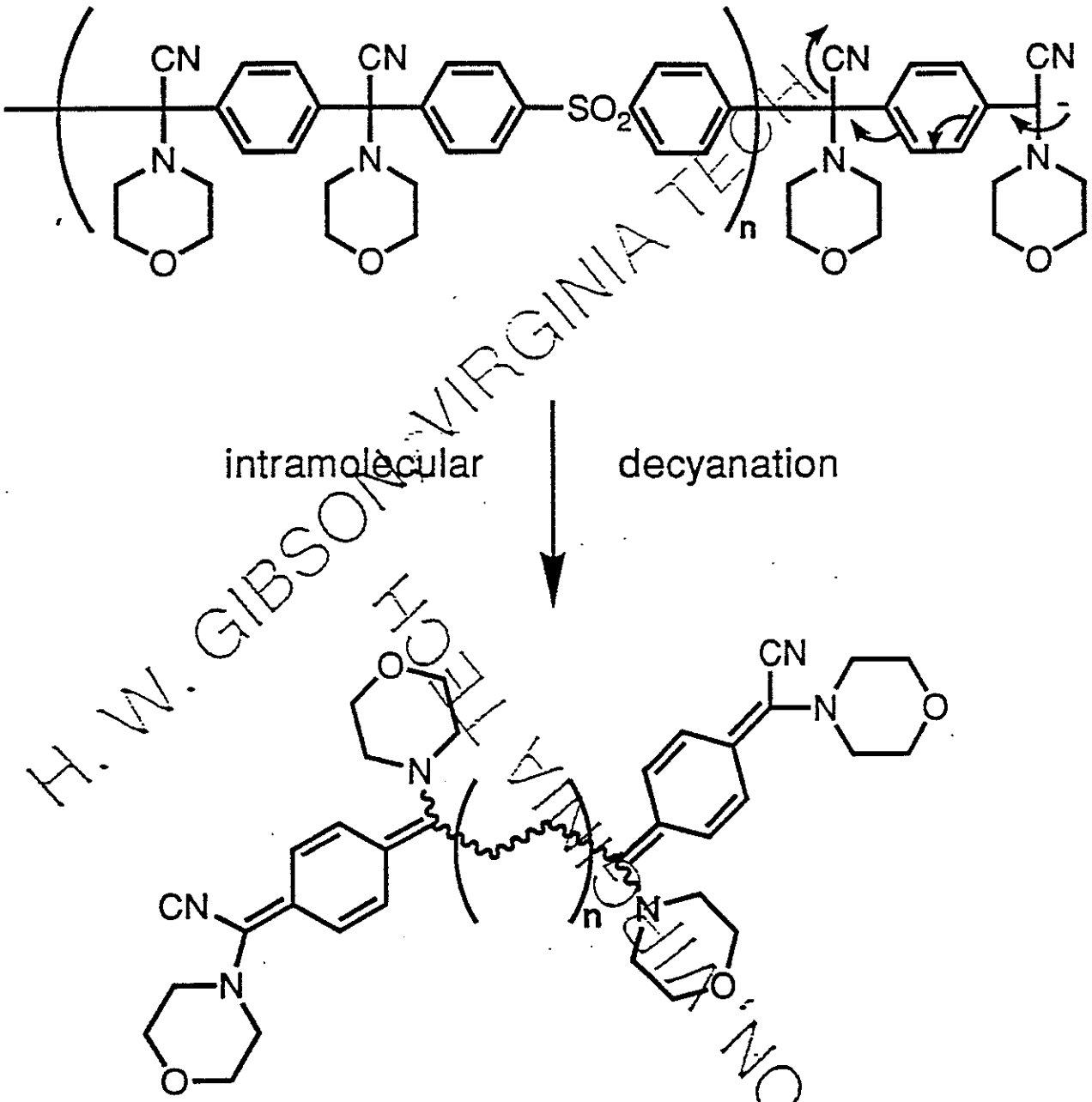

Proposed intramolecular decyanation side reaction leading to low molecular weights.

SYNTHESIS OF NOVEL POLYKETONE

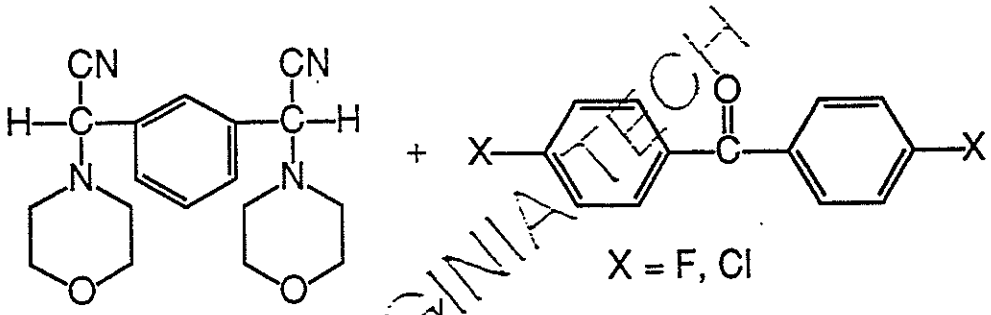

NaH, r.t.
DMF, N_2

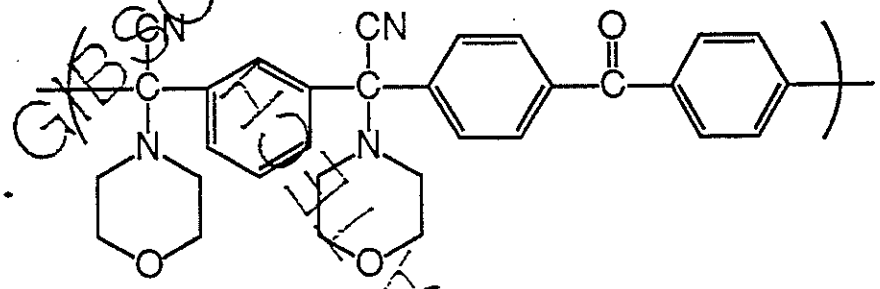

M_n=36K, M_w=75K (abs. MW, NMP, 60°C);
soluble in THF, $CHCl_3$, etc.;
DSC: T_g=69 °C; no T_m
TGA: 5% weight loss at 263 °C (air)

HCl
HOAc

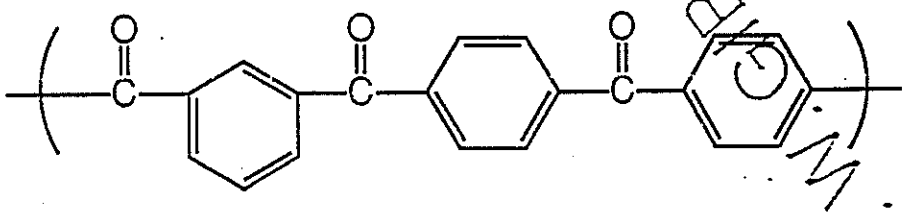

Only soluble in very strong acid, such as conc. H_2SO_4;
DSC: T_g=217 °C, T_m>525 °C;
TGA: 5% weight loss at 501 °C (air).

THE FTIR SPECTRA (KBr)

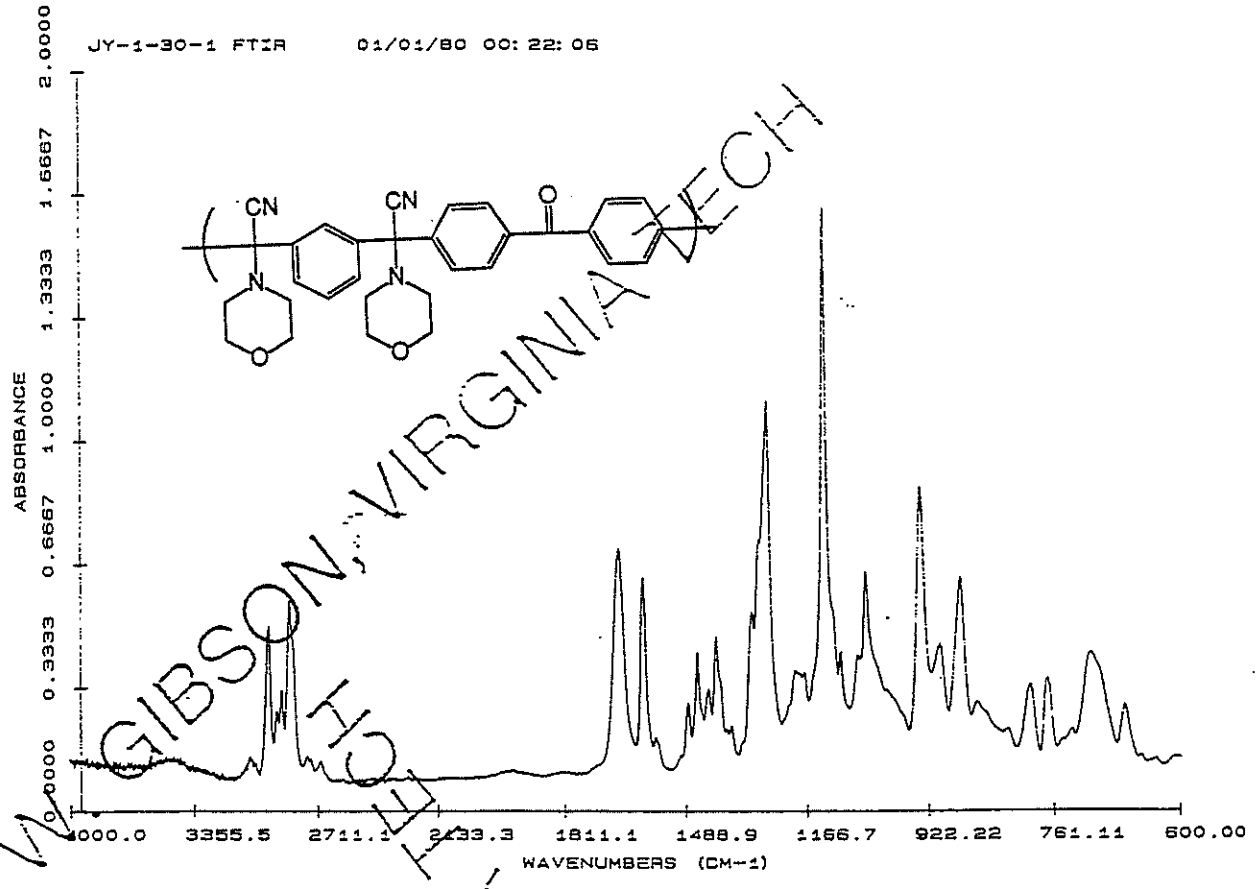

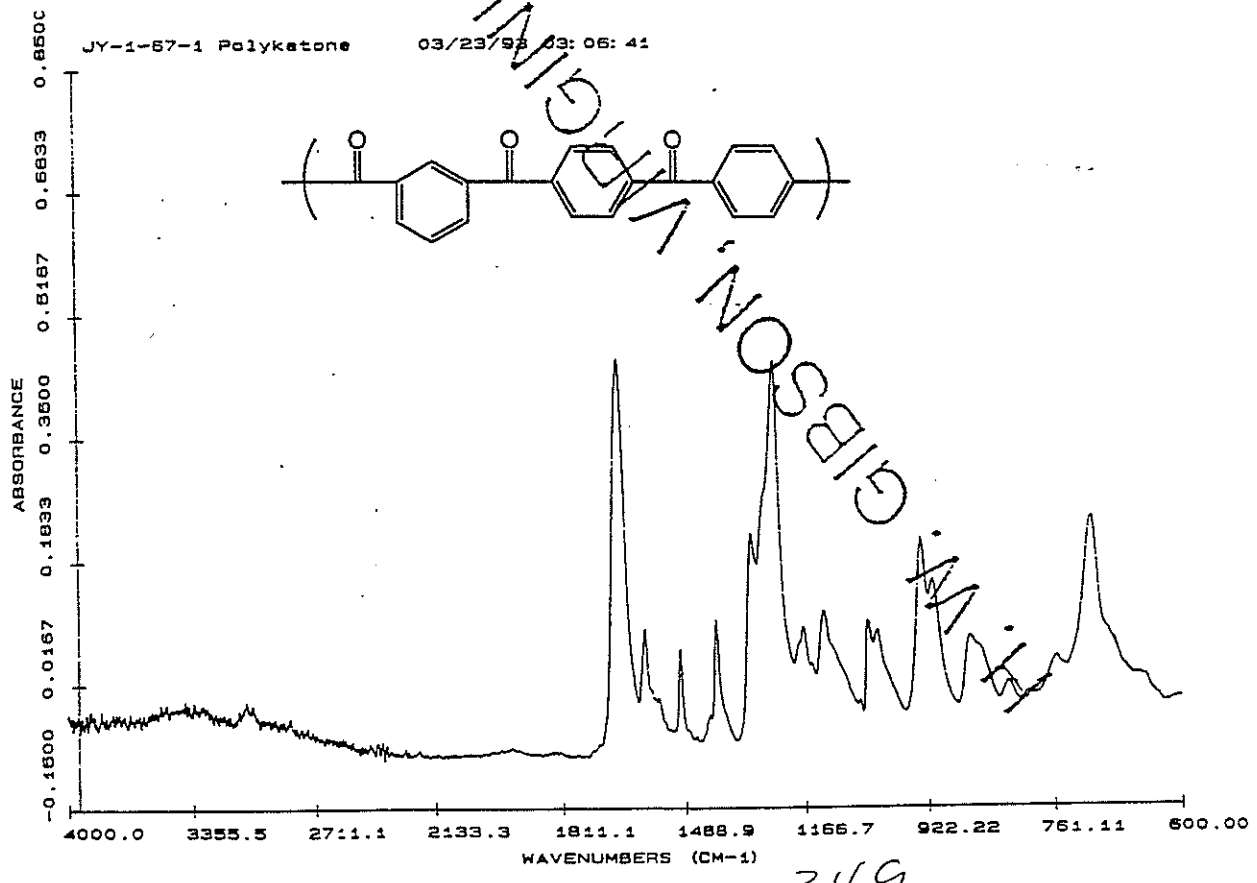

400 MHz ^{1}H NMR SPECTRUM ($CDCl_3$)

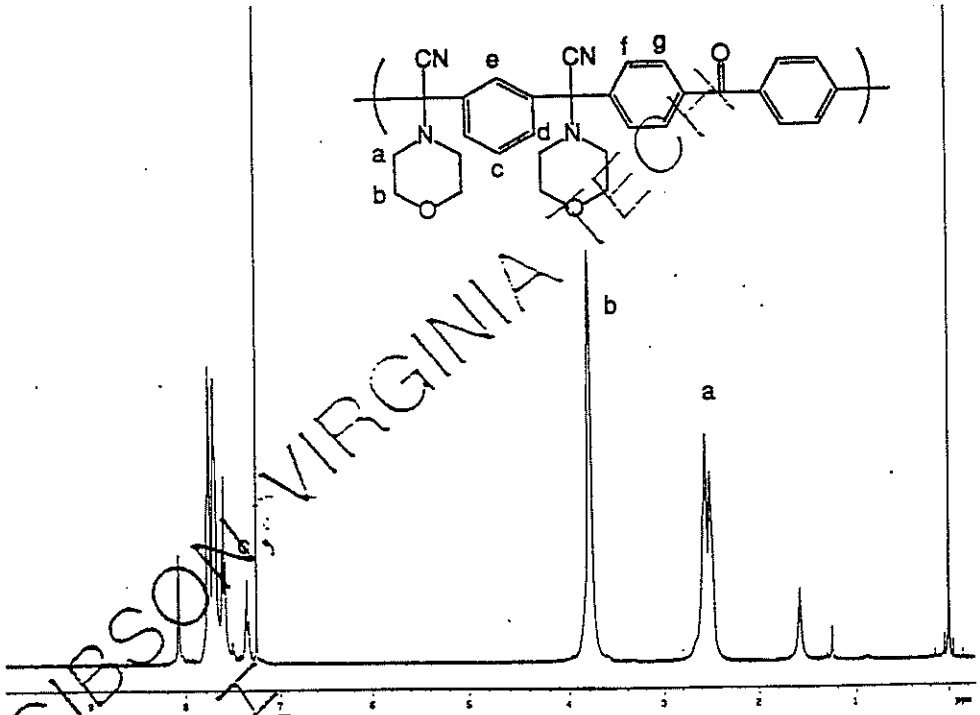

400 MHz ^{1}H NMR SPECTRUM (D_2SO_4)

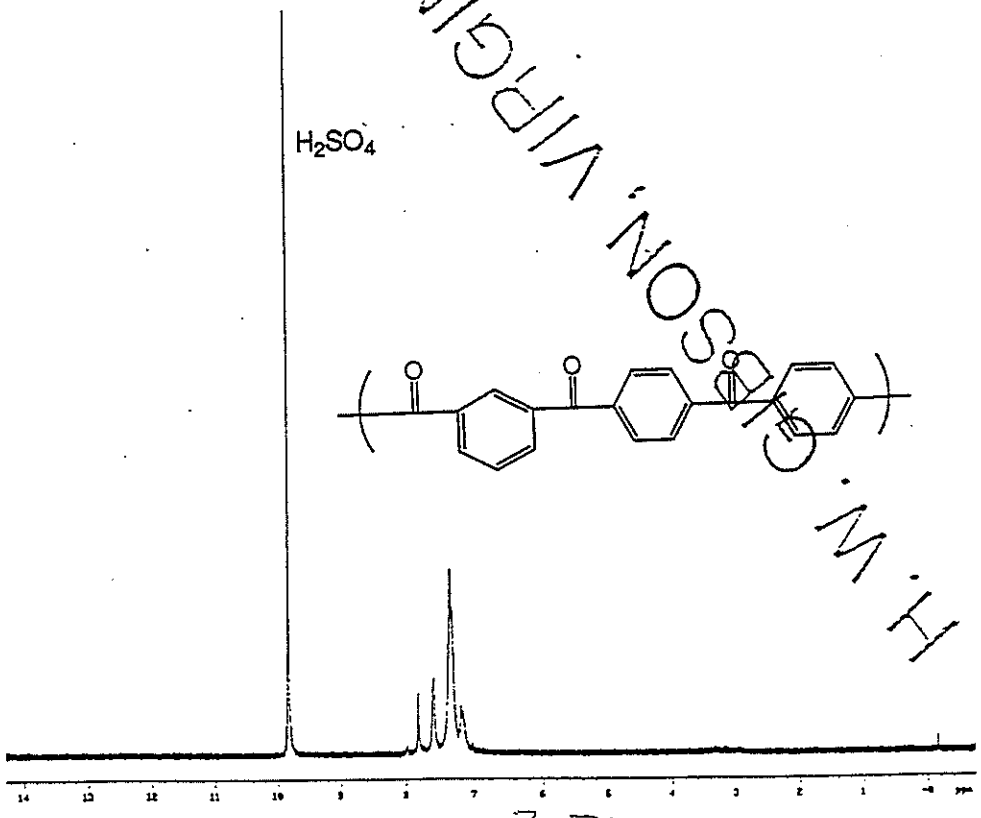

THE 2D-COSY SPECTRUM

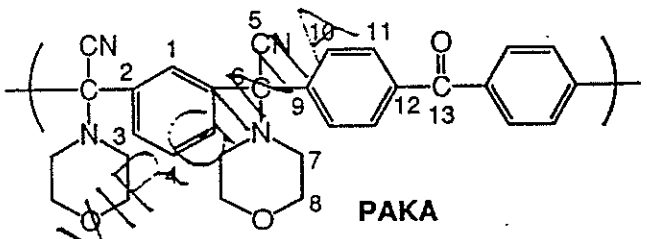

PAKA

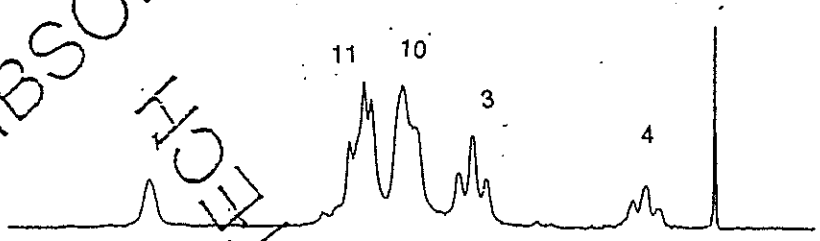

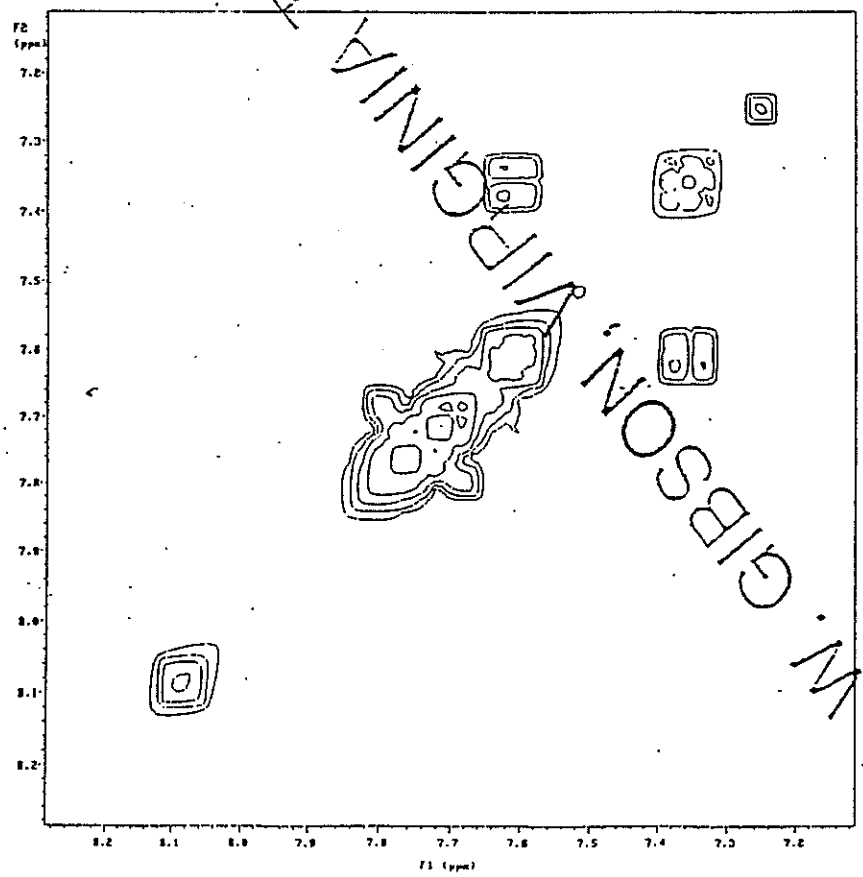

The APT SPECTRUM ($CDCl_3$)

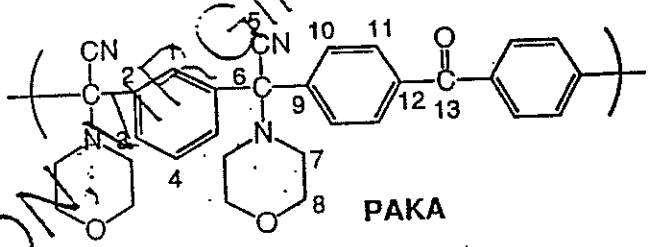

PAKA

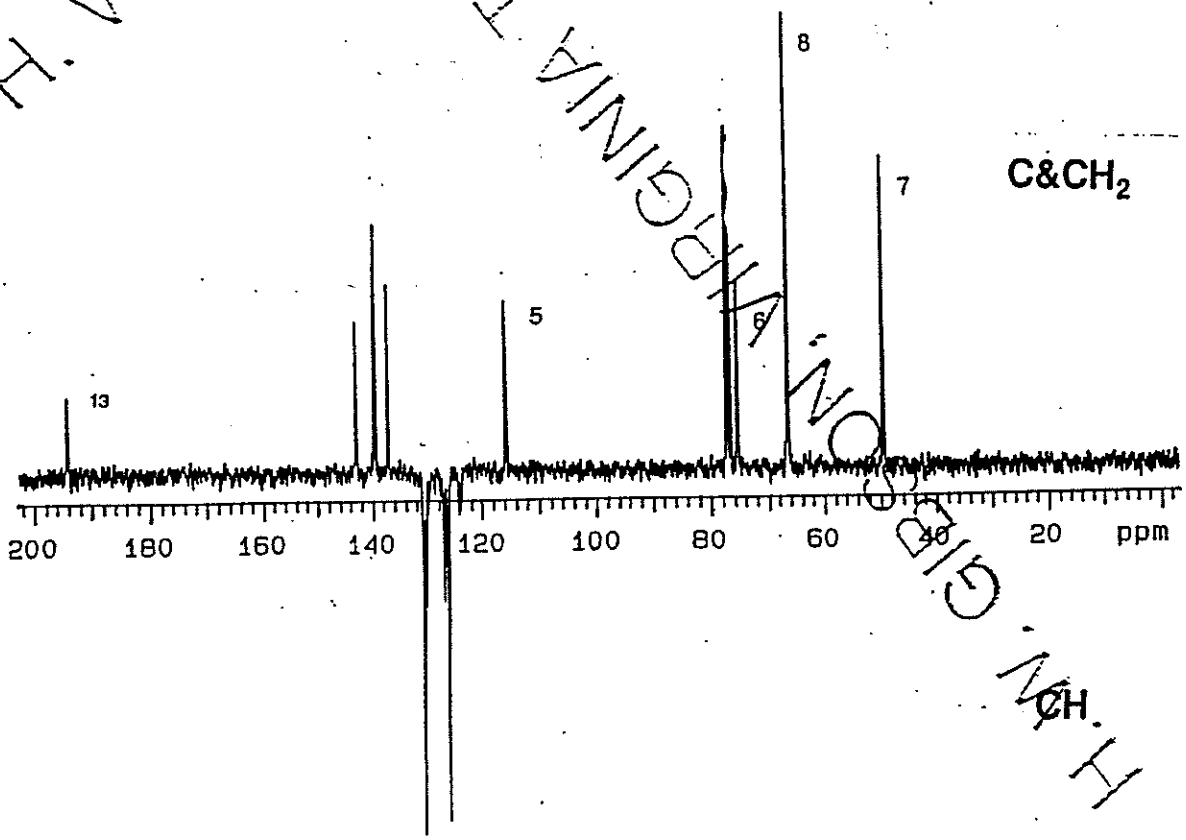

THE 2D-HETCOR SPECTRUM

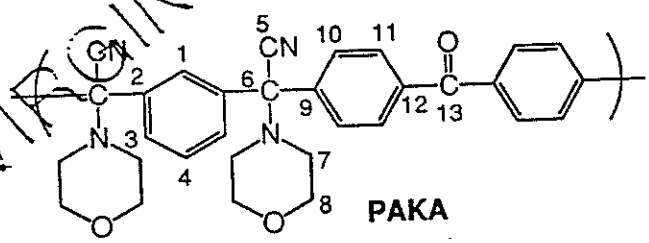

PAKA

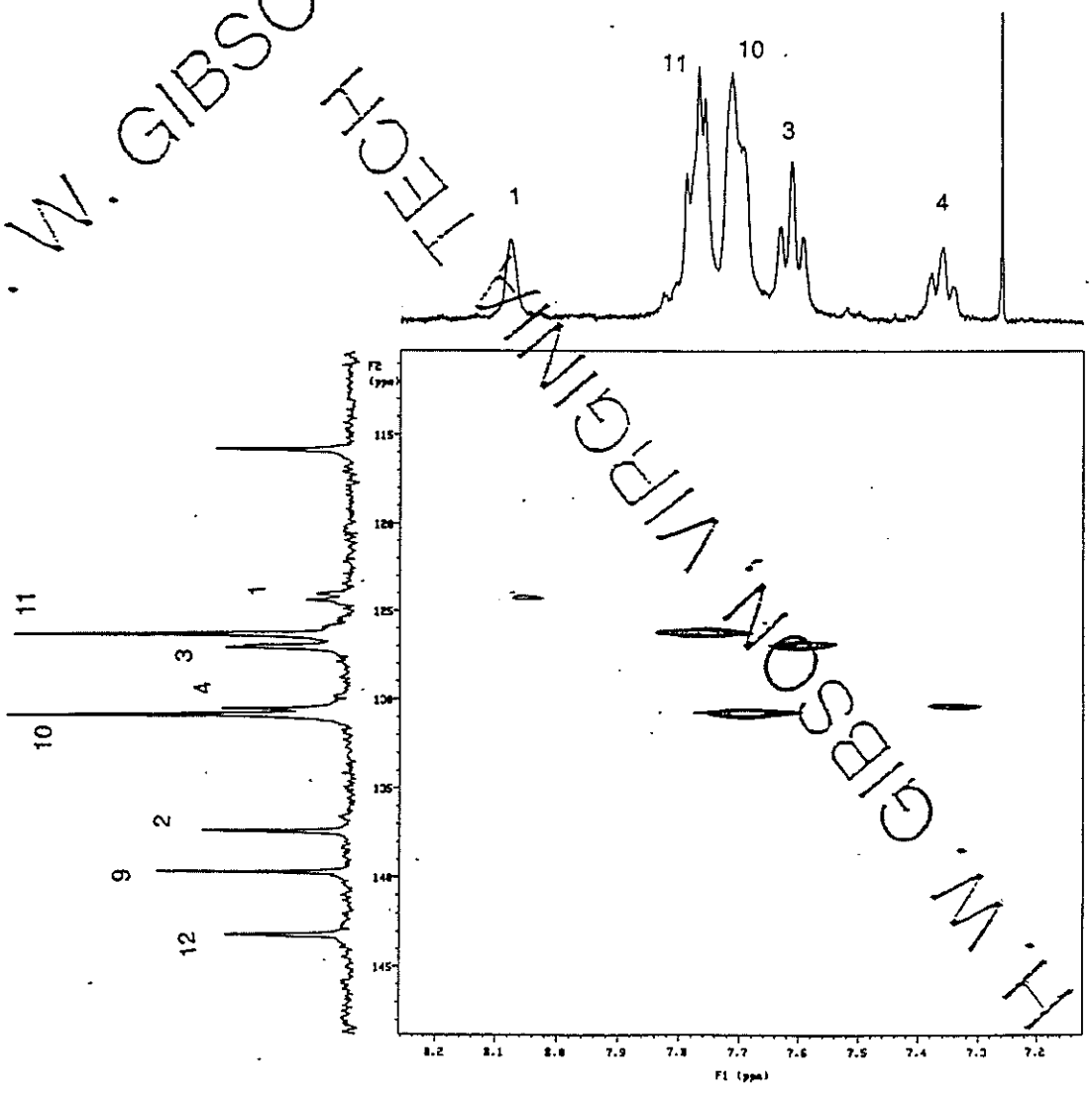

THE 2D-COSY SPECTRUM

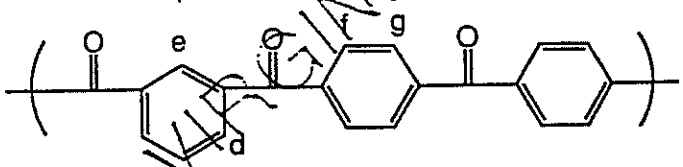

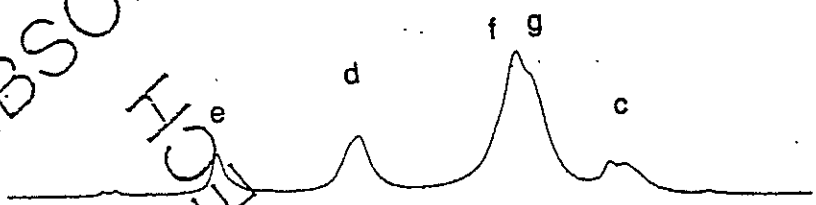

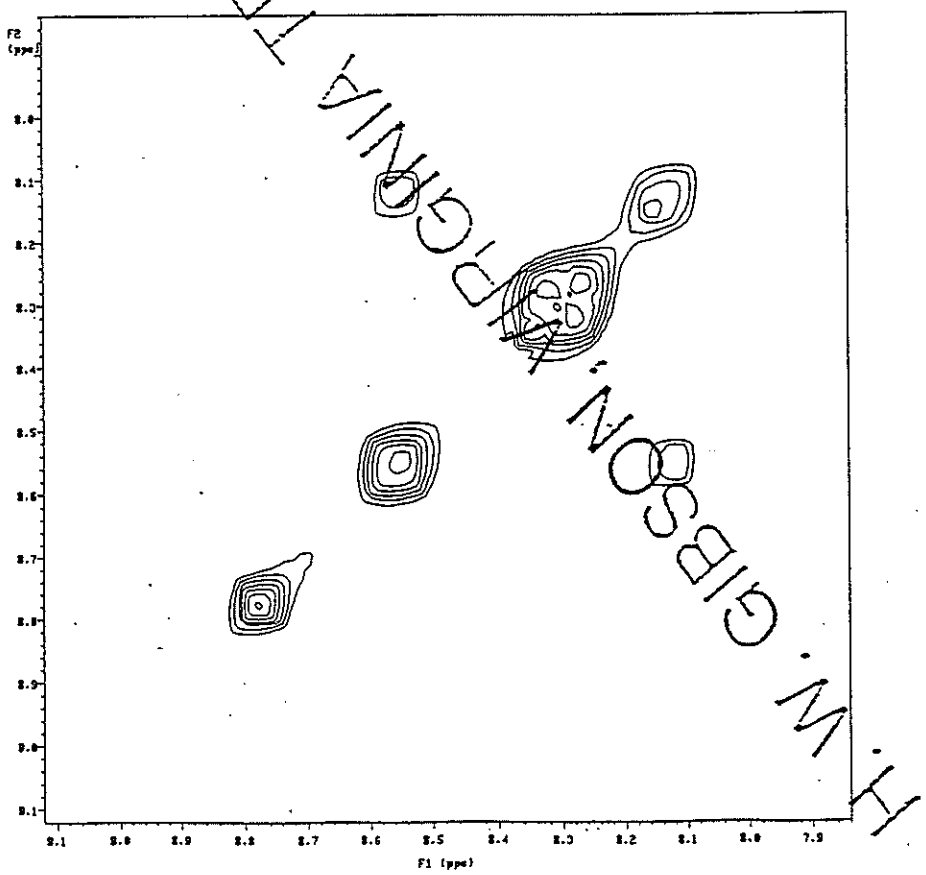

THE WIDE-ANGLE X-RAY PATTERN

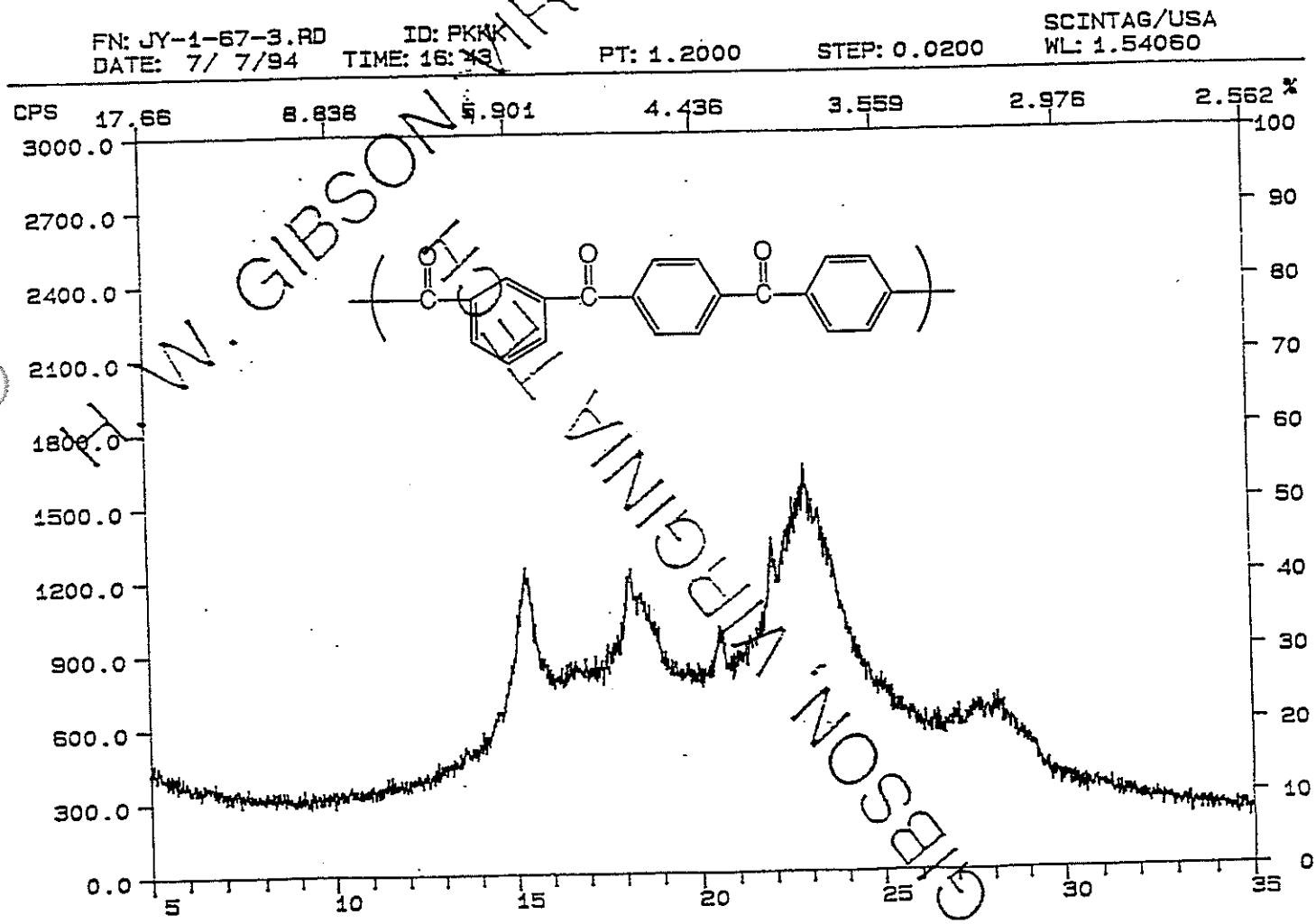

Synthesis of Novel Poly(ether ketone ketone ketone ketone) PEKKKK

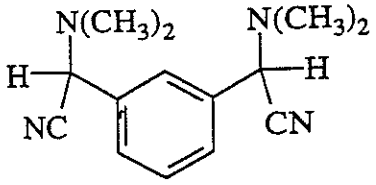

98% Yield

+

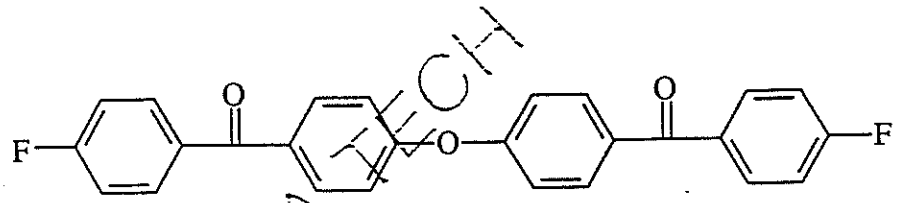

(From M. Chen, Gibson group)

NaH, DMF
85 °C

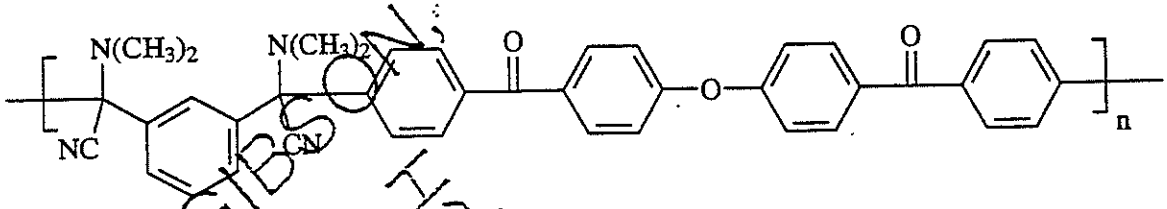

M_n= 7.2 x 10^3 g/mol, PS equivalents
Freely soluble in THF, acetone, chloroform
T_g= 146 °C, no T_m
5% Weight loss at 513 °C (N_2)

70% HOAc, HCl
90 °C

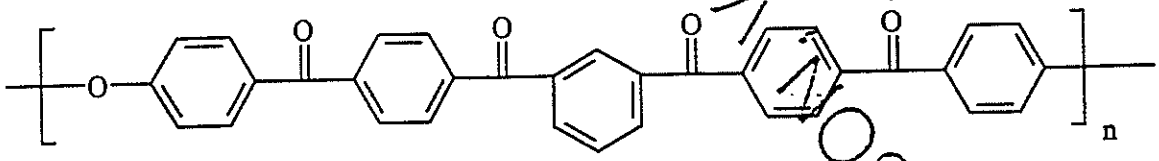

PEKKKK

Soluble only in conc. H_2SO_4, CF_3CO_2H
T_g= 185 °C, T_m= 343 °C
5% Weight loss at 492 °C (N_2)

The 2D-COSY NMR Spectrum in $CDCl_3$

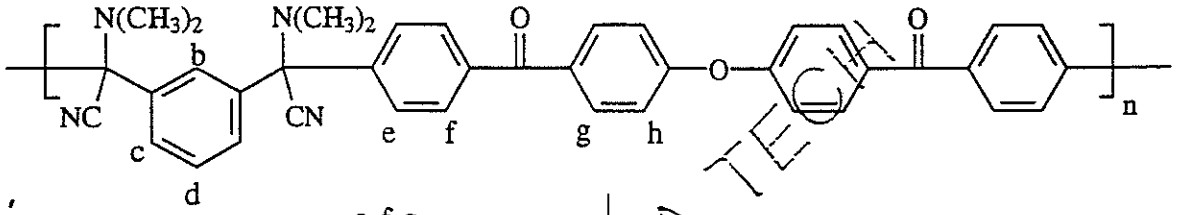

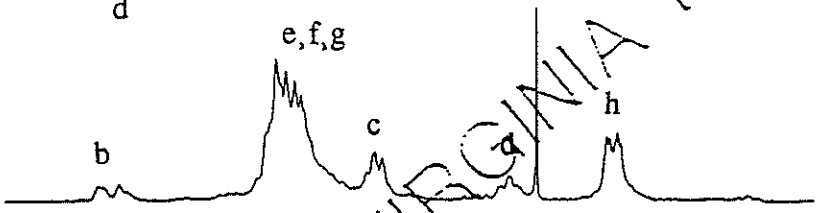

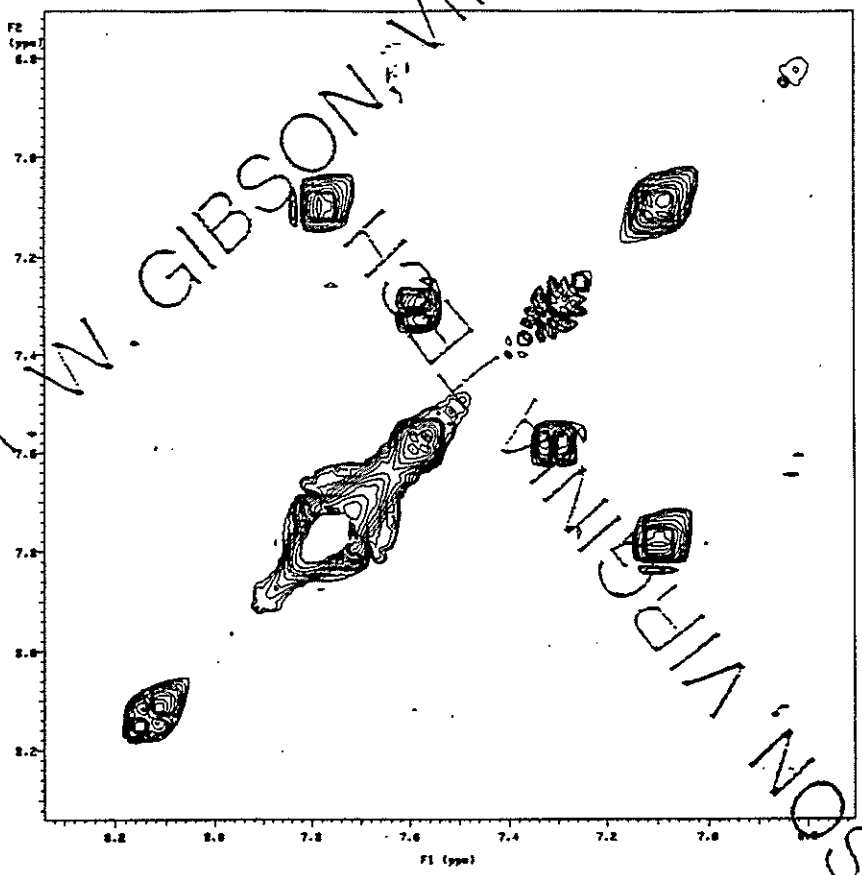

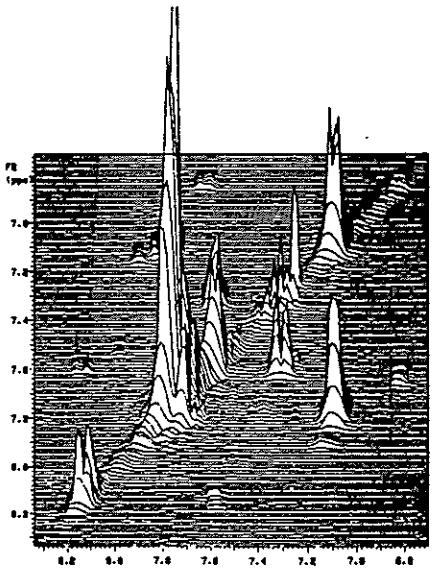

```
STANDARD 1H OBSERVE

exp1  pulse sequence: relayh

        SAMPLE                DEC. & UT
date      Apr 17 94   dfrq          399.961
solvent     CDCl3     dn               H1
file           exp    dpwr             38
   ACQUISITION        dof               0
sfrq       399.952    dn              mmm
tn              H1    dmm               c
at           0.254    dmf            2560
np             384    dseq      undefined
sw          852.8     dres      undefined
fb             400    homo              n
bs              16
ss              2       PROCESSING
tpwr           55     sb             0.000
pw           18.0     sbs        not used
pl           18.0     wtfile
d1           1.000    proc              ft
tof          582.8    fn              256
nt              16    math              f
ct              16    werr
fw               0    wexp
relay            0    wbs
slock            n    wnt
gain            20      2D PROCESSING
      FLAGS          lb1            0.005
il               n    lbs1       not used
in               n    wtfile1
dp               y    proc1             ft
hs              nn    fn1             256
  2D ACQUISITION
sw1          852.8
ni1           128
phase1          0
      DISPLAY
sp          2681.9
wp           852.8
vs             179
sc              89
wc             140
hzmm           4.66
is          500.00
rfl           213.8
rfp          2895.6
lh              0
ins          1.000
ai  cdc  av
    2D DISPLAY
sp1         2681.9
wp1          852.8
sc2             0
wc2           140
rfl1          213.8
rfp1         2896.6
```


357

Synthesis of a Water Soluble Wholly Aromatic Polyketone

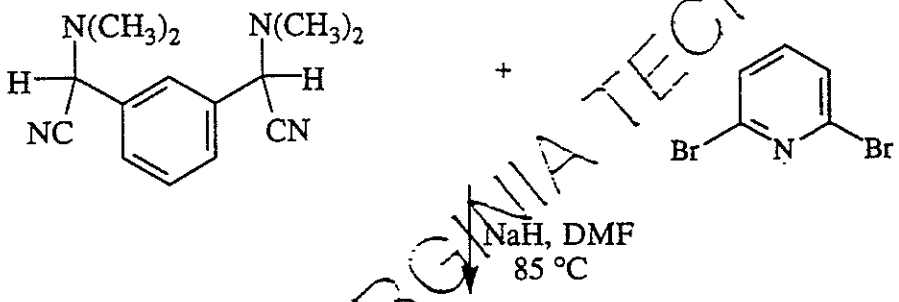

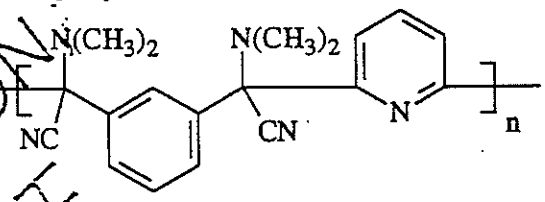

M_n= 13 x 10^3 g/mol (PS equivalents)
Freely soluble in MeOH, acetone, THF, chloroform
T_g= 94 °C, no T_m
5% Weight loss at 296 °C (N_2)

50% HOAc
90 °C

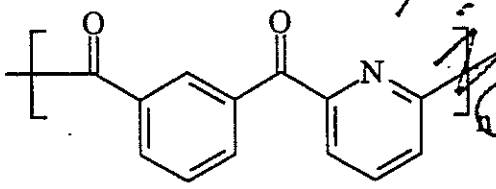

Soluble in hot DMSO, aqueous acetic acid (pH<6.0)
Insoluble in acetone, chloroform, THF
T_g= 129 °C, T_m> 170 °C
5% Weight loss at 242 °C (N_2)

SYNTHESIS OF BISFLUORO KETO MONOMERS FROM AMINONITRILES

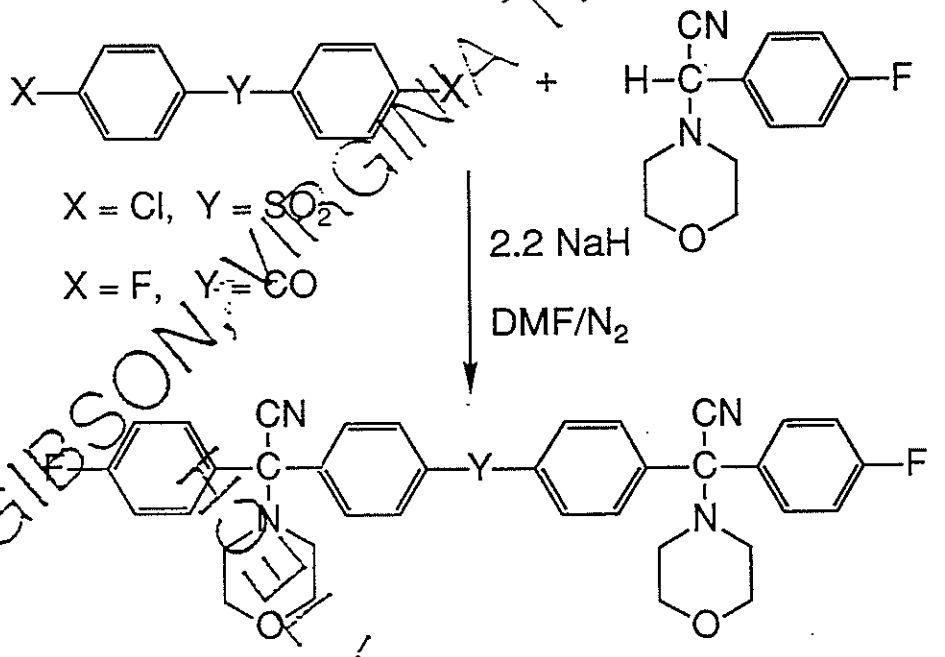

100% Yield ^{1}H NMR

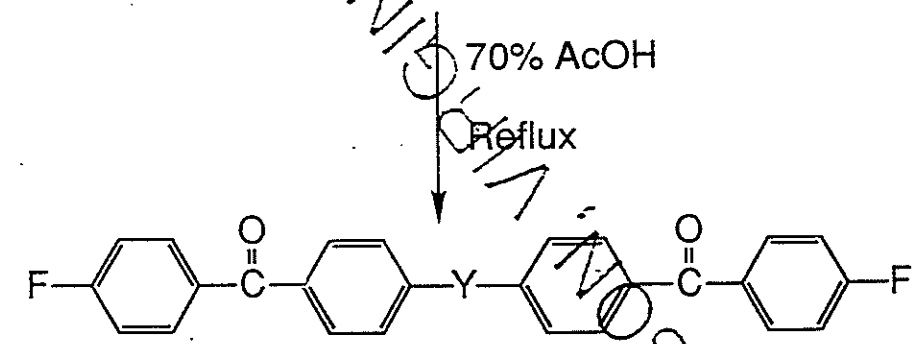

100% Yield ^{1}H NMR, FTIR

mp 183-4 °C (Y=SO_2, rep. 177-8 °C)

mp 294-5 °C (Y=CO, rep. 282-3 °C)

EXTENSIONS ARE POSSIBLE.

SYNTHESIS OF NOVEL POLY(KETONE SULFONE)

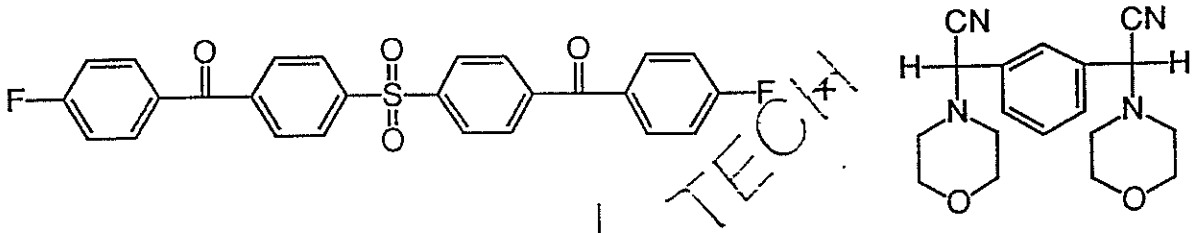

2.2 NaH
DMF/N_2
60 °C

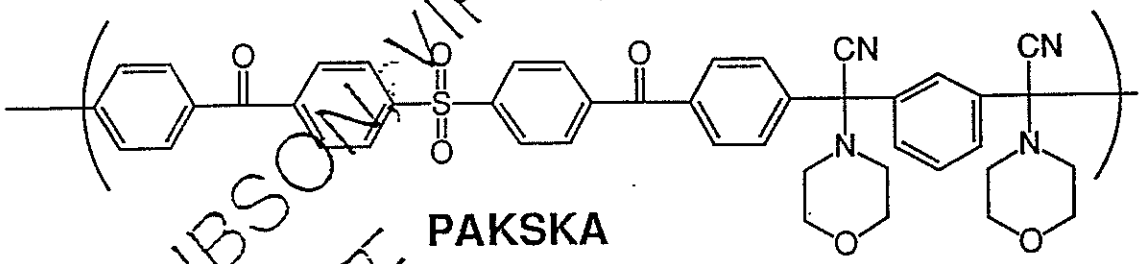

PAKSKA

M_n=17 Kg/mol, M_w=27 Kg/mol ($CHCl_3$, polystyrenes)
- NOT VERY SOLUBLE IN $CHCl_3$, SOLUBLE IN THF, DMF, DMSO, NMP, ETC.
^{1}H NMR, COSY, FTIR, ^{13}C NMR

HCl
HOAc
Reflux

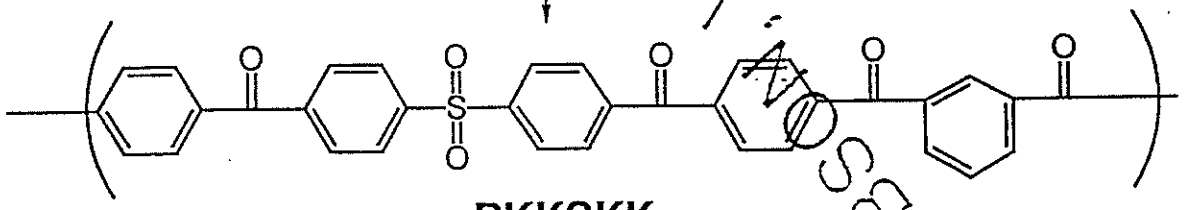

PKKSKK

INSOLUBLE IN MOST COMMON ORGANIC SOLVENTS, SOLUBLE IN CONC. H_2SO_4
^{1}H NMR (D_2SO_4), COSY, FTIR
TGA: 5% WEIGHT LOSS AT 514 °C(IN AIR)
DSC: T_g=195 °C; T_m>450 °C

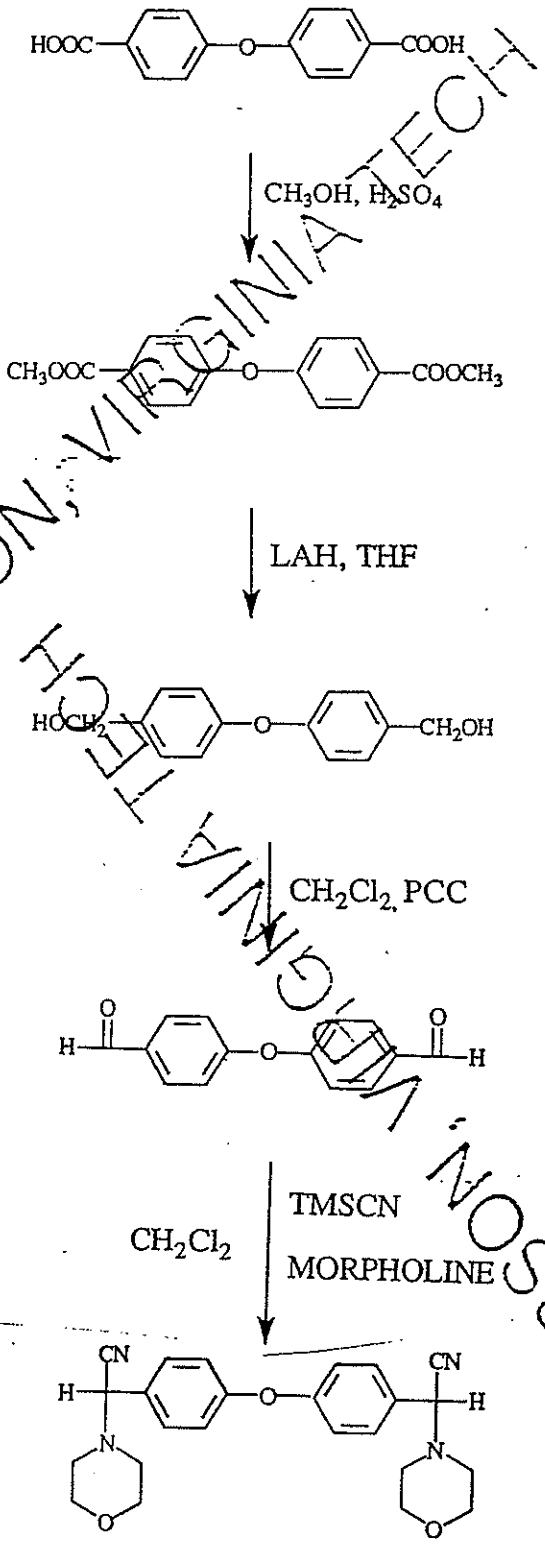

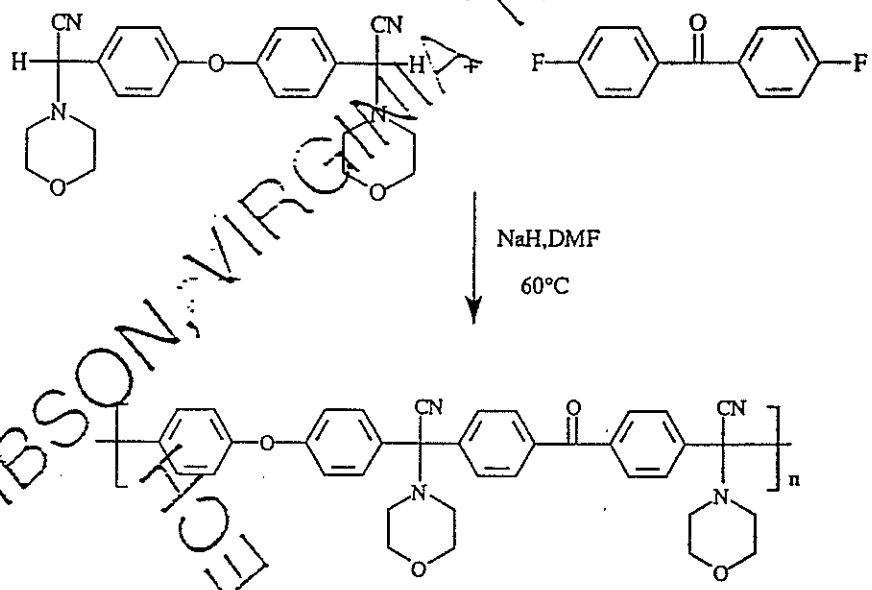

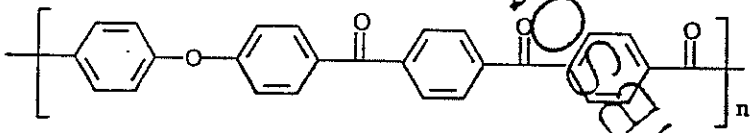

Mixed Aliphatic/Aromatic Polyketones From Soluble Poly(bis-α-aminonitrile)s

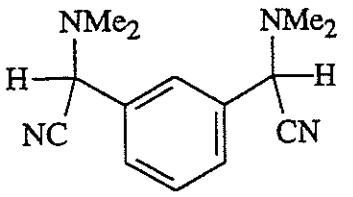

1

98% Yield

+

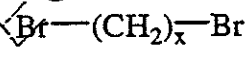

2 a: x= 4
b: x= 10

NaH, DMF
70 °C

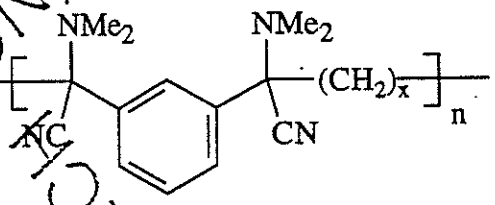

3a,b

Freely soluble in THF, acetone, chloroform
3a: T_g= 54 °C, no T_m ; 5% weight loss at 148 °C (N_2)
3b: T_g< 25 °C

50% HOAc
90 °C

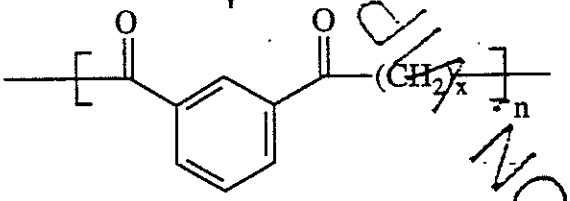

4a,b

4a: T_g= 105 °C, T_m= 207 °C; 5% weight loss at 212 °C (N_2), insoluble in organics
4b: T_g= 88 °C, T_m= 144 °C; 5% weight loss at 332 °C (N_2), soluble in hot DMSO

High molecular weights achieved (polymer **3a**: M_n= 42 x 10^3 g/mol, polymer **3b**: M_n= 32 x 10^3 g/mol, PS equivalents)

CONCLUSIONS

- The use of aminonitrile monomers allows efficient syntheses of polyketones via soluble precursors, reducing synthesis and processing problems associated with classical methods.
- The method is applicable to the production of aliphatic or aromatic or aliphatic/aromatic polyketones.
- New types of aromatic polyketones without ether linkages can be prepared in this way, possibly leading to higher performance materials.
- These materials appear to have potential as high performance adhesives and composite components.

ACKNOWLEDGEMENTS

MY COWORKERS:

Graduate Students: Jinlian Yang
Darin Dotson

Undergraduate Student:
Christie Sensenich

We sincerely appreciate financial support of this research by the American Chemical Society Petroleum Research Fund and the National Science Foundation Science & Technology Center for High Performance Polymeric Adhesives & Composites at Virginia Tech.

Chemistry for Rings and Pegs

Coleen Pugh
The University of Michigan
Department of Chemistry
Ann Arbor, MI 48109-1055

Rings

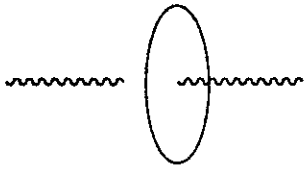

1) How to thread rings with chains which lack an enthalpic driving force.

Pegs

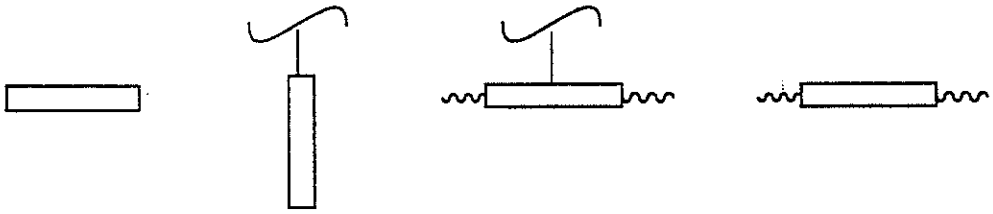

2) Prediction of mesophases formed / predetermined mesophases.
   - Backbone
   - Spacer
   - Mesogen
   - Molecular Weight
   - Polydispersity
   - Tacticity

3) Transformation / regulation of mesophases
   - Specific Interactions
   - Immiscible Components

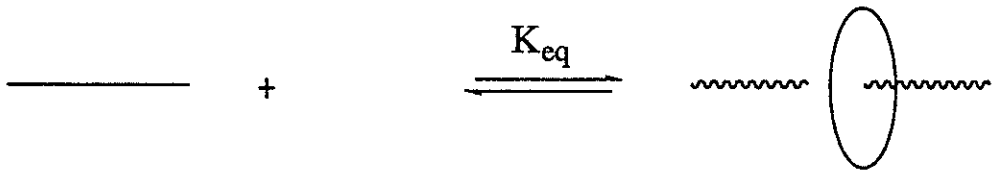

$$\Delta G = - RT \ln K_{eq}$$

$$\ln K_{eq} = \frac{\Delta S}{R} - \frac{\Delta H}{RT}$$

Threading Methods

1) Statistical Threading

strong attractive interactions absent

ΔS determines equilibrium

2) Directed / Template Threading

strong attractive interactions between cyclic & linear components

ΔH determines equilibrium

AMPHIPHILIC APPROACH

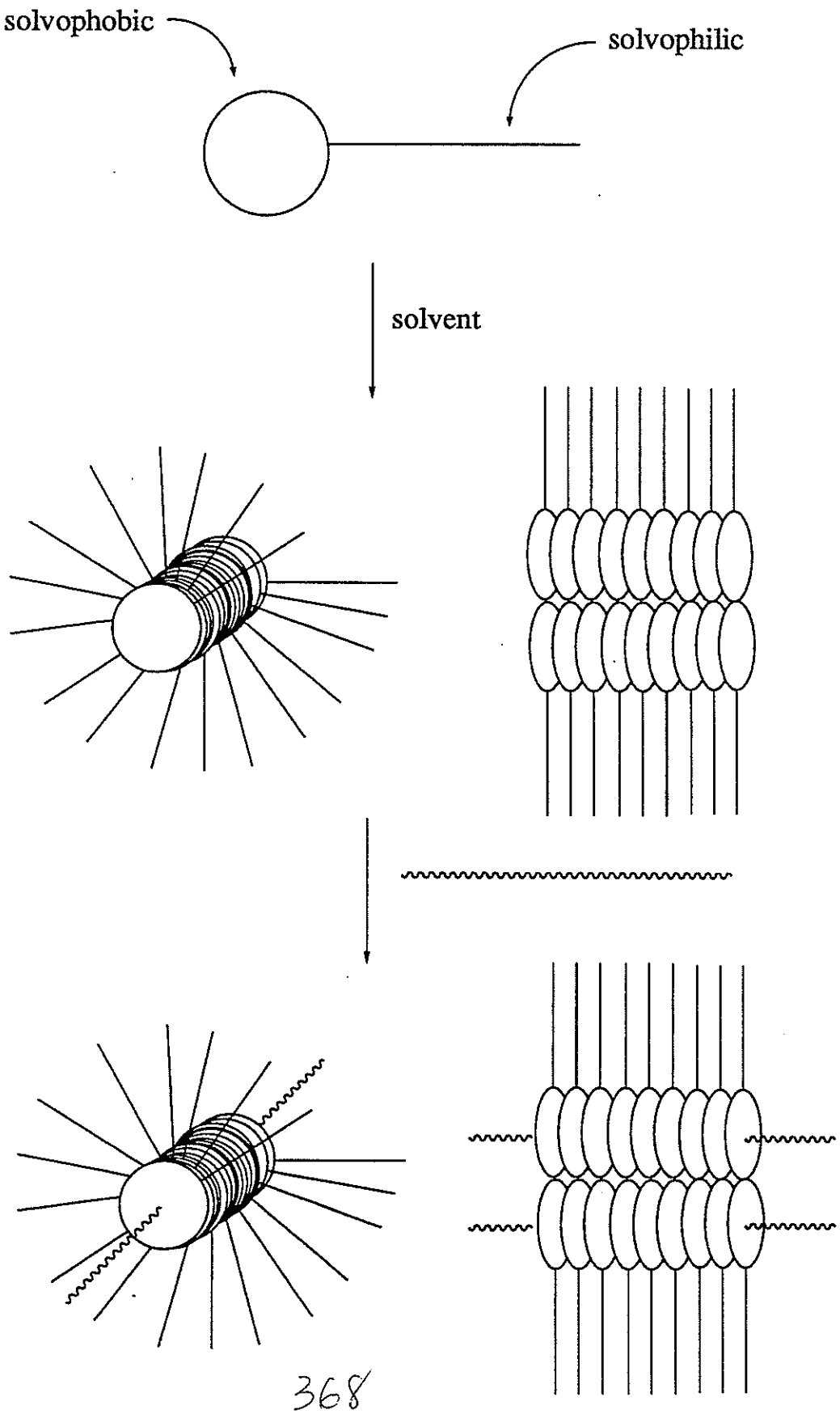

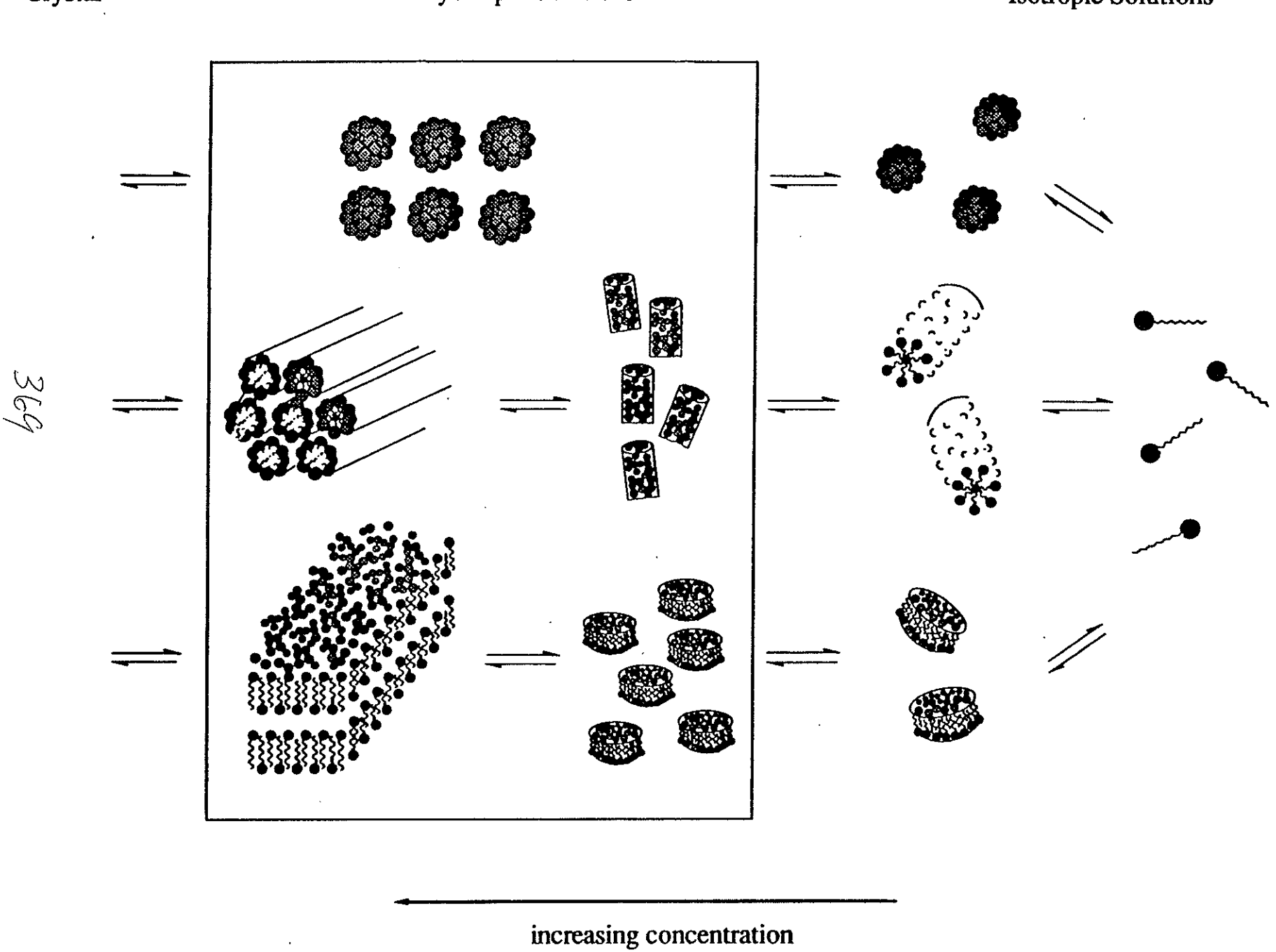
Crystal
Lyotropic Solutions
Isotropic Solutions
increasing concentration

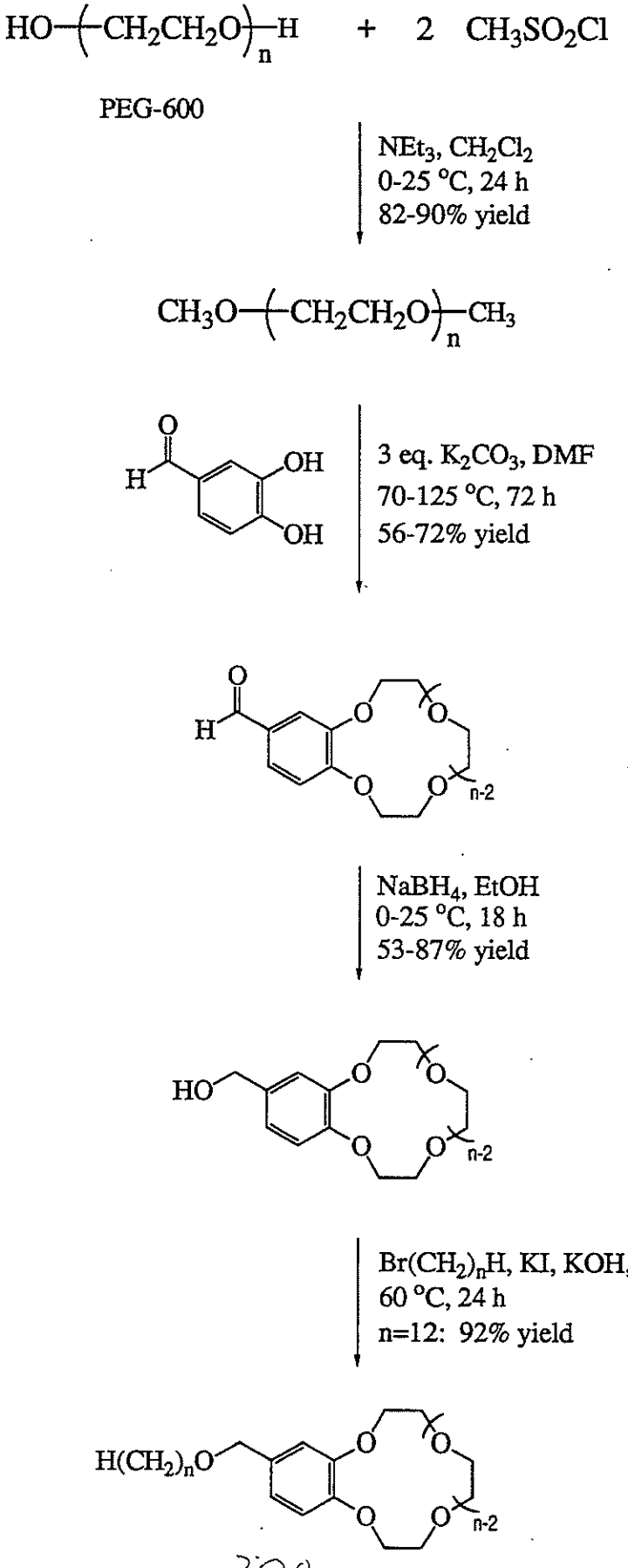
HO—(—CH2CH2O—)n—H + 2 CH3SO2Cl
PEG-600
NEt3, CH2Cl2
0-25 °C, 24 h
82-90% yield
CH3O—(—CH2CH2O—)n—CH3
3 eq. K2CO3, DMF
70-125 °C, 72 h
56-72% yield
NaBH4, EtOH
0-25 °C, 18 h
53-87% yield
Br(CH2)nH, KI, KOH, DMSO
60 °C, 24 h
n=12: 92% yield

Chemistry for Pegs

I. Prediction of Mesophases - Structural Variables in SCLCPs

Backbone	More thermally stable mesophases from flexible backbones. More ordered mesophases from flexible backbones.
Spacer	Doesn't completely decouple motions of mesogen and backbone. Better decoupling with increasing spacer length. Side chain crystallization at $n \geq 9$-11. Length determines nature of highest temperature mesophase.
Mesogen	
Molecular Weight	Phase transitions independent of molecular weight after 10-50 repeat units.
Polydispersity	
Tacticity	

II. Regulating / Transforming Mesophases

Specific Interactions

Immiscible Components

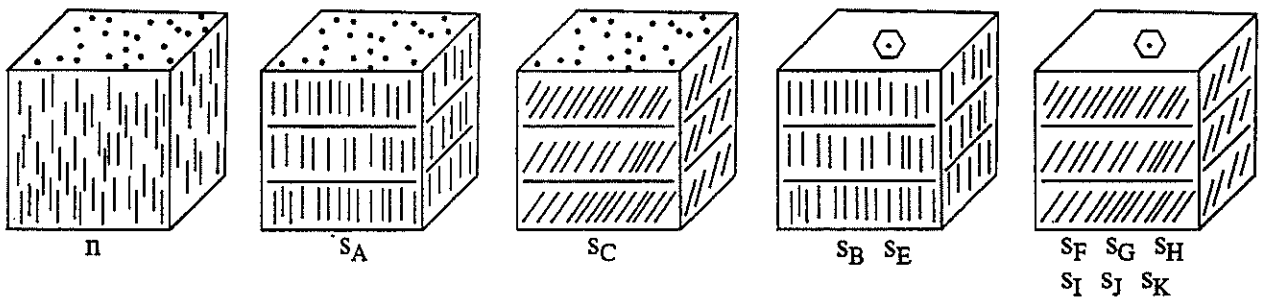

Polymer Backbone

General:

More ordered mesophases possible with more flexible backbones.

Exceptions:

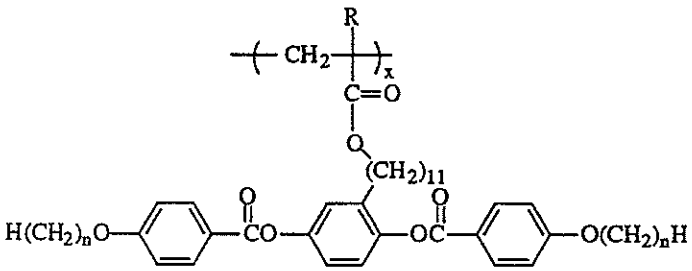

n	R = H	R = Cl	R = CH_3
1	g 14 n 44 i	g 36 n 59 i	g 38 n 62 i
2	(g 12 n 74) k 91 i	(g 31 n 79) k 92 i	(g 32 n 82) k 92 i
3	g 11 n 58 i		g 26 n 58 i
4	g 4 n 67 i	g 20 n 66 i	g 19 n 67 i
5			g 10 n 51 i
6	g -9 n 59 i		g 5 n 60 i
7			g 1 n 48 i
8	g -13 k 33 n 61 i	g 0 n 60 i	g -2 n 61 i

F. Hessel & H. Finkelmann, *Makromol. Chem.*, **189**, 2275 (1988).

F. Hessel & H. Finkelmann, *Polym. Bull.*, **14**, 375 (1985); F. Hessel, R.-P. Herr & H. Finkelmann, *Makromol. Chem.*, **188**, 1597 (1987).

Exception?

g 104 s_C 226 s_A 234 i

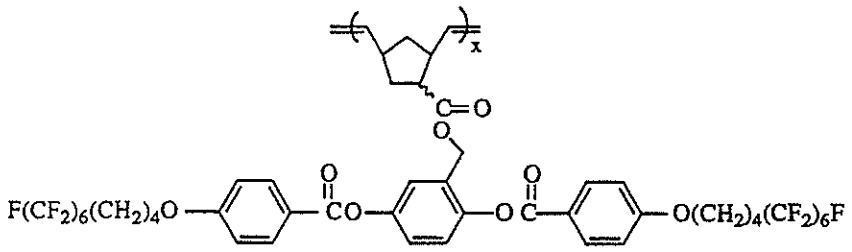

g 106 s_C 205 s_A 214 i

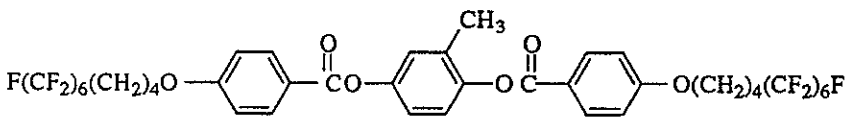

Nature of the Mesogen

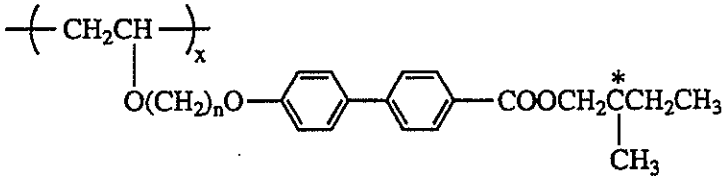

n = 6	g 30 s 58 s_A 110 i
n = 11	g 11 k 62 (s 26 s_C* 53) s_A 123 i

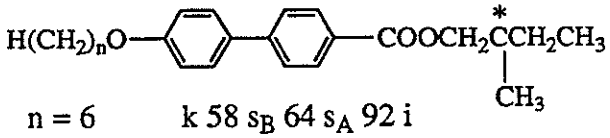

n = 6	k 58 s_B 64 s_A 92 i
n = 7	k 62 (s_C* 59) s_A 89 i
n = 10	k 54 (s_C* 49) s_A 82 i

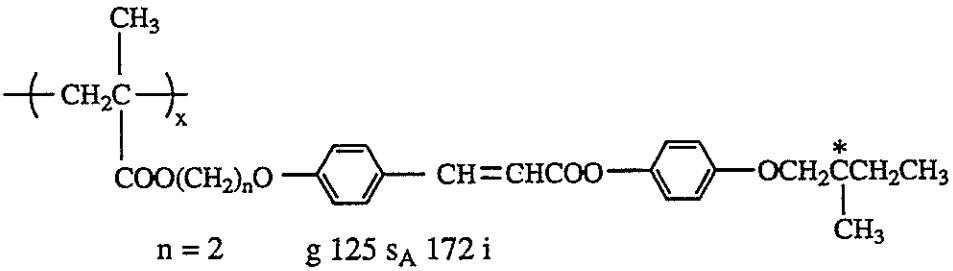

n = 2	g 125 s_A 172 i
n = 6	g 50 k 92 s_A 172 i
n = 11	g 35 k 65 s_C* 115 s_A 142 i

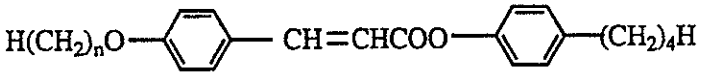

n = 1	k 82 n 93 i
n = 5	k 96 n 102 i
n = 7	k 65 s 86 n 111 i

n = 2	k 114 n 124 i
n = 6	k 72 n 109 i
n = 10	k 72 (s_C 58) s_A 109 n 109.5 i
n = 12	k 82 (s_C 58) s_A 107 i

PVE: V. Percec, Q. Zheng & M. Lee, *J. Mater. Chem.*, **10**, 229 (1991).
PMA: B. Messner & H. Finkelmann, *Makromol. Chem.*, **192**, 2383 (1991).
LMMLC: D. Demus & H. Zaschke, *Flussige Kristalle in Tabellen II*, VEB Deutscher Verlag, Leipzig, 1984.

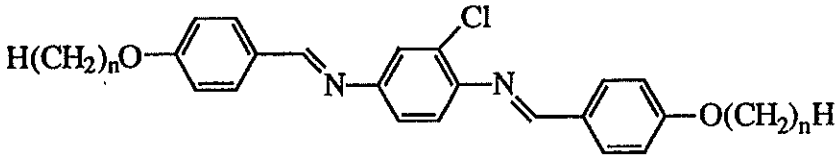

n=8	k	62	(s_C	60)	n	178	i			
10	k	64	s_C	110	n	166	i			

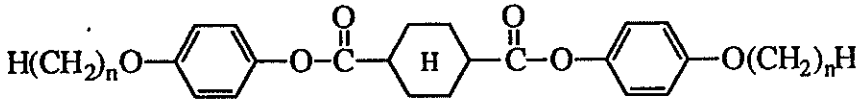

n=7	k	95	s	96	s_B	107	s_C	111	s_A	180 i
8	k	91	s	93	s_B	111	s_C	119	s_A	178 i
12	k	90			s	112	s_C	156	s_A	163 i
14	k	94			s_B	114	s_C	155	s_A	156 i
16	k	96			s_B	115	s_C	150		i

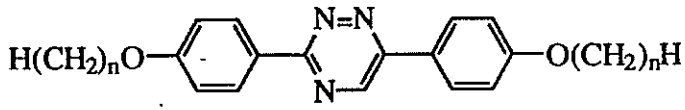

n=3	k	163	s_C	165	n	241	i			
4	k	147	s_C	193	n	240	i			
5	k	109	s_C	204	n	227	i			
6	k	92	s_C	208	n	219	i			
7	k	92	s_C	212	n	215	i			
8	k	86	s_C	213			i			
9	k	92	s_C	212			i			
10	k	95	s_C	211			i			

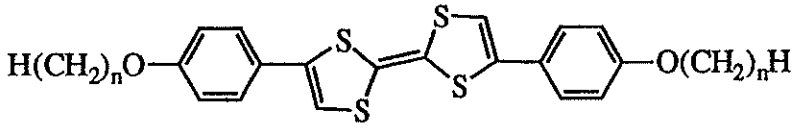

n=4	k	171	s_G	186			n	210	i	
8	k	146	s_G	156	s_C	172			i	
10	k	157			s_C	207			i	

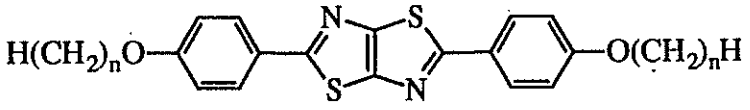

n=4	k	198			s_C	213	n	302	i	
5	k	145	s_E	180	s_C	228	n	277	i	
6	k	115	s_E	167	s_C	236	n	268	i	
7	k	105	s_E	160	s_C	240	n	256	i	
8	k	105	s_E	153	s_C	240	n	246	i	

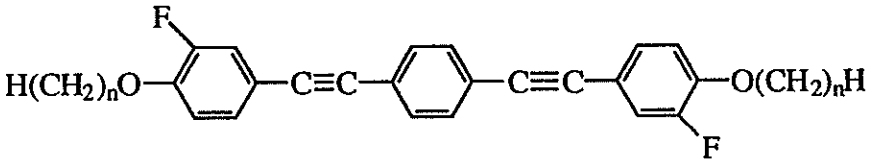

n=7	k	57	k	100	s_E	130	s_C	156	n	196	i	
8			k	99	s_E	128	s_C	159	n	183	i	
9			k	107	s_E	123	s_C	152	n	162	i	
10	k	86	k	95	s_E	117	s_C	156	n	169	i	
11	k	86	k	104	s_E	116	s_C	161	n	173	i	
12	k	70	k	104	s_E	112	s_C	154	n	158	i	

C. Pugh, S.K. Andersson & V. Percec, *Liq. Cryst.*, **10**, 229 (1991)

D. Demus & H. Zaschke, Flussige Kristalle in Tabellen II, VEB Deutscher Verlag, 1984.

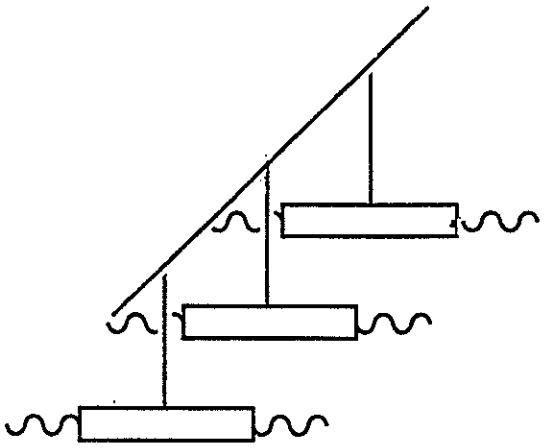

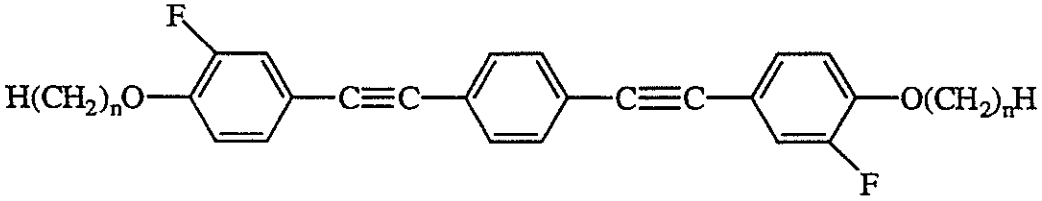
F
H(CH2)nO
C≡C
C≡C
O(CH2)nH
F

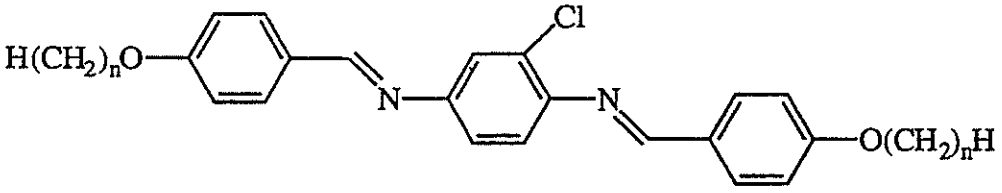
Cl
H(CH2)nO
N
N
O(CH2)nH

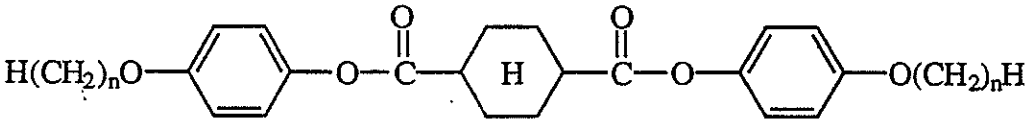
O
O
H(CH2)nO
O
C
H
C
O
O(CH2)nH

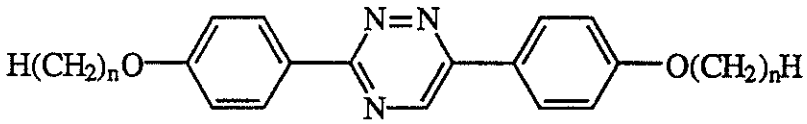
N=N
H(CH2)nO
N
O(CH2)nH

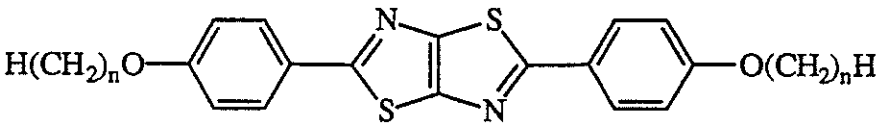
N
S
H(CH2)nO
S
N
O(CH2)nH

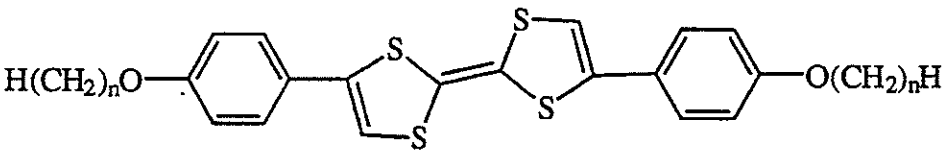
S
S
H(CH2)nO
S
S
O(CH2)nH

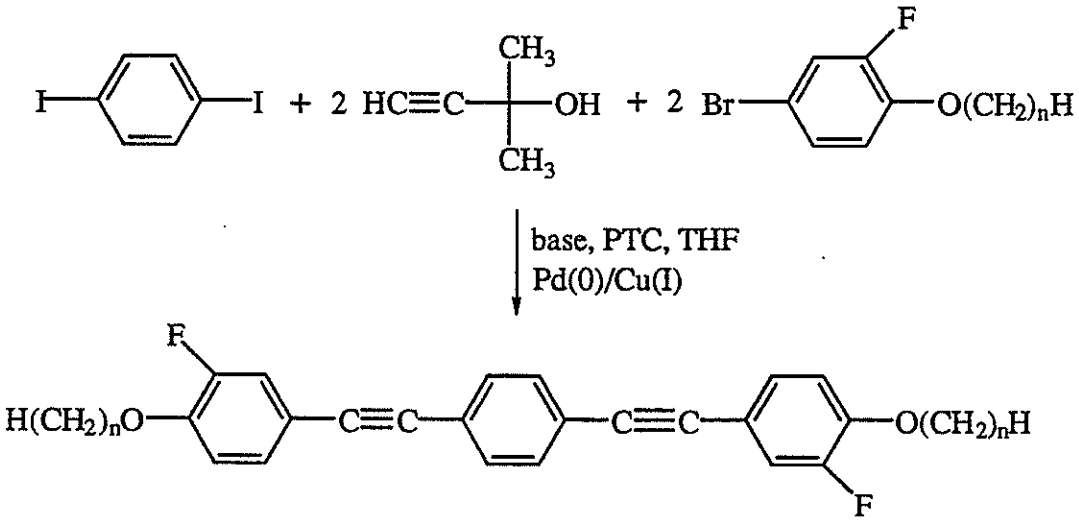

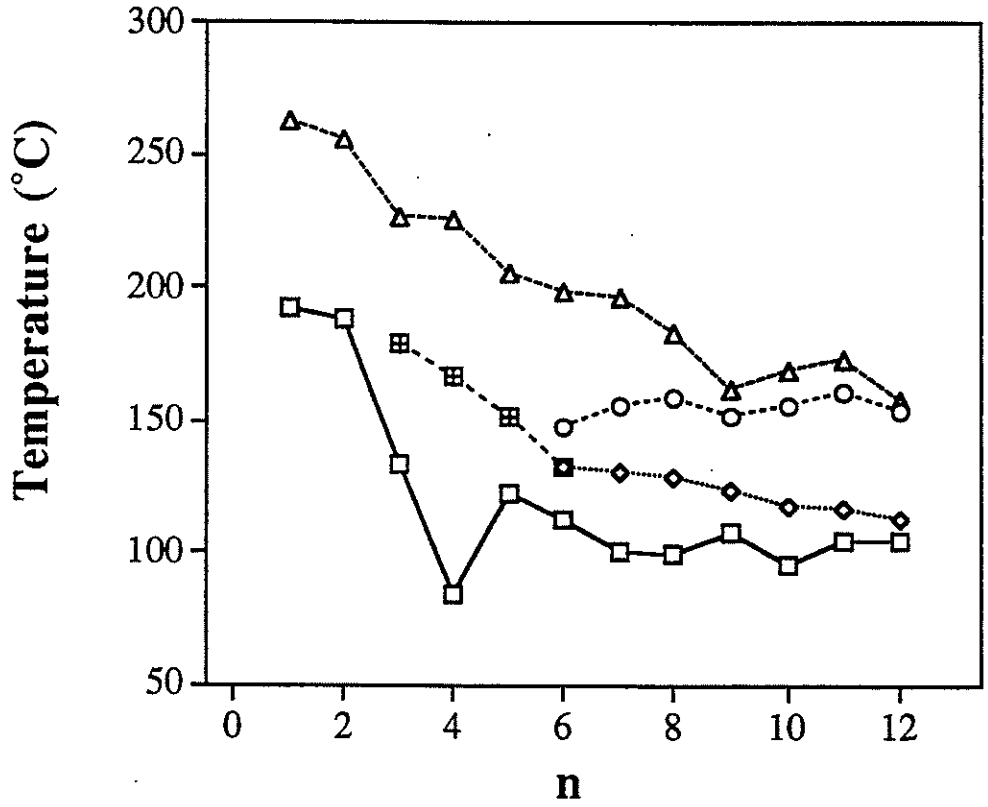

C. Pugh, S.K. Andersson and V. Percec, *Liq. Cryst.*, **10**, 229 (1991); C. Pugh, H. Liu, S.V. Arehart and R. Narayanan, *Macromol. Symp.*, in press.

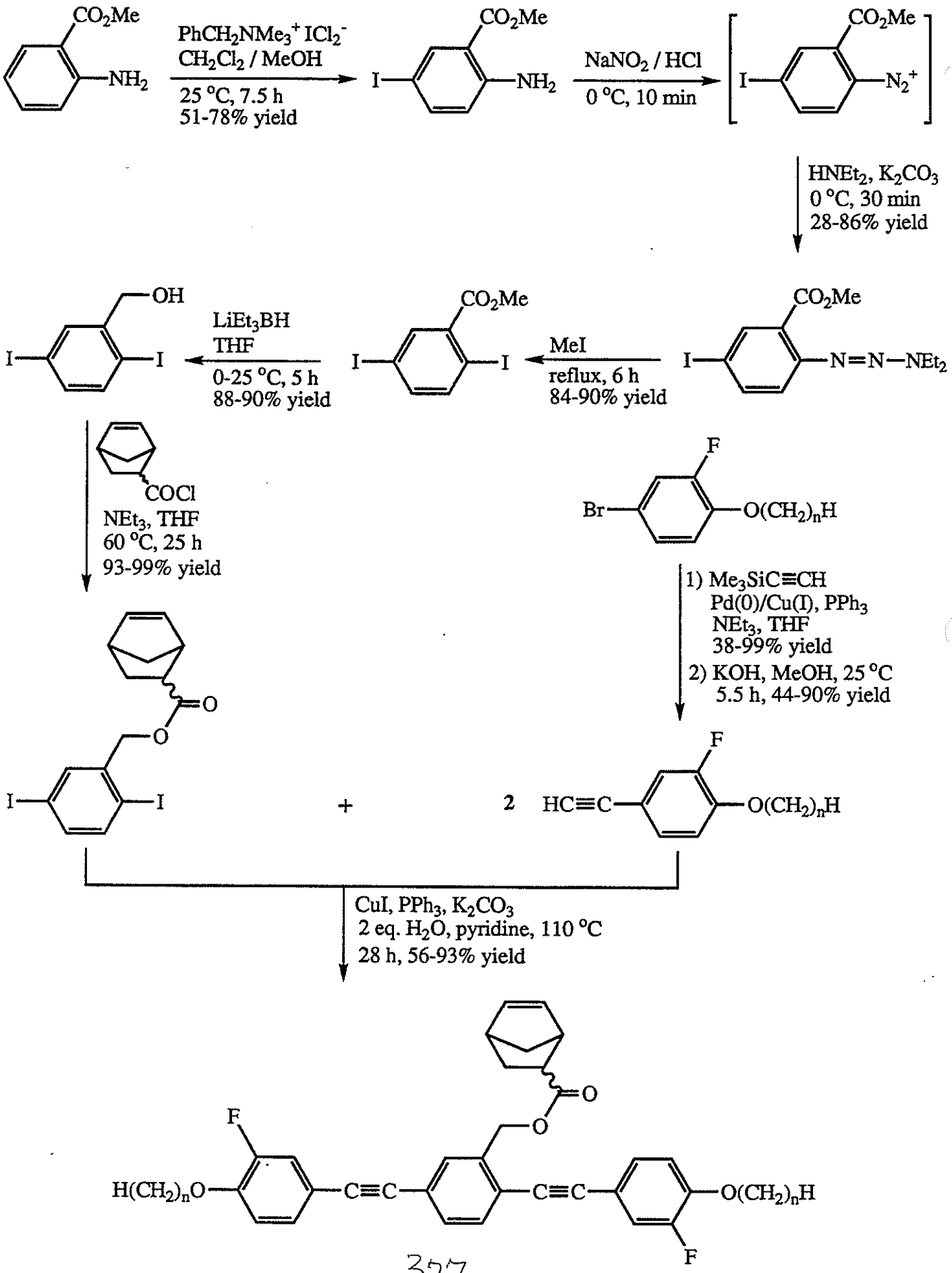
CO2Me
NH2
PhCH2NMe3+ ICl2-
CH2Cl2 / MeOH
25 °C, 7.5 h
51-78% yield
I
NaNO2 / HCl
0 °C, 10 min
N2+
HNEt2, K2CO3
0 °C, 30 min
28-86% yield
N=N—NEt2
MeI
reflux, 6 h
84-90% yield
OH
LiEt3BH
THF
0-25 °C, 5 h
88-90% yield
COCl
NEt3, THF
60 °C, 25 h
93-99% yield
F
Br
O(CH2)nH
1) Me3SiC≡CH
Pd(0)/Cu(I), PPh3
NEt3, THF
38-99% yield
2) KOH, MeOH, 25 °C
5.5 h, 44-90% yield
HC≡C
2
+
CuI, PPh3, K2CO3
2 eq. H2O, pyridine, 110 °C
28 h, 56-93% yield
H(CH2)nO
C≡C

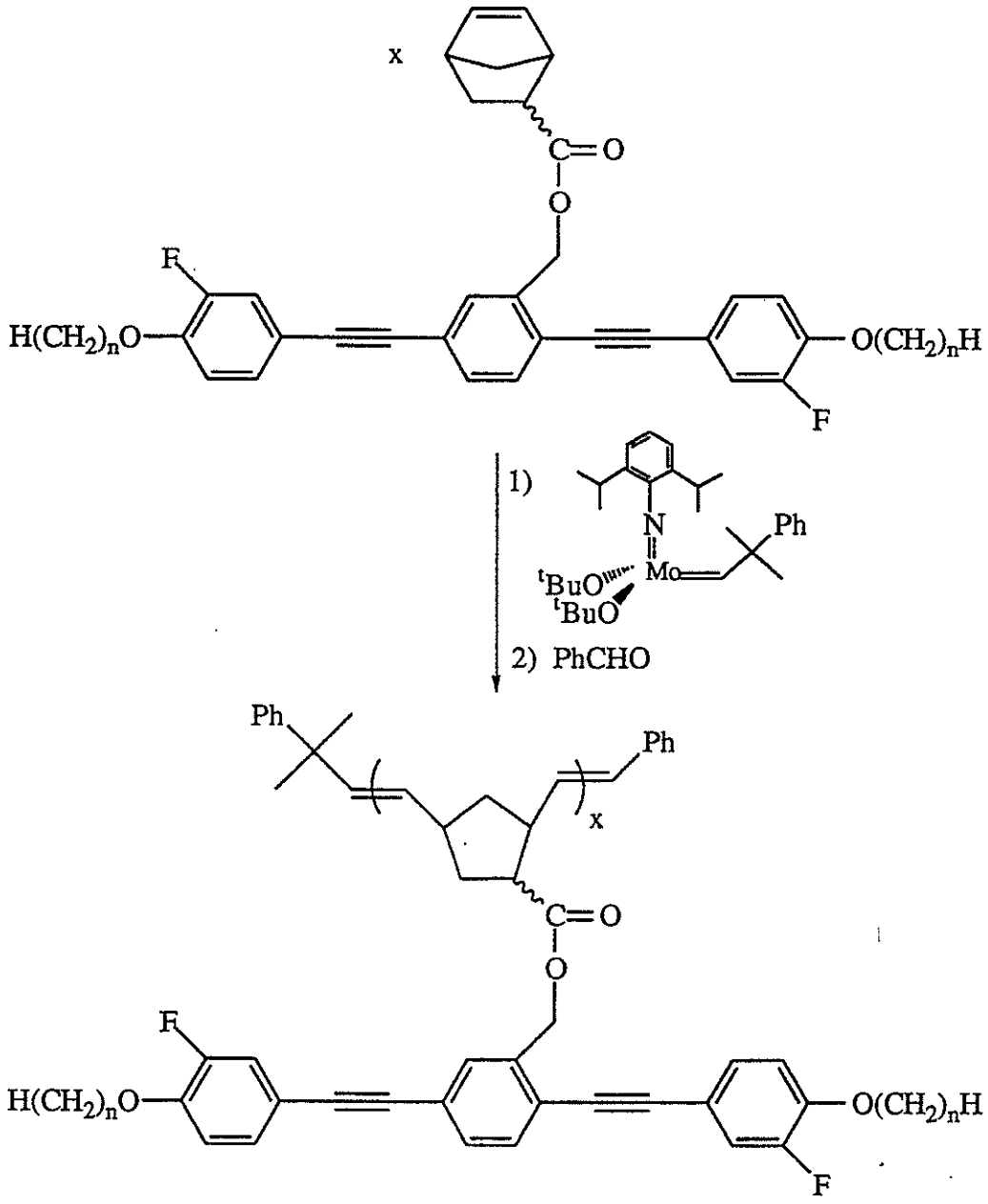

n	$[M]_0/[I]_0$	Theoretical $M_n x10^{-4}$	GPC		GPC/LS	
			$M_n x10^{-4}$	pdi	$M_n x10^{-4}$	pdi
1	44	2.3	2.7	1.12	5.6	1.18
2	51	2.8			4.0	1.17
3	50	2.9			5.2	1.35
4	50	3.0	3.6	1.12	6.6	1.04
5	50	3.2			3.9	1.07
6	50	3.3	2.9	1.16	4.6	1.18
11	50	4.0			4.9	1.19

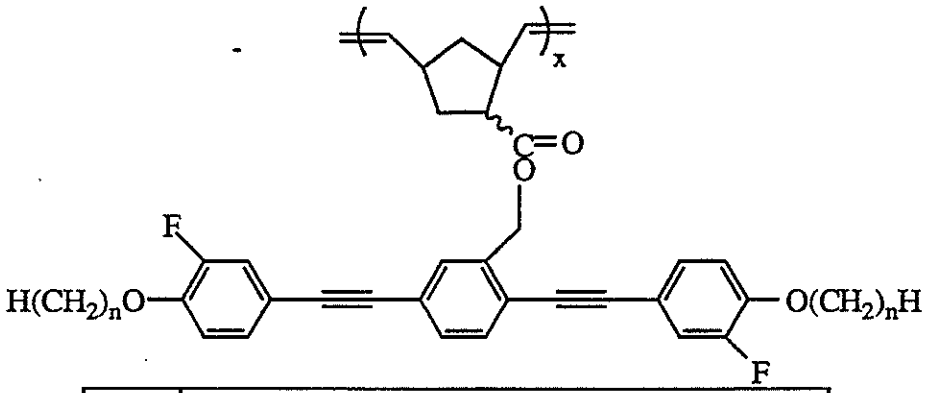

n	Phase Transitions (°C)		
1	g 93	n 120 (1.50)	i
2	g 82	n 134 (1.81)	i
3	g 71	n 113 (1.45)	i
4	g 64	n 115 (1.54)	i
5	g 56	n 106 (1.46)	i
6	g 55	n 107 (1.39)	i
7			
8			
9			
10			
11	g 40	s_C? 98 (2.50)	i
12			

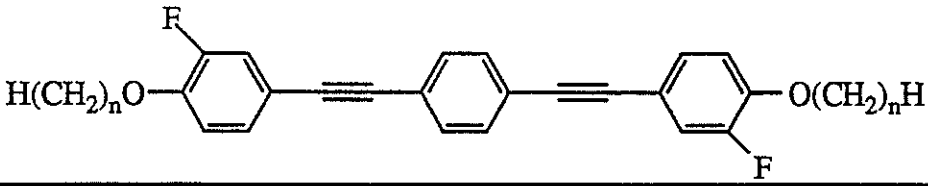

n	Phase Transitions (°C)			
1	k 192			n 263 i
2	k 188			n 256 i
3	k 134	s_E 179		n 226 i
4	k 84	s_E 167		n 225 i
5	k 122	s_E 152		n 205 i
6	k 112	s_E 132	s_C 148	n 198 i
7	k 100	s_E 130	s_C 156	n 196 i
8	k 99	s_E 128	s_C 159	n 183 i
9	k 107	s_E 123	s_C 152	n 162 i
10	k 95	s_E 117	s_C 156	n 169 i
11	k 104	s_E 116	s_C 161	n 173 i
12	k 104	s_E 112	s_C 154	n 158 i

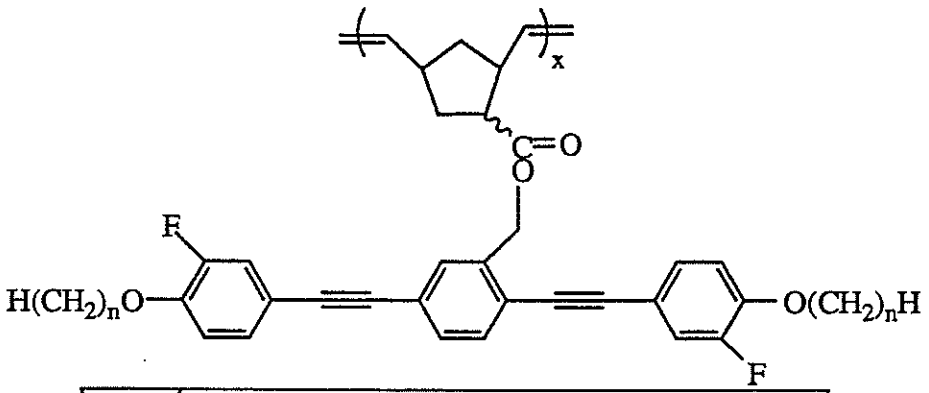

n	Phase Transitions (°C)		
4	g 64	n 115 (1.54)	i
5	g 56	n 106 (1.46)	i
7			
10			
11	g 40	s_C? 98 (2.50)	i

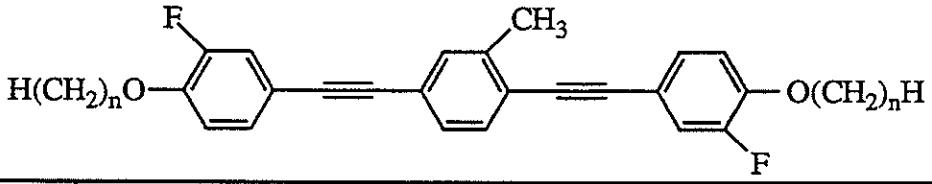

n	Phase Transitions (°C)	
4	k 101	n 177 i
5	k 88	n 201 i
7	k	i
10	k	i
11	k	i

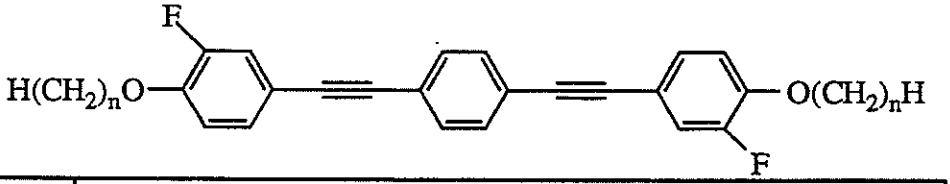

n	Phase Transitions (°C)			
4	k 84	s_E 167		n 225 i
5	k 122	s_E 152		n 205 i
7	k 100	s_E 130	s_C 156	n 196 i
10	k 95	s_E 117	s_C 156	n 169 i
11	k 104	s_E 116	s_C 161	n 173 i

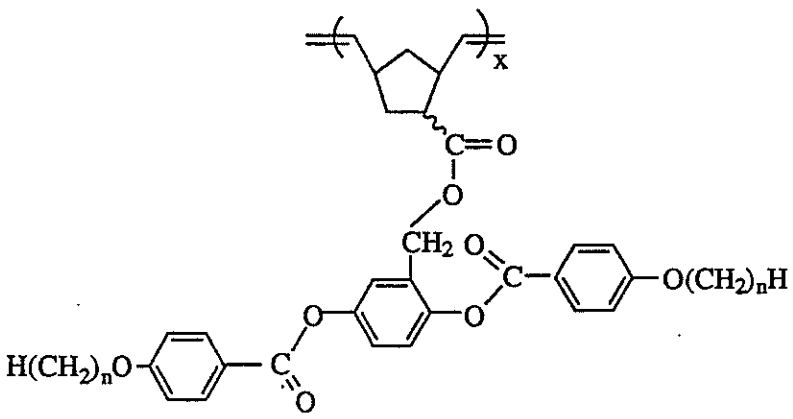

n	Phase Transitions (°C)
1	g 97 n 162 i
2	g 92 n 172 i
3	g 83 n 140 i
4	g 73 n 138 i
5	g 60 n 123 i
6	g 56 n 126 i

C. Pugh & R.R. Schrock, *Macromolecules*, **25**, 6593 (1992).

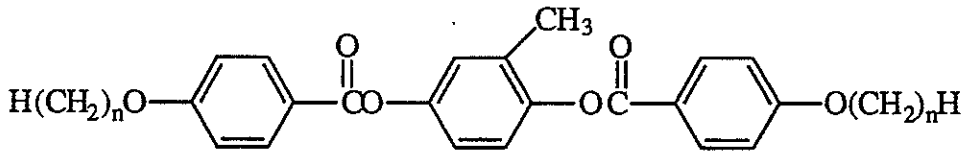

n	Phase Transitions (°C)	Ref.
1	k 166 n 252 i	1
2	k 187 n 248 i	1
3	k 138 n 209 i	1
4	k 115 n 206 i	1
5	k 90 n 178 i	1
6	k 88 n 173 i	1
7	k 86 n 161 i	2
8	k 40 n 157 i	2
9	k 79 n 148 i	2
10	k 83 n 139 i	2
11	k 81 (s_C 80) n 140 i	2
12	k 81 s_C 88 n 140 i	2

(1) D. Demus & H. Zaschke, *Flussige Kristalle in Tabellen II*, VEB Deutscher Verlag, Liepzig, 1984; (2) current.

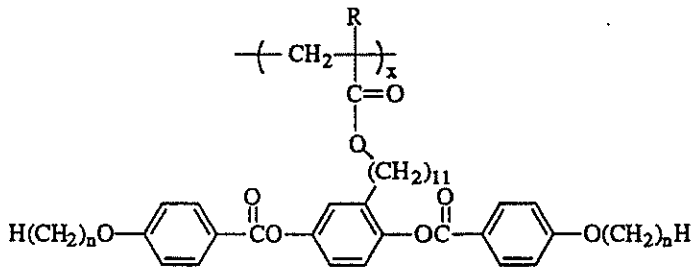

n	R = H	R = Cl	R = CH_3
1	g 14 n 44 i	g 36 n 59 i	g 38 n 62 i
2	(g 12 n 74) k 91 i	(g 31 n 79) k 92 i	(g 32 n 82) k 92 i
3	g 11 n 58 i		g 26 n 58 i
4	g 4 n 67 i	g 20 n 66 i	g 19 n 67 i
5			g 10 n 51 i
6	g -9 n 59 i		g 5 n 60 i
7			g 1 n 48 i
8	g -13 k 33 n 61 i	g 0 n 60 i	g -2 n 61 i

F. Hessel & H. Finkelmann, *Makromol. Chem.*, **189**, 2275 (1988).

F. Hessel & H. Finkelmann, *Polym. Bull.*, **14**, 375 (1985); F. Hessel, R.-P. Herr & H. Finkelmann, *Makromol. Chem.*, **188**, 1597 (1987).

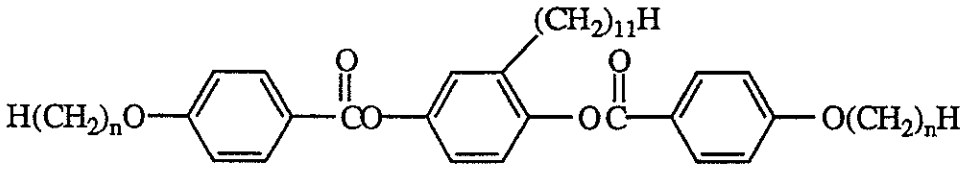

n	Phase Transitions (°C)
1	k 82 (n 58) i
2	k 121 (n 81) i
3	k 89 (n 56) i
4	k 74 (n 71) i
5	k 76 (n 62) i
6	k 71 (n 69) i
7	k 68 n 68 i
8	k 52 n 72 i

D. Demus & H. Zaschke, *Flussige Kristalle in Tabellen II*, VEB Deutscher Verlag, Leipzig, 1984.

Low Molar Mass Model Compounds

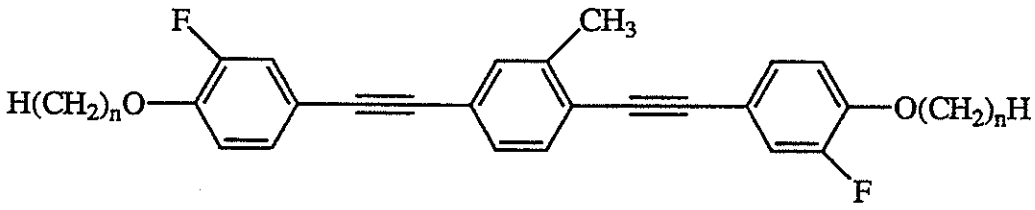

Most Appropriate for?

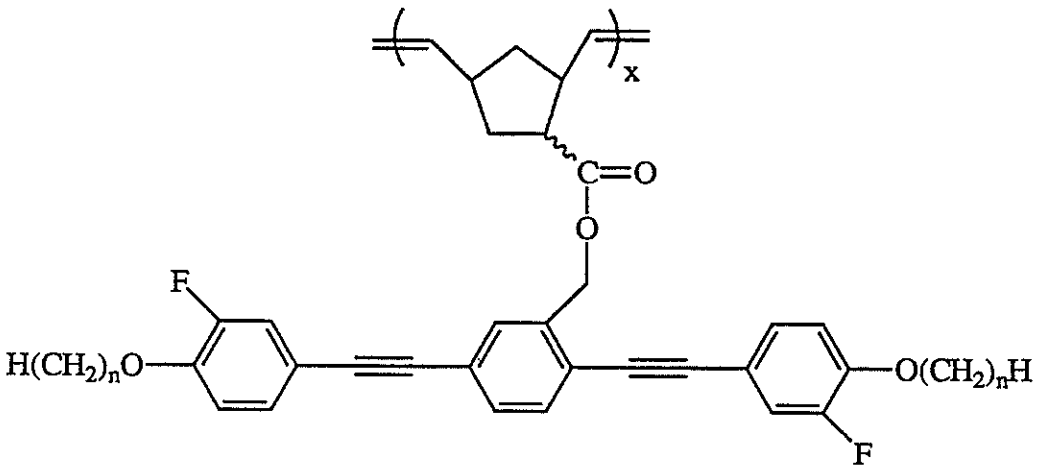

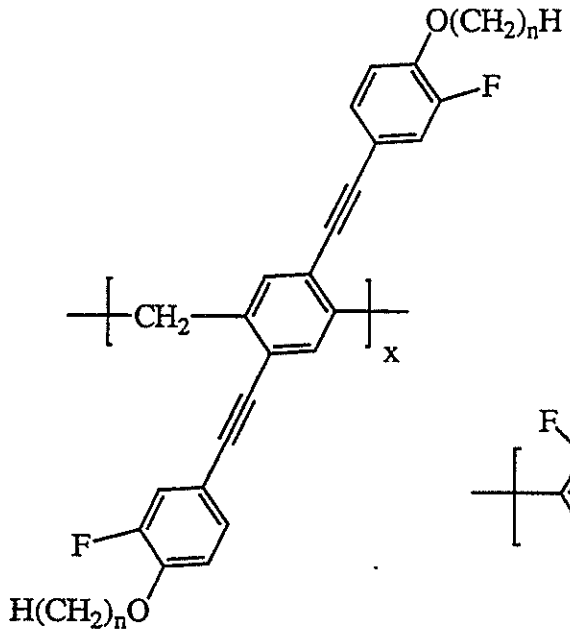

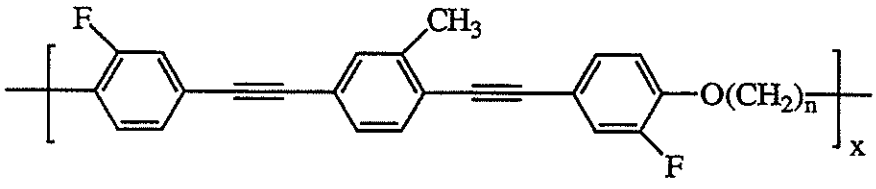

Polydispersity

Eg. S.G. Kostromin, R.V. Talroze, V.P. Shibaev & N.A. Platé, *Makromol. Chem., Rapid Commun.*, 3, 803 (1982).

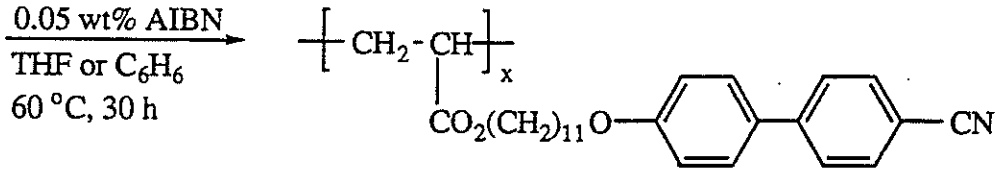

1c - original polymer separated into fractions (fractional precipitation of 1,2-dichloroethane with ethanol):

I	$[\eta] = 0.18$ dl/g	
II	$[\eta] = 0.11$	30 °C in 1,2-dichloroethane
III	$[\eta] = 0.08$	
IV	$[\eta] = 0.065$	

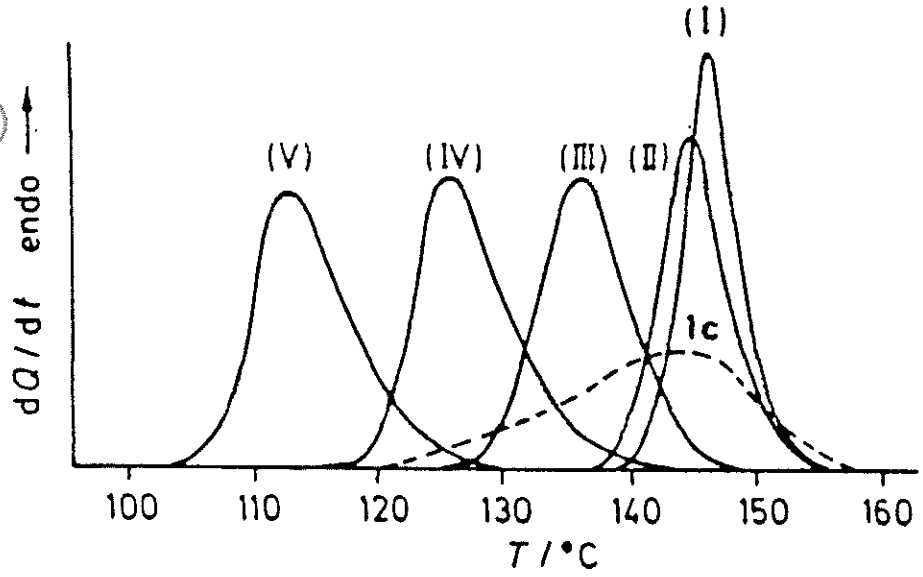

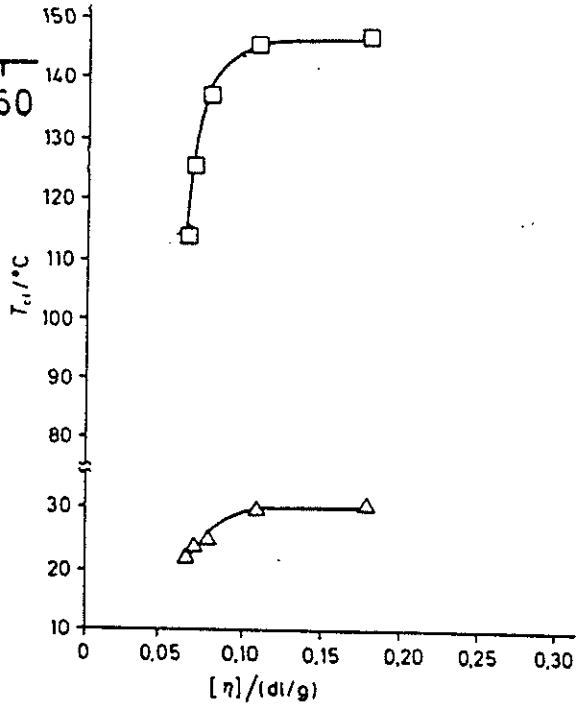

◇ S_A - i

Δ S_C - S_A

E. Komiya, C. Pugh & R.R. Schrock, Macromolecules, 25, 3609 (1992).

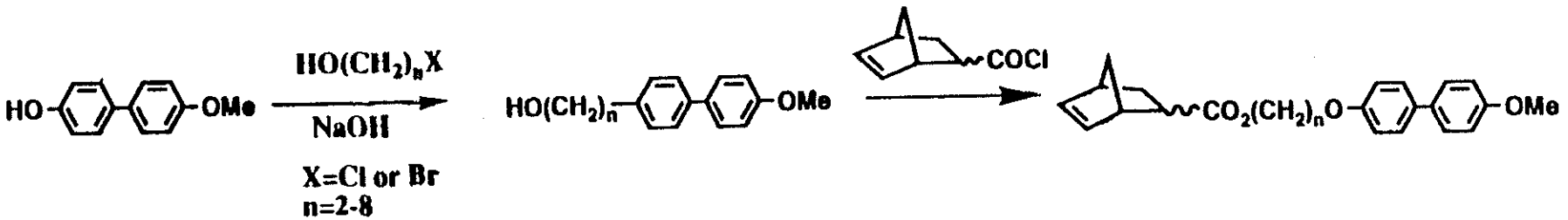

S85

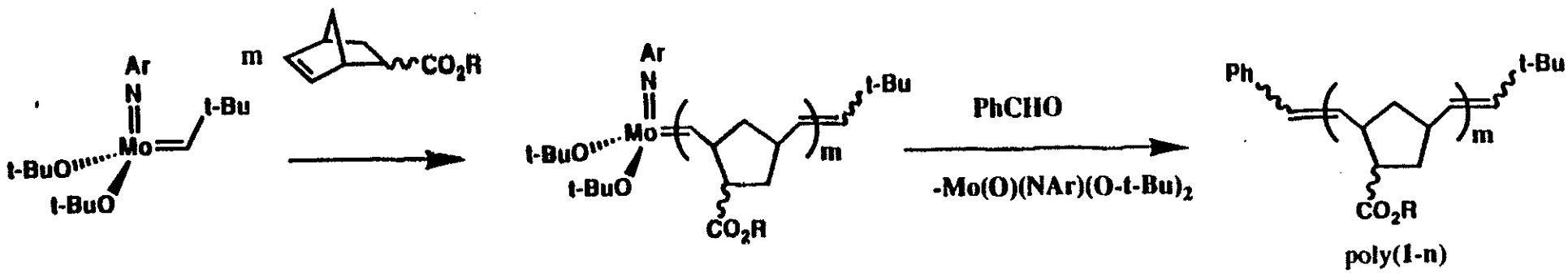

n = 2-8

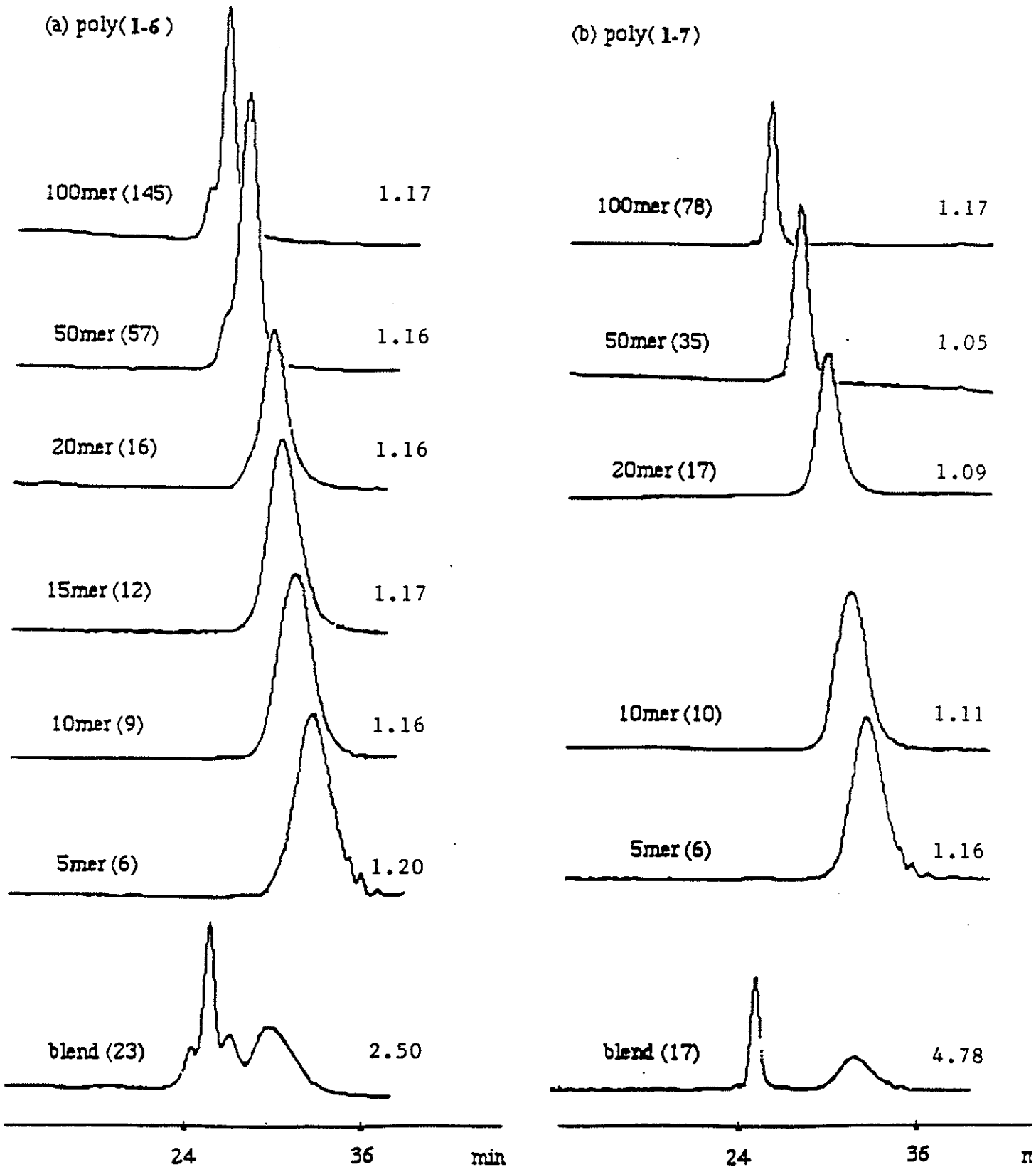
(a) poly(1-6)
100mer (145)
1.17
50mer (57)
1.16
20mer (16)
1.16
15mer (12)
1.17
10mer (9)
1.16
5mer (6)
1.20
blend (23)
2.50
24
36
min
(b) poly(1-7)
100mer (78)
1.17
50mer (35)
1.05
20mer (17)
1.09
10mer (10)
1.11
5mer (6)
1.16
blend (17)
4.78
24
36

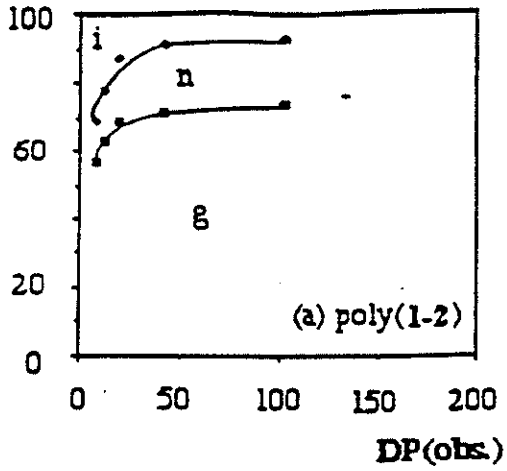
100
60
20
0
i
n
g
(a) poly(1-2)
0
50
100
150
200
DP(obs.)

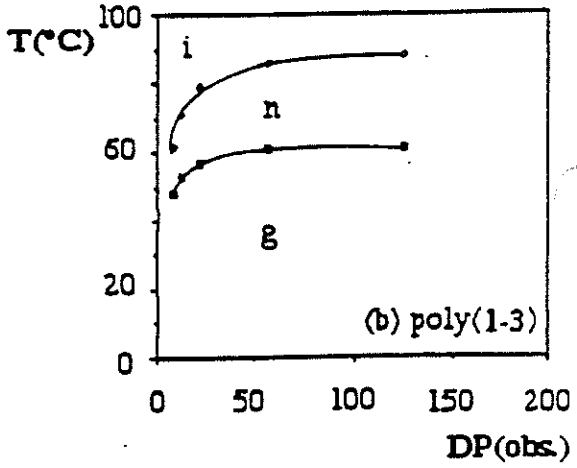
T(°C)
100
60
20
0
i
n
g
(b) poly(1-3)
0
50
100
150
200
DP(obs.)

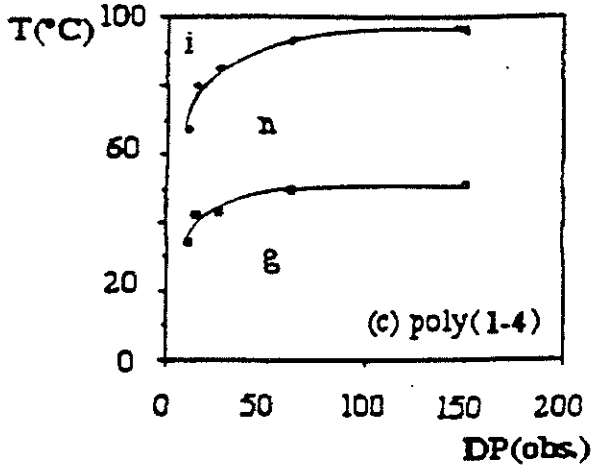
T(°C)
100
60
20
0
i
n
g
(c) poly(1-4)
0
50
100
150
200
DP(obs.)

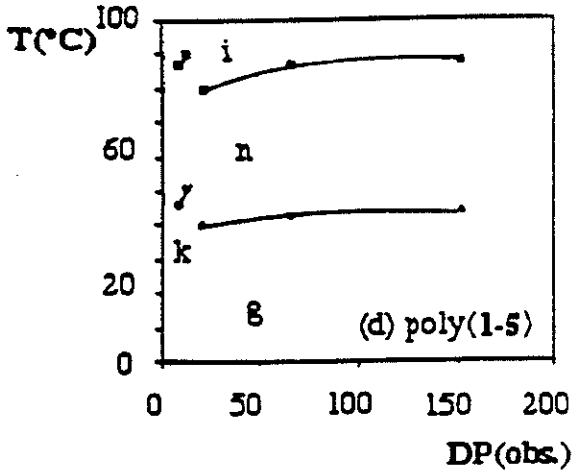
T(°C)
100
60
20
0
i
n
k
g
(d) poly(1-5)
0
50
100
150
200
DP(obs.)

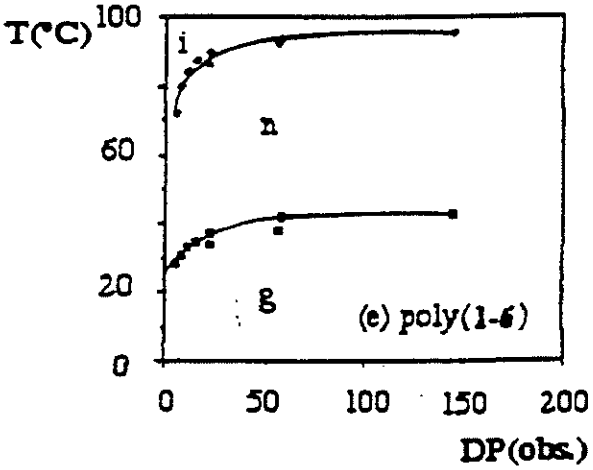
T(°C)
100
60
20
0
i
n
g
(e) poly(1-6)
0
50
100
150
200
DP(obs.)

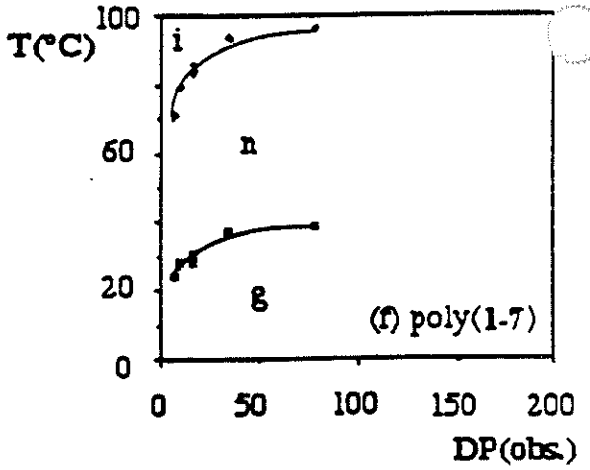
T(°C)
100
60
20
0
i
n
g
(f) poly(1-7)
0
50
100
150
200
DP(obs.)

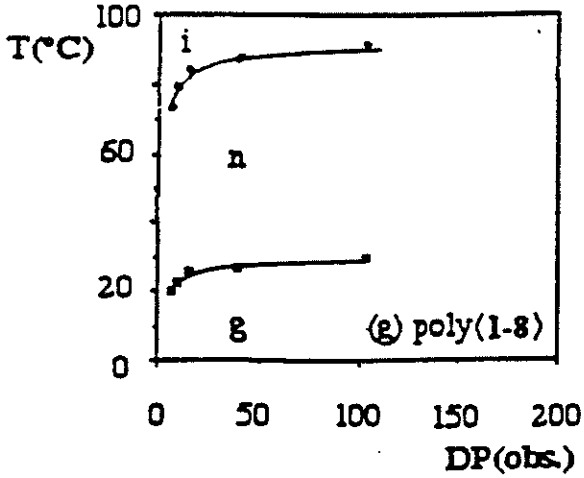
T(°C)
100
60
20
0
i
n
g
(g) poly(1-8)
0
50
100
150
200
DP(obs.)

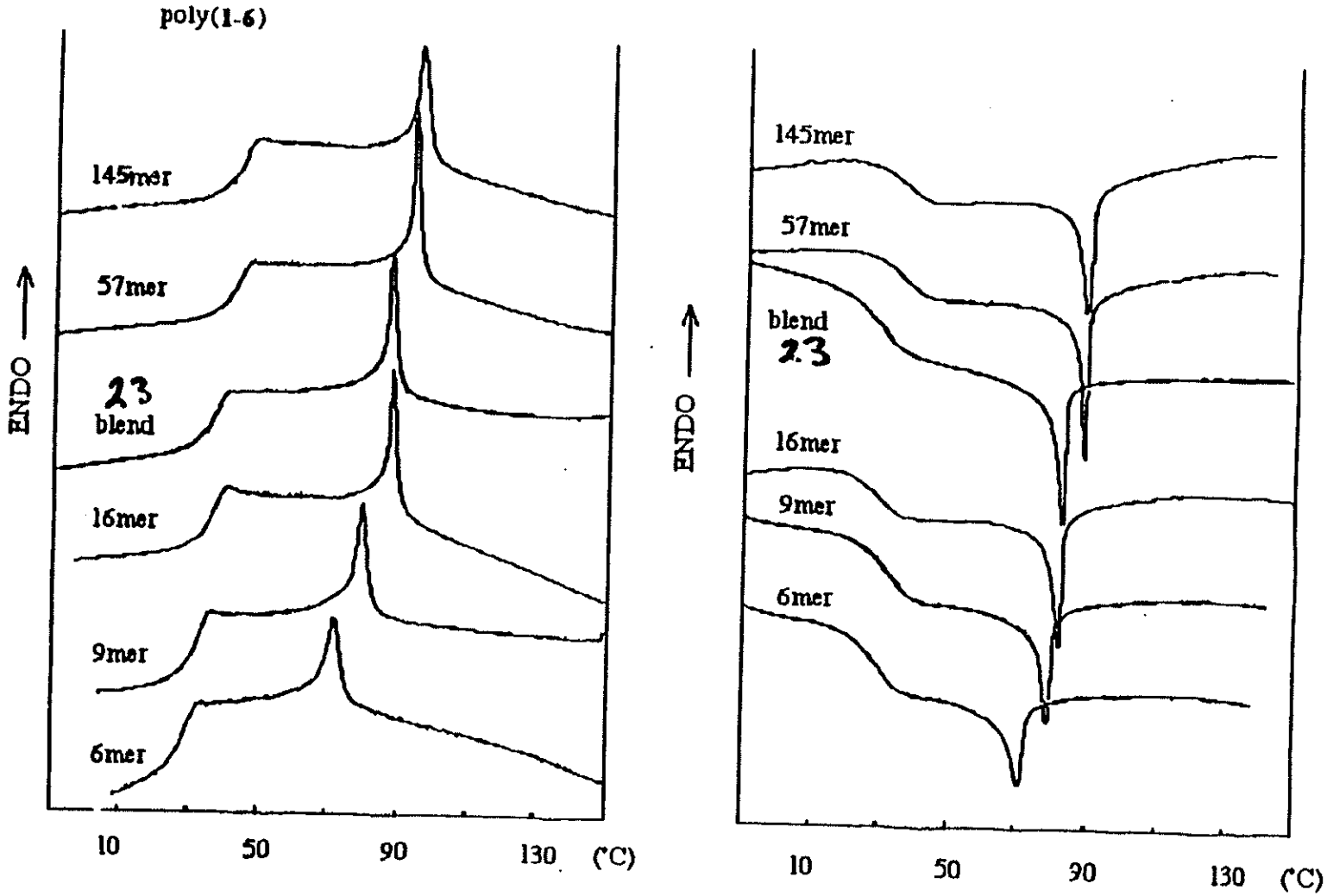
poly(1-6)
145mer
57mer
23
blend
16mer
9mer
6mer
ENDO
10
50
90
130
(°C)
145mer
57mer
blend
23
16mer
9mer
6mer
ENDO
10
50
90
130
(°C)

Polydispersity in Polystyrene

pdi	Polymerization Conditions
1.0	Living polymerization. Anionic: Na/naphthalene, in benzene, 25 °C
1.5	Free radical polymerization under conditions which avoid autoacceleration; incomplete conversion. (Termination by coupling.) AIBN, in benzene, 60 °C, 70% conversion.
2.0	Free radical polymerization under conditions which prevent termination by coupling of 2 chains (chain transfer agent); incomplete conversion. AIBN, *n*-BuSH, in benzene, 60 °C, 70% conversion.
5	Bulk radical polymerization at lower temperature to promote autoacceleration without chain transfer to polymer. AIBN/hν or redox (*t*-BuO-OH/Fe^{2+}), bulk, 25 °C, complete conversion.
>10	Free radical polymerization under conditions which promote chain transfer to polymer. AIBN, bulk, 60 °C, complete conversion.

Rod-Like Mesogens

MAIN CHAIN LCPs

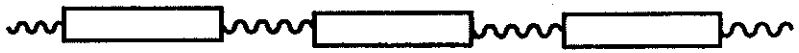

SIDE CHAIN LCPs

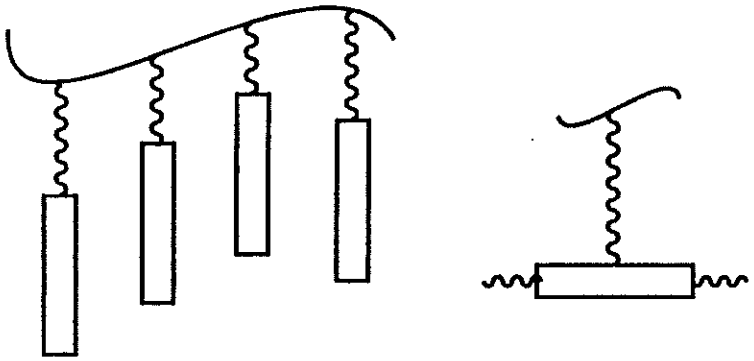

Polar Substituents: $-OCH_3$, -CN, -F, -Cl, $-NO_2$

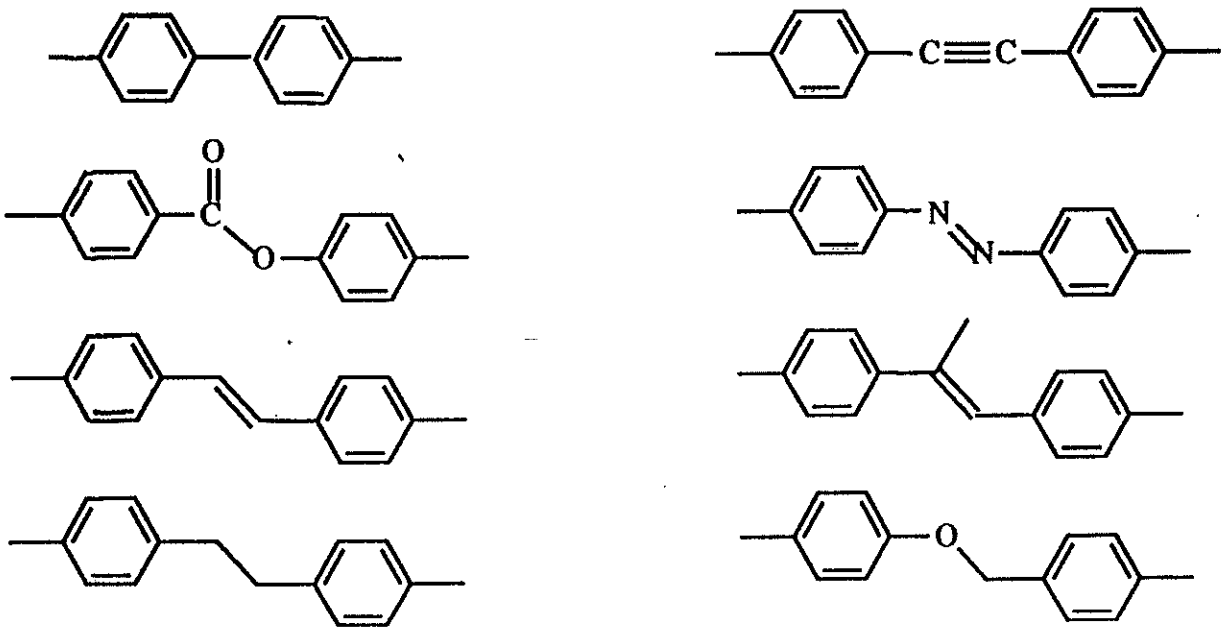

Chain Transfer Constants ($C_S=k_{tr}/k_p$) in Radical Polymerizations

Methyl Acrylate	$C_S \times 10^4$	T (°C)	Methyl Methacrylate	$C_S \times 10^4$	T (°C)
	0.45	80	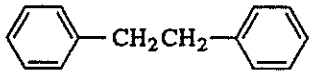	0	50
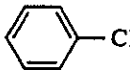	0.986	80	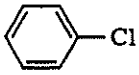	0.074	60
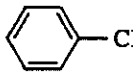	< 1	50	$CH_3CO_2CH_2CH_3$	0.13	60
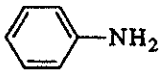	< 1	50	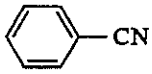	0.162	60
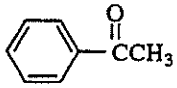	< 2.5	50		0.176	70
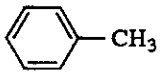	2.7	60	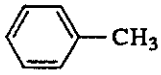	0.2	60
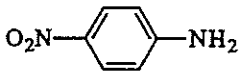	26.7	50	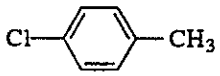	0.49	60
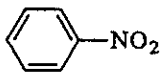	46.4	50	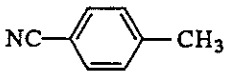	0.73	60
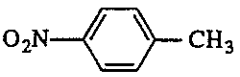	48.6	50	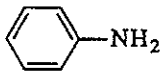	4.2	60
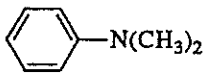	60	50	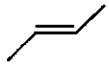	5.2	50
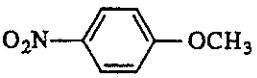	72.7	50	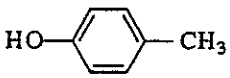	6.0	50
			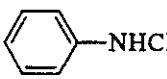	7.0	60
			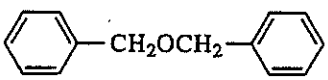	8.0	60
			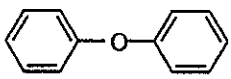	9.13	60
			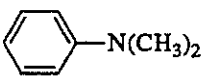	11.3	60
			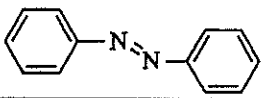	100	50

Radical Reactivity:

VAc· > AN· > MA· > MMA· > St·

Polydispersity

due to

- non-uniform mixture of linear chains
- chain branching / non-uniform mixture of molecular architectures

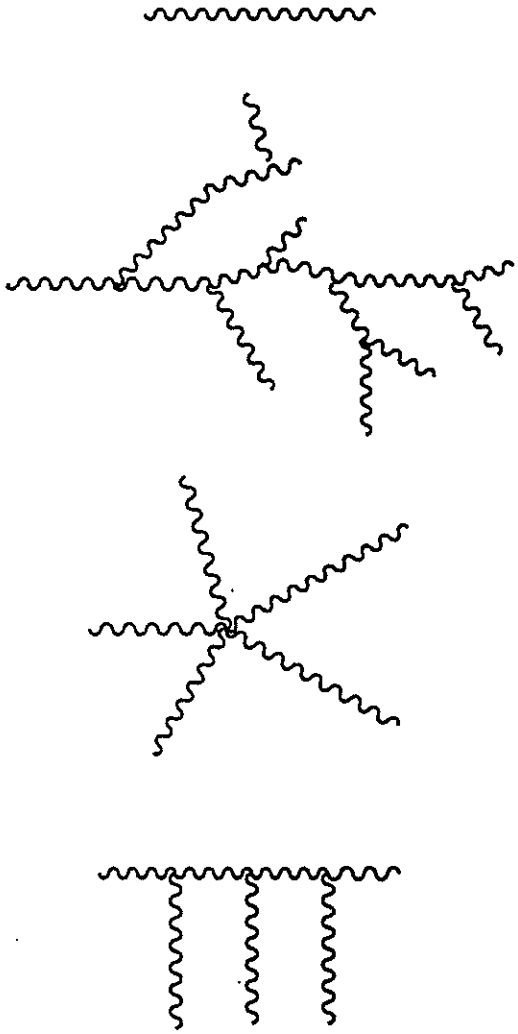

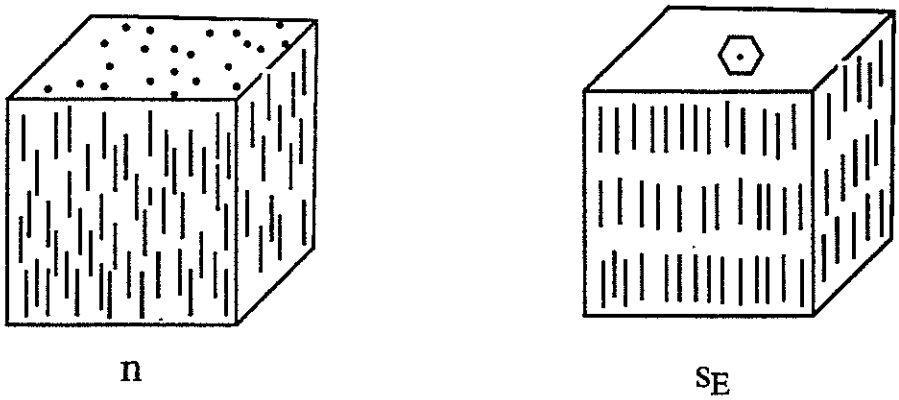

n s_E

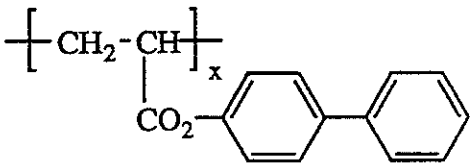

atactic g 110 s 280 i
isotactic g 110 s 233 i

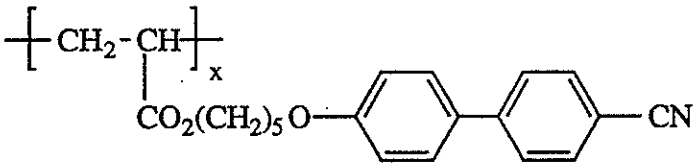

n 115 i

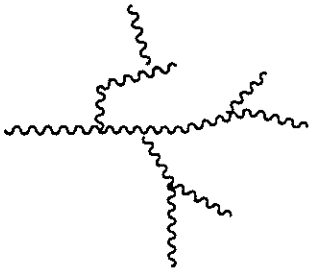

Literature and/or conventional free radical polymerization.

AIBN, in benzene, 60 °C, high conversion

(^{t}BuO)$_2$, bulk, 120 °C, high conversion

Atom transfer radical polymerization.

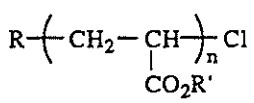

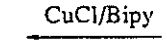

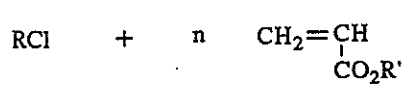

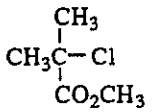

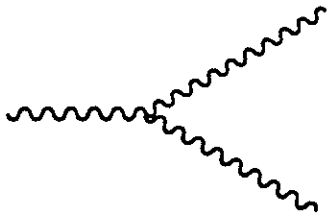

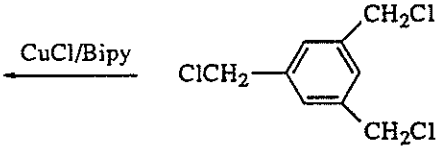

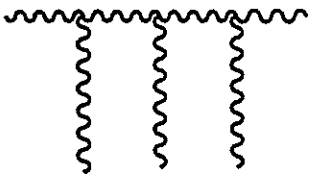

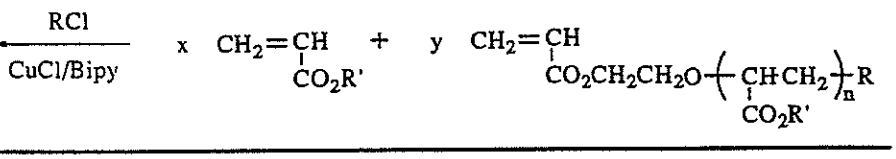

Regulating / Transforming Mesophases

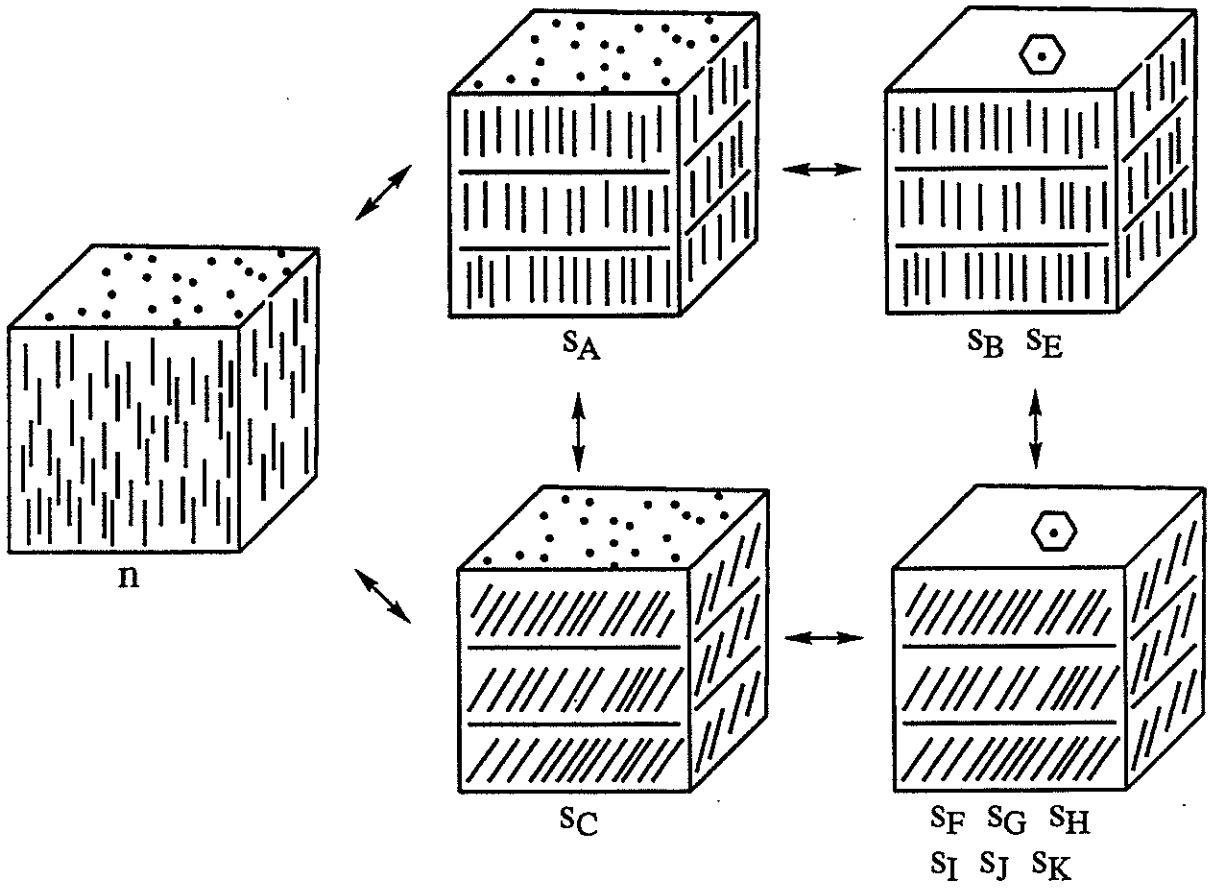

Eg. Nematic → Smectic

A. Specific Interactions

Electron - Donor Acceptor Interactions

Hydrogen Bonding

B. Immiscible Components

D. Demus, G. Pelzl, N.K. Sharma and W. Weissflog, *Mol. Cryst. Liq. Cryst.*, **76**, 241 (1981).

A 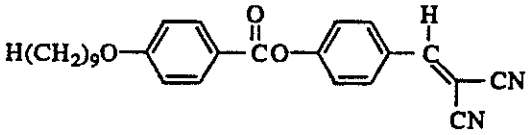

B 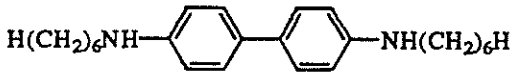

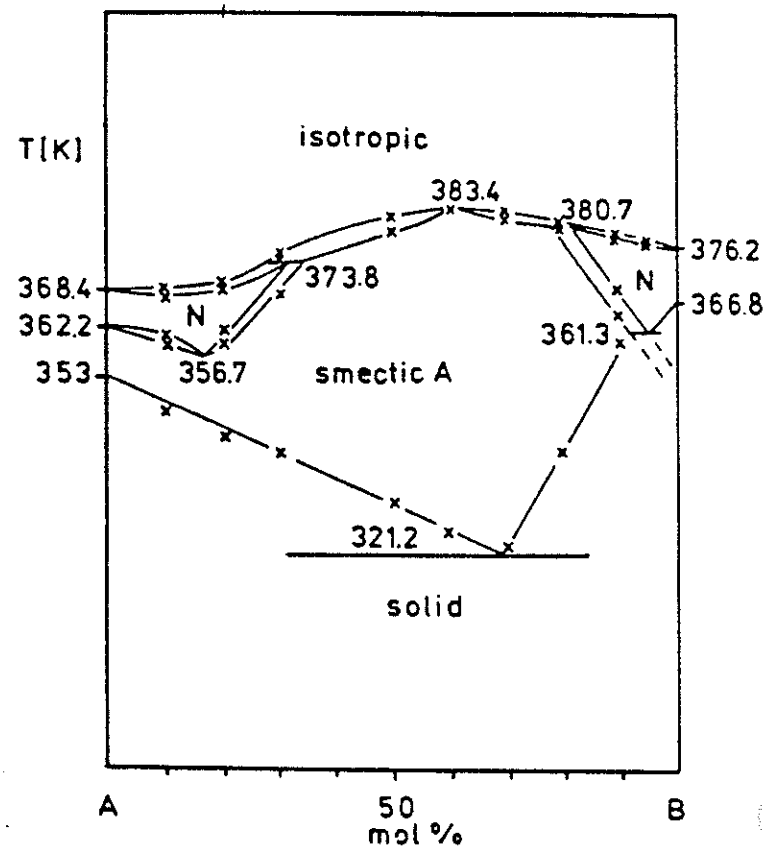

A 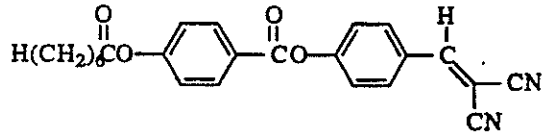

B 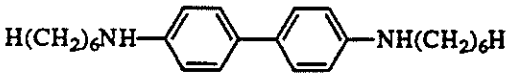

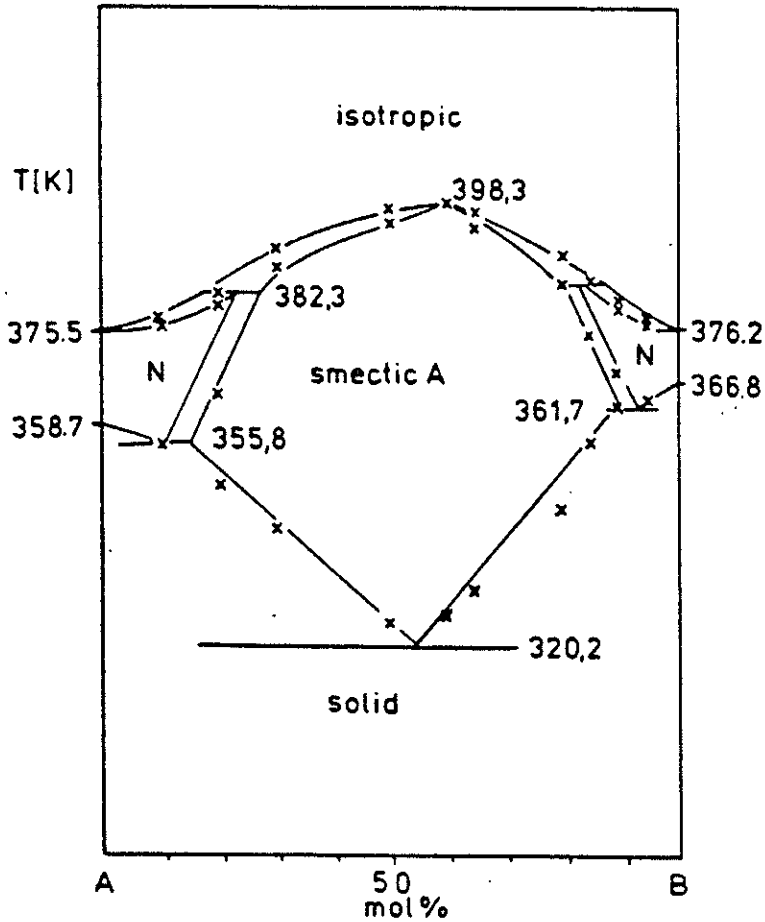

395

T. Schleeh, C.T. Imrie, D.M. Rice, F.E. Karasz and G.S. Attard, *J. Polym. Sci., Polym. Chem. Ed.*, **31**, 1859 (1993).

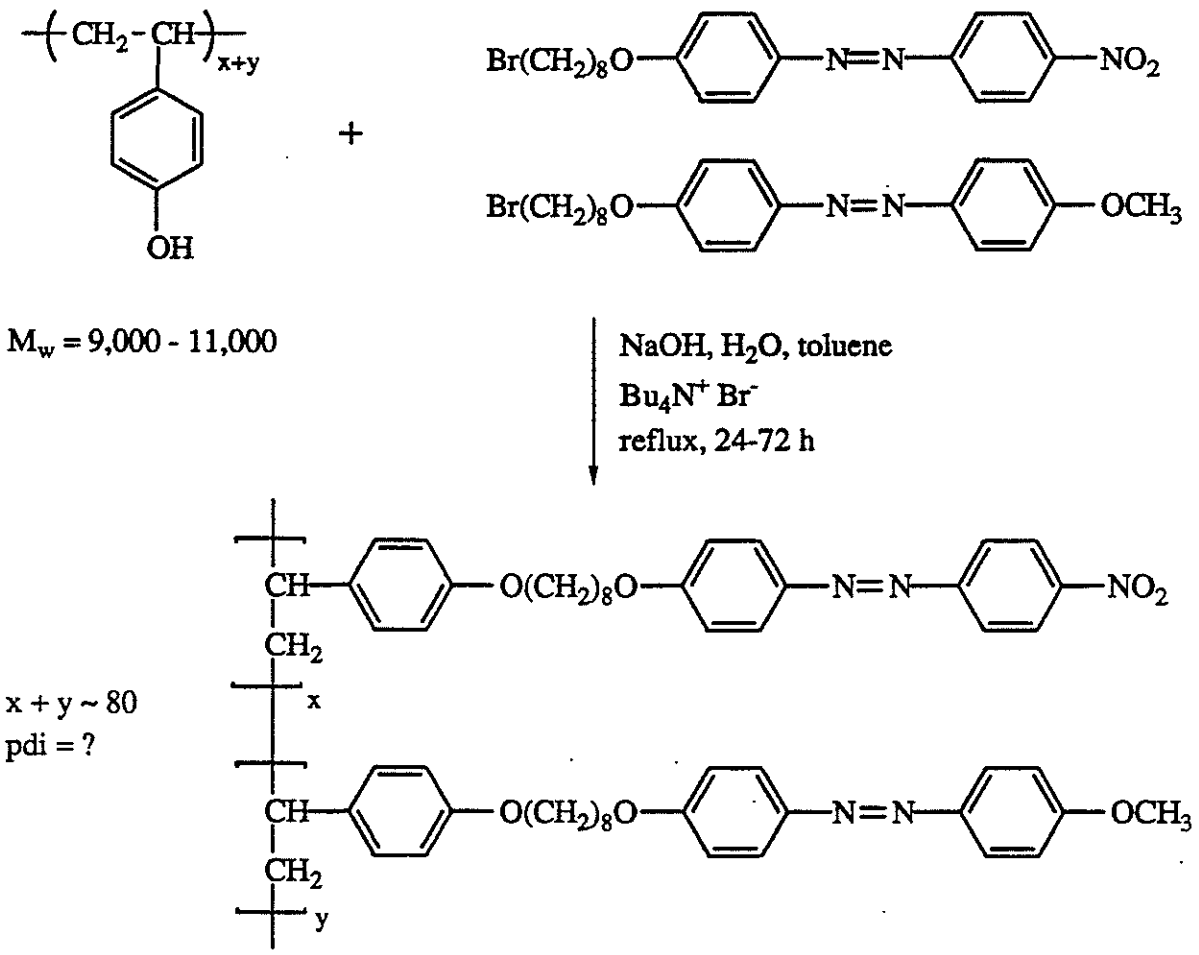

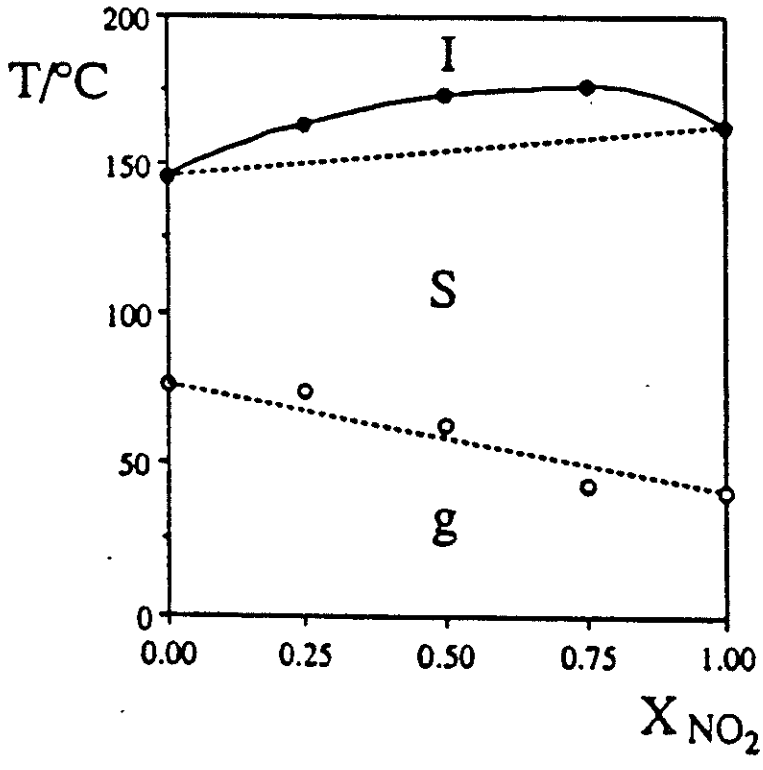

396

Y. Kosaka and T. Uryu, *Macromolecules*, **27**, 6286 (1994); *ibid*, **28**, 870 (1995).

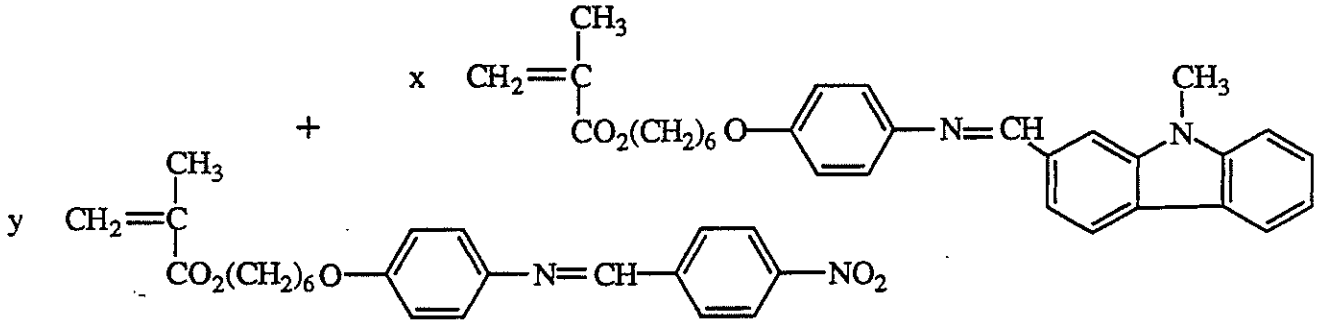

3 mol% AIBN
C_6H_6 or DMF
70 °C, 20 h

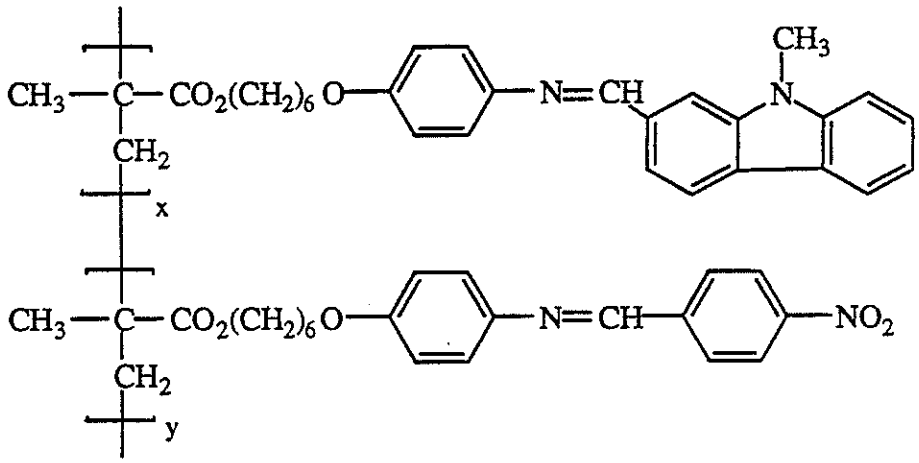

M_w = (1.62-2.75) x 10^4
pdi = 2.28-3.02

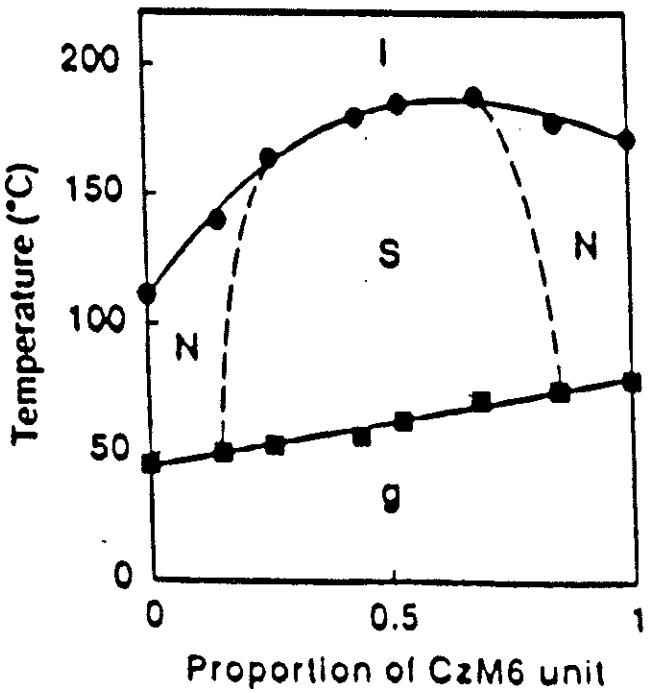

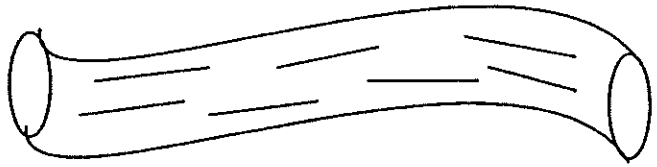

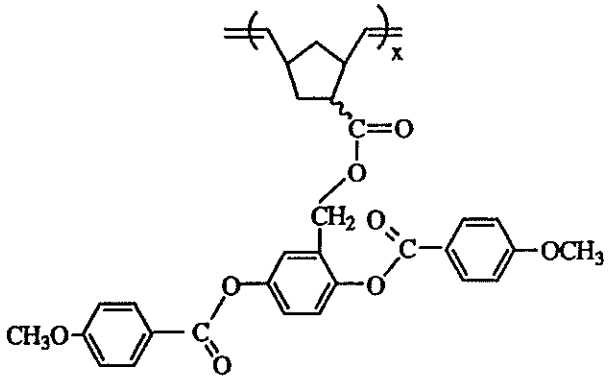

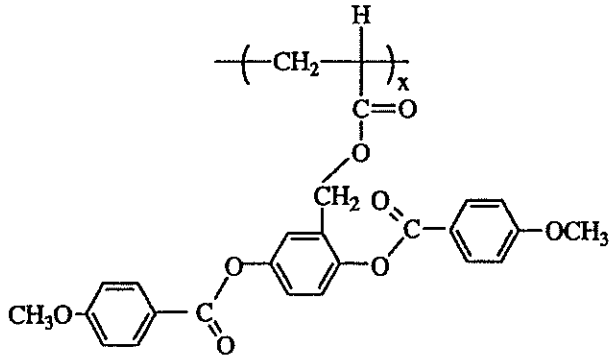

g 97 n 163 i [1]

g 103 n 160 i [2]

Poly(norbornene) T_g = 40 °C

Poly(methylacrylate) T_g = 5 °C

1) C. Pugh & R.R. Schrock, *Macromolecules*, **25**, 6593 (1992).

2) Q.-F. Zhou, H.-M. Li & X.-D. Feng, *Mol. Cryst. Liq. Cryst.*, **155**, 73 (1988); *Macromolecules*, **20**, 233 (1987).

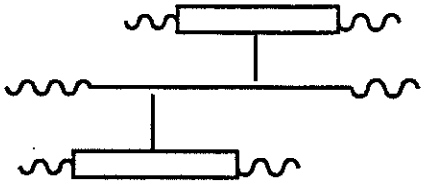

nematic

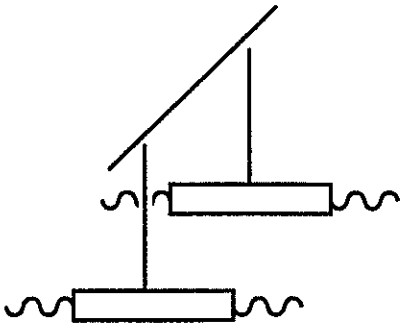

smectic

$n \geq 4\text{-}6,\ m > 6$

$$H(CH_2)_n(CF_2)_mF$$

n = 0	**m = 12**	**k 72 i**
2		**k 71 i**
4		**k 41 s 76 i**
6		**k 43 s 84 i**
8		**k 56 s 88 i**
10		**k 69 s 92 i**
12		**k 79 s 91 i**
14		**k 90 s 93 i**
16		**k 90 i**

$$F(CF_2)_m(CH_2)_n(CF_2)_mF$$

n = 8	**m = 10**	**k 114 i**
n = 10	**m = 12**	**k 98 s 129 i**

W. Mahler, D. Guillon & A. Skoulios, *Mol. Cryst. Liq. Cryst.*, 2, 111 (1985); T.P. Russel, J.F. Rabolt, R.J. Twieg, R.L. Siemens and B.L. Farmer, *Macromolecules*, **19**, 1135 (1986); J. Höpken, C. Pugh, W. Richtering & M. Möller, *Makromol. Chem.*, **189**, 911 (1987); C. Viney, T.P. Russell, L.E. Depero & R.J. Twieg, *Mol. Cryst. Liq. Cryst.*, **168**, 63 (1989).

L.M. Wilson and A.C. Griffin, *Macromolecules,* **26**, 6312 (1993); T. Davidson, A.C. Griffin, L.M. Wilson and A.H. Windle, *Macromolecules,* **28**, 354 (1995).

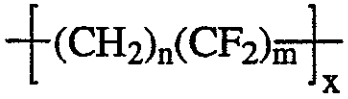

n	m	Phase Transitions (°C)
7	4	k 112 s_B 152 i
8		k 118 s_B 155 i
9		k 133 s_B 148 i
10		k 124 s_B 144 i
11		k 125 s_B 135 i
12		k 119 s_B 131 i
13		k 112 s_B 128 i
14		k 121 s_B 129 i
6	6	k 147 s_B 183 i
7		k 137 s_B 155 i
8		k 125 s_B 165 i
9		k 110 s_B 148 i
10		k 100 s_B 151 i
11		k 105 s_B 134 i
12		k 120 s_B 145 i
13		k 117 s_B 139 i
14		k 114 s_B 141 i

Molecular Phase Separation

≥ Two different structures

<u>form anisotropy</u>
structurally different

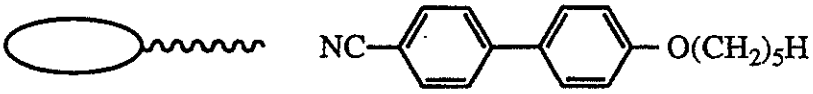

<u>chemical anisotropy</u>
amphiphiles

$F(CF_2)_m(CH_2)_nH$

thermotropic liquid crystals

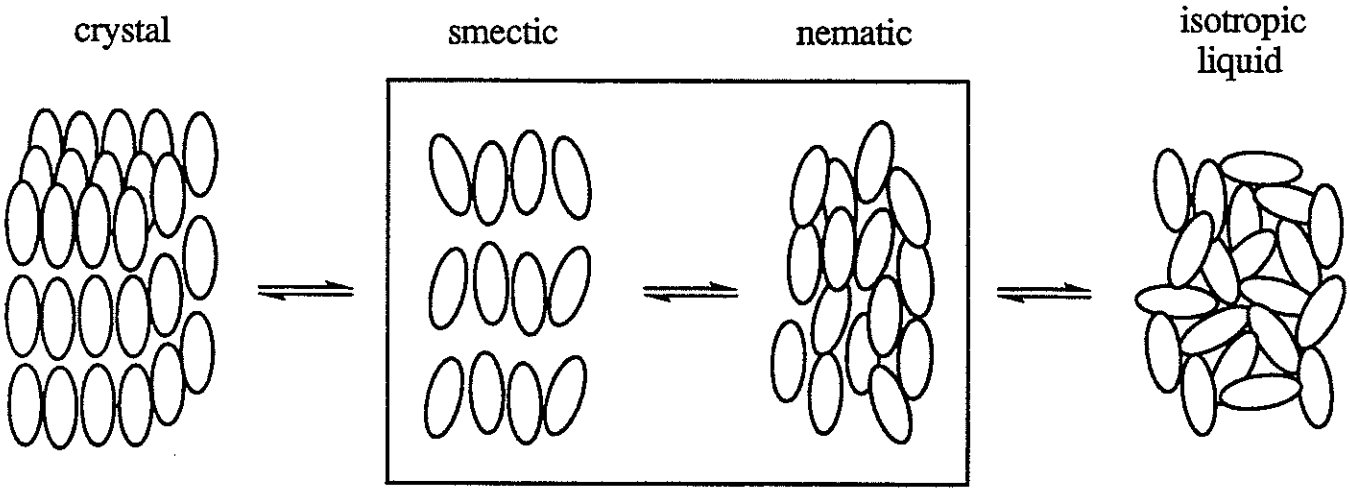

ORDER — ORDER and MOBILITY — MOBILITY

increasing temperature

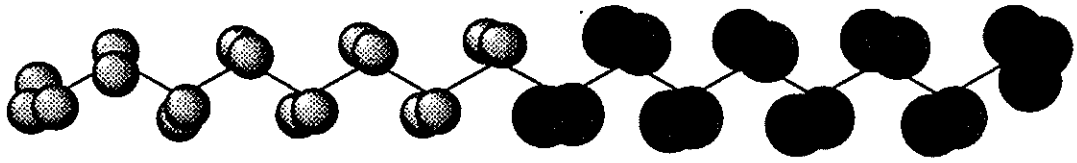

HYDROCARBON
oleophilic

FLUOROCARBON
oleophobic

	$-(CH_2)_x-$	$-(CF_2)_x-$
H, F van der Waals radii (Å)	1.2	1.35
Spatial Representation along the chain	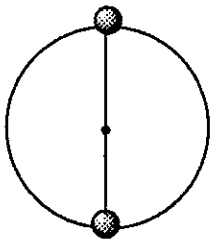	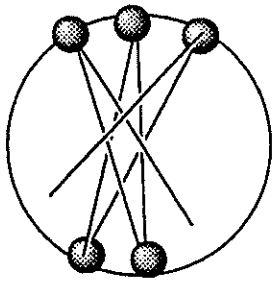
Distance between repeat units (Å)	2.539	
Helix type	1_1 (planar zigzag)	13_1
Torsion angle	0°	16°
Cross-sectional area ($Å^2$)	18.5	28.3

C. Bunn and E.R. Howells, *Nature*, **174**, 549 (1954); H.G. Elias, *Macromolecules. Structure and Properties*, 2nd Ed., Plenum Press: N.Y., 1984.

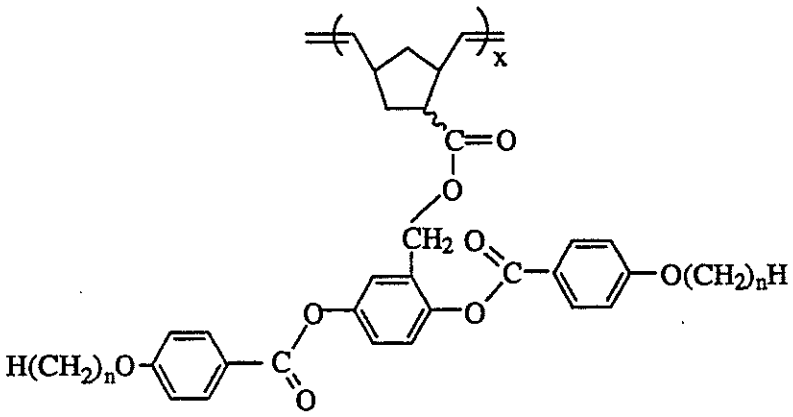

n	Phase Transitions (°C)
1	g 97 n 162 i
2	g 92 n 172 i
3	g 83 n 140 i
4	g 73 n 138 i
5	g 60 n 123 i
6	g 56 n 126 i

C. Pugh & R.R. Schrock, *Macromolecules*, **25**, 6593 (1992).

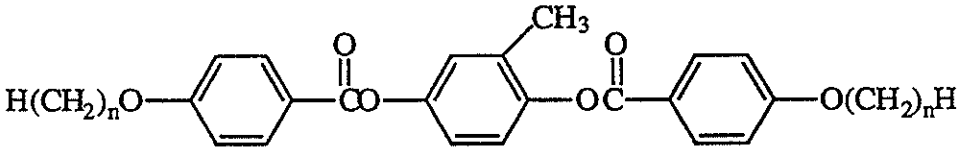

n	Phase Transitions (°C)	Ref.
1	k 166 n 252 i	1
2	k 187 n 248 i	1
3	k 138 n 209 i	1
4	k 115 n 206 i	1
5	k 90 n 178 i	1
6	k 88 n 173 i	1
7	k 86 n 161 i	2
8	k 40 n 157 i	2
9	k 79 n 148 i	2
10	k 83 n 139 i	2
11	k 81 (s_C 80) n 140 i	2
12	k 81 s_C 88 n 140 i	2

(1) D. Demus & H. Zaschke, *Flussige Kristalle in Tabellen II*, VEB Deutscher Verlag, Liepzig, 1984; (2) current.

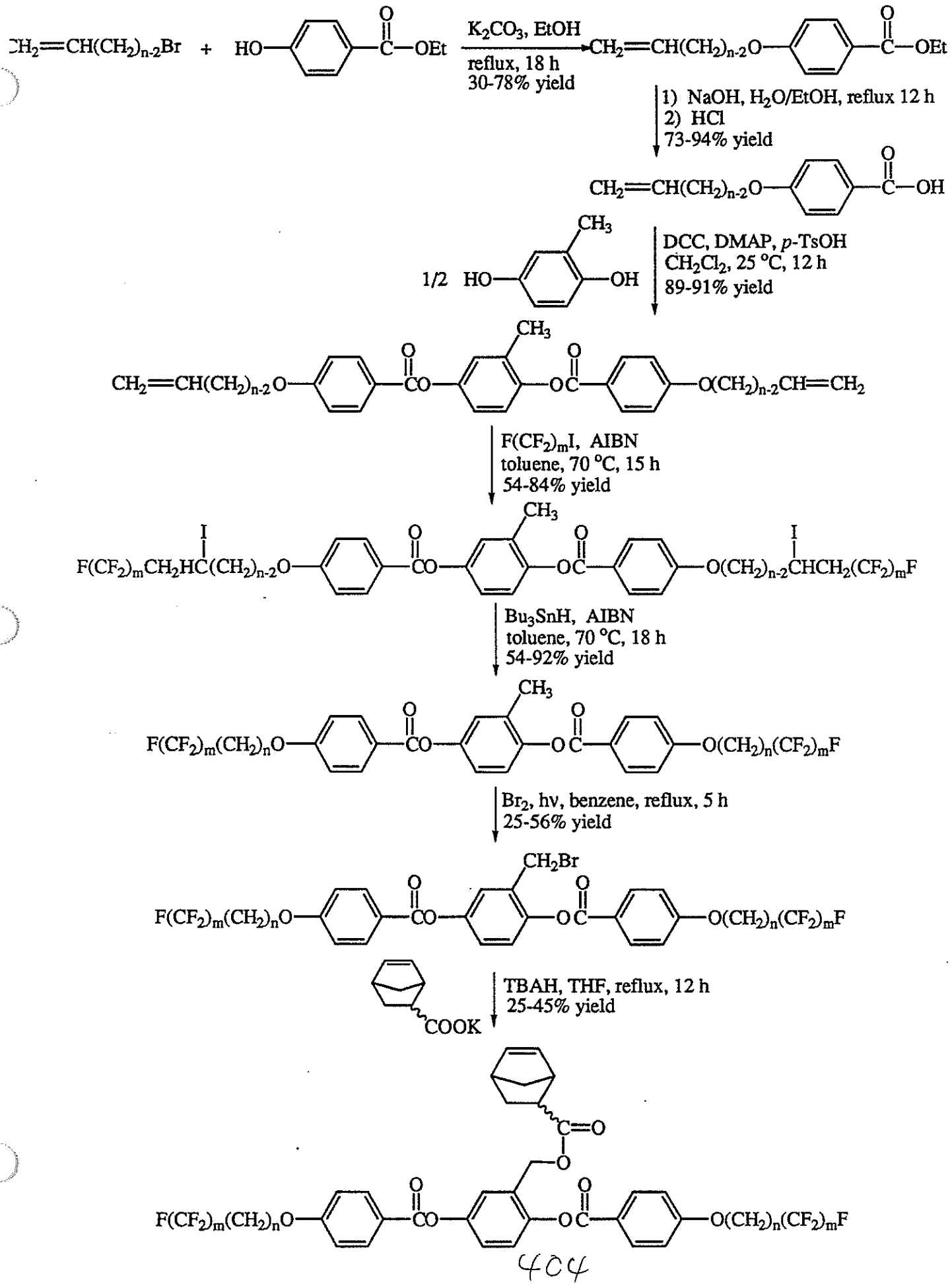
CH2=CH(CH2)n-2Br + HO-C6H4-C(=O)-OEt
K2CO3, EtOH
reflux, 18 h
30-78% yield
CH2=CH(CH2)n-2O-C6H4-C(=O)-OEt
1) NaOH, H2O/EtOH, reflux 12 h
2) HCl
73-94% yield
CH2=CH(CH2)n-2O-C6H4-C(=O)-OH
1/2 HO-C6H3(CH3)-OH
DCC, DMAP, p-TsOH
CH2Cl2, 25 °C, 12 h
89-91% yield
CH2=CH(CH2)n-2O-C6H4-CO-C6H3(CH3)-OC-C6H4-O(CH2)n-2CH=CH2
F(CF2)mI, AIBN
toluene, 70 °C, 15 h
54-84% yield
F(CF2)mCH2HC(I)(CH2)n-2O-C6H4-CO-C6H3(CH3)-OC-C6H4-O(CH2)n-2CH(I)CH2(CF2)mF
Bu3SnH, AIBN
toluene, 70 °C, 18 h
54-92% yield
F(CF2)m(CH2)nO-C6H4-CO-C6H3(CH3)-OC-C6H4-O(CH2)n(CF2)mF
Br2, hv, benzene, reflux, 5 h
25-56% yield
F(CF2)m(CH2)nO-C6H4-CO-C6H3(CH2Br)-OC-C6H4-O(CH2)n(CF2)mF
TBAH, THF, reflux, 12 h
25-45% yield
COOK
C=O
O
F(CF2)m(CH2)nO-C6H4-CO-C6H3(CH2-O-C=O)-OC-C6H4-O(CH2)n(CF2)mF

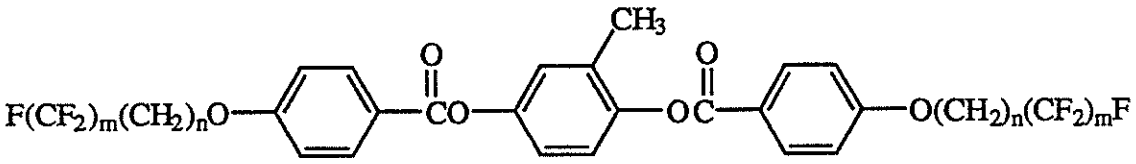

n	m	Phase Transitions (°C)					
5	3	k	89	s_C	123*	s_A 177	i
6	3	k	99	s_C	147*	s_A 171	i
8	3	k	107	s_C	176*	s_A 191	i
4	4	k	99	s_C	176*	s_A 191	i
5	4	k	92	s_C	162*	s_A 189	i
6	4	k	113	s_C	171*	s_A 185	i
8	4	k	95	s_C	169*	s_A 176	i
4	6	k	106	s_C	205	s_A 214	i
5	6	k	101	s_C	197	s_A 208	i
6	6	k	99	s_C	197	s_A 204	i
8	6	k	104	s_C	190	s_A 193	i
4	7	k	124	s_C	215	s_A 222	i
5	7	k	119	s_C	208	s_A 216	i
6	7	k	129	s_C	206	s_A 212	i
8	7	k	120	s_C	197	s_A 200	i
4	8	k	130	s_C	218	s_A 226	i
5	8	k	121	s_C	214	s_A 221	i
6	8	k	130	s_C	211	s_A 217	i
8	8	k	124	s_C	201	s_A 205	i

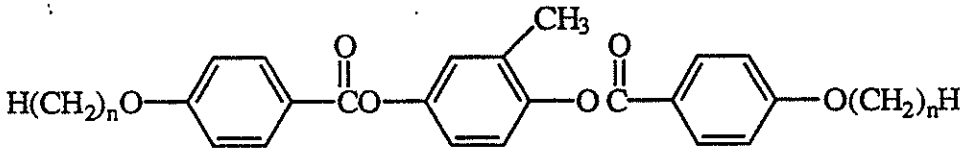

n	Phase Transitions (°C)			
1	k	166	n 252	i
2	k	187	n 248	i
3	k	138	n 209	i
4	k	115	n 206	i
5	k	90	n 178	i
6	k	88	n 173	i
7	k	86	n 161	i
8	k	40	n 157	i

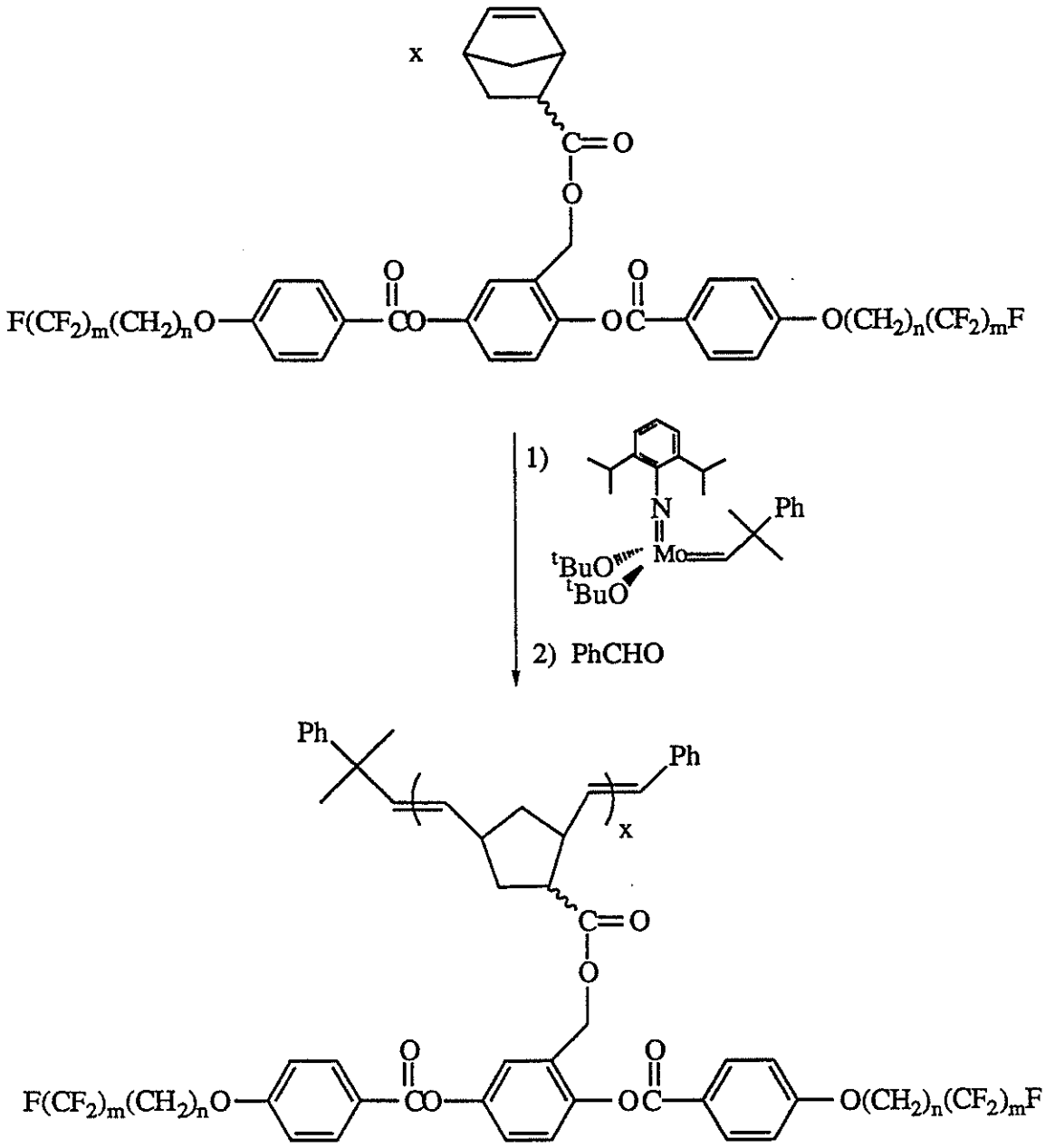

n	m	Solvent	Temp. °C	Solution	$[M]_0/[I]_0$	Theor. M_nx10-4	GPC M_nx10-4	GPC pdi
6	8	THF	25	turbid	32	4.8	0.2	2.1
6	7	CH_2Cl_2	25	turbid	40	5.5	2.9	1.3
6	7	toluene	25	precipitates	40	5.5	2.9	1.3
4	6	1,3-$(CF_3)_2$Ph	40	homogeneous	50	6.2	5.8	1.5

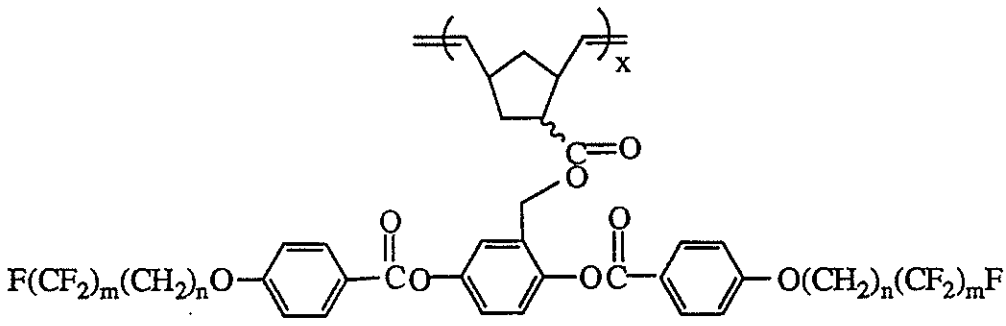

n	m	Phase Transitions (°C)
4	6	g 104 s_C 226 s_A 234 i
5	6	g i
6	6	g i
8	6	g i
4	7	g i
5	7	g i
6	7	g i
8	7	g i
4	8	g i
5	8	g i
6	8	g i
8	8	g i

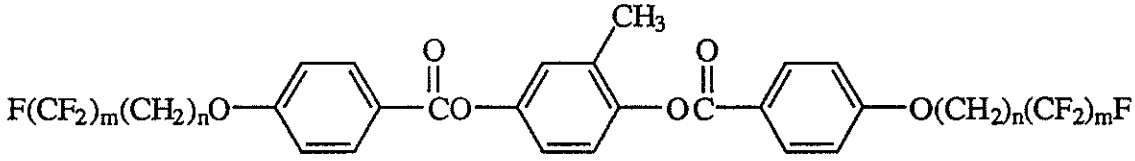

n	m	Phase Transitions (°C)
4	6	k 106 s_C 205 s_A 214 i
5	6	k 101 s_C 197 s_A 208 i
6	6	k 99 s_C 197 s_A 204 i
8	6	k 104 s_C 190 s_A 193 i
4	7	k 124 s_C 215 s_A 222 i
5	7	k 119 s_C 208 s_A 216 i
6	7	k 129 s_C 206 s_A 212 i
8	7	k 120 s_C 197 s_A 200 i
4	8	k 130 s_C 218 s_A 226 i
5	8	k 121 s_C 214 s_A 221 i
6	8	k 130 s_C 211 s_A 217 i
8	8	k 124 s_C 201 s_A 205 i

(C. Pugh & S.V. Arehart, unpublished results.)

Synthesis of Conjugated Macromolecules for Electronic Applications

James M. Tour
Department of Chemistry and Biochemistry
University of South Carolina
Columbia, SC 29208
Tel. 803-777-9517
Fax: 803-777-9521

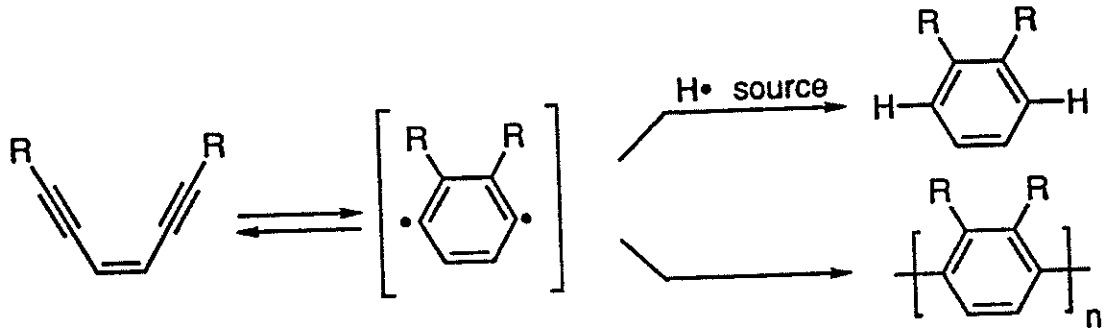

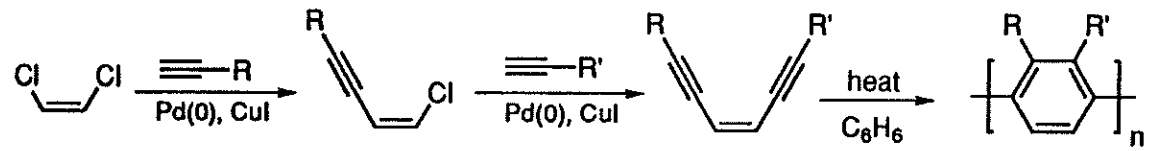

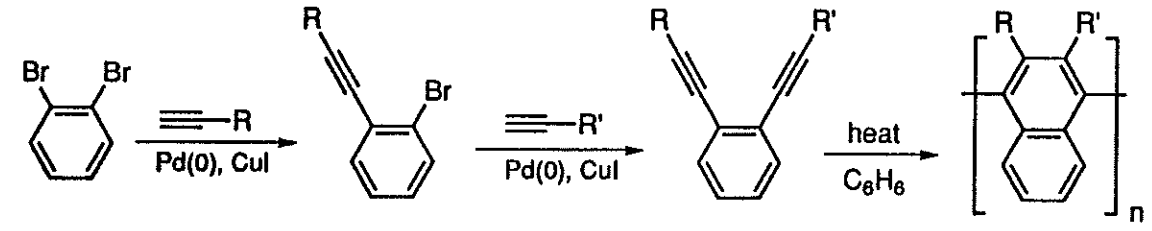

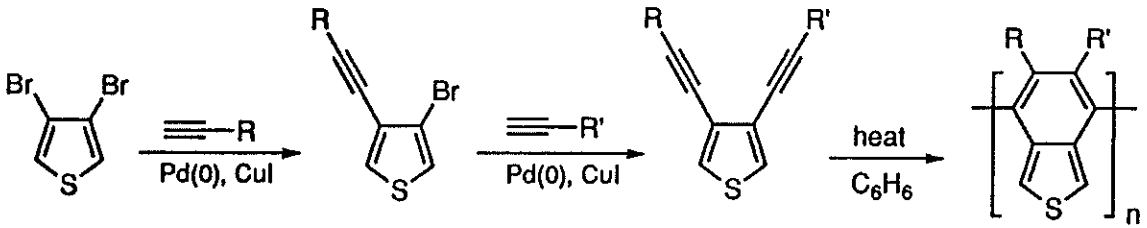

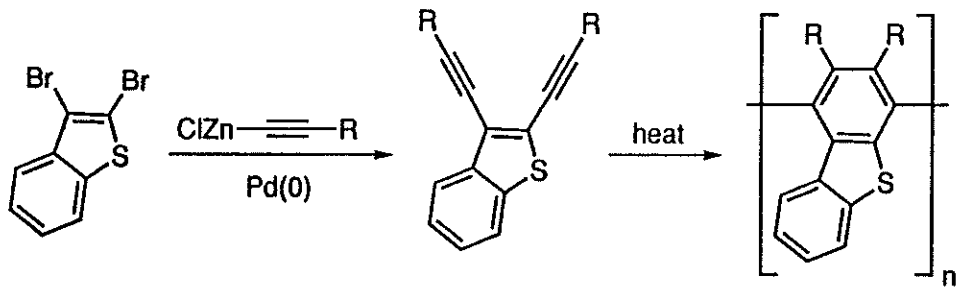

General SEC data:
M_n = 1000 - 9000
M_w = 2000 - 45,000
M_w/M_n = 2- 5

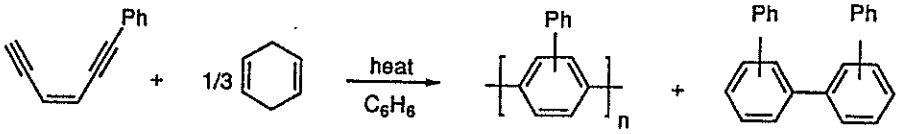

306 amu

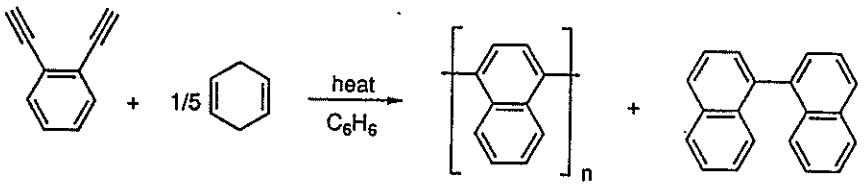

254 amu

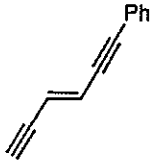

heat, C_6H_6 → Polymer but <u>not</u> a polyphenylene.
Missing IR bands at 935-810 and 880-795 cm^{-1}.

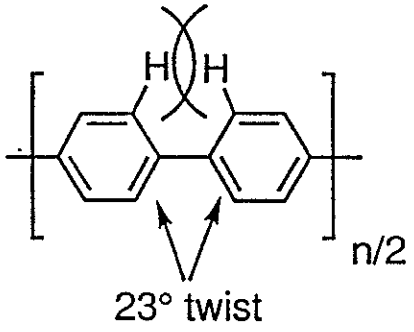

23° twist

22° twist by MMX (extended π–calculations)

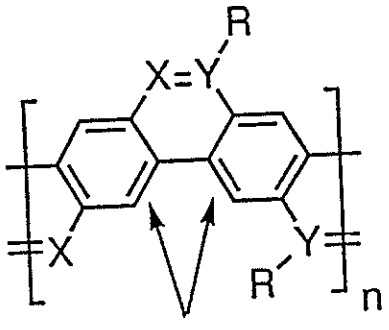

~0° twist

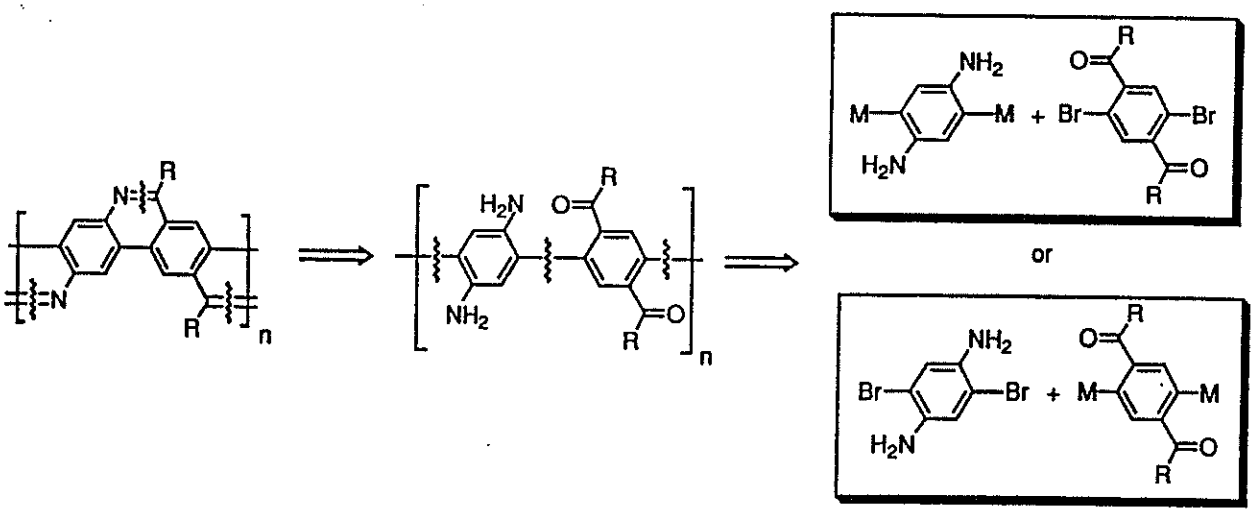
or

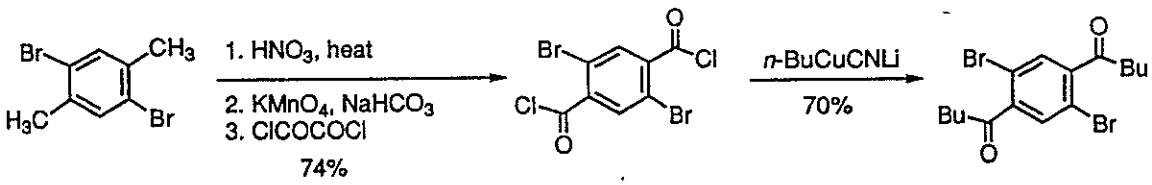
1. HNO3, heat
2. KMnO4, NaHCO3
3. ClCOCOCl
74%
n-BuCuCNLi
70%

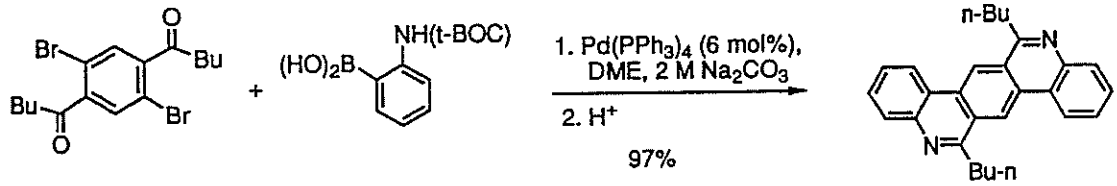
1. Pd(PPh3)4 (6 mol%), DME, 2 M Na2CO3
2. H+
97%
Very soluble

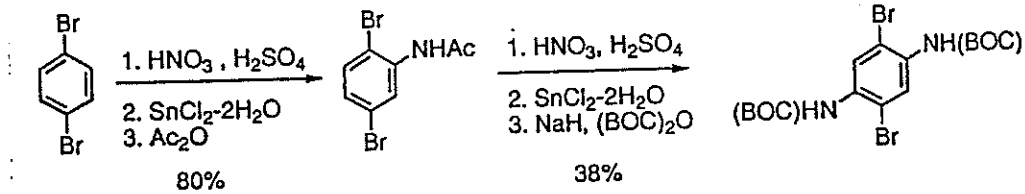
1. HNO3 , H2SO4
2. SnCl2-2H2O
3. Ac2O
80%
1. HNO3, H2SO4
2. SnCl2-2H2O
3. NaH, (BOC)2O
38%

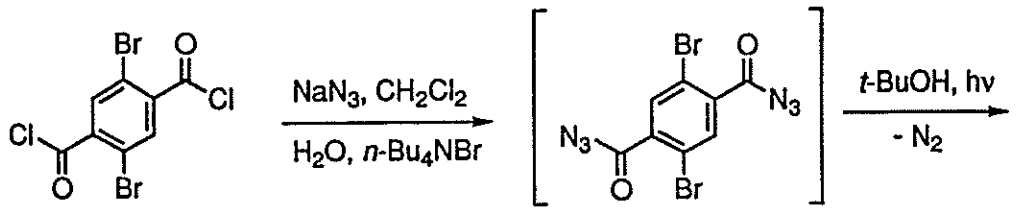

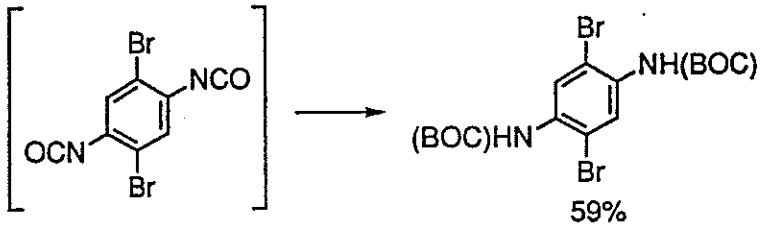

59%

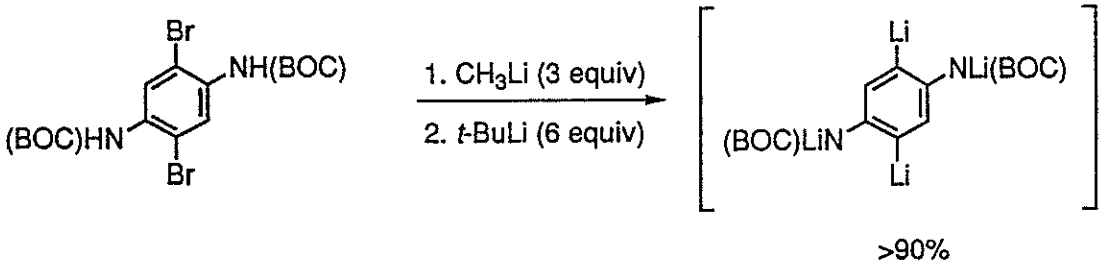

>90%

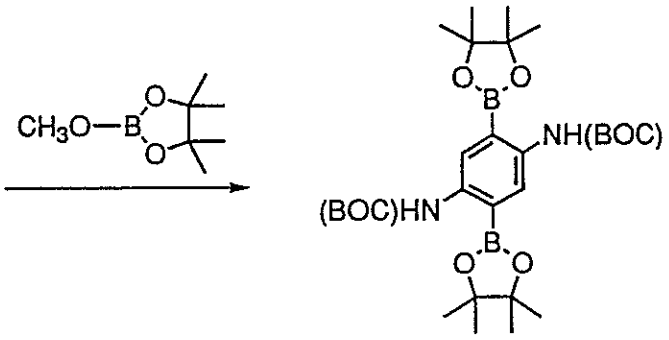

Bisboronic ester can be purified by chromatography on charcoal then crystallization (57% yield).

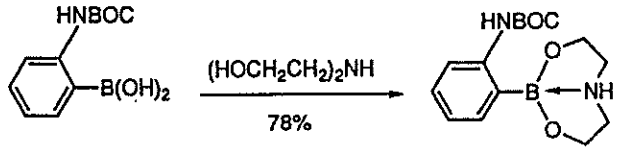
HNBOC
B(OH)2
(HOCH2CH2)2NH
78%
HNBOC
O
B
NH
O

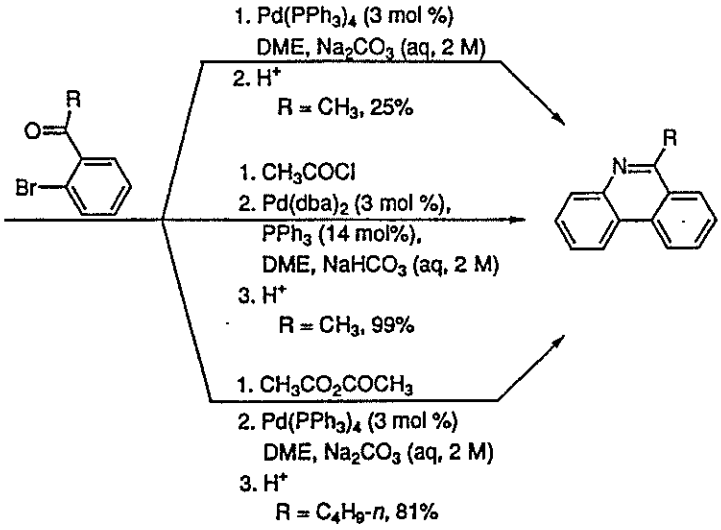
1. Pd(PPh3)4 (3 mol %)
DME, Na2CO3 (aq, 2 M)
2. H+
R = CH3, 25%
1. CH3COCl
2. Pd(dba)2 (3 mol %),
PPh3 (14 mol%),
DME, NaHCO3 (aq, 2 M)
3. H+
R = CH3, 99%
1. CH3CO2COCH3
2. Pd(PPh3)4 (3 mol %)
DME, Na2CO3 (aq, 2 M)
3. H+
R = C4H9-n, 81%
R
O
Br
N

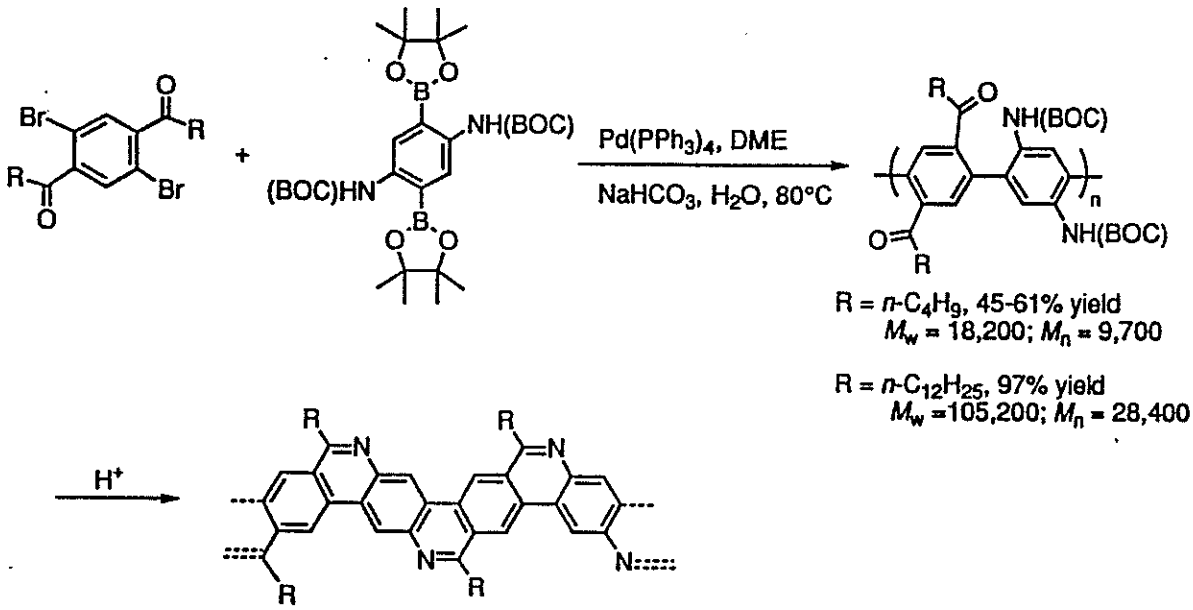
Br
O
R
Br
O
+
B
O
O
NH(BOC)
(BOC)HN
B
O
O
Pd(PPh3)4, DME
NaHCO3, H2O, 80°C
R
O
NH(BOC)
n
O
R
NH(BOC)
R = n-C4H9, 45-61% yield
Mw = 18,200; Mn = 9,700
R = n-C12H25, 97% yield
Mw =105,200; Mn = 28,400
H+
R
N
R
N
N
R
N
R

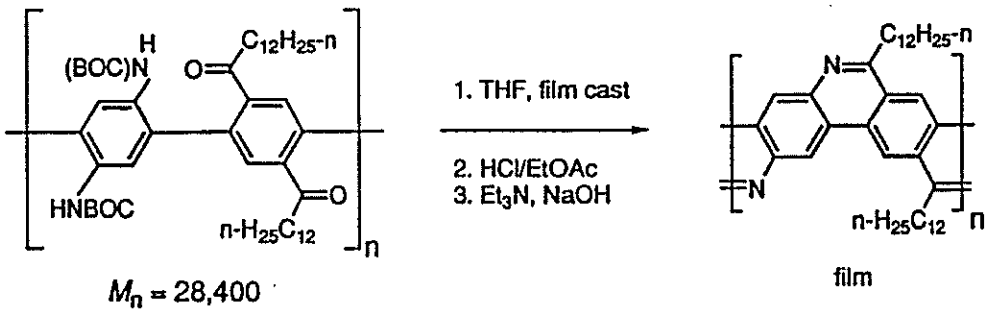
(BOC)N
H
O
C12H25-n
HNBOC
O
n-H25C12
n
Mn = 28,400
1. THF, film cast
2. HCl/EtOAc
3. Et3N, NaOH
C12H25-n
N
N
n-H25C12
n
film

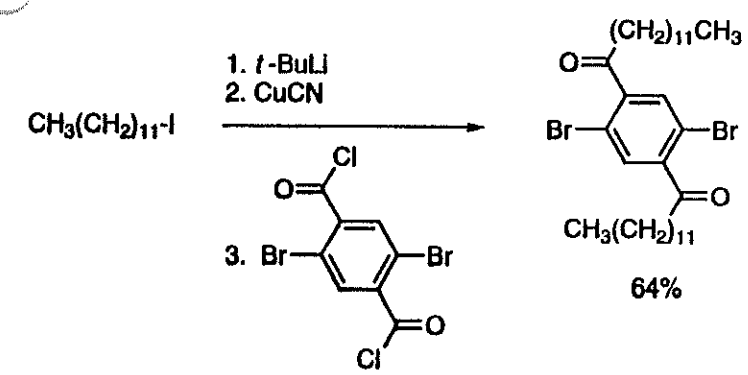
1. t-BuLi
2. CuCN
CH3(CH2)11-I
3.
64%

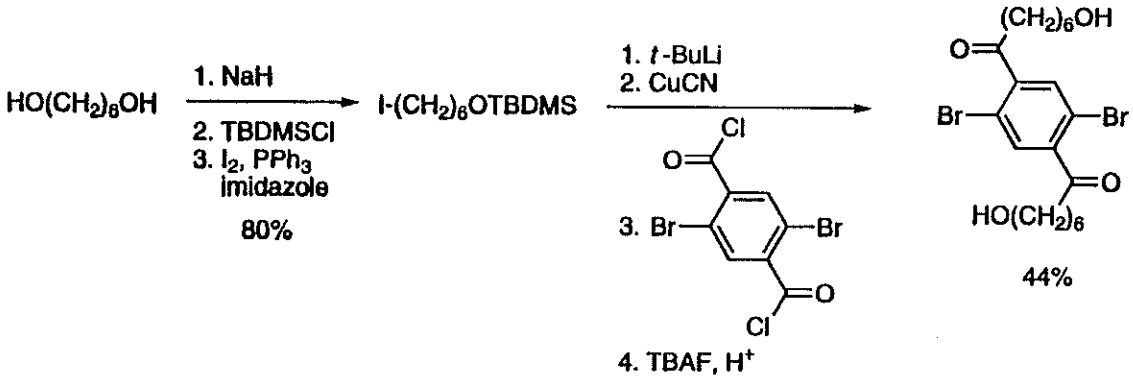
HO(CH2)6OH
1. NaH
2. TBDMSCl
3. I2, PPh3
imidazole
80%
I-(CH2)6OTBDMS
1. t-BuLi
2. CuCN
3.
4. TBAF, H+
44%

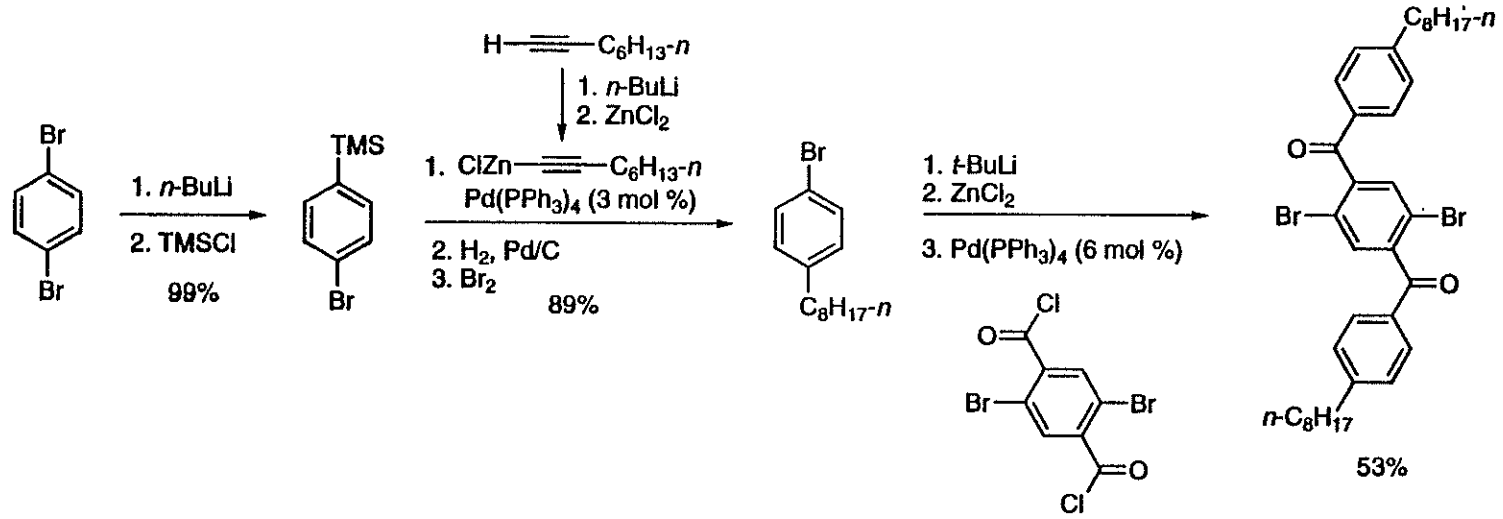
1. n-BuLi
2. TMSCl
99%
1. n-BuLi
2. ZnCl2
Pd(PPh3)4 (3 mol %)
2. H2, Pd/C
3. Br2
89%
1. t-BuLi
2. ZnCl2
3. Pd(PPh3)4 (6 mol %)
53%

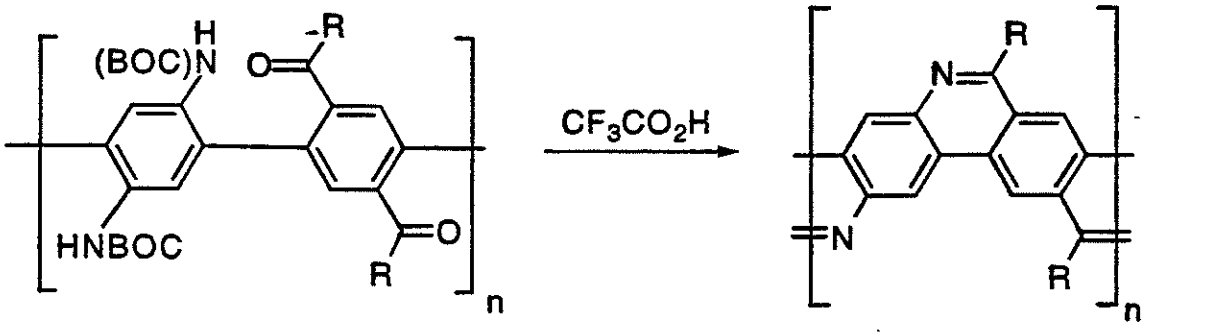

1, R = *n*-C_4H_9, 63%,
M_n = 9,850, M_w/M_n = 1.85
2, R = *n*-$C_{12}H_{25}$, 97%,
M_n = 28,400, M_w/M_n = 3.70
3, R = $(CH_2)_6OH$, 82%,
insoluble
4, R = *p*-(C_6H_4)-C_8H_{17}-*n*, 80%
M_n = 18,500, M_w/M_n = 2.75

5, R = *n*-C_4H_9, 90%
6, R = *n*-$C_{12}H_{25}$, 97%,
7, R = *p*-(C_6H_4)-C_8H_{17}-*n*, 99%

Optical Absorption Data

Compound	λ in solution (nm)	λ of solid (nm)
1	CH_2Cl_2: 250, 306 (sh)	248, 308
2	CH_2Cl_2: 250, 388	250, 398
4	CH_2Cl_2: 254	254
5	CH_2Cl_2/TFA: 374, 396, 426 (sh), 514, 520 (ed)	---
6	CH_2Cl_2/TFA: 376, 400, 428, 478, 516, 530 (ed)	463-490
7	CH_2Cl_2/TFA: 356, 376, 402, 458, 506, 549, 580 (ed)	482
p-sexiphenylene	$CHCl_3$: 318	---
PPP (calcd infinite M_n)	344	---

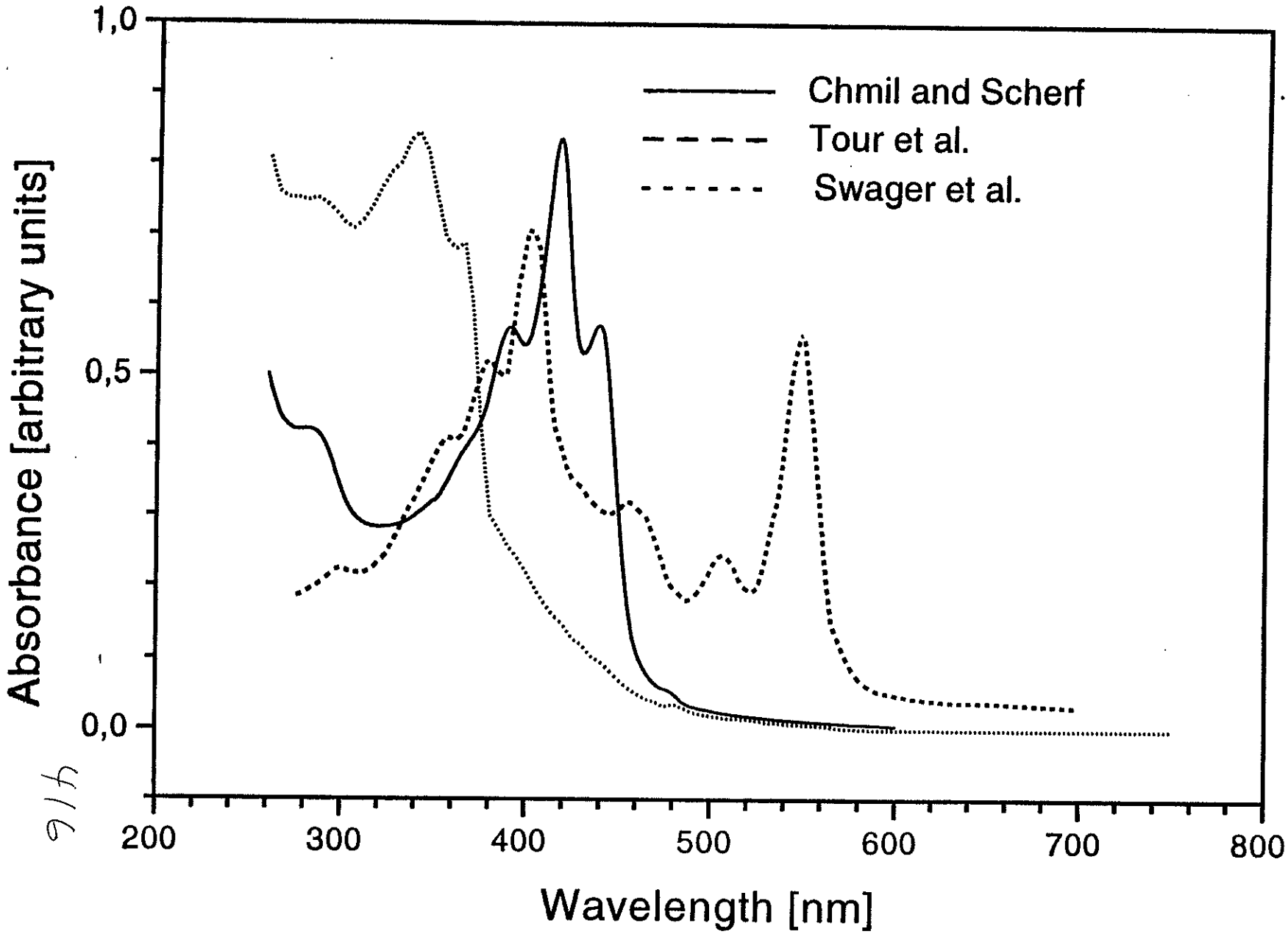
1,0
0,5
0,0
Absorbance [arbitrary units]
200
300
400
500
600
700
800
Wavelength [nm]
Chmil and Scherf
Tour et al.
Swager et al.

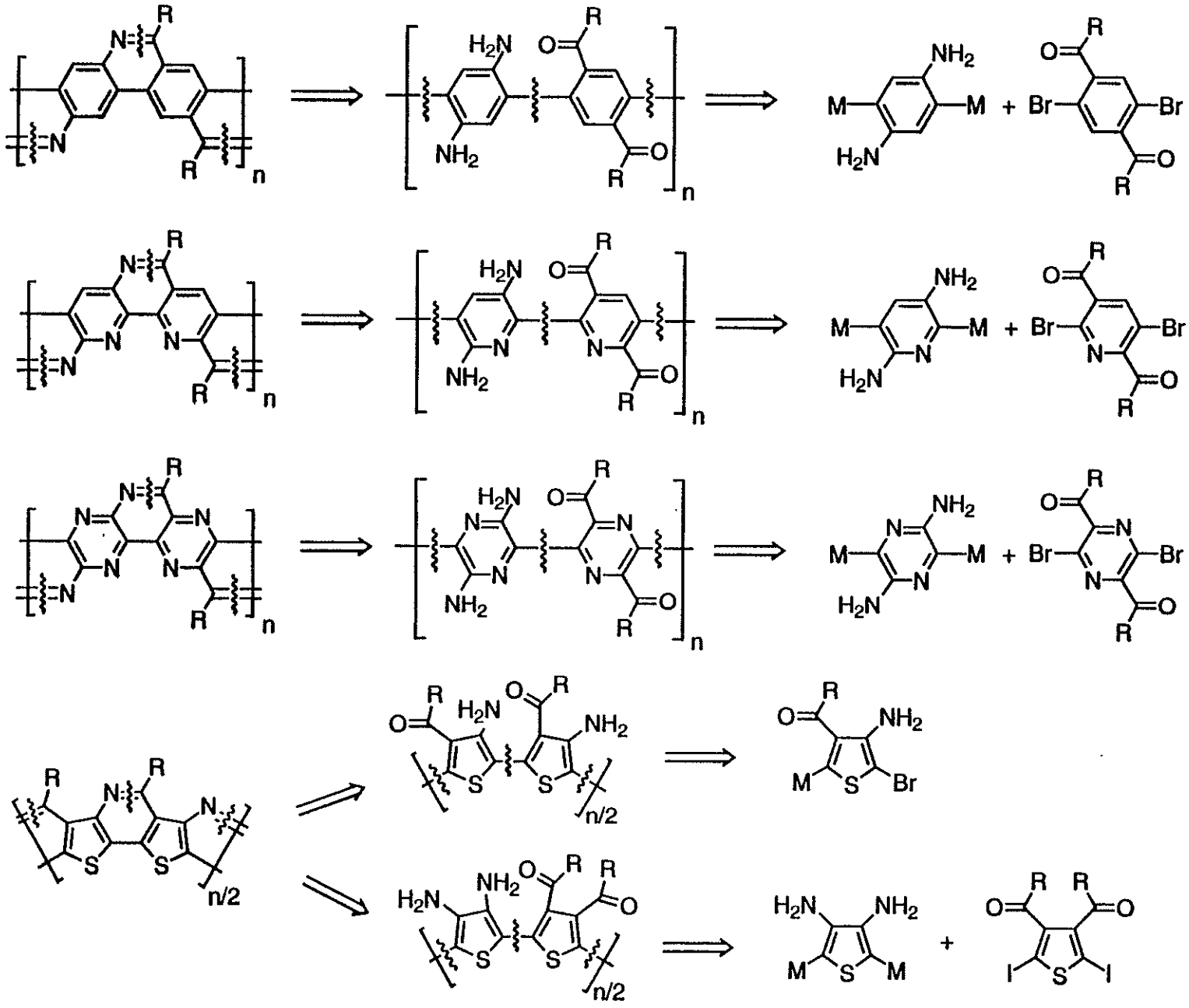

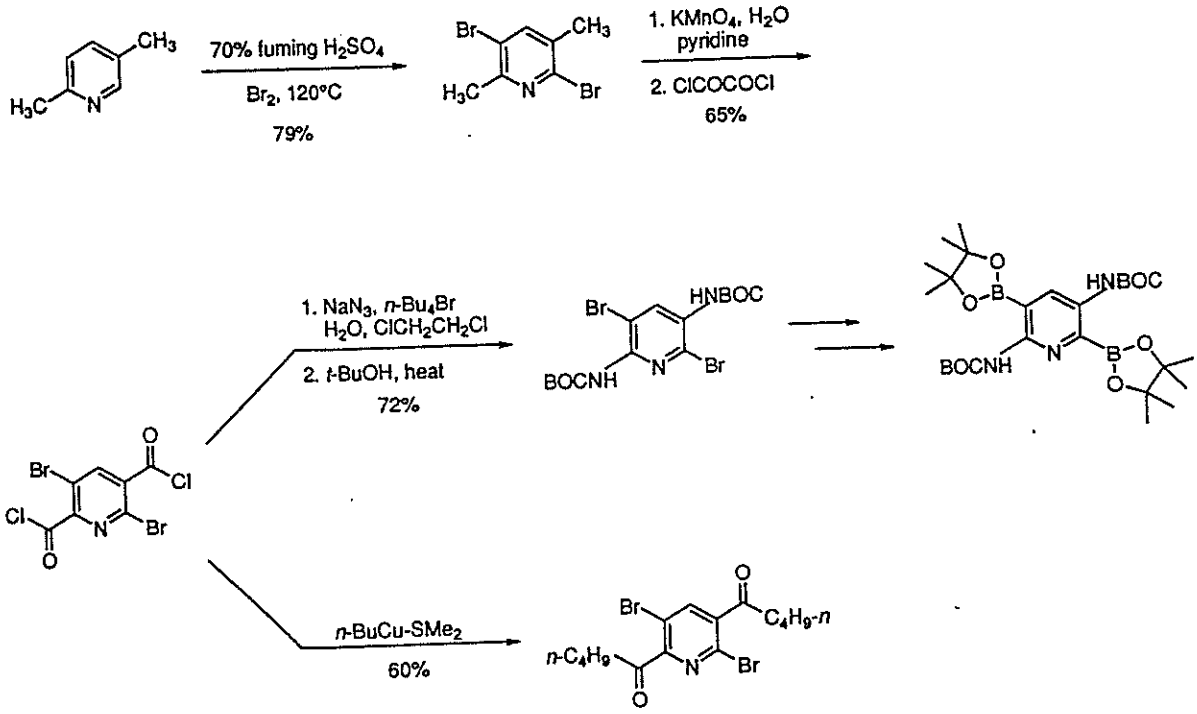
70% fuming H_2SO_4
Br_2, 120°C
79%
1. $KMnO_4$, H_2O
pyridine
2. ClCOCOCl
65%
1. NaN_3, n-Bu_4Br
H_2O, $ClCH_2CH_2Cl$
2. t-BuOH, heat
72%
n-BuCu-SMe_2
60%

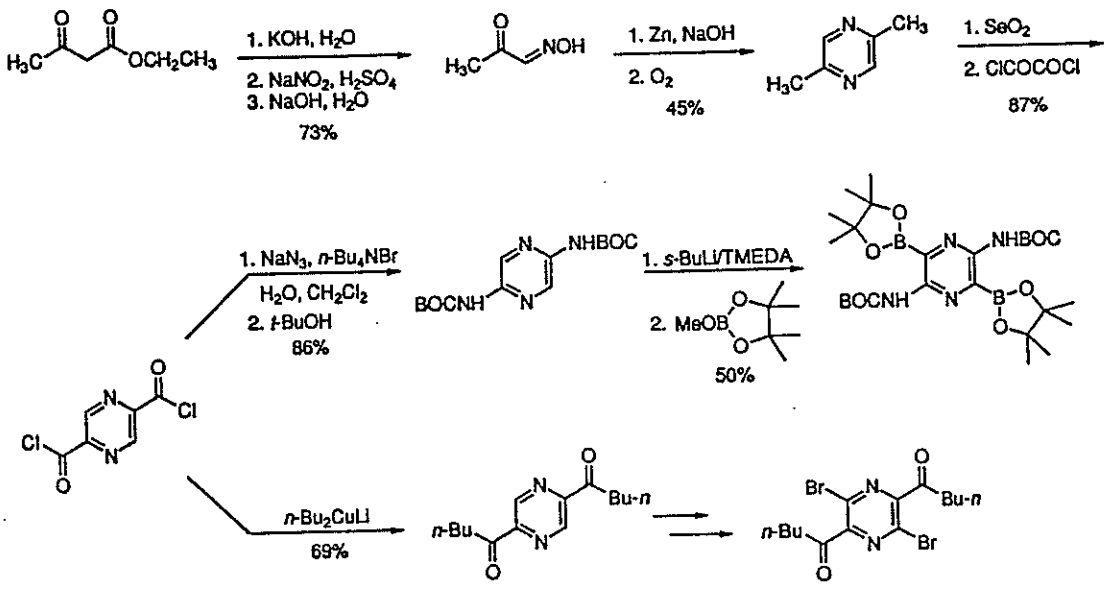
1. KOH, H_2O
2. $NaNO_2$, H_2SO_4
3. NaOH, H_2O
73%
1. Zn, NaOH
2. O_2
45%
1. SeO_2
2. ClCOCOCl
87%
1. NaN_3, n-Bu_4NBr
H_2O, CH_2Cl_2
2. t-BuOH
86%
1. s-BuLi/TMEDA
2. MeOB
50%
n-Bu_2CuLi
69%

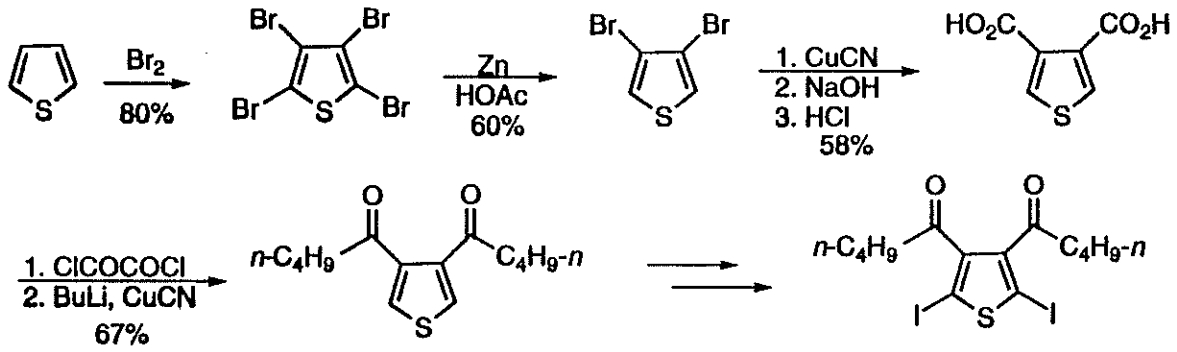
Br2
80%
Zn
HOAc
60%
1. CuCN
2. NaOH
3. HCl
58%
HO2C
CO2H
1. ClCOCOCl
2. BuLi, CuCN
67%
n-C4H9
C4H9-n

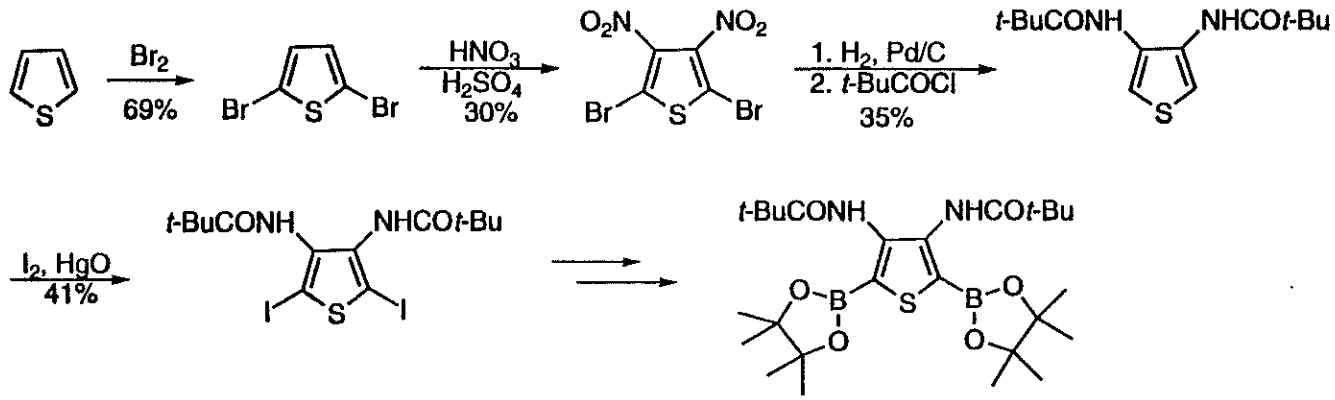
Br2
69%
HNO3
H2SO4
30%
O2N
NO2
1. H2, Pd/C
2. t-BuCOCl
35%
t-BuCONH
NHCOt-Bu
I2, HgO
41%

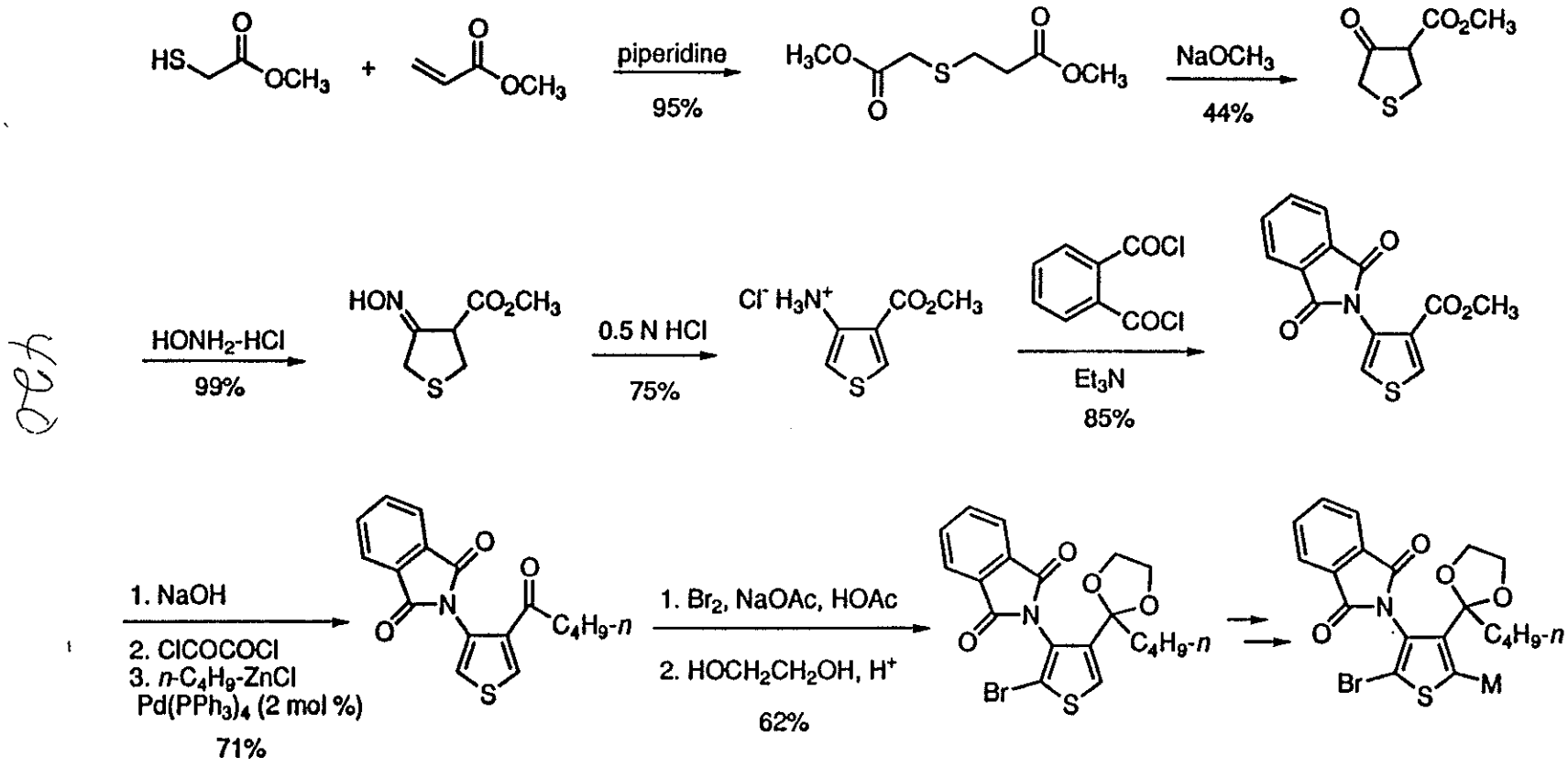
piperidine
95%
NaOCH3
44%
HONH2-HCl
99%
0.5 N HCl
75%
Et3N
85%
1. NaOH
2. ClCOCOCl
3. n-C4H9-ZnCl
Pd(PPh3)4 (2 mol %)
71%
1. Br2, NaOAc, HOAc
2. HOCH2CH2OH, H+
62%

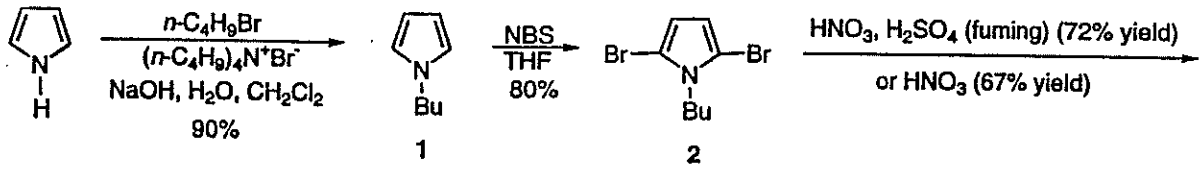

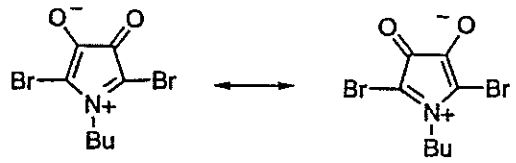

IR: 1718 cm^{-1}

MS: Calc'd: 311. Found: 311.

Elemental Analysis:

	Calc'd	Found
C_8	30.89	30.90
H_9	2.92	2.92
Br_2	51.39	51.25
N	4.50	4.48
O_2	10.29	10.45

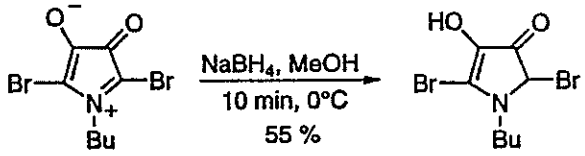

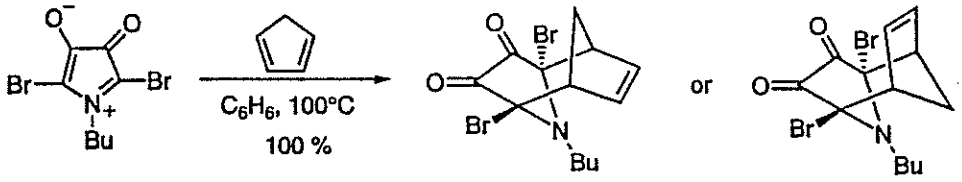

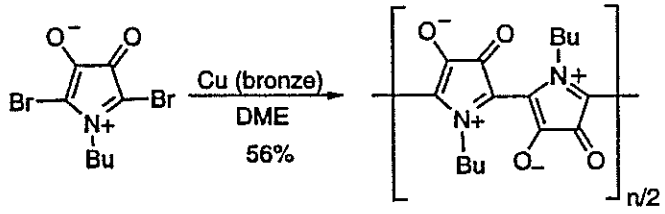

IR: 1697 cm^{-1} SEC: M_n = 5,000
M_w = 6,250
M_w/M_n = 1.25

Elemental Analysis:

	Calc'd	Found
C_8	63.57	63.40
H_9	6.00	6.71
N	9.26	8.06
O_2	21.17	21.83
Br	0.0	0.0

4-Point Probe Conductivity:
Intrinsic: 1.4 x 10^{-5} Ω^{-1} cm^{-1}
I_2 doped: 4.2 x 10^{-4} Ω^{-1} cm^{-1}

421

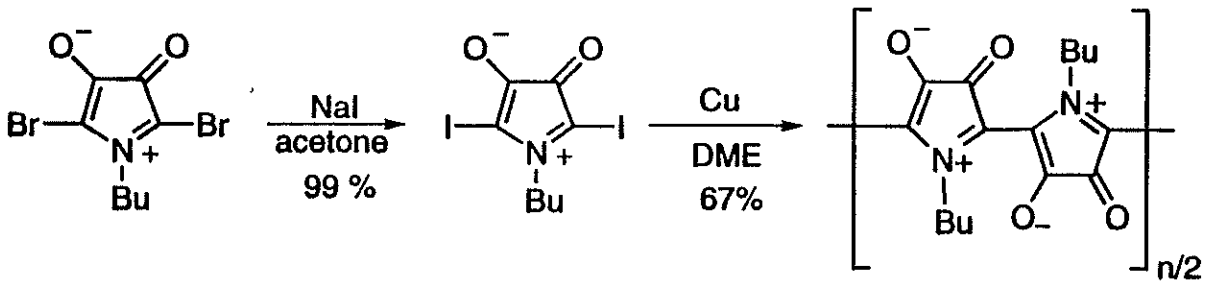
Br
Br
Bu
NaI
acetone
99 %
I
I
Bu
Cu
DME
67%
Bu
Bu
n/2

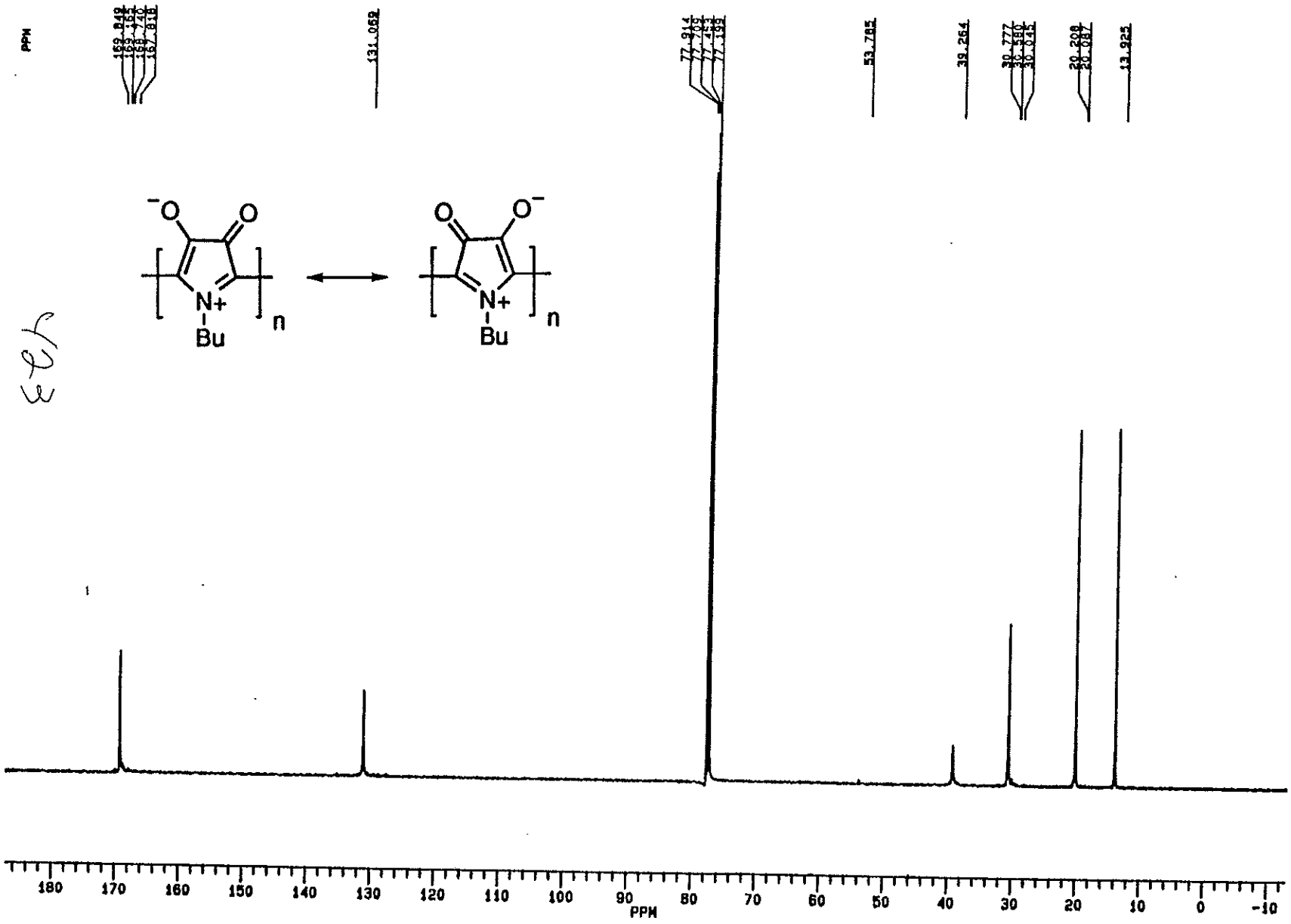

BRUKER

ID040F.106
AU PROG:
XO2.AU
DATE 4-10-93
TIME 17:36

SOLVENT CCl3
SF 125.759
SY 157.0
O1 52078.500
SI 65536
TD 65536
SW 38461.538
HZ/PT 1.174

AQ .852
RG 32768
NS 8192
TE 297

FW 48100
O2 7932.000
DP 17H CPD

LB 1.000
GB .500
CX 35.00
CY 18.00
F1 187.005P
F2 -12.990P
HZ/CM 718.605
PPM/CM 5.714
SR 35101.03

D5 .0010000
P9 90.10
S2 17H
D1 1.0000000
PO 1.60
RGA
AD 0.0
PW 0.0
DE 18.80
NS 8192
DS 2
NE 32

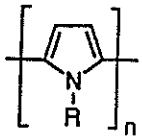

R = H, λ = 420 nm
R = *n*-C_4H_9, λ = 385 nm

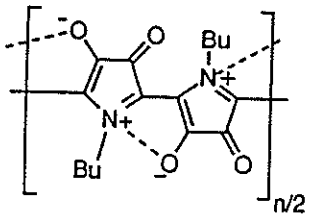

CCl_4, λ = 520 nm
THF, λ = 512 nm
EtOH/THF (1:1), λ = 503 nm
acetone, λ = 482 nm

Stabilization of the polar ground state increases the π-π* transition energy.

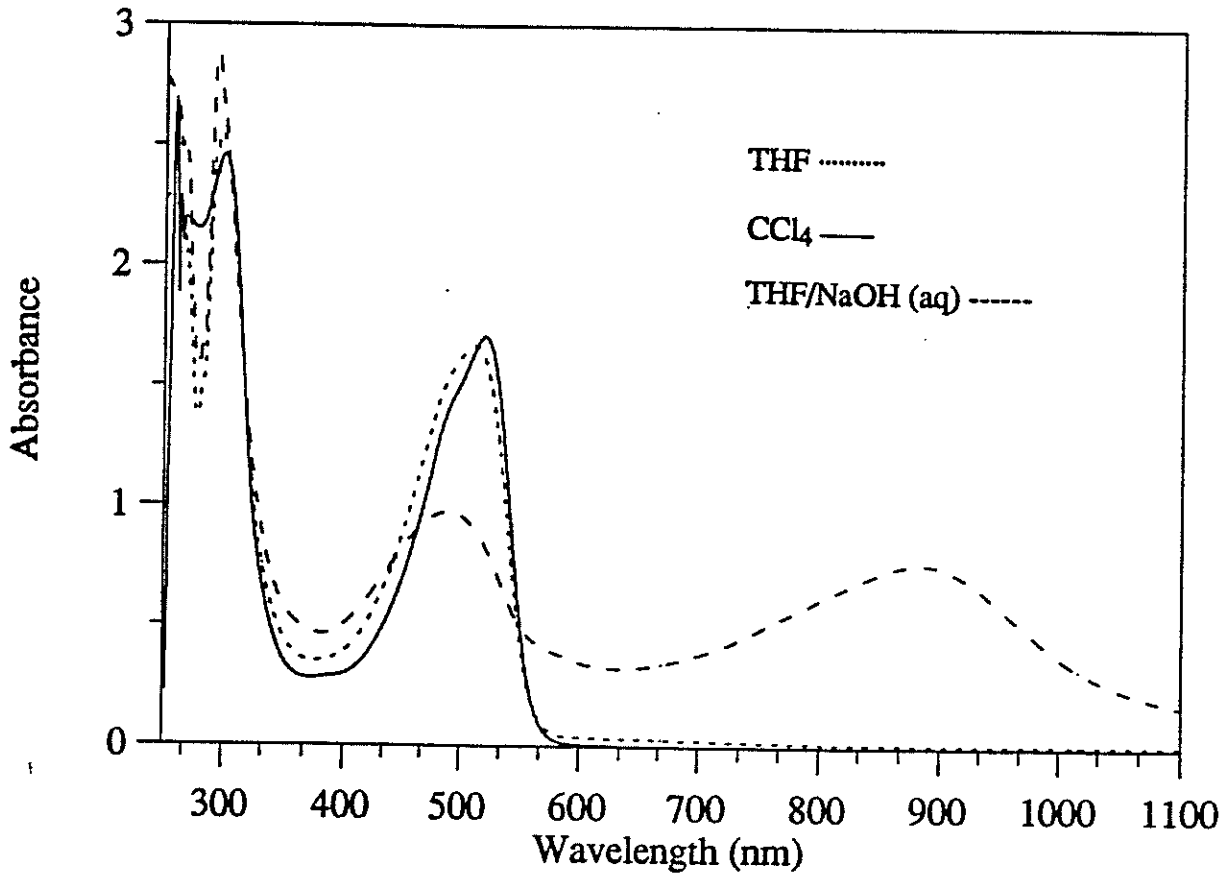

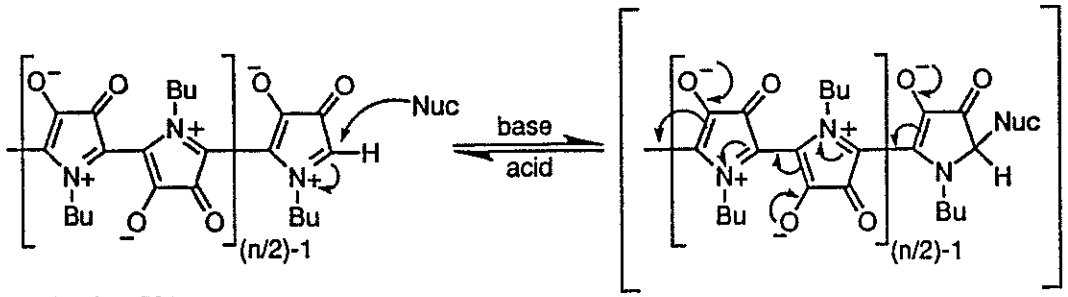

CCl_4, λ = 520 nm
THF, λ = 512 nm
EtOH/THF, (1:1) λ = 503 nm
acetone, λ = 482 nm

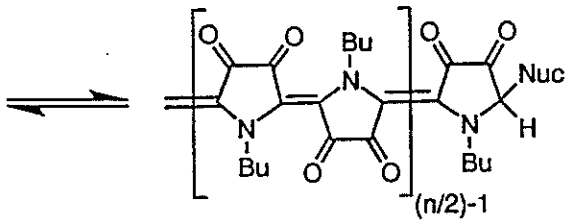

THF/NaOH (aq), λ = 881 nm
HMPA, λ = 901 nm
NMP, λ = 746 nm .

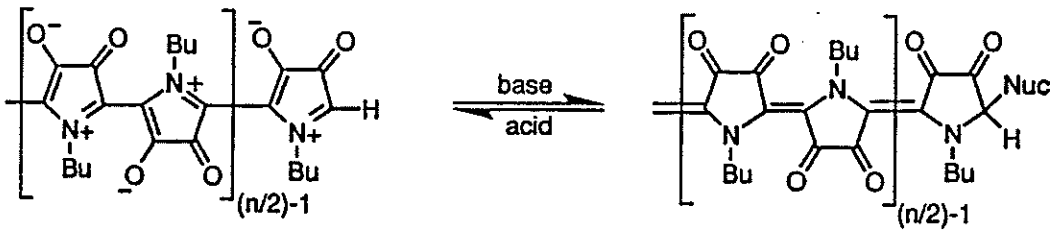

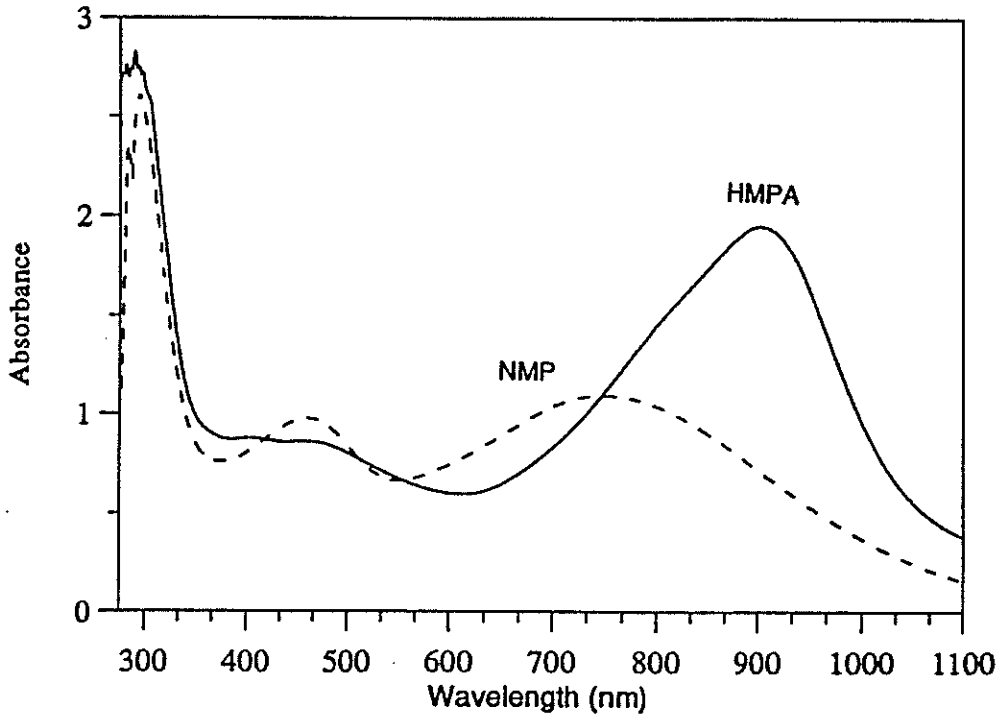

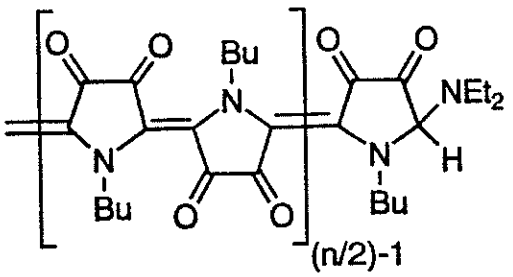

λ_{max} = 783 nm
Intrinsic conductivity: 6.9 x 10^{-5} Ω^{-1} cm^{-1}
I_2 doped conductivity: 3.5 x 10^{-3} Ω^{-1} cm^{-1}

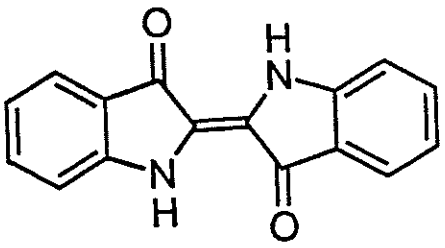

Indigo λ_{max} = 602 nm

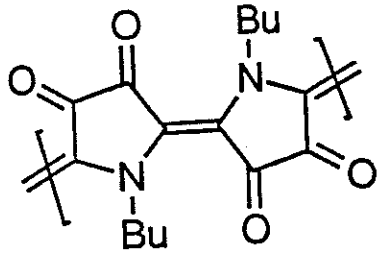

Indigo-like

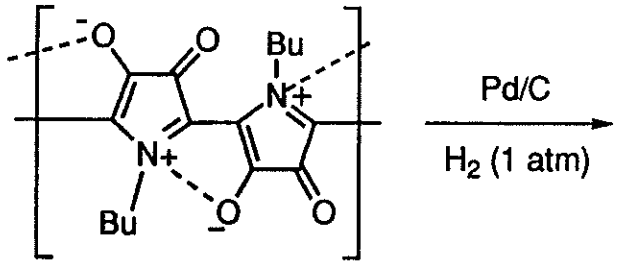

Pd/C

H_2 (1 atm)

THF, λ = 512 nm
DMSO insoluble

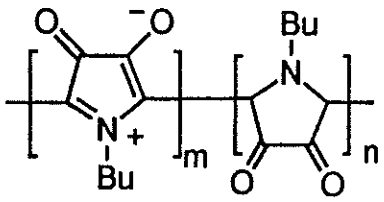

DMSO

THF

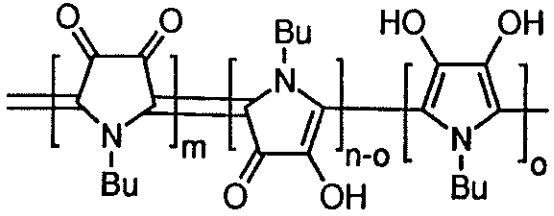

THF, λ < 290 nm

THF/NaOH (aq), λ = 618
DMSO, λ = 886

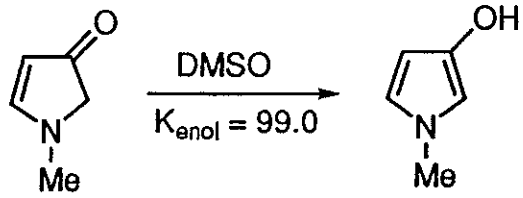

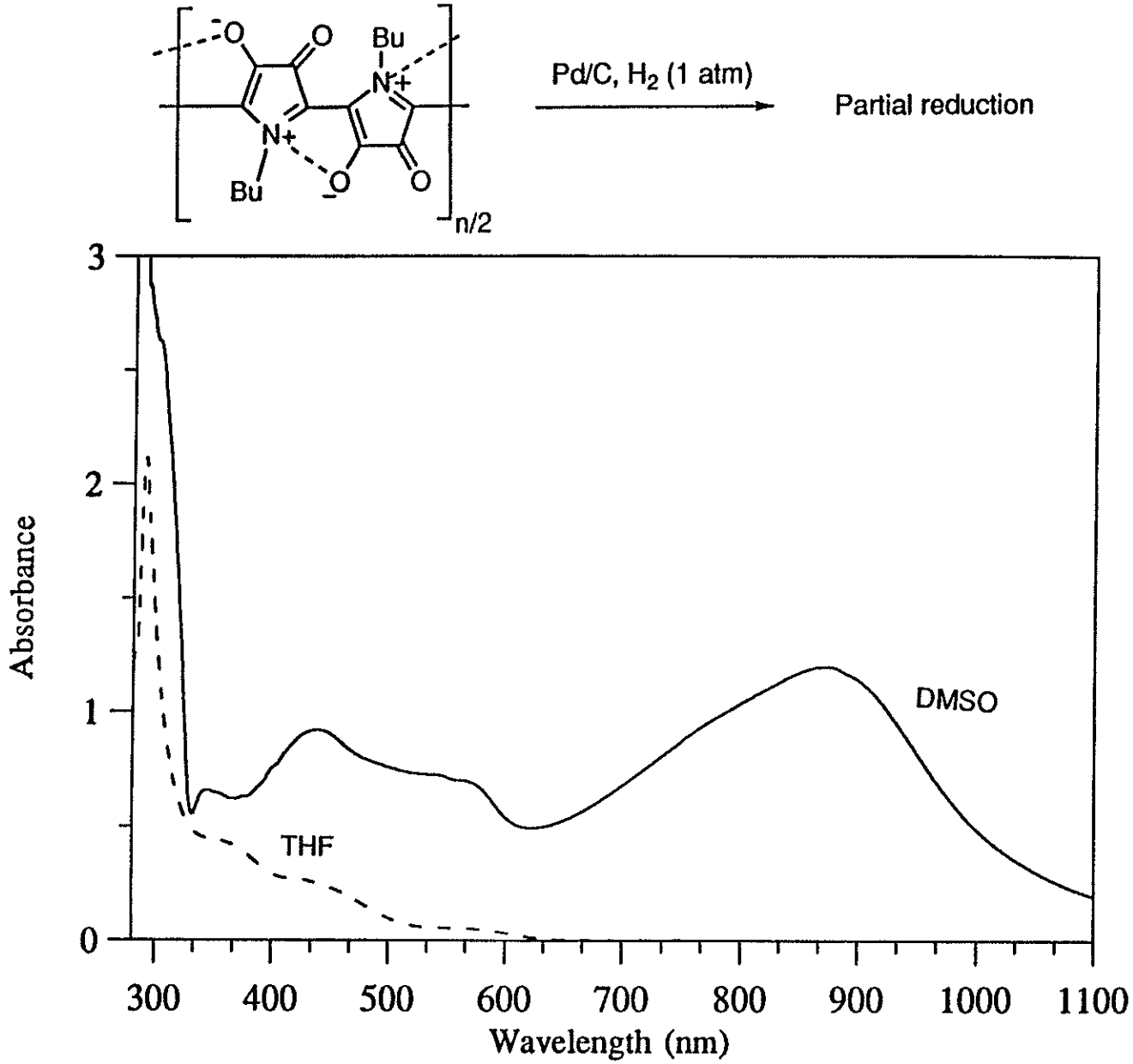
Pd/C, H2 (1 atm)
Partial reduction
Bu
Bu
n/2
Absorbance
Wavelength (nm)
DMSO
THF
0
1
2
3
300
400
500
600
700
800
900
1000
1100

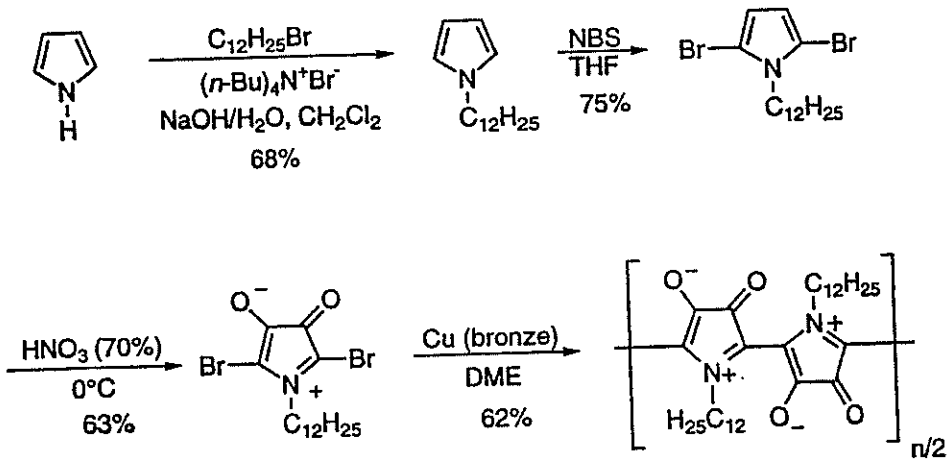

M_n = 8,650
M_w/M_n = 1.59

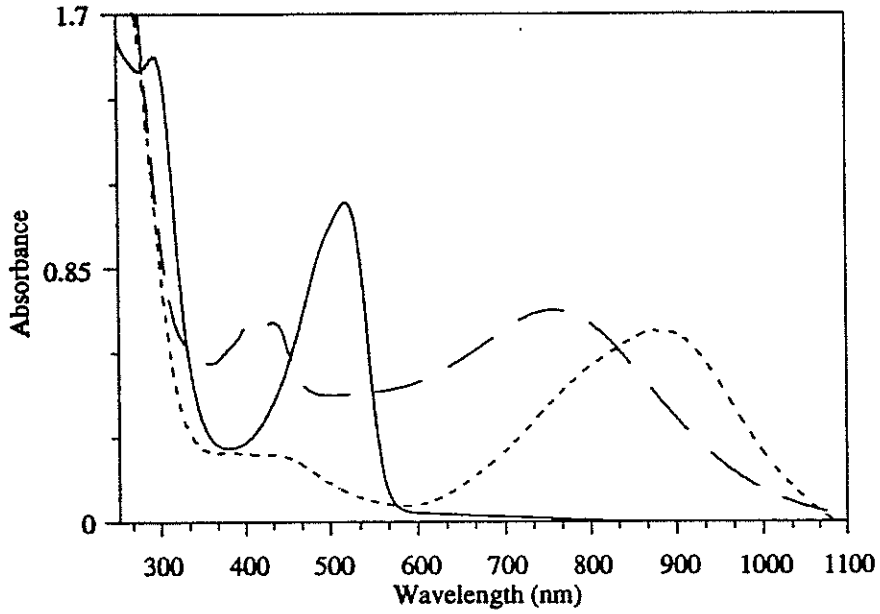

Spectrum of dodecyl-containing polymer in (a) CCl_4 (—), (b) THF/aqueous NaOH (— —), and (c) HMPA (- - -).

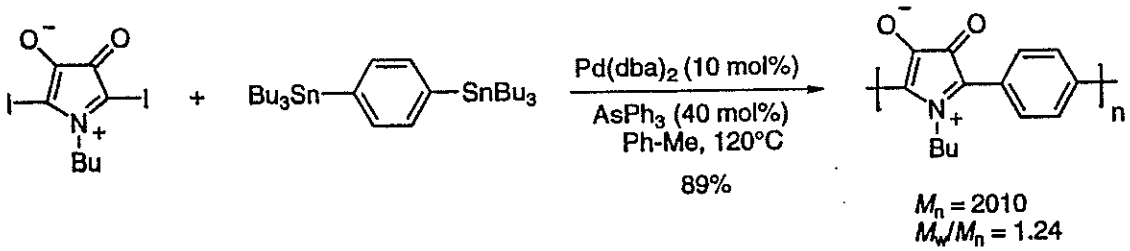

$M_n = 2010$
$M_w/M_n = 1.24$

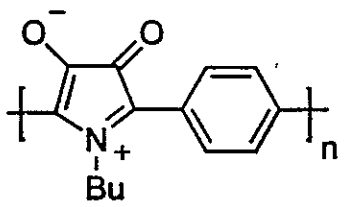

THF

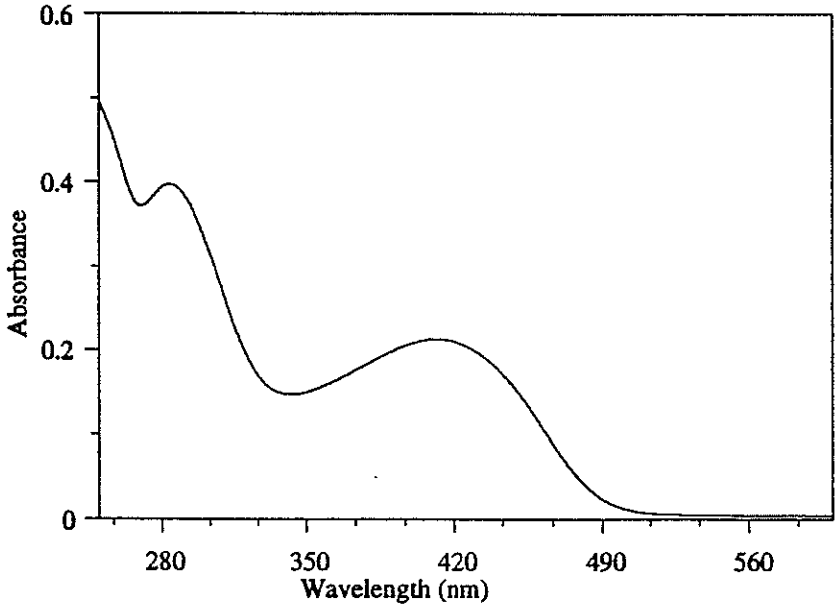

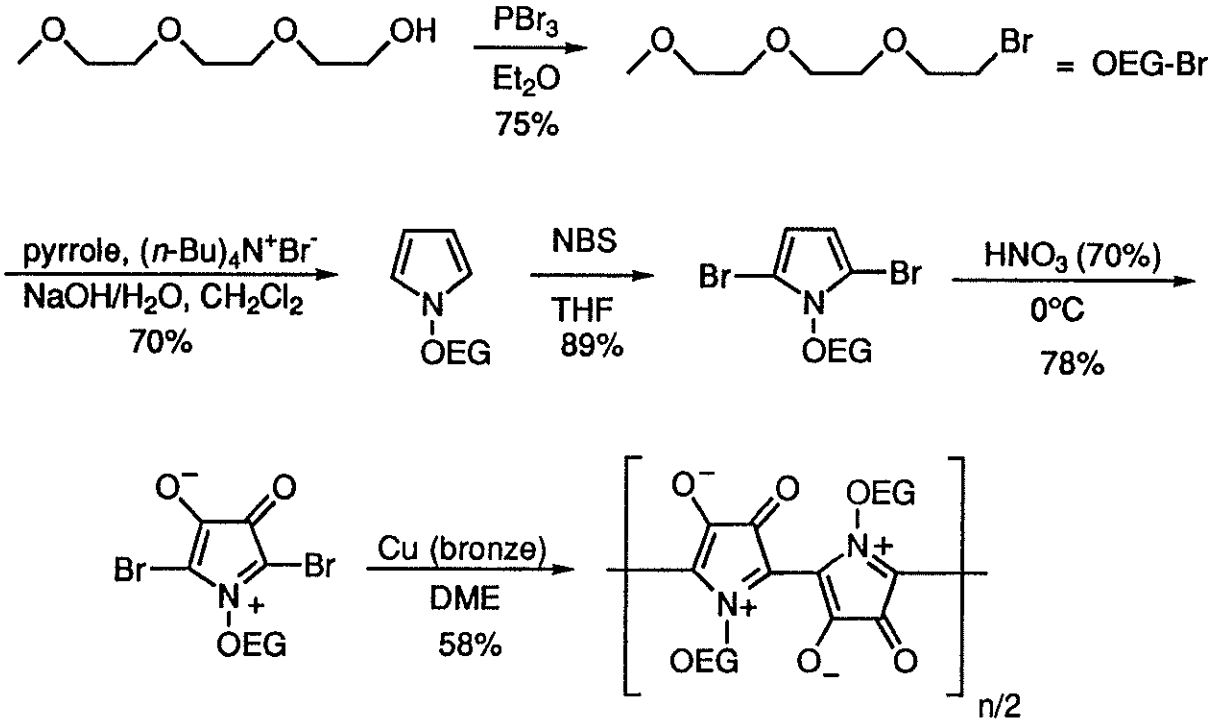

M_n = 8,650. M_w/M_n = 1.59. Anal. calc'd for $(C_{11}H_{15}NO_5)_n$: C, 54.76; H, 6.26; N, 5.85. Found: C, 54.18; H, 6.25; Br<0.5; N, 5.81.

Affect of Salts on the Optical Properties of Butyl- and OEG-Containing Polymers

Entry	Polymer	Solvent	Salt (0.2 M)	λ (nm)
1	**OEG**	MeOH	———	484
2	**OEG**	MeOH	$LiClO_4$	492
3	**OEG**	MeOH	$NaClO_4$	488
4	**OEG**	MeOH	$KClO_4$[a]	488
5	**OEG**	MeOH	LiF[a]	487
6	**OEG**	MeOH	LiCl	485
7	**OEG**	MeOH	LiBr	484
8	**OEG**	MeOH	NaF	486
9	**OEG**	MeOH	NaCl[a]	488
10	**OEG**	MeOH	NaBr	489
11	**OEG**	MeOH	KF	485
12	**OEG**	MeOH	KCl[a]	488
13	**OEG**	MeOH	KBr[a]	490
14	**OEG**	MeOH	LiI	480, 816
15	**OEG**	MeOH	NaI	459, 850
16	**OEG**	MeOH	KI	465, 876
17	**OEG**	CH_2Cl_2	———	518
18	**OEG**	CH_2Cl_2	TBAI[b]	518
19	**OEG**	CH_2Cl_2	$TMABF_4$[c]	518
20	**OEG**	CH_2Cl_2	$TBAPF_6$	517
21	**OEG**	MeOH/THF (9:1)	———	493
22	**OEG**	MeOH/THF (9:1)	LiI	476, 818
23	**OEG**	MeOH/THF (9:1)	NaI	474, 850
24	**OEG**	MeOH/THF (9:1)	KI	458, 863
25	**Butyl**	MeOH/THF (9:1)	———	480
26	**Butyl**	MeOH/THF (9:1)	LiI	477
27	**Butyl**	MeOH/THF (9:1)	NaI	479
28	**Butyl**	MeOH/THF (9:1)	KI	478
29	**Butyl**	CH_2Cl_2	———	518
30	**Butyl**	CH_2Cl_2	TBAI	516
31	**Butyl**	MeOH/THF (9:1)	NaI + 18-C-6	487
32	**Butyl**	MeOH/THF (9:1)	KI + 18-C-6	486

[a]This salt was only partially dissolved in MeOH. [b]TBA= tetrabutylammonium. [c]TMA = tetramethylammonium.

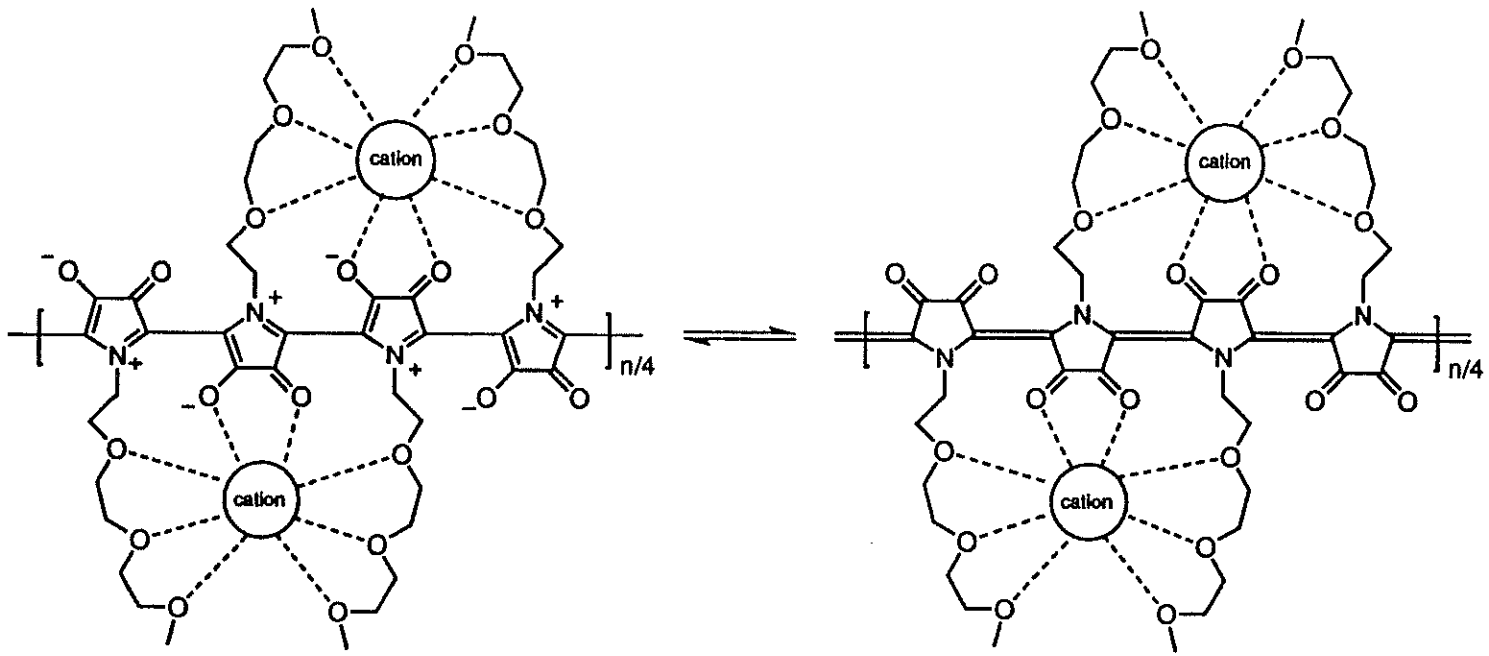
cation
cation
cation
n/4
n/4

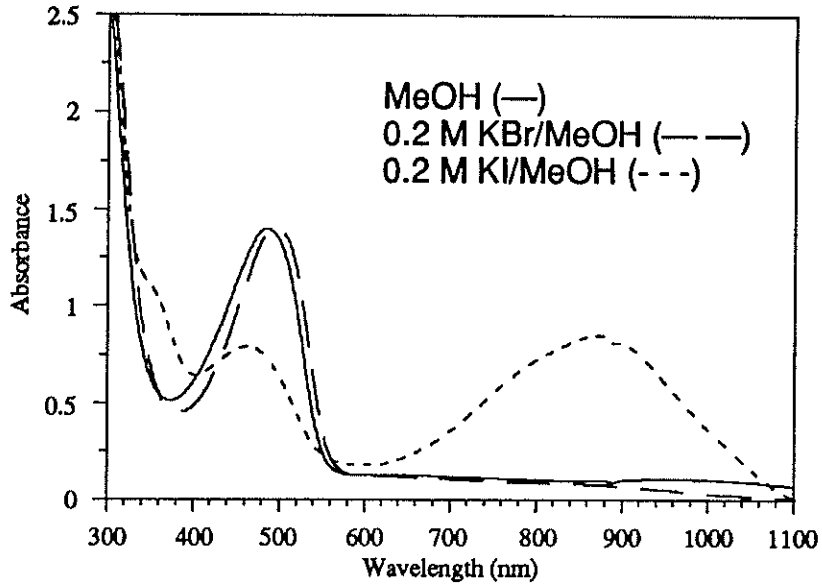
MeOH (—)
0.2 M KBr/MeOH (— —)
0.2 M KI/MeOH (- - -)
Absorbance
Wavelength (nm)
2.5
2
1.5
1
0.5
0
300
400
500
600
700
800
900
1000
1100

433

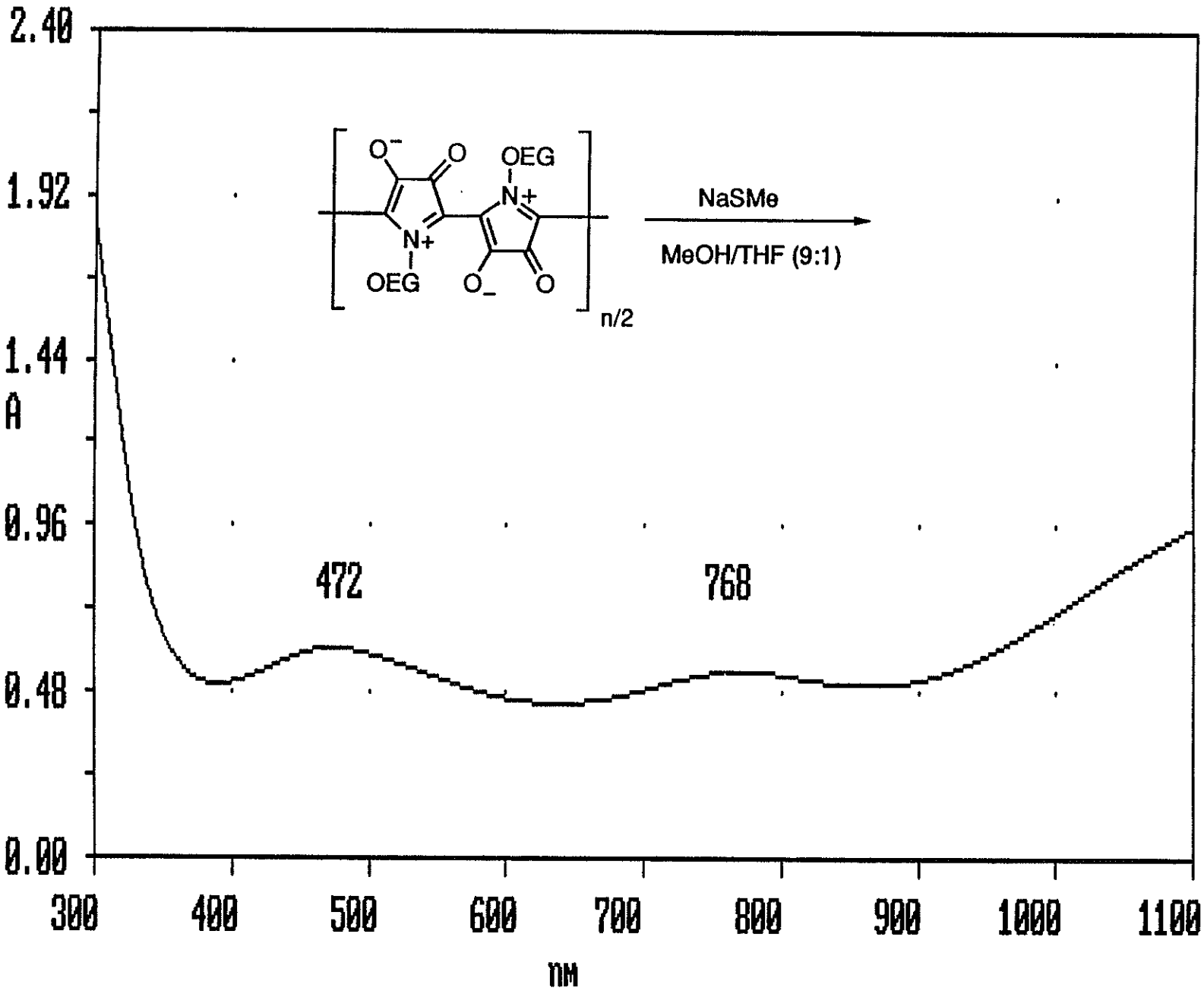
2.40
1.92
1.44
A
0.96
0.48
0.00
472
768
300
400
500
600
700
800
900
1000
1100
nm
O⁻
O
OEG
N+
N+
OEG
O_
O
n/2
NaSMe
MeOH/THF (9:1)

Molecular Electronics

Definition: A *single molecule* (not a film or crystal) functioning as a device (on/off).

Initial Obstacles:

(1) We must overcome the presumed hype barrier. Is molecular electronics simply science fiction or can we experimentally determine its potential?

(2) How do we address (attach to) a single molecule? Solution: nanoprobes.

(3) Can nanoprobes be fabricated or can a large enough molecule be synthesized? Solution: Nanoprobes down to the sub 100 Å regime can be fabricated and conjugated oligomers with precisely controlled length and constitution can be synthesized to these dimensions.

(4) How would we put the molecule in place between the probes? Solution: self-assembly or self-organization.

(5) How would we hold the molecule between the probes? Solution: molecular staples, for example, hydroxyl moieties attaching to an oxide surface.

(6) What would be the connecting units that would fasten the molecule to the probes? Solution: molecular-sized alligator clips, for example, thiol moieties binding to gold probes.

Plan of Attack:

(1) Physics (Drs. Tony Redondo and Brosl Hasslacher, LANL).
(2) Chemistry
(3) Nanofabrication/electronics (Professor Mark Reed, Yale University, EE Dept.).

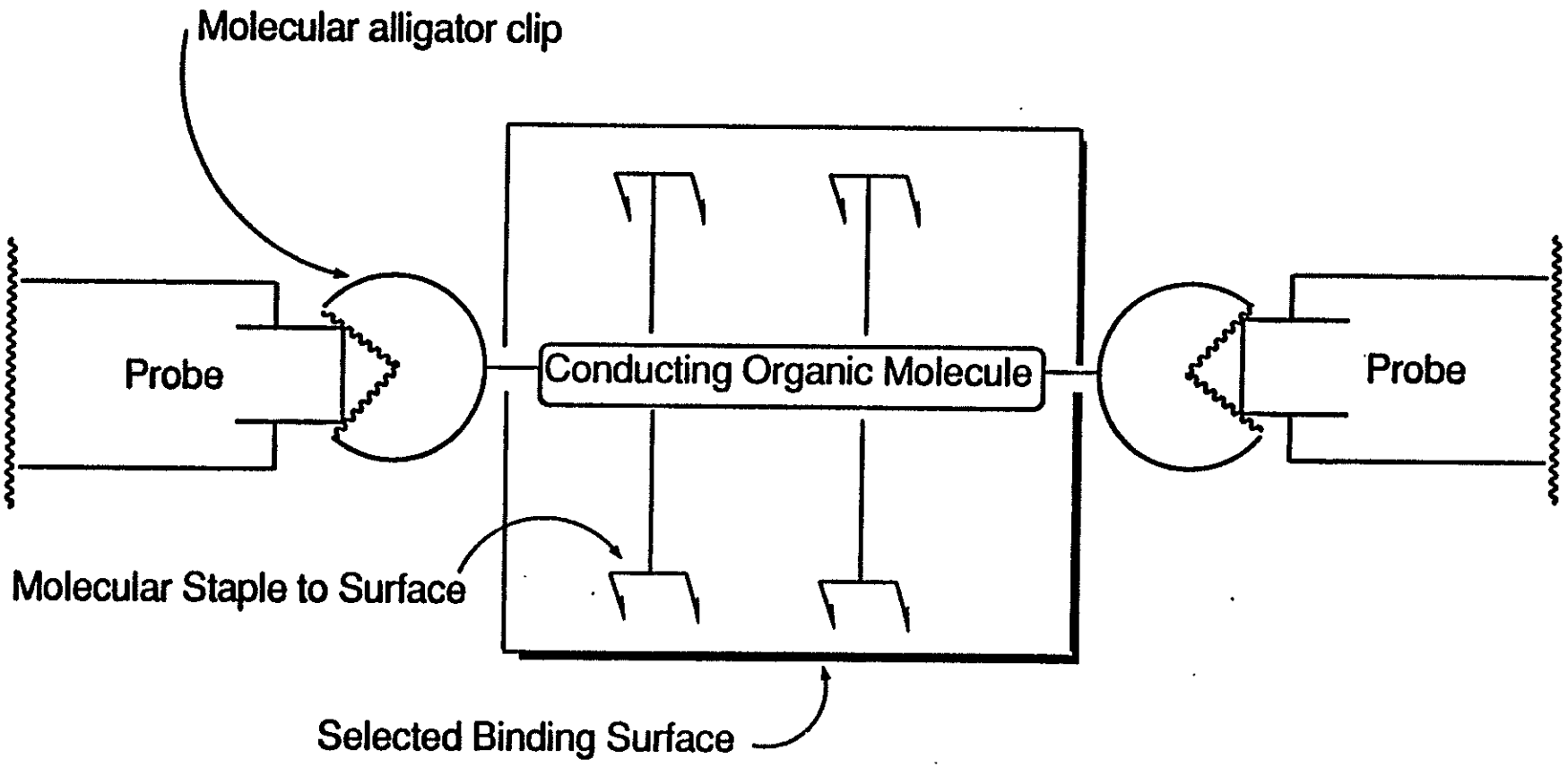
Molecular alligator clip
Probe
Conducting Organic Molecule
Probe
Molecular Staple to Surface
Selected Binding Surface

Deposition Cell

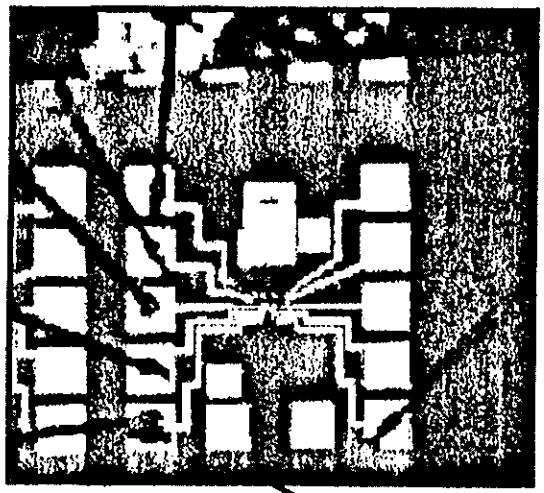

glass tube for solvent deoxygenation

inlet for oligomer solution injection

ribbon cable

electrical switch box

data acquisition

device on header in socket

solvent or oligomer solution

teflon base and support

glass cell

M. A. Reed
Microelectronics Center
Yale University

Electron Beam Lithography

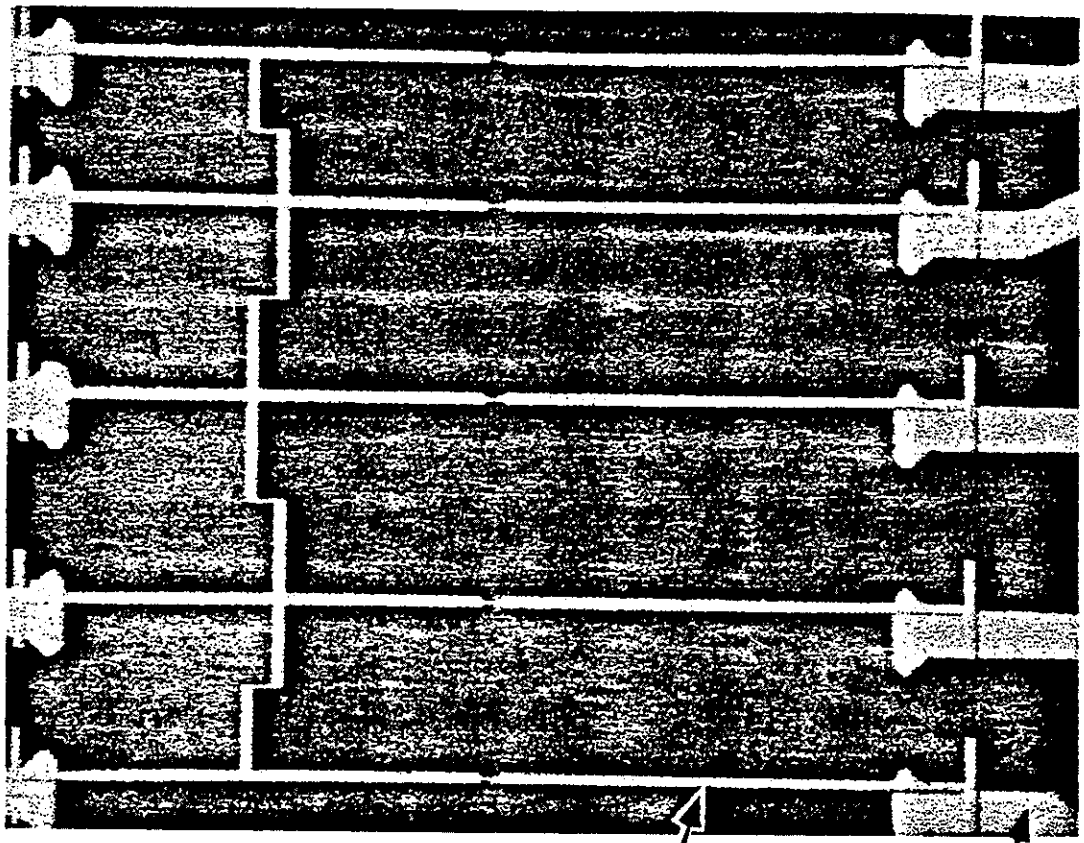

electron beam lithography

photolithography

Cross-Section:

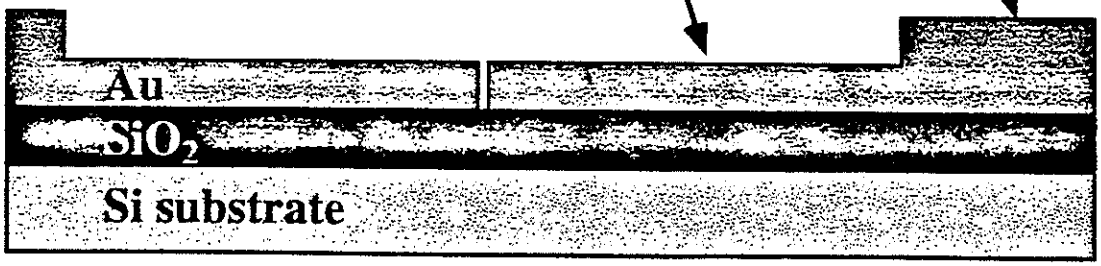

M. A. Reed
Microelectronics Center
Yale University

Angled Evaporation

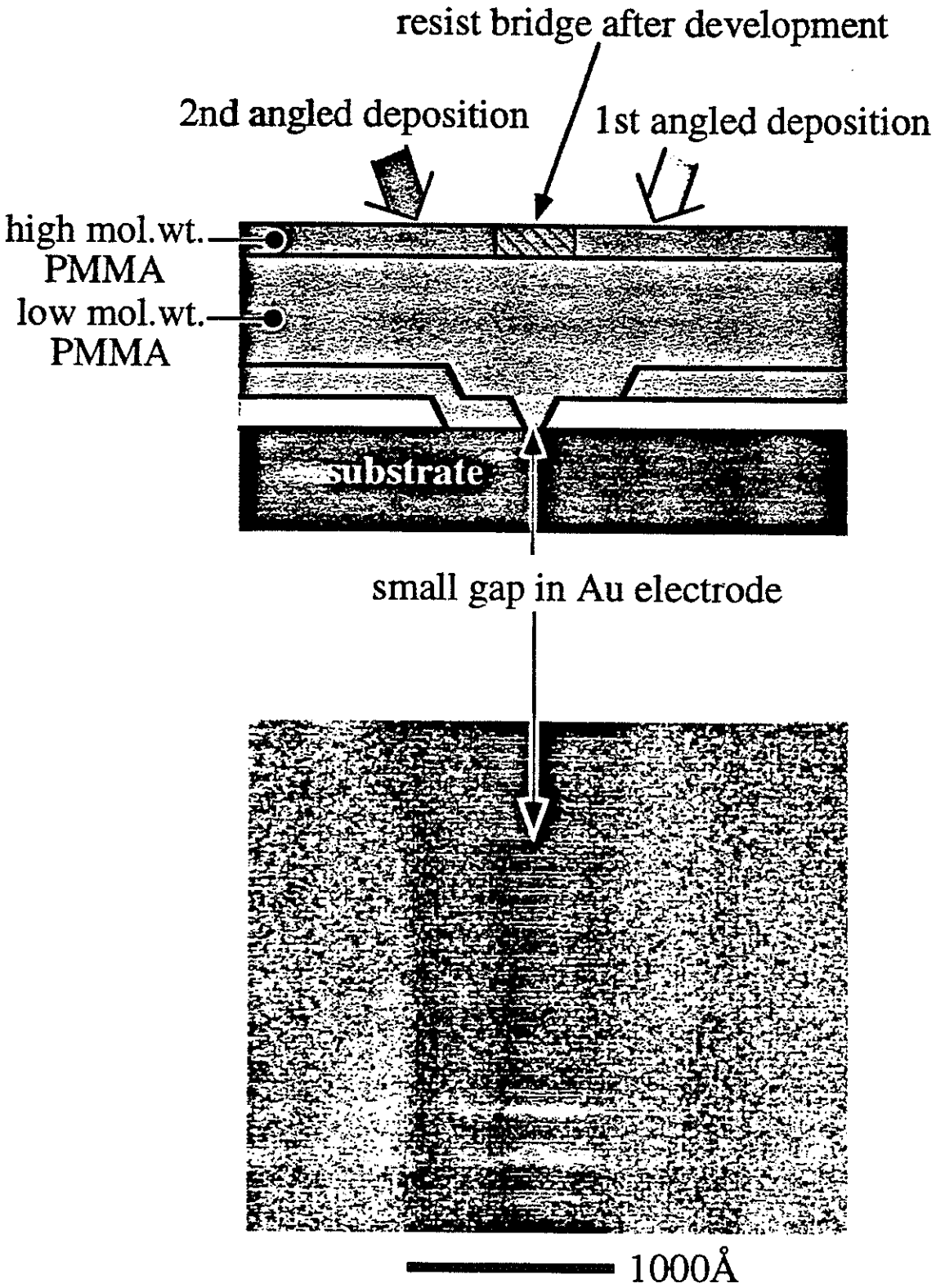

M. A. Reed
Microelectronics Center
Yale University

Small Gaps

3000Å nominal gap

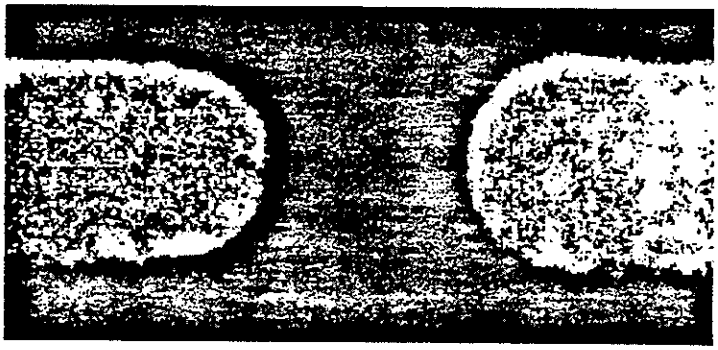

900Å

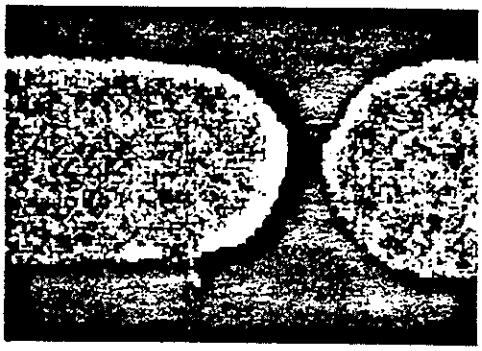

2000Å

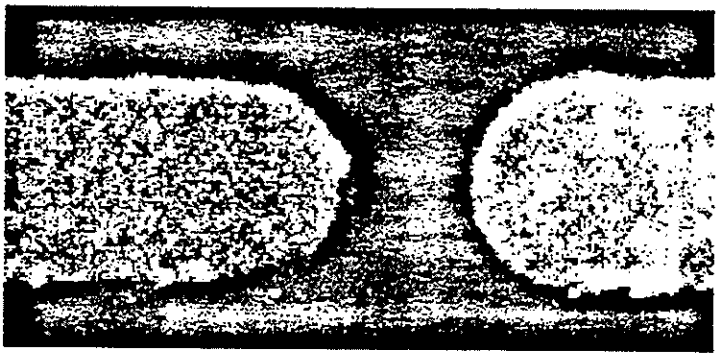

800Å

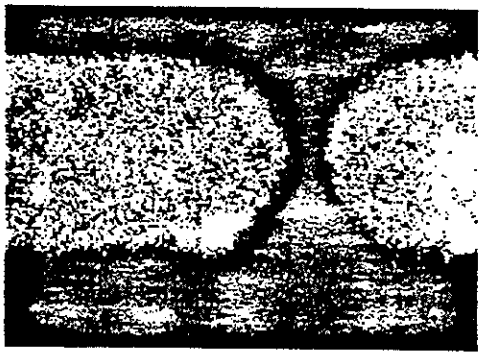

1000Å

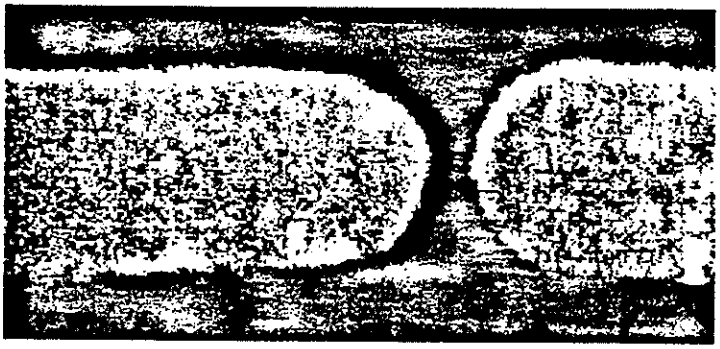

700Å

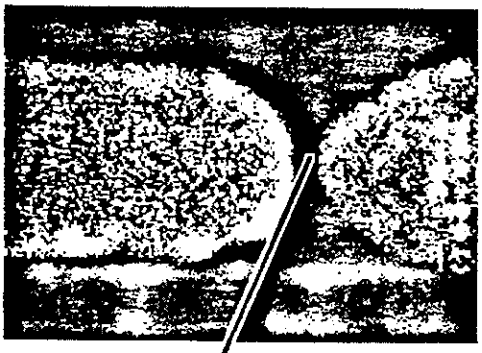

— 1000Å

200Å gap

440

M. A. Reed
Microelectronics Center
Yale University

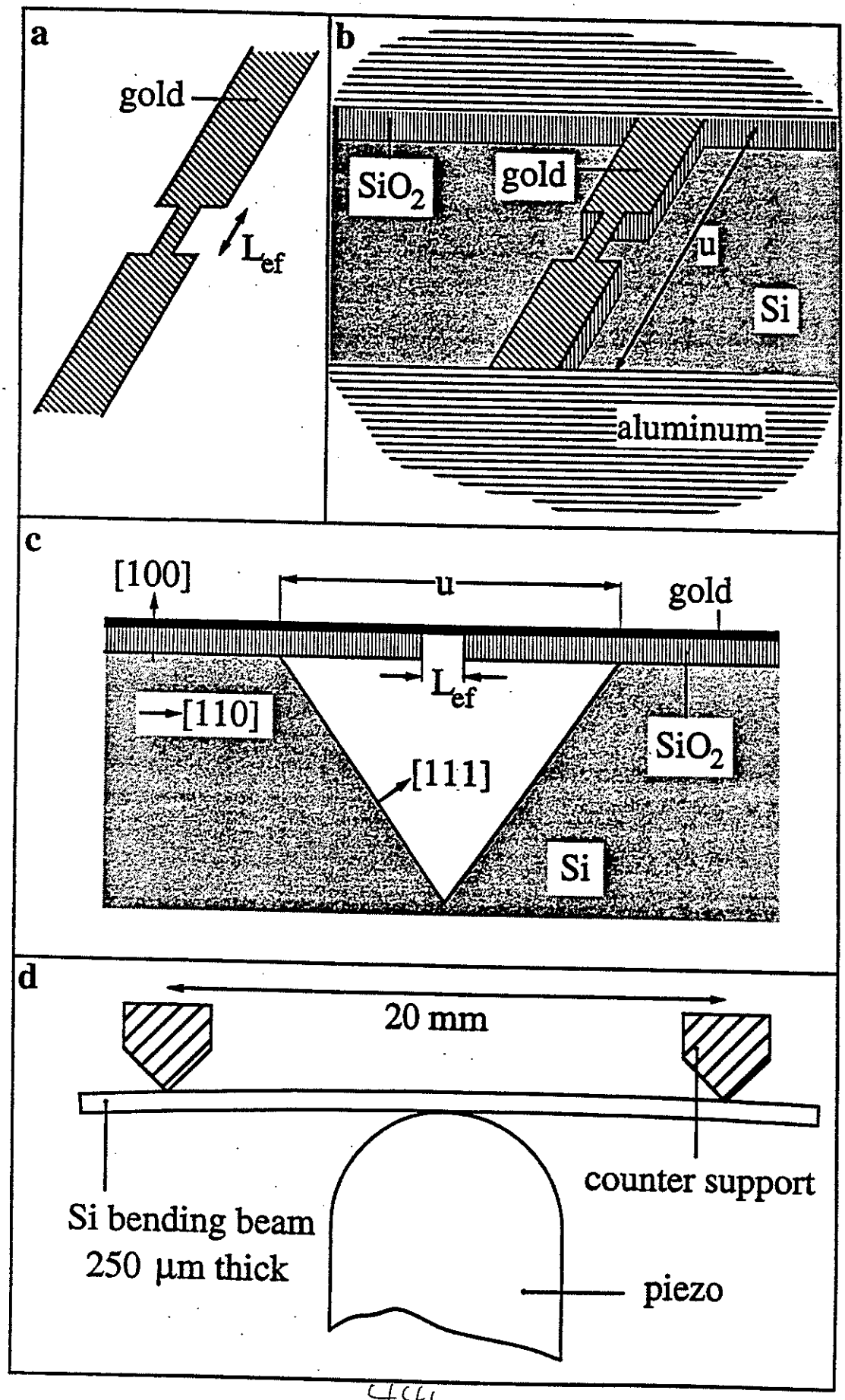
a
gold
L_{ef}
b
SiO_2
gold
u
Si
aluminum
c
[100]
u
gold
L_{ef}
[110]
SiO_2
[111]
Si
d
20 mm
counter support
Si bending beam
250 μm thick
piezo

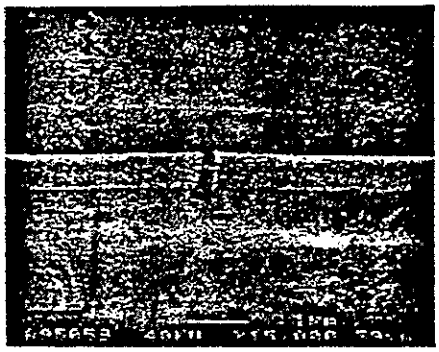

Figure 2a

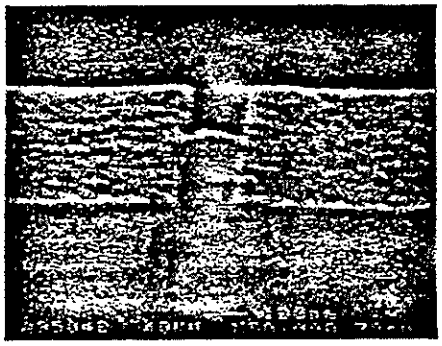

Figure 2b

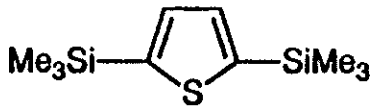

λ_{max} = 248
ε_{max} = 1.08 x 10^4
g = 6 x 10^{-36} esu by THG (L.-T. Cheng)
g = 4.1 x 10^{-36} esu by DFWM on
the unsubstituted system (Prasad)

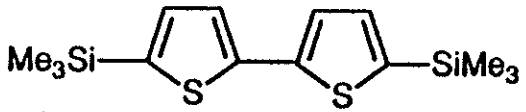

λ_{max} = 320 (305)
ε_{max} = 1.74 x 10^4
g = 15 x 10^{-36} esu by THG (L.-T. Cheng)
g = 22 x 10^{-36} esu by DFWM on
the unsubstituted system (Prasad)

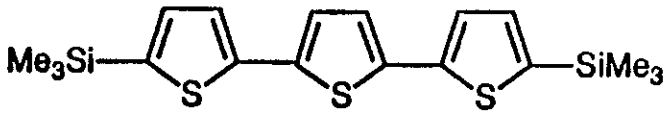

λ_{max} = 368 (360)
ε_{max} = 2.72 x 10^4
g = 41 x 10^{-36} esu by THG (L.-T. Cheng)
g = 160 x 10^{-36} esu by DFWM on
the unsubstituted system (Prasad)

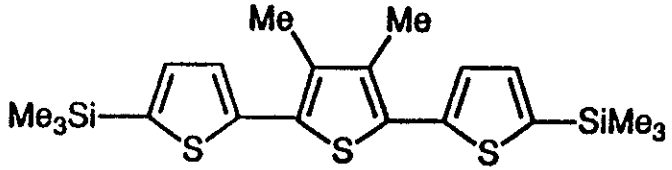

λ_{max} = 350
ε_{max} = 1.94 x 10^4

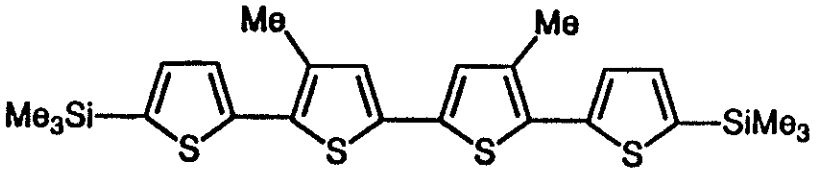

λ_{max} = 396 (391)
ε_{max} = 3.45 x 10^4
g = 142 x 10^{-36} esu by THG (L.-T. Cheng)
g = 800 x 10^{-36} esu by DFWM on
the unsubstituted system (Prasad)

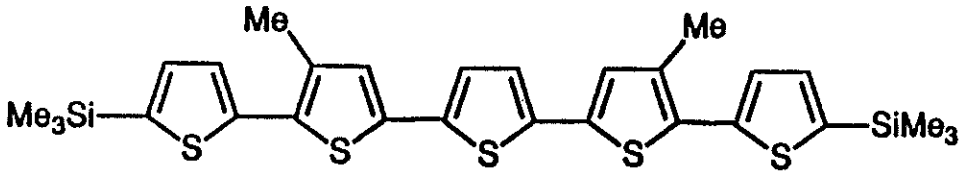

λ_{max} = 418 (416)
ε_{max} = 3.69 x 10^4
g = 249 x 10^{-36} esu by THG (L.-T. Cheng)
g = 2600 x 10^{-36} esu by DFWM on
the unsubstituted system (Prasad)

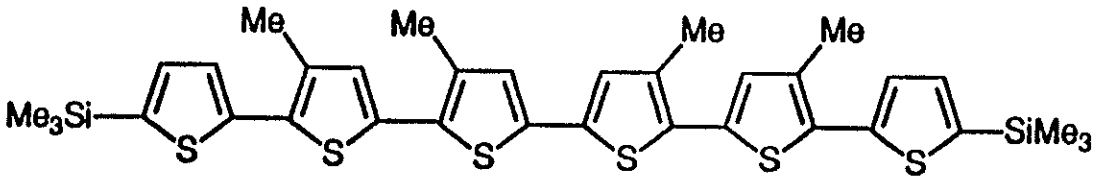

λ_{max} = 430 (438)
$\varepsilon_{max} = 4.06 \times 10^{4}$
$g = 320 \times 10^{-36}$ esu by THG (L.-T. Cheng)
$g = 10{,}000 \times 10^{-36}$ esu by DFWM on the unsubstituted system (Prasad)

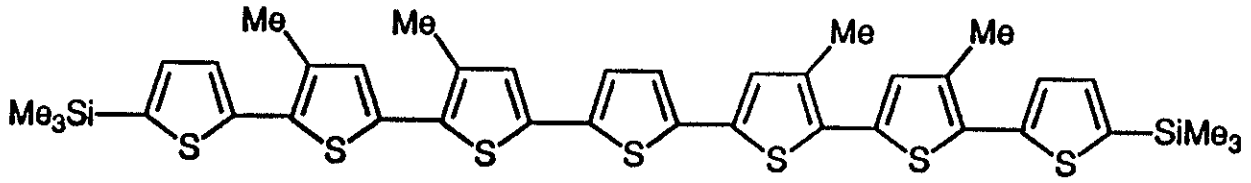

λ_{max} = 448 (440)
$g = 450 \times 10^{-36}$ esu by THG (L.-T. Cheng)

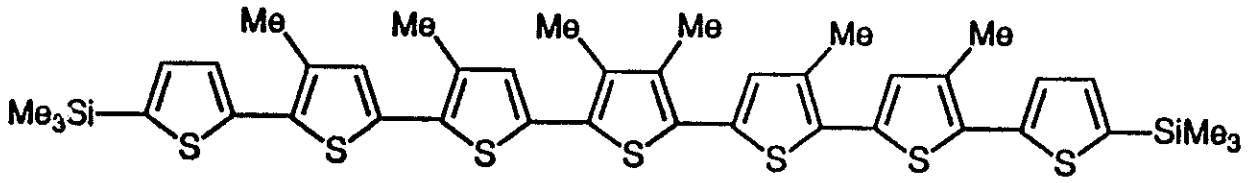

λ_{max} = 424 (440)
$\varepsilon_{max} = 4.13 \times 10^{4}$

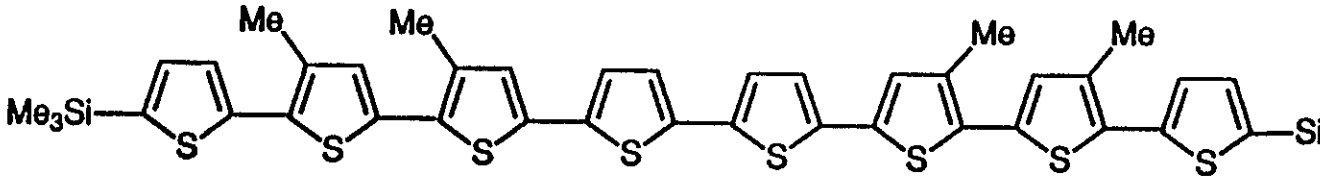

λ_{max} = 458
$\varepsilon_{max} = 6.09 \times 10^{4}$
$g = 620 \times 10^{-36}$ esu by THG (L.-T. Cheng)

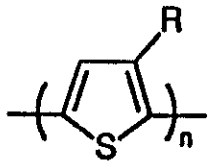

In solution λ_{max} = 430-440 nm
Films λ_{max} = 480-520 nm

Cheng exponent = 2.4
Prasad exponent = 4.05

RAPID SYNTHESIS OF CONJUGATED ORGANIC OLIGOMERS
SYNTHESIS OF "MOLECULAR WIRES" WITH END GROUP CONTROL

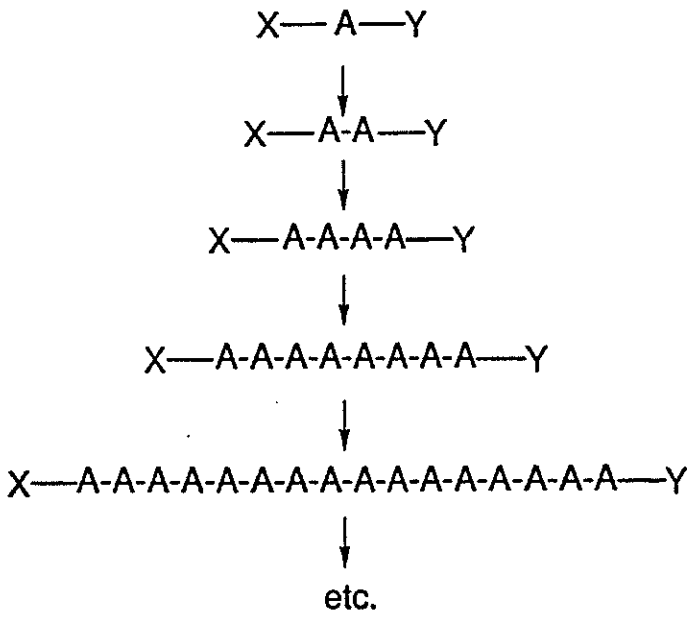

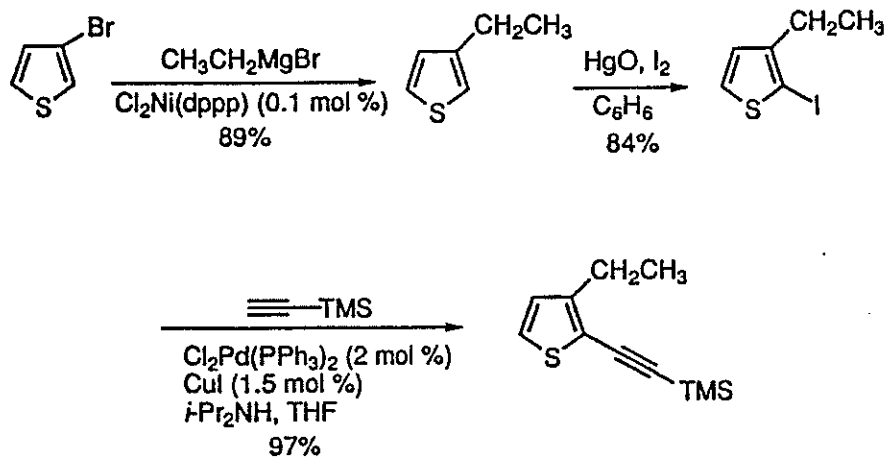

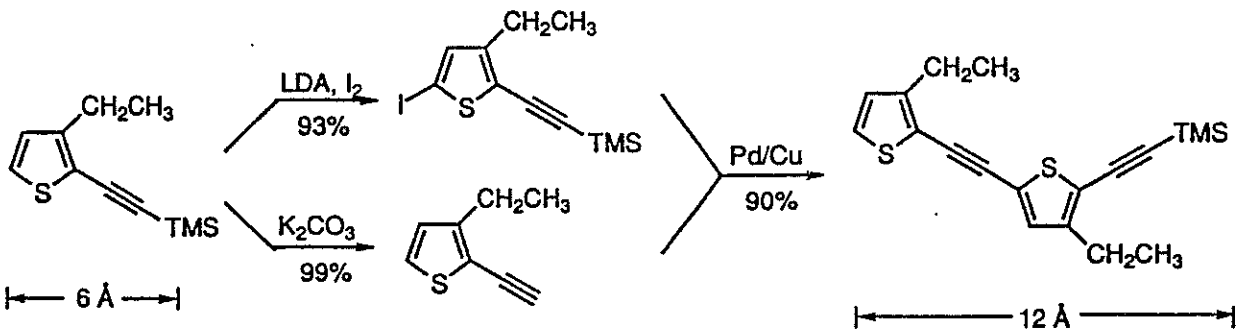

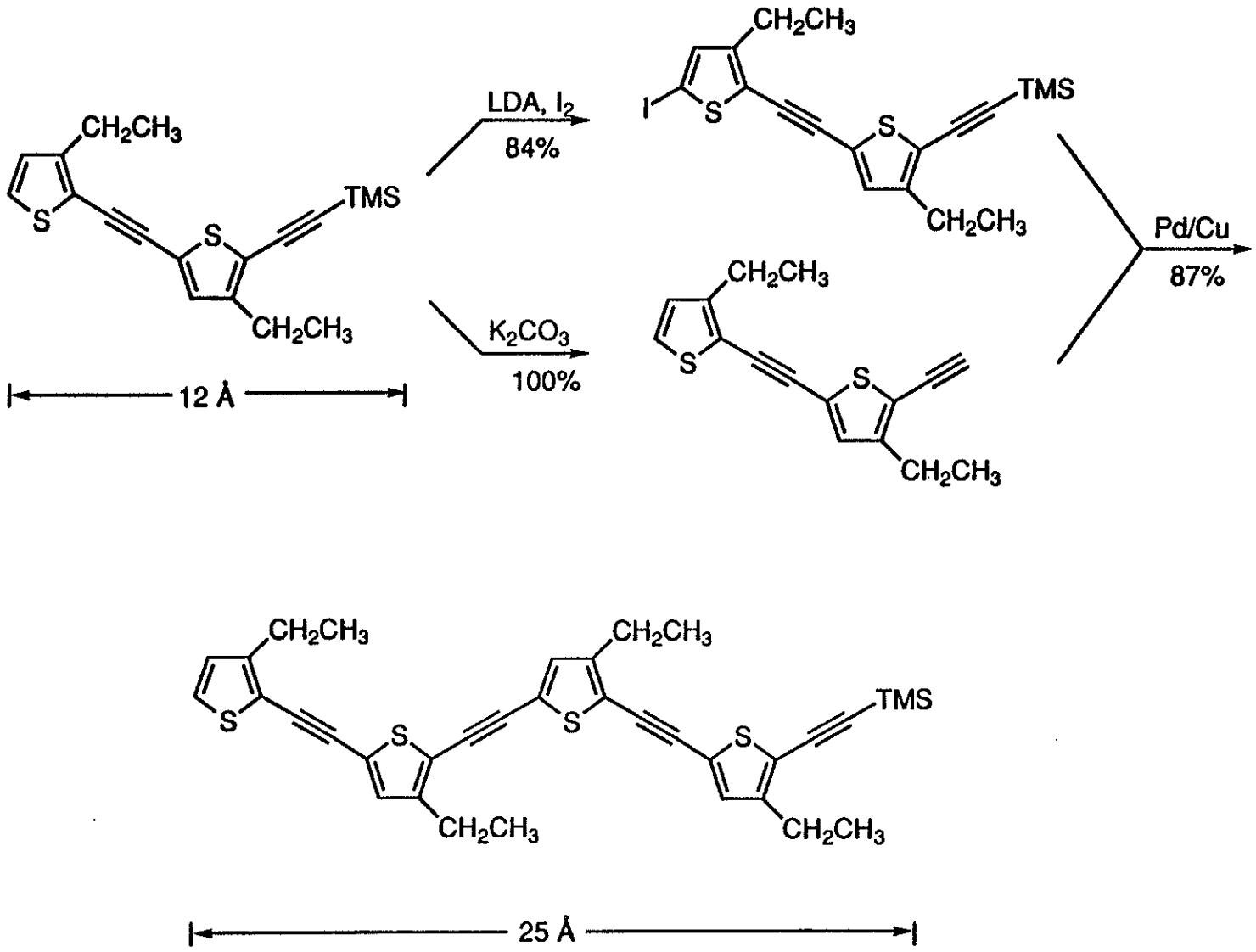
CH2CH3
TMS
S
S
CH2CH3
12 Å
LDA, I2
84%
K2CO3
100%
I
Pd/Cu
87%
25 Å

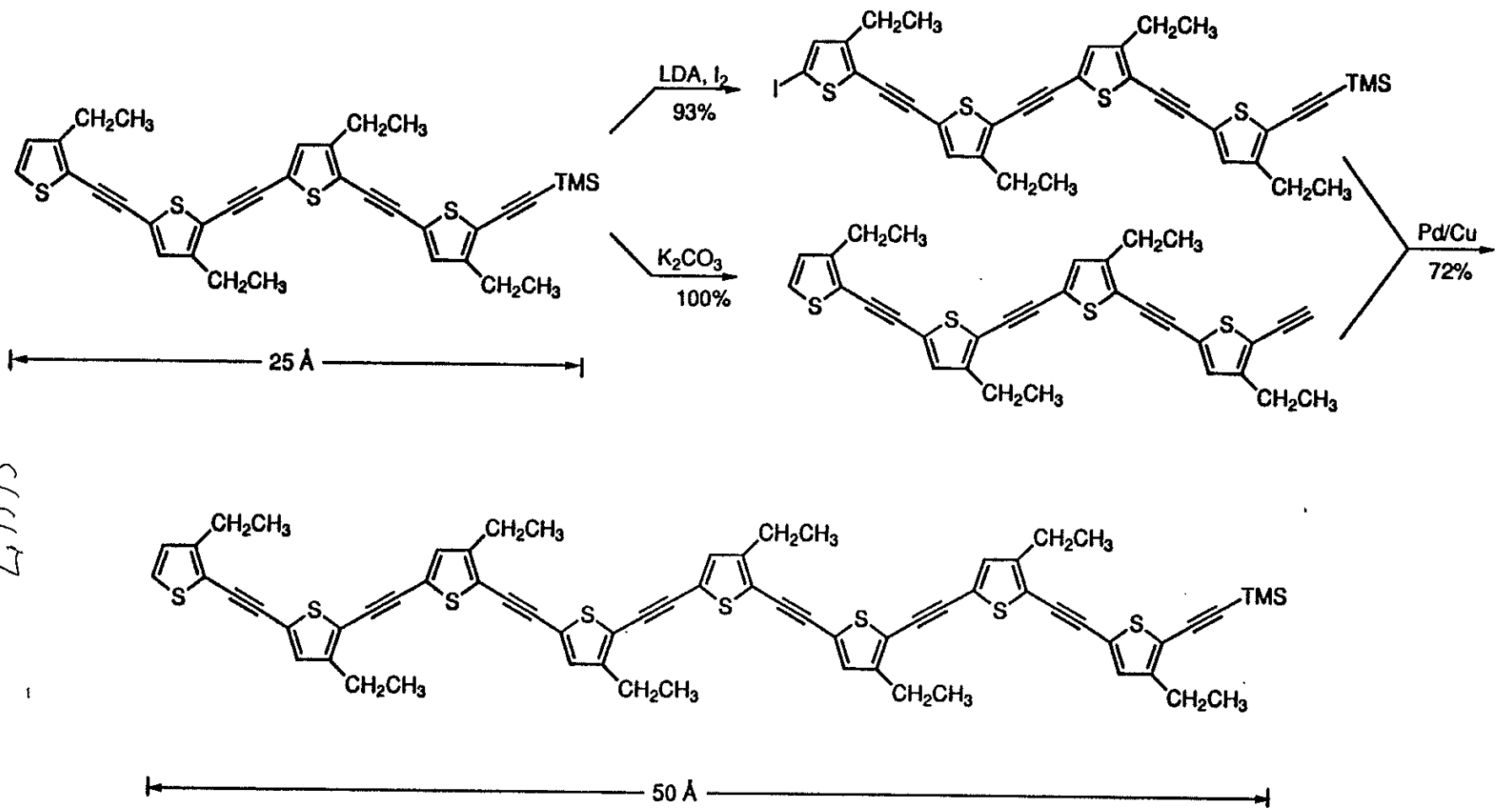
LDA, I2
93%
K2CO3
100%
Pd/Cu
72%
TMS
CH2CH3
25 Å
50 Å

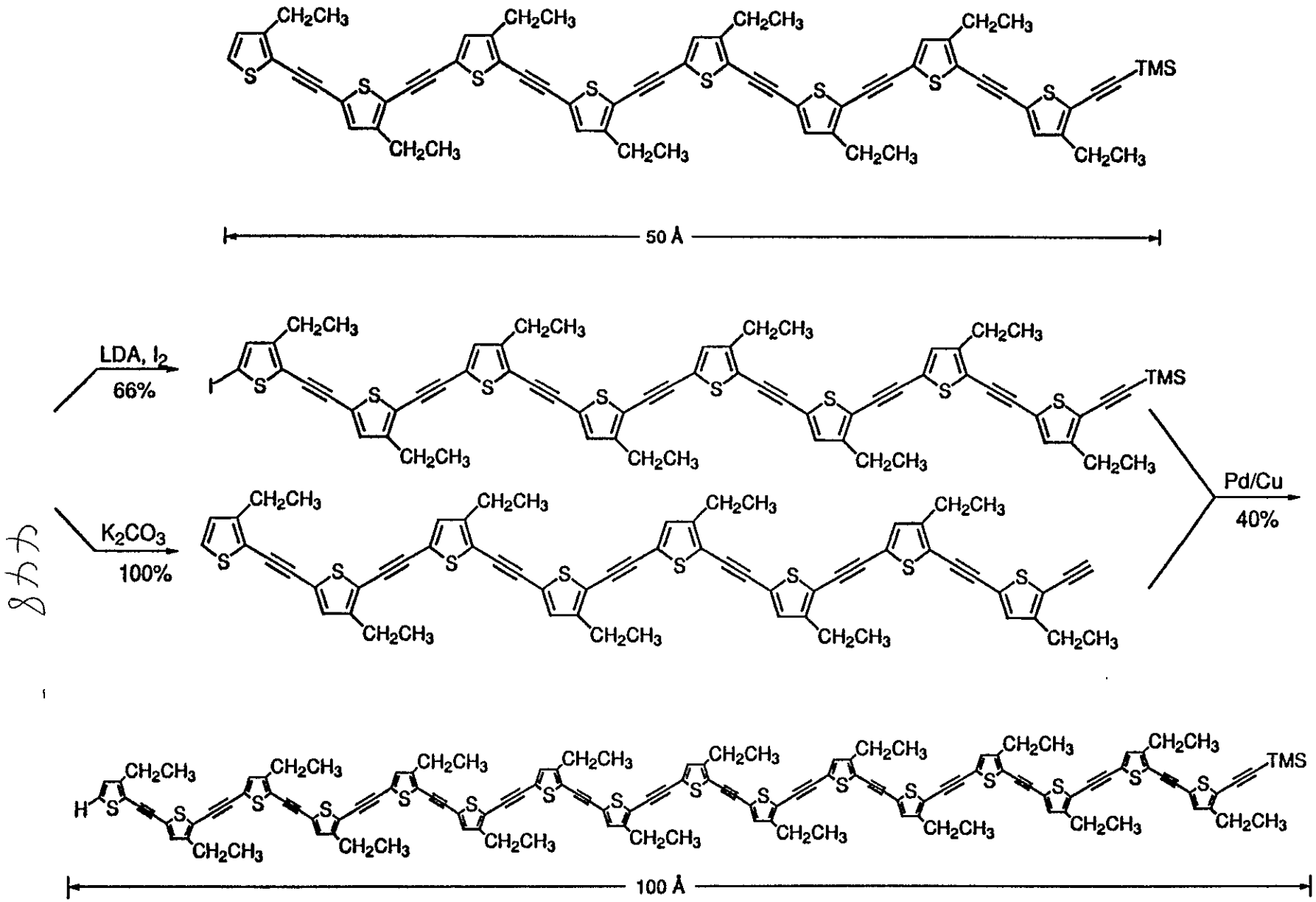
LDA, I2
66%
K2CO3
100%
Pd/Cu
40%
TMS
50 Å
100 Å

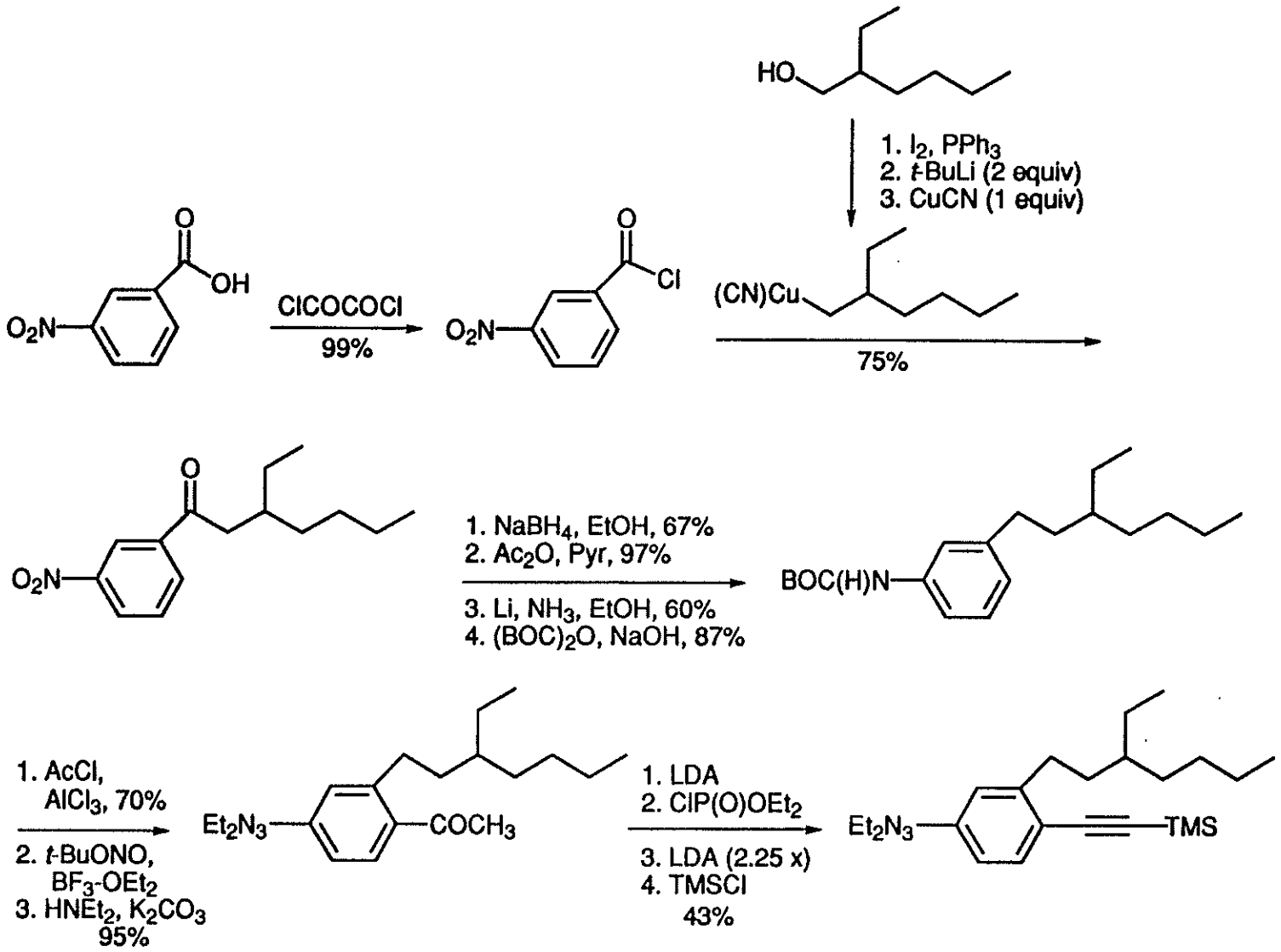
HO
1. I_2, PPh_3
2. t-BuLi (2 equiv)
3. CuCN (1 equiv)
O_2N
OH
O
ClCOCOCl
99%
Cl
(CN)Cu
75%
1. $NaBH_4$, EtOH, 67%
2. Ac_2O, Pyr, 97%
3. Li, NH_3, EtOH, 60%
4. $(BOC)_2O$, NaOH, 87%
BOC(H)N
1. AcCl, $AlCl_3$, 70%
2. t-BuONO, BF_3-OEt_2
3. $HNEt_2$, K_2CO_3
95%
Et_2N_3
$COCH_3$
1. LDA
2. $ClP(O)OEt_2$
3. LDA (2.25 x)
4. TMSCl
43%
TMS

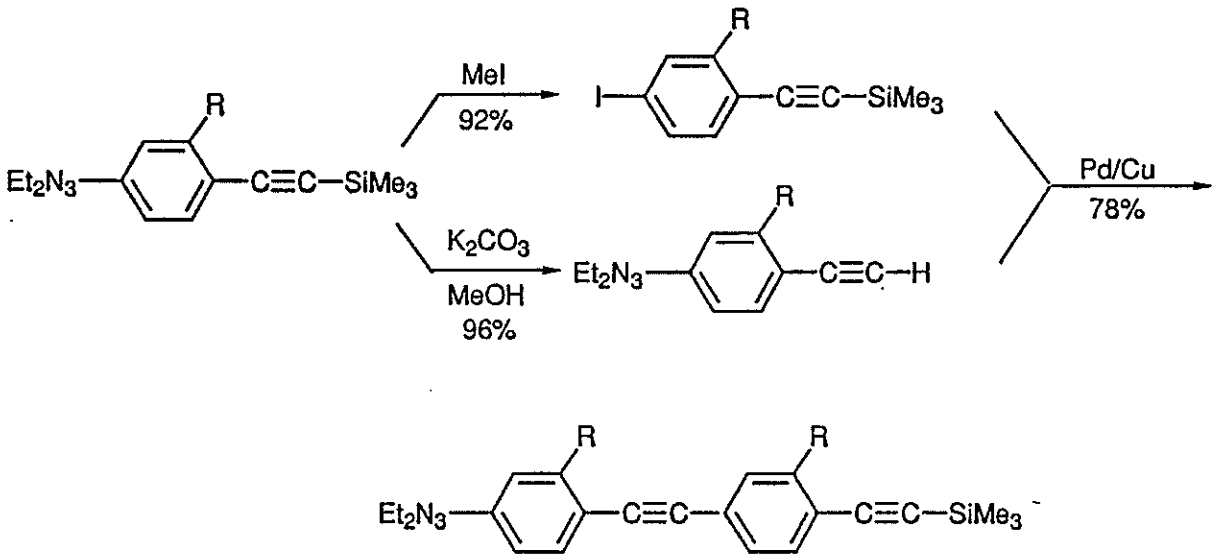

R = 3-ethylheptyl

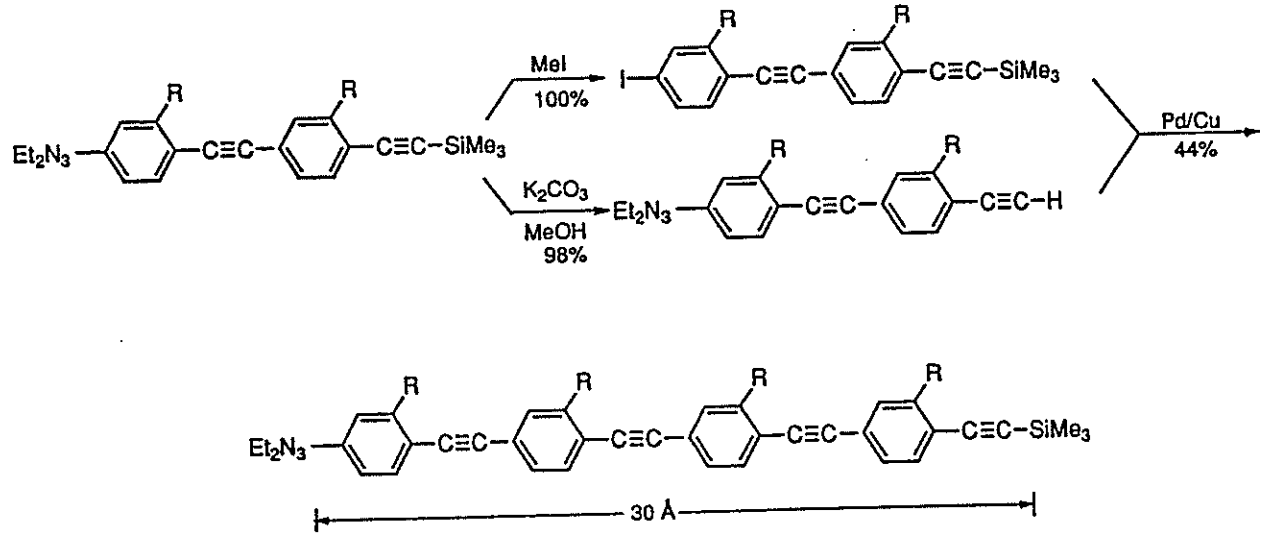

R = 3-ethylheptyl

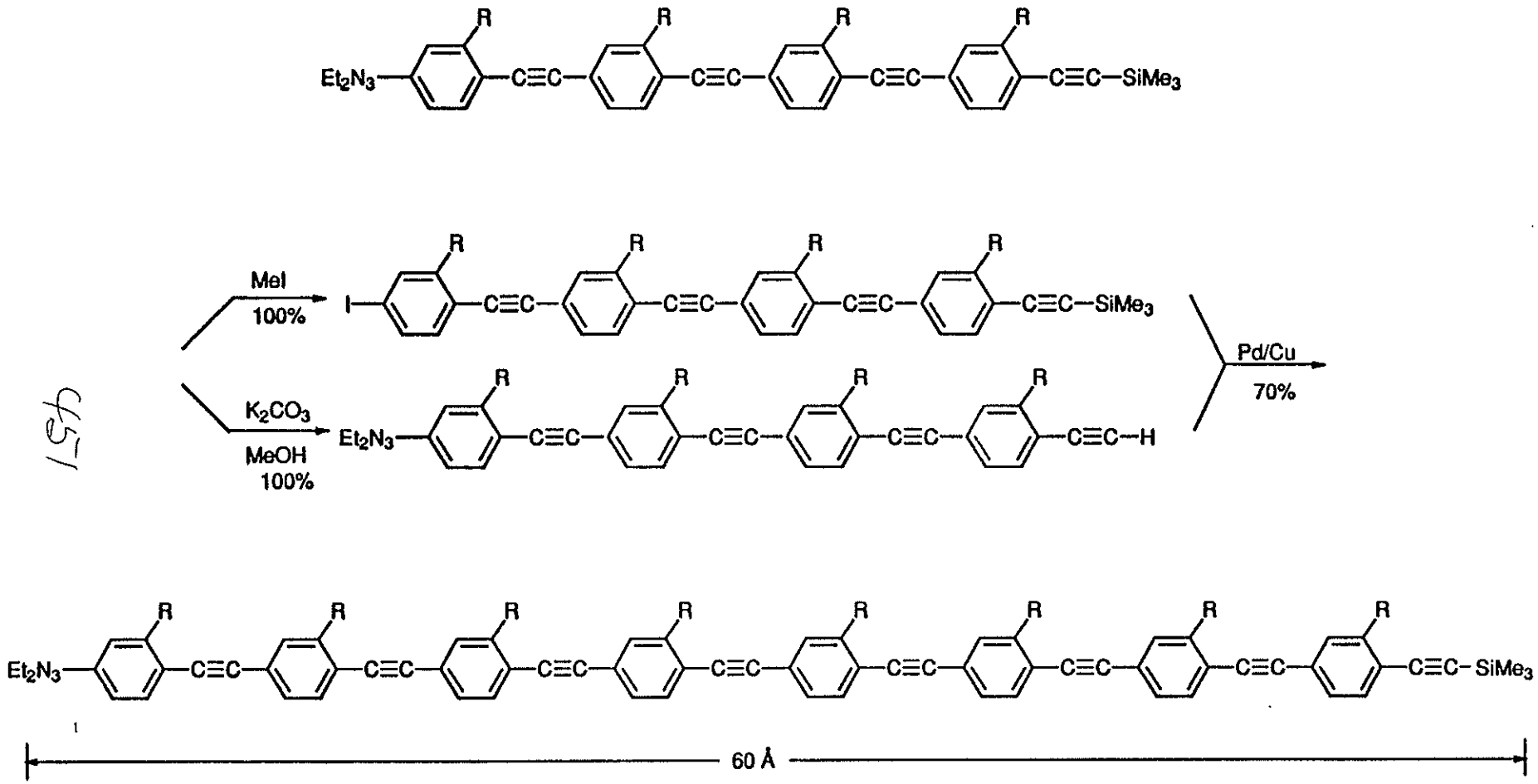
R
Et2N3
C≡C
SiMe3
MeI
100%
I
K2CO3
MeOH
100%
H
Pd/Cu
70%
60 Å
R = 3-ethylheptyl

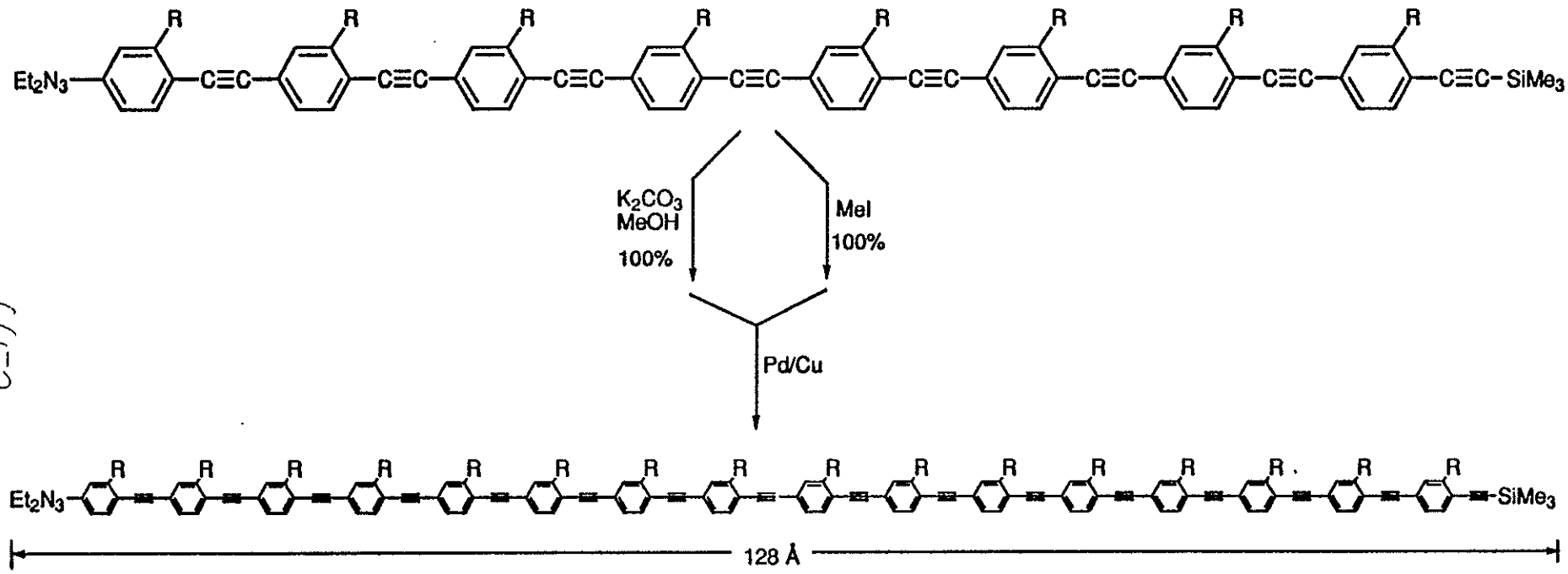

R = 3-ethylheptyl

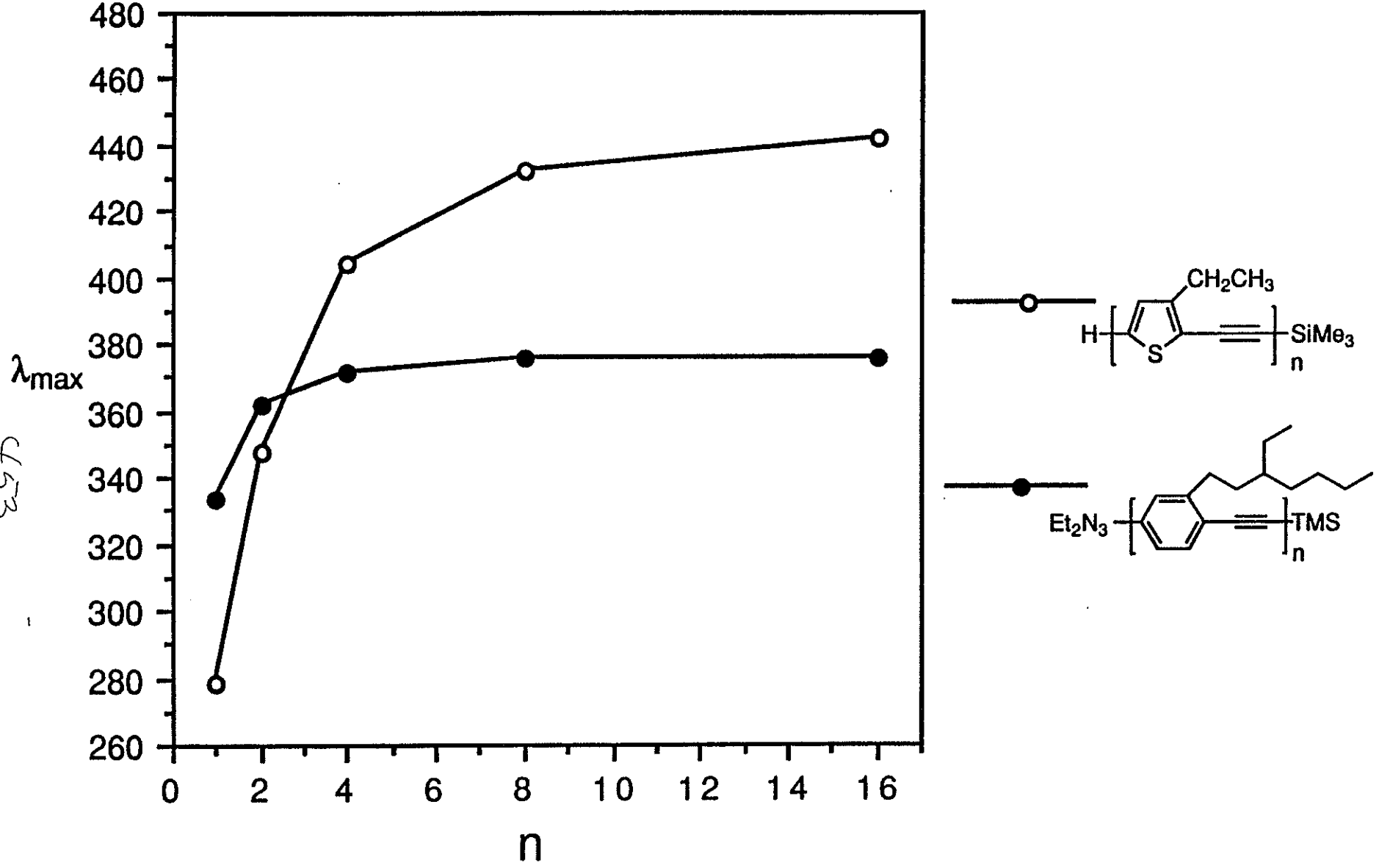
480
460
440
420
400
380
360
340
320
300
280
260
λmax
0
2
4
6
8
10
12
14
16
n
CH2CH3
H
S
SiMe3
n
Et2N3
TMS
n

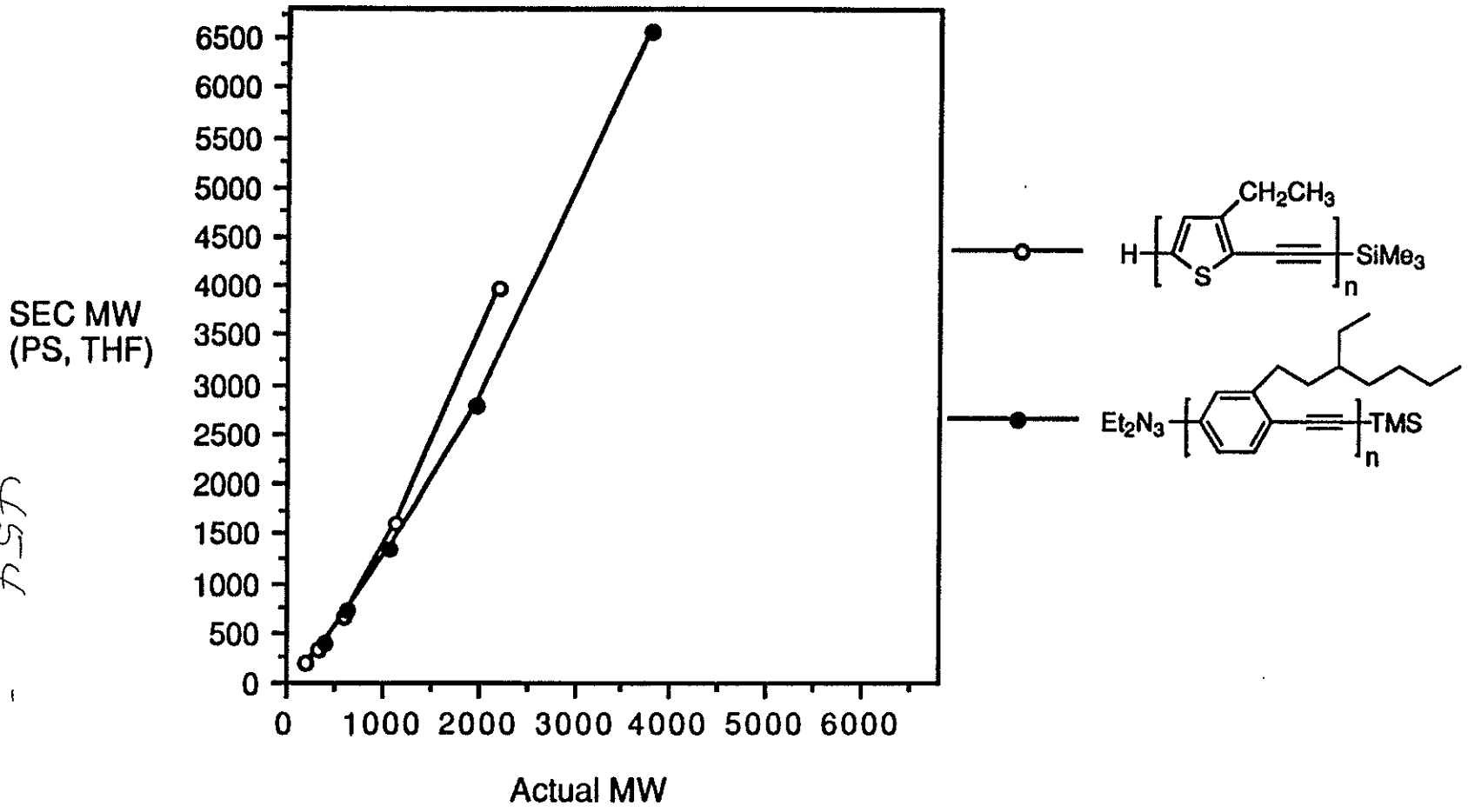
SEC MW
(PS, THF)
6500
6000
5500
5000
4500
4000
3500
3000
2500
2000
1500
1000
500
0
0 1000 2000 3000 4000 5000 6000
Actual MW
CH2CH3
H
S
SiMe3
n
Et2N3
TMS
n

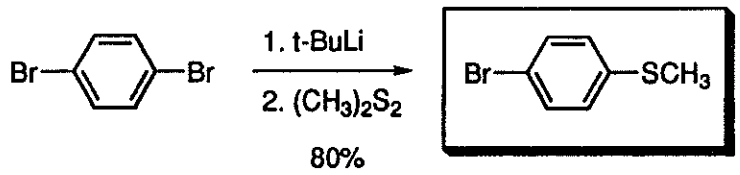
Br
Br
1. t-BuLi
2. $(CH_3)_2S_2$
80%
Br
SCH_3

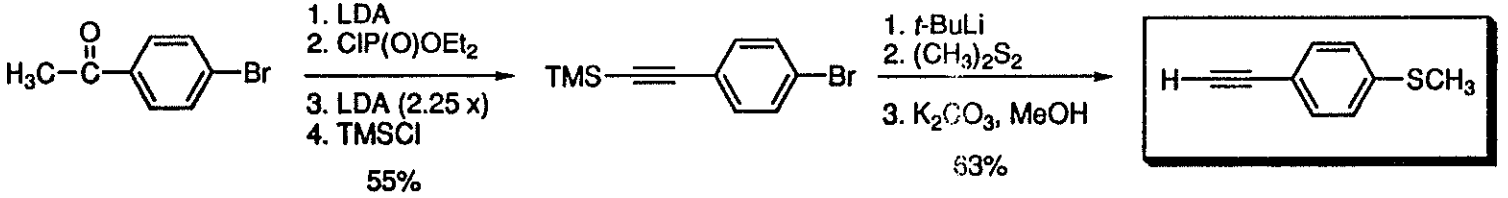
H_3C
C
O
Br
1. LDA
2. $ClP(O)OEt_2$
3. LDA (2.25 x)
4. TMSCl
55%
TMS
Br
1. t-BuLi
2. $(CH_3)_2S_2$
3. K_2CO_3, MeOH
63%
H
SCH_3

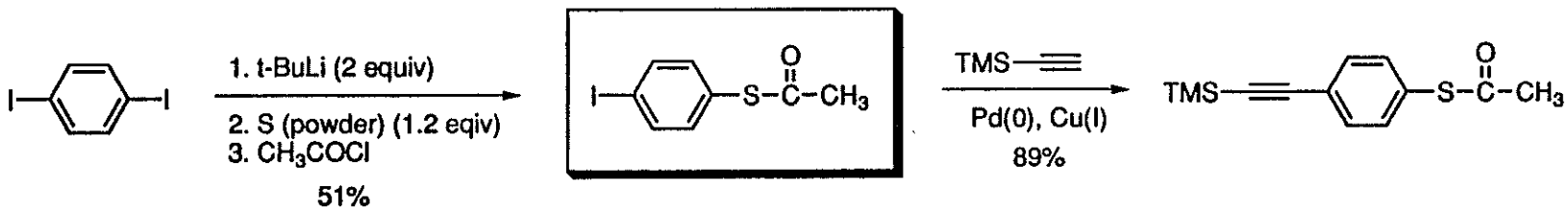
I
I
1. t-BuLi (2 equiv)
2. S (powder) (1.2 eqiv)
3. CH_3COCl
51%
I
S
C
O
CH_3
TMS
Pd(0), Cu(I)
89%
TMS
S
C
O
CH_3

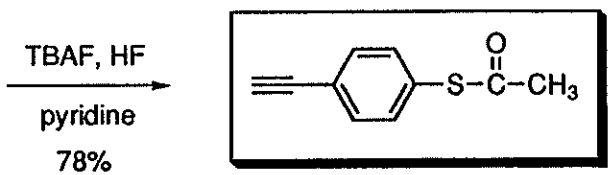
TBAF, HF
pyridine
78%
S
C
O
CH_3

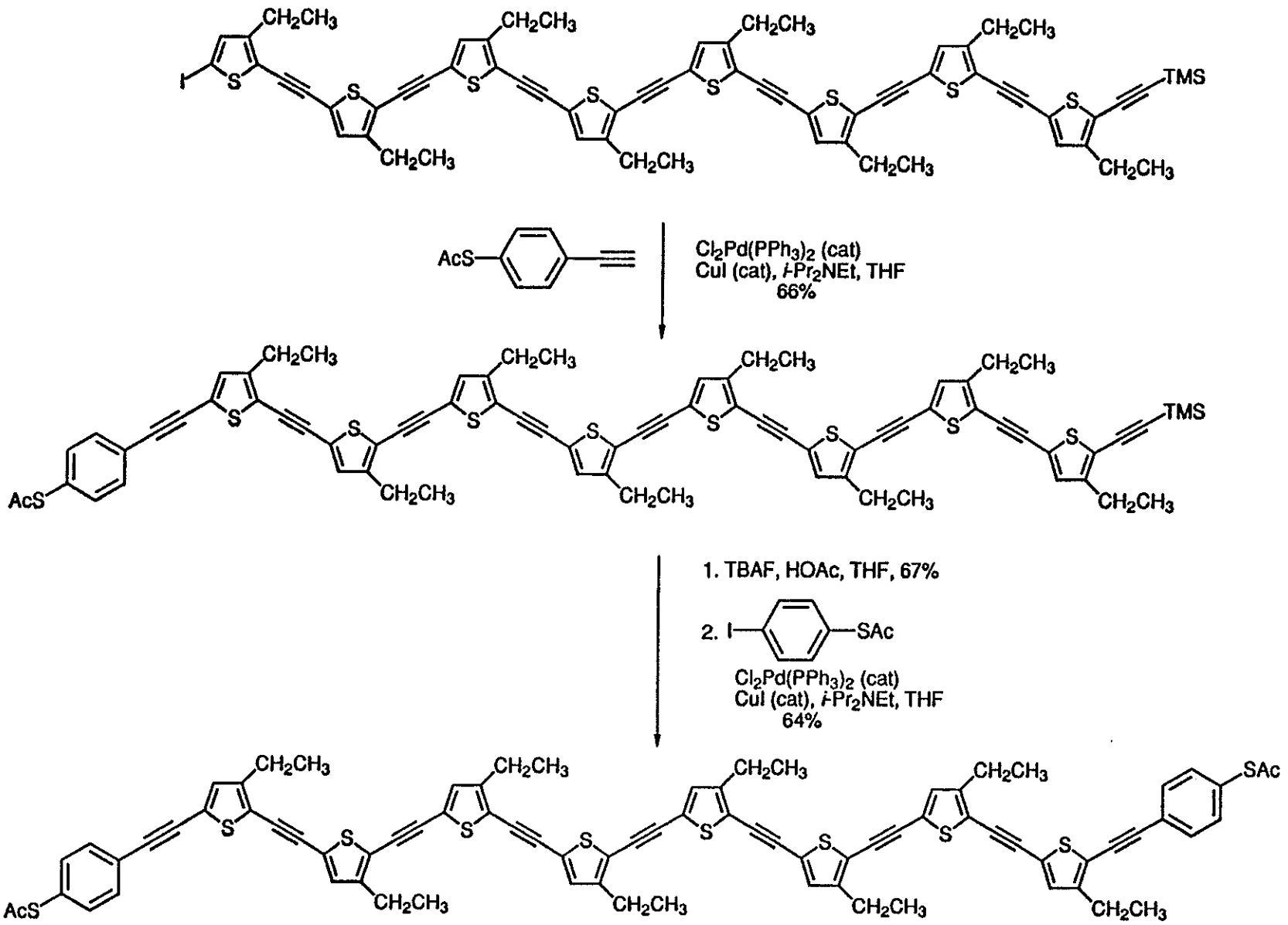
CH2CH3
S
TMS
AcS
Cl2Pd(PPh3)2 (cat)
CuI (cat), i-Pr2NEt, THF
66%
1. TBAF, HOAc, THF, 67%
2. I
SAc
Cl2Pd(PPh3)2 (cat)
CuI (cat), i-Pr2NEt, THF
64%

In situ deprotection of the thiols, during depositions, may solve the isolation and instability problems.

Model Studies:

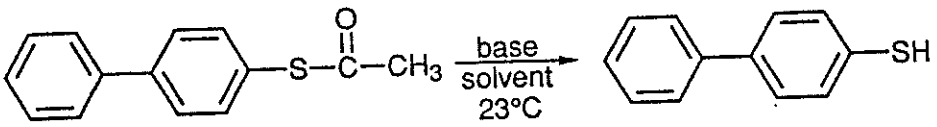

Base	Solvent	Ratio of acetate to thiol after 18 h
n-Pr_2NH	$CDCl_3$	1:5
n-Pr_2NH	$CDCl_3$, CH_3OH	1:4
n-Pr_2NH with AcOH	$CDCl_3$	1:9
n-Pr_2NH/DMAP (cat)	$CDCl_3$	0:10
NH_4OH	$THF\text{-}d_8$	0:10 **(10 min)**

Known in Self-Assembly on Gold

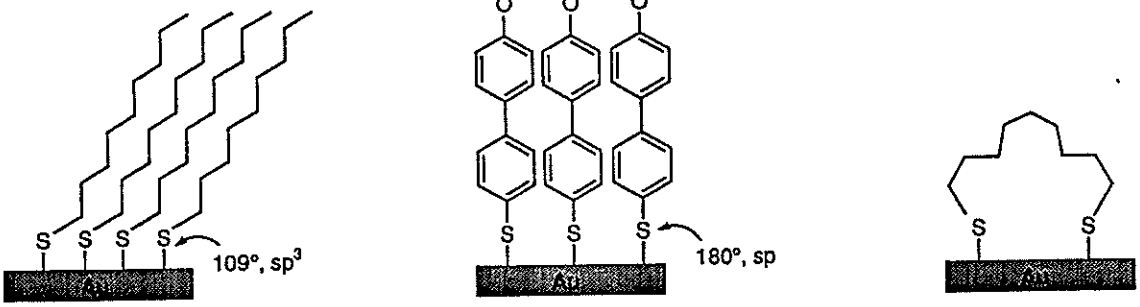

How will rigid-rod aromatic α,ω-dithiols order between gold probes?

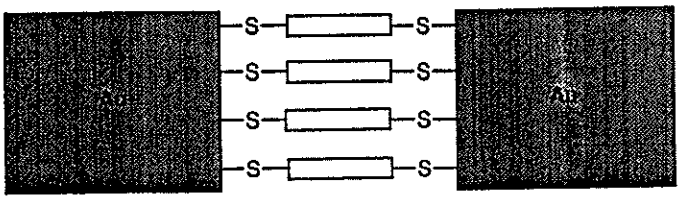

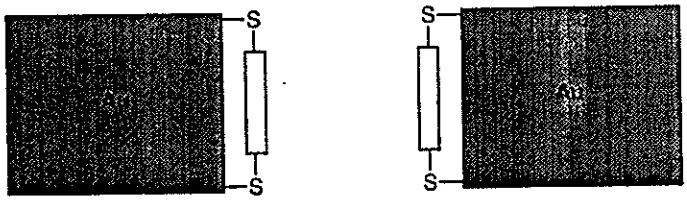

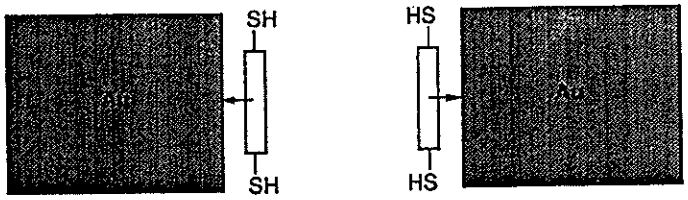

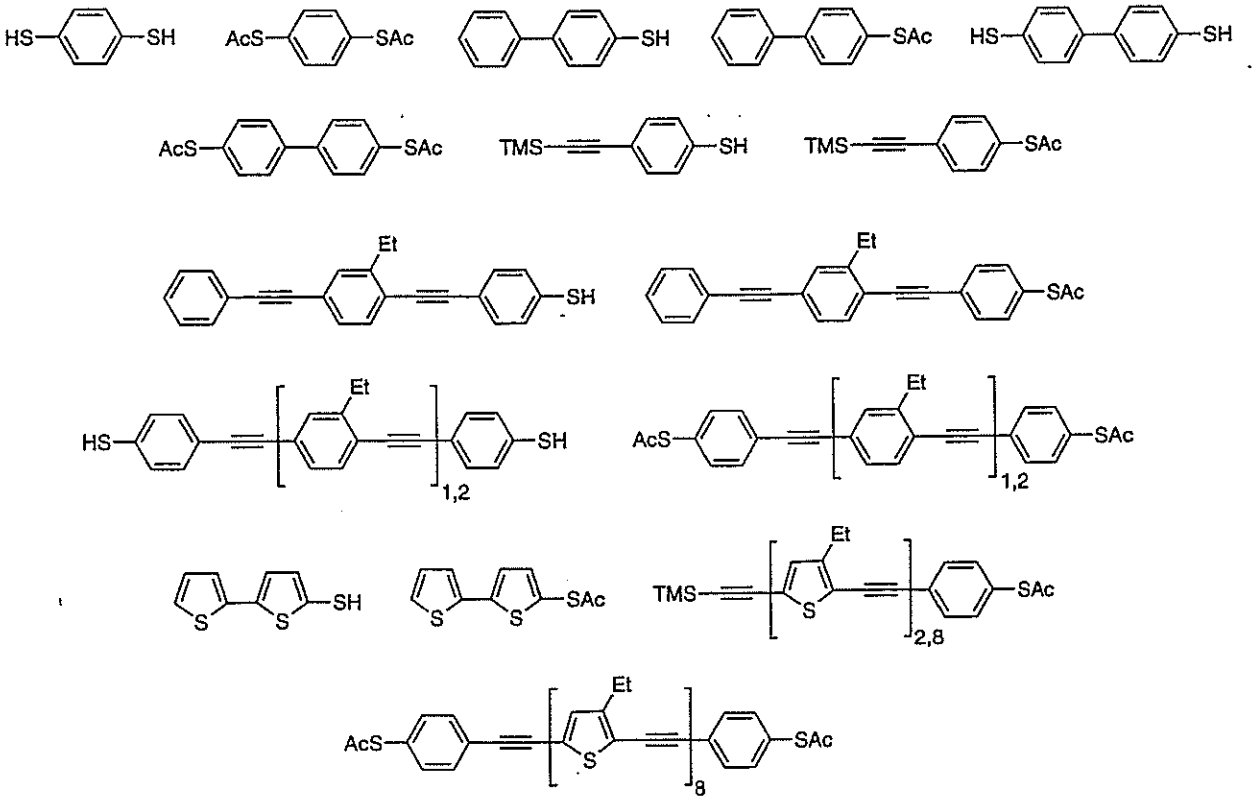

458

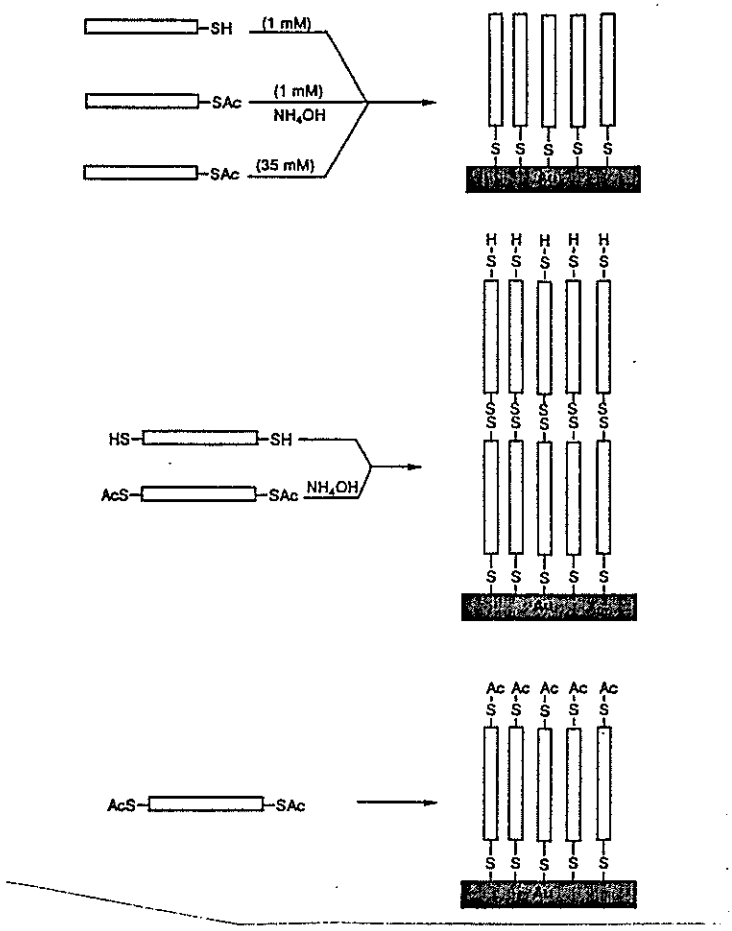

Molecular Electronics
Success Status

(1) Nanoprobes can be constructed. Mechanical break junctions provide a probe assembly for conductance testing of a single molecule.

(2) Molecular frameworks can be rapidly synthesized to the required dimensions.

(3) Self-assembly or self-organization appears to provide an approach to the required molecular placements.

(4) The molecules can be "stapled" into position with the proper functional groups.

(5) "Molecular alligator clips" can be constructed by proper functional group selection for the ends of the "molecular wires".

(6) Molecules with potential device-type properties can be synthesized.

Controlling PS Architecture During Free Radical Polym.

Irene Li and B. A. Howell
Central Michigan University

K. Matyjaszewski, T. Shigemoto
Carnegie Mellon University

P. Kastl, R. Koster, D. B. Priddy, Pat Smith
The Dow Chemical Company, Midland, MI

Outline

- Design of PS Architecture - Four Options
- Review Four Basic Styrene Polymerization Chemistries
- Review Free Radical Polymerization Chemistry
  - Effect of acid
- Broadening Dispersity by Design
- Narrowing Dispersity - Nitroxyl Mediated Styrene Polymerization

Architectural Control of PS

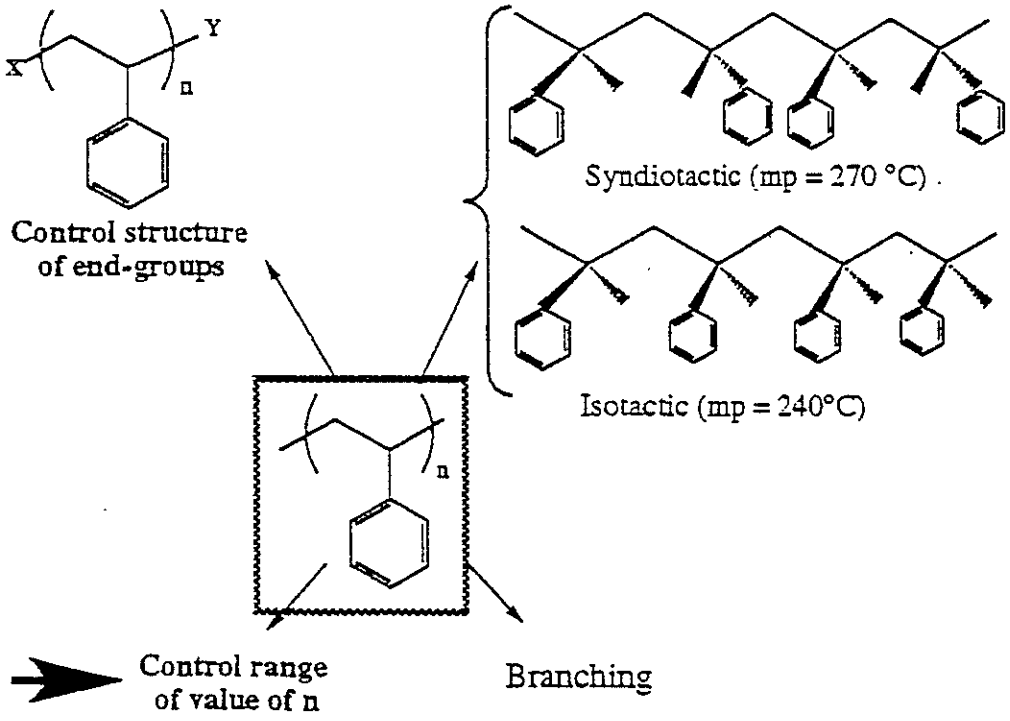

Comparison of Styrene Polym. Mechanisms

Anionic
- initiation, propagation, & termination steps are sequential
- narrow polydispersity (Mw/Mn < 1.1)
- termination step controlled –> control of end-group structure
- polymerization feed must be purified
- not yet commercial for homoPS

Cationic
- Used commercially to make very low MW PS
- polymerization feed must be purified

Ziegler
- Metal complexes - stereospecific polymerization
- polymerization feed must be purified
- being commercialized by Dow & IPC

► Free Radical
- initiation, propagation, & termination simultaneous
- broad polydispersity (Mw/Mn > 2)
- multiple termination paths lead to a variety of end-groups
- polymerization feed need not be purified

Free Radical Termination Mechanisms: Leads to Lack of Control of Architecture

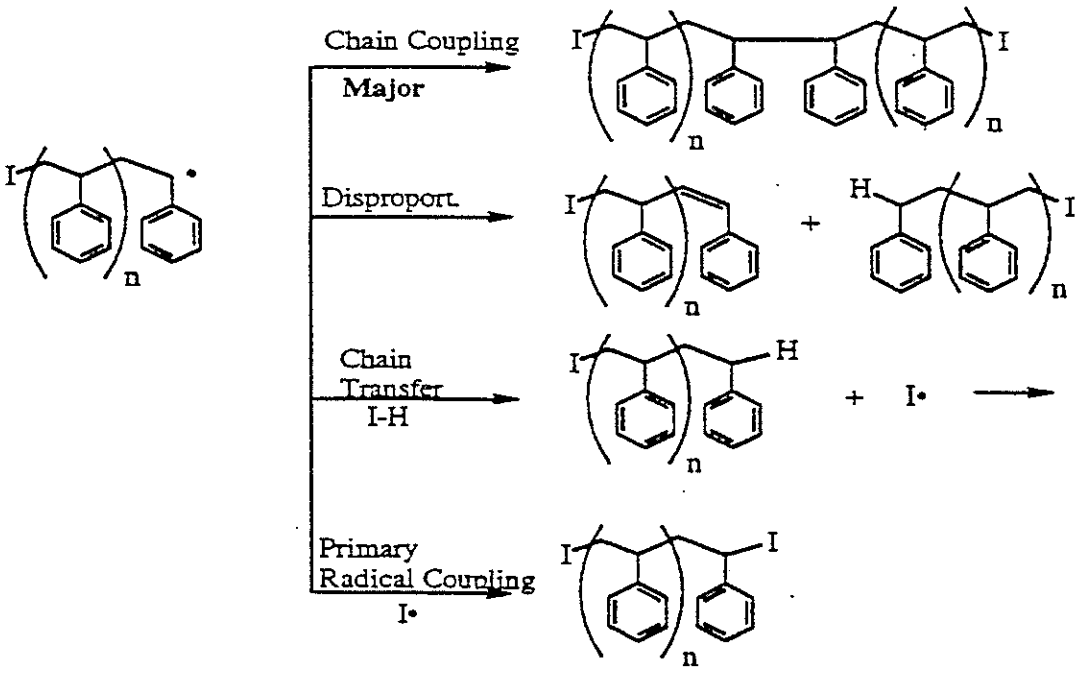

Styrene Spontaneous Polym.

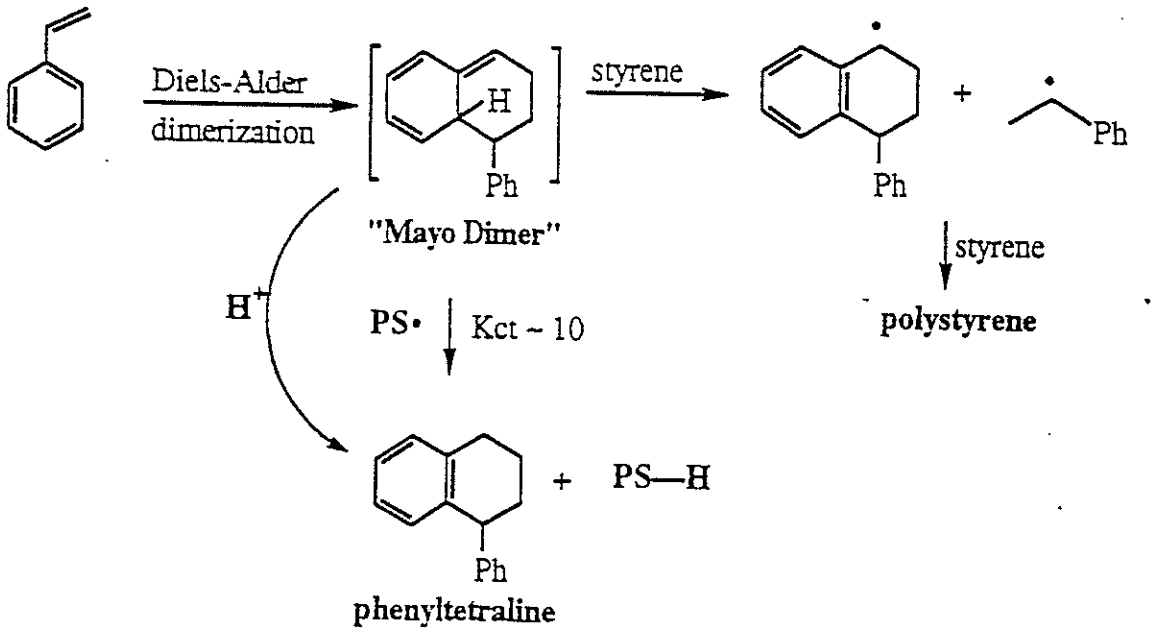

Acid Catalyzed Styrene Polym.

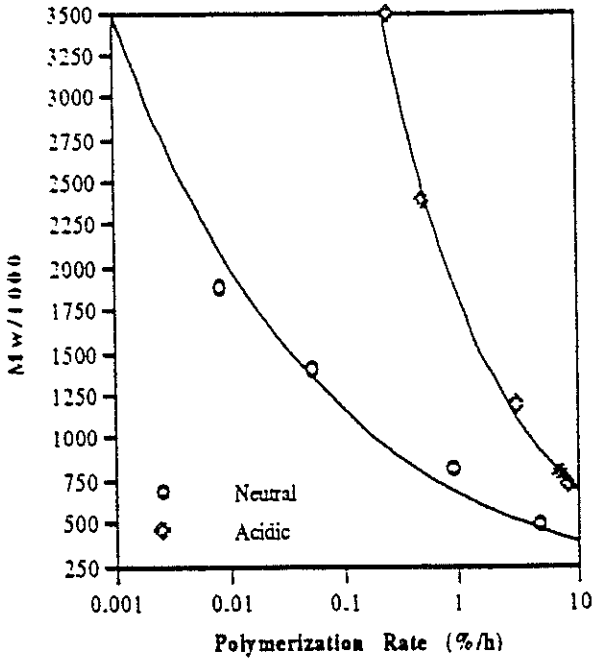

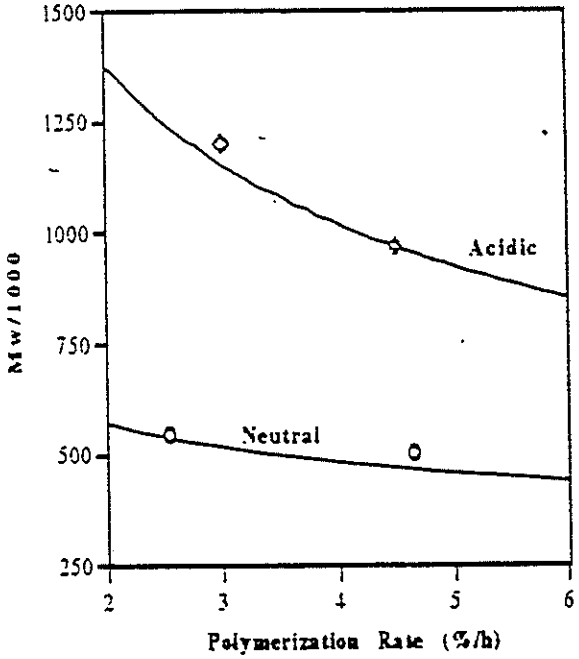

Nitroxyl Mediated Styrene Polym. (NMSP)

- Rizzardo & Solomon (Australia)

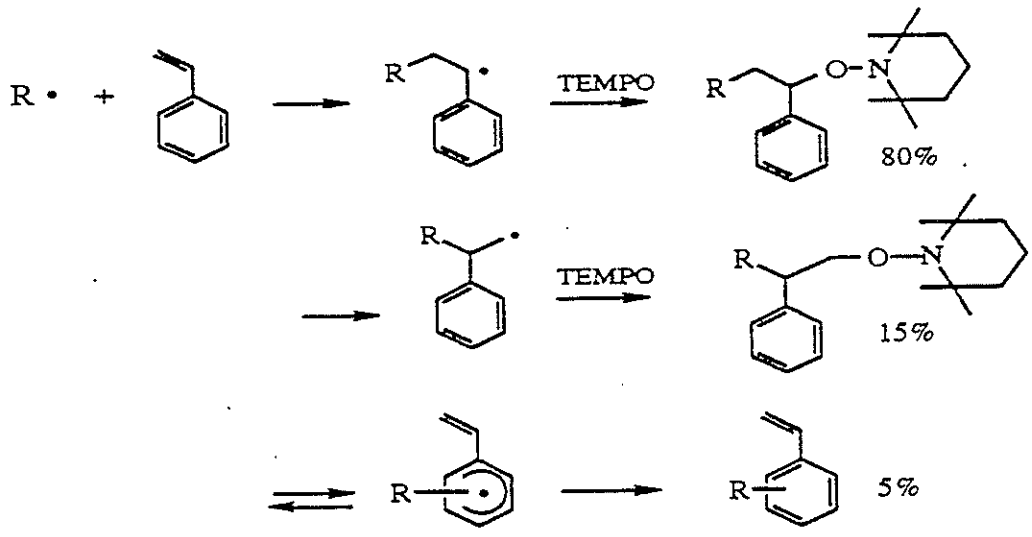

R = (a) Ph–C(=O)–O ; (b) Ph.

Rizzardo & Solomon

- 1984 EP Patent Appl

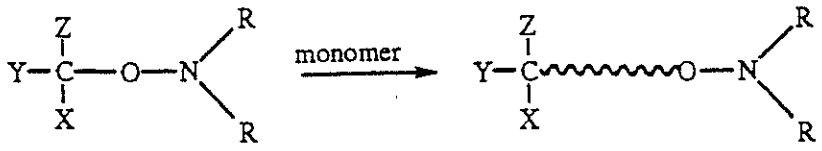

Georges et al - Xerox

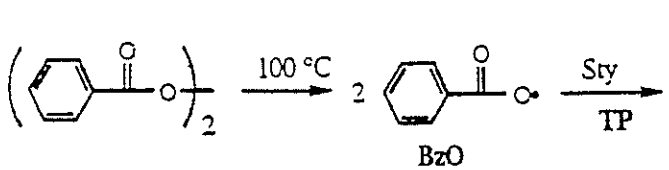

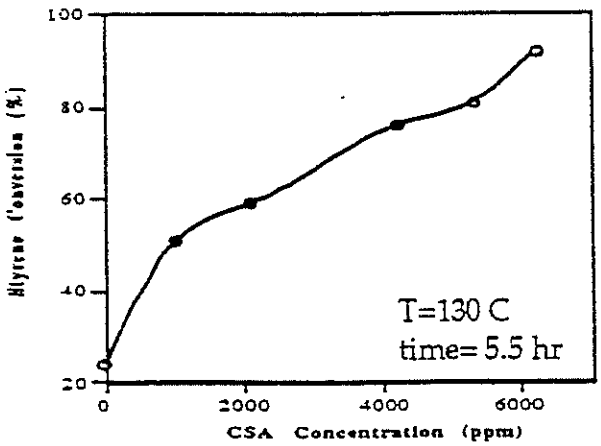

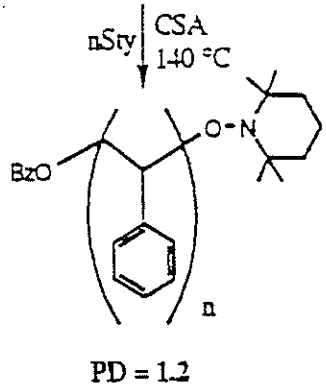

PD = 1.2

Acid increases polym. rate but also broadens PD!

Mw & PD Increase with Conv.

Spontaneous Styrene Polymerization at 140 °C
in the Presence of 5 mmolar TEMPO

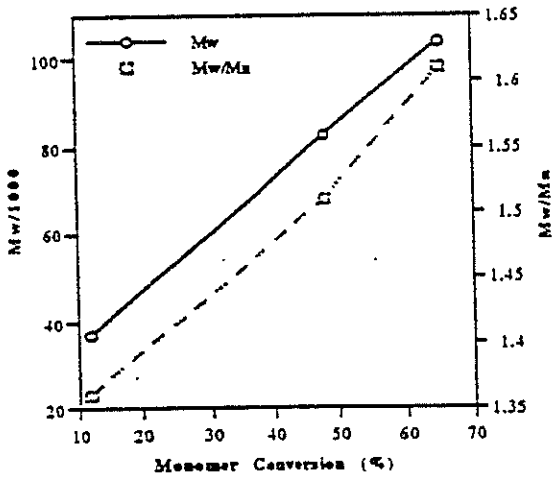

Mw & PD Limitations

Spontaneous Initiation - 140 °C

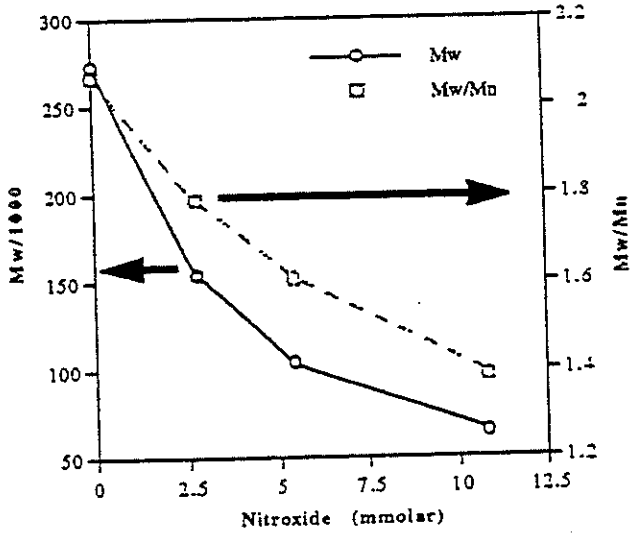

Hawker - IBM

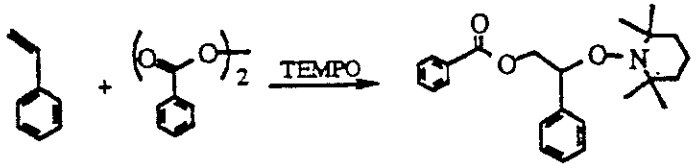

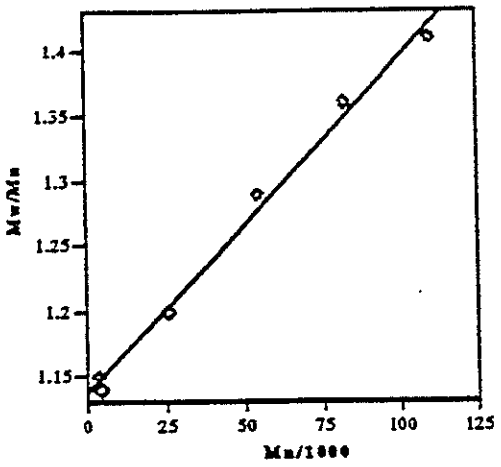

Questions

- Why does PD increase with conversion
- Why does PD increase when trying to make high MW
- Why does acid increase polym. rate
- Why does acid increase PD

Back to the Basics

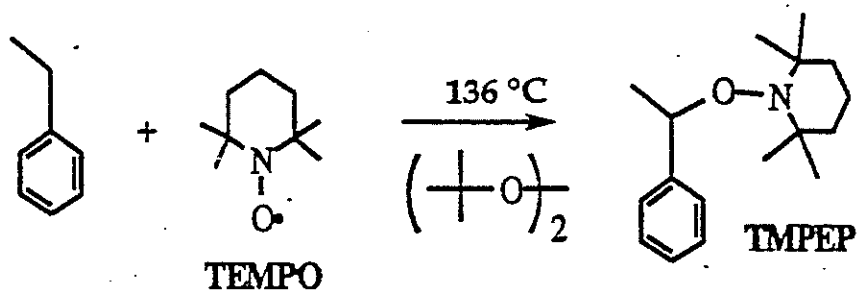

Chain-end Model
for NMSP

TMPEP Initiation - Acid vs Neut.

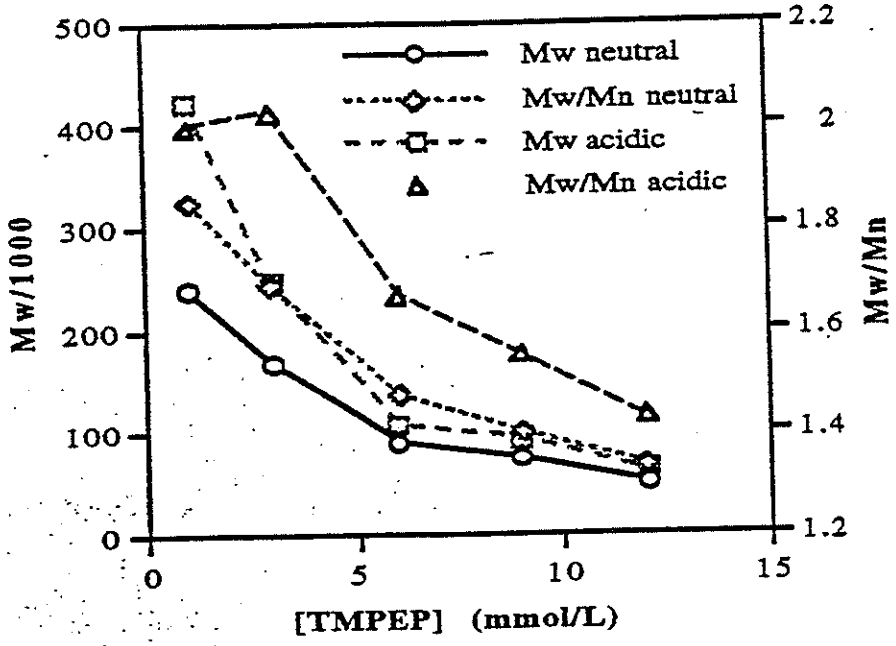

TMPEP Initiation - Acid vs Neut.

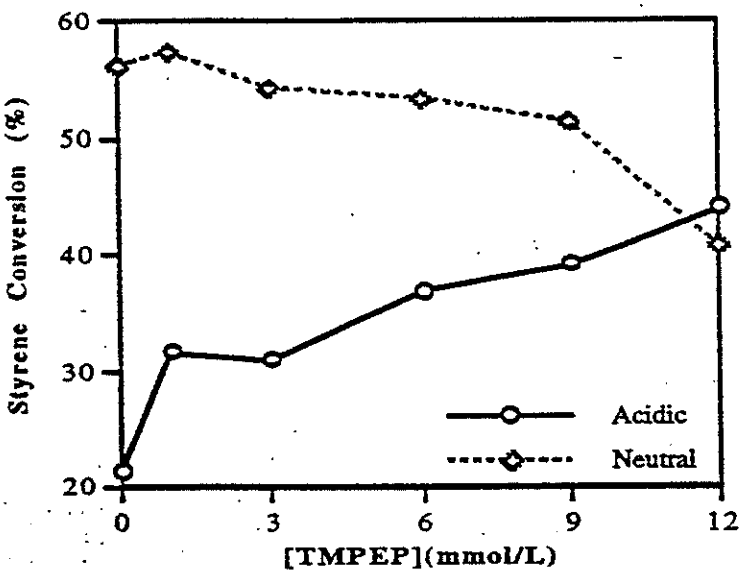

How Thermally Stable is Chain-end?

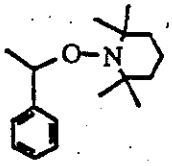

TMPEP

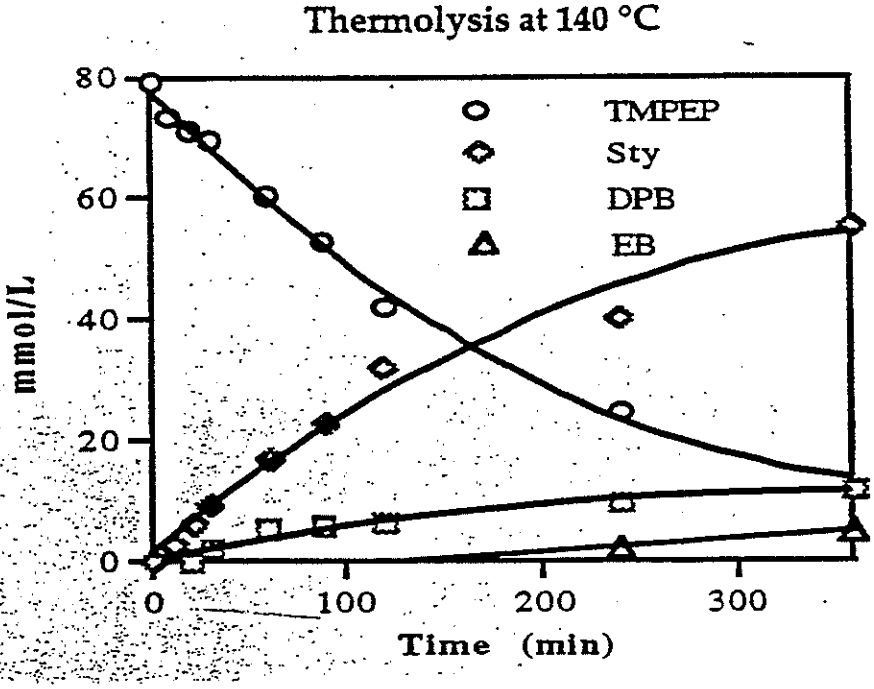

Decomposition Mechanism

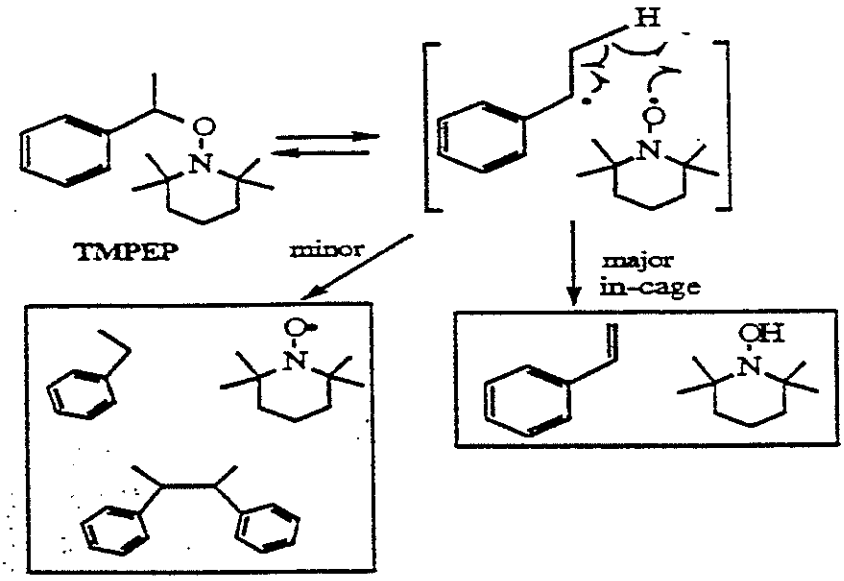

Ea of Thermal Decomp.

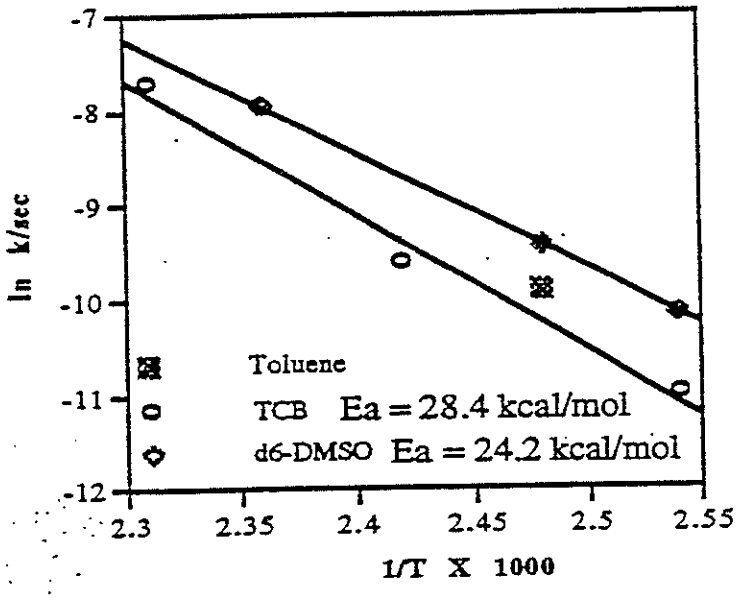

Is Chain-end Decomposition Significant?

Overlay of TMPEP Decomp. & Styrene Polym.
Kinetics Initiated using 12 mmolar TMPEP (140 °C)

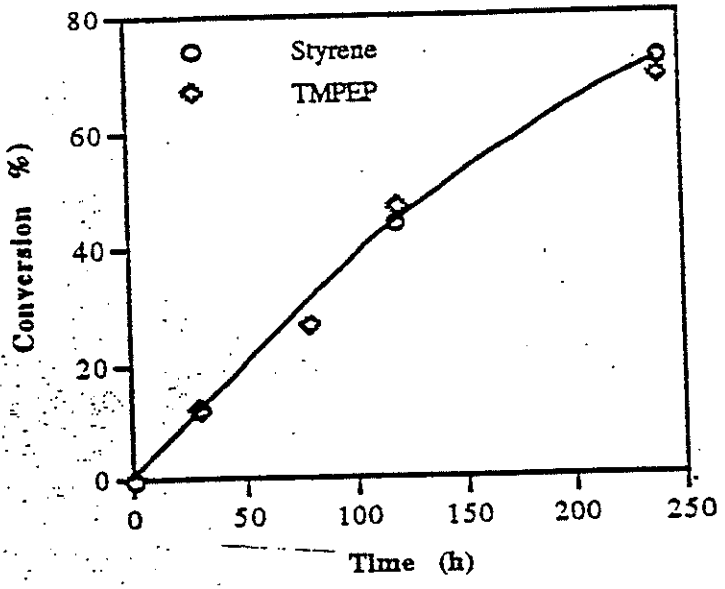

Effect of Air on TMPEP Decomp.

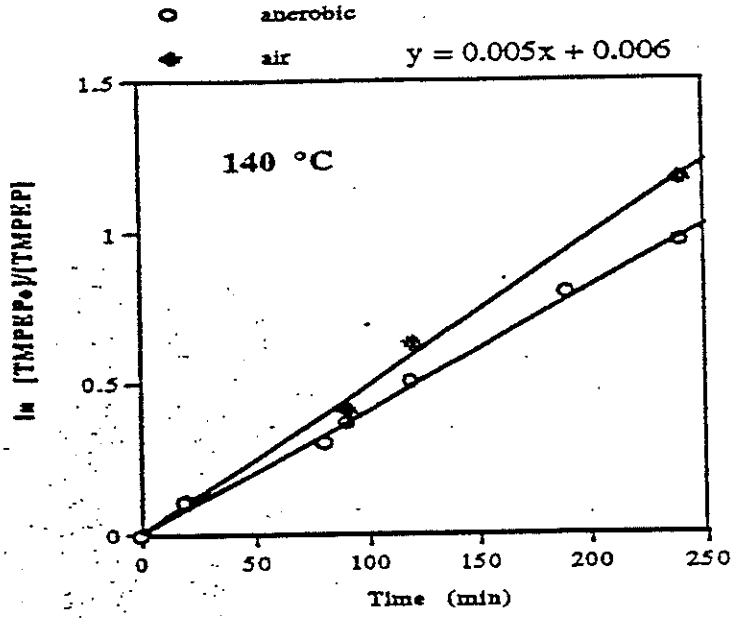

Effect of Air on NMSP

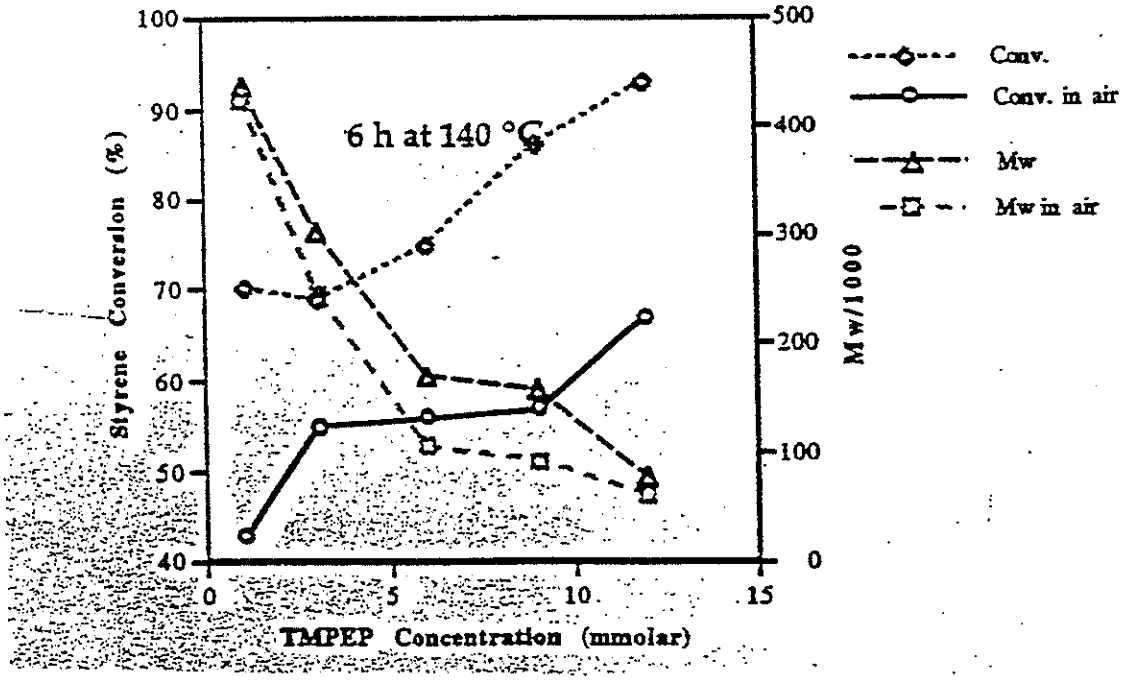

Conclusions & Challenges

Conclusions:

- Chains are constantly dying during NMSP
- Air accelerates the dying process

NMSP Research Challenges :

- How to make High Mw (>100K) PS with truly narrow PD (<1.1)
- Figuring out why acid broadens PD

RECENT ADVANCES IN FREE RADICAL COPOLYMERIZATION

H. JAMES HARWOOD
UNIVERSITY OF AKRON

DR. K. PLOCHOCKA
DR. O. H. JONES
M. ANATER
L. CHRISTOV
A. HUCKSTEP
DR. S. Y. KIM
DR. K. Y PARK
E/R. SANTEE
D.S. TUNG
O.O. WERSTLER
DR. R. BOCKRATH

THE TERMINAL MODEL

$$PM_1^{\cdot} + M_1 \xrightarrow{K_{11}} PM_1^{\cdot}$$

$$PM_1^{\cdot} + M_2 \xrightarrow{K_{12}} PM_2^{\cdot} \qquad r_1 = K_{11}/K_{12}$$

$$PM_2^{\cdot} + M_1 \xrightarrow{K_{21}} PM_1^{\cdot} \qquad r_2 = K_{11}/K_{21}$$

$$PM_2^{\cdot} + M_2 \xrightarrow{K_{22}} PM_2^{\cdot}$$

$$\frac{m_1}{m_2} = \frac{M_1}{M_2} \cdot \frac{r_1 M_1 + M_2}{M_1 + r_2 M_2}$$

CONDITIONAL PROBABILITIES

NO SOLVENT EFFECT

$$P(B/A) = \frac{1}{1 + r_A \frac{A_f}{B_f}}$$

SOLVENT EFFECT

$$P(B/A) = \frac{1}{1 + r_A K \frac{A_f}{B_f}}$$

n-Add Fraction

- written as $f_{\dot{B}A}$, $f_{A\dot{A}\dot{A}A}$, etc.
- fraction of monomer units of a given type that are centered in a particular n-add.

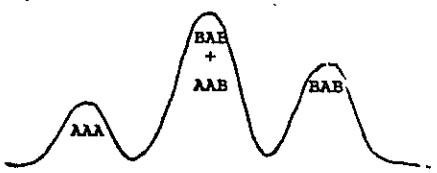

$$f_{BAB} = \frac{\text{BAB area}}{\text{Total area}}$$

SOLVENT EFFECTS IN COPOLYMERIZATION(1)

- IONIZABLE, CHARGED OR POLAR MONOMERS

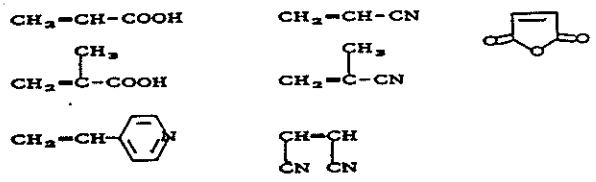

- MONOMERS CAPABLE OF HYDROGEN BONDING

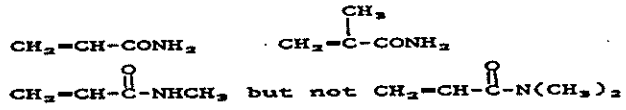

- DRAMATIC REACTIVITY RATIO VARIATIONS DEPENDING ON SOLVENT CHOICE OR pH
- ATTRIBUTED TO:
  a) ELECTROSTATIC REPULSION OF CHARGED MONOMERS.
  b) CHANGES IN MONOMER REACTIVITY (r-values).
  c) PARTICIPATION OF MONOMER COMPLEXES.
  d) HYDROGEN-BONDING OF MONOMER WITH SOLVENT.
  e) SOLVENT DIELECTRIC EFFECTS.

SOLVENT EFFECTS IN COPOLYMERIZATION

K. Plochocka, J. Macromol. Sci., Rev. Macromol. Chem., C20, 67 (1981).

L. Minsk, C. Kotlachik, R. Darlak, J. Polym. Sci., Polym. Chem. Ed., 11, 353 (1973).

K. Plochocka and H. J. Harwood, Polymer Preprints, 19, 2 (1978).

A. Chapiro, Europ. Polym. J., 9, 417 (1973).

A. Suggate, Makromol. Chem., 180, 679 (1979).

H. J. Harwood, Makromol. Chem., Makromol. Symp. 10/11, 331 (1987), cf PP 342-354.

K. Y. Park, E. R. Santee, H. J. Harwood, Eur. Polym. J. 25, 651 (1989).

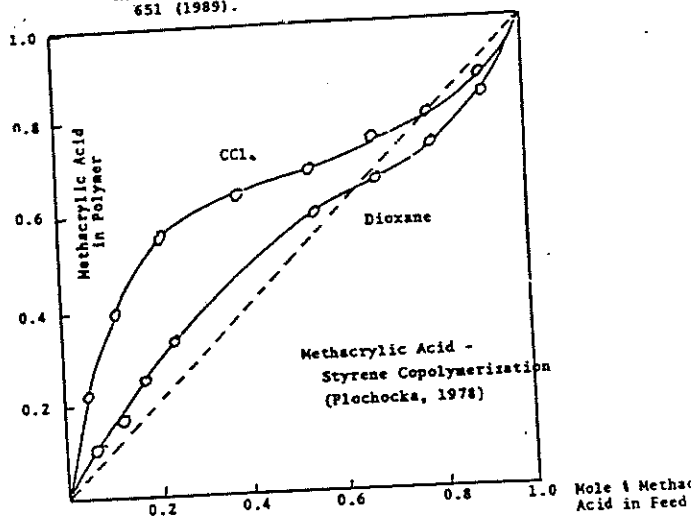

MAA-STYRENE

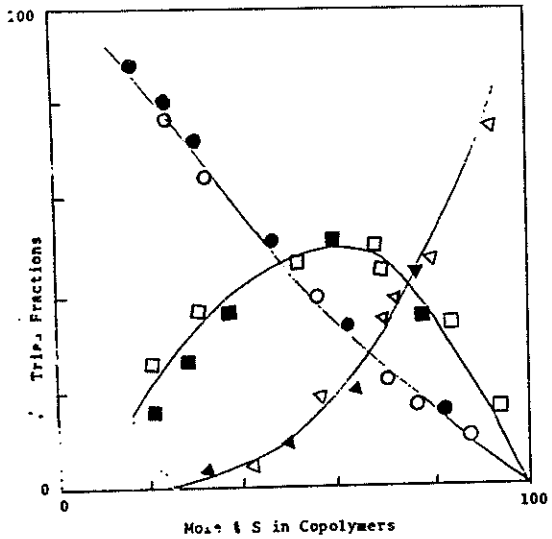

S-Centered Triad Fractions for S-MMA Copolymers in Dioxane (open points) and CCl_4 (solid points)

○, ● - f_{MSM}
△, ▲ - f_{SSS}
□, ■ - $f_{MSS+SSM}$

STYRENE-ACRYLAMIDE COPOLYMERIZATION
Minsk, Kolarchik, Darlak 1973

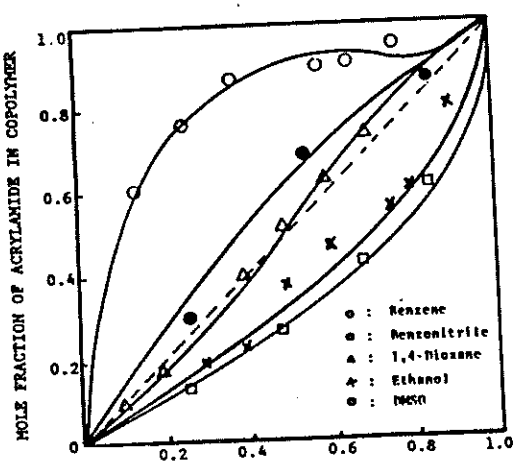

INTRASEQUENCE CYCLIZATION OF POLYACRYLAMIDE

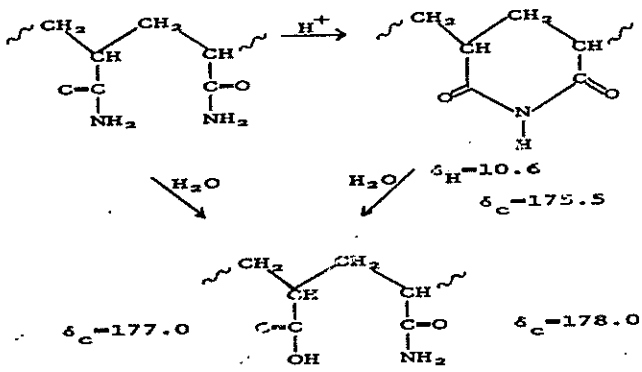

IF NO HYDROLYSIS,

$f_u = e^{-2} = 0.1356$

$\%_c = 1-e^{-2} = 0.8644$

MOLE FRACTION OF CYCLIZED IMIDE UNITS IN COPOLYMERS TREATED WITH HCl GAS VERSUS STYRENE CONTENT.

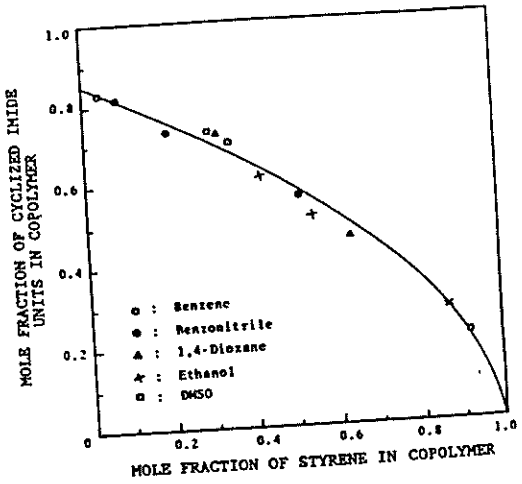

TRIAD FRACTIONS FOR VCl_2-MAN COPOLYMERS PREPARED IN CYCLOHEANONE AND HEXANE

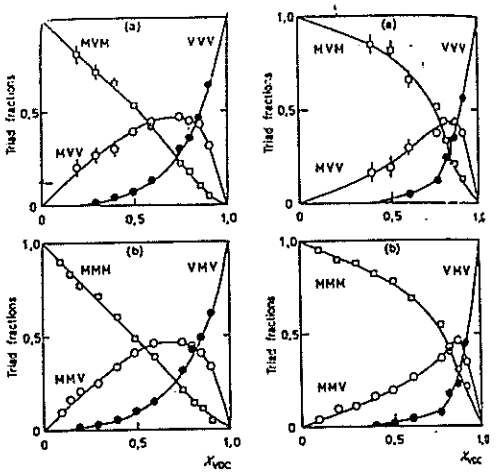

J.R. Suggate, Makromol. Chem., 180, 679 (1979).

VINYLIDENE CHLORIDE - MAN COPOLYMERS

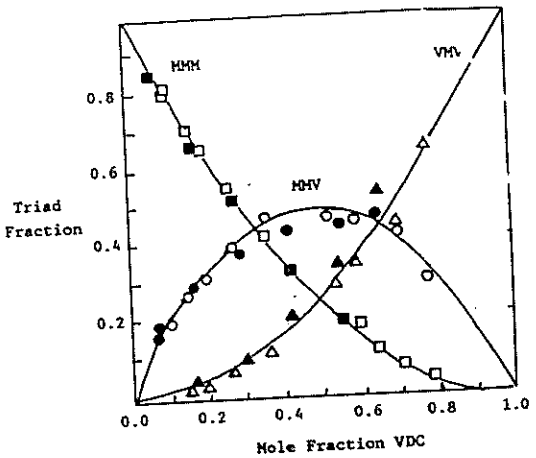

SOLVENT EFFECTS IN STYRENE - MMA COPOLYMERIZATION

T.P. Davis, Polym. Commun., 31, 442 (1990).

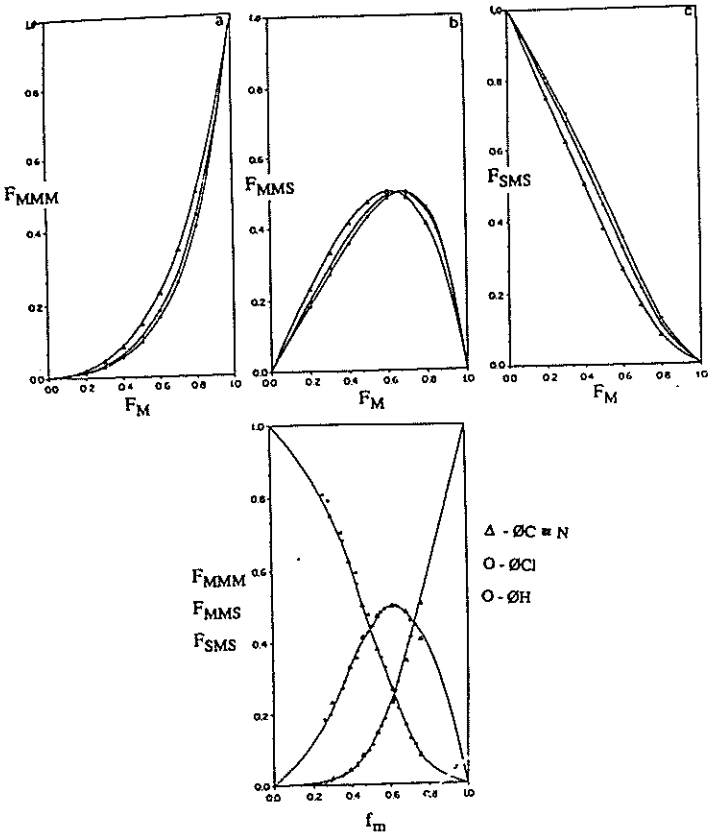

THE "BOOTSTRAP MODEL" FOR COPOLYMERIZATION

- POLYMERIZATION AND COPOLYMERIZ ARE POLYMER MODIFICATION REACTIONS
- THEY CAN BE INFLUENCED BY PARTITIONING OF REAGENT BETWEEN FREE SOLVENT, AND THE "DOMAINS OF POLYMER COILS"

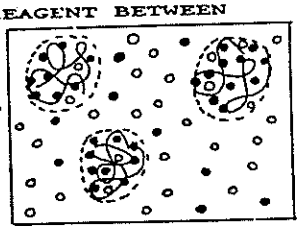

- IN POLYMERIZATION AND COPOLYMERIZATION, THE DOMAIN IS THAT OF A GROWING POLYMER CHAIN AND THE MONOMER IS THE REAGENT.
- THUS A GROWING COPOLYMER CHAIN CA CONTROL THE RELATIVE CONCENTRATIO OF MONOMERS IN THE VICINITY OF ITS PROPAGATING END AND INFLUENCE ITS OWN FORMATION.

CONSEQUENCES OF THE "BOOTSTRAP EFFECT"

- NONPOLAR SOLVENTS WILL FAVOR THE INCORPORATION OF POLAR MONOMERS INTO COPOLYMERS. (THE GROWING COPOLYMER PROVIDES A BETTER ENVIRONMENT FOR THE POLAR MONOMER THAN DOES THE SOLVENT-MONOMER COMBINATION).
- ALL REACTIVITY RATIOS REPORTED FOR POLAR MONOMER COPOLYMERIZATIONS ARE PROBABLY IN ERROR.
- PREVIOUSLY REPORTED PENULTIMATE EFFECTS MAY BE MANIFESTATIONS OF THE BOOTSTRAP EFFECT.
- NEW METHODS NEED TO BE DEVELOPED FOR EVALUATING REACTIVITY RATIOS WHEN POLAR MONOMERS ARE INVOLVED. EQUILIBRIUM DIALYSIS IS A POSSIBLE APPROACH.

FEATURES OF SYSTEMS INFLUENCED BY THE BOOTSTRAP EFFECT

- Selectivities of initiating radicals should be independent of solvent choice, even though reactivity ratios appear to depend on solvent choice.
- Sequence distributions of copolymers prepared from a given pair of monomers should be identical for copolymers having the same composition irrespective of the solvent used for their preparation.
- Copolymers should have "tapered" structures. The compositions of copolymers prepared from a given copolymerization should be dependent on chain length.
- Chain transfer reactions should also be influenced by solvent and by the bootstrap effect.
- The absolute rates of propagation reactions should be dependent on polymer radical size and on solvent choice.

SOLVENT EFFECTS ON COPOLYMERIZATION WHEN IDEAL COPOLYMERIZATION BEHAVIOR IS EXPECTED

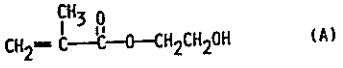

(A)

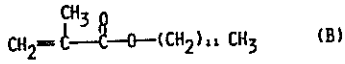

(B)

K. ITO, T. KITANI, E. YAMADA AND T. MATSUMOTO, POLYMER J., 17, 761 (1985)

HYDROXYETHYL METHACRYLATE /LAURYL METHACRYLATE COPOLYMERIZATION

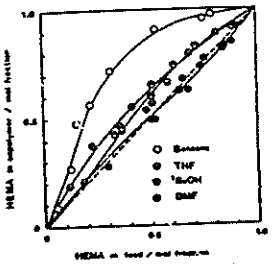

Figure 1. Composition curves for copolymerizations of HEMA and LMA in various solvents. Total monomer concentration = 0.5 mol l^{-1}.

Methyl Methacrylate-Methacrylic Acid Copolymerization

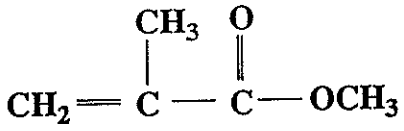

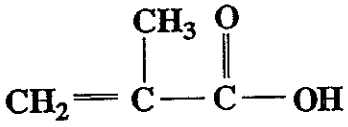

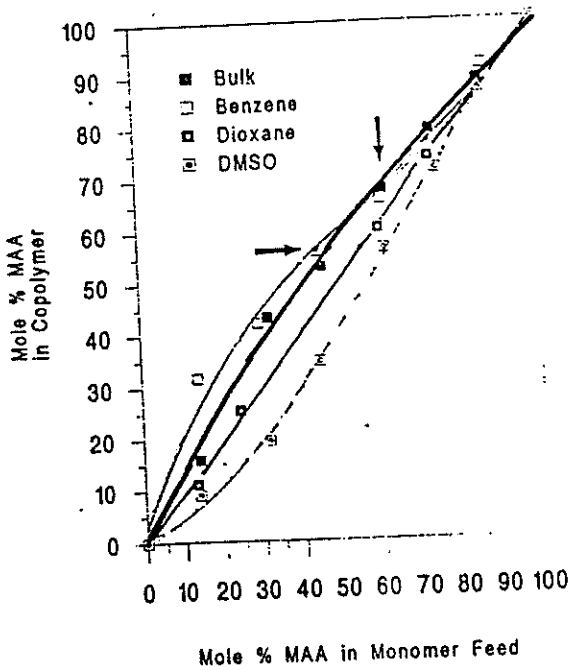

Copolymer Composition - Monomer Feed Plot

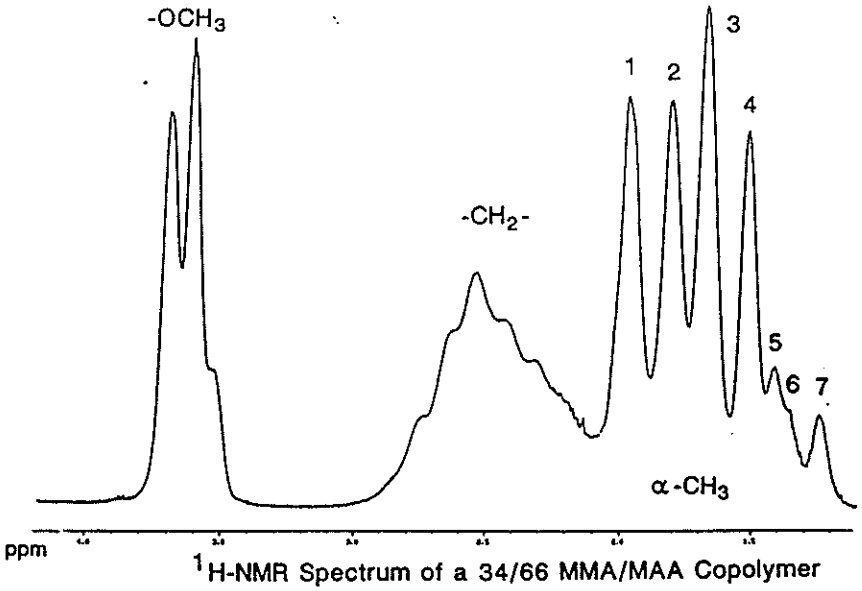

^{1}H-NMR Spectrum of a 34/66 MMA/MAA Copolymer

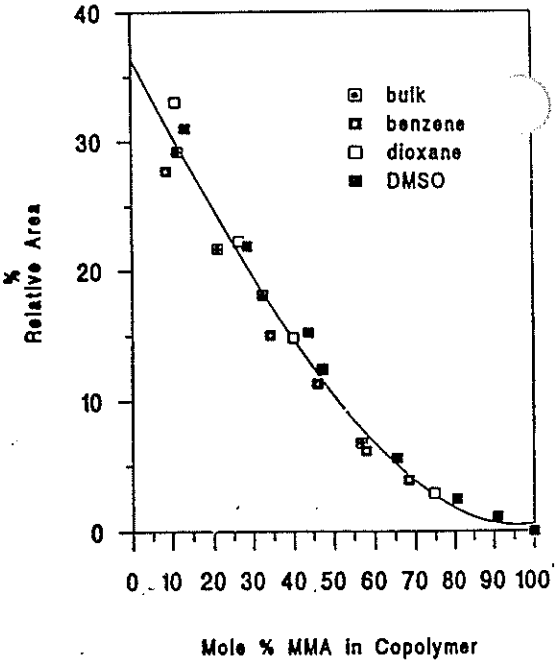

Fig. 12. Relative Resonance Area of Peak C3 as a Function of Copolymer Composition

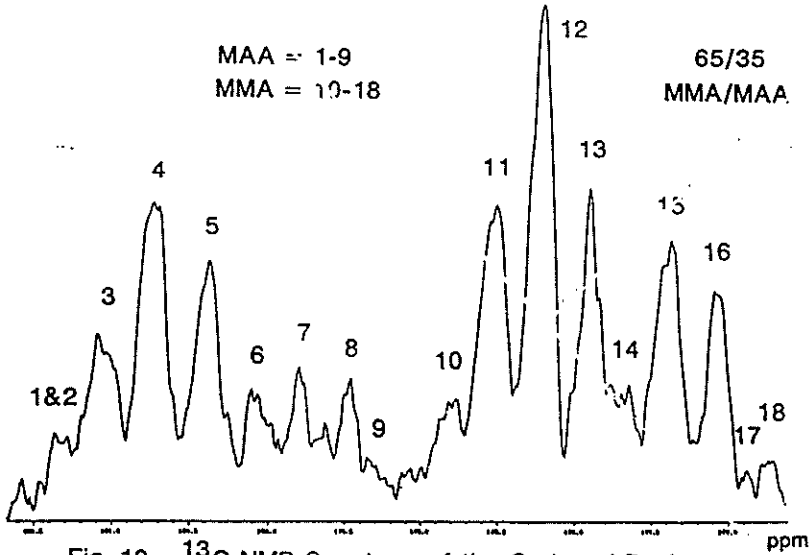

Fig. 10. ^{13}C-NMR Spectrum of the Carbonyl Region

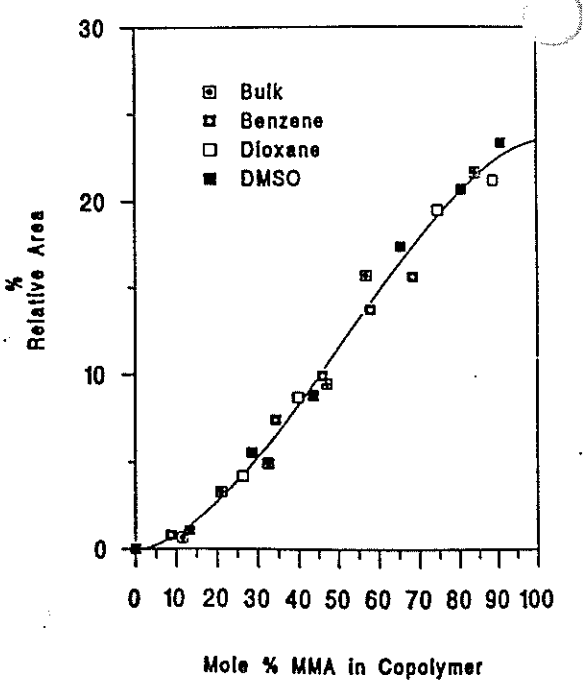

Fig. 17. Relative Resonance Area of Peak C12 as a Function of Copolymer Composition

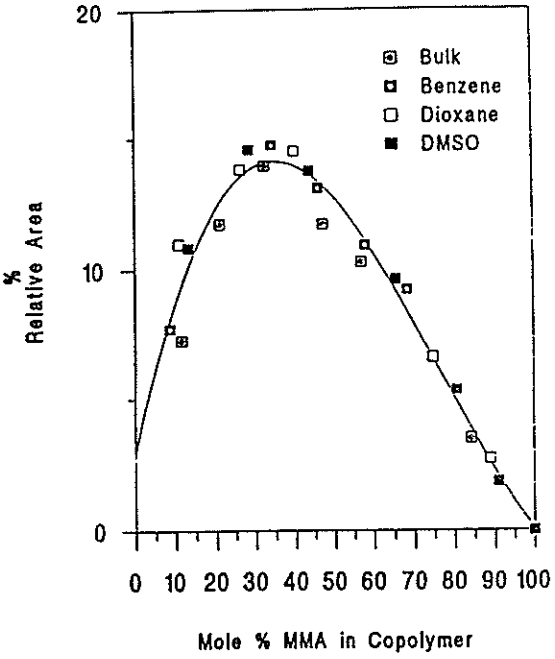

Fig. 13. Relative Resonance Area of Peak C4 as a Function of Copolymer Composition

Use of ^{13}C-Enriched AIBN to Investigate Effect of Solvent on The First Step in Copolymerization

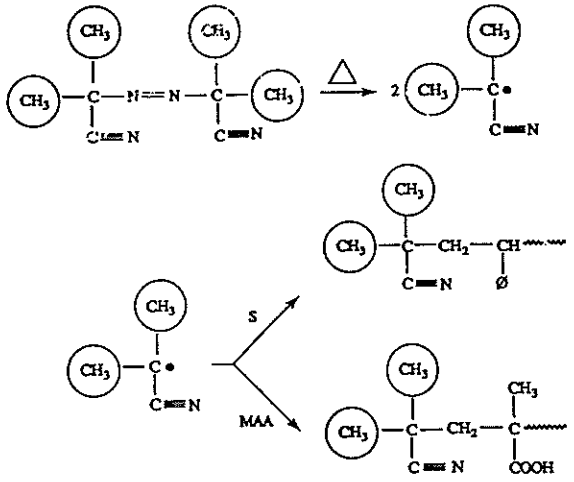

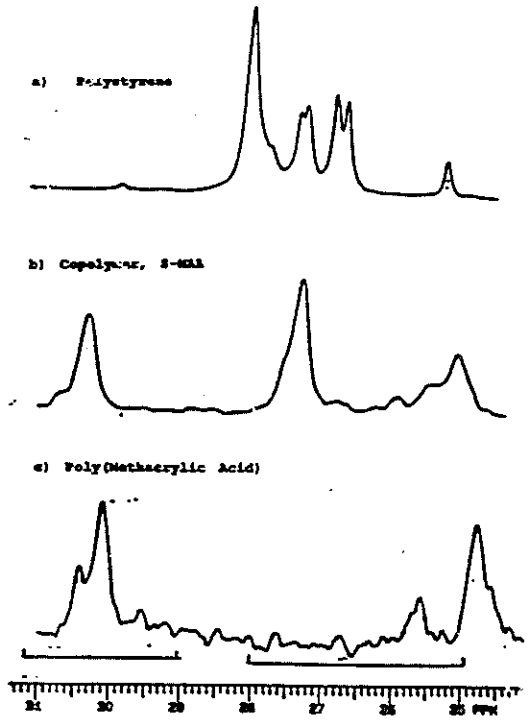

Figure 19: 200 MHz ^{13}C-NMR Resonances of ^{13}C-Enriched Initiator Fragments in a) Polystyrene, b) Copolymer S-MAA and c) Poly(Methacrylic Acid).

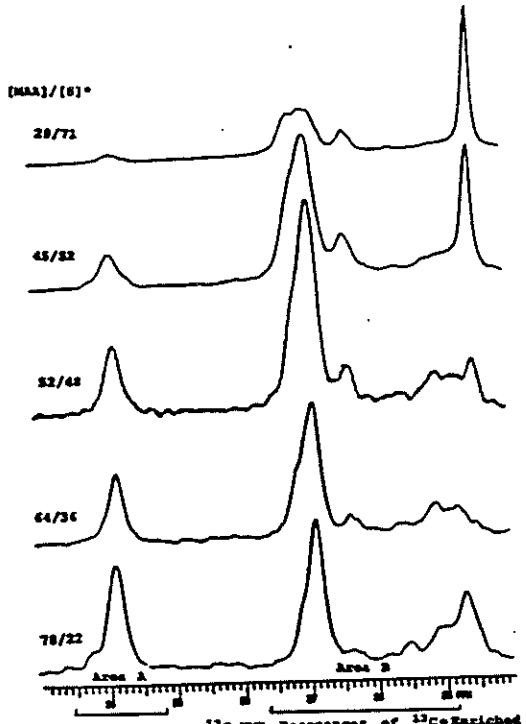

Figure 20: 200 MHz ^{13}C-NMR Resonances of ^{13}C-Enriched AIBN Initiator Fragments in Styrene-Methacrylic Acid Copolymers Prepared Using Methanol as a Solvent.

*Mole Percentages of Styrene and Methacrylic Acid in the Monomer Mixtures Used to Prepare the Copolymers

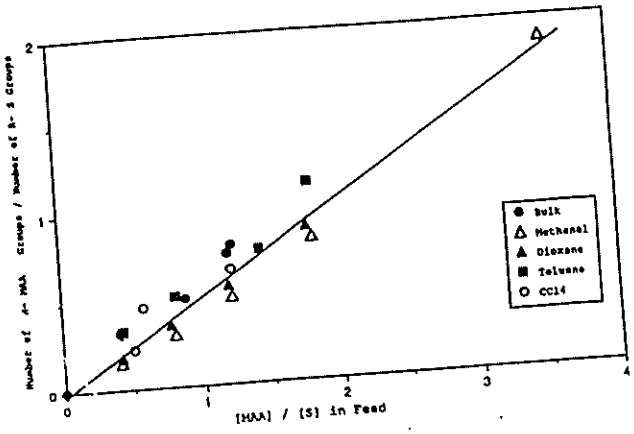

Figure 30 : Ratios of End Group Concentrations vs Monomer Feed Ratios for Copolymers Prepared in Various Solvents

RELATIVE REACTIVITIES OF INITIATOR RADICALS TOWARD MONOMERS IN VARIOUS SOLVENTS (30°C)

Radical	Solvent	k_{MMA}/k_{VAC}	k_S/k_{MMA}
$(CH_3)_2\dot{C}COOCH_3$	C_6H_6	46 ± 3	
$(CH_3)_2\dot{C}COOCH_3$	EtOAc	48 ± 2	
$(CH_3)_2\dot{C}COOCH_3$	CH_3OH	51 ± 1	
$(CH_3)_2\dot{C}CN$	C_6H_6	29 ± 2	1.8
$(CH_3)_2\dot{C}CN$	EtOAc	27 ± 3	1.8
$(CH_3)_2\dot{C}CN$	CH_3OH	26 ± 1	2.1

J. Kristina, G. Moad and D.H. Solomon, Eur. Polym. J., 28, 275 (1992).

INFLUENCE OF POLYMER RADICAL SIZE ON BOOTSTRAP EFFECT

Y.D. Semchikov, et al, Eur. Polym. J., 26, 883 (1990); Eur. Polym. J., 28, 681 (1992).

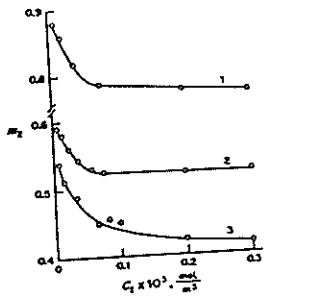

Fig. 1. The dependence of variation of chemical composition (m_2) of the copolymers: (1) 2M5VP–VA, (2) St–MAA and (3) St–AN upon the concentration of initiators: (1) BP, (2) AIBN, (3) DCC at (1,2) 333 K, (3) 313 K and (1,2) $M_2 = 0.5$; (3) 0.75. Here and in Figs 1–4, M_2 and m_2 represent respectively the mole fractions of 2M5VP, MAA or AN units in the monomer mixture and the copolymer derived from the monomer mixture by bulk polymerization to 5% conversion.

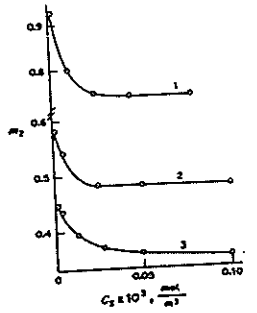

Fig. 2. The dependence of the compositions (m_2) of (1) 2M5VP–VA, (2) St–MAA and (3) St–AN copolymers prepared from equimolar monomer mixtures on the concentrations of chain transfer agent: (1) RSH, (2) Ph_3GeH, (3) CBr_4 at 333 K.

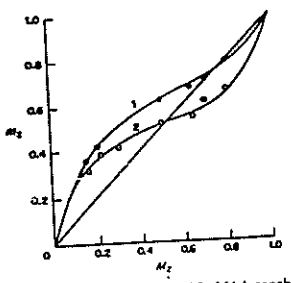

Fig. 3. The curves of composition of St–MAA copolymers prepared in the presence of [BP] = (1) 5 and (2) 200 mol/m³.

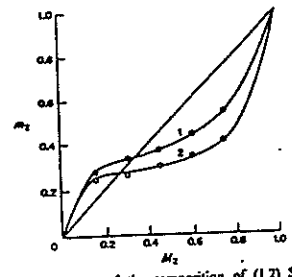

Fig. 4. The curves of the composition of (1,2) St–AN copolymers prepared in the presence of (1) [DCC] = 5 and (2) 100 mol/m³ at (1,2) 313 K.

DEPENDENCE OF S-MMA COMPOSITION ON MW

Y.D. Semchikov

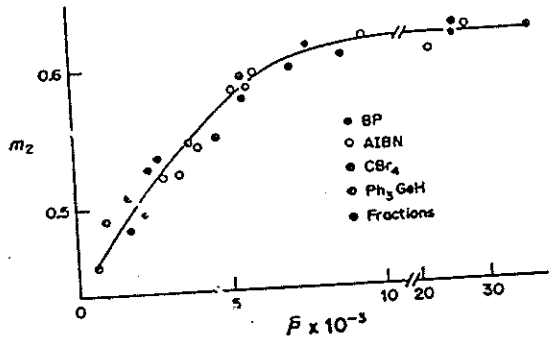

Fig. 5. The dependence of the composition (m_2) of St–MAA copolymer ($M_2 = 0.5$) upon the polymerization degree ($\bar{P}$), prepared at various concentrations of AIBN (○), BP (●) and chain transfer agents: CBr_4 (⊙), Ph_3GeH (◐) or obtained using fractional precipitation (⊗). Synthesis conditions for copolymers prepared in the presence of the chain transfer agents and for fractionation —[AIBN] = 5 mol/m³, 333 K, 5% conversion.

THE BOOTSTRAP EFFECT IN HOMOPOLYMERIZATION

J. PAVLINEC, S. FLORIAN AND V. PALENIK, EUR. POLYM. J., 11, 541 (1975).

J. PAVLINEC, M. JERGUSOVA AND S. FLORIAN, EUR. POLYM. J., 18, 279 (1982).

POLYMERIZATION RATE - INFLUENCED BY VISCOSITY AND RATIO OF SOLVENT AND MONOMER IN THE "DOMAIN OF THE POLYMER COIL."

DEPENDENCE OF R_p ON [M]- FIRST POWER AFTER CORRECTION FOR CONCENTRATION IN THE "DOMAIN OF THE POLYMER COIL."

INFLUENCE OF SOLVENT ON ABSOLUTE PROPAGATION RATES

B.R. Morrison, M.C. Piton, M.A. Winnik, R.G. Gilbert and D.H. Napper, Macromolecules, 26, 4368 (1993).

T.P. Davis, K.F. O'Driscoll, M.C. Piton and M.A. Winnik, Macromolecules, 22, 2785 (1989).

K.F. O'Driscoll, T.P. Davis, B. Klumperman and E.I. Madruga, Macromol. Rapid Commun., 16, 207 (1995).

S. Benermann, M. Buback and G.T. Russell, Macromol. Rapid Commun., 15, 647 (1994).

- **PULSED LASER POLYMERIZATION (OLAJ)**
  D.P. = k_p (M) t
- k_p at 25°C

Monomer	Solvent	k_p
Styrene	Bulk	84 L mole^{-1} sec^{-1}
	25% EtOH	76 L mole^{-1} sec^{-1}
	50% EtOH	80 L mole^{-1} sec^{-1}
	75% EtOH	101* L mole^{-1} sec^{-1}
	25% MeOH	70 L mole^{-1} sec^{-1}
MMA	Bulk	306/327 L mole^{-1} sec^{-1}
	25% EtOH	300 L mole^{-1} sec^{-1}
	50% EtOH	292 L mole^{-1} sec^{-1}
	75% EtOH	414* L mole^{-1} sec^{-1}
	ØCl	282/315 L mole^{-1} sec^{-1}
	ØCN	343/374 L mole^{-1} sec^{-1}

*Precipitation

INFLUENCE OF SOLVENT ON k_p FOR POLAR MONOMERS

V.F. Gromov and P.M. Khomikovskii, Russ. Chem. Rev., 48, 1040 (1979).

V.F. Gromov, et al, Eur. Polym. J., 16, 529 (1980).

Solvent	k_p
Acrylamide (30°C)	
Water (PH 7)	7.9
Water (PH 13)	5.8
Formamide	1.2
DMSO	0.37
Acrylic Acid (30°C)	
Water	31,900
Formamide	5,700
DMSO	760
Methacrylic Acid (40°C)	
Water	6,500
DMSO	310
Fluoracrylic Acid (20°C)	
Water	2,600
Formamide	2,200
DMSO	1,100

PROPAGATION RATES IN COPOLYMERIZATION

T. Fukuda, K. Kubo, Y-D Ma and H. Inagaki, Polym. J., 19, 523 (1987); Macromolecules, 18, 17, 26 (1985).

S-MMA Copolymerization

- Terminal Model Reactivity Ratios Adequate to Describe Copolymer Composites and Microstructure
- Termination Rates Linear Function of Composition
- Propagation Rates are Not Consistent with Terminal Model -- Penultimate Model Proposed

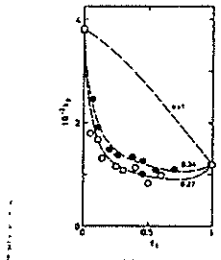

Figure 5. Plot of k_p vs. f_1 for the ST MMA/TOL/40°C system (open circles): the filled circles are for the bulk system,[1] and the curves were calculated with the penultimate model with the indicated values of $s(=s_1=s_2)$; clearly, the curve with $s=1$ corresponds to the terminal model.

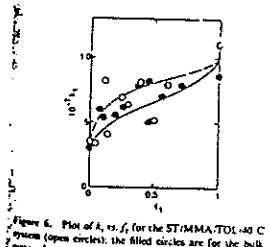

Figure 6. Plot of k_p vs. f_1 for the ST/MMA/TOL/40 C system (open circles); the filled circles are for the bulk system,[1] and the solid and the broken curves represent the North model[14] and the chemical model with $\phi=1$,[15] respectively.

PROPAGATION RATES IN COPOLYMERIZATION

I.A. Maxwell, A.M. Aerdts, and A.L. German, Macromolecules, 26, 1956 (1993).

S-MMA Copolymerization

- Triad Sequence Distribution Data Consistent with Terminal Model Reactivity Ratios
- Adjustment of Monomer Ratios Using a Single Bootstrap Parameter Enables Terminal Model to Accommodate Variations of Propagation Constants with Monomer Feed Composition

$$\frac{(M)}{(S)} = K\frac{(M_f)}{(S_f)}$$

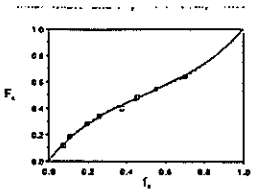

Figure 9. Fraction of styrene in copolymer versus fraction of styrene in feed. Experimental results (squares) from ref 5. Solid line is the fit of the simple bootstrap terminal model (SBTM) with $r_s = 2.41$, $r_m = 0.11$, and $K = 0.22$. Dashed line is the fit of the complex bootstrap terminal model (CBTM) with $r_s = 2.32$, $r_m = 0.05$, $K = 0.15$, and $z = 1.17$.

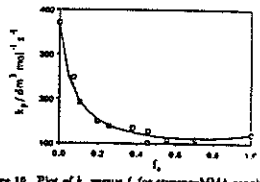

Figure 10. Plot of k_p versus f_s for styrene–MMA copolymerization at 40 °C. Experimental results (squares) from ref 5. Solid line is the fit of the simple bootstrap terminal model (SBTM) with $r_s = 2.41$, $r_m = 0.11$, and $K = 0.22$. Dashed line is the fit of the complex bootstrap terminal model (CBTM) with $r_s = 2.32$, $r_m = 0.05$, $K = 0.15$, and $z = 1.17$.

PENULTIMATE EFFECT IN S-AN COPOLYMERIZATION

D.J.T. Hill, A.P. Lang, P.D. Munro and J.H. O'Donnell, Polym. J., 28, 391 (1992).

- Model Radical Reaction Studies (D.A. Tirrell, et al) Indicate that γ-CN Groups Influence Radical Reactivity and Selection
- Sequence Distribution Studies Indicate Penultimate Effect
- Copolymerization Behavior with CH3CN as Solvent Resembles Bulk Copolymerizations when AN Concentration is High. Behavior in Toluene Resembles Bulk Copolymerizations When S Concentration is High

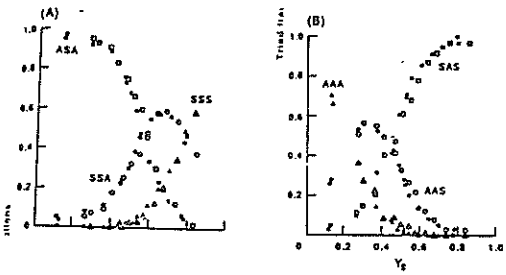

Fig. 6. Comparison between the triad fractions for the copolymerization of styrene and acrylonitrile in toluene and acrylonitrile at 60°C. The styrene-centred and acrylonitrile-centred triad fractions have been plotted against the copolymer composition, Y_S. (A) Styrene-centred triad fractions, ▲ ASA, ● SSA, ■ SSS. (B) acrylonitrile-centred triad fractions. ▲ ● ■. Triad fractions for the copolymerization in toluene; △ ○ □. triad fractions for the copolymerization in acetonitrile.

QUANTIFICATION OF THE BOOTSTRAP EFFECT

B. Klumperman and K.F. O'Driscoll, Polymer, 34, 1032 (1993).

B. Klumperman and I.R. Kraeger, Macromolecules, 27, 1529 (1994).

- Application to S-MMA, S-MAN, and S-AN Systems
- Reactivity Ratio Product Should Be Constant for All Solvents
- Quantification of K, Using Bulk System as a Reference State

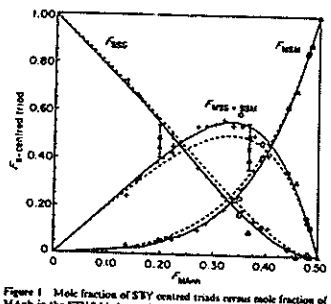

Figure 1 Mole fraction of STY centred triads versus mole fraction of MAnh in the STY/MAnh copolymer: (+) butanone, 110°C; (○) bulk, 60°C; (△) toluene, 60°C. Dashed curves are the Mayo–Lewis model predictions with $r_1r_2 = 0$. Drawn curves are the penultimate unit model predictions with $r_{11}/r_{21} = 0.63$